DESIGN OF GASTRO-RETENTIVE SYSTEMS FOR THE ERADICATION OF HELICOBACTER - PYLORI INFECTIONS IN THE TREATMENT OF PEPTIC ULCER

ADEOLA OMOLARA ADEBISI

B.Sc. (PHARM), M.Sc. (PHARMACEUTICS)

A THESIS SUBMITTED TO THE UNIVERSITY OF HUDDERSFIELD IN PARTIAL FULFILMENT OF THE REQUIREMENTS FOR THE DEGREE OF DOCTOR OF PHILOSOPHY

University of
HUDDERSFIELD

SEPTEMBER 2014

COPYRIGHT STATEMENT

THESIS SUMMARY

Obstacles to the successful eradication of *H. pylori* infections include the presence of antibiotic resistant bacteria and therapy requiring multiple drugs with complicated dosing schedules. Other obstacles include bacterial residence in an environment where high drug concentrations are difficult to achieve. Conventional oral formulations used in the treatment of *H. pylori* infections have a short gastric residence time, thus limiting the duration of exposure of drug to the bacteria. Gastro-retentive formulations such as floating and mucoadhesive systems can prolong the residence time of the formulation in the stomach and maintain a controlled release of drug. The purpose of this study was to prepare gastroretentive formulations such as alginate beads and ethylcellulose microspheres loaded with antibiotics such as clarithromycin (CMN) and metronidazole (MET). These formulations were characterized and evaluated for their gastro-retentive potential.

Drug-loaded beads were prepared by ionotropic gelation using 3 %w/w sodium alginate solution and 0.07 M calcium chloride solution as the gelling medium. The beads produced exhibited limited buoyancy, mucoadhesion and fast drug release especially MET beads with drug release complete within 3 – 4 h and CMN release complete within 8 h. These beads were modified in order to improve their floating / mucoadhesion characteristics and to control their release profile through addition of olive oil and/or coating with chitosan. Chitosan coating created an additional barrier on the surface of the beads, to sustain the release of drug from the beads and create a mucoadhesive surface on the beads. The addition of oil improved the buoyancy of the beads, which was useful for gastro-retentive applications. Beads that were modified both with oil and coated with chitosan, provided the best-combined buoyancy, mucoadhesive and drug release profiles, with the beads floating for at least 24 h, adhering to pig gastric mucosa for at least 12 h and drug release sustained beyond 12 h.

Clarithromycin-loaded ethylcellulose microspheres were prepared using the solvent evaporation method and the mucin-binding lectin, Concanavalin A (Con A), was successfully attached to the microspheres up to a maximum of 15.3 µg Con A per mg microsphere. The inclusion of CMN did not significantly reduce the amount of Con A bound to the surface of the microspheres, however, conjugation led to a reduction in the drug entrapment efficiency

(DEE) of the microspheres with more drug loss being observed with the S-10 series (microspheres from 10 cps ethylcellulose) than the S-46 series (microspheres from 46 cps ethylcellulose). Increasing chitosan concentration decreased the conjuation efficiency of Con A. *Ex vivo* mucodhesion studies and *in vitro* interactions with mucin confirmed the enhancement of mucoahesion due to the presence of lectin with conjugation increasing with increasing amount of Con A conjugated on the surface of the microspheres. The drug content, DEE, buoyancy and *in vitro* drug release in both the dissolution media and mucin dispersion were not compromised by the conjugation process. These conjugated microspheres demonstrated high buoyancy, improved mucoadhesion and sustained drug release thereby improving the formulations' gastro-retentive potential.

ACKNOWLEDGEMENT

First, I will like to thank God for his grace and blessings in my life. I will also like to thank the University of Huddersfield for providing the funding for this research without which this would have been impossible.

Special thanks also go to my supervisor, Prof. Barbara R. Conway, who provided useful and consistent advice, encouragement and supervision that made this work possible. She is greatly appreciated and I could not have wished for a better and more dedicated supervisor. I will also like to thank Dr Alan Smith for his contributions and valuable advice, which gave me some direction and insight in certain aspects of my research. I will not forget to mention the help of Dr Peter Laity for his help with the X-ray microtomography and SEM images, Dr Neil Mclay for his help with the NMR analysis and Dr Kofi Asare-Addo for his help with the P-XRD scans. Also, special thanks go to Ms Hayley Markham, Ms Margaret Scott and Mr Ibrahim George for their technical support and assistance. I will also like to thank my colleagues in the Pharmaceutics research laboratory for all their support and companionship.

I will also like to thank my dad - Dr G.S.O Adebisi, my mum- Mrs R.A Adebisi, my brothers – Dr Adewale Adebisi and Mr Babajide Adebisi for all their encouragement and support over all these years. You have all been wonderful and words cannot express how much I appreciate and love you all. Finally, I will like to thank my wonderful husband – Mr Oluwatumininu Alegbeleye, who has been my rock, support and who has shared my dreams and aspirations. Thank you for being there through it all, I really appreciate and love you.

DEDICATION

I would like to dedicate this thesis to my loving parents Dr G.S.O Adebisi and Mrs R.A Adebisi for all your support and dedication. I will always love you ….

Table of contents

List of Figures

List of Tables

List of Abbreviations

1-OCTS	1-Octanesulphonic acid
AAS	Atomic Absorption Spectroscopy
ALCS	Alginate beads modified with chitosan
ALGO	Alginate beads modified with vegetable oil
ANOVA	Analysis of variance
AUC	Area under curve
Con A	Concanavalin A
CMC	Carboxymethylcellulose
CMN	Clarithromycin
CNOM	Coated non oil modified beads
COM	Coated oil modified beads
CS	Chitosan
DDS	Drug delivery system
DEE	Drug entrapment efficiency
DF	Dosage form
DOPA	Dihydroxy-phenylalanine
DSC	Differential scanning calorimetry

EC	Ethylcellulose
EDAC	1-ethyl-3, 3-(dimethylaminopropyl) carbodiimide
EFMS	Effervescent floating matrix system
GG	Polyguluronic sequences
GI	Gastrointestinal
GIT	Gastrointestinal tract
GNP	Gliadin nanoparticles
GRDF	Gastro-retentive dosage form
GRDDS	Gastro-retentive drug delivery system
GRT	Gastric retention time
FITC	Fluorescein Isothiocyanate
FTIR	Fourier transform infrared
H. pylori	*Helicobacter-pylori*
HBS	Hydro-dynamically balanced system
HEC	Hydroxyethylcellulose
HPLC	High performance liquid chromatography
HPMC	Hydroxypropyl methylcellulose
IMMC	Inter-digestive myoelectric motor complex
LSC	Loose surface crystals
MAP	Mussel adhesive protein
MM	Polymannuronic sequences
MC	Methylcellulose
MET	Metronidazole
NaCMC	Sodium carboxymethylcellulose
NHS	N-hydroxysuccinimide

NMR	Nuclear magnetic resonance
NTA	Nanoparticle tracking analysis
PBS	Phosphate buffered saline
PEG	Polyethylene glycol
PGM	Pig gastric mucin
P-XRD	Powder X-ray diffraction
PVA	Polyvinyl alcohol
PVP	Polyvinylpyrrolidone
SAL	Sodium alginate
SEM	Scanning electron microscopy
SB	Sodium bicarbonate
SGF	Simulated gastric fluid
SLS	Sodium lauryl sulphate
SPH	Superporous Hydrogel
TGA	Thermo-gravimetric analysis
UEA	*Ulex europaeus*
USP	United States Pharmacopoeia
UV	Ultraviolet
WHO	World Health Organization
XμMT	X-ray microtomography

Chapter 1 INTRODUCTION

1.1 Oral drug delivery

Drug delivery to the human body can be *via* various routes such as oral, parenteral, topical, vaginal, nasal, *etc*. However, the oral delivery route is the most common of all these routes and accounts for more than half of the annual drug delivery market (Evers, 2001). This is partly because the gastrointestinal (GI) tract offers a wider range of flexibility in dosage form design (*e.g*. tablets, capsules, suspensions, solutions) than other routes and the ease of use by patients. It is also a convenient route of administration for easy access to the systemic circulation and drug administration *via* the mouth is generally well accepted. Orally administered formulations are convenient to use and can easily be used anywhere, which is not the case with the parenteral route which usually requires the assistance of trained health care personnel and the procedures can involve certain risks. Despite all these advantages, drug absorption *via* this route can be unsatisfactory and variable even following promising *in vitro* drug release profiles (Davis, 2005, Streubel *et al*., 2006). This makes it difficult to predict the *in vivo* performance of a drug delivery system (DDS), even though the *in vitro* data are reproducible. There are several physiological factors that could work against achieving effective absorption and successful drug delivery through the oral route and such factors include gastric emptying times, GI transit time of the dosage form, drug release from the dosage form and the absorption site of the particular drug. The unpredictability of gastric emptying times leads to non-uniform absorption profiles, partial drug release and shorter gastric residence of the dosage form.

1.2 Gastro-retentive drug delivery systems (GRDDS)

GRDDS are systems designed to be retained in the stomach for an extended duration in order to improve the residence time of dosage forms in the stomach, thereby enhancing the bioavailability of the drug. However, not all drugs are good candidates for gastro-retention, but those that have been formulated in a range of gastro-retentive systems include:

- Drugs that are primarily absorbed in the stomach, *e.g.* metronidazole (Adebisi and Conway, 2010, Adebisi and Conway, 2014)
- Drugs that are poorly soluble in alkaline pH, typical of the lower part of the GI tract, *e.g.* diazepam (Sheth and Tossounian, 1984) and verapamil hydrochloride (Streubel *et al.*, 2002), thereby preventing drug solubility from being the rate-limiting step to the absorption of the drug by prolonging the residence time in the stomach
- Drugs that have a narrow absorption window in the stomach or in the upper small intestine, *e.g.* levodopa (Erni and Held, 1987), para-amino benzoic acids (Ichikawa *et al.*, 1991) and furosemide (Menon *et al.*, 1994)
- Drugs that are absorbed rapidly from the GI tract, *e.g.* amoxicillin
- Drugs that degrade or are unstable in the colonic / intestinal environment, *e.g.* captopril (Matharu and Sanghavi, 1992, Nur and Zhang, 2000) and metronidazole (Searle and Willson, 1976, Nayak *et al*., 2010b)
- Drugs that act locally in the stomach and the proximal small intestine for the treatment of certain diseases *e.g.* misoprostol (Oth *et al.*, 1992), antacids (Fabregas *et al*., 1994) and antibiotics (Yang *et al.*, 1999, Whitehead *et al.*, 2000)
- Drugs used in the eradication of *Helicobacter-pylori (H. pylori)* in the treatment of peptic ulcer disease (Dave *et al*., 2004).

1.2.1 Requirements for gastro-retentive devices

There are certain conditions that must be satisfied for a DDS to achieve gastro-retention. One major requirement is that the DDS must be strong enough to withstand the peristaltic waves and contractions of the stomach, the contractions and forces within the stomach (1.5 -1.9 N (Kamba *et al*., 2000)). Another important requirement is that it must be easily removed from the stomach, once the drug content is completely released (Anilkumar, 2008).

1.2.2 Stomach

1.2.2.1 Physiology of the stomach

The stomach is involved in the liquefaction of food and it releases the churned food in a controlled manner into the intestines (Hoichman *et al.*, 2004). It is about 0.2 m in length, has a surface area of 0.2 m^2 and is divided into two major functional parts (Minami and McCallum, 1984). The fundus and the body of the stomach (Figure 1-1) produce contractions in the muscle walls and cause compaction of the stomach contents (Hoichman *et al*, 2004), while the antrum causes peristaltic phase movement leading to the comminution of the food into small particles of about 2 mm. The particle size should be within the range of 1 - 2 mm (Deshpande *et al.*, 1996) to be able to pass through the pyloric valve into the small intestine.

In the fasted state, the stomach has a residual volume of about of 25 - 50 ml (Waugh *et al.*, 2001) with a small amount of fluid and a pH ranging from 1 to 3 (Bowman *et al.*, 1968). However, in the fed state - the volume of the stomach varies according to the amount of distension up to 1500 ml (Bannister, 1995). The stomach pH in the fasted state is 1.1 ± 0.15 while in the fed state it is 3.6 ± 0.4 (Mojaverian, 1996). Another study reported gastric pH in the human gastric lumen has a median 24 h intra-gastric pH of 1.4 (Bloom and Polak, 1980).

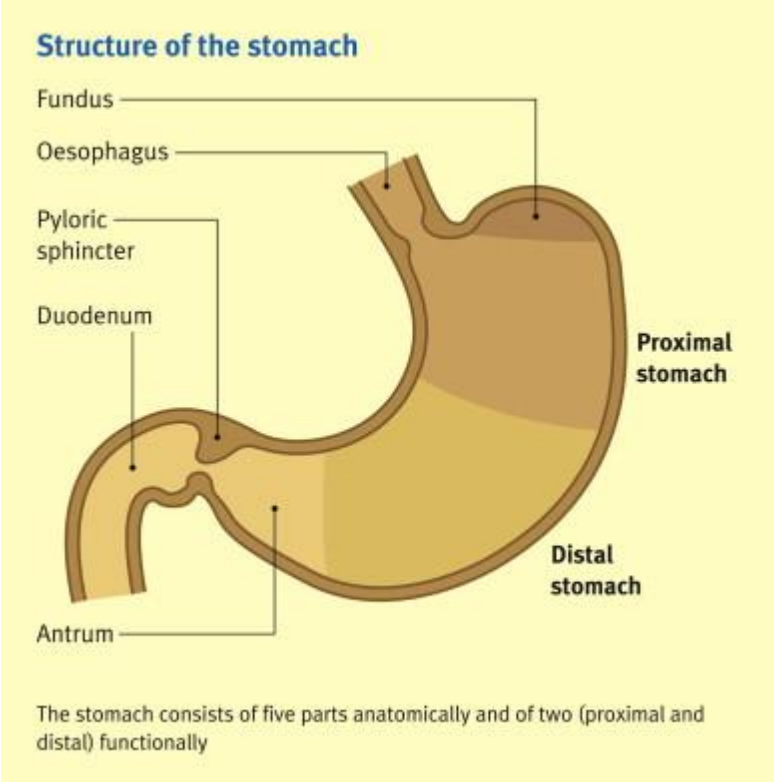

Figure 1-1: Structure of stomach

(Campbell, 2012) (Used with permission)

1.2.2.2 Gastric motility

The GI tract is in a state of continuous motility. The motility is in two modes: the inter-digestive myoelectric motor complex (IMMC) and digestive motility pattern (Anilkumar, 2008). The IMMC presides in the fasted state, with its main function being the clearing of the stomach of the residual contents of the upper GI tract. It is organised in cycles of activity and quiescence (Deshpande *et al.*, 1996). Each of the cycles lasts for a period of 90 to 120 min, consisting of four phases and the duration of the phases depends on the concentration of

the hormone motilin. Motilin is produced from endocrine M cells of the duodenal mucosa to regulate the motility of the digestive tract. The full cycle begins in the lower oesophageal sphincter/gastric pacemaker, spreading over the whole stomach, the duodenum and jejunum and terminating at the ileum. Phase I (basal phase) lasts for 45 - 60 minutes with rare or relatively few contractions and a period of quiescence compared to Phase II and III. Phase II (pre-burst phase) lasts for approximately 40 - 60 min, exhibiting intermittent action potential, amplitude contractions (Minami and McCallum, 1984) and involves bile secretion (Gruber *et al*., 1987)**.** Phase III, or the housekeeper wave, lasts for 4 - 6 min and consists of strong intense contractions, which help to remove undigested food contents from the stomach (Soppimath *et al*., 2001) with maximal pyloric opening (Ehrlein, 1988). Phase IV lasts for a maximum of 5 minutes and occurs between Phase III and Phase I of consecutive cycles. The ingestion of food interferes with the inter-digestive motility cycle and the digestive cycle takes over. The digestive cycle is induced 5-10 minutes after the ingestion of food and remains active for as long as there is food in the stomach. Therefore, the larger the meal, the longer the period of fed activity, with usual times being 2 - 6 h and more usually 3 - 4 h with contractions similar to Phase II of IMMC (Pawar *et al*., 2011)**.** For a formulation to be gastro-retentive, it must be able to resist the pressures and forces of the IMMC for a considerable period of time. The gastric retention time (GRT) of a particular formulation will depend on which stage of the IMMC is active at the time of drug administration. In the fed state, after the comminution of food to minute sizes, the residence time of the food depends on the type of food consumed. Liquids and small food particles will be easily transferred into the duodenum, while solids and larger food particles are released much more slowly (Conway, 2005).

.

1.2.2.3 Gastric mucus

Gastric mucus plays a cyto - protective role by protecting the stomach surface mucosal cells (Glass, 1964) from a wide range of ingested substances, secreted acid, enzymes and refluxed contents of the duodenum. It is a viscoelastic, gel-like, stringy slime consisting mainly of glycoproteins. It serves as a lubricant for the passage of solids and as a barrier to antigens, bacteria and viruses (Chawla *et al.*, 2003). The gel like nature of mucus is due to the presence of the glycoprotein – mucin (Table 1-1). The surface of the stomach mucosa is covered by a single layer of mucus-secreting epithelial cells punctuated by gastric 'pits' which occupy almost half of the stomach surface. The mucosal layer in the GI tract provides a barrier to acid in the stomach by presenting an unstirred layer into which bicarbonate ions are secreted by the surface epithelium. These bicarbonate ions neutralise hydrogen ions which are secreted by parietal or oxyntic cells as they diffuse towards the epithelium from the lumen (MacAdam, 1993). The mucus layer also prevents digestion of the GI tract by presenting a diffusional barrier to enzymes such as pepsin. Mucus is continually secreted from goblet cells and its rheological properties changes from a secretory low viscosity solution to a viscoelastic gel. This gel keeps the mucus layer intact due to its constant loss from enzymatic degradation and physical erosion (Allen, 1981). It is difficult to measure the exact turnover time accurately and it varies considerably. The turnover time of mucus gel layer in rats has been reported to be between 4 and 6 h (Allémann *et al.*, 1998, Galindo-Rodriguez *et al.*, 2005, Lehr *et al.*, 1991) and this has been reported to be similar to humans (Lai *et al.*, 2009). The glycoprotein component of mucus (mucin) is responsible for the viscosity, adhesive and cohesive properties of the mucus. Mucins (Figure 1-2) are large molecules with molecular weights ranging from 0.5 MDa to over 50 MDa (Bansil and Turner, 2006, Berry *et al.*, 1996, Dodd *et al.*, 1998, Harding *et al.*, 1999). They contain large amounts of carbohydrate (for GI mucins 70 – 80 % carbohydrate, 12 – 25 % protein and up to 5 % ester sulphate).

Table 1-1: Composition of gastric mucus

(Johnson *et al*., 1987)

Component	% content
Water	> 95 %
Glycoproteins	0.5 – 5 %
Lipids	<0.5 %
Mineral salts	1 %
Free proteins	0.5 -1 %

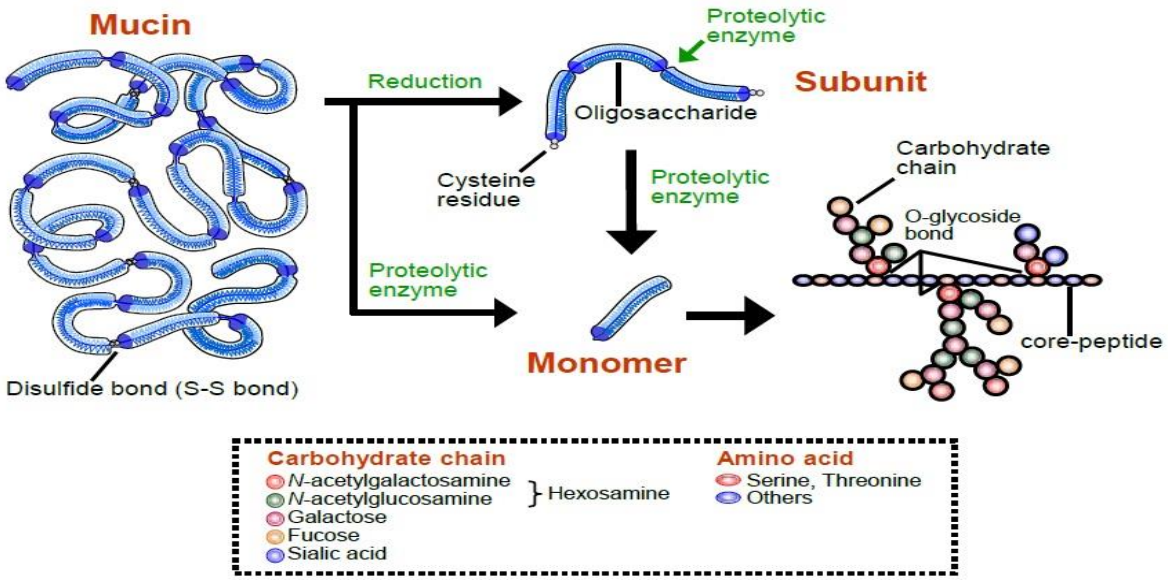

Figure 1-2: Polymeric structure of mucin molecules

(Takafumi and Kazuhiko, 2011)

1.2.3 Factors affecting gastric residence time

Several factors affect the GRT of dosage forms (Gruber *et al*., 1987) and they include:

- Fed or fasted conditions - GRT is longer in the fed state than in the fasted state. In the fasted state, the GRT of dosage forms is mostly less than 1 h and it is common for dosage forms to move rapidly through the small intestine, with duration of not more than 3 h (Naisbett and Woodley, 1995, Khandai *et al*., 2010). This phenomenon occurs because the IMMC moves the undigested food material from the stomach and if the time of drug administration occurs around the time of IMMC, the formulation will be expelled out of the stomach, leading to a short GRT. However, in the fed state, the presence of food causes a delay in the housekeeper wave with only Phase II - like contractions predominating and thus the IMMC (related to fasted state) is delayed, thereby increasing GRT. Kaniwa *et al.* (1998) reported the prolongation of gastric emptying of dosage forms of various sizes or densities due to the presence by food. When 3 - 7 mm diameter tablets were taken with a meal, the emptying process was delayed in humans (Khosla *et al.*, 1989). In humans, swelling tablets with dimensions of 4 x 4 mm or 6 x 6 mm (length x diameter) showed rapid emptying from the stomach in less than 1 h in the fasted state. However, after a heavy breakfast of 1500 kcal, 80 % of the tablet contents were retained for 4 h and in 50 % of subjects (*n=10*), the tablets were retained for 6 h or more. In 8 of the subjects, the tablets were retained for 10 h or more (Shell *et al.*, 2002).
- Density of formulation - The density of a dosage form (DF) has an impact on its ability to stay in the stomach for a prolonged period (Figure 1-3). A high density formulation, *e.g.* coated pellets, which have a density greater than that of gastric contents (density = 1.004 g/cm^3) will sink to the lower part of the stomach. This high density coating is achieved by the use of heavy inert material such as barium sulphate, zinc oxide, and titanium dioxide (Patel, 2007). Also, a low density formulation with a

density less than the density of the gastric contents is expected to remain buoyant in the gastric fluid (Singh and Kim, 2000). A study reported that the hypotensive action of diltiazem was heightened when administered to humans in a floating controlled release tablet compared to an equivalent non-floating tablet (Gu *et al*., 1992). However, some studies have given contrasting results with formulations of differing densities having similar GRTs, *e.g.* it has been reported that particles of different densities ranging from 0.5 to 2.9 g/cm^3, emptied from the stomach of dogs in a similar manner (Gruber *et al*., 1987). These results by Gruber and co-workers are similar to those of other researchers who observed no differences between the rate of gastric emptying of floating (density = 0.96 g/cm^3) and non-floating (density = 1.96 g/cm^3) single unit dosage forms in fasted human (Davis *et al*., 1986). The inconsistencies and variability in results is likely to be a consequence of fed *versus* fasted conditions in the stomach, thereby limiting the impact of density on gastro-retention.

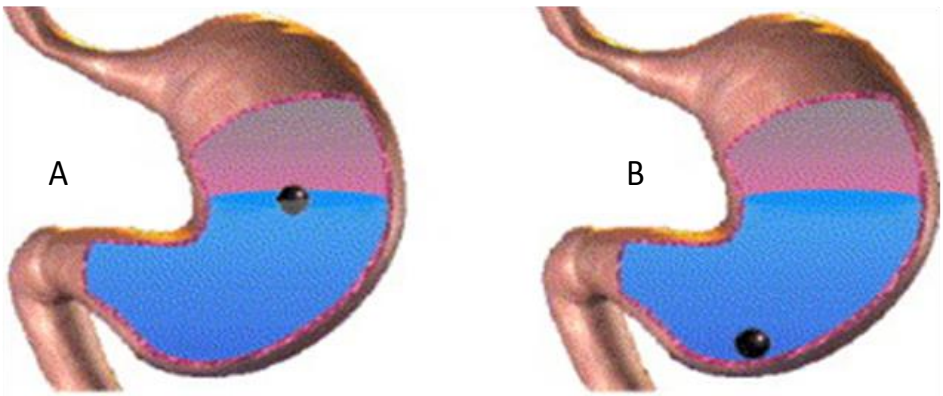

Figure 1-3: Schematic localisation of (A) intra-gastric floating system and (B) high density system in the stomach.

Adapted from (Bardonnet *et al.*, 2006) (Used with permission)

- Size of formulation – A DF larger than the diameter of the pylorus is likely to be retained in the stomach, even during the housekeeper wave. The DF is initially of a smaller size to facilitate swallowing, then it increases in size when it gets to the stomach (Streubel *et al.*, 2006). The size of the dosage form required may be greater than 5 cm in length and a diameter greater than 3 cm (Klausner *et al.*, 2003c). A diameter of more than 7.5 mm has been reported to be more likely to be retained than DFs with diameters greater than 9.9 mm (Timmermans and Moes, 1994).
- Shape of formulation - The shape of the DF has an effect on its gastro-retentive ability. Ring shaped and tetrahedral devices have been shown to be retained longer in the stomach than with DF of other shapes (Garg and Sharma, 2003). In addition, ring-shaped GRDDS with a flexural modulus of 22.5 kilo pounds per square inch and tetrahedral GRDFs with a flexural modulus of 48 kilo pounds per square inch (psi) were reported to have over 90 % retention at 24 h, compared to those with shapes defined as continuous stick, planar disc, planar multi-lobe and string (Pawar *et al.*, 2011).
- Single or multiple unit formulations - Multiple unit formulations show more predictable and more reliable gastric emptying than single unit formulations. Single unit formulations exhibit the "*all or none concept*'' and failure of the unit, while in the case of multiple unit systems, the particles are distributed more freely throughout the GI system and their distribution or movement is less affected by the transit time (Bechgaard and Ladefoged, 1978, Whitehead *et al.*, 1998). In addition, as the drug release kinetics and gastric emptying profiles of multiple unit systems are more predictable, there is a reduced likelihood of localized mucosal damage and dose dumping (Rouge *et al.*, 1997). Multiple unit systems also enable the co-administration of units with different release profiles or those containing substances that are incompatible (Ishak *et al.*, 2007).

- Nature of meal and food intake - Several factors such as the nature of food, frequency of feeding and caloric content have important effects on GRT. Fatty acid salts and indigestible polymers such as cellulose, poly-dextrose and raffinose extend GRT. In addition, it has been reported that a high fat meal may delay gastric emptying for about 3 to 5 h (Gad, 2008). The retention of water was reported to follow an expediential pattern with a half-life ($t_{1/2}$) of 10 minutes (Hunt and Knox, 1968). An increase in the volume of water increases the gastric emptying; however, gastric emptying of a liquid meal can be affected by the chemical and osmotic properties of the meal. Foods high in proteins and fats can increase GRT by 4 - 10 h. Enteric-coated or enteric matrix tablets may be retained longer, if administered with heavy meals or breakfast (Gad, 2008).
- Gender - Females have been reported to exhibit a comparatively lower mean ambulatory GRT than males. The gastric emptying time of a Heidelberg capsule was observed to be slower in women than in men (Mojaverian *et al.*, 1988). In addition, the mean GRT in females (4.6 ± 1.2 h) was higher than in males (3.4 ± 0.6 h) of the same age and race.
- Posture - A study reported that posture does not have a significant effect on GRT (Mojaverian *et al.*, 1988); however, another study showed that for both floating and non-floating systems, the GRTs of the DF vary depending on the subject's posture (Van Gansbeke *et al.*, 1991). Floating systems taken by subjects in an upright position floated for a longer period, thereby extending GRT. However, non-floating systems settled to the bottom of the stomach and were easily evacuated by stomach contractions. However, in a supine position, the reverse was observed with the floating units being easily emptied from the stomach than the non-floating units (Timmermans and Moes, 1994).
- Concomitant drug administration - Drugs such as anti-cholinergic drugs *e.g.* atropine; opiates, *e.g.* codeine and pro-kinetic drugs, *e.g.* metoclopramide prolong GRT. However, drugs like octreotide (a somatostatin analogue and an inhibitor of motilin secretion) and erythromycin (motilin receptor agonist) enhance gastric emptying.

- Biological factors - Crohn's disease and diabetes have been associated with delayed gastric emptying (Grill *et al.*, 1985, Annese *et al.*, 1995). 30 - 50 % of patients with long standing diabetes experience delayed gastric emptying (Horowitz *et al.*, 1996). Duodenal ulcer leads to an increase in gastric emptying, while gastric ulceration reduces antral motility causing a normal emptying of liquids but results in delayed emptying of solids (Miller *et al.*, 1980).
- Age - The effect of age on the gastric residence of the Heidelberg capsule was assessed in 12 healthy elderly males over 65 years. It was observed that the mean GRT after a 500 kcal breakfast was significantly longer, compared to that observed in young male volunteers (Mojaverian *et al.*, 1988).

1.3 Gastro-retentive dosage forms (GRDF)

Various approaches have been explored to achieve gastro-retention. Passage delaying agents, such as triethanolamine myristate (Gröning and Heun, 1984), have been used to influence GRT of DDS based on the fact that the lipid vehicles tend to reduce the motility of the stomach. However, this deliberate slowing down of gastric motility may have an effect on the emptying of the entire stomach contents, not just the DDS. Several categories of DDSs have been developed to achieve gastro-retention and these include bioadhesive systems (Ponchel and Irache, 1998); expandable systems (Urguhart and Theeuwes, 1994); high density systems (Rednick and Turner, 1970); floating systems (Deshpande *et al.*, 1996) and modified shape systems (Fix *et al.*, 1993) (Figure 1-4).

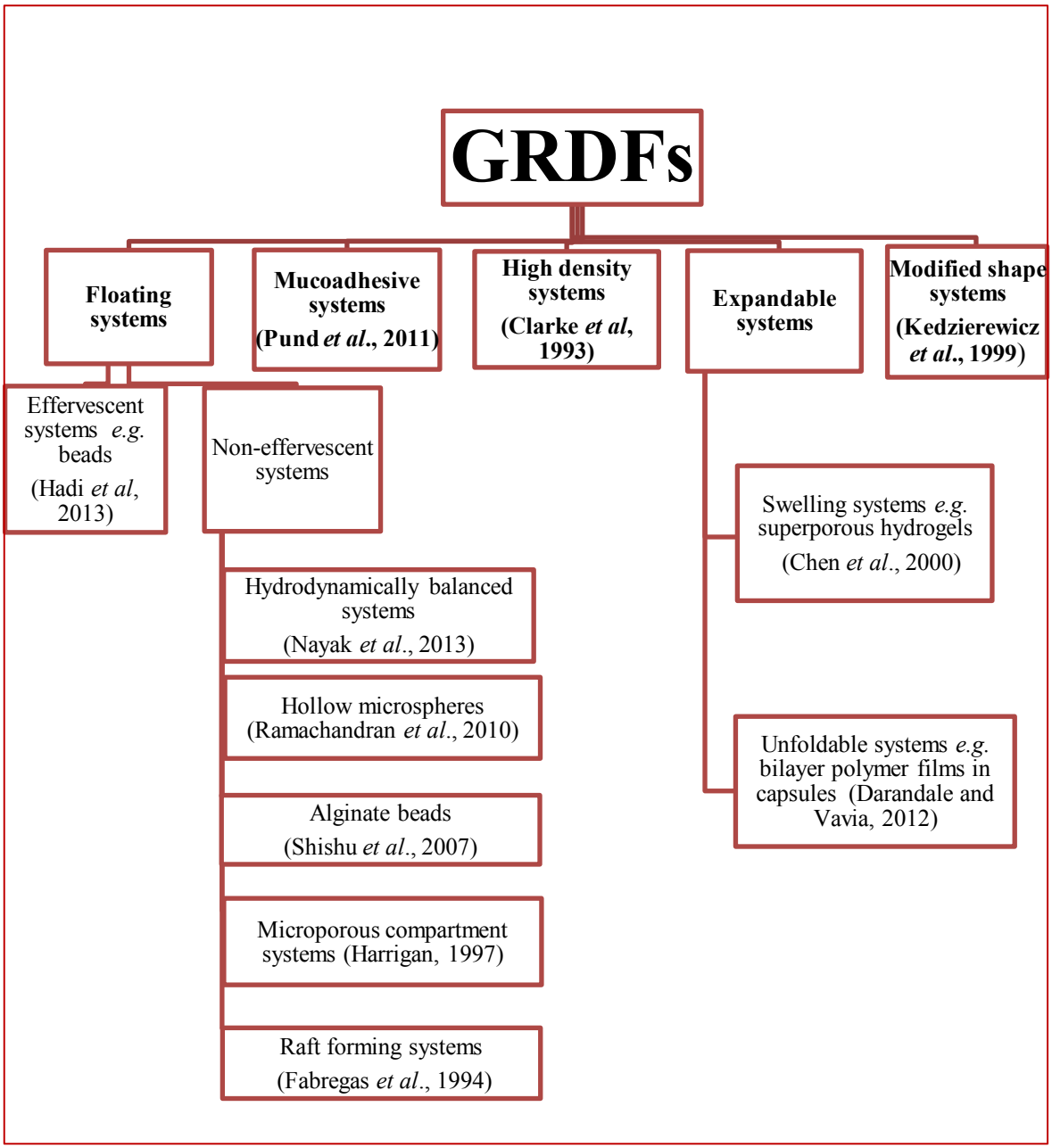

Figure 1-4: Gastro-retention techniques

1.3.1 Bioadhesive / mucoadhesive systems

Bioadhesive DDS, was introduced in the 1980s and they adhere to epithelial surfaces, thus maintaining a more intimate contact with the biological barrier (Park and Robinson, 1984) thereby prolonging GRT. A subset of bioadhesive systems is mucoadhesive systems, which adhere to the thick mucus gel layer that covers mucosal surfaces in the stomach (Conway, 2005) mouth, nostril *etc*. and provide a controlled release of drugs such as antibiotics. Polymers such as chitosan and Carbopol® have been used to achieve mucoadhesion (Lehr *et al*., 1992a) and adhesion to porcine stomach (Gåserød *et al.*, 1998a) in some formulations. The process of mucoadhesion is complex and its mechanism has been explained through various theories including electrical, adsorption, wetting (Figure 1-5), fracture (Figure 1-6) and diffusion theories (Figure 1-7) (Peppas and Buri, 1985, Park and Robinson, 1987, Rillosi and Buckton, 1995). Mucoadhesion has been reported to occur in two stages, the contact stage also known as the wetting stage and then the consolidation stage where adhesive interactions are established (Figure 1-8) (Smart, 2005) The mucosal surface is negatively charged; therefore, a polymer that has a positive charge might assist the mucoadhesion process. An initial step of mucoadhesion could be electrostatic attraction, followed by mechanical interlocking of the polymer chains, van der Waals force, hydrogen bonding and other forces (Lehr *et al.*, 1993). The different mechanisms of bioadhesion are summarized in Table 1-2. One drawback associated with such systems is that the mucus on the stomach walls is constantly being renewed, thereby making adherence of a formulation to this mucus unpredictable (Chun *et al.*, 2005). In addition, the contents of the stomach are highly hydrated, thereby reducing the level of adhesiveness of the polymers. Other factors that can affect effective *in vivo* mucoadhesion include the composition of mucus, different behaviour of mucoadhesive devices over the pH range, and disease conditions (Vasir *et al.*, 2003). Also, the prospect of oesophageal binding might be daunting, regarding the safety aspects of such formulations (Wang *et al.*, 2000). The specificity of the formulation could also be a major

drawback, as it is difficult to specifically target mucoadhesive polymers to the gastric mucosa, for example, Carbopol® will adhere to various surfaces (Khosla and Davis, 1987). The advantages of such systems in the treatment of *H. pylori* infections may outweigh these concerns, because they have the potential to maintain contact with the mucus layer and provide controlled release of drugs in a localised environment. An additional consideration with this application is the avoidance of any local drug overdose, which could lead to irritation of the gastric mucosa (Ch'ng *et al.*, 1985).

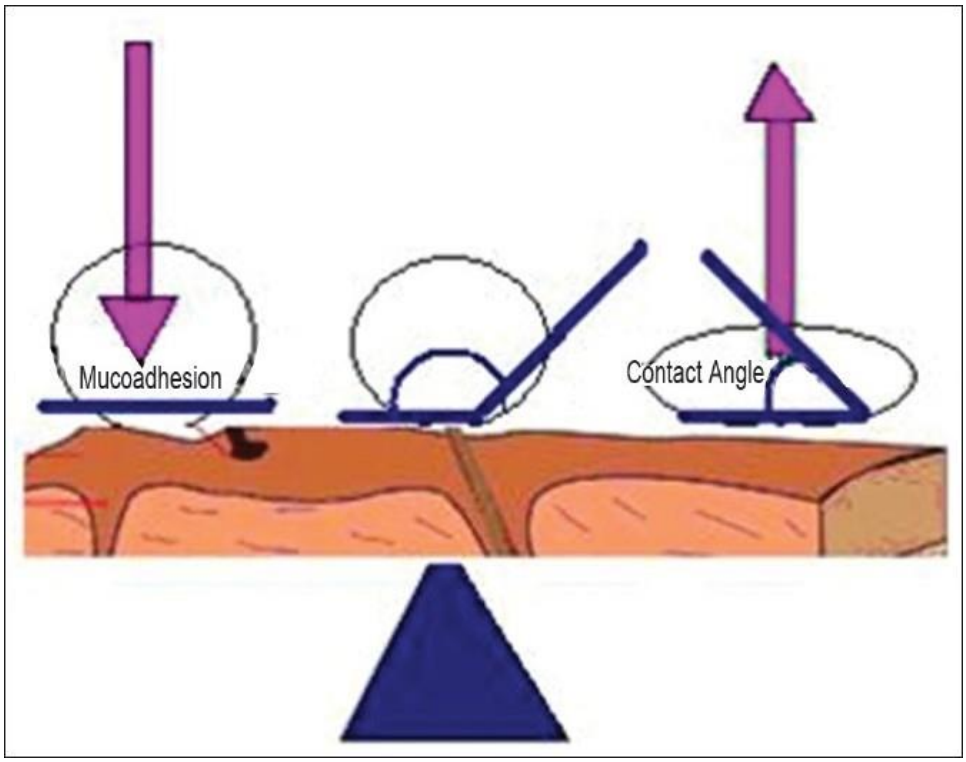

Figure 1-5: Wetting theory of mucoadhesion

(Boddupalli *et al.*, 2010)

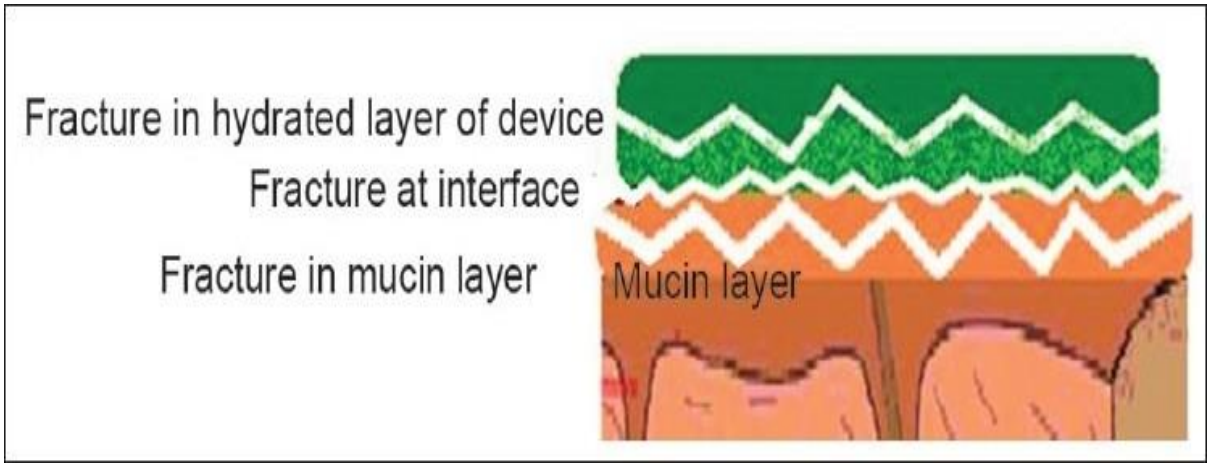

Figure 1-6: Fracture theory of mucoadhesion

(Boddupalli *et al*., 2010)

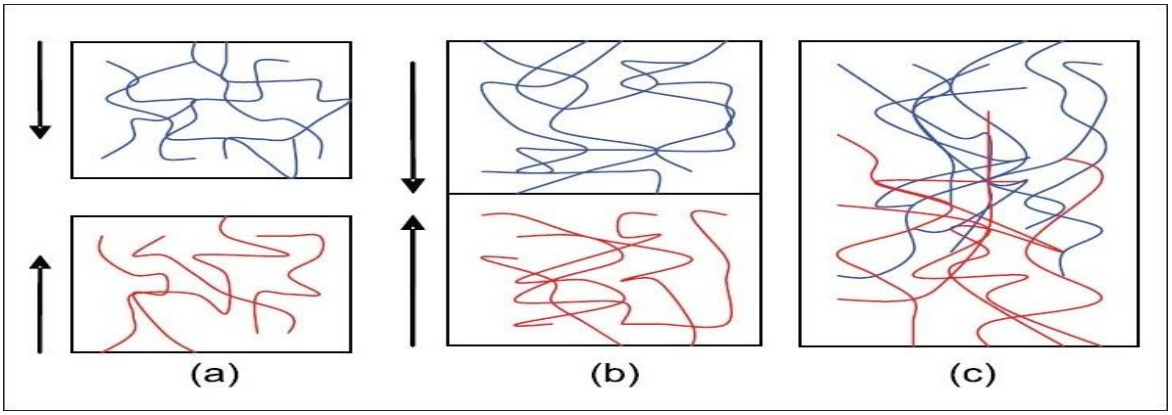

Figure 1-7: Diffusion theory of mucoadhesion

(Shaikh *et al*., 2011)

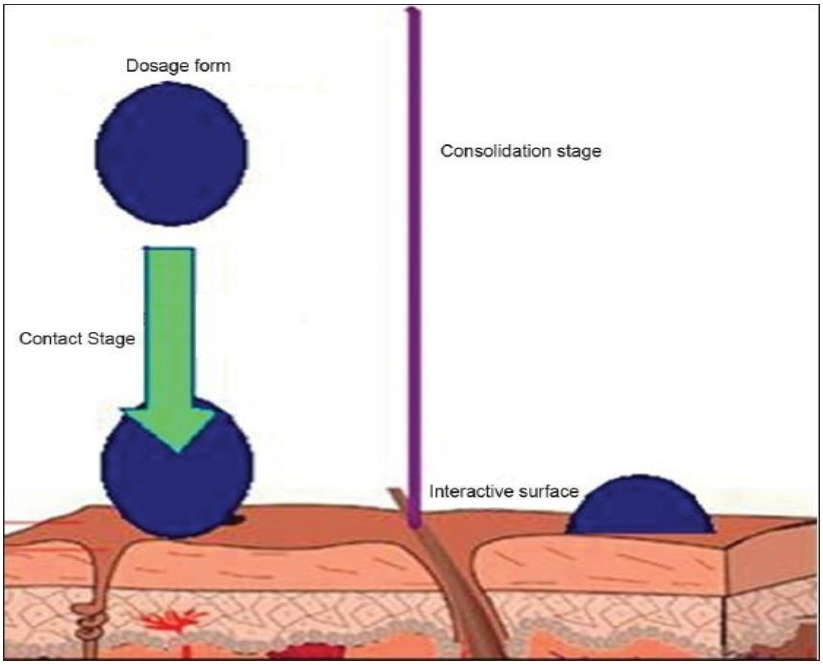

Figure 1-8: Stages of mucoadhesion

(Boddupalli *et al*., 2010)

Table 1-2: Theories of mucoadhesion.

Adapted from Vasir *et al*, 2003. (Used with permission)

Theory	Mechanism of adhesion	Comments
Electronic theory	There are attractive electrostatic forces between the glycoprotein mucin network and the bioadhesive material	Electron transfer occurs between the mucin and the bioadhesive material forming a double layer of electric charge at the interface (Derjaguin *et al.*, 1977, Derjaguin *et al.*, 1994)
Adsorption theory	There are surface forces resulting in chemical bonding	The surface forces include strong primary forces which are covalent bonds and weak secondary forces, which include ionic bonds, hydrogen bonds and van der Waal's forces (Kinloch, 1980, Chickering and Mathiowitz, 1999)
Wetting theory	The ability of bioadhesive polymers to spread and develop intimate contact with the mucus membranes	Spreading coefficients of polymers must be positive. Contact angle between polymer and cells must be near to zero (Lehr *et al.*, 1993, Lehr *et al.*, 1992b)
Diffusion theory	Physical entanglement of mucin strands and the flexible polymer chains	For maximum diffusion and best bioadhesive strength; solubility parameters (δ) of the bioadhesive polymer and the mucus glycoproteins must be similar interpenetration of mucin strands into the porous structure of the polymer substrate (Park and Robinson, 1985, Leung and Robinson, 1990)
Fracture theory	Analyses the maximum tensile stress developed during detachment of the bioadhesive drug delivery system from mucosal surfaces	Does not require physical entanglement of bioadhesive polymer chains and mucin strands, hence appropriate to study the bioadhesion of hard polymers which lack flexible chains (Kinloch, 1980)

1.3.2 Expandable systems

Swelling systems exploit the restrictions on the removal of large particles from the stomach if they are larger than the opening of the pyloric sphincter (Nayak *et al.*, 2010b). For a formulation to be retained in the stomach, the size required may be greater than 5 cm with a diameter larger than 3 cm (Klausner *et al.*, 2003c). Important features of these formulations are that the DF must be small enough to be easily swallowed; the onset of swelling must be fast, so as to prevent its evacuation from the stomach before getting a chance to swell (Conway, 2005). In addition, it must not cause any form of gastric obstruction, either singly or by accumulation (Nayak *et al.*, 2010b) and must regain a size small enough to be evacuated easily after complete drug release (Gröning *et al.*, 2007).

The increase in size of the DF is normally achieved by swelling (through the process of osmosis) or by unfolding on contact with the contents of the stomach (Klausner *et al.*, 2002). The process of unfolding can be achieved through mechanical shape memory, which involves the production of the formulation in a large size, which is then folded into a pharmaceutical drug carrier such as a gelatin capsule, to ensure convenience of intake. However, the mechanical shape memory is relatively fleeting. When the formulation gets into the stomach, the carrier dissolves and the formulation opens up to achieve an extended size (Pawar *et al.*, 2011). Hydrogels, which are hydrophilic polymers, may be useful candidates for these formulations, as they absorb large amounts of fluids and swell in the process. Such DFs should not possess sharp edges or cause local damage to the stomach on extension and the system must be made from biodegradable polymers. There are several drawbacks to the use of this kind of system, as large single unit dosage forms may cause obstruction, intestinal adhesion, and gastropathy (Klausner *et al.*, 2003c). The storage of such types of polymers may be difficult (Torrado *et al.*, 2004) due to stability issues.

1.3.3 High density systems

High density systems have a density greater than that of normal stomach contents (Figure 1-3b). The density of the formulation should be close to 2.5 g/cm^3 for it to be retained in the stomach for any considerable length of time (Clarke *et al.*, 1993). Rouge *et al.* (1998) also reported that densities greater than 2.4 - 2.8 g/cm^3 ensures retention in the lower part of the stomach. Inert materials used to increase the density of DF are either used to coat the DF or by mixing the material with the drug (Vyas and Khar, 2006). On addition of such inert materials, the formulation density can increase by up to 1.5 - 2.4 g/cm^3 (Clarke *et al.*, 1993). However, one major drawback is that they are difficult to manufacture, requiring relatively large quantities of active drug as the dry material constituent of the formulation reacts with the gastric fluid to release its contents. There is no formulation utilising this strategy currently in the market (Nayak *et al.*, 2010b, Garg and Sharma, 2003) and *in vivo* data in animals or clinical studies are also rather scarce.

1.3.4 Floating systems

Studies based on floating systems date as far back as 1968 (Davis, 1968). Floating DDS (Figure 1-3a) have a bulk density less than that of gastric contents and therefore remain buoyant in the stomach, without affecting the intrinsic gastric emptying rate for a prolonged period. A floating DDS could lead to high drug levels in the fundal area of the stomach and this may be a useful strategy for the delivery of narrow spectrum antibiotics for peptic ulcer disease (Umamaheswari *et al.*, 2002) and for drugs that are primarily absorbed in the stomach or the upper small intestine (Sungthongjeen *et al.*, 2006), *e.g.* metronidazole. The drug content of the DDS should be released slowly as the DDS remains floating on the gastric contents. At the end of the release period, the DDS should exit from the stomach. This type of

DDS has been demonstrated to increase gastro-retention and reduce fluctuations in drug plasma concentrations (Singh and Kim, 2000).

1.3.4.1 Specific criteria for a floating drug delivery system

Floating DDS include designs such as hydrodynamically balanced systems (HBS), gas-generating systems, raft-forming systems and hollow microspheres. Hollow microspheres are achieved by entrapping air into the formulation (Kawashima *et al.*, 1991, Krogel and Bodmeier, 1999). Other methods of achieving buoyancy include the inclusion of oils or fatty materials with bulk density less than $1g/cm^3$ (Reddy and Murthy, 2002, Sriamornsak *et al.*, 2004, Adebisi and Conway, 2014) or formation of foam powder (Streubel *et al.*, 2002). Floating DDS include granules (Yuasa *et al.*, 1996), powders (Dennis and Timmins, 1992), capsules (Franz and Oth, 1992), tablets (Sheth and Tossounian, 1979) and laminated films (Machida *et al.*, 1989). There are several advantages attributed to the use of floating DDS and this includes improvement in patient compliance; achievement of better therapeutic effect of drugs with a short half-life; enhancement of absorption of drugs, which are soluble primarily in the stomach and achievement of site-specific delivery of drug to the stomach (Pawar *et al.*, 2011).

Specific criteria for floating dosage systems include:

- It must have a structure to form a cohesive gel barrier
- It must maintain a density lower than that of gastric contents ($1g/cm^3$)
- It should dissolve slowly enough to serve as a drug depot (Desai, 2007)

The limitations to the use of these formulations, include the requirement for the presence of fluids in the stomach (Floating DDS is typically administered with fluid of about 200 - 250

ml (Soppimath *et al.*, 2001)), in order to maintain the buoyancy effect of the formulation in the stomach. Drugs that cause gastric mucosa irritation and those that have solubility and/or stability issues in gastric fluids like biomolecules such as proteins and peptides (which are liable to proteolysis in gastric fluid) are not suitable for incorporation into this type of DDS. In addition, drugs that are well absorbed along the entire GI tract (*e.g.* isosorbide dinitrate) and undergo significant first pass metabolism are not suitable candidates, since the slow gastric emptying could lead to a reduction in systemic bioavailability (Pawar *et al.*, 2011).

1.3.4.2 Formulations for floating systems

Floating systems can be divided into two categories: gas-generating systems and non-effervescent systems (Garg and Gupta, 2008).

1.3.4.2.1 Gas-generating /effervescent systems

These are systems designed so that on contact with gastric contents, gas bubbles are released causing the DF to float on gastric contents. This is achieved by the incorporation of vacuum, air or an inert gas into a floatation chamber (Iannuccelli *et al.*, 1998). The gas can be included in the formulation by the volatilization of an organic solvent such as ether or cyclopentane, causing inflation on contact with gastric fluid. CO_2 can also be produced in the DF due to the chemical reaction between organic acids and carbonate-bicarbonate salts (Sakr, 1999) on contact with gastric fluid. These formulations make use of swellable polymers such as methylcellulose (MC) and hydroxyl-propylmethylcellulose (HPMC); polysaccharides (*e.g.* chitosan) and effervescent materials, such as sodium bicarbonate ($NaHCO_3$), citric acid (Rubinstein and Friend, 1994), tartaric acid or floating chambers that contain liquids that turn

into gas at body temperature (Pawar *et al.*, 2011). The required stoichiometric ratio of citric acid and $NaHCO_3$ for gas generation has been reported to be 0.76:1 (Garg and Sharma, 2003).

Floating mini-capsules with a diameter of 0.1- 0.2 mm were developed containing $NaHCO_3$, coated with an inner HPMC layer and an outer pepstatin layer (Umezawa, 1978). On contact with gastric fluid, there was a release of CO_2 leading to a GRT of about 3 - 5 h and prolonged drug release from these mini-capsules. Other floating formulations include those using a combination of sodium alginate and $NaHCO_3$ (Stockwell *et al.*, 1986); floating mini-capsules consisting a core of $NaHCO_3$, lactose and polyvinyl-pyrrolidone (PVP), coated with HPMC and systems produced using ion exchange resin technology (Garg and Gupta, 2008). The main problem associated with these systems is that they do not float immediately after swallowing due to the lag time between swallowing and the release of gas. In order for the formulation to be effective, the lag time has to be as low as possible to avoid premature removal from the stomach (Streubel *et al.*, 2003a). There are several commercially available floating formulations such as Gaviscon®, Madopar® HBS capsule (Singh and Kim, 2000), Cifran O.D®, Glumetza®, Cytotec® and Baclofen GRS®.

1.3.4.2.2 Non-effervescent systems

In non-effervescent systems, the air entrapped in the swollen polymer lowers the density and confers buoyancy on the DDS. The systems absorb gastric fluid on contact, swell and form a colloidal gel barrier (Sheth and Tossounian, 1979), which limits the rate of fluid absorption into the DDS and subsequently drug release (Sheth and Tossounian, 1984). A common way of incorporating drug into this type of formulation is by mixing the drug with a gel that swells on contact with gastric fluid, while still maintaining its integrity of shape and a bulk density less than that of gastric contents. Commonly used polymers for this type of formulation include, cellulosic hydrocolloids such as HPMC and matrix-forming polymers such as poly-

acrylate, polycarbonate, polystyrene and poly-methacrylate. Other excipients include polyvinyl acetate, Carbopol®, agar, sodium alginate, polyethylene oxide and polycarbonates (Garg and Gupta, 2008). Non-effervescent systems are sub-divided into HBS, alginate beads, microporous compartment systems and hollow microspheres.

A) Hydrodynamically balanced systems (HBS)

HBS was introduced in 1975 by Sheth and Tossounian as single unit dosage forms, containing the active ingredient with one or more gel forming hydrocolloids, which remain floating on stomach contents. Excipients commonly used in this type of formulations include HPMC, hydroxyethylcellulose (HEC), sodium carboxy-methylcellulose (NaCMC), polycarbophil, polyacrylate, polystyrene, agar, carrageenans or alginic acid (Hwang *et al*., 1998, Reddy and Murthy, 2002, Nayak *et al*., 2010b). Formulations can be prepared by mixing the drug with the polymer followed by administration in a HBS capsule (Figure 1-9). The capsule dissolves on contact with liquid gastric contents and then swells to form a gelatinous barrier which makes the dosage form float on the gastric contents for an extended period of time of about 3 – 4 h (Shah *et al*., 2009b, Nayak *et al*., 2010b). The continuous erosion of the surface facilitates water penetration into the inner layers of the dosage form, thereby maintaining surface hydration and buoyancy to the dosage form (Reddy and Murthy, 2002). The addition of fatty excipients confers buoyancy to the formulation, thereby limiting erosion. Examples of suitable fatty excipients include: a purified grade of beeswax; fatty acids; long chain fatty alcohols, myristyl alcohol, stearyl alcohol, glycerides such as glyceryl esters of fatty acids or hydrogenated aliphatic acids such as, for example, glyceryl monostearate, glyceryl distearate, glyceryl esters of hydrogenated castor oil; and oils such as mineral oil *etc*. (Sheth and Tossounian, 1979).

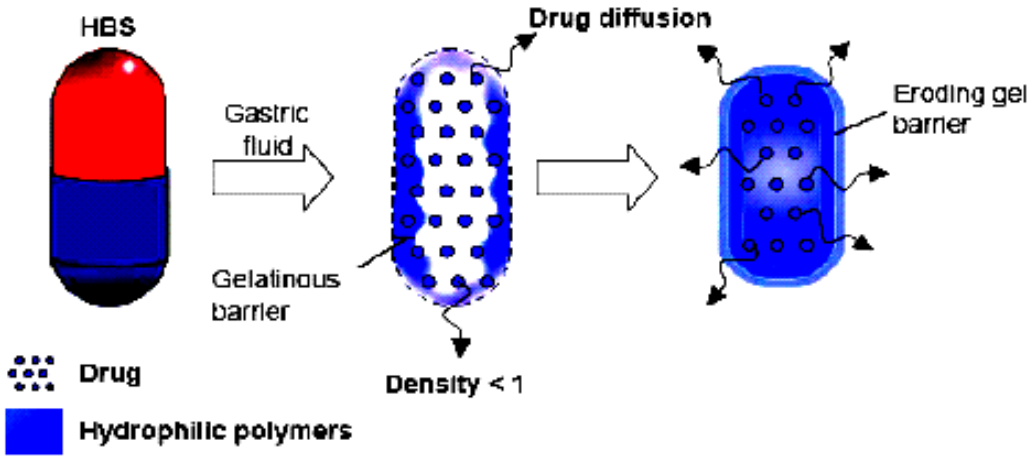

Figure 1-9: Hydrodynamically balanced systems (HBS)

B) Floating alginate beads

Floating alginate dosage forms were introduced in the 1980s (Stockwell *et al.*, 1986). Alginate is a favourable biodegradable polymer for drug delivery because gel beads are prepared easily in aqueous solutions without the use of organic solvents at room temperature and without the use of complicated equipment. In addition, alginate gels dissolve in alkaline conditions (pH > 6) and are biocompatible; therefore, they are useful as a DDS for bioactive compounds. Alginates are linear anionic block copolymer hetero-polysaccharides made up of monomers of (β-D-mannuronic acid) (M) and its C-5 epimer (α-1-guluronic acid) (G) residues, linked to one another by 1, 4- glycosidic linkages (Figure 1-10). They are extracted from the cell walls of various species of brown algae (Sanford and Baird, 1983). Alginates from different seaweeds can have different ratios of G and M monomers. The ratio and the distribution of the monomers in the alginate chain have an effect on gel formation and strength. Hydrogel formation occurs by ionotropic gelation on reaction with bivalent alkaline earth metals such as Ca^{2+}, Sr^{2+} and Ba^{2+} or trivalent Fe^{3+} and Al^{3+} ions, due to an ionic interaction and intra-molecular bonding (Figure 1-10) between the carboxylic acid groups

present on the polymer backbone and the cations (Patel *et al.*, 2006). Beads produced from sodium alginate have been demonstrated to extend GRT to beyond 5.5 hours (Whitehead *et al.*, 1998, Garg and Gupta, 2008).

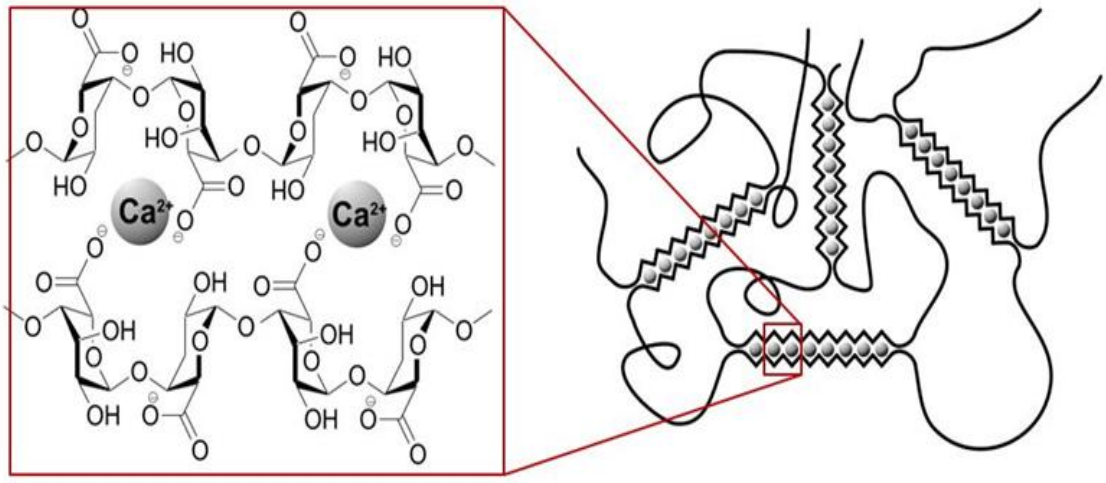

Figure 1-10: Calcium cross-linked alginate formation reaction

C) Microporous compartment systems

In microporous compartment systems, the drug reservoir is inside a compartment containing pores within the surrounding membrane (Harrigan, 1977). The peripheral walls are completely sealed in order to avoid any direct contact of the undissolved drug with the gastric fluids. The entrapped air in the floatation chamber causes buoyancy over gastric fluids (Vyas

and Khar, 2006). The gastric fluid passes through the apertures, dissolving the drug, thereby providing a reservoir of dissolved drug for continuous drug transport and absorption.

D) Hollow microspheres

Microspheres have been widely researched in the area of gastro-retention. Floating microspheres or hollow microspheres combine the advantages of floating systems along with those of multiple unit systems as described in section 1.2.3. At present, hollow microspheres are promising buoyant systems because they combine the advantages of multiple unit system with good floating properties.

1.3.5 Advantages of gastro-retentive systems

Gastro-retentive systems (Figure 1-11) can:

- improve the bioavailability of drugs that are metabolised in the upper GIT (Garg and Gupta, 2008). The bioavailability of riboflavin from a GRDF was significantly enhanced in comparison to non-GRDF formulations. Different processes related to absorption and the movement of drug in the GI tract act to enhance the extent of drug absorption (Klausner *et al.*, 2003c)
- reduce the frequency of dosing and this is useful for drugs with a relatively short biological half-life ($t_{1/2}$). A reduction in the frequency of dosing may help to improve patient compliance and thereby improvement in drug therapy (Garg and Gupta, 2008)
- target therapy for local delivery in the upper GI tract especially locally to the stomach and the small intestine.
- reduce the amount of drug that reaches the colon thereby limiting the drug adverse activity of the drug on the colon. This gives a rationale for gastro-retentive systems

for β-lactam antibiotics, that are usually absorbed in the small intestine but there is the possibility of development of antibiotic resistance in the colon.

- reduce drug wastage as most, if not all, the drug content of the formulation is released where it is expected relative to conventional DFs.
- maintain the therapeutic plasma levels of the drug over an extended period with less fluctuation in therapeutic levels thereby, minimizing the risk of resistance especially in case of antibiotics *e.g.* β-lactam antibiotics (penicillins and cephalosporins) (Anilkumar, 2008). It is also of special importance for drugs with narrow therapeutic index (Hoffman, 1998).
- improve solubility profile of drugs that are less soluble in a high pH environment.
- provide better availability of new products with new therapeutic possibilities and substantial benefits for patients (Arora *et al.*, 2005)
- increase bioavailability of sustained release delivery systems intended for once-a-day administration *e.g.* ofloxacin.

1.3.6 Limitations of gastro-retentive systems

There are several limitations to the use of GRDFs and they include:

- Floating systems require fluid in stomach
- Swelling systems require to be swollen before gastric emptying occurs
- Drugs that irritate the stomach are not suitable candidates for delivery using this approach
- They do not offer an advantage for drugs that are unstable in acidic pH

- Mucus on stomach wall undergoes constant renewal and causes problems for muco-adhesive systems especially in the acidic environment of the stomach.

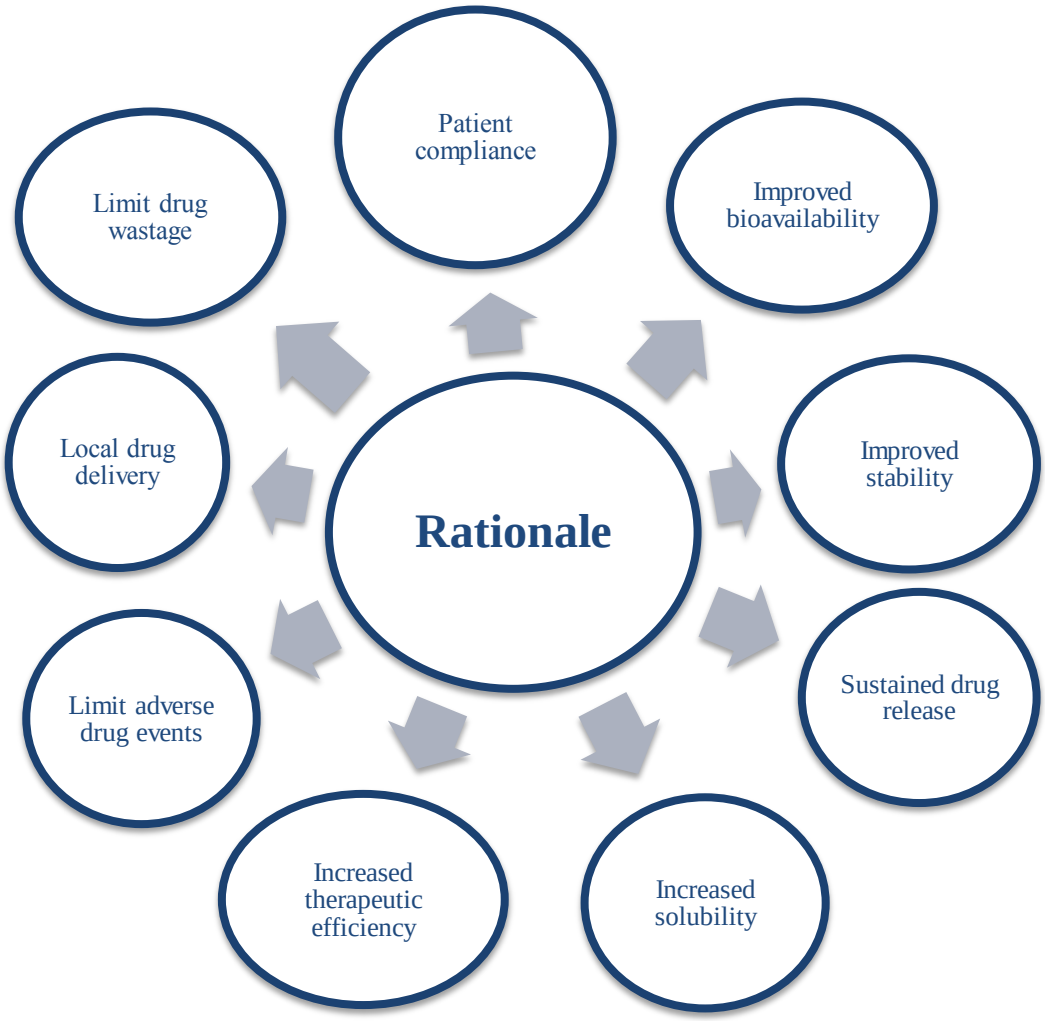

Figure 1-11: Rationale for GRDDS

(Nayak *et al*., 2010b)

1.4 Gastro-retentive applications in drug delivery

Oral drug delivery is limited by the short GRT of the formulations. Therefore, the use of gastro-retentive formulations tends to permit the localisation of the drug component in the GI mucosal membrane for an extended period. This improves the bioavailability, leading to a reduction in the dose and frequency of administration. The control of the location of a delivery system at a particular site in the GI tract, especially the upper GI tract, often improves the absorption of the drug and the therapeutic effect of the drug (Singh and Robinson, 1988).

1.4.1 Mucoadhesive formulations

Mucoadhesive microspheres are a useful and promising DDS, adhering to the mucosal layer, while releasing their drug contents in a sustained manner (Illum, 1998). These microspheres either can consist entirely of a mucoadhesive polymer or can be coated with a mucoadhesive polymer (Figure 1-12). Mucoadhesive microspheres can be modified to adhere to any form of mucosal tissue and have the added advantage of efficient absorption and improved bioavailability of drug content due to the high surface-to-volume ratio, an intimate contact with the mucosal layer and they could help target specific absorption sites (Lehr *et al*., 1992a, Henriksen *et al*., 1996, Bhaskara and Sharma, 1997, Chowdary and Rao, 2003). Several studies have shown improved bioavailability of drugs from mucoadhesive formulations. Such drugs include testosterone and its esters, vasopressin (Morimoto *et al.*, 1991), dopamine (Ikeda *et al.*, 1992), insulin (Nagai *et al.*, 1984) and gentamicin (Illum *et al*., 1989). However, there are challenges in the development of particles with adequate drug loading for their intended application. Low drug contents associated with these microspheres raise concerns about both the efficiency of the process and the amount of material that would need to be

delivered to achieve therapeutic levels (Liu *et al.*, 2005), *e.g.* drug loadings of 26 % observed with amoxicillin mucoadhesive microspheres. Acyclovir microspheres were prepared by an emulsion-chemical cross-linking technique using mucoadhesive polymers such as chitosan (CS), thiolated CS, Carbopol® 71G and Methocel® K15M (Dhaliwal *et al.*, 2008). The microspheres released 78.8 ± 3.9 % of their drug load in 12 h compared with dissolution of 90.5 ± 3.6 % in 1 h using the drug as a powder. The thiolated CS, CS, Carbopol® and Methocel® formulations microspheres showed gastric retention at 8.0 ± 0.8 h, 3.1 ± 0.4 h, 1.1 ± 0.2 h and 0.2 ± 0.1 h respectively (Dhaliwal *et al.*, 2008). Studies also showed that the administration of thiolated CS microspheres could maintain plasma levels for about 24 h compared to 5 h after administration in solution and showed a nearly four-fold higher AUC_{0-24} value. Lacidipine loaded CS microspheres prepared using glutaraldehyde as the cross-linking agent has been evaluated *in vitro* for the treatment of pylorospasm. The drug entrapment efficiency (DEE) was between 14 % and 40.8 % and the microspheres exhibited mucoadhesion of over 70 % in the *in vitro* wash-off test using rat stomach mucosa. The DEE and the mucoadhesion depended on the polymer concentration, volume of cross-linker and the stirrer speed. The optimal formulation showed controlled release for more than 6 h and release followed Higuchi kinetics (Sultana *et al.*, 2009). Mucoadhesive tablets containing atenolol using Carbopol® 934P and sodium carboxymethylcellulose showed high bioadhesive strength measured as force of detachment from porcine gastric mucosa. This high bioadhesive strength is likely to increase the GRT and bioavailability. The formulation also exhibited zero order drug release and can be employed as a once-a-day oral controlled drug delivery system (Singh *et al.*, 2006).

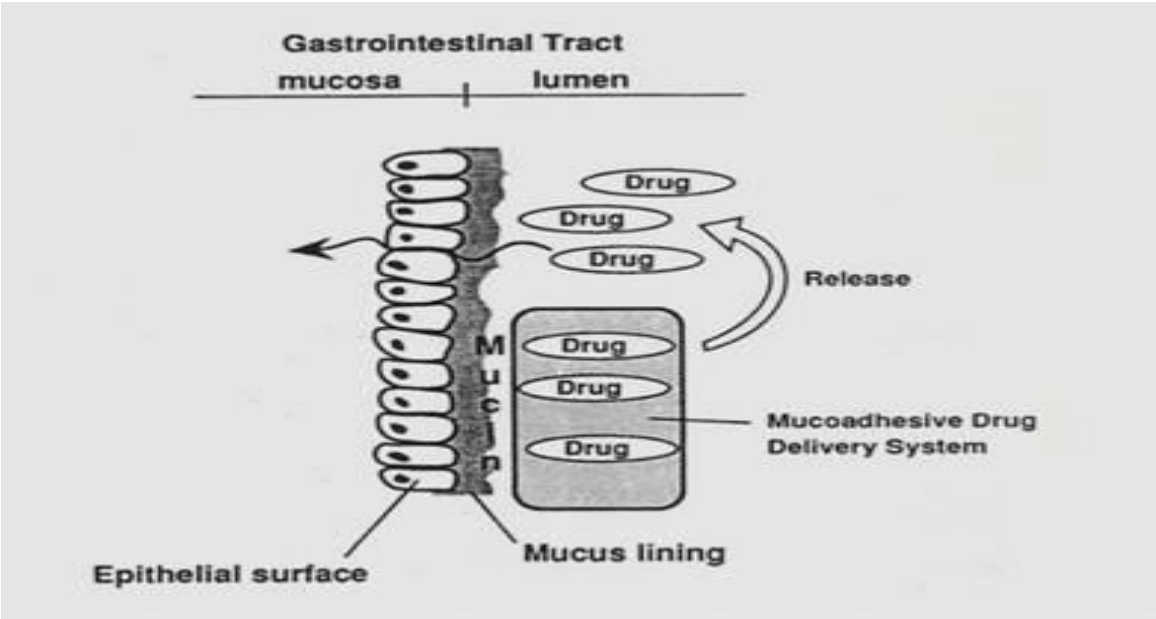

Figure 1-12: Interaction of mucoadhesive delivery system with the mucosal layer of the GI tract (Ganga and Bafna, 2007)

1.4.2 Floating formulations

Floating bilayer tablets were prepared with one layer of the tablet made from polymers HPMC 4000, HPMC 100 and carboxymethylcellulose (CMC) and the drug – furosemide (Ozdemir *et al.*, 2000). The second layer consisted of an effervescent mixture of sodium bicarbonate and citric acid Radiographic studies in volunteers showed that the floating tablets were retained in the stomach for 6 h. Corresponding blood analysis showed the bioavailability of furosemide was enhanced by about 1.8 times than that of conventional tablets and peak diuretic effect was prolonged with the floating tablets. Gas forming agents were incorporated into an expandable tablet containing a mixture of polyvinyl lactams and

polyacrylates that can swell rapidly in an aqueous environment. As soon as the gas formed, the density of the system was reduced with the system floating on the gastric environment (Penners *et al*., 1997). A once-daily formulation was developed for the oral administration of ciprofloxacin containing sodium alginate, xanthum gum, sodium bicarbonate and cross-linked polyvinyl pyrrolodine (PVP). The PVP and the gel forming polymers formed a hydrated gel matrix that entrapped the gas, leading to the buoyancy and gastric retention of the tablets (Talwar *et al*., 2001). Streubel *et al*. (2003b) prepared floating tablets based on Accurel MP 1000® (a polypropylene foam powder) and matrix forming polymer. The highly porous foam powder in the tablets provided a lower density than the release medium and remained floating for at least 8 h in the medium. The drug release profile of the tablets may be altered by varying the ratios of the matrix forming polymers and the foam powder. Wu *et al*. (1997) prepared floating nimodipine sustained release tablets using HPMC and PEG 6000. Nimodipine was initially incorporated into a Poloxamer-188 solid dispersion before it was directly compressed into floating tablets. The optimized tablets were buoyant for over 10 h *in vitro*, with GRT of the floating tablets in fed and fasted states being 5 h and 3 h respectively, in comparison with the GRT of conventional tablets in fed and fasted states being 3 h and 2 h respectively. Drug release followed zero order release kinetics and drug bioavailability was double that of non-floating tablets. Iannuccelli *et al*. (1998) prepared air compartment multiple unit systems. Each unit, with diameter of about 3.7 mm was composed of an alginate core separated from a calcium alginate / polyvinyl alcohol (PVA) membrane by an air compartment. In the presence of water, the PVA leaches out and increases membrane permeability thereby preventing shrinkage of the air compartment. The PVA-containing units floated immediately upon contact with artificial gastric juice, with 100 % buoyancy lasting more than 24 h. The units without PVA did not float due to shrinkage of the air compartment. Ma *et al*. (2008) produced floating alginate microsphere by ionotropic gelation method with calcium carbonate as the gas-forming agent. Chitosan was added to the gelation medium to modify drug release and increase drug entrapment and Eudragit was used as the coating material. It was observed that the formulations, either coated or uncoated, floated continuously in simulated gastric fluid (SGF) for 24 h *in vitro*. GRT of optimised coated

floating microspheres in healthy volunteers was over 5 h while the non-floating microspheres were emptied within 2.5 h. An effervescent floating matrix system (EFMS) was designed to cause tablets to float in gastric fluid and was used to significantly improve the release of a new synthetic flavonoid (DA-6034). The EFMS was formulated using swelling polymers (HPMC, Carbopol® 934P and Kollidon® CL), a gas generating agent (sodium bicarbonate (SB)), eroding polymers (Eudragit L100-55 or alginic acid), and solubilizers (Poloxamer F68 and sodium lauryl sulphate (SLS)) and this mixture was compressed to form tablets following the addition of a lubricant. The therapeutic limitations of this flavonoid were due to its low solubility in acidic media but with the use of EFMS, drug was released continuously. This was attributed to the effect of the solubilizers and the alkalinising agent such as SB used as a gas generating agent. DA-6034 EFMS tablets showed enhanced gastro-protective effects in gastric ulcer-induced beagle dogs, indicating the therapeutic potential of EFMS tablets for the treatment of gastritis (Jang *et al.*, 2008). Chen *et al.* (2013) developed gastro-retentive tablets combining both floating and swelling properties. These losartan tablets were formulated with hydroethylcellulose (HEC), CS and SB. Results showed that formulations at HEC:CS (5:5) showed optimal floating lag time, floating duration and swelling. Addition of SB improved the buoyancy and the optimized formulation, containing 20 mg SB, resulted in the tablets floating for < 16 h and an adjustable drug release profile.

Floating tablets of ciprofloxacin hydrochloride were prepared by direct compression and evaluated for physical, swelling, floating and drug release properties. *In vivo* studies were also carried out on the optimized floating and non-floating tablets in healthy volunteers. The duration of floating were predominantly > 24 h and floating lag times < 20 s for the floating tablets. The drug release followed zero order kinetics. C_{max}, T_{max}, and $AUC_{0-\infty}$ of floating *versus* non-floating tablets were 0.945 ± 0.29 *versus* 2.1 ± 0.46 μg/ml; 6.0 ± 1.42 *versus* 1.42 ± 0.59 h and 8.54 ± 1.87 *versus* 9.45 ± 2.12 μg/ml/h, respectively. These parameters indicate that the developed gastro-retentive formulation extended the pharmacokinetic profile achieved with the conventional tablets (Mostafavi *et al.*, 2011).

1.4.3 Expandable formulations

Expandable formulations were initially designed for veterinary use (Laby, 1974) for the controlled release of bloat-preventing surfactants in bovines. A unique super-porous hydrogel (SPH) (Poly (acrylamide-co-3-sulfopropyl acrylate) (P(acrylamide-co-potassium salt of 3-sulfopropyl acrylate containing $NaHCO_3$)) composites was designed which combined a high swelling rate at a ratio of more than 100 times the original weight of the dried matrix with substantial mechanical strength (Chen *et al*., 2000, Chen and Park, 2000). Inside these SPHs, water flows through an open channel system with pores of a few hundred micrometres by capillary action with rapid swelling occurring within 20 minutes. This is in contrast to the conventional hydrogels, which have relatively small pore sizes, and equilibrium swelling is achieved after several hours through diffusion of the aqueous media. The rapid swelling of SPH prevents premature emptying from the stomach by IMMC. Whilst SPHs are characterised by low mechanical strength, the addition of a super-disintegrant, *e.g.* Ac-Di-Sol®, increases the cross-linking density, yielding an SPH composite. An *in vivo* study in beagles showed that the SPH composite, previously shown to swell in SGF to a size of 3.5 x 2.4 cm (length x diameter), was retained in the fed stomach for more than 24 h. However, administration to a fasting dog showed rapid evacuation.

Gastro-retention was enhanced with the use of a rectangular-shaped unfolding GRDF, which used a combination of rigid components with large dimensions *e.g.* 5 x 2 cm (Klausner *et al*., 2002, Klausner *et al*., 2003a). The formulations were compounded from thin polymeric membranes with a drug polymer matrix being surrounded by rigid polymeric strips, all covered from both sides in a sandwich form by identical membranes which connected and maintained the structure intact. Each component was designed for rapid removal from the stomach, while the whole combination in this formulation yielded a prolonged gastro-retention. These GRDFs were retained in the stomach of humans and dogs for extended periods of at least 5 h. The use of both soluble and poorly soluble drugs in this formulation has shown *in vitro* controlled release. In dogs, formulations incorporating riboflavin and

levodopa had increased bioavailability in comparison with non-gastro-retentive DFs. Studies in healthy volunteers showed enhanced pharmacodynamic activity such as diuresis and natriuresis with furosemide (Klausner *et al.*, 2003d) and with levodopa – an extended absorption phase by 2 h in comparison to a non-gastro-retentive DF Sinemet CR® (Klausner *et al.*, 2003b). Several researchers have exploited the physiological fact that the fed mode prolongs gastro-retention. Therefore, these DFs are administered with food and swell to a certain size that enhances gastro-retention, while releasing the drug in a controlled manner. GRDFs designed with dimensions of 19 x 8 mm (length x diameter) were administered to fasting beagle dogs and these were retained for less than 90 min in the stomach with prolongation of GRT to 4 - 5 h. Arza *et al.* (2009) developed a combined swellable and floating ciprofloxacin hydrochloride tablet. These tablets employed a combination of polymers such as HPMC, swelling agents (crosprovidone sodium, starch glycolate and croscarmellose sodium) and an effervescent substance (SB). The swelling ratio increased to about 400 % of the dried tablet weight. The mean residence time of the tablet in healthy volunteers was found to be 320 ± 48.99 min (n=6).

1.4.4 High density formulations

Compared to other gastro-retentive systems, research into high density formulations has been rather limited. High density microspheres with loose bulk density between 0.42 - 0.74 g/cm^3 were prepared by a coacervation phase separation technique for the sustained release of famotidine with the addition of titanium dioxide (Ahad *et al.*, 2011). However, there were no *in vivo* studies or *in vitro* studies to demonstrate the actual sinking of the microspheres in physiological fluids for a considerable length of time, since the bulk and tapped densities were all less than the density of gastric contents (Ahad *et al.*, 2012). A high density propafenone HCl gastric-resident tablet was developed employing zinc oxide (ZnO) as the

density-increasing agent, increasing density up to 1.63 g/cm^3. ZnO increases the system density making the system resident in the stomach to prolong the drug delivery time in absorption zone. The device released its drug content over 12 h and maintained its conformation over this period (Ashoka *et al.*, 2013).

1.5 *Helicobacter-pylori* (*H. pylori*) infections

1.5.1 Aetiology of *H. pylori* infections

H. pylori is a spiral gram-negative micro-aerophilic bacterium, with two to six unipolar, sheathed flagella (Figure 1-13). The flagella provide motility and the ability to penetrate the gastric mucosa, resist gastric rhythmic contractions and remain in the gastric mucosa. It is 2.4 - 4.0 µm long and 0.5 - 1.0 µm wide (Blaser, 1992, Brown, 2000). This bacterium was initially identified in autopsied dogs in 1893, described in humans in 1906 (Rothenbacher and Brenner, 2003) and successfully isolated in 1983 (Marshall and Warren, 1984). Infection is silent and *H. pylori* is implicated in the development of chronic active gastritis, peptic ulcer disease, gastric mucosal-associated lymphoid tissue lymphoma and gastric carcinoma (Peterson, 1991, Dunn *et al*., 1997, Ernst and Gold, 2000, Suerbaum and Michetti, 2002). This bacterium affects half the world's population (Dunn *et al.*, 1997). *H. pylori* infection has also been associated with coronary artery and ischemic heart disease (Mendall *et al*., 1994, Cammarota *et al*., 1998). About half a million new cases per year of gastric cancer, about 55 % of the total cases worldwide, have been linked to *H. pylori* and has been predicted to be one of the top ten leading causes of death worldwide by 2020 (Murray and Lopez, 1997, Kawahara *et al*., 2005). Due to the various conditions associated with *H. pylori*, the World Health Organisation (WHO) International Agency for Research on Cancer classified *H. pylori* as a class 1 carcinogen in humans (Sherman, 2004).

Figure 1-13: *H. pylori* strain

(Image adapted from (Bouyssou, 2014) Used with permission)

Even though only a small proportion of individuals carrying this bacterium ever develop clinical sequelae, the infection is asymptomatic (Petersen and Krogfelt, 2003) and if left untreated the infection is lifelong (Czinn, 2005). The prevalence of infection with *H. pylori* varied between 7 % in a study conducted among children in the Czech Republic (Sýkora *et al.*, 2009) and 87 % in South Africa (Dube *et al.*, 2009). In Europe, the prevalence varied between 7 and 33 % (Breckan *et al.*, 2009, Sýkora *et al.*, 2009) between 48 and 78 % in South American studies (Santos *et al.*, 2009) and between 37.5 and 66 % in Asian studies (Hirai *et al.*, 2009, Zhang *et al.*, 2009, Ford and Axon, 2010).

1.5.2 Mechanism of *H. pylori* infection

H. pylori infections occur mainly from childhood (Imrie *et al.*, 2001, Rowland *et al.*, 2006), between the ages of 1 to 5 years. The primary route of infection has yet to be confirmed, but several routes have been proposed and they include gastric-oral, oral-oral (Megraud, 1995), faecal-oral, zoonotic (Fox, 1995) and water/food-borne (Hulten *et al.*, 1996, Herrera, 2004). However, one of the major risk factors for infection with *H. pylori* is contamination of food by human faecal material (Hopkins *et al.*, 1993). A major route of transmission in developing countries is through intra-familial transmission (Nahar *et al.*, 2009, Salih, 2009). Acute infection most likely occurs as a result of ingestion of the organism which is most commonly asymptomatic, but may be associated with epigastric burning, abdominal distension or bloating, belching, nausea, flatulence, and halitosis. The principal reservoir for *H. pylori* infection appears to be the human stomach, especially the antrum. *H. pylori* attaches to the gastric epithelial cells and one of the major features of its infection is that it causes progressive injury to the gastric mucosa and its function (Suzuki and Ishii, 2000, Lehmann *et al.*, 2002). The injurious effect of the bacterium is further enhanced by the production of a vacuolating cytotoxin VacA (Farthing, 1998). *H. pylori* is a very diverse species and cancer risks may be increased with strains having virulence-associated genes (cytotoxin-associated gene, CagA), host genetics and environmental factors (Rothenbacher and Brenner, 2003). *H. pylori* produce several enzymes and have a high urease activity. In the acidic environment of the stomach, urea (CH_4N_2O) breaks down into bicarbonate (CHO_3^-) and ammonia (NH_3) that shields the bacterium in the acidic environment of the stomach (Owen, 1998). The ammonium ions produced from the urea breakdown can be toxic to the gastric superficial epithelial cells, thereby causing further injury. Urease enhances inflammatory cytokine production and activates mononuclear phagocytes (Dunn *et al.*, 1997). On colonisation, the host immune system is stimulated and there is an increase in secretory IgA (sIgA) detected in the gastric mucosa; raised specific IgG and the host is unable to rid itself of the bacterium (Shah *et al.*, 2009a). This colonisation causes persistent gastric inflammation; however the clinical course of the bacterial infection varies from patient to patient (Atherton, 2006).

1.5.3 Treatment of *H. pylori* infections

Table 1-3: Therapies used for treatment of *H. pylori*

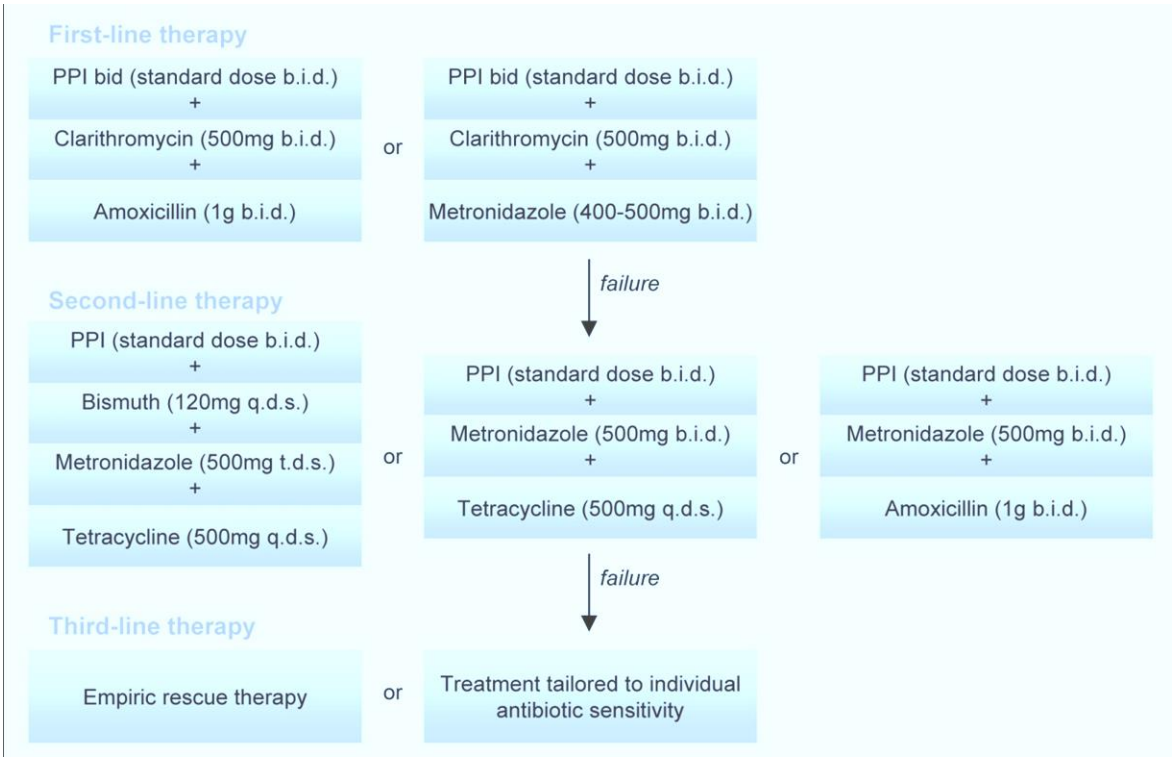

H. pylori is sensitive to many antibiotics *in vitro*; however no single agent is effective alone *in vivo* (Bazzoli *et al.*, 2002), therefore, there is a need for a combination therapy to effectively eradicate the bacterium (Table 1-3). A minimum of two antibiotics in combination

with gastric acid inhibitors is therefore used in the treatment. The major problem relating to the antibiotic treatment is that after infection the bacterium resides below the gastric mucus adherent to the gastric epithelium; therefore, the access of drugs to this particular site is rather limited. In addition, due to bacterial resistance, the bacteria might have acquired resistance to the commonly used antimicrobial drugs (Iijima *et al.*, 2004). Therefore, for a regimen to achieve a high eradication rate, it is necessary that the drug is delivered to the entire surface of the stomach and must reach high concentrations for a sufficient time to efficiently kill the bacteria (Midolo *et al.*, 1996). If eradication is not achieved, the bacteria can re-colonize the gastric epithelium, resulting in treatment failure (Atherton *et al.*, 1995). The first line therapy for the treatment of this infection is the use of a triple therapy consisting of an adjuvant and two antibiotics *e.g.* clarithromycin, amoxicillin and metronidazole (Laheij *et al.*, 1999, Malfertheiner *et al.*, 2007, Georgopoulos *et al.*, 2012). The antibiotics have to be used in combination, as one antibiotic cannot achieve adequate eradication and there is a requirement for adjuvant therapy (Chang *et al.*, 2003). The adjuvant therapy consists of drugs that increase alkalinity of the stomach in order to allow local action of antibiotics that are not stable in the acidic pH of the stomach. An example of the adjuvant drugs is the proton pump inhibitors (PPI) *e.g.* omeprazole which is used at a dose of 20 mg twice daily. Increasing intra-gastric pH by the co-administration of potent gastric acidity inhibitors has been reported to significantly improve eradication (Moayyedi *et al.*, 1995). In patients for whom the PPI-based triple therapy fails, different regimens (sequential, quadruple, concomitant and hybrid therapies) and various combinations of new and old antibiotics are becoming increasingly popular (Hsu *et al.*, 2008, Basu *et al.*, 2011). Quadruple therapies include colloidal bismuth subcitrate, tetracycline, metronidazole and omeprazole (De Boer, 2001). The recommended regimens are not very effective and have an eradication efficacy of 60 – 80 % (Georgopoulos *et al.*, 2002, Chi *et al.*, 2003). This is due to several factors such as the persistent rise in resistance of this bacterium to these antibiotics; the hostile environment of the stomach that leads to inactivation of drugs such as clarithromycin which is degraded in the lumen mainly through the action of acid and pepsin with a half-life of less than 1 h; reduction of antibiotic bioavailability at the site of action (Megraud, 2004, Batchelor *et al.*, 2007). Other factors

include the formation of biofilms by *H. pylori* on the gastric mucosa epithelium, which can all lead to treatment failures (Cammarota *et al.*, 2012). In addition, other major problems with this regimen include patient compliance and side effects due to the number of drugs and frequency of dosing (Table 1-3). Patient compliance with this type of complicated regimen of four drugs may be improved by combining all the different drugs in a single dosage form. This idea resulted in the development of the formulation Pylera®. Pylera® has been approved in the United States and it contains bismuth subcitrate potassium (140 mg), metronidazole (125 mg) and tetracycline (125 mg).

One other major problem in the eradication of *H. pylori* in the stomach is the limited gastric residence of conventional controlled release formulations, which, even if designed to ensure release of drug over longer periods, may not be retained in the stomach for that long. The average residence time of formulations in the stomach depends on the type of dosage form with tablets, pellets, capsules and solutions having an average time of 2.7 ± 1.5 h , 1.2 ± 1.3 h, 0.8 ± 1.2 h and 0.3 ± 0.07 h respectively (Chawla *et al.*, 2003). Therefore, the duration of drug release from controlled drug delivery system such as oral matrix/osmotic systems is dependent on the GI transit time and so is unpredictable and limited to around 12 h maximum. For controlled release formulations, especially those containing drugs with a narrow absorption window in the upper GI tract *i.e.* stomach and small intestine, this can be a problem. This is due to the relatively short transit time of the DS in these parts of the GI. Therefore, after only a short period of less than 6 h, the controlled release DS would have left the upper GI tract and the drug is released in non-absorbing segments of the GI tract. This results in a short absorption phase and lower bioavailability (Klausner *et al.*, 2003c).

1.5.4 Resistance of *H. pylori* to antimicrobials

There is global concern regarding acquired resistance to the commonly used antibiotics in the eradication of *H. pylori* (Megraud, 2007, Chang *et al*., 2009, Graham and Fischbach, 2010, Kao *et al*., 2014) as this has been suggested to be a major cause of the treatment failure. The standard triple regimens showed eradication rates of 40 – 80 % in southern European countries (Graham and Fischbach, 2010). The prevalence rate of clarithromycin (CMN) (17.2 %), metronidazole (MET) (26.7 %), amoxicillin (11.2 %) and levofloxacin (16.2 %) resistance increased from Europe to Asia, America and Africa, with tetracycline resistance low (<3 %) in all countries, but was 43.9 % in Africa (De Francesco *et al.*, 2010). Just as *H. pylori* infection is associated with geographical areas, so also the prevalence of the resistance rates appear to be partly determined by geographical factors (Wu *et al.*, 2012). An analysis of 59 independent studies (56 in adults, 2 in children and 1 in both groups in Latin America) published from 1988 till October 2013, showed prevalence of antimicrobial primary resistance among adults varied by antibiotic. Resistance varied from 12 % for CMN (35 studies), to 53 % for MET (34 studies), to 4 % for amoxicillin (28 studies), to 6 % for tetracycline (20 studies) to 3 % for furazolidone (6 studies), to 15 % for fluoroquinolones (5 studies) and to 8 % for dual CMN and MET (10 studies). Resistance prevalence varied significantly by country, but not by year of sample collection (Camargo *et al.*, 2014). Elevated primary resistance to CMN (20 to > 40 %) and quinolones (20 to > 33 %) has been observed in developed countries, while high primary resistance to MET (≥76 %), tetracycline (≥ 15 %), and amoxicillin (> 30 %) has been found in developing countries. In addition, secondary resistance is more common (Boyanova *et al*., 2011). The prevalence of CMN and MET resistance in China has both increased from 12.8 to 23.8 % and 12.8 to 56.6 % respectively between 2000 and 2009 (Gao *et al.*, 2010). An increase in the duration of treatment (Streubel *et al.*, 2003a) and combination of different antibiotics with different mechanisms of actions (Chaudhuri *et al.*, 2003) has been used to reduce the prevalence of resistance. CMN is effective and is the key component of most combination therapies and resistance to CMN has become one of the main reasons for eradication failures (De Francesco

et al., 2009) Resistant strains to CMN are emerging, but the instances are comparatively lower than MET (Logan *et al.*, 1994, Boyanova *et al*., 2011, Mansour *et al*., 2010). Resistance to CMN has been detected more in patients living in the south (up to 20 %) than in those living in the north of Europe (Koletzko *et al*., 2006, Janssen *et al*., 2006, Storskrubb *et al*., 2006). Spain has one of the highest levels of CMN resistance of about 35.6 % observed in Europe (Agudo *et al*., 2009). Administration of CMN with a PPI significantly increases its concentration in the antral mucosa and the mucus layer (Meurer and Bower, 2002). In cases where CMN therapies fail, this drug should not be used in second-line therapies and a regimen containing amoxicillin, MET and a PPI can be used or a levofloxacin - based triple therapy which has proven to be a superior therapy to quadruple therapy and fewer side effects (Liou *et al*., 2010). A high dose of amoxicillin is required in either dual therapy or in second-line treatment regimens as a result of the low local concentrations of amoxicillin at its site of action. An example is seen in a case where levels above the minimum inhibitory concentration have been detected for CMN in gastric juice, mucosa and serum after 6 hours following oral dosing with a triple therapy regime of omeprazole, CMN and amoxicillin. However, following a 1g dose of amoxicillin, it was only detected for two hours in gastric mucosa (Conway, 2005).

1.6 Gastro-retentive applications in the treatment of peptic ulcer

1.6.1 Mucoadhesive formulations

Patel and Chavda (2008) developed amoxicillin microspheres using Carbopol® 934P as the mucoadhesive polymer and ethylcellulose (EC) as the carrier polymer. The microspheres produced were spherical, free flowing and with DEE ranging from 20 % to 56 %. The microspheres adhered to gastric mucus layer over an extended period and drug release from these microspheres was sustained for more than 12 h. In addition , i*n vivo* tests showed that these microspheres exhibited better *H. pylori* clearance than amoxicillin powder. In another study by Yellanki *et al.* (2010), amoxicillin-trihydrate microspheres were prepared using Carbopol® 934P and EC with the DEE between 78 and 86 %. The particle size ranged from 500 to 560 µm for all the batches produced. *In vitro* tests carried out using sheep gastric mucosa showed retention of more than 84 % of the microspheres on the tissue. Drug release was biphasic, with an initial burst release followed by a slow release with more than 80 % drug released after 6 h. Liu *et al.* (2005) prepared EC microspheres with Carbopol® 934P as the mucoadhesive polymer and amoxicillin as the active drug. The sizes of microspheres ranged from 400 to 1000 µm. The microspheres had a dense but porous inner core and the release was pH dependent. In acidic medium (HCl - pH 1.0), 90 % of the drug was released in 4 h, while in phosphate buffer (pH 7.8), the release was about 50 %. *In vitro* mucoadhesion studies showed that 93.5 % of the microspheres containing Carbopol® were retained in the gastric mucosa of rats, compared with 85.8 ± 5.3 % of those without Carbopol®. *In vivo* studies in rats showed that the mucoadhesive microspheres containing Carbopol® were retained for longer, gastric amoxicillin concentrations were higher and there was enhanced clearance of *H. pylori*. Another study reported that gastric retention of amoxicillin microspheres prepared by dispersing Carbopol® in waxy hydrogenated castor oil in rats was about three times higher than that obtained using amoxicillin suspension containing 0.5 %w/v

methylcellulose. After 2 and 4 h, about 47 % and 20 % of the microspheres were retained respectively compared with only 17 % and 6 % respectively retained for the amoxicillin suspension. In addition, the mucoadhesive microspheres achieved a 10 times higher bactericidal activity than the amoxicillin suspension in rats (Nagahara *et al.*, 1998).

In a study by Patel and Patel (2007), the *in vitro* and *in vivo* characteristics of chitosan microspheres loaded with amoxicillin were evaluated. *In vitro* mucoadhesion tests showed that these microspheres were retained more strongly on the gastric mucous layer and could be retained in the GI tract for an extended period. The best formulation produced in this research exhibited a high DEE of 70 % and swelling index (which is a ratio of the change in weight of microspheres on exposure to SGF and the initial weight of the microspheres) of 1.39. The retained microspheres was ~ 80 % after 1 h and drug release was sustained for more than 12 h. The *in vivo* clearance studies showed that mucoadhesive microspheres had a better clearance effect on *H. pylori* than amoxicillin powder. Following administration of a dose of 4 mg/kg amoxicillin mucoadhesive microspheres, the colony counts (a measurement of the growth of *H. pylori*) were 23 ± 7.07, and as the doses increased to 7.5 and 15 mg/kg, the colony counts reduced to 5.5 ± 0.70 and 2 ± 0, respectively. However, following administration of amoxicillin powder (4 mg/kg), the colony counts were 78 ± 8.48, and as the doses increased to 7.5 and 15 mg/kg, they were 29 ± 5.65 and 17.5 ± 17.67, respectively. Wang *et al.* (2000) produced modified gelatin microspheres using aminated gelatin by surfactant-free emulsification in olive oil, followed by a cross-linking reaction with glutaraldehyde. These modified microspheres exhibited a greater gastric mucoadhesion than the unmodified gelatine microspheres; thereby, presenting a likely candidate DDS for the eradication of *H. pylori*. There are however safety concerns in using glutaraldehyde as a cross-linking agent and residual levels need to be controlled.

Ramteke *et al.* (2006) prepared mucoadhesive nanoparticles of CMN for oral delivery. The maximum DEE was 73 %, while the nanoparticle recovery was reported to be 88 %. The drug formulation was shown to be retained in the stomachs of rats for a longer period than CMN

suspensions or conventional drug formulations, as some nanoparticles were still retained in the stomach of rats 6 h after administration. Cuna *et al.* (2001) prepared amoxicillin-loaded ion-exchange resins encapsulated in mucoadhesive polymers such as polycarbophil and Carbopol® 934. An oil-in-oil solvent evaporation technique was modified to produce these microparticles containing multiple amoxicillin - resin cores. Polycarbophil microparticles were spherical, while those containing Carbopol® were irregularly shaped. *In vitro* release of amoxicillin was rapid despite the polymer coating. GI transit in rats was investigated by fluorescence microscopy, using particles loaded with fluorescein instead of amoxicillin; GRT was longer, and the particles were more evenly distributed over the stomach when uncoated. In addition, it was observed that Carbopol® did not enhance the GRT of the microspheres. Such discrepancies may be due to the method of administration, the amount of polymer used and the swelling of the formulation.

1.6.2 Improving targeting of mucoadhesive formulations

Targeted drug delivery is a selective and effective localisation of drugs at specific targets in therapeutic concentrations, while restricting its access to other sites, thus minimising the toxic effects and maximising the therapeutic index and efficiency (Gregoriadis and Florence, 1993). Mucoadhesive polymers generally exhibit the ability to stick to wet mucosal surfaces by non-specific physicochemical mechanisms, such as hydrogen bonding. With this non-specific binding, the polymer is unable to differentiate between adherent or shed-off mucus and binds to both types of mucus, limiting their ability to target a specific mucosal tissue. The development of DDS coupled with cell-specific ligands has increased the therapeutic benefits and enhanced the possibility of effective site-specific drug delivery (Chowdary and Rao, 2004). Any ligand that has a high binding affinity for mucin can be linked covalently to DDS such as microspheres. Examples of such ligands include lectins, adhesins, antibodies and certain amino acid sequences.

1.6.2.1 Lectins

Lectins have the ability to bind specifically to membrane-bound sugar moieties located at the cell surface of epithelial cells, enhancing the adherence of DDS to the intestinal epithelium and improving the absorption of drugs (Lee *et al.*, 2000b). Lectins are found in plants, vertebrates (Ashwell and Harford, 1982, Stockert and Morell, 1983), bacteria and invertebrates (Lis and Sharon, 1986) but the plant lectins are the largest known group. Based on their molecular structure, lectins are divided into three categories:

- Monolectins – those having only one carbohydrate recognising domain
- Hololectins – those with two or more carbohydrate recognising domains
- Chimerolectins – those with additional unrelated domains

Lectins have the potential to target drugs to different parts of the GI tract or even to different cells (*e.g.* complex-specific lectins for parietal cells or fuco-specific lectins for M cells). Binding of polystyrene microparticles to enterocytes have been demonstrated to be enhanced by coating the microparticles with tomato lectins (Gabor *et al.*, 1997). They exhibit strong binding to nuclear pore membranes following cellular uptake (Haas and Lehr, 2002). Another important advantage of lectins in mucoadhesive drug delivery to the GI tract is their resistance to digestion within that environment. Montisci *et al.* (2001) investigated the behaviour of two lectin-particle conjugates after oral administration. The two different plant lectins - *Lycopersicon. esculentum L.* and *Lotus. tetragonolobus,* are specific for oligomers of N-acetyl-D-glucosamine and L-fucose, respectively, and they were conjugated to small poly(lactide) microspheres. The overall GI transit of the particles was delayed when the microspheres were conjugated to the lectins, mainly due to the gastric retention of the particles. A significant proportion of the conjugated particles adhered to the gastric and

intestinal mucosa. There were no significant differences after a preliminary incubation of lectin-microsphere conjugate with specific sugars showing that the activity of the lectins could be maintained. Jain and Jangdey (2009) prepared and characterised lectin conjugated CMN microparticles for the effective treatment of colonisation of *H. pylori*. DEE was about 70 % and conjugation with Concanavalin A (Con A) was confirmed by infrared (IR) spectroscopy and differential scanning calorimetry (DSC). Con A is a lectin isolated from the jack bean, *Canavalia ensiformis* and binds specifically to mono, oligo- and polysaccharides with terminal non-reducing α-D-mannopyranosyl-, α-D-glucopyranosyl- or β-D-fructofuranosyl residues. Maximum mucoadhesion of 85 % was observed for Con A conjugated EC microspheres on stomach mucosae of rats, compared with 12 % observed for a non-conjugated control formulation. A GRT of over 6 h was reported for Con A conjugated microspheres of CMN in rabbits, while it was 3 h for an optimised CMN tablet formulation In another study by Umamaheshwari and Jain (2003), lectin conjugated nanoparticles were prepared as a means of attaching an acetohydroxamic acid delivery system on the carbohydrate receptors of *H. pylori*. *Ulex europaeus* Agglutinin I (UEA I) and Con A lectins were bound to gliadin nanoparticles (GNP) by a two-stage carbodiimide coupling technique. The binding efficacy of the lectin to the carbohydrate receptors was evaluated and this showed strong agglutination patterns with mannose-specific Con A-GNP and (L)-fucose specific UEA–GNP formulations. The lectin conjugated nanoparticles completely inhibited *H. pylori* binding to human stomach cells. The antimicrobial activity of the conjugated nanoparticles was evaluated by % growth inhibition (% GI) studies by using isolated *H. pylori* strain. The inhibitory efficacy of UEA–GNP and Con A-GNP was approximately two-fold higher compared to the unconjugated nanoparticles.

1.6.2.2 Bacterial adhesins

Bacterial fimbriae are long lectin-like proteins found on the surface of many bacterial strains, through which they attach to the epithelial surfaces of enterocytes. Their presence has been

associated with pathogenicity. Therefore, DDS based on this approach could be an efficient mechanism to enhance adhesion of bioadhesive DDS to epithelial surfaces (Lee *et al.*, 2000b). Bernkop-Schnurch *et al.* (1995) covalently attached a fimbrial protein-K99 to poly (acrylic acid) polymer in order to improve the adhesion of the DDS to the GI epithelium. K99 was isolated from an *Escherichia coli* strain harbouring the fimbriae-encoding plasmid pR19906. In this research, the function of the fimbrial protein was tested using a haemagglutination assay, along with equine erythrocytes expressing the same K99-receptor structures as those of GI-epithelial cells. A 10-fold slower migration of the equine erythrocytes through the K99-poly(acrylic acid) gel compared to the control gel without the fimbriae was demonstrated, indicating the strong affinity of the K99-fimbriae to their receptor on the erythrocytes.

1.6.2.3 Amino acid sequences

Some amino acid sequences have complementary parts on the target cell and on the target mucosal surfaces and when they are attached to microparticles; this can enhance binding to specific cell surface glycoproteins (Vasir *et al.*, 2003). In disease states, the cell surface glycoproteins are altered and these altered protein sequences can be targeted by complementary amino acid sequences attached to DDS. Dihydroxy-phenylalanine (DOPA), an amino acid, is found in mussel adhesive protein (MAP) and is believed to contribute to the adhesive process. DOPA has been combined with Pluronics® to enhance its adhesion (Huang *et al.*, 2002). MAP has a favourable safety profile and is a suitable compound for the development of mucoadhesive DDS, preferably if these can be manufactured and stored under non-oxidative conditions (Schnurrer and Lehr, 1996). Antibodies can be produced against some selected molecules present on mucosal surfaces and could be a rational choice

for designing site-specific mucoadhesive DDS, due to the high level of specificity of the antibodies. This could be especially useful in targeting drugs to tumour tissues.

1.6.3 Floating formulations

Floating acetohydroxamic acid microspheres were prepared by the emulsion solvent evaporation technique using polycarbonate as the polymer. *In vitro* analysis showed that the microspheres exhibited buoyancy with over 70 % of the microspheres floating over SGF (pH 1.2) containing Tween 20 after 12 h (Umamaheshwari *et al.*, 2003). An increase in the concentration of polymers led to a reduction in buoyancy of the microspheres due to an increase in bulk density. In addition, the microspheres required a reduced drug dose to achieve anti-*H. pylori* activity in rat models, when compared to the unencapsulated drug. These microspheres cleared *H. pylori* more effectively than the unencapsulated drug, due to buoyancy of the microspheres leading to prolonged GRT.

There is little research reported on the use of floating microspheres in the eradication of *H. pylori* in the treatment of peptic ulcer and this is an area of research that is promising. However, floating beads have been extensively researched for eradication of *H. pylori* and these results may be used to inform subsequent studies involving microparticles. MET was incorporated into chitosan-treated alginate beads by the ionotropic gelation method (Ishak *et al.*, 2007). A (3 x 2 x 2) factorially designed experiment was used, in which three viscosity-imparting polymers (methylcellulose, Carbopol 934P and κ-carrageenan); two concentrations (0.2 and 0.4 %w/v) of chitosan as encapsulating polymer and two concentrations (2.5 and 5 %w/w) of the low-density magnesium stearate as a floating aid were tested. The bead formula containing 0.5 % κ-carrageenan, 0.4 % chitosan and 5 % magnesium stearate showed immediate buoyancy, optimum DEE and extended MET release. The histopathological examination of mice stomachs and *in vivo H. pylori* clearance tests were carried out by orally administering MET alginate beads or MET suspension to *H. pylori*-infected mice under fed conditions as a single daily dose for three successive days in different doses (5, 10, 15 and 20

mg/kg). Mice groups receiving MET in the form of floating alginate beads at doses (10, 15 and 20 mg/kg) showed better *H. pylori* eradication than the corresponding suspension form. The *in vivo H. pylori* clearance tests showed that MET floating beads with a dose of 15 mg/kg provided 100 % *H. pylori* clearance, whereas the MET suspension at a dose of 20 mg/kg gave only 33.33 % clearance efficacy. Rajinikanth and Mishra (2009) prepared floating gellan gum CMN beads. Formulation variables such as concentrations of gellan, calcium carbonate and drug loading influenced the *in vitro* drug release. There was good antimicrobial activity against the isolated *H. pylori* strain, with complete growth inhibition after 12 h. About 80 %, 60 % and 50 % of the beads remained floating in rabbit stomachs after 1 h, 4 h and 6 h, respectively. The stability of beads was unaffected by storage at a temperature of 40 ℃ and 75 % relative humidity for 6 months. These preliminary results suggest that gellan beads can be used to incorporate antibiotics like CMN and may be effective when administered locally in the stomach for the eradication of *H. pylori*. MET-loaded alginate beads containing calcium silicate as a porous carrier or $NaHCO_3$ as a gas-forming agent were prepared for local eradication of *H. pylori* (Javadzadeh *et al.*, 2010). The silicate-based beads had a slower rate of MET release, compared to the gas-forming beads due to the strengthening effect of the calcium silicate on the network structure. In addition, the $NaHCO_3$ based beads had a shorter buoyancy lag time, because the $NaHCO_3$ produced larger pores than those of silicate-treated ones. DEE was over 60 % for all the formulations. In another study, two types of floating MET-loaded alginate beads were prepared. The first set of alginate beads contained vegetable oil (ALGO) with the oil enhancing its buoyancy. The second set of beads had chitosan dispersed within the bead matrix (ALCS). When ALCS containing MET was administered orally to guinea pigs, the beads floated over the gastric contents and released MET into the pig stomachs. In addition, the concentration of MET at the gastric mucosa after administration of ALCS was higher than that obtained from MET solution, though MET serum concentration was the same, regardless of which set of gel beads

were administered. These release characteristics of alginate gels are applicable not only for sustained release of drugs, but also for targeting the gastric mucosa (Murata *et al.*, 2000).

1.6.4 Dual gastro-retentive formulations

Dual gastro-retentive formulation is achieved by exploring two gastro-retentive techniques. Floating bioadhesive microparticles dual functioning systems is achieved through a combination of both the floating and bioadhesive systems, which can be exploited to achieve synergy and help to overcome the drawbacks associated with each system. Chitnis *et al.* (1991) initially explored this theory and it was proposed that these dual functioning systems target *H. pylori*-induced infected sites more effectively and could serve to optimise antibiotic monotherapy of *H. pylori*-based infections. In the research by Umamaheswari *et al.* (2002), floating microspheres containing acetohydroxamic acid were prepared and were coated with polycarbophil. The microspheres floated for longer than 12 h, due to the low bulk densities of the formulation (0.61 – 0.85 g/cm^3). Polycarbophil coating reduced the release rate of the acetohydroxamic acid and they exhibited a better *in vitro* and *in vivo* percentage *H. pylori* growth inhibition.

Zheng *et al.* (2006) explored this dual strategy with chitosan-alginate-EC microparticles. The formulation was prepared through a combination of emulsification/evaporation and internal/ion gelation methods. *In vitro* tests showed that 74 % of the microspheres remained floating in acetate buffer solution for 8 h and 90 % of the drug content was released in a sustained manner over this period. *In vivo* mucoadhesion tests showed that 61 % of the microparticles were retained in the stomach of male Sprague–Dawley rats for 4 h. Pre-treatment with omeprazole led to an increase in CMN concentration for the microparticles in the gastric mucosa compared to CMN solution. A floating-bioadhesive system was developed for the eradication of *H. pylori* with EC as matrix polymer and Carbopol 934P as the mucoadhesive polymer (Rajinikanth *et al.*, 2008). These microspheres exhibited both strong mucoadhesive and good buoyancy profiles. They also demonstrated significant anti-*H. pylori*

effect *in vivo* in Mongolian gerbil. In addition, on comparison with conventional CMN suspension, this formulation required a lower dose of drug for eradication of the microorganism. The microspheres also improved the gastric stability of CMN and eradication of *H. pylori* from the GI tract more than conventional formulations, due to the prolonged GRT of the formulation (Rajinikanth *et al.*, 2008). In a randomised clinical trial, floating bioadhesive microspheres were compared with conventional clarithromycin suspension. In 876 patients, it was observed that at low doses of 60 and 90 mg/kg of CMN, *H. pylori* was mostly cleared with a 98 – 100 % clearance rate and 83 % inhibition at CMN dose of 30 mg/kg. This formulation exhibited a better eradication profile than the suspension and the microbial clearance was further confirmed by polymerase chain reaction analysis (Vaiciunas *et al.*, 2010). Gattani *et al.* (2010) developed alginate / HPMC-based floating-mucoadhesive beads containing CMN to extend the contact time of the antibiotic with *H. pylori*. The beads were prepared by the ionic-gelation technique with calcium chloride as the gelating agent and liquid paraffin (LP) was incorporated to aid the floating of the beads. DEE was more than 80 % for all batches of the formulation with particle sizes within the range 0.7 – 1.1 mm. SEM images of the beads exhibited a rough surface with characteristic large wrinkles and micropores. Buoyancy of the beads depended upon the proportion of LP in the beads. The beads without LP were not buoyant and those containing more than 10 % LP showed 100 % buoyancy. As the concentration of LP increased, CMN release rate decreased. *In vitro* mucoadhesion studies showed that alginate beads exhibited up to 80 % mucoadhesion and LP had no effect on the mucoadhesive properties of the beads, while Alginate-HPMC beads showed 100 % mucoadhesion. *Ex vivo* mucoadhesion studies showed that floating-mucoadhesive beads of Alginate-HPMC have a better mucoadhesive effect in the stomach and might be retained for longer in the stomach for more effective H. pylori clearance. *In vivo* X-ray imaging studies showed that the Alginate-HPMC beads of CMN remained buoyant for at least 6 h in rabbit stomach and that they had good floatability *in vivo*. Sahasathian *et al.* (2010) prepared amoxicillin-loaded alginate gel beads, coated with 0.5 %w/v chitosan and the

beads exhibited DEE and mucoadhesion, which was over 90 %. Excellent buoyancy (100 %) was achieved and the beads demonstrated sustained release of amoxicillin for over 6 h in simulated gastric fluid.

1.7 Common polymers used in gastro-retentive formulations

1.7.1 Alginates

In the pharmaceutical industry, alginates (Figure 1-14) have been used in formulations as tablet binders, disintegrants, gastric emptying delaying substances, gelling agents, sustained release matrices, stabilizers and viscosifiers (Daigo *et al*., 1981, Bodmeier and Paeratakul, 1989, Hwang *et al.*, 1993). Advantages of alginate include the fact that it is cheap and abundant, since it is derived from natural sources; it is stable at low pH, thereby making it a good choice for gastro-retentive drug delivery; it is easy to produce; it forms a gel and re-swells (Haug *et al*., 1963, Yotsuyanagi *et al*., 1987, Hwang *et al*., 1993, Tomida *et al*., 1993), has excellent biocompatibility and total degradation without any toxic by-products when taken orally.

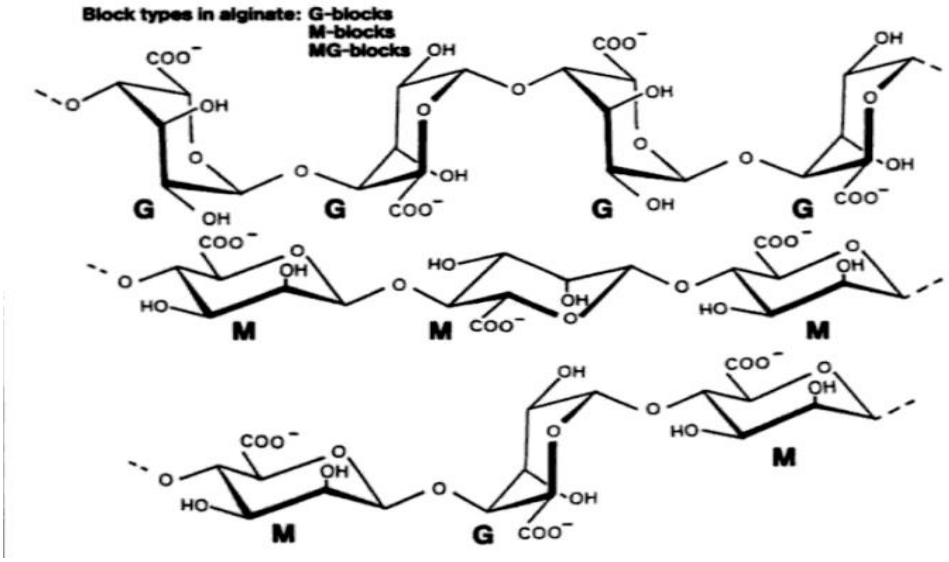

Figure 1-14: Structure of alginates

Due to the inert environment within the network of the alginate and the mild encapsulation conditions (encapsulation at room temperature in aqueous medium), sensitive drugs (Grassi *et al.*, 2001) and other molecules have been incorporated into these delivery systems. Examples include gastro-irritant non-steroidal anti-inflammatory drugs, cells and enzymes (Tomida *et al.*, 1993, Sugawara *et al.*, 1994, Blandino *et al.*, 2000), peptides/proteins (Hari *et al.*, 1996, Wee and Gombotz, 1998, Kierstan and Bucke, 2000) ophthalmic drugs (Cohen *et al.*, 1997), spermatozoa (Torre *et al.*, 2000) and used with chitosan salts to adsorb bile acids (Murata *et al.*, 1999). Calcium alginate is also used in wound dressings (Kneafsey *et al.*, 1996) and scaffolds for tissue engineering (Leor *et al.*, 2000). Calcium alginate beads can be formulated as single or multiple units and this can be with or without the inclusion of other hydrogels or polymers. The major limitation associated with the use of calcium alginate beads as a delivery system is that drug release from such systems is rapid (Whitehead *et al.*, 1996). The control of the drug release from these porous beads can be achieved through modifications to the matrix.

1.7.2 Chitosan

Chitosan is a polymer of ß- (1-4)-linked 2 –acetamido-2-deoxy-D-glucopyranose; however, some of the gluco-pyranose residues are de-acetylated and occur as 2-amino-2-deoxy-D-glucopyranose (Figure 1-15). Chitosan is derived from the alkaline de-acetylation of chitin. Chitin is found in plankton and in the exoskeleton of crustaceans such as shrimp, lobster or crab. Chitin is called chitosan if more than 50 % of its units are de-acetylated (Hudson and Jenkins, 2001)

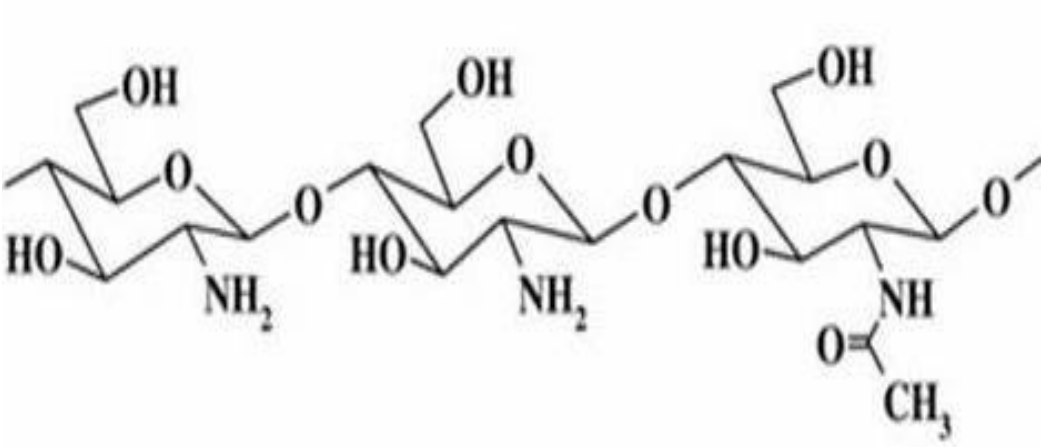

Figure 1-15: Structure of chitosan

(Image adapted from (Pandya, 2008)

Chitosan is becoming a very important excipient in pharmaceutical formulations due to its relatively low toxicity and its abundance in nature and similar attributes to alginates. It has been used for delivery of drugs through the nasal, ocular, parenteral, transdermal and oral routes. Being a cationic polymer, it protonates at acidic pH and also adheres to mucus and porcine stomach (Gåserød *et al.*, 1998a), making it quite useful in the delivery of drugs to such areas. Chitosan has also been useful for the sustained release of water-soluble drugs and for improving the bioavailability of poorly water-soluble substances. Large chitosan

microspheres and beads (with diameters up to a few millimetres) have been proposed for the controlled release of drugs (Sezer and Akbuga, 1999). The use of chitosan and alginate polyelectrolyte complexes has been studied (Lee and Min, 1995, Gåserød *et al.*, 1998a). Chitosan can be used as a coating agent for alginate beads as it alters the rate of diffusion of the encapsulated drug (Anal and Stevens, 2005). In addition, it can be used as an additive for the modification of the alginate bead structure (Gotoh *et al*., 2004, Lin *et al.*, 2005).

1.7.3 Ethylcellulose

Ethylcellulose (EC) is an inert non-biodegradable, biocompatible hydrophobic polymer that is essentially stable, non-toxic, odourless, tasteless, colourless and soluble in a wide range of organic solvents. It is an ethyl ether of cellulose and is a long chain polymer of β- anhydro-glucose units joined together by acetal linkages (Rowe *et al.*, 2003) (Figure 1-16). The specific properties of the polymer depend on the number of anhydro-glucose units in the polymer chain and the degree of ethoxyl-substitution.

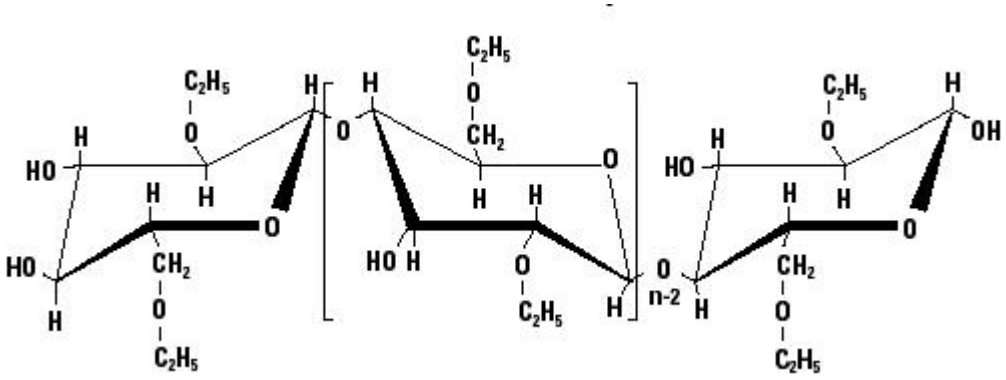

Figure 1-16: Structure of ethylcellulose

EC is widely used in controlled release matrix and coating systems. Dissolution times of various dosage forms may be extended or modified by varying the amount of EC in the formulation. Its melting range is between 240 - 255 ℃. Even though EC is water insoluble, it can take up water (Joshi and Wilson, 1993). This property is due to the hydrogen bonding potential with water attributable to the polarity difference between the oxygen atom and the ethyl group of the polymer (Agrawal *et al.*, 2003, Emeje *et al.*, 2006). Like most hydrophobic polymers, EC requires the use of release modifiers such as carrageenan (Siepmann *et al*., 2007b), HPMC (Frohoff-Hülsmann *et al*., 1999), synthetic poly(vinylalcohol)-poly(ethyleneglycol) graft copolymer (Siepmann *et al*., 2007a) and propylene alginate glycol (Siepmann *et al*., 2008) for drug delivery. These modifiers craft channels in the matrix which improves drug diffusion out of the matrix or enhance the wetness of the matrix (Emeje *et al*., 2006).

1.8 Research aims and objectives

The aim of this study was to develop gastro-retentive controlled release formulations for the delivery of antibiotics such as clarithromycin and metronidazole over an extended period of 12 - 24 h. Such formulations would have the advantage of supplying high concentrations of these drugs into the gastric mucosa, where the bacterium (*H. pylori)* is resident, leading to better eradication of this microorganism and reduction in drug dose (Ishak *et al*., 2007). The gastro-retentive properties of these formulations were assessed using both *in vitro* and *ex vivo* models. The formulations were modified to improve their gastro-retentive and controlled release properties by addition of hydrophobic components or surface modification of the formulations. Surface modification was achieved by either coating of the formulation or by conjugation with lectins, exploring the potential synergy of combining targeting strategy *e.g*. mucoadhesive polymer with lectin.

These were achieved through the evaluation of the outlined objectives:

- study the effect of different variables on formulation parameters such as drug entrapment efficiency, drug content, *in vitro* buoyancy profile and mucoadhesion
- characterisation of the structure of the prepared formulations through observation and determination of morphology, sizes, weights, density, flow properties and moisture content
- determination of the *in vitro* buoyancy profile and lag times of the formulations
- determination of the *ex vivo* mucoadhesion profile of the formulations
- evaluation of the swelling properties of the formulations in different simulated physiological media
- thermal studies involving the use of differential scanning calorimetry (DSC) and thermo-gravimetric analysis (TGA) to study the drug-polymer interactions and compatibility of the formulation components
- *in vitro* release studies of the drugs from formulations

Chapter 2 MATERIALS AND METHODS

2.1 Chapter overview

This chapter gives a brief overview of the experimental methods and techniques commonly used in this research. Some other methods that are specific to each chapter are included in the appropriate chapter and section. All the results presented are expressed as the mean ± standard deviation of at least three separate readings. All materials were obtained from Sigma Aldrich UK and Discovery Fine Chemicals UK and were of analytical grade unless otherwise specified.

2.2 Statistical analysis

Statistical analysis were performed including the one way analysis of variance (ANOVA) Dunnetts test or Tukey test. The analysis was carried out using the Graph-pad Instat 3.10 software.

2.3 Techniques and methods

2.3.1 Ionotropic gelation

Ionotropic gelation occurs based on the ability of polyelectrolytes to cross link in the presence of counter ions (such as calcium, potassium, aluminium and zinc) to form three

dimensional hydrogel beads through the diffusion of the cations into the polymer droplets. These polyelectrolytes contain ions that form a meshwork structure by combining with the counter ions and induce gelation by cross-linking. The hydrogel beads are spherical, swell in simulated physiological fluids and are a known means of microencapsulation of drugs. Drug release from these gels can be controlled through polymer relaxation. Common polymers that undergo ionotropic gelation include sodium alginate, fibrin, chitosan, pectin *etc*. The beads are normally prepared by dropping a drug-loaded polymeric solution into an aqueous solution of polyvalent cations (Patil *et al.*, 2012).

2.3.2 Microencapsulation by solvent evaporation

Microspheres can be prepared through a method of solvent evaporation. This method involves four major stages (Figure 2-1): stage 1 involves the dissolution or suspension of the drug in a solution of the encapsulating polymer in an organic solvent; stage 2 involves the emulsification of the organic phase in a continuous aqueous phase which is generally immiscible in the organic phase; stage 3 involves the extraction of the organic solvent from the dispersed phase which is optionally accompanied by solvent evaporation leading to formation of solid microspheres and stage 4 involves the collection and drying of the solid microspheres (Freitas *et al.*, 2005). The properties of the microspheres can be modified by the concentration of polymers used, the stirring time and speed, volume of the organic and aqueous phases *etc*.

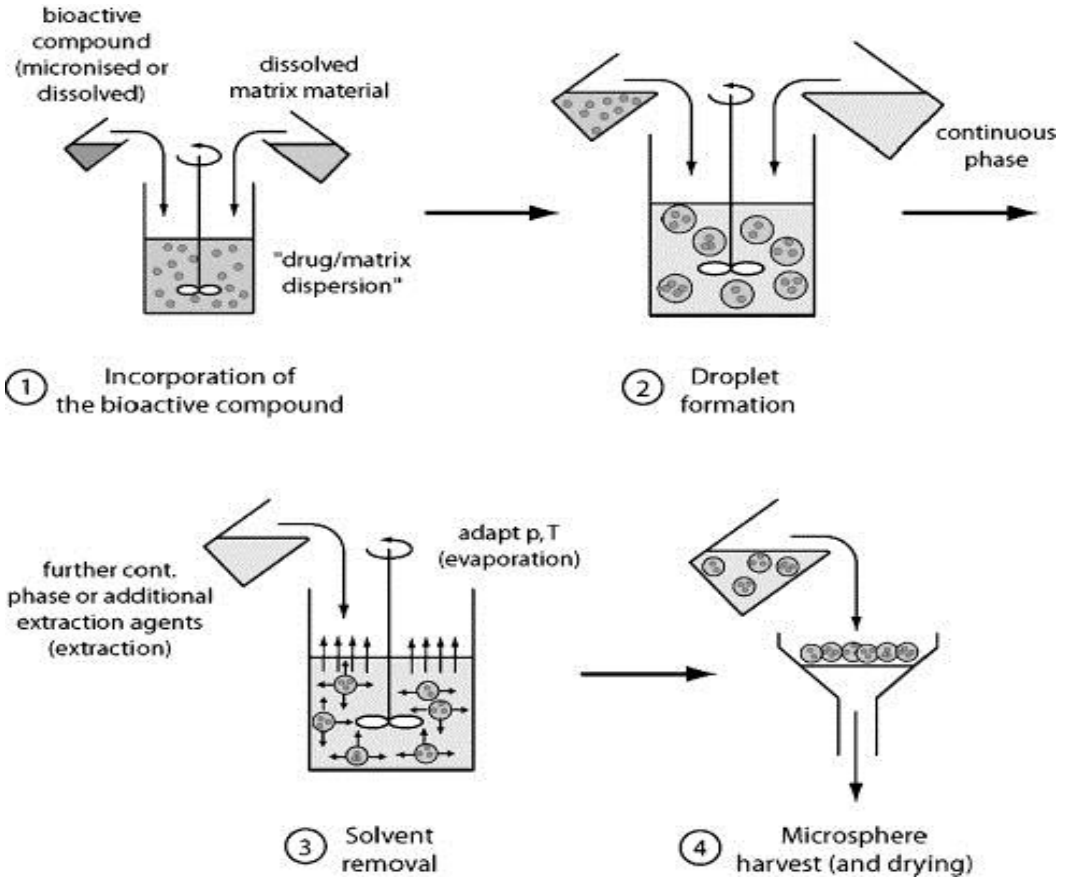

Figure 2-1: Solvent evaporation technique

(Freitas *et al*., 2005)

2.3.3 Freeze drying

Alginate beads produced using the ionotropic gelation method were freeze-dried in order to maintain the shape and size and enhance the porosity of the beads. Freeze drying is the process of removal of solvents often water, associated with a particular material through freezing by direct sublimation of the liquid under vacuum from the solid phase to the gaseous phase, without passing through the liquid phase. This is done without the application of any heat for the evaporation process. There are 3 stages involved in the freeze drying process

which are freezing, primary drying and secondary drying (Wang, 2000, Pikal, 2002). The freezing stage is a very important stage of this process (Willemer, 1992) as the sublimation and the qualities of the finished product depend on this stage. Once frozen the structure and shape of the sample cannot be changed during the drying stages (Pikal, 1990). Primary drying involves the removal of the free moisture that has been frozen (Cameron, 1997) at a low temperature under reduced pressure. The main driving force for sublimation of water is the temperature difference of about 20 ºC between the product and the condenser (Franks, 1992). However, the products are not sufficiently dry for long term storage, having a residual moisture content of about 5 – 7 % (Ward *et al.*, 2008). The secondary drying stage involves desorption of bound moisture (Cameron, 1997, Arakawa *et al.*, 2001). At the end of the drying process, the sample is porous and retains its initial form, volume and original structure as well as its physical, chemical and biological properties. The sample beads were freeze-dried using an Edwards Mudolyo bench-top freeze dryer (West Sussex , UK) maintained at a temperature of – 40 º C and a pressure of 80 N m^{-2} for 24 h (Stops *et al.*, 2008).

2.3.4 High performance liquid chromatography (HPLC) techniques

Chromatographic separation was performed on a Shimadzu System equipped with a SPD-20 AV Prominence UV/VIS detector, an LC 20 AT pump, and SIL-20A Prominence autosampler. The data acquisition was carried out on a LC solution software integrator. The separation was performed using a SphereClone 5µm ODS (2) column (150 x 4.6 µm) (Phenomenex, UK). The HPLC software generated the data and this was analysed using Microsoft Excel 2007 to generate calibration curves and process the sample results.

2.3.4.1 HPLC methods

All chemicals used were of analytical grade; solvents were HPLC grade and were used as received without further treatment. HPLC grade water was used in the preparation of the mobile phases, while deionised water was used in the preparation of sample solutions. All samples were analysed immediately unless otherwise stated. The mobile phase was filtered and degassed by sonication (Fisher Scientific Ultrasonic bath FB15050). Calibration standards were prepared and run with each assay and the area under the curve (AUC) was integrated for each concentration. Calibration curves were determined by direct linear regression. Separation of the peaks of interest was observed for all the compounds tested and the total run time was below 10 minutes for all compounds of interest. Precision and linearity over the concentration range were assessed. Precision was calculated from the relative standard deviation (RSD) of the standard curve and linearity was assessed from the linear regression. All compounds were identified by comparison of retention times obtained from sample and standard solutions

2.3.4.2 Metronidazole assay

The mobile phase for MET comprised methanol – 50mM KH_2PO_4, pH 2.5 (40:60, vol/vol) and the pH was adjusted with phosphoric acid (Wu and Fassihi, 2005). The HPLC conditions are presented in Table 2-1.

Stock solutions of MET were prepared by dissolving 10 mg drug in 10 ml 0.1 M HCl and then made up to 50 ml with deionised water. Standards solutions were prepared in concentrations between 2 µg/ml and 100 µg/ml by diluting the stock solution with the mobile phase and were analysed in triplicate. Figure 2-2 shows a sample chromatogram, Figure 2-3 shows a typical calibration curve constructed from peak area against concentration and Table 2-2 shows the HPLC method validation for the assay.

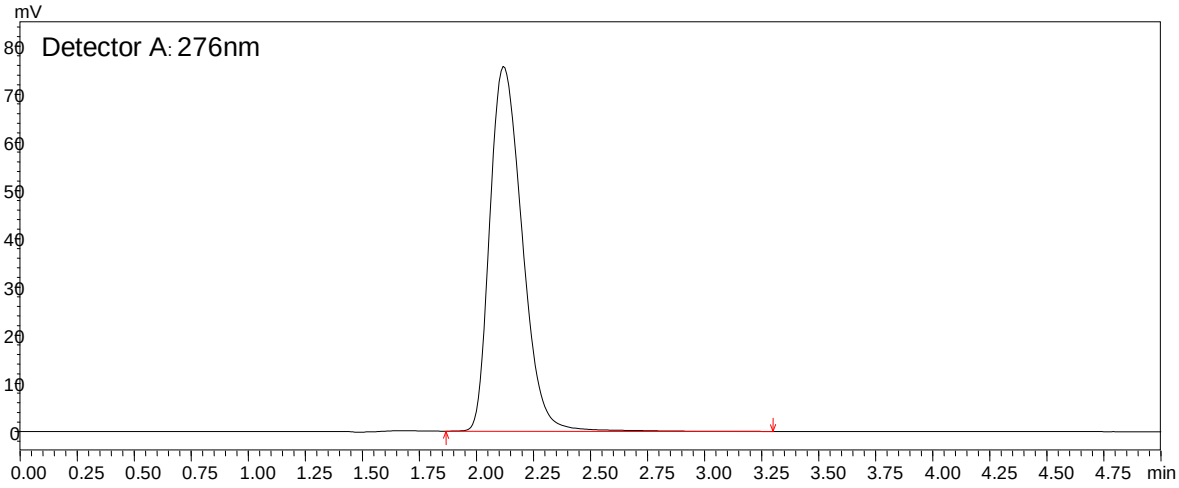

Figure 2-2: Typical chromatogram of MET at 276 nm

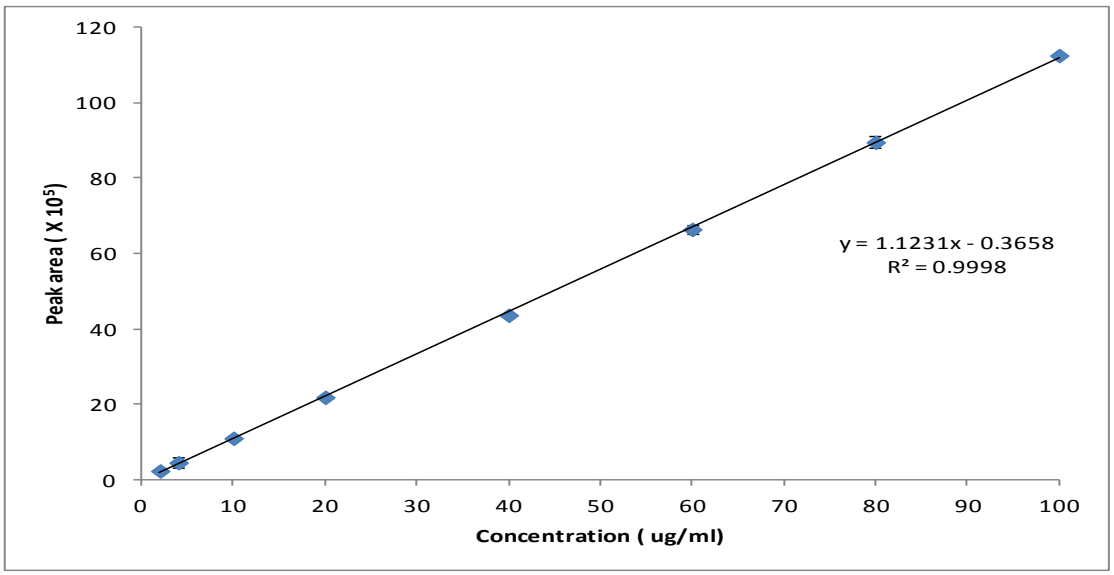

Figure 2-3: Calibration curve for MET HPLC assay at 276 nm

Table 2-1: HPLC conditions for MET assay

Injection volume	**10 µl**
Wavelength	276 nm
AUFS	0.01
Flow rate	1 ml/min
Run time	5 minutes

Table 2-2: HPLC method validation for MET assay

Theoretical plate	**1421**
Tailing factor	0.93
Retention time	2.1 minutes
LOD	0.62 ± 0.005 µg/ml
LOQ	1.90 ± 0.016 µg/ml
Precision and accuracy	RSD < 4 %

2.3.4.3 Clarithromycin assay

The mobile phase for CMN comprised 50 mM KH_2PO_4:ACN, pH 4.6 (50:50 v/v) containing 5 mM 1-Octanesulphonic acid (1-OCTS) and the pH was adjusted with phosphoric acid (Erah *et al.*, 1996). The HPLC conditions are presented in Table 2-3.

Stock solutions of CMN were prepared by dissolving 10 mg drug in 10 ml 0.1 M HCl and then made up to 50 ml with deionised water. Standards solutions of CMN were prepared in

concentrations between 10 µg/ml and 250 µg/ml by diluting the stock solution with the mobile phase and were analysed in triplicate. Figure 2-4 shows a sample chromatogram of CMN, Figure 2-5 shows a typical calibration curve constructed from peak area against concentration and Table 2-3 shows the HPLC method validation for the assay.

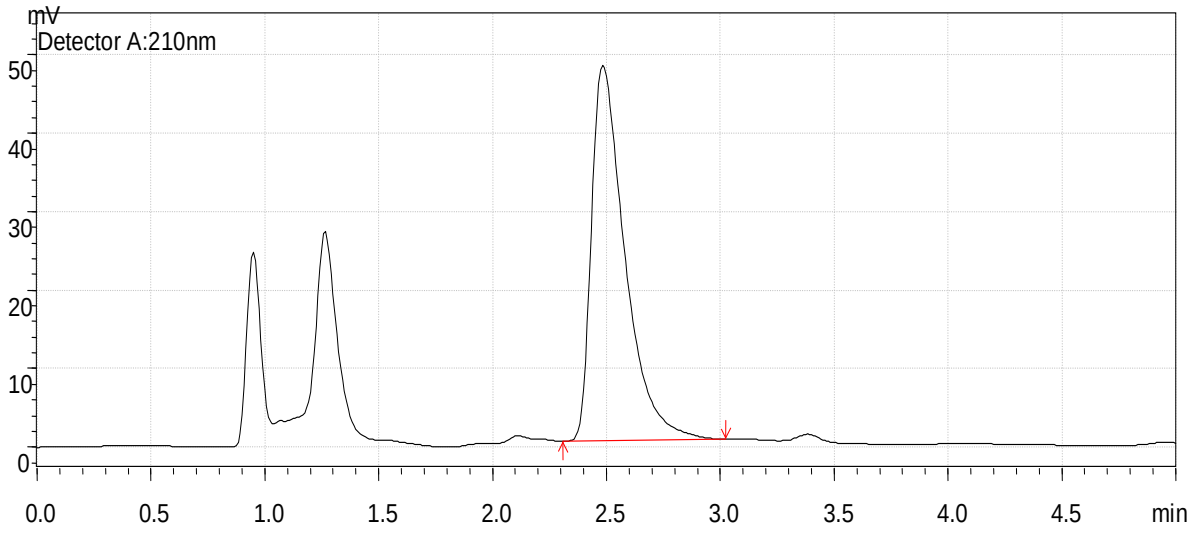

Figure 2-4: Typical chromatogram of CMN at 210 nm

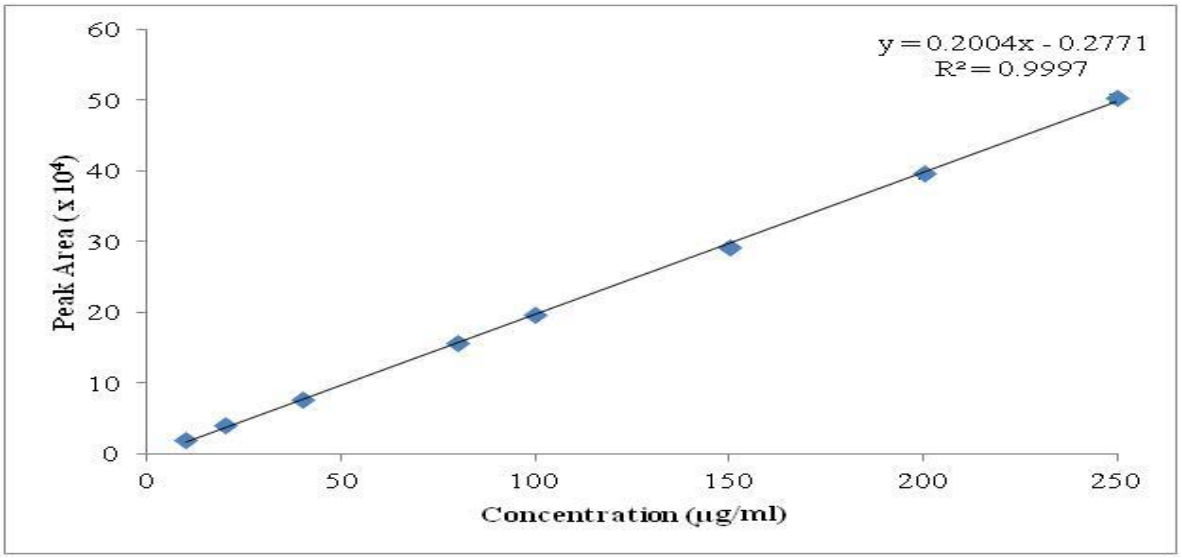

Figure 2-5: Typical calibration curve for CMN assay

Table 2-3: HPLC conditions for CMN assay

Temperature	**50 ºC**
Injection volume	50 µl
Wavelength	210 nm
AUFS	0.01
Flow rate	1.5 ml/min
Run time	5 minutes

Table 2-4: HPLC method validation for CMN assay

Theoretical plate	**1818**
Tailing factor	0.91
Retention time	2.52 minutes
LOD	1.85 ± 0.01 µg/ml
LOQ	5.63 ± 0.05 µg/ml
Precision and accuracy	RSD < 5 %

2.3.5 Drug content and drug entrapment efficiency (DEE)

The formulations (100 mg) were digested using PBS (phosphate buffered saline) (100 ml) under agitation at 37 ℃ over 24 h. The solution was filtered and assayed by HPLC and the parameters calculated using Equation 2-1 and Equation 2-2.

$$Drug\ content\ \left(\%\frac{w}{w}\right) = \frac{amount\ of\ drug\ in\ sample\ (mg)}{sample\ weight\ (mg)}\ x\ 100 \text{.....} \quad \text{Equation 2-1}$$

$$DEE\ (\%) = \frac{\%\ drug\ content}{\%\ theoretical\ drug\ content}\ x\ 100 \text{.....} \quad \text{Equation 2-2}$$

DEE describes the ability of the method of preparation to incorporate drug into the carrier system. High drug content with a minimum nominal drug loading is the aim, since this enhances the DEE. In addition, the quantity of drug entrapped determines the performance and lifetime of the DDS, since this influences the rate and extent of drug release. The drug content and DEE depend on the physicochemical properties and the interactions between the drug, carrier and the surrounding medium.

2.3.6 *In vitro* drug release studies

Unless stated otherwise, drug release from formulations was carried out in 0.1 N HCl (pH 1.2) or PBS (pH 7.4). Formulations equivalent to 100 mg drug were immersed in 900 ml media at 37 ± 1 °C under agitation at 100 rpm using the USP Type 1 (basket) dissolution apparatus (Pharmatest PTWS 610). Aliquots of 5 ml sample media were withdrawn at predetermined time intervals and replaced with fresh, warm dissolution media of equal volume. Samples were analysed by HPLC (see section 2.3). The times for 25 %, 50 %, 75 % drug release from the formulation were recorded and denoted as $t_{25\%}$, $t_{50\%}$ and $t_{75\%}$ respectively and were averages of 3 determinations.

2.3.7 *In vitro* drug release kinetics

In order to describe the drug release kinetics, various mathematical equations were used. Zero order kinetics (Equation 2-3) result from systems where the drug release rate is independent of its concentration (Najib and Suleiman, 1985). First order kinetics (Equation 2-4) describe release from systems where release rate is concentration dependent (Desai *et al.*, 1966). Higuchi described the drug release from insoluble swellable matrices being dependent on the square root of time based on Fickian diffusion (Higuchi, 1963) (Equation 2-5). The Hixson – Crowell cube root law (Equation 2-6) represents release from systems where there is a change

in surface area and diameter of the particles or tablets characterised by polymer erosion and dissolution (Hixson and Crowell, 1931, Abdou, 1989).

$$Q_t = k_0 t \quad \text{..... Equation 2-3}$$

$$ln\ Q_t = ln\ Q_0 - k_1 . t \quad \text{..... Equation 2-4}$$

$$Q_t = K . S \sqrt{t} = k_H . \sqrt{t} \quad \text{..... Equation 2-5}$$

$$\sqrt[3]{Q_0} - \sqrt[3]{Q_t} = k_{HC} . t \quad \text{..... Equation 2-6}$$

where, Q_t is the amount of drug released in time t, Q_0 is the initial amount of the drug in tablet, S is the surface area of the tablet, and k_0, k_1, k_H and $k_{HC,}$ are release rate constants for zero order, first order, Higuchi and Hixson-Crowell respectively.

2.3.8 *In vitro* drug release mechanisms

The Korsmeyer – Peppas model (Equation 2-7) was derived to describe drug release from a polymeric system to distinguish between competing release mechanisms: Fickian release (diffusion-controlled release), non-Fickian release (anomalous transport), and case-II transport (relaxation-controlled release). For spheres, a value of $n \leq 0.43$ indicates the Fickian release. Fickian diffusion indicates a gradient – dependent drug release. The n value between 0.43 and 0.85 is an indication of non-Fickian release, which indicates a dual mode of drug release with diffusion controlled, and swelling controlled drug release. When, $n \geq 0.85$, it is case-II transport and this involves polymer dissolution and polymeric chain enlargement or relaxation during gel swelling (Siepmann and Peppas, 2001, Ritger and Peppas, 1987). In order to investigate the release mechanism, drug release data up to 60 % were fitted to Equation 2-7:

$$F = K_P \,.\, tn$$ ..... Equation 2-7

where, F is the fraction of drug released in time t, with K_P being the release rate constant and and *n* is the release exponent indicative of the drug release mechanism.

2.3.9 Dissolution profile comparison using similarity factor, f_2

A model independent mathematical approach was proposed in 1996 (Moore and Flanner, 1996) to compare the dissolution profiles using the factor, f_2 for modified release dosage forms. f_2 can be defined as the logarithmic reciprocal square root transformation of one plus the mean squared (the average sum of squares) differences of drug percent dissolved between the test and the reference products (Murtaza *et al*., 2009) as expressed in Equation 2-8.

$$f_2 = 50 \log\left[\left(1 + \frac{1}{n}\sum_{n-1}^{n}(R_t - T_t)^{\,2}\right)^{-0.5} * 100\right]$$

..... Equation 2-8

where, f_2 is similarity factor, n is the number of sampling time , R_t is average percentage drug dissolved from reference formulation and T_t is average percentage drug dissolved from test formulation. Generally, an average of twelve observations is used for calculating f_2 and it is inversely proportional to the average squared difference between the two profiles, with the emphasis on the larger difference among all the time points. f_2 measures the closeness between the two dissolution profiles and to have a measure of which is more sensitive to large differences at any particular time point. When the two profiles are identical, f_2 = 100. An average difference of 10 % at all measured time points result in f_2 value of 50. A standard f_2 value of 50 – 100 indicates a similarity between two dissolution profiles (Costa and Lobo, 2001).

2.3.10 *In vitro* drug release in mucin suspension

In order for release studies to better reflect the environment in the stomach, *in vitro* diffusion of formulations through a 3 % pig gastric mucin (PGM) solution at pH 2 and pH 5 was studied using vertical Franz diffusion cells (effective diffusion surface area = 2.77 cm^2) (Figure 2-6). The receptor compartment was filled with previously degassed 30 ml buffer, maintained at 37 °C using a circulating water jacket and agitated by stirring with a magnetic stirrer. Dialysis membrane (cut off MW 14,000) was mounted between the donor and receiver cells with the mucin dispersion representing an unstirred layer of mucus gel layer and 1 ml of receptor fluid was sampled, replaced and analysed by HPLC. All experiments were performed in triplicate.

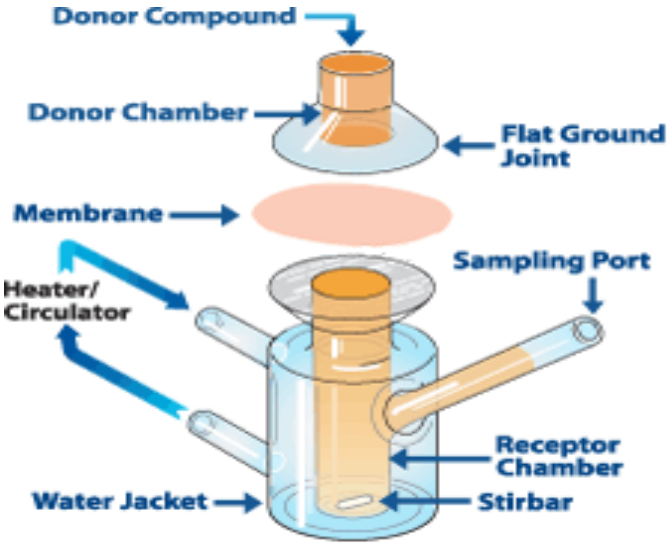

Figure 2-6: Franz diffusion cell

2.3.11 Particle sizing / weight

Unless stated otherwise, the particle sizes (*n*=50) of triplicate batches of beads were determined using an electronic digital calliper (Linear tools-49-923-150) (Murata *et al.*, 2000). The mean diameters and standard deviations were recorded. The weight of a sample of beads (*n=100*) was determined in triplicate. The particle sizes of microspheres were determined using Mastersizer 2000 (Malvern Mastersizer, UK). Approximately, 10 – 20 mg microspheres were dispersed in water into the Hydro SM unit containing a surfactant and the volume mean diameter were determined by Malvern software.

2.3.12 Density measurements and porosity

To estimate the bulk density (P_b) (Bai and Li, 2006), the weight of the volumetric flask was initially measured (W_1), the beads were dried and filled to the 10 ml mark of the volumetric flask and weighed (W_2). The P_b of the beads was calculated using equation 2-9:

$$P_b = \frac{W_2 - W_1}{10} \quad \text{..... Equation 2-9}$$

where, W_2 is the total weight of the porous beads and the flask, and W_1 is the weight of the flask only. The true densities (P_t) of the beads were determined using a helium pycnometer (Quantachrome multipycnometer (Model MVP-D160-E)) with a 5 cm^3 micro sample cup. The porosity *P* of the beads was determined using equation 2-10:

$$P = 1 - \frac{P_b}{P_t} \quad \text{..... Equation 2-10}$$

(Gal and Nussinovitch, 2007, Smrdel *et al*., 2008b)

2.3.13 Determination of calcium content of alginate beads by atomic absorption spectroscopy (AAS)

Atomic spectroscopy is one of the most common methods for quantitative elemental analysis to determine the presence of metals such as Fe, Cu, Al, Pb, Ca, in liquid samples. An aqueous solution of sample is vaporised and decomposed into gaseous free atoms in a flame or furnace. The concentrations of atoms present in the sample are measured because metals, in their elemental form, will absorb UV light when they are excited by heat. The sample solution is aspirated into the flame. If that metal is present in the sample, it will absorb some of the light, thereby reducing its intensity. The instrument measures the change in intensity, which is then converted into absorbance.

A stock solution of calcium was prepared by dissolving 2.5 g of dry calcium carbonate ($CaCO_3$) in a small volume of deionised water. A small volume of concentrated HNO_3 was added to dissolve the $CaCO_3$ and deionised water used to make up 1000 ml volume. Standard solutions of calcium concentrations ranging from 1 to 5 ppm were prepared by diluting the stock with deionised water and were analysed in triplicate for Ca^{2+} ion at 422.7 nm. Figure 2-7 shows a typical calibration curve constructed from the absorbance against concentration and Table 2-5 shows the assay validation parameters.

The amount of calcium that cross-linked with the polymer during gelation was determined by dissolving 100 mg of the beads in 10 ml concentrated HNO_3 by heating at 50 °C (El-Kamel *et al*., 2003). Upon dissolution, the samples were diluted and analysed for Ca^{2+} ion at 422.7 nm AAS (Perkin Elmer AAnalyst 100).

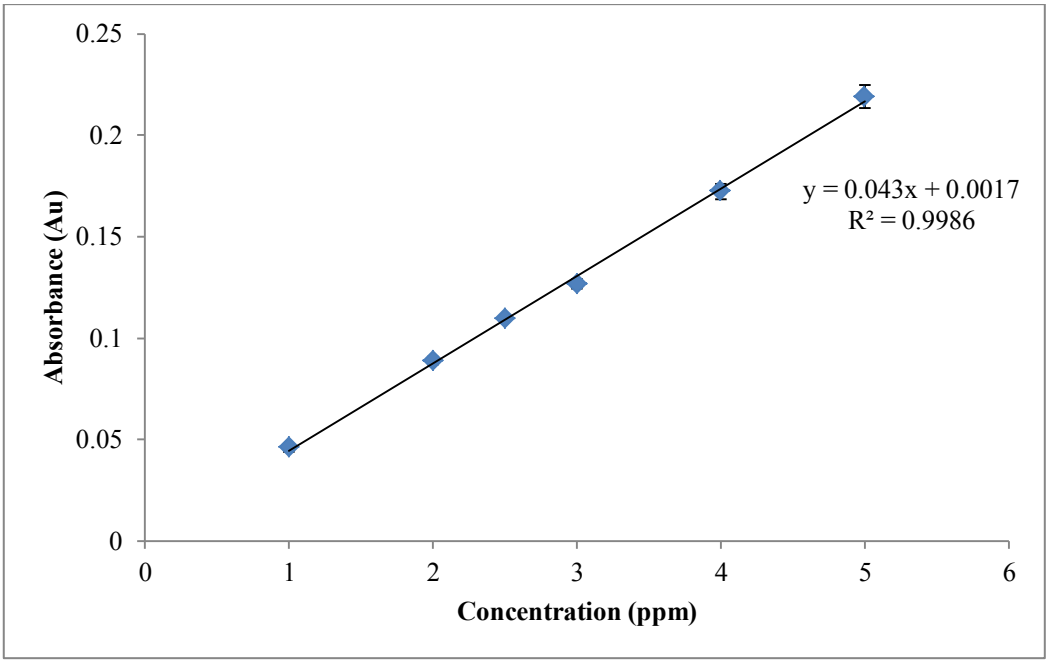

Figure 2-7: Calibration curve of calcium measured at 422.7 nm

Table 2-5: UV method validation for calcium ion assay

Wavelength	**422.7 nm**
Correlation coefficient (R^2)	0.99
LOD	0.39 ± 0.04 ppm
LOQ	1.18 ± 0.13 ppm
Precision and accuracy	RSD < 4 %

2.3.14 Determination of loose surface crystals

The determination of the loose surface crystals (LSC) was to estimate the actual drug amount present in the beads rather than on the surface of the beads. The drug present on the surface should show immediate release into the dissolution medium. 100 mg beads were suspended in 100 ml of phosphate buffer (pH 7.4) simulating the dissolution medium. The samples were shaken vigorously for 5 minutes in a mechanical shaker. The amount of drug that leached out was assayed and the percentage of drug released relative to the entrapped drug in each sample was recorded (Rastogi *et al*., 2007).

2.3.15 X-ray microtomography (XμMT)

Three-dimensional structures of formulations were obtained using X-ray microtomography (Nikon XTH225 X-Ray Microtomography) in order to obtain an insight into the surface and internal structure of the beads. This presents a non-destructive technique of assessing the structure of formulations, has high penetration ability and provides a reasonable level of resolution (5 - 20 μm). X-ray beams are directed from a high-power source toward a sample, and a detector on the opposite side of the sample measures the intensity of these transmitted X-rays. A two-dimensional "shadow" image is generated by accurately rastering the X-ray beam across the sample. The sample is carefully rotated relative to the X-ray beam and the process is repeated to produce additional two-dimensional images from different viewpoints. Using a sophisticated Fourier transform algorithm, these two-dimensional images are then combined to generate a complete three-dimensional image of the sample (Hancock and Mullarney, 2005).

2.3.16 Scanning electron microscopy (SEM)

The surface morphology of the formulations were examined using SEM. Samples were mounted on aluminium stubs using double sided carbon tape attached to a stub and coated with a gold film under vacuum in a sputter coater through the use of an Emscope SC 500 (Emscope, UK). The study was carried out under magnification with a Stereoscan 90 Scanning Electron Microscope (Cambridge, UK).

2.3.17 Determination of moisture content

Thermogravimetric analysis (TGA) is a simple and easy method that can also be used to determine the moisture content of polymers and formulations. In addition, it can give information about the threshold decomposition temperature upon heating which is important to determine the highest processing and handling temperature that can be used (Mano *et al.*, 2003). The TGA was allowed to equilibrate for 10 minutes before analysis and samples (5 - 6 mg) were heated from 25 ℃ to 200 ℃ at a heating rate of 10 ℃/min using a Perkin Elmer Thermo-gravimetric Analyzer (Perkin Elmer, Germany). All TGA runs were performed in an open previously tarred crucible with purge and protective N_2 gas flow of 20 ml/min. The moisture content was determined as the loss of mass resulting from loss of water between 50 to 150 ℃ (Nassar *et al.*, 2003, Mai *et al.*, 2012).

2.3.18 Differential scanning calorimetry (DSC)

DSC measures the energy required to produce a near zero temperature difference, between two materials (sample and reference materials), when they are both exposed to similar temperatures. The difference in heat input between both the sample and the reference material, per unit time, is measured and this is plotted as a curve of heat flux, $\Delta H/dt$, *versus*

the average sample temperature (or time), to which the sample and reference were raised. This difference is compensated for by the system, which regulates the power output to the heaters and supplies different amounts of heat to each specimen in order to maintain both at the same temperature.

Thermal analysis of the formulations was carried out using DSC-1 Mettler Toledo (Mettler-Toledo, Switzerland) calibrated with an indium standard. Approximately 5-10 mg of the beads / microspheres were weighed and sealed in standard aluminium pans. The samples were held at 25 ℃ for 1 min and heated from 25 ℃ to 300 ℃ at a rate of 10 ℃ / min under N_2 atmosphere equipped with an intra-cooler. A similar empty aluminium pan sealed in the same way was used as a reference sample. The characteristic endothermic peaks and the melting points of the samples were recorded. In order to characterise the physical status of the drug in the beads, thermograms of the drug, blank formulation, drug loaded formulations and the physical mixture of the components were obtained.

2.3.19 Determination of *in vitro* buoyancy lag time and duration

Lag times until the onset of floating were determined by placing a sample of the formulation (normally beads) in a beaker containing 100 ml of 0.1N HCl, pH 1.2 (unless stated otherwise), 0.02 %w/v Tween 20 maintained at 37 ± 1 ℃. The time taken by the sample to float on the surface was determined and the sample was considered to have passed the test if the lag time was ≤ 2 min (Ishak *et al.*, 2007). The buoyancy properties of the formulations were determined by placing a sample of the formulation in a container to which 100 ml of 0.1N HCl containing 0.02 %w/v Tween 20 had been added. The container was stoppered and agitated at 100 rpm for 24 hours in a water bath shaker maintained at 37 ± 1 ℃. The duration of floating of the beads and the percentage of floating sample were recorded. The sample was considered to be buoyant only when all formulation (*e.g.* beads) floated on the test solution

for the prescribed period (Tang *et al.*, 2007). The experiment was conducted in triplicate for each batch.

2.3.20 Swelling studies

The extent of swelling was measured in terms of % weight gain of the beads. 100 mg beads from each batch of the formulation was weighed formulations and immersed in 300 ml of 0.1N HCl or PBS and at fixed time intervals the formulations were removed from the media. Upon removal from the media, the sample were dried with filter paper to remove the excess liquid drops adhering to the surface and weighed. The dynamic weight change of the sample was calculated using Equation 2-11:

$$Weight\ change\ (\%) = \frac{W_s - W_i}{W_i}\ X\ 100 \quad \text{..... Equation 2-11}$$

where, W_s is the weight of sample in the swollen state and W_i is the initial weight of the beads (Pasparakis and Bouropoulos, 2006).

2.3.21 Powder X-ray diffraction analysis (P-XRD)

The effect of encapsulation on the crystallinity of the drug in the formulations was assessed by P-XRD. X-ray diffractograms of drug, polymers, blank formulations and drug loaded formulations were recorded with a Bruker diffractometer (Bruker D2 Phase, UK). Powdered samples were placed in a stainless steel holder and the surface of powder was levelled manually to create a flat surface for analysis. The sample was exposed to X-ray radiation (Cu

Kα) with a wavelength of 1.5406 Å. Samples were scanned between 5 and 40 of 2θ with a step size of 0.019° and a step time of 32.5 s. X-rays are generated when a focused electron beam accelerated across a high voltage field in a sealed vacuum bombards a solid anode target whether stationary or rotating. As the electrons collide with atoms in the target and slow down, a continuous stream of X-rays are emitted. Commonly used targets in X-ray tubes include Cu, Cr, Fe, Co and Mo, which emits 8 keV and 14 keV X-rays with wavelengths of 1.54 Å and 0.8 Å, respectively. In diffraction applications, only short wavelength X-rays up to a maximum of 0.1 Å are used. The peaks in an X-ray diffraction pattern are directly related to the atomic distances. The X-ray diffractometer measures powders and thin films in the two theta (2θ) configuration.

2.3.22 Fourier transform infrared (FT-IR) spectroscopy

Infrared (IR) spectroscopy measures the infrared intensity against the wave number of light. Traditional IR spectroscopy analyses samples by means of transmitting the IR beam directly through the sample; however, Attenuated total reflectance (ATR) uses the reflectance of the sample instead. FTIR-ATR is FTIR spectroscopy that involves the use of a sampling technique that enables samples to be examined without any further preparation *e.g.* diluting with an IR transparent salt such as potassium bromide. The main benefit of ATR sampling is the very thin sampling path length and depth of penetration of the IR beam into the sample. The IR radiation passes through an IR transmitting crystal *e.g.* diamond, germanium or zinc selenide with a relatively high refractive index, allowing the radiation to reflect within the ATR element several times. The surface of the sample is in intimate optical contact with the top surface of the crystal and the IR radiation passes into and reflects through the crystal and penetrates the sample with each reflection along the top surface, through the top surface *via* "evanescent" wave that protrudes the sample (0.5 – 5 µm). Some of the energy of the

evanescent wave is absorbed by the sample and the reflected radiation is returned to the detector. Different crystals have different refractive indices depending on the material used and are applied to different transmission ranges (ZnSe for 20,000 - 650 cm^{-1}, Ge for 5,500 - 800 cm^{-1}). The samples were scanned from 400 - 4000 cm^{-1} at ambient temperature using a Thermo Nicolet 380 FTIR with Diamond ATR. The characteristic peaks of IR transmission spectra were recorded in triplicate.

2.3.23 Determination of surface charge

Suspensions of the formulations (2 %w/v) in 0.1N HCl (pH 2.0) and PBS (pH 7.4) were sonicated for 12 h and injected into the capillary cell to determine the zeta potential (Z_p) using Zetasizer Nano Z (Malvern Instruments Ltd., UK). Each sample was analysed at least six times to obtain an average value and a SD.

2.3.24 Mucoadhesion studies

2.3.24.1 Preparation of pig gastric mucosa segments

Pig stomachs were obtained fresh from a local abattoir in Huddersfield and emptied of its contents followed by washing with distilled water. The required porcine mucosa was separated from the underlying muscle. The gastric mucosa was cut into strips of 5 cm long by 3 cm wide. These were washed with non-ionic isotonic solution of 0.25 M sucrose solution and flash-frozen in liquid nitrogen and stored at – 20 °C to maintain cell integrity. When required, the tissues were defrosted overnight in sucrose solution. Freezing the tissue minimises tissue damage and the effects of bacterial and enzymatic degradation (Young and Smart, 1998, Riley *et al.*, 2002). Pig is considered to be a suitable animal model because it

resembles humans more than any other non-primate animal species with regard to the eating behaviour, anatomy, and physiology of the gastrointestinal tract (Davis *et al.*, 2001).

2.3.24.2 *Ex vivo* wash off mucoadhesion tests

2.3.24.2.1 Humidity cabinet

A 5 cm long and 3 cm wide piece of porcine gastric mucosa was mounted onto a Perspex mounting block using cyanoacrylate glue. The samples were spread evenly onto the wet surface of the tissue specimen, and allowed to equilibrate for ~ 20 minutes in an adapted humidity cabinet at high humidity (> 90 % RH) to facilitate the interaction between the sample and the mucosa (Figure 2-8). The slide was positioned at an angle of 30 ° (mimicking the inclination angles in the antrum) and maintained at 37 ± 1°C. HCl (0.1 N, pH 2.0) and PBS (pH 7.4) as appropriate previously warmed to 37 °C were circulated over the tissue at a rate of 1 ml/min (mimicking the flow of gastric contents) supplied *via* a peristaltic pump (Watson Marlow model 202) for 12 h. The flow was split into three channels to provide an even distribution of the media over the entire tissue section. The material washed from the surface of the tissue was collected at various time intervals. The beads remaining on the tissue surface after each hour were counted and the percentage of the remaining beads was calculated using Equation 2-12:

$$\%\ Mucoadhesion = \frac{N_0 - N_i}{N_0} \quad \text{.....Equation 2-12}$$

where, N_0= number of beads applied initially and N_i = number of beads rinsed from the tissue.

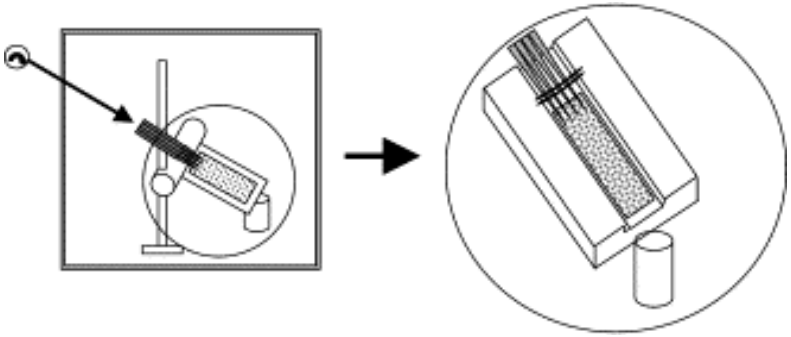

Figure 2-8: Schematic representation of the *ex vivo* mucoadhesion tests

Adapted from (Batchelor *et al*., 2002) (Used with permission)

2.3.24.2.2 Disintegration apparatus

The mucoadhesivity of the drug-loaded beads was also assessed by another wash-off method. Freshly excised pieces of pig gastric mucosa were mounted on a glass slide with cyanoacrylate glue. 20 beads were spread out on each piece of mucosa and brought into direct contact with the mucus layer of the stomach tissues using a weight of 25 g on the glass-slide for 2 minutes and allowed to equilibrate for ~ 20 minutes. The slide was then hung onto the arm of a tablet disintegration apparatus. The tissue specimen was given agitated vertically in a 1L vessel containing either HCl (0.1 N, pH 2.0) or PBS (pH 7.4) medium maintained at 37 °C. The beads remaining adhered to underlying mucosa were counted up to 6 hours. The percentage mucoadhesion was calculated using the equation 2-12.

2.3.24.3 *In vitro* interactions with pig gastric mucin (Type III)

The binding capacity of formulations with PGM was determined by mixing 10 ml (1 mg/ml) of PGM suspension in PBS (pH 7.4) with equal volumes of the sample suspension. After incubation at different time intervals at room temperature and at 37 ℃, the samples were centrifuged at 10,000 rpm for 10 min. The amount of bound mucin was determined by UV spectroscopy at 251 nm (Agilent Cary 60 UV-Vis Spectrophotometer). The PGM binding efficiency of the samples was calculated using Equation 2-13:

$$Bound\ PGM\ (\%) = \frac{C_0 - C_s}{C_0}\ X\ 100 \quad \text{..... Equation 2-13}$$

where, Co is the initial concentration of the PGM used for incubation and Cs is the concentration of free PGM in the supernatant. The reference consisted of the same amount of PGM present in the samples (Yin *et al.*, 2006).

2.3.25 Concanavalin A assay

2.3.25.1 Folin- ciocalteu method

This assay is based on two reactions; the first reaction involves the formation of a copper ion complex ("Biuret" chromophore) with the Con A amide bonds in alkaline solutions due to the reduction of Cu^{2+} to Cu^{+}. The second reaction involves the reduction of Folin-Ciocalteu reagent (phosphomolybdate and phosphotungstate) by tyrosine and tryptophan residues of Con A. This reduced Folin-Ciocalteu reagent is blue in colour and thus detectable at a UV of 750 nm (Lowry *et al.*, 1951). The reagents used include ‘Reagent A’ (2 g Na_2CO_3 in 100 ml of 0.1N NaOH); ‘Reagent B’ (0.5 g of $CuSO_4$. $5H_2O$ in 100 ml, 1 % sodium/potassium

tartrate); 'Reagent C' (50 ml of Reagent A with 1 ml of Reagent B) and 'Reagent D' (1:1 dilution of Folin – Ciocalteu phenol reagent with water). 10 ml of Reagent C was added to standard solutions of Con A, mixed thoroughly and allowed to stand for 30 minutes. 1 ml of Reagent D was added and mixed rapidly. After 30 minutes, the solution was filtered and absorbance was measured against a blank (without lectin) using a UV-Vis spectrophotometer at 750 nm (Jain and Jangdey, 2009). Figure 2-9 shows a typical calibration curve constructed from absorbance intensity against concentration and Table 2-6 shows the method validation parameters.

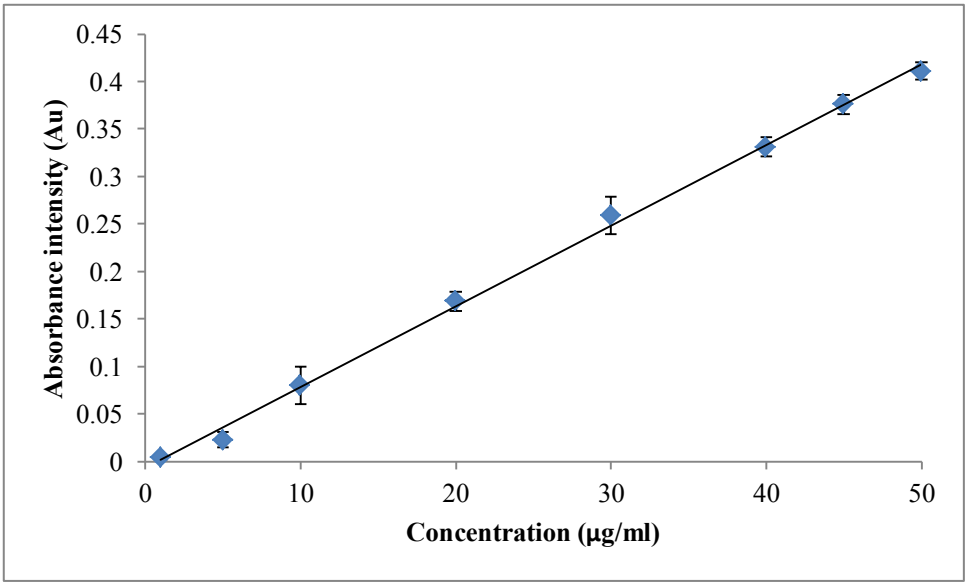

Figure 2-9: Calibration curve of Con A

Table 2-6: Spectrophotometric method validation for Con A assay

Wavelength	**750 nm**
Slope	0.0085
Intercept	0.0069
Correlation coefficient (R^2)	0.99
LOD	0.59 ± 0.02
LOQ	1.77 ± 0.09
Precision and accuracy	RSD < 3 %

2.3.25.2 Fluorescence spectroscopy

Fluorescence spectroscopy measures the intensity of photons emitted from a sample at a wavelength after it has absorbed photons at another wavelength. It involves the use of a light beam, which excites the electrons in molecules of some compounds and causes them to emit light but not necessarily, visible light. The emission occurs from the ground vibrational level of the excited electronic state and transits to an excited vibrational state of the ground electronic state. Therefore, fluorescence signals are observed at longer wavelengths than absorbance. Information about the structure and the environment of the fluorophores can be obtained from the energies and the relative intensities of the fluorescence signals. Fluorophores exhibit specific excitation (absorption) and emission (fluorescence) wavelengths. Both wavelengths are determined *via* the collection of two spectra, an excitation spectrum and an emission spectrum. The fluorescence emission spectrum is normally recorded when the excitation wavelength is held constant and the emission beam is scanned as a function of wavelength (λex). However, the excitation spectrum is recorded as a function

of wavelength, when the emission is held at a constant wavelength (λem). Although the approximate excitation and emission wavelengths for many molecules are solutions known, these wavelengths should be optimized for the specific experimental conditions. Once these wavelengths have been determined, the fluorescence intensity of standard solutions as a function of concentration is determined and constructed into a calibration curve. FITC Con A has an excitation and emission spectrum peak wavelengths of approximately 493 nm and 516 nm, respectively. All determinations were subsequently carried out at these wavelengths. A stock solution of FITC Con A was prepared in phosphate buffer (pH 5.8) and this was used to prepare standard solutions of concentrations ranging from 1 to 50 µg/ml FITC Con A. Figure 2-10 shows a typical calibration curve constructed from fluorescence intensity against concentration and Table 2-7 shows the method validation parameters.

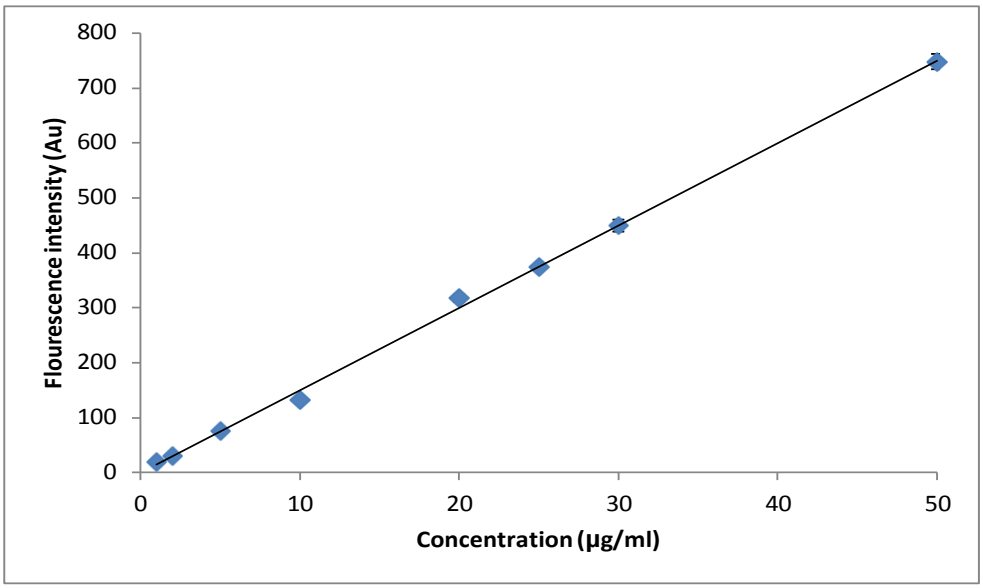

Figure 2-10: Calibration curve of FITC Con- A in phosphate buffer (pH 5.8)

Table 2-7: Spectrophotometric method validation for FITC Con A assay

Wavelength	**Excitation λ = 493 nm** **Emission λ = 516 nm**
Slope	15.01
Intercept	0.07
Correlation coefficient (R^2)	0.99
LOD	0.37 ± 0.003 µg/ml
LOQ	1.15 ± 0.01 µg/ml
Precision and accuracy	RSD < 3 %

2.3.26 Nanoparticle tracking analysis (NTA)

The interaction between PGM and a mucoadhesive polymer was assessed using Nanosight LM 10 (Figure 2-11) and NTA 2.2 analytical software (Nanosight, UK). This equipment uses the principles of nanoparticle tracking analysis (NTA). NTA uses the properties of both light scattering and brownian motion to obtain particle size distributions of samples in a liquid suspension (Carr and Wright, 2013). It offers the ability to directly visualize size and count nanoparticles (Figure 2-12); and is ideally suited for the real time analysis of polydisperse systems ranging from 10 - 20 nm up to 1 - 2 µm in size. A laser beam is passed through a prism edged flat glass within the sample chamber into the sample suspension. The angle of incidence and refractive index of the glass is designed so that the laser beam emerges from the interface between the glass and the sample above it. This beam refracts to an intense low profile resulting in a compressed beam with a reduced profile and a high power density. The nanoparticles in suspension in the path of this beam then scatters the light in such a way that they can easily be visualized through a long working distance with a x 20 magnification

microscope objective fitted to a conventional microscope and a highly sensitive camera which operates at 30 frames/second. The camera captures a video file (typically 30 - 60 seconds duration) of particles moving under brownian motion within a field of view of approximately 100 µm x 80 µm x 10 µm. The NTA software simultaneously identifies and tracks the centre of each particle on a frame-by-frame basis. The software then determines the average distance moved by each particle in the x and y directions. This value allows the particle diffusion coefficient (Dt) to be determined and from which if the sample temperature T and solvent viscosity are known, the sphere – equivalent hydrodynamic diameter, *d*, of the particle can be identified using the Stokes-Einstein equation (Equation 2-14):

$$Dt = \frac{TKB}{3\Pi\eta d} \text{.....Equation 2-14}$$

Figure 2-11: Nanosight LM -10

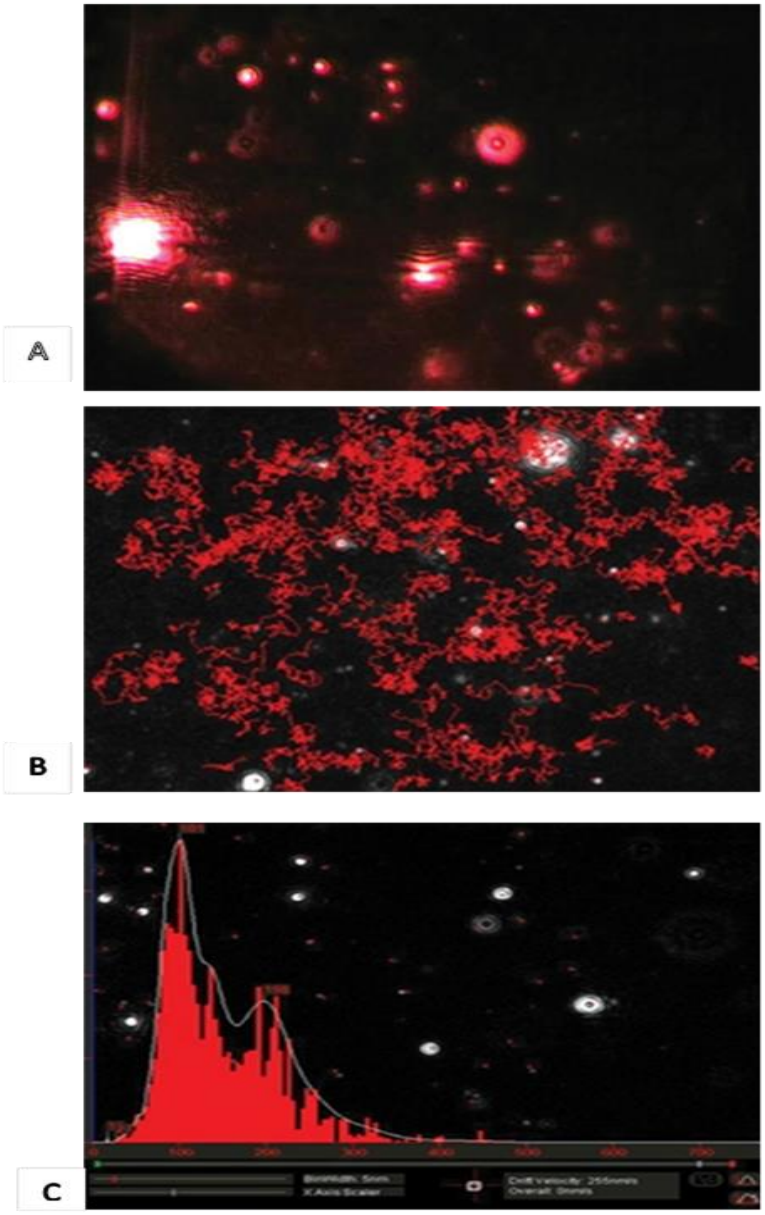

Figure 2-12: A) The sample nanoparticles illuminated by the laser beam; B) Tracks of Individual particles and C) The particle size distribution of the sample

(Philippidis, 2013).

Chapter 3 ALGINATE BEADS: PREPARATION, OPTIMISATION AND CHARACTERISATION

3.1 Chapter overview

Drug encapsulation in alginate beads is an easy, cheap, safe and non-destructive method of drug encapsulation therefore does not require any specialist equipment or solvents. The complexation of the polyguluronic sequences (G block) of alginate by Ca^{2+} ions results in the formation of a three-dimensional network usually described by the ‘egg box’ junction (Grant *et al.*, 1973, Park and Sharaby, 1993), giving rise to formation of calcium alginate hydrogels. The buckled chain of the guluronic acid units is a two-dimensional analogue of a corrugated egg-box (Figure 1-10), with interstices in which the calcium ions may pack and be coordinated (McHugh, 1987). "The analogy is that the strength and selectivity of co-operative binding is determined by the comfort with which 'eggs' of a particular size may pack in the 'box', and with which the layers of the box pack with each other around the eggs". The divalent cations bind to the α-guluronic acid blocks in a highly cooperative manner and the size of the cooperative unit is < 20 monomers (Smidsrod and Skjak-Braek, 1990). It has been suggested that the MG blocks also contributes to the junction zone in addition to the G block (Donati *et al.*, 2005) in the presence of excess cations.

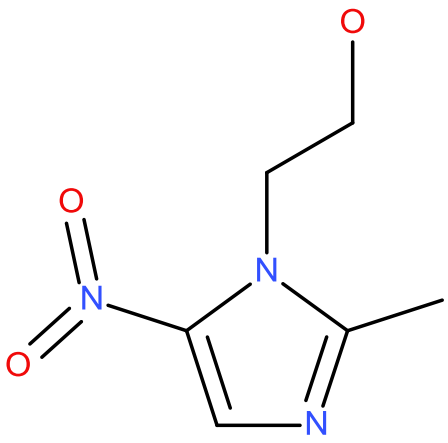

Figure 3-1: Structure of metronidazole

Metronidazole (MET) (Figure 3-1) is a synthetic nitro-imidazole antimicrobial drug, also known as 2-methyl-5-nitroimidazole-1-ethanol. Nitro-imidazoles are a group of antibiotics initially introduced in 1957 and they are imidazole heterocycles with a nitro group that is used to fight anaerobic bacterial and parasitic infections. Other drugs in this class of drugs include secnidazole, tinidazole and nimorazole. MET occurs as white to pale-yellow crystals or a crystalline powder with an average melting point of 160 °C (Reynolds, 1993) and is slightly soluble in water (Bempong *et al.*, 2005). It has been widely used to prevent the recurrence of peptic ulcer disease, a phenomenon that is typical of *H. pylori* infection (Sorberg *et al.*, 1998). The mechanism of action of MET is mediated by its reduced metabolites, where the nitro moiety of MET (RNO_2) is reduced to a radical anion (RNO_2^-) and possibly nitroso (RNO) and hydroxylamine derivatives (RNHOH) (Lindmark and Muller, 1976, Moreno *et al.*, 1983, El-Gibaly, 2002).

$$RNO_2 \Longrightarrow RNO_2^{\cdot -} \Longrightarrow RNO \Longrightarrow RNHOH$$

These reduction products have been demonstrated to cause DNA damage resulting in cell death (Lindmark and Muller, 1976, El-Kamel *et al*., 2001). MET diffuses into cells (Eltom *et al*., 1984), but due to its low redox potential (486 mV) (Alvarez-Elcoro and Enzler, 1999), formation of reduced metabolites is limited to cells with electron donors (anaerobic cells) with a good low redox potential and a suitable intracellular redox potential (Eltom *et al*., 1984). The on-going reduction of MET maintains a favourable concentration gradient of drug facilitating further diffusion into the cell (El-Gibaly, 2002). MET is rapidly and completely absorbed from the GI tract with 100 % oral bioavailability (Ralph, 1983, Dupuy *et al*., 1994). Following administration, t_{max} is 1 to 2 h, and C_{max} is 25 mg/ml. Oral bioavailability is not affected by food, but peak serum levels will be delayed to 2 h. MET has limited plasma protein binding (< 20 %), but is well distributed in most tissues and body fluids (Schwartz *et al.*, 1979, Sattar *et al.*, 1982, Nagar *et al.*, 1989). It diffuses across the blood-brain barrier, crosses the placenta and appears in the saliva and breast milk of nursing mothers in concentrations equivalent to those found in the plasma. It is extensively metabolised by the liver to form two primary oxidative metabolites - the hydroxyl and acetic acid metabolites. It is eliminated *via* urine (60 – 80 %) and faeces (6 -15 %). The half-life is 8 h in healthy adults and the hydroxyl-metabolites half-life is 15 h. The kidney eliminates a small fraction of the parent drug and the removal of the metabolites from the body depends on kidney function (Davey, 1991).

In this chapter, alginate beads were prepared using the ionotropic gelation method with calcium chloride ($CaCl_2$) as the gelation agent. Various concentrations of both sodium alginate (SAL) and $CaCl_2$ were used in order to determine the ideal concentrations to be used in formulations. MET was entrapped in the beads and the efficiency of the formulation as a gastro-retentive DDS was assessed.

3.2 Materials and methods

Sodium alginate (SAL) (Molecular weight 120,000 - 190,000 g/mol), calcium chloride dihydrate ($CaCl_2.2H_20$), MET, phosphate buffered saline (PBS) HCl, methanol, potassium dihydrogen phosphate (KH_2PO_4), phosphoric acid were obtained from Sigma Aldrich (UK). Liquid nitrogen (N_2) was obtained from BOC (UK).

3.2.1 Preformulation studies

3.2.1.1 Hydrolysis of sodium alginate

10 g SAL (M:G ratio - 1.56) was suspended in 500 ml HCl (0.3 M) and maintained at a temperature of 100 °C in a water bath for 5 h to ensure cleavage of the SAL. The suspension was filtered and the undissolved fraction was reconstituted with water. The pH of the suspension was adjusted to pH 3.3 to generate monomers of high purity and yield. This was left overnight, after which it was centrifuged at 4000 rpm for 10 minutes to ensure complete separation. The precipitate was collected and freeze dried. The pH of the filtrate was re-adjusted to pH 1.3 and the precipitate collected and freeze dried (Simensen *et al.*, 1998).

3.2.1.2 Chemical composition analysis of sodium alginate by nuclear magnetic resonance (NMR)

The polymer sample and its monomer components (10 mg) were dissolved in 1 ml of deuterium oxide (D_2O). The spectra were recorded using a Bruker Avance 500 MHz NMR spectrophotometer (Bruker, UK) with a 5 mm PABBO probe at 297 K, with an acquisition

time of 3.17 seconds and 1.09 seconds for ^{1}H and ^{13}C, respectively and a 2-second cycle delay.

3.2.1.3 Viscosity and pH measurements

The pH of various concentrations of SAL in deionised water was measured using a pH meter (Mettler Toledo). The viscosities of solutions of increasing concentrations of SAL from 0.1 to 2 %w/w were measured using a CS-50 rheometer (Bohlin Instruments, USA) at 25 ˚C with a gap of 150 µm at a single shear rate of 10 s^{-1}. Small volumes of samples were added to the lower plate (4 cm diameter) and the upper cone (4 ° cone angle) re-adjusted to lie above the sample.

3.2.1.4 Solubility of metronidazole in buffers and gelling medium

The saturation solubility profile of MET was assessed in different media from pH 1.2 to 8, maintained at 37 ± 1 ℃. Excess MET was added to 100 ml medium and agitated continuously for 8 hours in a shaking water bath. Small volumes of these MET solutions were diluted, filtered and analysed by HPLC. The solubility of MET in $CaCl_2$ solutions was also determined by adding excess amounts of MET to 100 ml solution of 1 to 0.34 M $CaCl_2$ and allowed to dissolve in the solution by shaking constantly for 12 hours, while being maintained at 37 ± 1 °C. These samples were filtered, diluted and analysed.

3.2.2 Preparation of gel beads

Quantities of SAL were dissolved in deionized water to give the desired final concentration of SAL solution. The solution was allowed to hydrate for 4 h. 10 g of this solution was

extruded drop-wise through a needle into calcium chloride ($CaCl_2$) solution using a peristaltic pump (Minipuls 3-Gilson (Anachem Ltd) Model M312) (Figure 3-2) (Takka *et al.*, 1998) at a flow rate of 0.5 ml/min. The needle was kept at a distance of approximately 6 cm from $CaCl_2$ solution (Smrdel *et al*., 2008b). The beads formed were cured in the gelling medium, filtered, washed, snap-frozen in liquid nitrogen and freeze dried (Edwards Modulyo, England) at - 40 °C for 24 hours. Drug loaded beads were prepared by dispersing the drug evenly in the SAL solution before extrusion into the $CaCl_2$ solution. The suspension of the drug in SAL was to obtain higher drug loadings (Whitehead *et al.*, 2000).

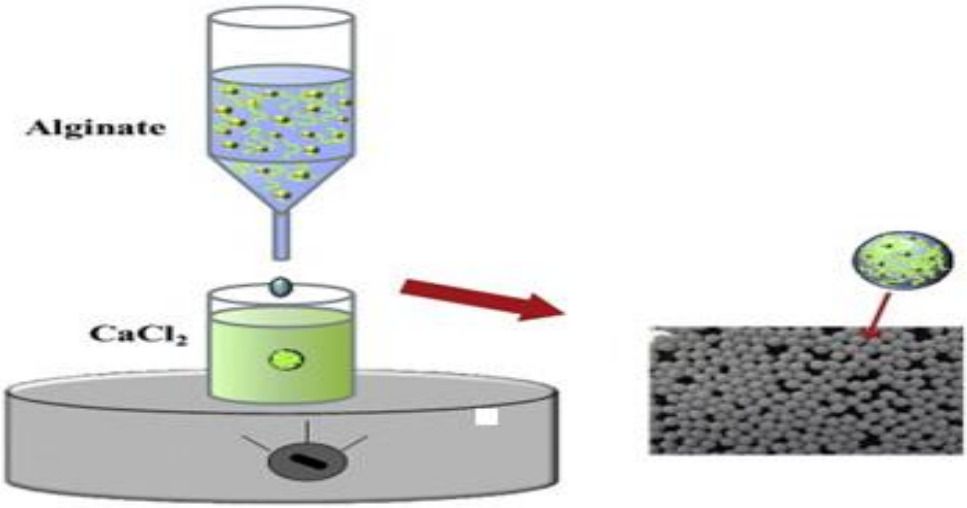

Figure 3-2: Schematic representation of the preparation of calcium alginate beads.

Adapted from Li *et al* (Li *et al.*, 2011)

3.2.3 Optimization of the MET- loaded beads

3.2.3.1 Effect of concentration of SAL and $CaCl_2$

Various concentrations of SAL (1 %, 2 %, 3 %, 5 % w/w) were extruded into different concentrations of $CaCl_2$ solutions (0.03 M, 0.07 M, 0.34 M), in order to determine the optimum levels required for the formation of discreet and spherical beads. The beads produced were assessed based on their structure, buoyancy, drug content and DEE.

3.2.3.2 Effect of curing time on drug content of MET beads

The effect of curing time on the drug content of the beads was assessed with the curing time being varied over 5, 15 and 30 minutes. The drug content, DEE and the drug release of these beads were compared to determine the impact of curing times on these parameters.

3.2.3.3 Effect of drug loading on DEE of MET beads

The effect of the amount of drug added to SAL solution on the bead drug content, DEE and the release studies was assessed. Various MET loadings between 0.5 – 15 %w/w (with respect to the SAL concentration) were added to the SAL solution**.**

3.2.3.4 Determination of MET loss in gelling medium

The amount and percentage of drug loss in the gelling medium were determined by measuring the MET concentration in the $CaCl_2$ solution after curing of the beads.

3.2.4 Bead formulations of MET beads

After optimisation, alginate beads were prepared using a 3 %w/w SAL solution cross-linked with a 0.07 M $CaCl_2$ solution and the beads were cured for 15 minutes unless stated otherwise. Bead formulations were prepared based on Table 3-1.

Table 3-1: MET loadings and corresponding codes of bead samples

Code	MET (% w/w)
$\mathbf{M_0}$	-
$\mathbf{M_{0.5}}$	0.5
$\mathbf{M_1}$	1
$\mathbf{M_2}$	2
$\mathbf{M_3}$	3
$\mathbf{M_5}$	5
$\mathbf{M_{10}}$	10
$\mathbf{M_{15}}$	15

3.3 Results and discussion

3.3.1 Pre-formulation studies

3.3.1.1 Hydrolysis of sodium alginate

The hydrolytic process breaks the alginate into its three different fractions which include guluronic acid (G block), mannuronic acid (M block) and alternating blocks (MG block) (Figure 3-3). The MG block is the first product of the hydrolysis (Haug, 1974) and is filtered out after boiling in HCl, leaving the residual undissolved M and G blocks. pH adjustment to pH 3.3 dissolves the M block with the G block undissolved, further pH adjustment of filtrate to pH 1.3 precipitates out the M block fractions. The determination of the presence of the guluronic acid component of SAL is important since the gel forming capacity of SAL depends on the presence of homopolyguluronic acid chains (Grant *et al.*, 1973).

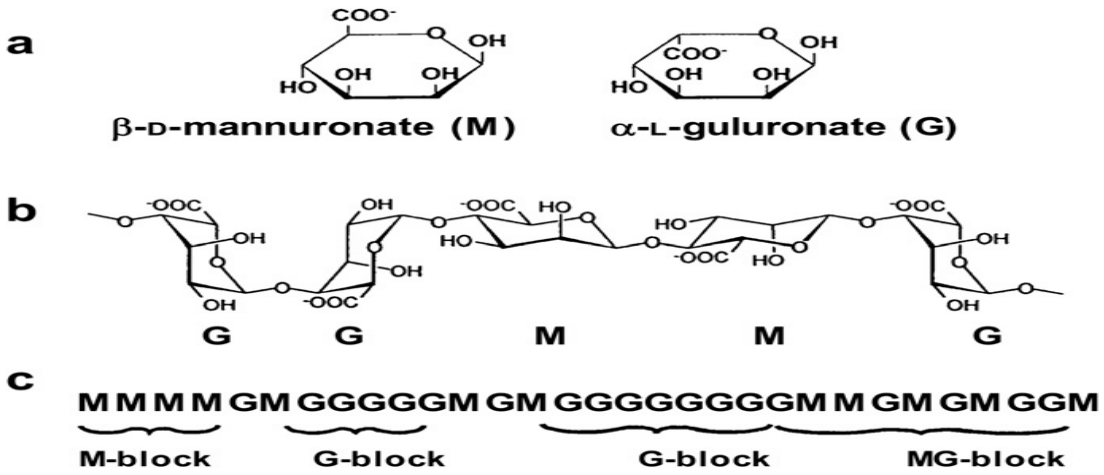

Figure 3-3: Structural characteristics of alginates: (a) alginate monomers, (b) chain conformation, (c) block distribution

(Draget and Taylor, 2011)

3.3.1.2 ^{1}H AND ^{13}C NMR analysis of hydrolytic products of SAL

In the ^{1}H NMR spectrum of SAL, there were many peaks in the region between 3 and 5 ppm (Figure 3-4), this is typical of polysaccharide spectra and could make interpretation of the spectra difficult especially with polysaccharides containing many similar sugar residues (Cui, 2005). The signals between 3.5 to 4.3 ppm can be assigned to non-anomeric photons (H2 – H6). Also, the signals between 4.3 to 4.9 ppm and 4.9 to 5.2 ppm come from β-anomeric and α-anomeric protons respectively (Cui, 2005). Similar peaks were observed in Figure 3-5 and 3-8a. The ^{13}C spectrum showed signals between 60 and 90 ppm which are from the bulk of the ring *C-OH* carbons (C2 - C5) (Figure 3-5). The C1 anomeric carbons gave signals between 90 and 110 ppm. Similar peaks were observed in the monomer units and they corresponded to data from previous studies with ^{13}C chemical shifts for mannuronate and guluronate in each block as follows (in ppm): MM-1 (98.47), MM-2 (68.78), MM-3 (70.06), MM-4 (76.05), MM-5 (74.40), MM-6 (173.99) (Figure 3-8b); GG-1 (99.71), GG-2 (63.55), GG-3 (67.71), GG-4 (78.99), GG-5 (68.58) and GG-6 (174.21) (Figure 3-7) (Penman, 1972, Grasdalen, 1979, Grasdalen, 1981, Grasdalen, 1983, Heyraud *et al.*, 1996, Sakugawa *et al.*, 2004).

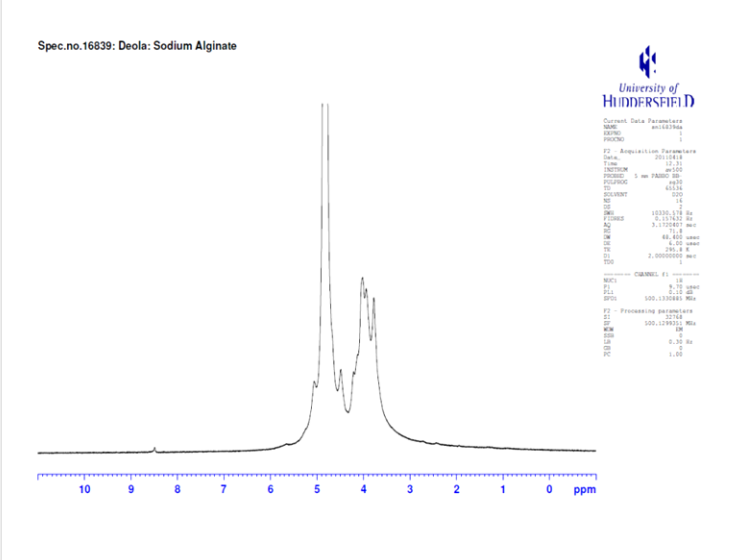

Figure 3-4: ^{1}H NMR spectrum of sodium alginate

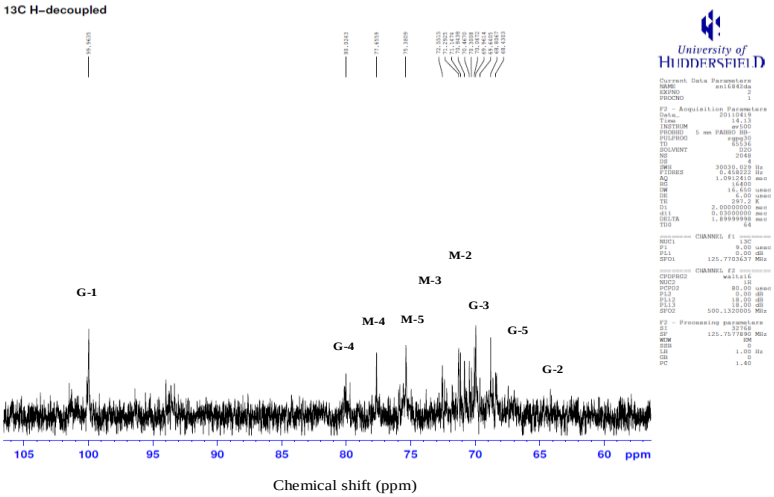

Figure 3-5: ^{13}C NMR spectrum of sodium alginate- G-i and M-i are the different carbons of the guluronic and mannuronic units, respectively

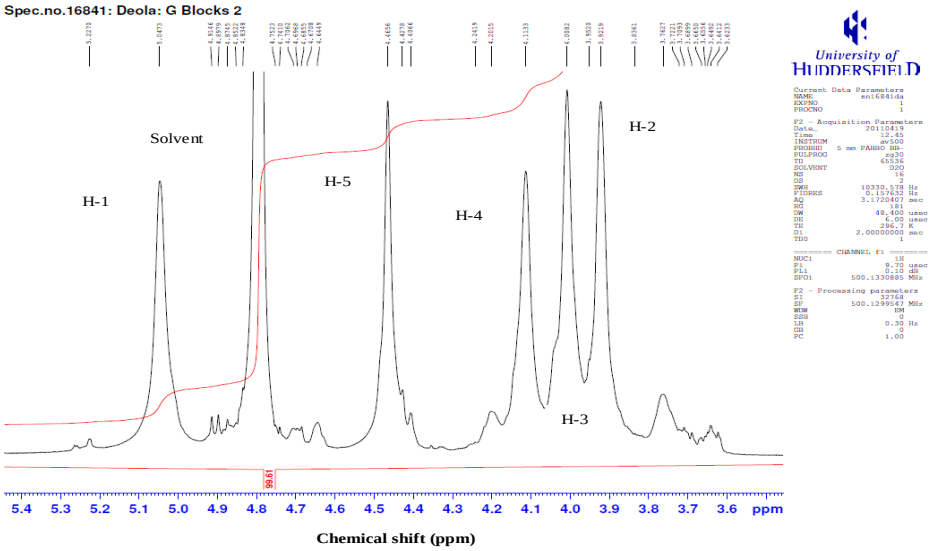

Figure 3-6: ^{1}H NMR spectrum of G block monomer

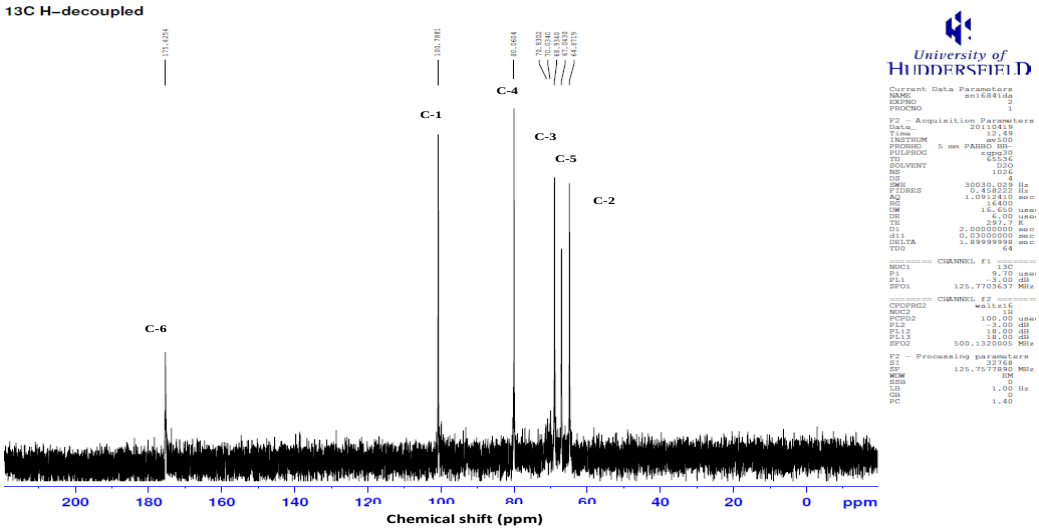

Figure 3-7: ^{13}C NMR spectrum of G block monomer

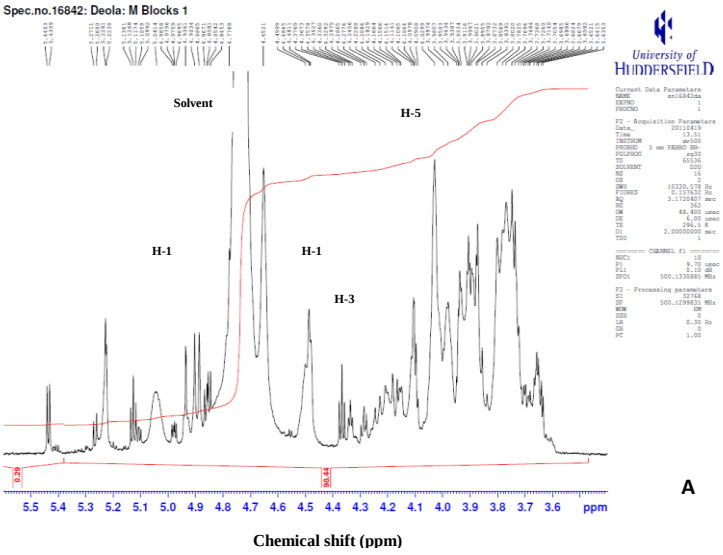

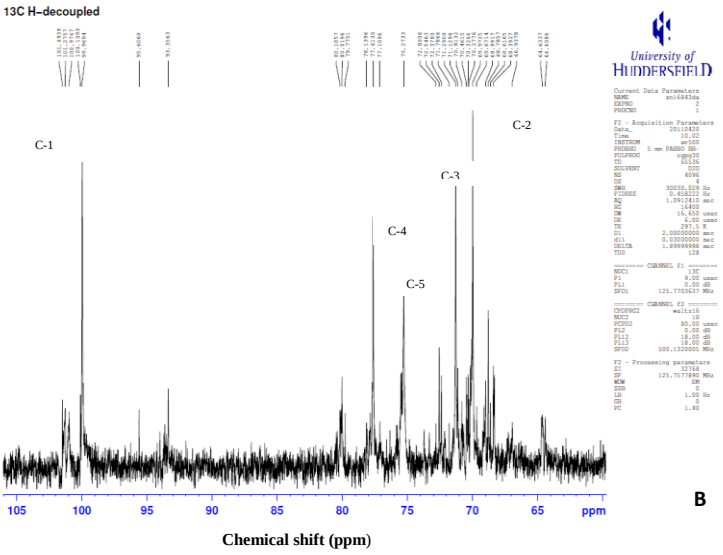

Figure 3-8: A) ^{1}H and B) ^{13}C NMR spectrum of M block monomer

3.3.1.3 Viscosity and pH measurements

Table 3-2: Viscosity and pH of SAL solutions

Concentration (%w/v)	pH	Viscosity (mPa.s)
0.2	7.13 ± 0.01	18 ± 7
0.4	7.15 ± 0.04	49 ± 12
0.5	7.21 ± 0.07	60 ± 9
1.0	7.07 ± 0.01	102 ± 15
2.0	7.17 ± 0.01	211 ± 23

The viscosity of the SAL solution increased with an increase in SAL concentration as expected with polymers (Table 3-2) (Venugopal, 2011). The pHs of the SAL solutions are generally neutral and similar to the reported pH of a 1 %w/v SAL solution at pH 7.2 (Tafaghodi *et al.*, 2006, Thompson and Davidow, 2009, Rasel and Hasan, 2012). At this pH the carboxylic acid group of SAL (pK_a = 3.4 - 4.4) are slightly dissociated. In aqueous alginate solutions, two kinds of interactions play important roles; the first interaction is charge repulsion between broken carboxylic groups and the second interaction is the formation of hydrogen bonds between acid carboxylic and ionized carboxylic groups (Bu *et al.*, 2005). It was important to determine the pH of the SAL solutions as this will influence both solubility and stability of the drugs suspended in the polymer solutions.

3.3.1.4 pH solubility profile of metronidazole

MET is a weak base (pK_a = 2.62), therefore it is ionised in acidic medium leading to an increase in solubility of the drug at low pH, as seen in Figure 3-9. As the pH increased, the solubility of the drug reduced due to a reduction in the ionization of the drug, however, there was no significant difference in solubility of MET across a pH range of 3-8 (~ 10 mg/ml). Therefore, MET has its highest solubility at the lowest pH studied (pH 1.2). Solubility of MET has been reported to be maximal at pH ≤ 2, with the solubility of MET at pH 1.2 reported to be 64.80 mg/ml and ~ 20 mg/ml at pH 2 (Wu and Fassihi, 2005). Another study reported the solubility of MET in 0.1N HCl to be 64.6 mg/ml (Koteshwara *et al*., 2011). These results are similar to the result obtained in this study.

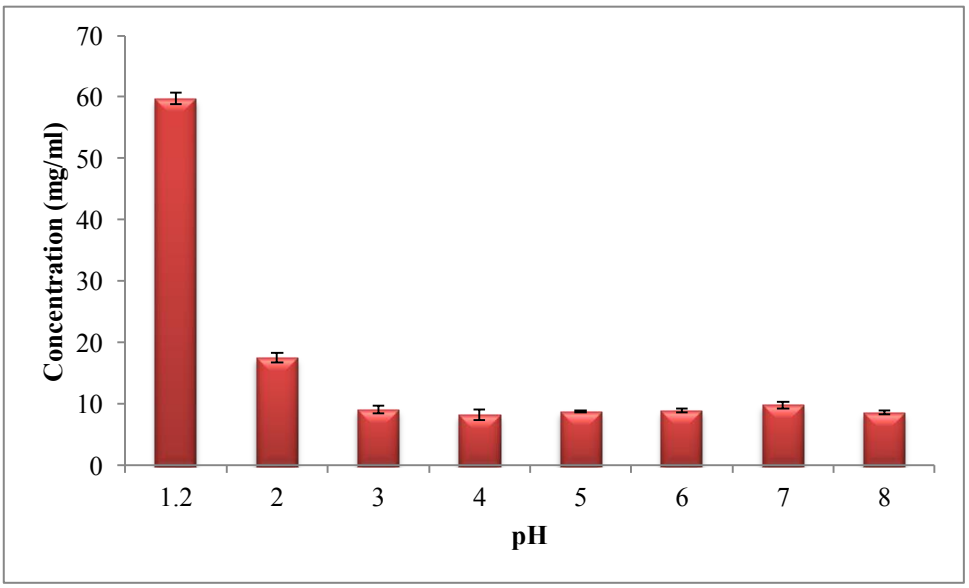

Figure 3-9: Solubility of MET over the pH range 1.2 – 8

3.3.2 Bead optimisation

The beads produced are required to be able to fit some criteria and these include that the:

- beads maintain a level of sphericity and structure both when wet and dry with no fragmentation of the beads on drying
- incorporation of drug into these beads should have minimal effect on the bead shape and structure
- desired bead formulation should be able to encapsulate sufficient amount of drug within the bead structure with high drug content and DEE.
- desired bead formulation must be able to float on the SGF
- desired bead formulation must be able to completely release its entrapped drug content

3.3.2.1 Effect of sodium alginate concentration on bead formation

Beads produced with 1 %w/w SAL across the different $CaCl_2$ concentrations were irregularly shaped and formed clumps when wet and dry. The beads produced using a 2 %w/w solution across the different $CaCl_2$ concentrations gave relatively stronger beads with a spherical shape but there was fragmentation of the beads after drying. The flattening and fragmentation of the beads on drying is likely to be a consequence of their fragility and low mechanical strength. This is due to inadequate cross-linking as a result of low concentration of SAL (Table 3-3). The most structurally stable of this range after drying were those obtained using the 3 %w/w solution and the sphericity of beads improved due to the increase in SAL concentration.

Table 3-3: Optimisation of MET beads

SAL (w/w)	$CaCl_2$		
	0.03 M	**0.07 M**	**0.34 M**
1 %	No beads	No beads	No beads
2 %	Flattened beads	Flattened beads	Flattened beads
3 %	Brittle Beads	Beads	Beads
5 %	Beads with tails	Beads with tails	Beads with tails

The presence of drug reduced the gel formation for the 1 % and 2 %w/w alginate beads with these beads collapsing in the gelling medium. However, this was not observed with beads produced using the 3 %w/w solution. This may be due to the fact that beads were adequately cross-linked therefore, were able to entrap drug within their matrix, whereas this was not achieved for lower SAL concentrations. Smrdel *et al* (2008b) reported that calcium alginate beads could be regularly shaped and spherical when wet, but on drying the shape of the beads could flatten out, become less regularly shaped, like ellipsoid spheres or remain spherical depending on the concentration of the SAL solution and the drying process. Increasing the SAL concentration increases the viscosity of the solution as observed in Table 3-2; therefore 5 %w/w SAL solution had an increased viscosity and was difficult to pump, thereby hindering droplet formation (Ishak *et al.*, 2007). In addition, the beads formed using this concentration had tails which occurs due to the hardening of the bridge that forms during droplet formation at the needle tip as observed in Figure 3-10. This was observed by other

researchers (Haeberle *et al.*, 2008, Chan *et al.*, 2011a) at high SAL concentrations. Therefore, the use of this concentration and other higher concentrations was abandoned.

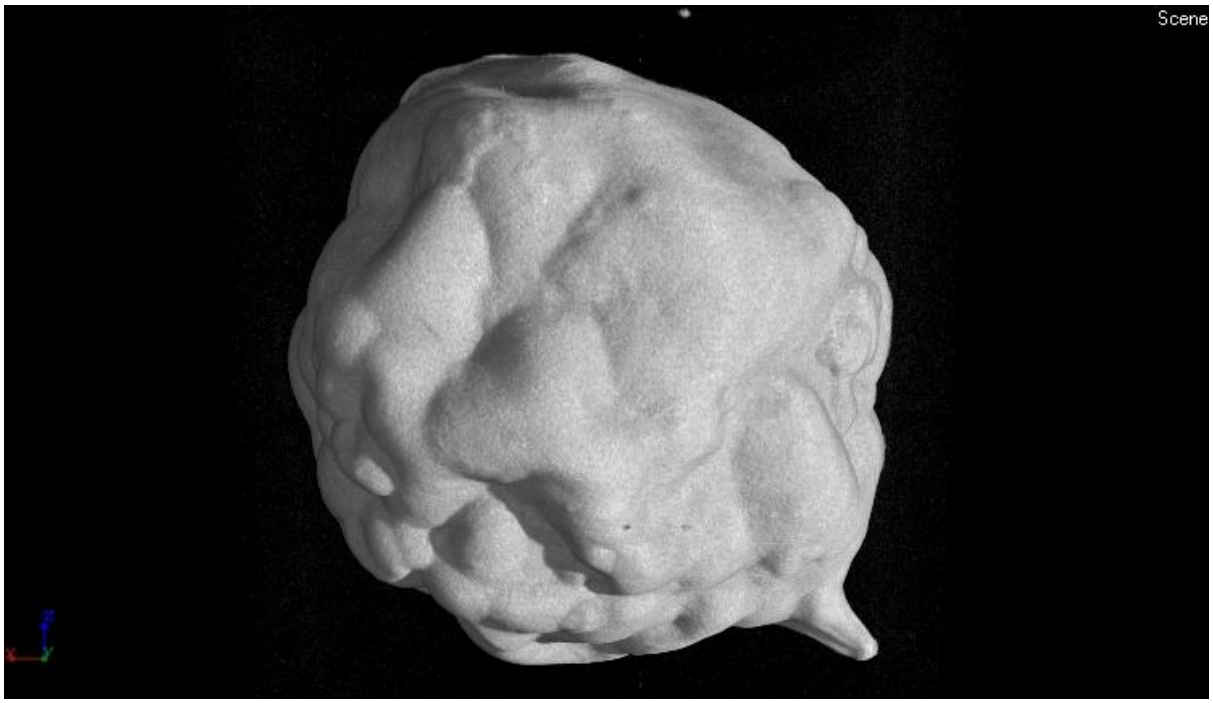

Figure 3-10: XμMT image of bead prepared with 5 %w/v SAL showing tails

3.3.2.2 Effect of $CaCl_2$ concentration on bead formation and calcium content

The $CaCl_2$ concentration affects the amount of Ca^{2+} in the gel beads (Soni *et al.*, 2010) (Figure 3-11), the structure and mechanical strength of the beads (Wan *et al.*, 2008). Beads produced with 0.03 M $CaCl_2$ did not form well-structured beads and this may be due to low calcium ion concentration, which would likely cause loose gel formation. Those formed using 0.07 M $CaCl_2$ solution resulted in a more consistent bead structure with little or no fragmentation (even on loading with drug), while those made from a higher concentration (0.34 M), were less spherical with irregular surfaces and relatively smaller beads than those obtained from 0.07 M solution. This observed reduction in bead size (1.91 mm (0.07 M $CaCl_2$) *versus* 1.67 mm (0.34 M $CaCl_2$) was also reported by other researchers (Sankalia *et al.*, 2005, Giri *et al.*, 2013, El-Kamel *et al.*, 2003, Mandal *et al.*, 2010); with the observed size reduction being a result of syneresis (water loss) (Martinsen *et al.*, 1989) and shrinkage of the gel due to a higher level of cross-linking. Bead gelation process starts radially from the surface of the beads to its centre. As the gelation process continues, water is continuously expelled due to cross-links being formed leading to contraction of the gel volume. Increasing SAL concentrations at constant $CaCl_2$ concentration causes an increase in calcium content of the bead, as a result of the presence and availability of more calcium binding sites (Figure 3-11). Soni *et al* (2010) also reported an increase in Ca^{2+} ions of alginate microspheres on increasing the polymer concentration.

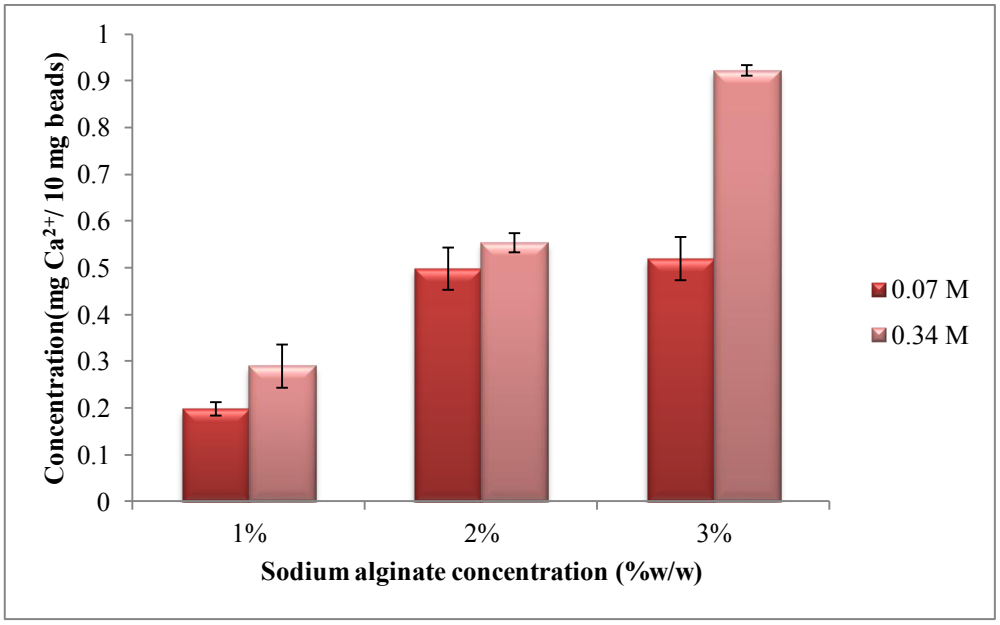

Figure 3-11: Calcium content of beads produced using 0.07 M and 0.34 M $CaCl_2$.

3.3.2.3 Effect of SAL and $CaCl_2$ concentration on metronidazole entrapment

Formation of the calcium alginate gels occurs due to cross-linking between SAL and Ca^{2+} ions in the $CaCl_2$ solution, therefore, these two parameters are important for drug entrapment. It is assumed that higher concentrations of both components may improve DEE. Increasing SAL concentration from 1 % to 2 %w/w and 3 %w/w, whilst maintaining $CaCl_2$ concentration and drug loading at 0.07 M and 1 %w/w respectively, with respect to the SAL concentration, led to a 55.7 ± 9.8 % and 238.7 ± 21.2 % increase in DEE respectively ($p < 0.05$) (Figure 3-12). There have been several reports of increasing DEE on increasing SAL concentrations (Ishak *et al.*, 2007, Peeush *et al.*, 2010, Halder *et al.*, 2005). This may be due

to an increase in polymer viscosity and the greater availability of active calcium – binding sites in the polymeric chains and consequently, the greater degree of cross-linking as the quantity of SAL increased (El-Kamel *et al.*, 2003), creating an increased space for the drug molecules to be retained throughout a larger cross-linked network of bead (Bera *et al.*, 2009). Increasing SAL concentration led to a significant reduction in the LSC (Figure 3-13) of the beads due to a higher entrapment of the drug as a result of the denser matrix. On increasing the alginate concentration from 1 %w/w to 2 %w/w and 3 %w/w, the LSC decreased by 28 ± 4.3 % and 66.9 ± 2.9 % respectively ($p < 0.05$).

Increasing $CaCl_2$ concentration with varying MET loading - 0.5 %w/w and 2 %w/w - at a constant SAL concentration (3 %w/v) led to no significant change in DEE ($p > 0.05$) (Figure 3-14). At higher drug loadings (5 %w/v), increasing $CaCl_2$ concentration led to a slight decrease in DEE (Figure 3-15). There was about 14 % and 7 % decrease in DEE on increasing the $CaCl_2$ concentration from 0.07 M to 0.34 M for beads loaded with 5 and 10 w/w % MET, respectively ($p > 0.05$). This is in contrast to an increase in DEE observed by some researchers (Sorberg *et al*., 1998, Mandal *et al*., 2010, Manjanna *et al*., 2013). Manjanna *et al* (2013) reported ~ 20 % increase in DEE of aceclofenac sodium on increasing the $CaCl_2$ from 1 to 5 %w/v; however, increasing $CaCl_2$ concentration beyond 5 %w/v, did not enhance drug entrapment. The increase in DEE may be as a result of the increased level of cross-linking and compactness in the bead matrix thereby making the beads able to entrap the drug better than beads cross-linked with a lower $CaCl_2$ concentration. Some studies however documented a reduction in DEE on increasing $CaCl_2$ concentration (Østberg *et al*., 1994, Halder *et al*., 2005, Ishak *et al.*, 2007, Peeush *et al.*, 2010, Chowdhury *et al*., 2011). Ishak *et al* (2007) reported ~ 9 % reduction in MET content of beads on increasing $CaCl_2$ from 1 to 5 %w/v. The reported decrease could be due to competition between calcium ions and the drug for the same binding sites on SAL. A high concentration of $CaCl_2$ causes significant number of pores on the surface of beads (Sankalia *et al.*, 2005) and increased loss of dissolved drug (Aslani and Kennedy, 1996) leading to a reduction in DEE. The solubility, molecular size and the ionic nature of the drug determines the DEE and the drug release

(Pawar *et al.*, 2008) of the encapsulated drug from the polymer matrix. Drugs with a high water solubility and low molecular mass generally have poor entrapment compared to insoluble and higher molecular mass drugs (Liu *et al.*, 2003, Shilpa *et al.*, 2003, Patil *et al.*, 2006, Aslani and Kennedy, 1996, Lee *et al.*, 1999). $CaCl_2$ (0.07 M (~ 1 %w/v)) was used as the gelling medium for further studies to determine the impact of other variables. This concentration was chosen in several other studies as an ideal concentration for cross-linking alginate (Ishak *et al*., 2007, Narra *et al*., 2012, Malviya *et al*., 2013).

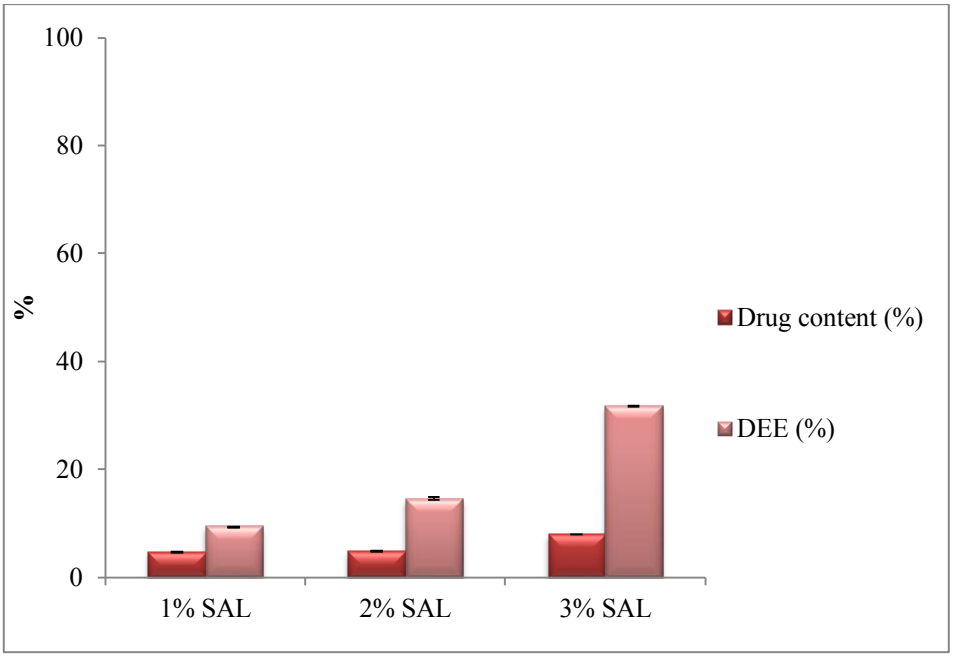

Figure 3-12: Effect of SAL concentrations on DEE using 1 %w/w MET and 0.07 M $CaCl_2$

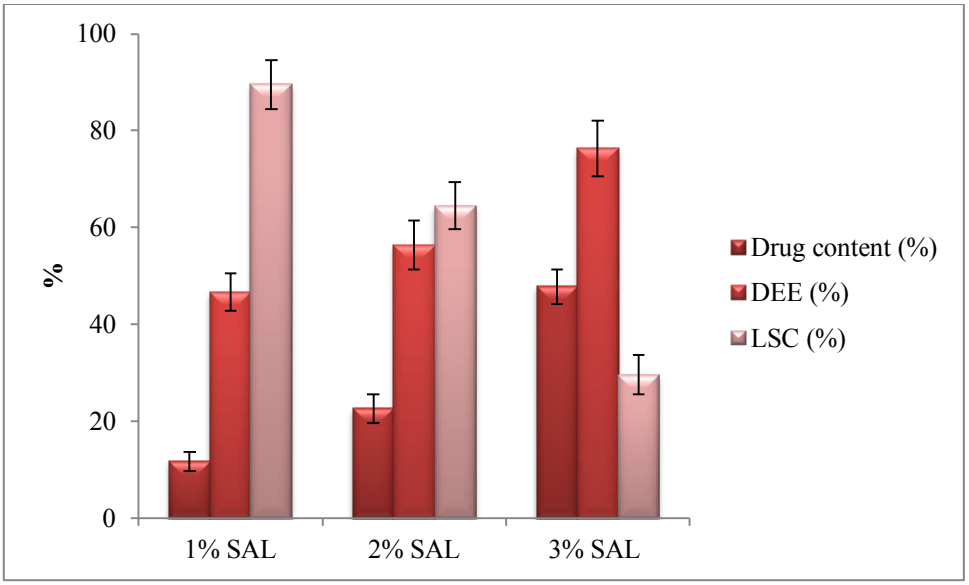

Figure 3-13: Effect of SAL concentrations on DEE using 5 %w/w MET and 0.07 M $CaCl_2$

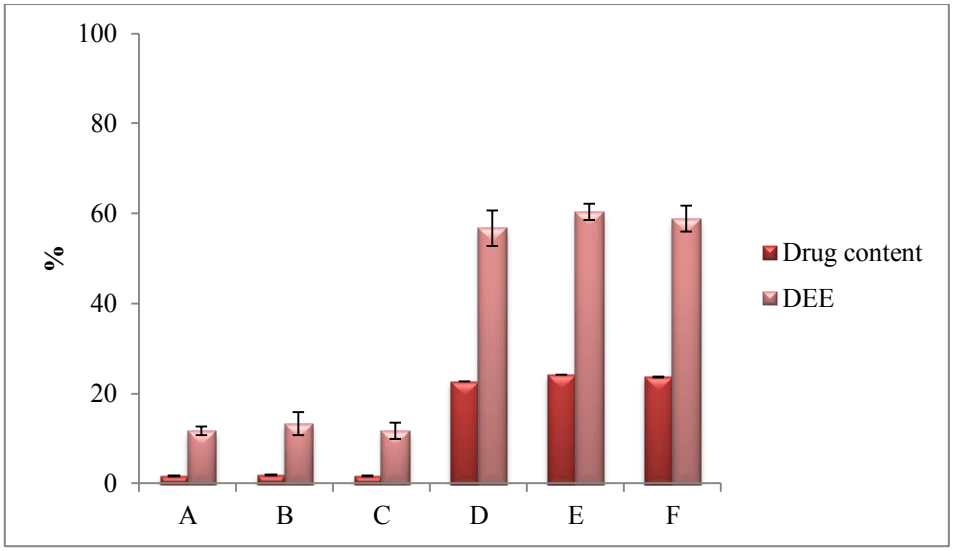

Figure 3-14: Effect of $CaCl_2$ concentration on drug content and DEE with 3 % SAL containing 0.5 % MET cross-linked with (a) 0.03 M $CaCl_2$, (b) 0.07 M $CaCl_2$, (c) 0.34 M $CaCl_2$; 3 % SAL containing 2 % MET cross-linked with (d) 0.03 M $CaCl_2$, (e) 0.07 M $CaCl_2$, (f) 0.34 M $CaCl_2$.

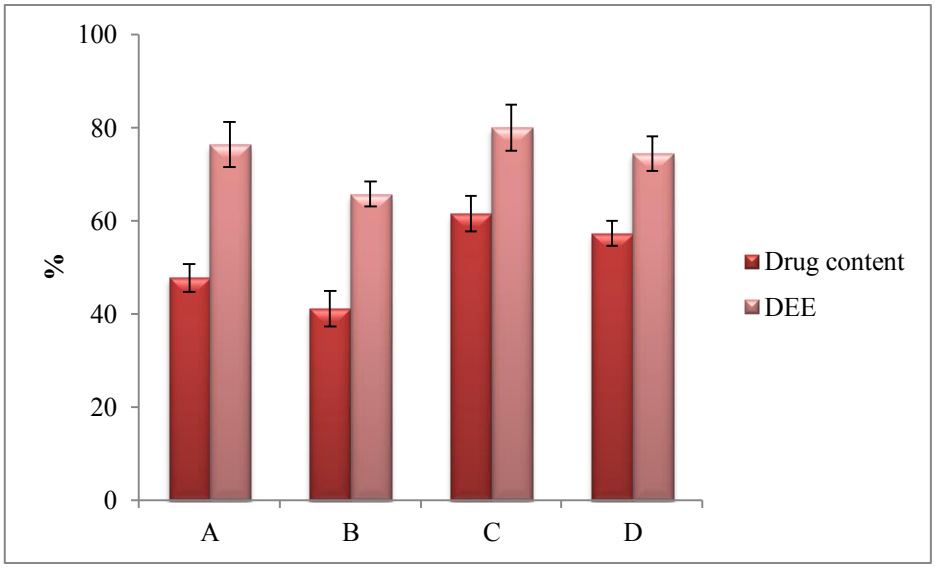

Figure 3-15: Effect of $CaCl_2$ concentration on drug content and DEE with 3 % SAL containing 5 % MET cross-linked with (a) 0.07 M $CaCl_2$, (b) 0.34 M $CaCl_2$; 3 % SAL containing 10 % MET cross-linked with (c) 0.07 M $CaCl_2$, (d) 0.34 M $CaCl_2$.

3.3.2.4 Effect of drug-polymer ratio and $CaCl_2$ concentration on calcium content of MET loaded beads

An increase in drug-polymer ratio decreased the calcium ion content of the beads. The blank beads had the highest amount of Ca^{2+} of 5.2 ± 0.4 %w/w, while the beads loaded with 10 %w/w MET had a calcium content of 2.1 %w/w ± 0.1 %w/w for beads cross-linked with 0.07 M $CaCl_2$. The reduced Ca^{2+} content did not correspond to reduced cross-linking in the drug loaded beads relative to blank beads, but this is due to the fact that the calculations were carried out based on weight of the bead which includes the drug content (Figure 3-16). This is similar to the increased Ca^{2+} content of beads observed at low drug/polymer ratio by other researchers (Basu and Rajendran, 2008, Rajendran and Basu, 2009, Takka *et al.*, 1998). Increasing $CaCl_2$ concentration from 0.07 M to 0.34 M led to an increase in the calcium content of the beads with an increase of 77.4 % in blank beads. There were also corresponding increases with the drug-loaded beads with an increase of 74 % and 47.1 % in beads loaded with the 1 %w/w and 5 %w/w MET, but at 10 % MET, there was only 13 % increase in calcium content on increasing $CaCl_2$ concentration from 0.07 M to 0.34 M (Figure 3-16). This was expected, as more calcium was available for cross-linking when SAL is reacted with a higher concentration of $CaCl_2$. Takka *et al.* (1998) reported an increase in calcium content from 0.522 ± 0.006 to 0.661 ± 0.032 mg Ca^{2+}/10 mg beads on increasing the $CaCl_2$ concentration from 0.1 M to 0.5 M. This may be attributed to the availability of more binding sites in the beads at low drug/polymer ratios (Anal *et al.*, 2003).

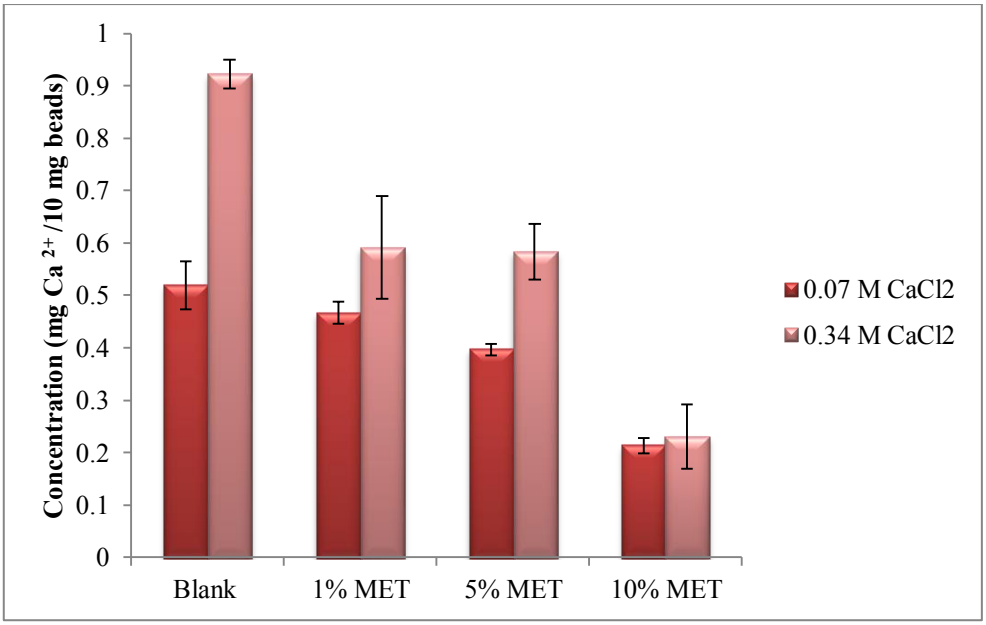

Figure 3-16: Calcium content of blank and drug loaded beads.

3.3.2.5 Effect of curing time on calcium content of alginate beads

The curing time is the period required for gelation and cross-linking of the alginate matrix with calcium ions. Ionic gelation occurs during this period and increasing the curing time from 5 to 15 minutes led to an increase of about 9 % and 17 % for 0.07 M and 0.34 M $CaCl_2$ respectively. Extending the curing time to 30 minutes had a negligible effect on calcium content with an increase of only 1.8 % and 0.4 % for 0.07 M and 0.34 M $CaCl_2$ respectively (Figure 3-17). This result is similar to results obtained from previous studies (Kim and Lee, 1992, Lim and Wan, 1997, Pillay and Fassihi, 1999), where increasing curing times led to negligible increases in calcium content of calcium alginate gels.

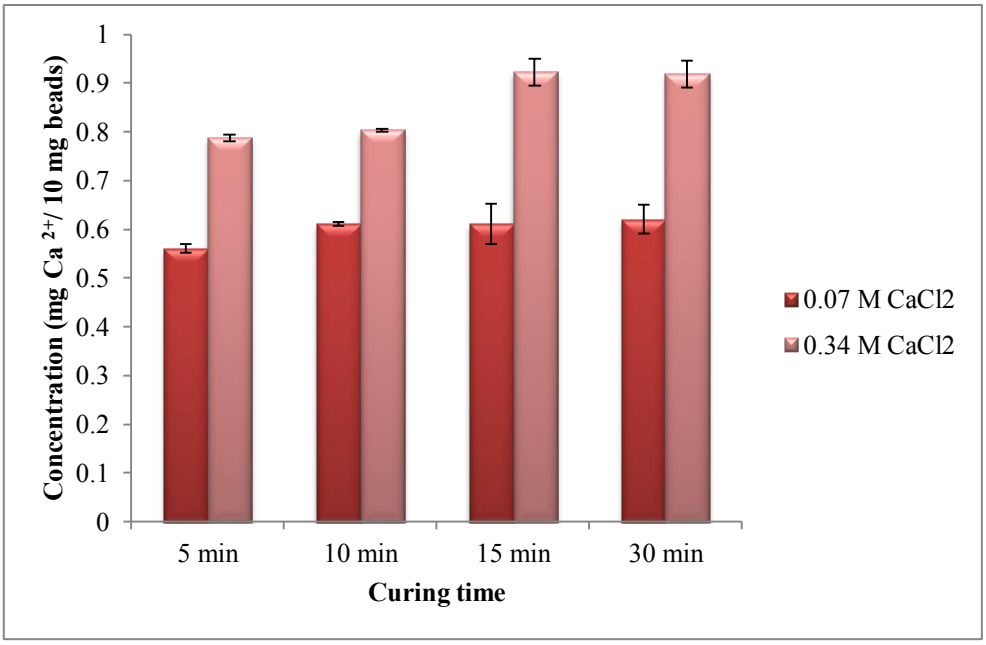

Figure 3-17: Effect of curing time on calcium content

3.3.2.6 Effect of curing time on MET entrapment

The solubility of MET in 0.07 M $CaCl_2$ was determined to be 9.2 ± 0.1 $mgml^{-1}$ at 37 °C. This is similar to the solubility of MET in water which was reported to be 10 $mgml^{-1}$ at 20 °C (O'Neil 2006) and 10.5 $mgml^{-1}$ at 25 °C (Mahfouz and Hassan, 2001). Due to the inherent aqueous solubility of MET, the curing time should be kept as short as possible to limit drug loss in the aqueous $CaCl_2$ solution. It was observed that the drug content of the beads reduced with an increase in curing time ($p < 0.05$). As shown in Figure 3-18, MET content decreased from 10.4 ± 0.9 %w/w to 5.9 ± 0.8 %w/w, on extension of curing time from 5 minutes to 30 minutes for the 1 %w/w drug-loaded beads. In addition, for the 10 %w/w drug-loaded beads, MET content reduced from 76.7 ± 4.6 %w/w to 59.6 ± 2.9 %w/w over the same time interval. This result correlates with earlier findings (Patel *et al.*, 2006, Manisha *et al.*, 2010). It has

always been assumed that the incorporation of water-soluble drug in beads would be problematic due to the surrounding aqueous environment in which they are produced. This aqueous environment leads to poor encapsulation and fast drug release governed by the pore size of the beads and the inherent solubility of drug in a matrix system. These issues make the determination of the ideal curing time a crucial factor in ensuring a high drug content and DEE (Kulkarni *et al.,* 1999, Murata *et al.,* 2000). The solubility of MET in the gelling medium has been identified as the main cause of drug loss into the $CaCl_2$ solution over time. Some researchers have attempted to minimise or prevent drug loss into the gelation media and improve DEE by pre-saturating the $CaCl_2$ solution with the drug (Javadzadeh *et al*., 2010, Giri *et al*., 2013). Drug loss starts during the gel formation and continues as more fluid is exuded from the beads, *e.g.* during gelation and drying. In order to achieve adequate cross-linking of the matrix and high DEE, a curing time of 15 minutes was chosen for all subsequent bead formulations, unless otherwise stated. This was because there was no significant increase in the calcium content at times > 15 minutes (Figure 3-17) and the drug content and DEE at this time were still sufficiently high especially at high drug-polymer ratios (Figure 3-18). This time has been chosen as an ideal curing time for alginate beads in several other studies (Bone *et al*., 1997, Pasparakis and Bouropoulos, 2006, Giri *et al*., 2013, Malakar *et al*., 2013, Rajalakshmi *et al.*, 2013), while some have chosen a considerably longer time (El-Kamel *et al.*, 2003, Caballero *et al.*, 2014, Al-Kassas *et al*., 2007, Tang *et al.*, 2007). This ideal time depends mostly on the solubility of the encapsulated material in the cross-linking medium.

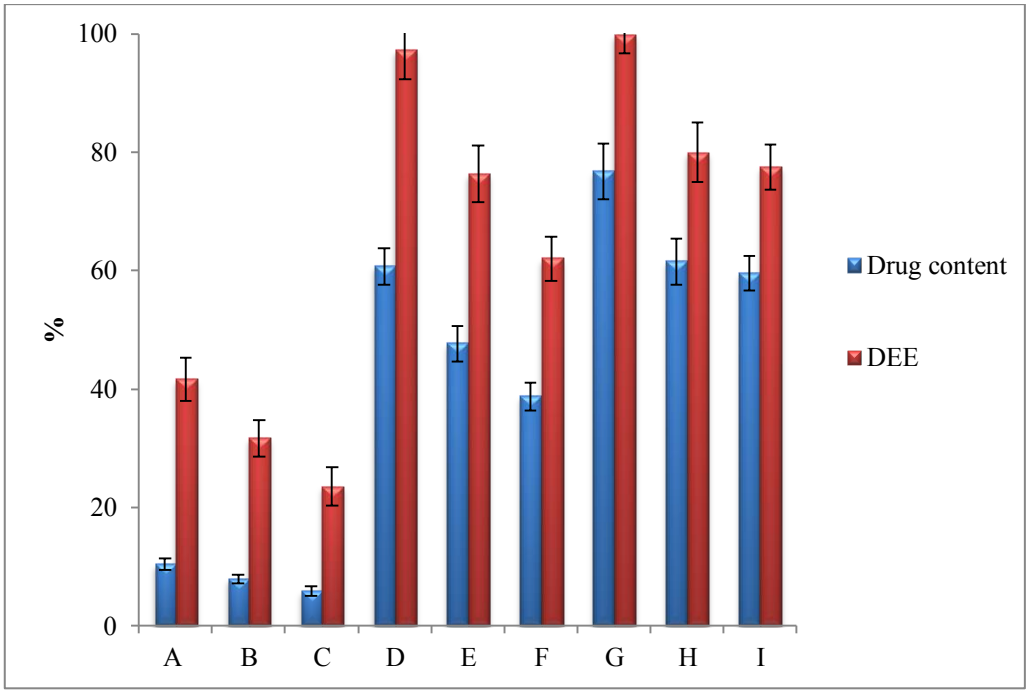

Figure 3-18: Effect of curing time on DEE of formulation of 1 % MET cured for a) 5 min (b) 15 min (c) 30 min; 5 % MET cured for (d) 5 min (e) 15 min (f) 30 min and 10 % MET cured for (g) 5 min (h) 15 min (i) 30 min

3.3.2.7 Effect of drug-polymer ratio on drug entrapment

The pH of SAL solutions was ~ 7; therefore, this suggests that MET is in suspension in the SAL solution rather than in solution when added in high amounts. With an increase in drug-polymer ratio, more drug leached into the gelling medium, as seen in Figure 3-19b, with ~ 68 mg MET being lost with M_1 while with M_{10} and M_{15} there was about 180 mg and 195 mg MET loss. At high drug loadings, however, (M_{10} and M_{15}) there was a reduction in the extent of drug loss, which might be due to MET saturation of the gelling medium. Drug loss was confirmed by measuring the MET concentration in the gelling medium after curing. The LSC

gives an indication of the amount of drug on the surface of the beads that has not been properly encapsulated in the beads and is an indication of the loss of drug during processing. The DEE increased with an increase in drug-polymer ratio ($p < 0.05$) (Figure 3-19a) and this result correlates with earlier findings (Ishak *et al.*, 2007), where DEE of MET increased from 22.76 to 79.08 % by increasing the MET/SAL ratio from 1:1 to 4:1, respectively. The drug content in M_{10} beads (drug-polymer ratio = 3.3:1) was ~ 62 % and ~ 68 % in M_{15} beads (drug-polymer ratio = 5:1). Both of these are lower than the drug content of MET beads (drug-polymer ratio = 3:1) developed by Ishak *et al* (2007) using similar SAL and $CaCl_2$ concentrations, which was reported to be ~ 78 %. Another study by Patel *et al* (2006), reported a higher DEE of MET (> 87 %) for beads prepared using 2 % SAL and 4 % $CaCl_2$. This variation can occur due to differences in the M/G ratio, source and molecular weight of SAL, concentration of $CaCl_2$ used and the bead preparation and recovery techniques.

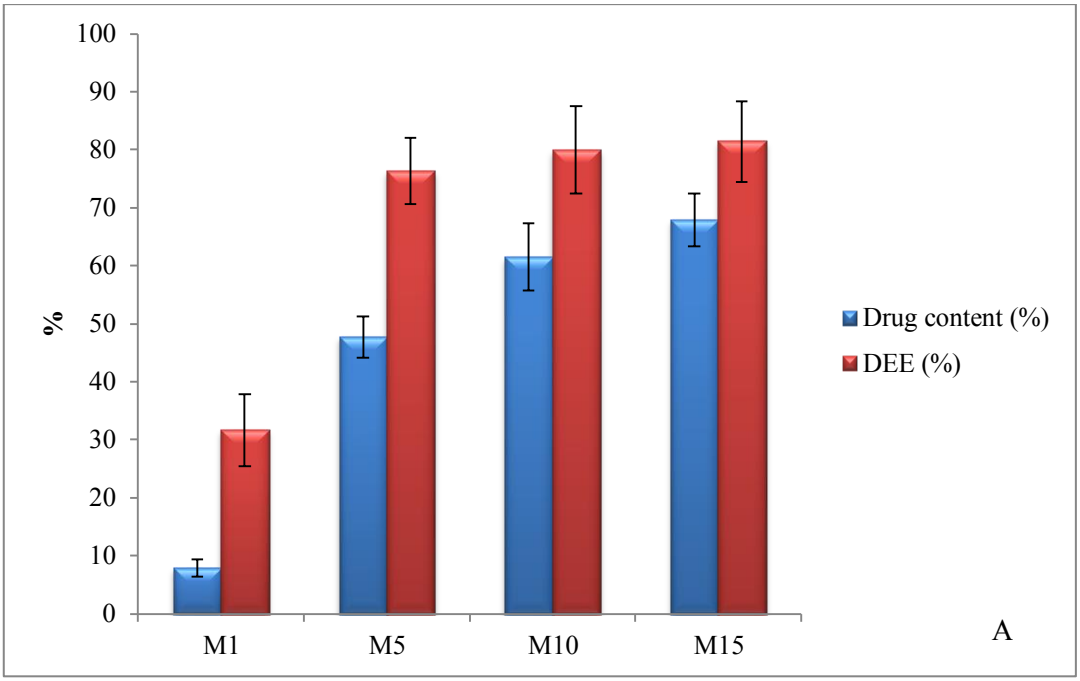

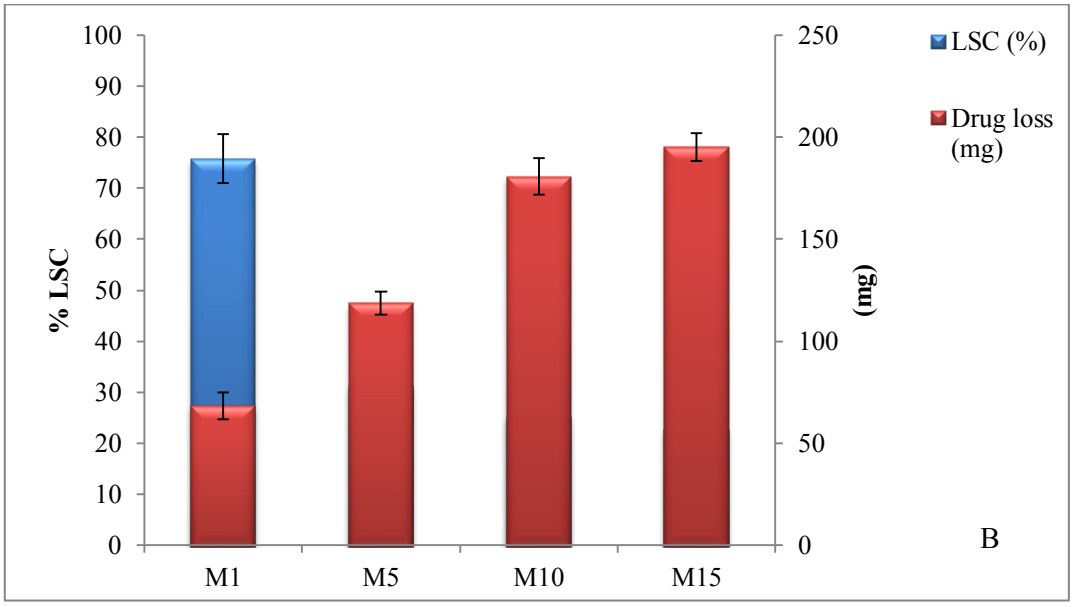

Figure 3-19: Effect of drug-polymer ratio on A) drug content and DEE and B) drug loss

3.3.3 Characterisation of MET beads

3.3.3.1 Morphology and structure of metronidazole beads

Calcium alginate beads were spherical in nature as shown in Figures 3-20 to 3-21. The surface of the M_0 (unloaded) bead appeared slightly wrinkled relative to the surface of the drug - loaded beads; see M_5 as an example in Figure 3-20. A cross section of an M_0 bead showed a collapsed inner core with sheath-like layers in the inner structure (Figure 3-20b and d). This supports the theory of the radial formation of gels during curing. These cavities, noticeable in the core, are areas of former ice crystals (Fennema, 1975) and are a result of freeze-drying. These are unique to alginate beads and aid buoyancy of the beads (Stops *et al.*, 2008). M_5 beads had a spongy texture and denser core (Figure 3-21b and d), relative to M_0 with a crude and rough outer surface, as verified with the XμMT images (Figure 3-20a and c). When there are differences in the density of a sample, variations in the X-ray's attenuation (*i.e.*, absorption and scattering) produce a contrast in the sample image with the white areas corresponding to the alginate and the black areas representing the voids (Chan *et al.*, 2011b). This is similar to previous studies (Rastello De Boisseson *et al.*, 2004, Nussinovitch and Zvitov-Marabi, 2008, Chan *et al.*, 2011b). XμMT analysis showed distribution of the drug particles within the core. XμMT images of M_5 show that MET particles were concentrated in a portion of the bead (Figure 3-21d), rather than homogenously dispersed throughout the bead. MET particles can also be observed on the surface of the beads (Figure 3-21c), which may be as a result of the drug leaching out of the beads. MET particles are assumed to have accumulated at the bottom of the alginate droplet during droplet formation at the needle tip before dropping into the gelling medium. Whitehead and co-workers (2000) also, reported this unexpected distribution of drug in alginate beads, where amoxicillin was concentrated in the centre of the beads and not evenly distributed within the bead as expected.

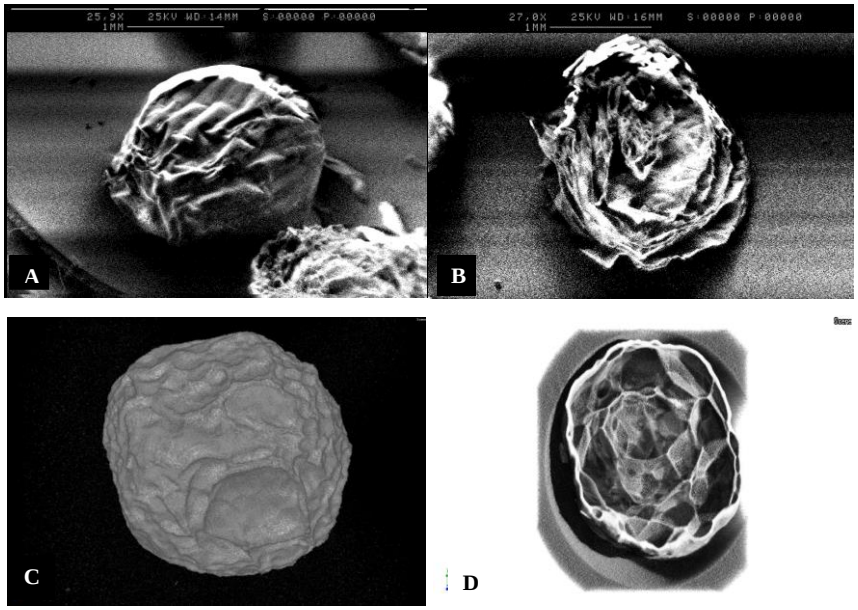

Figure 3-20: SEM images of A) external surface and B) cross-section of M_0 beads and XµMT images of C) external surface and D) Internal surface of M_0 beads (M_0 beads contains no drug)

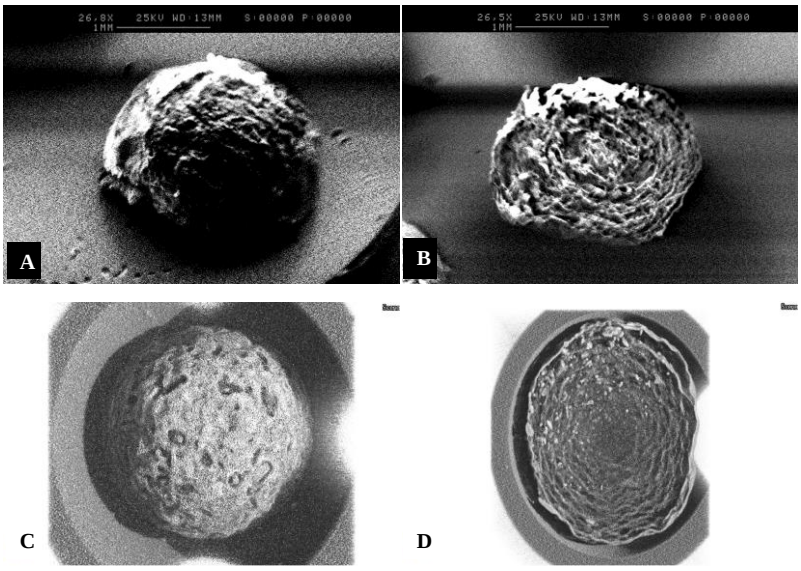

Figure 3-21: SEM images of A) external surface and B) cross-section of M_5 beads and XµMT images of C) external surface and D) internal surface of M_5 beads. (M_5 beads loaded with 5 %w/w MET)

3.3.3.2 Physical properties of metronidazole beads

The beads had a white colour with slight yellowish tinge present in the MET loaded ones, with the diameter increasing with an increase in drug-polymer ratio. The size of the beads increased by about 20 % for M_3 beads compared with M_0 beads or by 51 % for M_{15} beads ($p < 0.05$) (Table 3-4). These beads were cured for 15 min, but those cured for 5 min were observed to have a slightly larger diameter than those cured for 15 min. Smrdel *et al* (2008a) observed a reduction in diameter with increasing curing time with a reduction in diameter from 1.91 mm to 1.33 mm on increasing the curing time from 1 to 30 minutes. The weight of the beads also increased with increasing drug content ($p < 0.05$) (Table 3-4). This could be due to lower drug content since there was a significant decline in MET content with increasing curing time. The bulk density of the beads ranged between 0.11 - 0.26 g/cm^3, with all the beads exhibiting a bulk density less than 1.004 g/cm^3. The true density ranged from 0.45 - 1.55 g/cm^3, with the true density increasing with increasing drug-polymer ratio and porosity was above 70 % for all beads. The relatively high porosity is due to the freeze drying process. Freeze drying leads to the least shrinkage and structural changes within the beads and creates pores in areas of former ice crystals (Fennema, 1975). Various authors have observed a relationship between the processing parameters in production of alginate beads and their influence on the size on the beads (Whitehead *et al*., 1998, Klokk and Melvik, 2002). Since the process parameters were kept constant during the production of the beads, it can be deduced that the changes observed in the beads are due to the addition of the drug in the formulation (Stops *et al*., 2008).

3.3.3.3 Moisture content of metronidazole beads

The residual moisture content (%) of the beads ranged from 2.1 ± 0.2 to 3.1 ± 0.8 %w/w. This was measured as the % weight loss when the sample was heated up to 150 ℃, which is an indication that the weight loss was due to bound water. A high moisture content will affect the physico-chemical characteristics and storage stability of the beads (Nimase and Vidyasagar, 2010). Several studies have reported similar moisture content of alginate beads to be ≤ 4 %w/v (Nimase and Vidyasagar, 2010, Mallick *et al*, 2013, Asha *et al*, 2011).

Table 3-4: Physical properties of MET-loaded beads

Code	Diameter (mm)	True density (g/cm^3)	Weight (g) (*n=100*)	Bulk density (g/cm^3)	Porosity (%)	Ca^{2+} content (mg/10mg bead)
M_0	1.91 ± 0.3	0.49 ± 0.02	0.05	0.11 ± 0.02	77.55	0.52 ± 0.04
$M_{0.5}$	1.88 ± 0.5	0.45 ± 0.02	0.05	0.09 ± 0.04	80.01	0.54 ± 0.03
M_1	2.05 ± 0.2	0.59 ± 0.01	0.06	0.12 ± 0.02	79.66	0.49 ± 0.02
M_2	2.12 ± 0.4	0.54 ± 0.03	0.08	0.12 ± 0.01	77.78	0.44 ± 0.03
M_3	2.29 ± 0.2	0.64 ± 0.02	0.11	0.14 ± 0.02	78.12	0.41 ± 0.01
M_5	2.45 ± 0.2	0.92 ± 0.01	0.14	0.18 ± 0.05	80.43	0.39 ± 0.01
M_{10}	2.71 ± 0.1	1.43 ± 0.01	0.24	0.23 ± 0.01	83.99	0.21 ± 0.01
M_{15}	2.89 ± 0.3	1.55 ± 0.02	0.31	0.26 ± 0.02	83.22	0.17 ± 0.03

3.3.3.4 Differential scanning calorimetry of metronidazole beads

DSC analysis was to assess the thermal behaviour of MET, SAL and MET-loaded beads. Pure MET showed a single, sharp endothermic peak with an average onset at 160.41 ± 0.59 ℃ (*n=3*), which corresponds to its melting point which is reported as 160 ℃ (Reynolds, 1993). The temperature at peak height was 162.75 ± 0.72 ℃. An exothermic peak was also observed at 284.63 ± 0.64 ℃ (*n=3*) which corresponds to the complete degradation / crystallisation of MET (Kiss *et al.*, 2006) (Figure 3-22). The MET scan did not show any additional peaks indicating the purity of the MET sample. The physical mixture of MET and SAL showed an endothermic peak at 161.45 ± 0.23 ℃ (*n=3*) similar to that of the pure MET sample. SAL and M_0 did not show any peaks within the range of analysis, while the MET loaded beads showed melting endotherms at 165.32 ± 0.91℃ (*n=3*), representing the presence of MET in the samples analysed. These findings confirm the dispersion of the drug in the polymer matrix with the drug maintaining its crystalline nature in the formulation as observed in the XμMT images (Section 3.3.3.1). The absence of any additional peaks or significant shift in melting endotherms of MET in the samples suggested there was no obvious interaction between drug and excipients or instability of drug during the process of bead formation. The complete degradation of MET observed at ~ 285 ºC was also similarly observed in the physical mixture and the formulations with the onset of degradation of MET in bead formulations not significantly different from that of the pure drug. Similar findings of the presence of drug peak and the absence of drug-polymer interaction in alginate beads were reported by other researchers (Rajendran and Basu, 2009, Patel *et al.*, 2010, Satishbabu *et al.*, 2010, Hadi *et al.*, 2013). Other studies show the absence of drug peaks on analysis of the drug loaded beads as a result of the amorphous dispersion of the drug with the drug molecularly dispersed in the polymer matrix (Giri *et al.*, 2013, Smrdel *et al.*, 2006, Olukman *et al.*, 2012, Khames *et al.*, 2014). These differences might be due to the method of preparation of the beads. If the drug is completely dissolved in the SAL mixture, then there

will most likely be the absence of drug peak on the scan, however, if the drug is not soluble in the SAL and was just dispersed in the polymer solution as in this study, the drug peak should be detected.

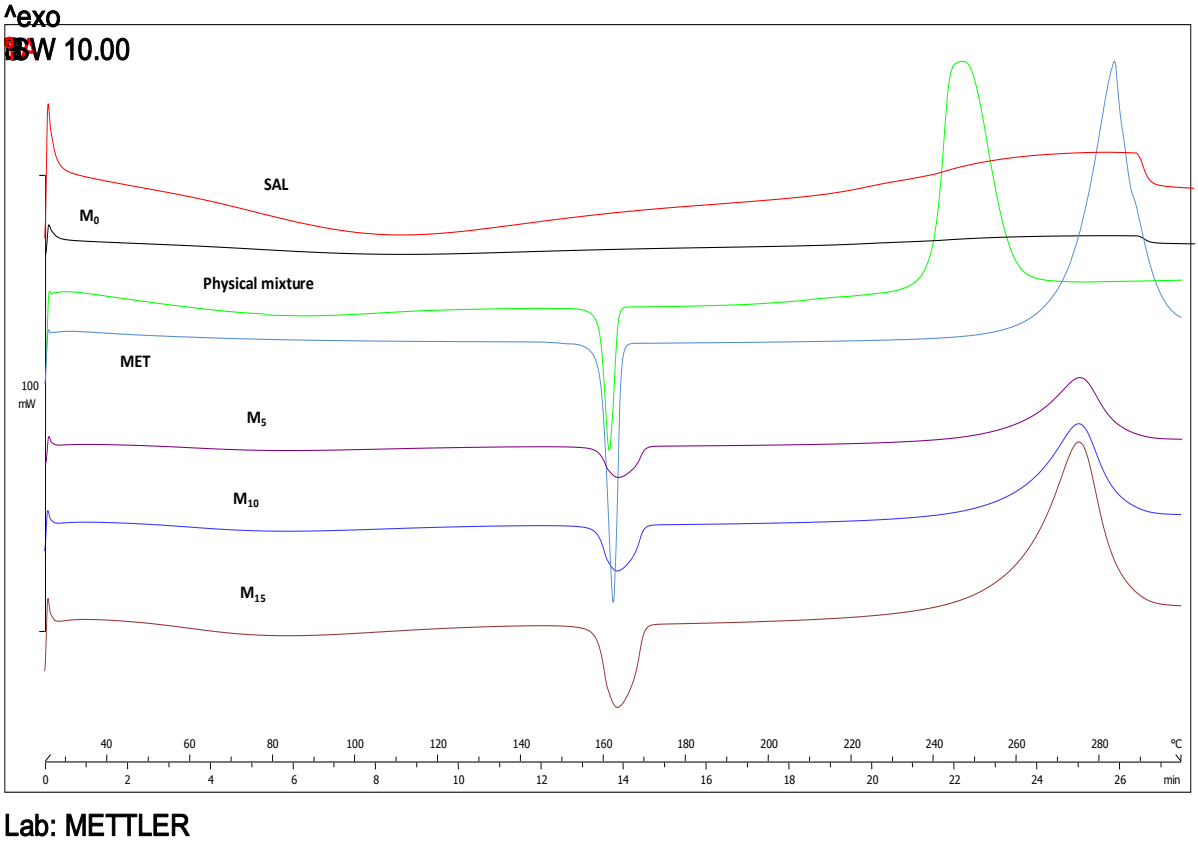

Figure 3-22: DSC thermograms of SAL, MET, physical mixture of SAL and MET, unloaded and MET- loaded beads

3.3.3.5 Powder X-ray diffraction analysis of metronidazole beads

The diffractograms of SAL and M_0 did not show any sharp peaks reflecting their amorphous nature. MET exhibited a P-XRD pattern of a highly crystalline material with no amorphous component with peaks at 12°, 14°, 17°,18°, 24°, 27°, 29°, 33° 2θ which may be attributed to the highly ordered molecular structure (Gates, 1999, Ramukutty and Ramachandran, 2012, Giri *et al*., 2013, Singh *et al.*, 2014). The P-XRD pattern of the physical mixture of SAL and MET (Figure 3-23) showed similar characteristic peaks observed in MET, though the intensity of the peaks was markedly reduced. This reduction in intensity was also observed for MET-loaded beads with MET retaining its crystalline nature in the beads. The reduction in intensity was because the proportion of polymer was higher relative to the proportion of drug in the formulation. This reduction in intensity of drug peaks on incorporation into polymer matrices have been reported by several authors (Singh *et al.*, 2014, Fontes *et al.*, 2013, Tabbakhian *et al.*, 2014, Chatap *et al.*, 2013, Rajendran and Basu, 2009, Moreira *et al.*, 2014). The absence of any significant changes in the position of the peaks indicates that the drug maintained its crystallinity in the polymer (further confirming results from the DSC studies) and the absence of polymer-drug interaction and the physical stability of the drug in the matrix. Some researchers also reported the absence of drug characteristic peaks in drug-loaded formulations due to the molecular dispersion of the drug in the polymer matrix, which were in good agreement with the DSC (Giri *et al*., 2013, Mandal *et al.*, 2010, Mladenovska *et al*., 2007).

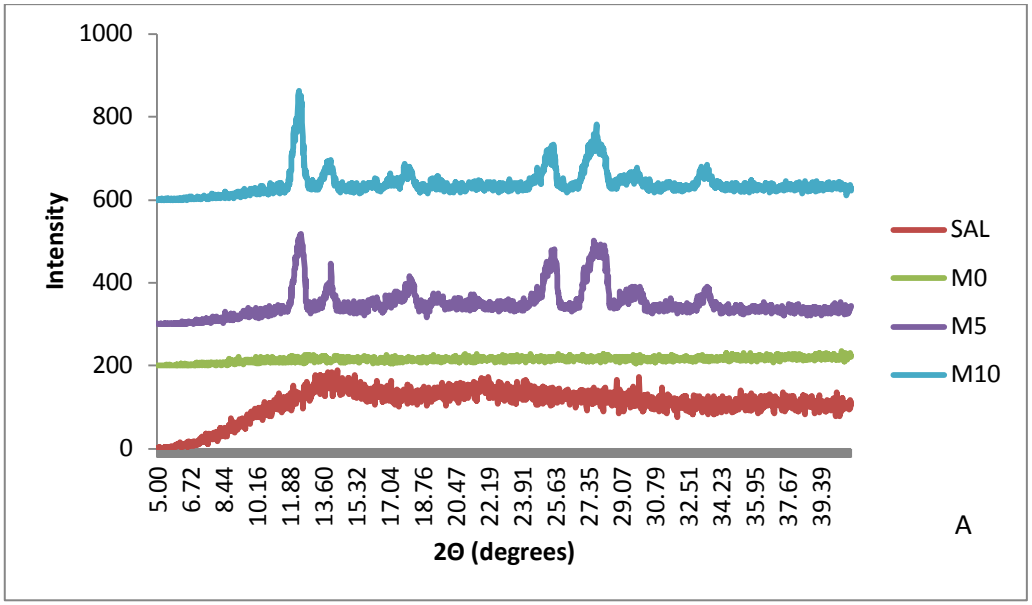

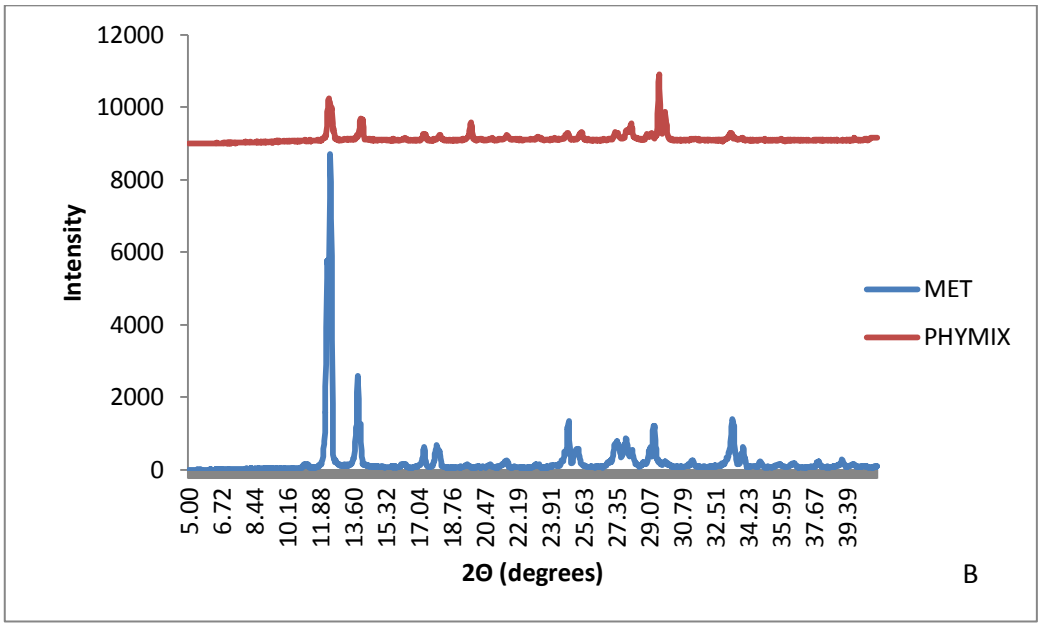

Figure 3-23: P-XRD of SAL, MET, physical mixture of SAL and MET, unloaded and MET- loaded beads

3.3.3.6 Fourier transform infrared (FT-IR) analysis of metronidazole beads

Characteristic bands of M_0 in Figure 3-24, were at 3418.2 cm^{-1} representing the O - H band, 1607.1 cm^{-1} and 1428.6 cm^{-1} representing the asymmetric band of the carboxylate ion (Lawrie *et al*., 2007)**,** the band at 1034.9 cm^{-1} is given by the guluronic units (Pereira *et al*., 2003), and 823.5 cm^{-1}, identified in the literature as the combination of three possible vibrational modes (tCO+dCCO+dCCH) (Dupuy *et al.*, 1994). The FTIR spectra of MET shows characteristic vibrational peaks such as O − H str*et*ch (3201.3 cm^{-1}), C = CH (alkene) stretch (3098.7cm^{-1}), NO_2, N − O (nitro) stretch (1534.1 cm^{-1}; 1367.2 cm^{-1}), CH_2/CH_3 (alkane) (2844.8 cm^{-1}; 2940.3cm^{-1}), C – N (imines) (1158.2 cm^{-1}, 1264.5 cm^{-1}) C − OH, C − O bend (1072.3cm^{-1}; 1426.9 cm^{-1}), C − NO_2, C − N stretch (824.6cm^{-1}) (Silverstein and Webster, 1996, Sravani *et al*., 2011, Al-Abdulla *et al*., 2012, Choudhury *et al*., 2012, Ramukutty and Ramachandran, 2012). M_{10} beads showed similar bands to that of the pure drug and SAL with no significant change in the wavenumber of the peak bands. The O - H stretch (3217.5 cm^{-1}), C = CH, C − H stretch (3100.6 cm^{-1}), NO_2, N − O stretch (1538.2 cm^{-1}; 1372.8 cm^{-1}), CH_2/CH_3 (2857.5 cm^{-1}; 2932.1 cm^{-1}), C - N (1160.4 cm^{-1}, 1267.0 cm^{-1}) C − OH, C − O bend (1075.7 cm^{-1}; 1431.4 cm^{-1}), C − NO_2, C − N stretch (826.4 cm^{-1}) characteristic of MET were present in the drug loaded beads (M_{10}). Previous studies observed the presence of similar peak bands of encapsulated drug in formulations (Mandal *et al.*, 2010, Verma *et al*., 2013, Olukman *et al.*, 2012, Fontes *et al.*, 2013, Halder *et al*., 2005, Kulkarni *et al.*, 2001) confirming the stability of the drug in the formulations and the absence of any chemical interactions between the drug and the polymer. This further confirms results observed from the DSC and P-XRD analysis.

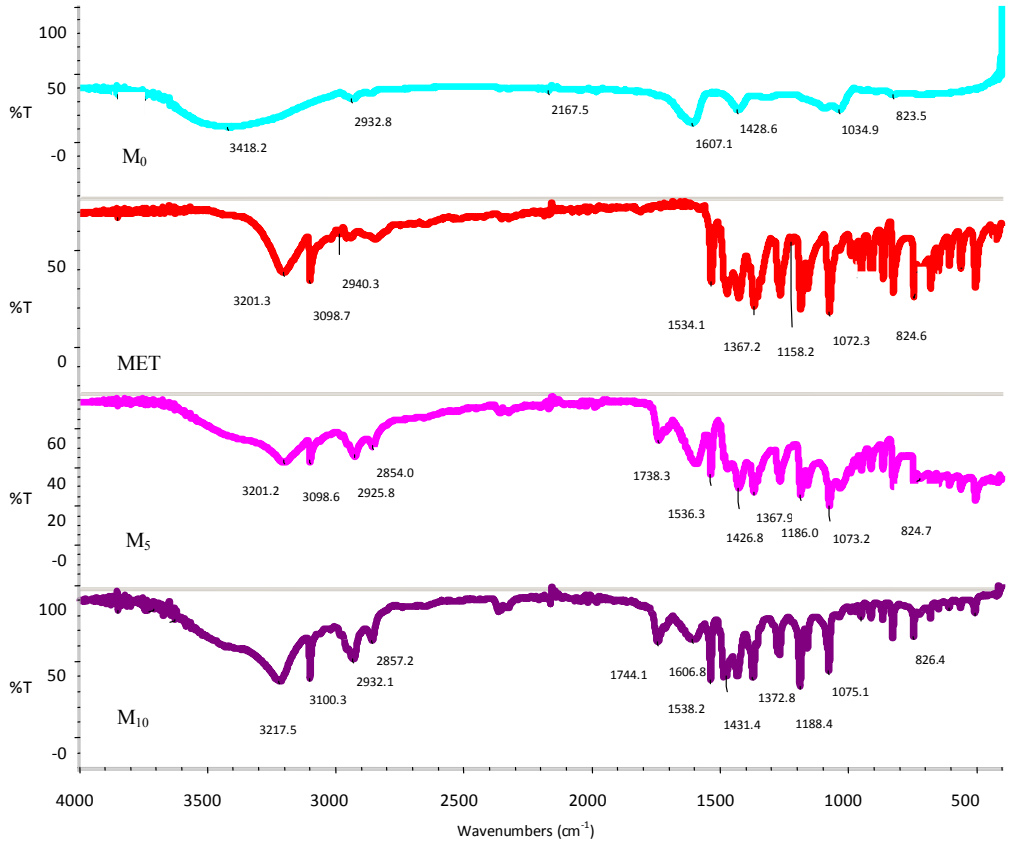

Figure 3-24: FTIR scans of MET, unloaded and loaded bead samples

3.3.3.7 *In vitro* buoyancy lag time and duration of metronidazole beads

On contact with the medium, the beads floated almost immediately with the floating lag time ranging between 2 and 3 minutes. Several of the beads began to sink with agitation as a result of water absorption into the beads. All samples both blank and drug loaded, failed the test

because on visual inspection after the first hour, between 10 – 55 % of the beads sank and at subsequent time intervals with increased water absorption into the beads, the proportion of beads sinking continued to increase. After a 12 hour period, more than 40 - 80 % of all the bead formulations sank and after 24 hours, the percentage of beads floating was just between 5 – 40 % (Table 3-5). Due to the low bulk density of the beads (0.11 - 0.26 g/cm^3), they were expected to float on the medium for a longer period. This indicated that, even though bulk density is a major criterion for floating formulations, it is not a good predictor of the lasting buoyancy of a formulation because the magnitude of floating strength may vary as a function of time and gradually decrease on contact with fluid as a result of development of a hydrodynamic equilibrium (Bhardwaj and Harikumar, 2013). This result is consistent with the findings of Murata *et al* (2000), where the blank beads steeped in water, physiological saline (0.9 % NaCl) or HCl sank in these media. Other studies also corroborated this observation (Choi *et al*., 2002, Ishak *et al*., 2007, Bera *et al*., 2009) with only beads modified with oil, magnesium stearate, CO_2 gas forming agents ($CaCO_3$ or $NaHCO_3$) respectively floating for the duration of the studies. However, some other studies reported buoyancy for alginate beads (Whitehead *et al*., 1996, Whitehead *et al*., 1998, Stops *et al*., 2008). Stops *et al* (2008) reported that the alginate beads floated for more than 13 hours, with the buoyancy determined using the resultant weight apparatus, which measures a change in the weight of objects when in an immersed condition as a function of time (Timmermans and Moës, 1990). This method is different from the visual method used in this study and the other studies quoted above, so this may account for the difference in results. The presence of drug impaired the buoyancy of the beads ($p < 0.05$) with less drug-loaded beads floating compared with the blank beads especially at high drug – polymer ratios over time. It should be noted, however, that blank beads also sank in the medium. These beads have a short lag time to onset of floating, but a shorter lag time is desirable so that the beads are not emptied from the stomach before the onset of floating. It can be inferred that the voids in the beads were insufficient to maintain the buoyancy of the beads, which may be as a result of water

penetrating into the beads and filling the inert pores, thereby increasing the density of the beads beyond that of the media in which the beads were dispersed. Based on the results obtained, it is assumed that on oral administration, the bead formulation will sink to the bottom of the stomach within a short time interval and will be evacuated from the stomach before completely releasing their drug content at the target site.

Table 3-5: Floating profile of unloaded and MET-loaded beads

Sample	Lag time (min)	%Floating (1h)	% Floating (12h)	% Floating (24h)
M_0	< 3	80 ± 10	50 ± 10	30 ± 10
$M_{0.5}$	< 3	85 ± 15	60 ± 15	30 ± 5
M_1	< 3	70 ± 5	40 ± 10	30 ± 5
M_2	< 3	85 ± 10	40 ± 5	20 ± 5
M_3	< 3	65 ± 10	45 ± 10	10 ± 5
M_5	< 3	65 ± 5	25 ± 5	10 ± 5
M_{10}	< 3	55 ± 10	30 ± 5	15±5
M_{15}	< 3	50 ± 15	30 ± 10	15 ± 10

3.3.3.8 Swelling profile of metronidazole beads

Swelling of the beads is mainly attributed to the hydration of the hydrophilic groups of alginate (Hoffman, 2002). Free water penetrates into the beads filling the inert pores, thereby contributing to a greater swelling degree. In PBS (pH 7.4), M_0 showed peak swelling of about 2500 % weight change at ~ 120 minutes, after which time, the beads started to disintegrate, leading to a reduction in weight beyond 120 minutes (Figure 3-25a). Increasing the drug-polymer ratio slightly reduced the swelling of the beads ($p > 0.05$) with M_5 and M_{10} exhibiting maximum swelling of ~ 2200 % and 2100 % respectively. The swelling and degradation in alkaline pH occurs due to several mechanisms:

- the displacement of Ca^{2+} ion binding (mainly in the poly-mannuronate sequences at the initial stage) by Na^{+} ions in PBS through an ion –exchange process. This leads to an increase in the electrostatic repulsion between the ionized $–COO^{-}$ (Bajpai and Sharma, 2004). At the latter stages, the ion exchange occurs in the polyguluronate sequences; this is because the polyguluronate sequences have a strong auto-cooperative binding of Ca^{2+} ions (Smidsrød, 1974) and serve as a stable cross-linking structure within the gel, while the polymannuronate sequences show no specificity for ion binding (Kikuchi *et al.*, 1999) The hydrogen bonds between $-COO^{-}$ and H_2O are formed, causing the beads to absorb water and swell.
- the sequestering effect of phosphate on Ca^{2+}, which makes the calcium alginate gel structure loose and soluble. This solubility is due to the formation of calcium phosphate and causes turbidity in the medium (Bajpai and Tankhiwale, 2006).

In PBS, the water uptake and swelling seem to be due to the presence of sodium and phosphate in the buffer and not the pH of the media. Bajpai and Sharma (2004), reported almost no swelling of beads in a Tris-HCl buffer (pH 7.4), thus supporting the hypothesis that

water uptake of beads is due to ion exchange between Ca^{2+} ions and Na^{+} ions from the sodium phosphate buffer.

In HCl, it was observed that there was limited swelling of the hydrogels and water uptake was low and independent of time, relative to the observed uptake in PBS. Swelling did not exceed ~ 330 % of the original size and they remained at this size, without disintegrating, throughout the study period (Figure 3-25b). When these beads are steeped in media with a pH < 4.0, the Ca^{2+} ions are displaced from the alginate network and the carboxyl residues of alginate are protonised to alginic acid (Østberg *et al.*, 1994, Pasparakis and Bouropoulos, 2006). The presence of MET also reduced the degree of swelling in acidic media with M_0 beads exhibiting maximum swelling of ~ 350 % weight change, while M_5 and M_{10} exhibited maximum swelling of ~ 250 % and 150 % weight change respectively.

This conversion to alginic acid may cause disruption to ionic linkages with the electrostatic repulsion, resulting in the shrinkage of the bead matrix. The swelling profiles in both media suggest that the beads will swell slightly in the acidic stomach and as they move down the GI tract into the more alkaline small intestine, the beads will begin to swell more and ultimately disintegrate in the large intestine. Since this polymer does not degrade in acidic media, it reduces the risk of dose dumping or excessive swelling of polymer in the stomach.

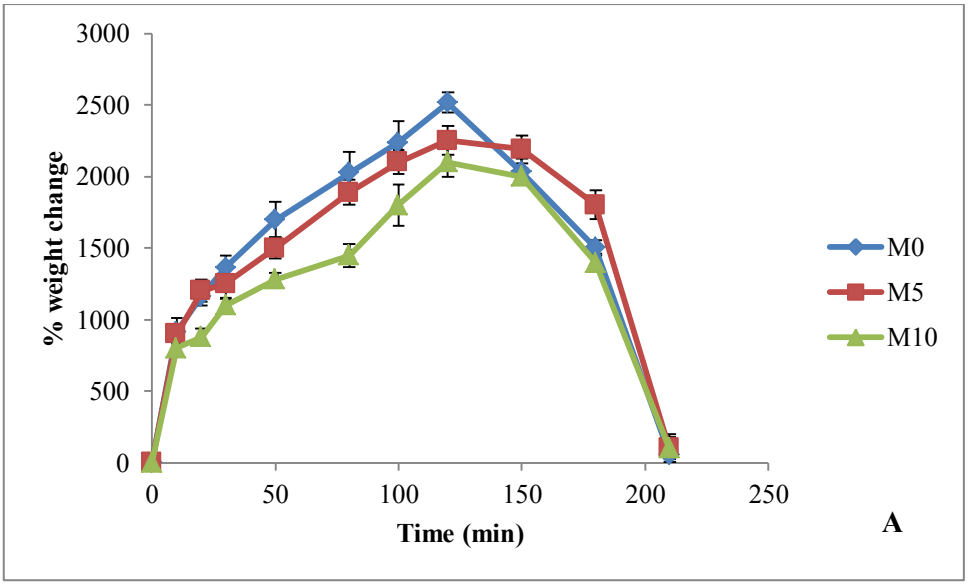

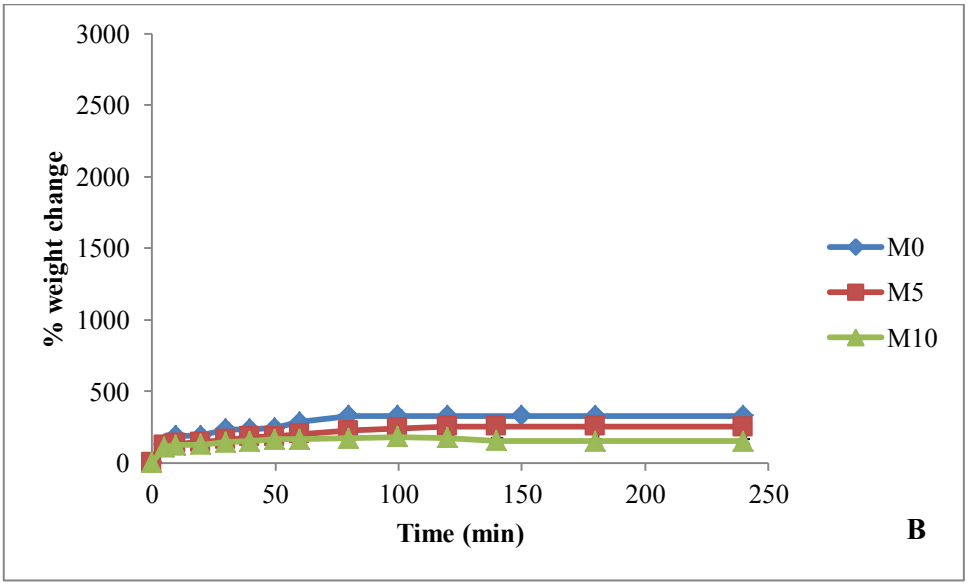

Figure 3-25: Swelling profile of unloaded and MET- loaded beads in a) PBS and b) 0.1N HCl

3.3.3.9 Determination of calcium ion release in PBS

The release of Ca^{2+} from the beads was determined in order to correlate the Na^{+}/Ca^{2+} ion-exchange process with the swelling profile of the beads through AAS (Kikuchi *et al*., 1999). Another method which has been used to assess Ca^{2+} release from calcium alginate complexes is the EDTA method (Chen and Wang, 2001, Bajpai and Sharma, 2004). The Ca^{2+} ion content of the beads was released over a period of 150 minutes for beads analysed in PBS (Figure 3-26). In M_0, there was ~ 50 % Ca^{2+} release within 30 min with the remaining Ca^{2+} ions being released over the next 120 min. A slightly slower release was observed between 20 and 60 min after which time, the release rate increased. These times correlate with the swelling profiles of the beads in PBS. Time for complete release of Ca^{2+} ions coincides with the time for complete disintegration of the beads. The presence of drug retarded the Ca^{2+} release ($p < 0.05$), which may be as a result of the drug limiting the exposed surface area of the bead matrix to the buffer. It has been reported that Ca^{2+} ions are present in two different environments within the calcium alginate gel. The first set of Ca^{2+} ions is found within the buckled egg box junction reacting with the polyguluronate sequences. The phenomenon of the egg-box junction is detailed in section 3.1. The second set of Ca^{2+} ions are those interacting with other carboxylate anions within the polymer, *i.e*. the polymannuronate sequences. The amount of Ca^{2+} released over time depends on the guluronic /mannuronic composition of the alginate (Bajpai and Sharma, 2004). The ratio of mannuronic acid to guluronic acid residues of the alginate used in this study is 1.56, therefore indicating that the alginate contains ~ 60 % mannuronic acid and 40 % guluronic acid. As the Na^{+} ions from the PBS penetrate the gel bead, the Ca^{2+} ions bound to the mannuronic acid content, estimated to be ~ 60 % of the Ca^{2+} ion load of the bead is released during the first stage. This is the slow release observed within the first 60 minutes of the release study and is mainly diffusion controlled being proportional to the square root of time (Figure 3-26). There was negligible alginate disintegration probably due to the relatively stable association of Ca^{2+} ions with polyguluronate sequences, which serve as cross-linking points within the gels. There is also the possibility of the released Ca^{2+} ions re-binding to polyguluronate sequences (Kikuchi *et*

al., 1999). In the latter stage, the remaining ~ 40 % Ca^{2+} ion load involved in the formation of the egg-box junction starts to exchange with Na^{+} and diffuse outward into the release medium. There is a slow dissociation of Ca^{2+} ions from the polyguluronate sequence accounting for the initial slow release of Ca^{2+} ions in the first 60 min before the rapid release apparent after 60 min. It is at this stage of final calcium release that the disintegration of the gel bead starts to occur due to excessive swelling of the gels as a result of the electrostatic repulsion between the carboxylate anions (Yotsuyanagi *et al*., 1991, Sugawara *et al*., 1994, Kikuchi *et al*., 1999). This electrostatic repulsion causes the dissociation of the gel into soluble alginate molecules (Kikuchi *et al*., 1999).

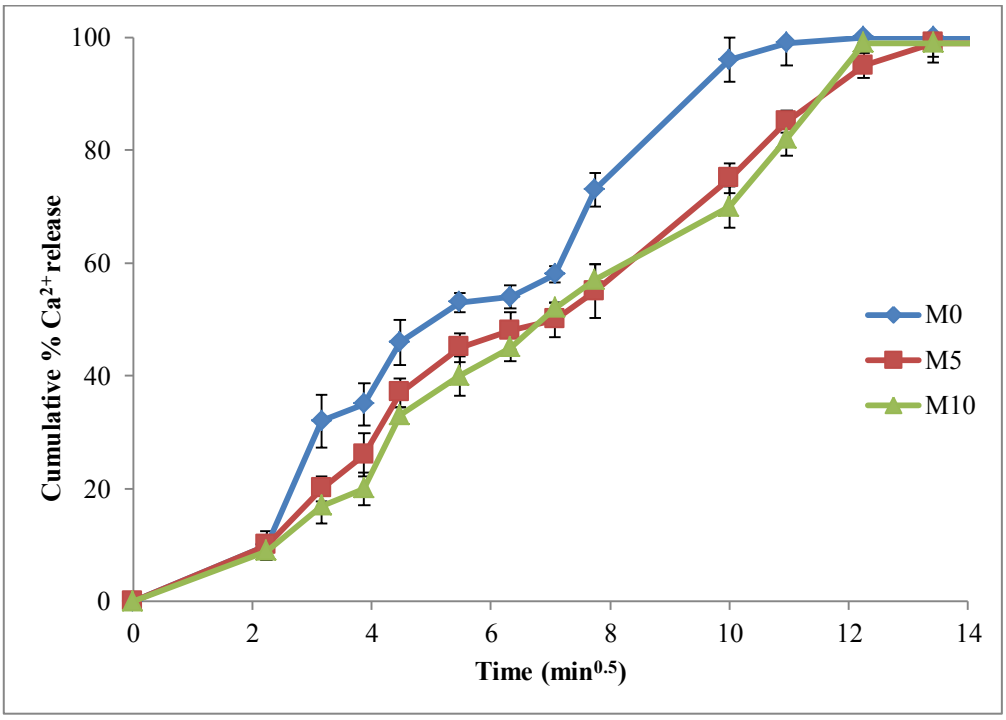

Figure 3-26: Calcium ion release from MET-loaded beads in PBS

3.3.3.10 *In vitro* drug release of metronidazole from beads

The release of drug from the beads was assessed across a range of pHs to represent the pH range of the stomach in the fed (pH 1.2) and fasted state (pH 4.0). In addition, drug release was assessed in intestinal pH (pH 7.4).

3.3.3.10.1 Release of metronidazole from beads in acidic medium – (0.1N HCl (pH 1.2) and acetate buffer (pH 4)

The dissolution of the unencapsulated drug was rapid at pH 1.2, with complete dissolution achieved within 5 minutes (Figure 3-27a). Drug release from the beads at this pH was fast and most of the drug content was released over a period of 3 h, with a larger proportion of the release occuring in 2 h. There was no difference in the dissolution profiles of the unencapsulated drug and beads with low drug-polymer ratios ($M_{0.5}$ – M_1). There was more than 90 % release within 10 minutes with $M_{0.5}$ – M_1 beads, and there was complete release of MET from these beads after 30 minutes. There was no significant difference between the release from these beads at low drug-polymer ratio. This is probably due to the low drug content of the beads which limits the lifetime of the DDS and easy diffusion of water into the beads through the less occupied spaces within the bead leading to a faster drug dissolution and diffusion out of the beads. At higher drug-polymer ratios (M_5 - M_{15}), drug release decreased ($p < 0.05$), with ~ 60 % , 55 % and 50 % drug released after 10 min with M_5, M_{10} and M_{15} beads, respectively. Also, after 30 minutes, drug release was ~ 80 %, 69 % and 65 % with M_5, M_{10} and M_{15} beads, respectively. In comparison, the release profile of M_5 and M_{10} (f_2 = 54.6) ; M_{10} and M_{15} (f_2 = 64.9) were similar, however there was a significant difference in the release profiles of M_5 and M_{15} (f_2 = 44.7). The difference in the release profiles of M_5 *versus* M_{15} highlights the effect of drug content on the rate of drug release from calcium alginate beads, with beads containing more drug releasing drug at a slower rate compared to faster rate of drug release from beads containing less drug. This reduction in release rate with

an increase in drug-polymer ratio was also reported by Basu and Rajendran (2008). Drug release profiles from the beads at pH 4.0 (Figure 3-27b) was similar to that observed at pH 1.2, but was at a slightly slower rate ($p > 0.05$) (Table 3-6), with an initial burst release and a subsequent slow release. In comparison, the release profiles of M_{10} at pH 1.2 and pH 4.0 (f_2 = 59.1) and M_{15} at pH 1.2 and pH 4.0 (f_2 = 59.9) were similar , however the release profiles of M_5 at both pHs were different (f_2 = 47.1). This difference observed in release from M_5 can only be due to the difference in solubility of MET in the different media and the effect of the high drug content of M_{10} and M_{15} was more dominant than the effect of pH. Overall, drug release from the beads was biphasic, with an initial burst release, followed by a slower release (Figure 3-26; Table 3-6). The initial part of drug release is driven by two concurrent mechanisms, *i.e.* swelling (Figure 3-25b) and diffusion (Pasparakis and Bouropoulos, 2006). An initial high burst release reduces the effective lifetime of a drug delivery device (Huang and Brazel, 2001). Drug released at this stage may not be utilised effectively leading to drug wastage. The major causes of burst release in formulations include, surface adsorption of drug molecules on the matrix, uneven distribution of drug within the matrix (observed in these beads in section 3.3.3.1), and porous matrix morphologies (Kim and Park, 2004). In this case, due to the hydrophilic nature of MET, it rapidly diffuses out to the outermost layers and the surface of the bead structure during the curing period; therefore burst release is the release of the adsorbed particles of drug left on or near the surface of the beads during the curing and freeze-drying period. The second phase of drug release was a more moderated release as a result of slow diffusion of the entrapped drug from the core of the alginate matrix with the swelling of the beads at this stage being relatively constant (Figure 3-25b) (Pasparakis and Bouropoulos, 2006). This biphasic pattern of drug release is typical of matrix diffusion kinetics (Rajinikanth and Mishra, 2008). Drug release from alginate beads has been said to be governed mainly by the solubility of the drug in the dissolution medium and not dependent on the gel properties of the beads (Patel *et al.*, 2006). This means that the more soluble the drug is in the acidic media, the faster the drug release rate as observed with the MET beads.

MET solubility at pH 1.2 was determined to be 59.7 ± 0.9 mg/ml (section 3.3.1.4) and a combination of this high solubility in acidic media, the existence of sink conditions and the porous nature of the alginate beads (Fennema, 1975), all contributed to fast MET release. Another reason for this is the physical state of the drug in the beads. It has been reported that drug suspended in SAL is rapidly released from the beads than when the drug is dissolved in SAL (Whitehead *et al.*, 2000). Rapid drug release observed from these beads is similar to that observed by other researchers (Østberg *et al*., 1994, Murata *et al*., 2000, Whitehead *et al*., 2000, Pasparakis and Bouropoulos, 2006, Patel *et al*., 2006). Murata *et al* (2000) reported complete MET release from the beads within 30 minutes while Whitehead *et al* (2000) observed ~ 80 % amoxycillin release within 80 minutes.

Table 3-6: Release parameters of MET-loaded beads

	$t_{25\%}$ (min)	$t_{50\%}$ (min)	$t_{75\%}$ (min)	$t_{25\%}$ (min)	$t_{50\%}$ (min)	$t_{75\%}$ (min)
Formulation		pH 1.2			pH 4.0	
$M_{0.5}$	< 5	< 5	< 5	< 5	< 5	< 5
M_1	< 5	< 5	< 5	< 5	< 5	< 5
M_2	< 5	< 5	< 5	< 5	< 5	5 - 10
M_3	< 5	< 5	5 - 10	< 5	< 5	15 - 20
M_5	< 5	5 - 10	15 - 20	< 5	10 - 15	30 - 40
M_{10}	< 5	5 - 10	30 - 40	< 5	10 - 15	40
M_{15}	< 5	10 - 15	50 - 60	< 5	15 - 20	50

3.3.3.10.2 Release kinetics of metronidazole from beads in acidic medium (pH 1.2)

It is important to study drug release kinetics as this has a strong influence on drug bioavailability, dosage intervals and the development of toxic side effects (Shah *et al.*, 1998). On examination of the coefficient of determination (R^2) of the various plots of the drug release models, it was observed that the release kinetics followed a diffusion-controlled mechanism. The *in vitro* release data was in favour of Higuchi-diffusion kinetics (R^2 = 0.96 – 0.99) (Table 3-7). The Higuchi square root equation describes drug release from systems where the solid drug is dispersed in an insoluble matrix, and the rate of drug release is related to the rate of drug diffusion. This model is consistent with the release of drug from a granular or porous matrix (Whitehead *et al.*, 2000). The Higuchi model has previously been used to describe drug release from alginate beads (Murata *et al.*, 2000, Rajinikanth and Mishra, 2008, Bera *et al.*, 2009, Jahan *et al.*, 2012). The 'n' value, which is indicative of drug release mechanism, was < 0.43, indicating Fickian diffusion.

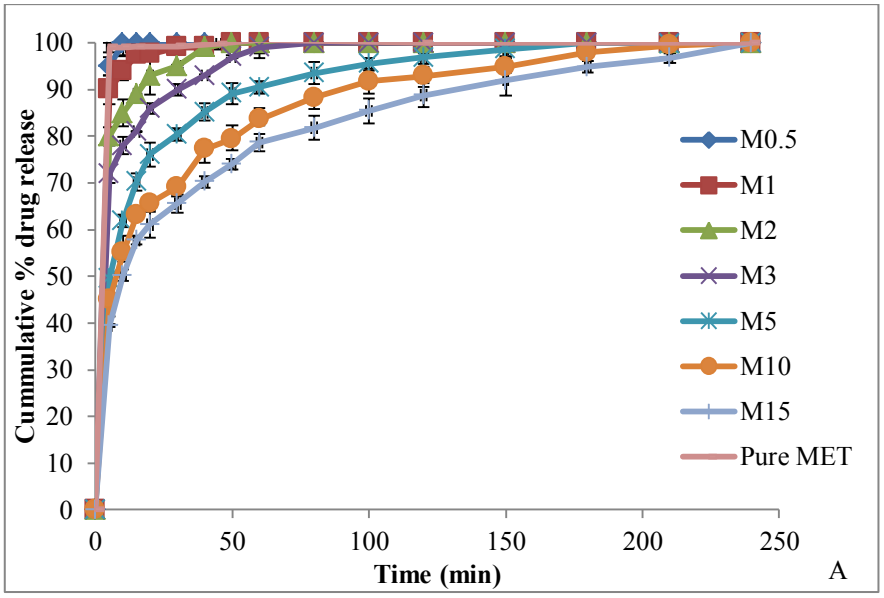

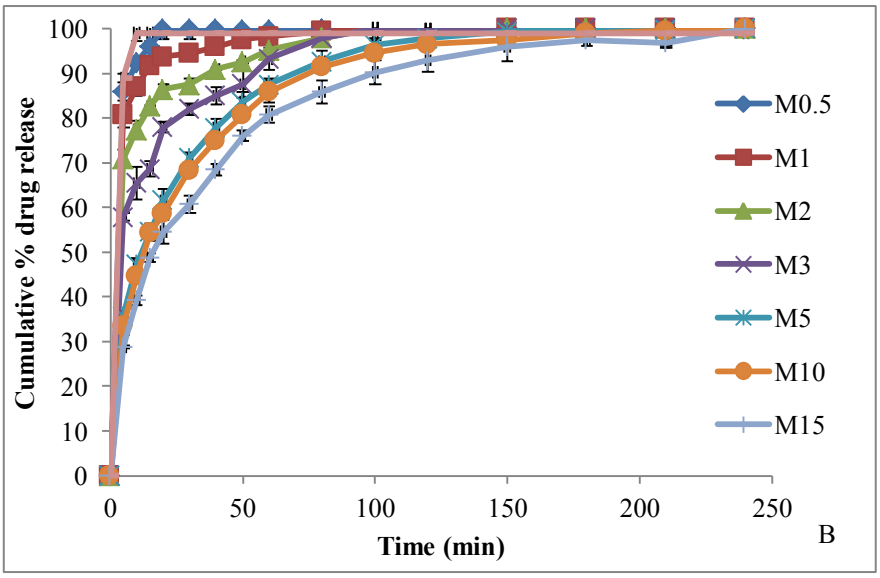

Figure 3-27: Release of MET from beads in A) 0.1N HCl (pH 1.2) and B) acetate buffer (pH 4.0)

Table 3-7: Release kinetics of beads in 0.1N HCl (pH 1.2)

Code	Zero order		1st order		Higuchi		Hixson-Crowell		Peppas	
	$K_0(min^{-1})$	R^2	$K_1(min^{-1})$	R^2	$K(min^{1/2})$	R^2	k	R^2	n	R^2
M_2	0.603	0.913	0.025	0.974	4.827	0.988	0.041	0.959	0.101	0.986
M_3	0.711	0.958	0.018	0.981	5.620	0.989	0.035	0.985	0.125	0.989
M_5	1.198	0.885	0.016	0.952	9.684	0.985	0.039	0.932	0.279	0.982
M_{10}	0.921	0.845	0.009	0.893	7.507	0.968	0.026	0.878	0.247	0.966
M_{15}	0.997	0.878	0.009	0.925	8.075	0.981	0.026	0.910	0.289	0.978

3.3.3.10.3 Release of metronidazole from beads in alkaline medium – phosphate buffered saline (pH 7.4)

Drug release in PBS was also biphasic, similar to drug release in acidic media (pH 1.2), however, the order was reversed with an initial slow release followed by a subsequent fast release. The initial slow release was probably due to reduced solubility of MET in this media, which was determined to be 8.4 ± 0.4 mg/ml, which is significantly lower than the solubility at pH 1.2. Overall, there was a significant difference in the MET release profiles in both media (pH 1.2 and 7.4), and comparison of release profiles of M_5, M_{10} and M_{15} beads in both media yielded f_2 values of 34.4, 45.1 and 45.0, respectively. Drug release was mostly complete within 150 minutes for all beads (Figure 3-28) (Table 3-8). This correlates with the swelling studies, where disintegration of the beads which enhances drug release starts to occur at ~ 120 minutes, but prior to this time, the beads are swollen allowing easy access of

water into the bead through the pores, allowing easy diffusion of the drug out of the beads through these pores. Drug release from alginate beads in alkaline media has already been reported to be controlled by the swollen gel (Patel *et al.*, 2006), rather than by diffusion as observed in acidic medium with the swelling increasing the pore size/volume thereby ensuring fast drug release (Al-Kassas *et al.*, 2007). Beads agglomerate on contact with the alkaline medium and after about ~ 120 minutes, they started to dissolve completely and were completely dissolved within 180 minutes. This is unlike the observation in acidic medium where the beads remained intact for the entire period of the dissolution test.

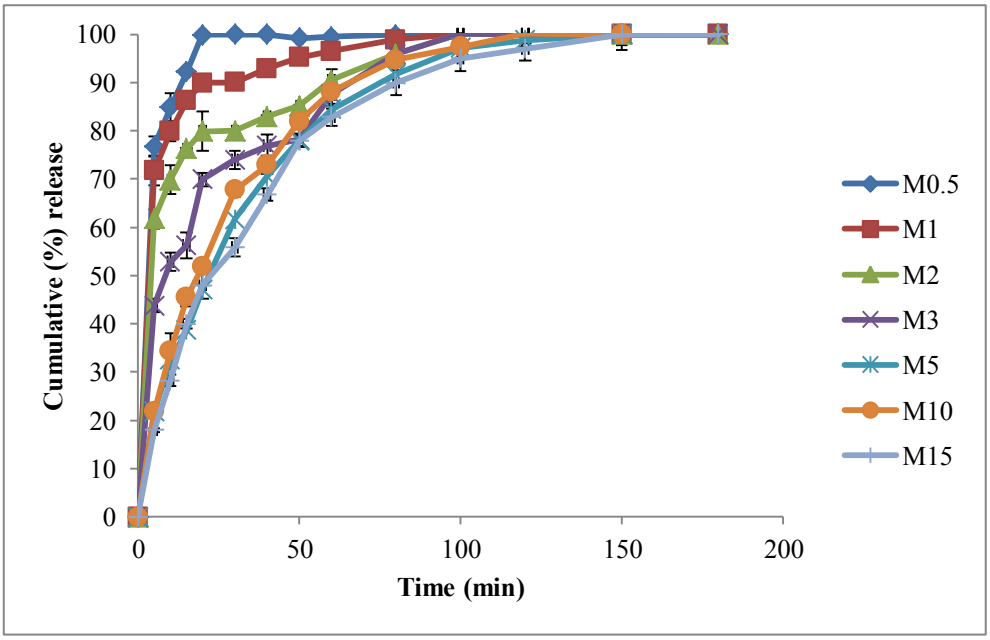

Figure 3-28: Release profile of metronidazole from beads in PBS

Table 3-8: Release parameters of MET-loaded beads

Formulation	$t_{25\%}$(min)	$t_{50\%}$(min)	$t_{75\%}$ (min)
$M_{0.5}$	< 5	< 5	< 5
M_1	< 5	< 5	5-10
M_2	< 5	< 5	10 - 15
M_3	< 5	5 - 10	30 - 40
M_5	5 - 10	20 - 30	40 - 50
M_{10}	5 - 10	15 - 20	40 - 50
M_{15}	10 - 15	30 - 40	60 - 80

3.3.3.10.4 Release kinetics of metronidazole beads in PBS

The release kinetics of MET from beads in PBS followed Higuchi kinetics with the release exponent 'n' being less than 0.43, indicating Fickian diffusion for beads with a low drug-polymer ratio (M_2 and M_3). At high drug-polymer ratios (M_5, M_{10} and M_{15}), n < 0.85 indicating non-Fickian diffusion (Table 3-9), thus, both diffusion and swelling controlled drug release. Therefore, increasing the drug-polymer ratio changed the drug release kinetics of the formulation in PBS, unlike release kinetics in acidic media, which was constant for all drug-polymer ratios. Once the beads leave the acidic environment of the stomach into the less acidic enviroment of the small intestine and colon, the beads dissolve in the fluid of the intestines, through which it is readily eliminated from the body.

Table 3-9: Release kinetics of beads in PBS (pH 7.4)

Code	Zero order		1st order		Higuchi		Hixson-Crowell		Peppas	
	$K_0(min^{-1})$	R^2	$K_1(min^{-1})$	R^2	$K(min^{1/2})$	R^2	k	R^2	n	R^2
M_2	1.217	0.974	0.019	0.994	8.249	0.998	0.044	0.989	0.188	0.995
M_3	1.637	0.949	0.017	0.914	10.819	0.992	0.045	0.928	0.309	0.922
M_5	1.563	0.995	0.012	0.993	12.116	0.995	0.036	0.996	0.569	0.991
M_{10}	1.795	0.983	0.015	0.996	14.072	0.998	0.043	0.996	0.631	0.993
M_{15}	1.343	0.954	0.011	0.988	11.901	0.991	0.032	0.981	0.634	0.989

3.3.3.10.5 Effect of calcium concentration and curing time on metronidazole release

Increasing $CaCl_2$ concentration did not have a major effect on MET release from the beads ($p > 0.05$) with the beads cross-linked with 0.07 M and 0.34 M $CaCl_2$ showing similar fast MET release profiles (f_2 = 55 - 66) (Figure 3-29a). This further confirms the similarity in DEE of beads cured at both concentrations (Figure 3-16). During bead formation, a high concentration of $CaCl_2$ may cause the development of a densely cross-linked polymeric layer on the surface of droplets thereby preventing Ca^{2+} ions diffusion into the bead core, which subsequently may lead to the formation of beads with partially reacted cores. These might be the reason for the similarity in the release profiles of beads cured with both concentrations of $CaCl_2$. Even though the beads cured with 0.34 M $CaCl_2$ contained ~ 30 % more Ca^{2+} ions than those of 0.07 M $CaCl_2$, these did not have an impact on drug release. These results are similar to the observation of Basu and Rajendran (2008), where increasing $CaCl_2$ from 2 to 5 % led to an even faster nateglinide release from the beads which may be as a result of the

increase in porosity and swelling properties of beads prepared with a higher concentration of $CaCl_2$. This is contrary to results obtained by Badwan and co-workers (1985) where the higher the concentration of $CaCl_2$, the slower the release of sulphamethoxazole from beads. Other studies also reported a decrease in drug release on increasing $CaCl_2$ concentration (Tavakol *et al.*, 2013, Rajalakshmi *et al.*, 2013).

Similarly, the curing time had little effect on MET release with the results obtained from the release profiles of beads cured for 30 minutes being similar to those cured for 5 and 15 minutes (Figure 3-29b). The f_2 values were between 64 - 94 for the M_5 and M_{10} beads. This result is similar to a study by Kim and Lee (1992), where there was little variation in blue dextran release from alginate gel beads cured for more than 6 minutes. However, it was contrary to results obtained by another study, where it was observed that beads cured for 5 minutes and 25 minutes gave a more rapid release rate, when compared with release rate of beads cured for 15 minutes (Patel *et al.*, 2006). This release profile was attributed to the porosity of the beads and surface deposition of leached drug. Overall, these results demonstrate that for a water-soluble drug like MET, its solubility in the dissolution media had more impact on its release from the beads than the calcium content of these beads and the extent of cross-linking in these formulations.

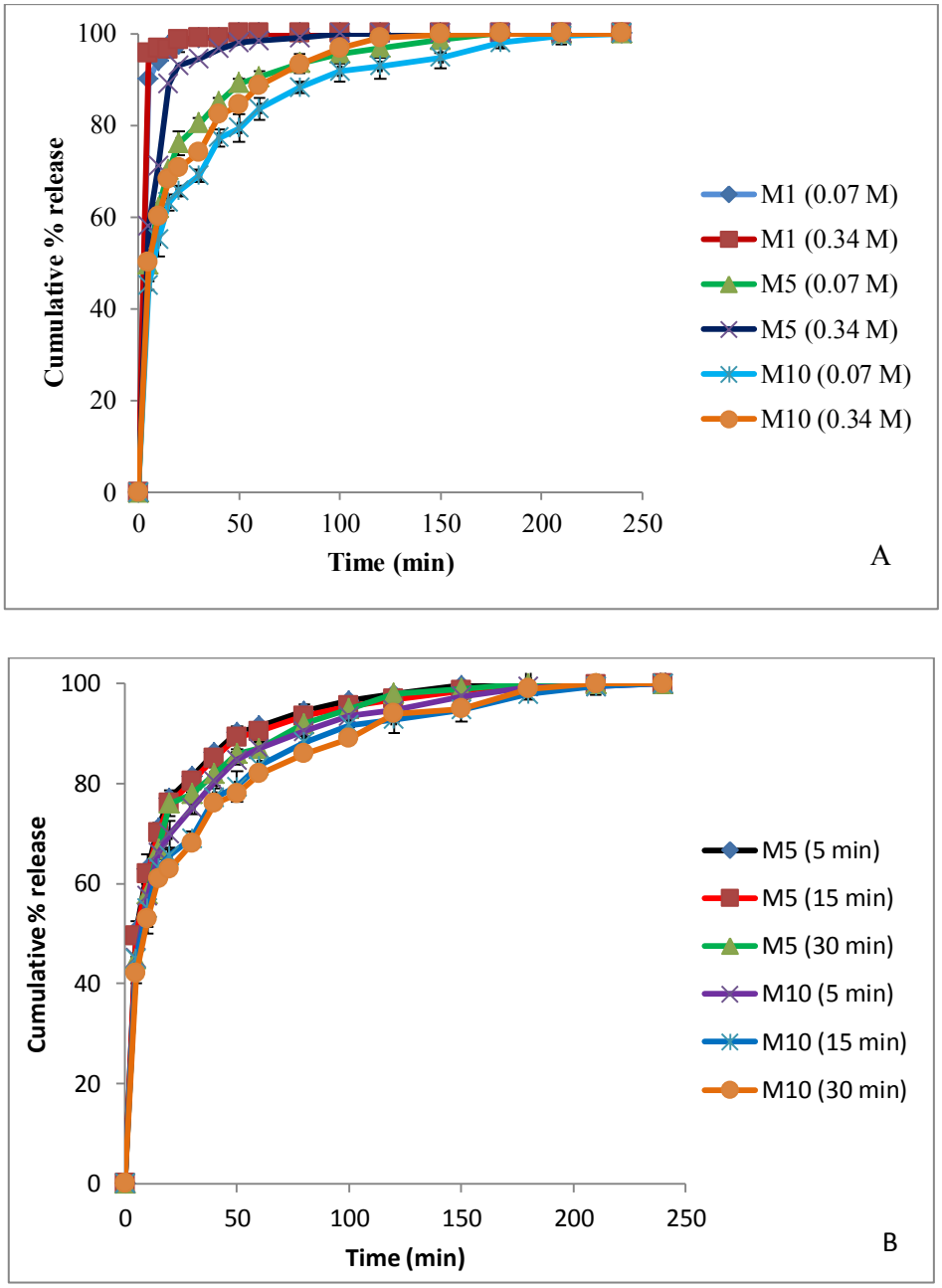

Figure 3-29: Comparison of release profiles of beads cured a) with 0.07 M and 0.34 M $CaCl_2$ and b) at times 5, 15 and 30 min

3.3.3.10.6 *In vitro* release of metronidazole beads in mucin suspension

Mucus contains mostly mucin, secretory IgA, lysozyme, lectoferrin, lipids, polysaccharides and ions. Pig gastric mucin was used because it is available commercially, well characterised and because pigs have a physiology similar to man. The bacteriostatic action of mucus is due to its non-mucin components (Allen and Snary, 1972). Non-mucin components are also reported to contribute to the "weakening" of mucus, as they interrupt fibre associations and also play a role in impeding solute transport (Bell *et al*., 1985, Sellers *et al*., 1987, Larhed *et al*., 1998). Mucins are negatively charged poly-electrolytes with heavily O-glycosylated serine/threonine-rich (Evans and Koo, 2009) glycoproteins that are responsible for the viscous and gel-forming nature of mucus (Allen and Snary, 1972, Meyer and Silberber, 1978). Mucins can be divided into two classes: the membrane bound mucins and the secreted mucins which differ based on the fact that membrane bound mucin contain a hydrophobic domain anchoring the molecules in the plasma membrane (Sigurdsson *et al.*, 2013) and also lack intermolecular associations through disulphide bridges (Hicks *et al*., 1998). Mucins contribute to a barrier layer through which foreign molecules *e.g.* drug molecules must diffuse to gain access to intracellular drug targets. The barrier function of mucus is dependent on the physicochemical properties of the drug and the tertiary conformation of the mucin, the latter also being dependent on environmental factors such as pH, ionic strength and the presence of other agents (Khanvilkar *et al*., 2001). Mucus presents a particular barrier to diffusion for drugs and nutrients with a capacity for binding. The mucus layer of the stomach is reported to be 50 - 600 µm (Lee and Nicholls, 1987, Norris *et al*., 1998, Khanvilkar *et al*., 2001) with the thickness of antral mucus being 200 µm (Gu *et al.*, 1988) and the target microorganism *H. pylori* reside in the mucus gel and at the mucus-epithelial cell surface (Hessey *et al.*, 1990). For many solutes, there is a reduction in effective diffusion coefficient and passive diffusion fluxes when they cross the mucus layer (Desai *et al.*, 1991, Korjamo *et al*., 2009). An administered antimicrobial drug would need to permeate through the gastric

mucus layer to reach the target microorganism in bactericidal concentrations. Therefore, the rate and extent of drug transport through gastric mucus can be an important determinant of the efficacy of a formulation and better represents and mimics *in vivo* dissolution of drug in the gastric lumen and its subsequent penetration into the gastric mucus layer than dissolution tests in SGF. In these experiments, a 3 % mucin solution was used due to this concentration being equivalent to mucin concentration in gastric mucus (Bansil *et al*., 2013). The saturated solution of MET (60 $mgml^{-1}$) at pH 1.2, had a 6-fold higher diffusion rate through mucus than drug encapsulated in the beads (Table 3-11). The concentration gradient between the donor and receiver solutions was the driving force for the diffusion of molecules between both solutions. The presence of mucin restricted the movement of drug as the flux was ~ 26 % lower than the flux observed with the 0.1N HCl. This is similar to an earlier study which reported ~ 25 % reduction in permeability of MET loaded chitosan microspheres in gastric mucin *versus* gastric fluid (Shah *et al.*, 1999). Also, diffusion into PBS was slower compared with that of 0.1N HCl (reduced by ~ 40 %) (Figure 3-30). The diffusion of drug through mucin is dependent on several factors which include the relative size of the drug molecule, the effective mesh spacing of the gel, and any interaction (binding, partitioning, reaction *etc*.) between the drug and the mucin (Khanvilkar *et al*., 2001). MET is a small sized molecule (Nau *et al.*, 2010), so its transport through the mucin suspension was fast and complete, further confirming the absence of significant MET binding with mucin in all the samples. Drug binding to mucus gives an indication of the proportion of antibiotic available for diffusion into the surrounding mucus environment thereby rendering the bound antibiotic bacteriologically inactive. As observed in the dissolution studies, the beads remained intact in studies at acidic pH with minimal swelling, while at alkaline pH, the beads swelled and almost completely dissolved by the end of the study. There were lag times in the onset of diffusion through mucin into both the acidic (~ 15 min) and alkaline (~ 40 min) medium, and the difference was probably due to the low solubility of MET in alkaline media.

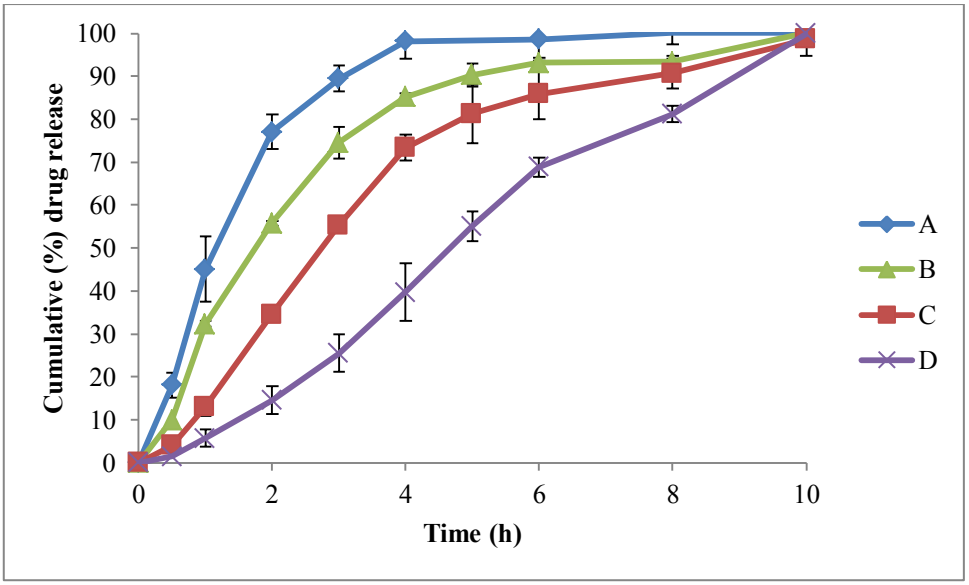

Figure 3-30: Franz cell diffusion studies with a) saturated MET solution / 0.1N HCl receiver cell b) M_{10} in 0.1N HCl / 0.1N HCl (c) M_{10} in 3 % mucin (pH 1.2) / 0.1N HCl (d) M_{10} in 3 % mucin/PBS (pH 7.4)

Table 3-10: Franz cell diffusion studies of beads in mucin dispersion

Donor cell	Receiver cell	Sample	Flux ($mgcm^{-2}h^{-1}$)	Lag time (h)
Saturated solution	0.1N HCl (pH 1.2)	-	8.46	0
0.1N HCl (pH 1.2)	0.1N HCl (pH 1.2)	M_{10}	1.26	0
3 % Mucin (pH 1.2)	0.1N HCl (pH 1.2)	M_{10}	0.94	0.25
3 % Mucin (PBS)	PBS	M_{10}	0.58	0.67

3.4 Conclusion

It was demonstrated that calcium alginate beads can efficiently encapsulate a highly soluble drug, MET, which has been a main concern due to leaching of MET into the cross-linking solution. These beads had a high drug content up to 67 %w/w and high DEE up to 81 % with both parameters increasing with increases in drug-polymer ratio. Solid state chracterisation showed no polymer-drug interaction and stability of MET in the beads with the drug maintaining its crystallinity in the beads. The entrapped drug can subsequently be released in both acidic and alkaline media, with drug release being rapid and complete in both media within an average of 4 hours. The fast drug release and limited buoyancy (< 24 h) of these formulations have been well documented and these properties do not fit the controlled release profile expected of a gastro-retentive formulation for the eradication of *H. pylori*. Therefore, in order to improve the buoyancy of these beads and control MET release from the beads, there is a need for modification of the formulation.

Chapter 4 CLARITHROMYCIN BEADS - PREPARATION AND CHARACTERISATION

4.1 Chapter overview

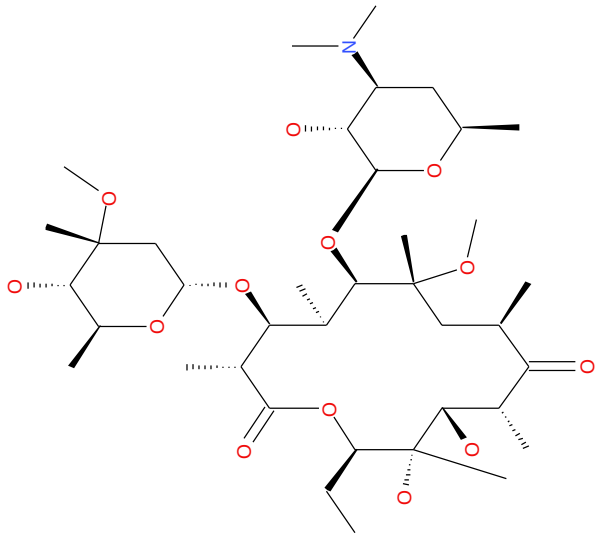

Figure 4-1: Structure of clarithromycin

(MW = 747.95 g/mol)

Clarithromycin (CMN) is a semi synthetic antibiotic also known as 6-O-methyl erythromycin and was first developed in the 1970s, through the substitution of the C6 hydroxy group of erythromycin with a methoxy group (Figure 4-1). It belongs to a group of antibiotics called the macrolides. Other members of this group include erythromycin and azithromycin. CMN is more chemically stable than erythromycin (Davey, 1991, Tsang *et al*, 1994); better tolerated with few GI side effects (Neu, 1991) and has a broader spectrum of activity than erythromycin (Sturgill and Rapp, 1992, Alvarez-Elcoro and Enzler, 1999). CMN occurs as a white to off-white crystalline powder. CMN is a drug of choice in treating peptic ulcer as *H. pylori* resistance is much lower compared to antibiotics such as amoxicillin and tetracycline (Gattani *et al.*, 2010). CMN exerts its antimicrobial activity by reversibly binding to the 50S subunit of the bacterial ribosome. This inhibits RNA-dependent protein synthesis by preventing transpeptidation and translocation reactions (Sturgill and Rapp, 1992). CMN is well absorbed in the GI tract and has an oral bioavailability of 55 % (Neu, 1991) due to the first pass metabolism. Due to the short half-life of CMN (4 - 5 h), immediate release formulations require twice daily dosing (Piscitelli *et al.*, 1992). It has a high plasma protein binding (60 - 70 %) and is metabolized in the liver to an active metabolite, 14 - hydroxyl CMN and six other products. 30 – 40 % of an oral dose of CMN is excreted in the urine either unchanged or as the active 14-hydroxy metabolite (Hardy *et al.*, 1992). The remainder is excreted into the bile.

In the previous chapter, MET, a BCS class I drug (high solubility and high permeability) was successfully incorporated into calcium alginate beads. In this chapter, CMN, a BCS class II drug (low solubility, high permeability) was incorporated in these gel beads and characterised. This was to compare the structure, drug distribution, physical properties, DEE, buoyancy and drug release profiles of beads prepared with poorly soluble and highly soluble drugs.

4.2 Materials and methods

Sodium alginate (SAL), calcium chloride dihydrate ($CaCl_2.2H_20$), phosphate buffered saline (PBS), HCl, acetonitrile, potassium dihydrogen phosphate (KH_2PO_4), 1-octane-sulphonic acid (1-OCTS), phosphoric acid, sodium acetate, acetic acid were obtained from Sigma Aldrich (UK). Liquid nitrogen (N_2) was obtained from BOC (UK). CMN was obtained from Discovery Fine Chemicals (UK).

4.2.1 Pre-formulation studies

4.2.1.1 Stability of CMN and determination of degradation rate constant (*k*)

CMN (50 mg) was dispersed in 100 ml buffers at pH 1.2 - 7.0 maintained at 37 ± 1 ℃ and stirred at 100 rpm. Samples were taken at different time intervals and the pH was adjusted to pH 5.0 to minimise degradation of the drug during HPLC analysis. Samples were analysed by HPLC as described in section 2.3.4.3. The degradation of CMN in acidic media is assumed to follow pseudo-first order kinetics and the half-life ($t_{1/2}$) of CMN was determined from the pseudo-first order degradation rate constant (k) using Equation 4-1(Venkateswaramurthy *et al.*, 2012).

$$C = C_0 e^{-kt} \quad \text{Equation 4-1}$$

in which C, is the concentration of drug remaining at time t, C_0 is the initial concentration of drug of drug and k is the degradation constant. The half-life ($t_{1/2}$) was determined from the degradation constant.

Equation 4-2 was used to estimate the amount of CMN released by the CMN-loaded beads in acidic media:

$$\frac{dC}{dt} = \frac{dQ}{V\,dt} - kC \quad \text{..... Equation 4-2}$$

where, *C* is the concentration of the drug at time *t*, *Q* the total amount of the drug released at time *t*, *V* the volume of the release medium, and *k* the first order degradation rate constant.

4.2.1.2 Solubility of clarithromycin

Solubility of CMN was determined in buffers with pH ranging from 1.2 to 8 maintained at 37 ± 1 ℃. Excess CMN was added to 100 ml buffer and agitated continuously for 1 h in a water bath. Samples were filtered, diluted and analysed by HPLC. Solubility of CMN in $CaCl_2$ solutions was determined by adding excess amounts of CMN to 100 ml solution of 0.07 M to 0.34 M $CaCl_2$ and allowed to dissolve in the solution by shaking constantly for 12 hours, while being maintained at 37 ± 1 ℃. These samples were filtered, diluted and analysed by HPLC.

4.2.2 Bead preparation

Beads were prepared as outlined in Sections 3.2.2 and 3.2.4 based on the formulation table (Table 4-1).

Table 4-1: CMN loading and corresponding codes of bead samples

Code	CMN (w/w) %
C_0	-
$C_{0.5}$	0.5
C_1	1
C_2	2
C_3	3
C_5	5
C_{10}	10
C_{15}	15

4.3 Results and discussion

4.3.1 Solubility and stability profile of clarithromycin

CMN is a weak base containing one ionisable group with a pK_a of 8.99; therefore, it exists in an ionized state in an acidic and neutral pH environment. Solubility of CMN is pH dependent with a decrease in solubility with increasing pH and the highest solubility observed at the lowest pH measured – pH 1.2 (Figure 4-2). CMN is slightly water soluble and resists wetting with fluids with only a fraction of the potentially available surface area of CMN powder being in contact with fluids (Grubel and Cave, 1998). Stability of CMN at different pHs was assessed because of its known instability in acidic pH (Nakagawa *et al.*, 1992, Erah *et al*., 1997, Venkateswaramurthy *et al.*, 2012) and non-distinguishing techniques may underestimate release (Rajinikanth and Mishra, 2008) (Table 4-2) (Figure 4-3). It has been reported that decomposition of the CMN molecule occurs *via* cleavage of the neutral cladinose sugar at low pH (Morimoto *et al.*, 1990). The highest stability of CMN was

observed at pH 5 – 7, while it was least stable at the lowest pH studied which is pH 1.2. In buffer pH 1.2, there was ~ 94 % CMN degradation within 1 h while at pH 7, there was less than 0.5 % degradation within this same time interval. Therefore, at pH values < 2, which easily occurs in the stomach, CMN will undergo rapid degradation, which may significantly affect the antimicrobial activity of the drug. These results correspond to results obtained by other researchers (Nakagawa *et al*., 1992, Erah *et al*., 1997, Chun *et al*., 2005).

Table 4-2: Degradation constants of CMN at different pHs

pH	Degradation rate constant (k) (h^{-1})	Half life ($t_{1/2}$) (h)
1.2	1.45 ± 0.13	0.47 ± 0.04
2.0	0.45 ± 0.01	1.53 ± 0.01
3.0	0.055 ± 0.007	12.65 ± 1.72
4.0	0.0030 ± 0.0006	> 100
5.0	0.0028 ± 0.0003	> 100

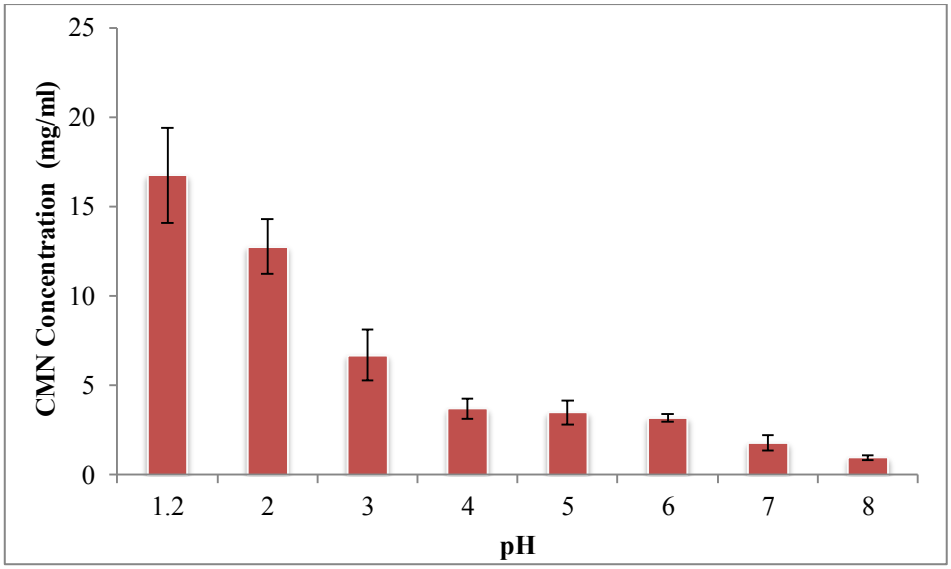

Figure 4-2: pH solubility profile of CMN at 37 ℃

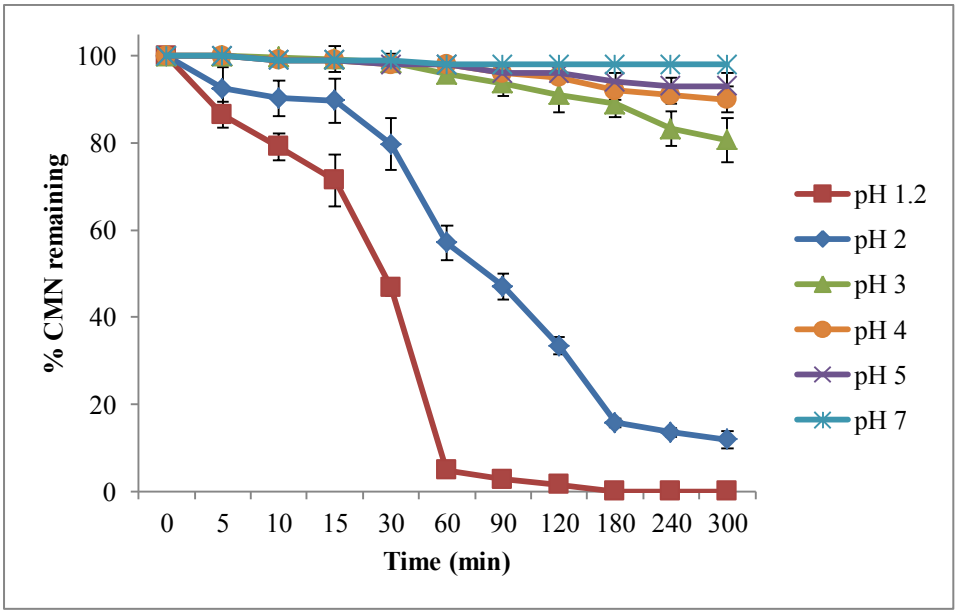

Figure 4-3: pH stability profile of CMN at 37 ℃

4.3.2 Characterisation of clarithromycin beads

4.3.2.1 Morphology and structure of clarithromycin beads

Similarly, to MET-loaded beads, the CMN beads were spherical and porous as seen in Figure 4-4. The major difference between the internal structures of both MET and CMN – loaded beads is obvious from the XμMT images. XμMT images of MET beads (Figure 3-20d) showed MET particles concentrated in a portion of the bead, however this phenomenon was not observed with the CMN beads because the CMN beads showed a more even distribution of the drug particles throughout the beads (Figure 4-4b). This is probably due to the finer particle sizes of the CMN particles, which were better dispersed in the SAL solution and did not have a tendency to sediment when left to stand like MET in SAL solution. The very distinct, thick, layered internal structure of the beads also gave an indication of the viscosity of the CMN-SAL solution, which appeared more viscous than the corresponding MET-SAL solution, hence the thin layers observed in the internal structure of MET beads (Figure 3-20d).

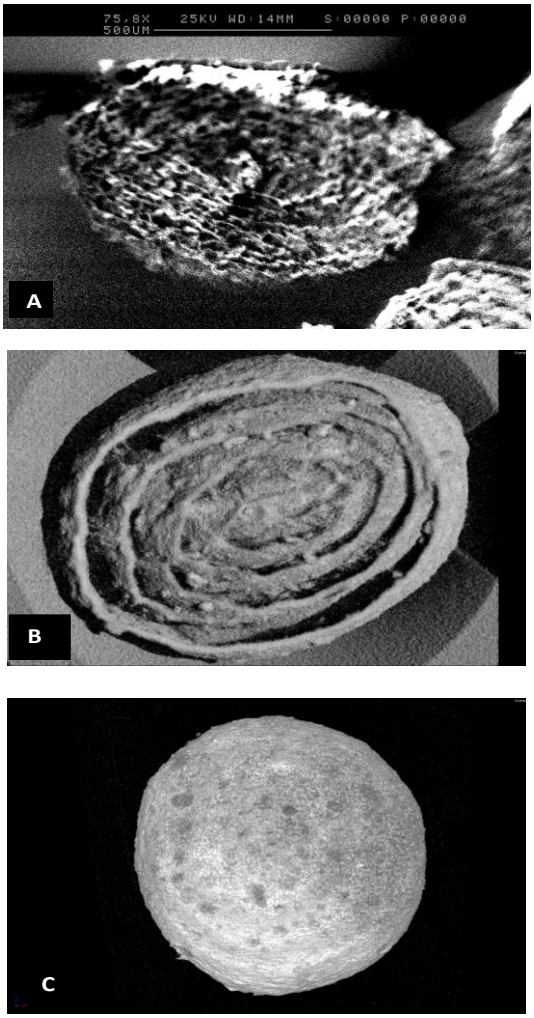

Figure 4-4: A) cross section of CMN loaded bead; XμMT images of B) internal surface and C) external surface of C_{10} (C_{10} beads loaded with 10 %w/w CMN).

4.3.2.2 Physical properties of clarithromycin beads

The beads had a whitish colour with the size, weight and density of the beads increasing with an increase in drug-polymer ratio ($p < 0.05$) as expected, however there was no significant difference in these properties when loaded either with MET or CMN ($p > 0.05$) (Table 4-3). The porosity, moisture content and calcium content were also similar to those observed in MET beads ($p > 0.05$).

Table 4-3: Physical properties of CMN - loaded beads

Code	Diameter (mm)	True density (g/cm^3)	Weight (g) *(n=100)*	Bulk density (g/cm^3)	Porosity (%)	Ca^{2+} content (mg/10mg bead)
$C_{0.5}$	1.94 ± 0.3	0.49 ± 0.04	0.06 ± 0.01	0.11 ± 0.02	79.59	0.50 ± 0.07
C_1	2.09 ± 0.5	0.61 ± 0.03	0.07 ± 0.01	0.12 ± 0.03	80.33	0.51 ± 0.05
C_2	2.21 ± 0.4	0.63 ± 0.06	0.11 ± 0.01	0.13 ± 0.03	79.36	0.41 ± 0.06
C_3	2.32 ± 0.3	0.68 ± 0.08	0.13 ± 0.01	0.15 ± 0.02	77.94	0.38 ± 0.08
C_5	2.49 ± 0.5	0.95 ± 0.06	0.16 ± 0.01	0.18 ± 0.02	81.05	0.36 ± 0.04
C_{10}	2.75 ± 0.4	1.39 ± 0.04	0.27 ± 0.01	0.24 ± 0.04	82.73	0.23 ± 0.05
C_{15}	2.93 ± 0.5	1.57 ± 0.05	0.33 ± 0.01	0.24 ± 0.01	82.80	0.21 ± 0.04

4.3.2.3 Drug content and DEE of clarithromycin beads

The drug content and DEE were high for all the beads (Figure 4-5) with the DEE being > 85 % in all cases, probably due to the limited solubility (the solubility of CMN in $CaCl_2$ was determined to be ~ 2.1 ± 0.82 mg/ml), which minimises drug loss/ leaching during drug encapsulation (Wagner, 1977, Nimase and Vidyasagar, 2010). The drug-polymer ratio had no significant effect on DEE ($p > 0.05$), but did on drug content ($p < 0.05$). This was different from the observation in MET loaded beads with increasing DEE on increasing drug-polymer ratio. LSC was minimal < 5 % at all drug-polymer ratios, indicating there was a low amount of drug present at or near the bead surface after encapsulation and that the drug was well encapsulated in the bead matrix**.** LSC values were lower than the MET beads (the lowest being ~ 22 %) at the higher drug-polymer ratio, as more MET was lost due to its higher solubility in $CaCl_2$ solution (9.2 ± 0.1 $mgml^{-1}$ at 37 °C). The drug contents of both MET and CMN beads were significantly different ($p < 0.05$) at low drug-polymer ratios as observed in $C_{0.5}$ – C_3 and high drug loading in C_{15} *versus* $M_{0.5}$ – M_3 and M_{15}. There was no difference observed in DEE of C_5 and C_{10} when compared with equivalent MET beads ($p > 0.05$). This was because at low drug-polymer ratios ($C_{0.5}$ – C_3 / $M_{0.5}$ - M_3), the difference in solubilities had a high impact on drug entrapment/ drug content, but at intermediate drug-polymer ratios (C_5 - C_{10}/ M_5 - M_{10}) due to saturation of the gelation medium with MET leading to lower drug loss into the gelation medium, the difference in solubility had very little impact on drug entrrapment/content. At high drug-polymer ratio (C_{15} and M_{15}), the difference in drug entrapment/content might then be due to solubility differences and drug particle packing in the beads. The high DEE observed have been previously reported by other researchers (Gattani *et al.*, 2010, Nimase and Vidyasagar, 2010, Raj and Pillai, 2013, Rajinikanth and Mishra, 2009). Gattani *et al* (2010) reported DEE of ~ 82 – 89 % of CMN loaded beads, which is similar to the DEE achieved in this study. This high DEE is common in BCS Class II drugs entrappped in alginate beads with over 70 % DEE observed for diclofenac beads

(Goudanavar *et al.*, 2010) and over 80 % DEE reported for diclofenac alginate microspheres (Maiti *et al.*, 2012).

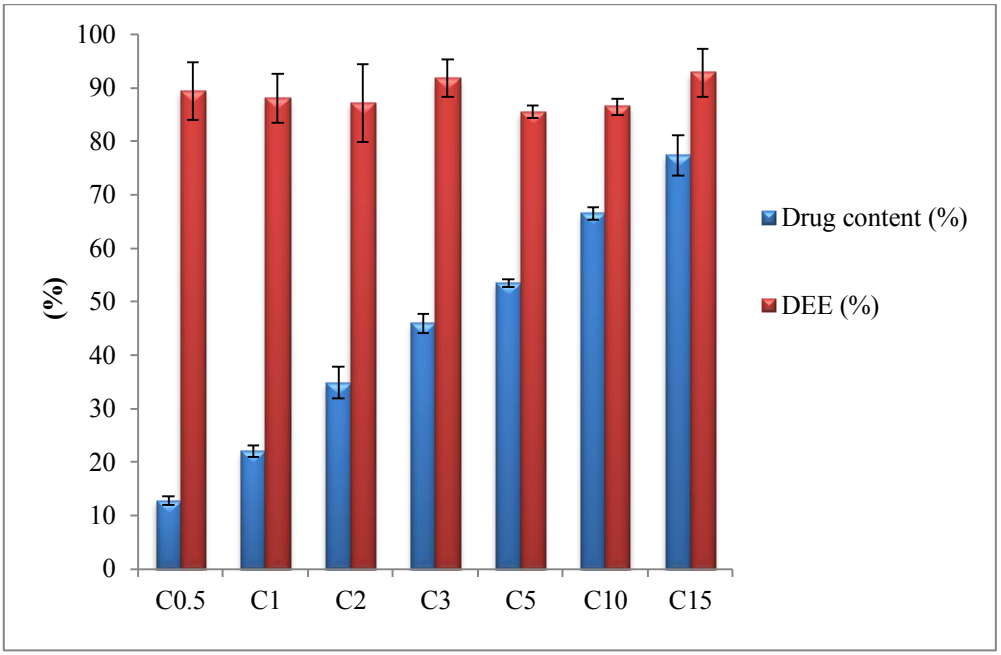

Figure 4-5: Drug content and DEE of CMN beads.

4.3.2.4 Differential scanning calorimetry of clarithromycin beads

CMN showed a single, sharp endothermic peak with an average onset at 227.5 ± 0.32 °C (*n*=3), which corresponds to the documented melting point of the CMN polymorph form II (Gómez-Burgaz *et al.*, 2009, Tozuka *et al.*, 2002), this was followed by the onset of degradation of the drug at ~ 280 °C (Sohn *et al.*, 2000). The polymorphic form II of CMN has been reported to be the most stable form of the drug (Sohn *et al.*, 2000). The physical mixture of CMN and SAL had a similar endothermic peak at 226.74 ± 0.78 °C (*n*=3) . The drug-loaded beads C_5 and C_{10} exhibited a melting endotherm at 226.56 ± 0.89 °C (*n*=3) and 225.98 ± 0.93 °C (*n*=3), respectively (Figure 4-6) though the peaks were broader and had a lower intensity. This reduction in intensity and broader peak indicate that there was a little

molecular dispersion of the drug in the polymer with the drug still maintaining its crystallinity in the formulation. Similar results were obtained by other researchers (Novoa *et al*., 2005, Javadzadeh *et al*., 2008, Gattani *et al*., 2010). The absence of any significant shifts of the melting endothermic peaks of CMN showed the absence of solid-state interaction between drug and polymers after the cross-linking process over the whole drug/polymer ratio range.

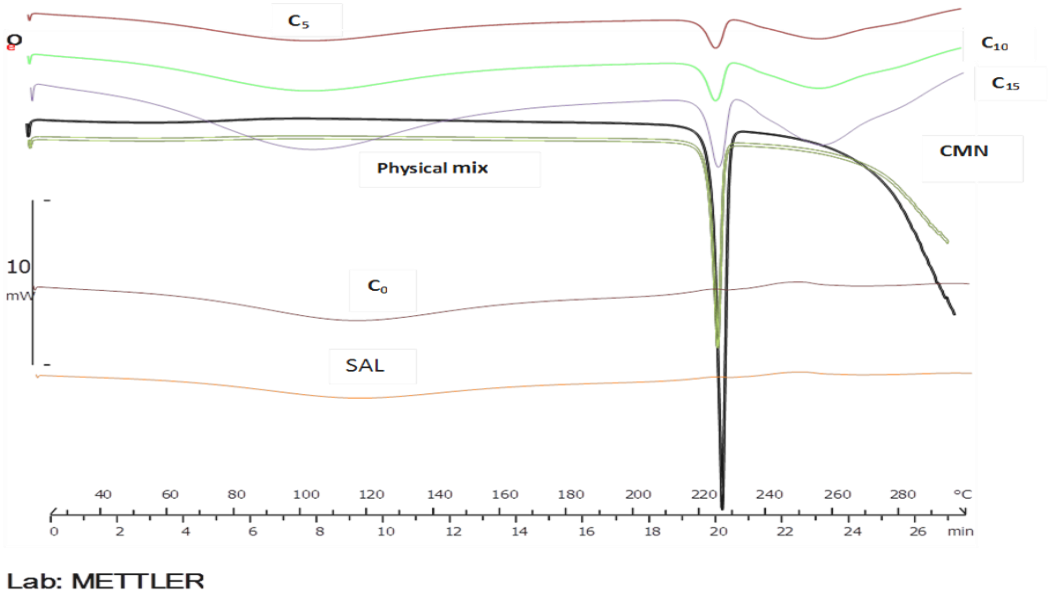

Figure 4-6: DSC thermograms of SAL, CMN, physical mixture of SAL and CMN, unloaded and CMN- loaded beads

4.3.2.5 Powder X-ray diffraction analysis of clarithromycin beads

The diffractograms of the polymer and blank samples showed indistinct, clustered peaks reflecting the amorphous nature of the samples, which is common with polymers. CMN exhibited a pattern characteristic of a highly crystalline material with no amorphous component with peaks appearing at 2θ values of 8.52 ° / 9.57 °/ 10.94 ° / 11.55 °/ 12.35 °/ 13.27 °/13.81 °/ 15.27 °/ 16.70 °/ 17.39 °/ 18.33 ° which are peaks attributed to the stable CMN form II (Liu and Riley, 1998, Inoue *et al.*, 2007). The P-XRD pattern of the CMN loaded beads (Figure 4-7) showed the characteristic peaks (especially the peak at ~ 8.6 2θ (Tozuka *et al.*, 2002)) observed in CMN, though there was a significant reduction in the intensities of the peaks as the proportion of polymer was high relative to the drug in the formulation. The presence of these peaks and the absence of any major peak position shift indicated that CMN maintained its crystallinity in the beads. This is similar to results for the MET-loaded beads.

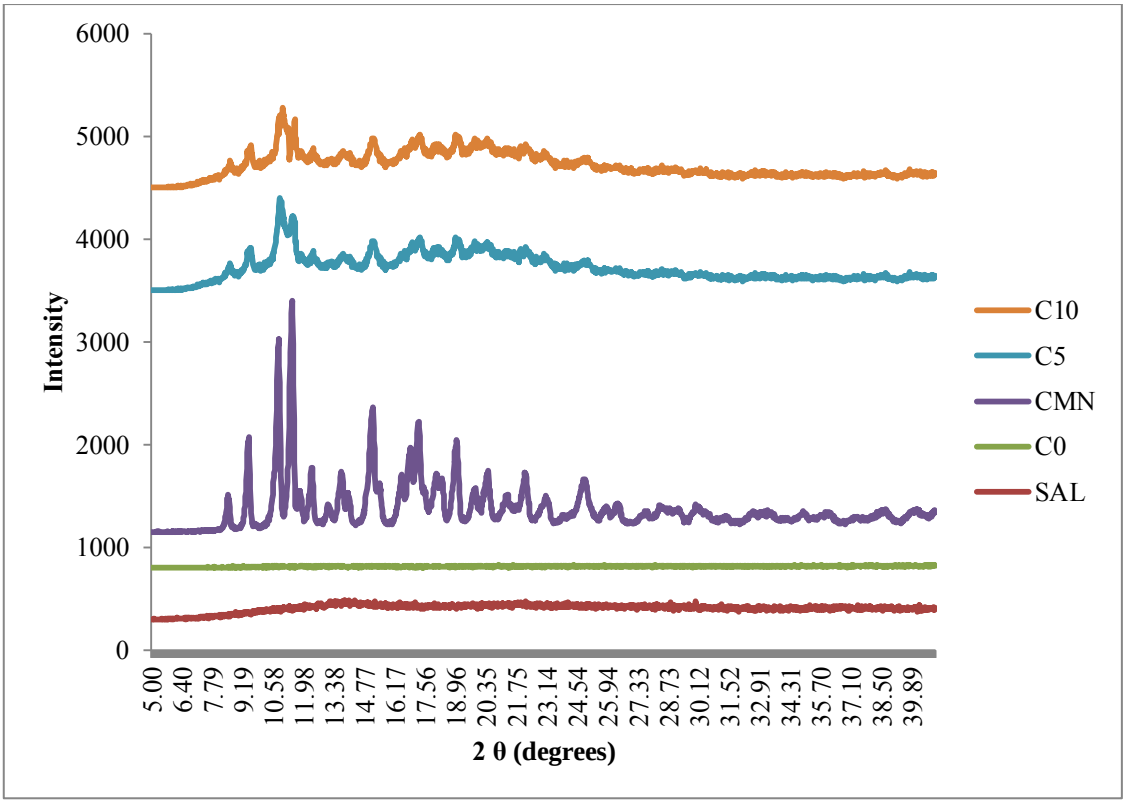

Figure 4-7: P-XRD of SAL, CMN, unloaded and CMN - loaded beads.

4.3.2.6 Fourier transform infrared (FT-IR) analysis of clarithromycin beads

The IR spectrum of CMN showed the characteristic band of hydrogen bonds between –OH groups vibration at 3479.5 cm^{-1}. Bands such as hydroxyl (OH) stretch at 2941.2 cm^{-1}, C=O vibration of the lactone group at 1732.9 cm^{-1}, strong absorption band at 1692 cm^{-1} belonging to the carbonyl ketone peak for N-CH_3 stretching of aromatic ring at 1457.7 cm^{-1} and the aliphatic –CH stretching were also detected in CMN (Figure 4-8) (Akre *et al.*, 2012, Venkateswaramurthy *et al.*, 2012). Similar peaks at 1732.3 cm^{-1} (lactone carbonyl), 1692.6

cm^{-1} (ketone carbonyl), 3422.1 cm^{-1} (hydrogen bonding between OH Groups), and 1379.9 cm^{-1} (CH_2), were observed in CMN loaded beads indicating that the encapsulation process did not cause any alteration of the drug. There was however slight broadening and reduction in intensity of these peaks as a result of the relative proportion of CMN to the polymer in the beads. This result confirms the results obtained from both DSC and P-XRD analysis indicating the stability of the drug in the bead matrix, with no drug – polymer interactions and the drug maintaining its crystalline nature in the beads as observed in MET beads. Other researchers also observed this (Gattani *et al.*, 2010, Raj and Pillai, 2013), where it was reported that encapsulation of CMN did not alter the crystallinity of the encapsulated drug.

4.3.2.7 *In vitro* buoyancy of clarithromycin beads

The beads floated immediately on contact with the medium with a lag time of < 3 minutes for all the formulations. The beads failed the buoyancy test because, after the first hour, between 20 – 65 % of the beads sank and at subsequent time intervals, the proportion of beads sinking continued to increase. After a 12 hour period, more than 35 - 70 % of all the bead formulations sank and after 24 hours, the percentage of beads floating was just between 10 and 25 % (Table 4-4). The floating behaviour of CMN beads was similar to those observed with the MET loaded beads ($p > 0.05$) and was also similar to reports by other researchers (Rajinikanth and Mishra, 2009, Gattani *et al.*, 2010, Patel *et al.*, 2014). Gattani *et al* (2010) reported 0 % buoyancy with CMN loaded beads exposed to 0.1M HCl at 37 ºC for 10 h.

Table 4-4: Floating profile of unloaded and CMN - loaded beads

Sample	Lag time (min)	%Floating (1h)	% Floating (12h)	% Floating (24h)
M_0	< 3	70 ± 10	40 ± 5	20 ± 5
$M_{0.5}$	< 3	75 ± 5	50 ± 15	15 ± 5
M_1	< 3	70 ± 5	40 ± 0	15 ± 5
M_2	< 3	60 ± 10	40 ± 5	20 ± 5
M_3	< 3	55 ± 10	55 ± 10	15 ± 5
M_5	< 3	65 ± 5	40 ± 5	15 ± 5
M_{10}	< 3	65 ± 10	35 ± 5	20 ± 5
M_{15}	< 3	50 ± 15	40 ± 10	20 ± 5

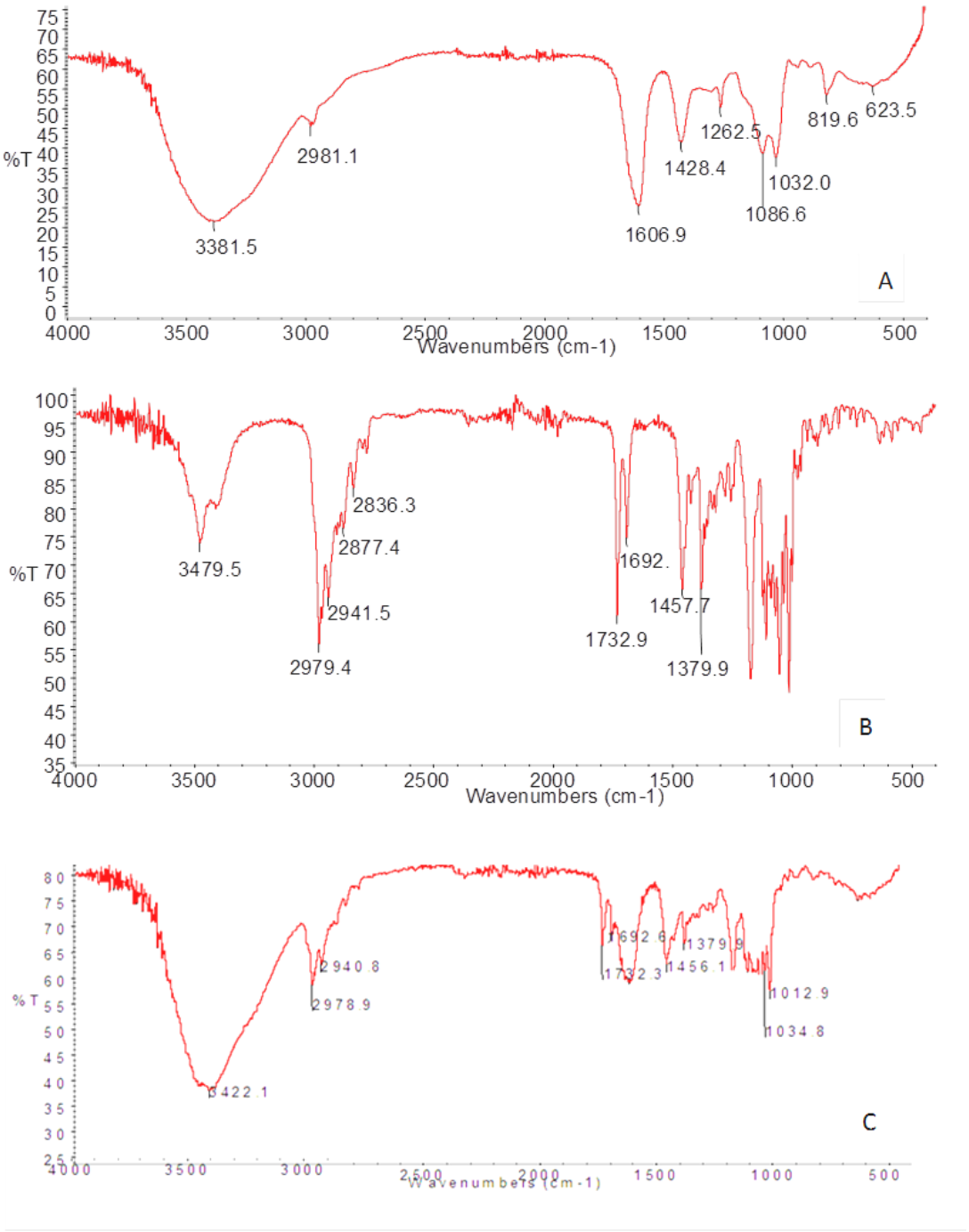

Figure 4-8: FTIR scans of a) C_0 beads; b) pure CMN and c) C_5 beads

4.3.2.8 Swelling profile of clarithromycin beads

Water uptake into the beads was similar to that observed with MET-loaded beads, with minimal swelling observed in the beads in acidic media with about 150 - 200 % weight change (Figure 4-9). However, in PBS maximal swelling was observed with an average of 2000 % weight change at the maximum and the beads started to disintegrate at times beyond 150 minutes and complete dissolution was observed at ~ 240 minutes. The reasons for the major differences in swelling in both media has been fully discussed in section 3.3.3.8.

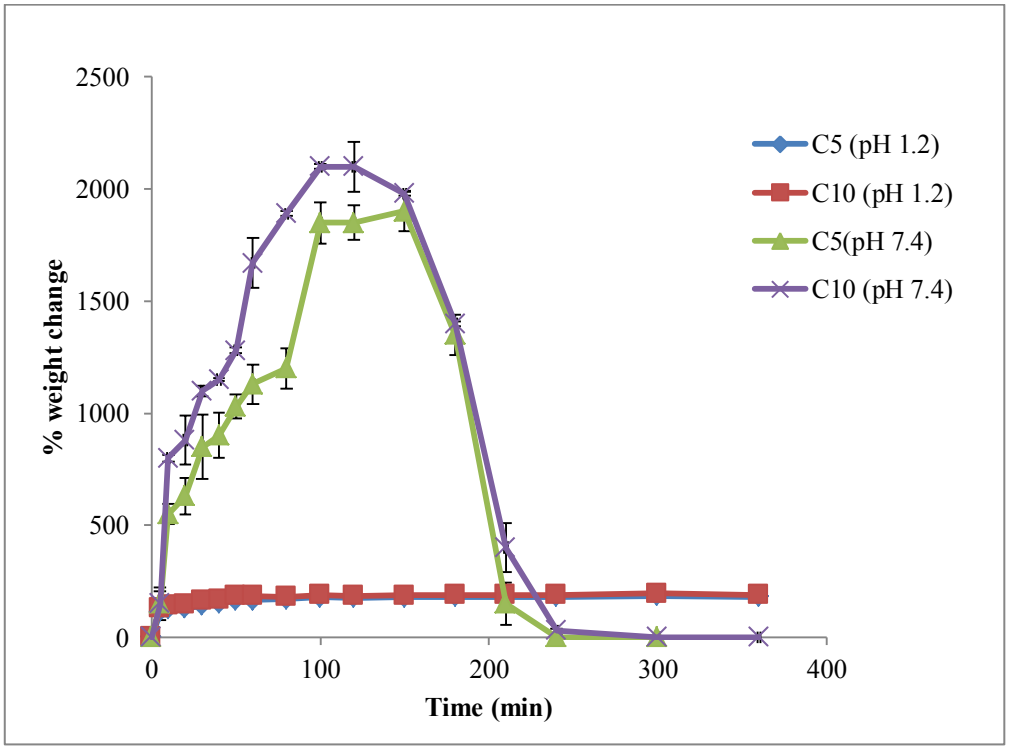

Figure 4-9: Swelling profile of CMN - loaded beads in acidic and alkaline media.

4.3.2.9 *In vitro* drug release of clarithromycin beads

Drug release was determined in acidic media (pH 2.0 and 4.0) and in PBS (pH 7.4).

4.3.2.9.1 Release of clarithromycin beads in acidic medium - 0.1N HCl (pH 2.0)

CMN release from beads increased initially with time but then gradually appeared to fall (Figure 4-10). This apparent decrease was due to the degradation of CMN at this pH. At the start of the drug release studies, the release rate dominated over the degradation rate of CMN, however after about an average of 60 - 90 minutes (C_2 - C_{15}), and about 30 minutes ($C_{0.5}$ – C_1), the degradation rate dominated (Table 4-5). CMN release was corrected with Equation 4-2 to determine the actual amount released and the uncorrected and corrected data at pH 2.0 are both presented in Figure 4-10 and Figure 4-11a respectively. Overall, there was an initial burst release with these beads as a result of surface – associated drug followed by a slower release. The burst release observed was more pronounced at low drug-polymer ratios than at high drug - polymer ratios. As observed from Figure 4-11a, drug – polymer ratio had an effect on drug release across the range of formulations. Formulations with a high drug – polymer ratio (C_5, C_{10}, C_{15}) exhibited a more controlled drug release than formulations with a relatively lower drug – polymer ratio ($C_{0.5}$, C_1, C_2). This difference in release profiles was also obvious in the f_2 values of C_1 and C_5 (f_2 = 36.7); C_2 and C_{10} (f_2 = 36.1) and C_3 and C_{15} (f_2 = 38.2). Therefore, the higher the drug content of the beads, the slower its release rate from the bead. This is similar to the observation in the MET beads. CMN release at pH 2.0 (Table 4-5) occurred over a period of 6 - 8 h with a larger proportion of the release within the first 3 h. Gattani *et al* (2010) reported a slightly lower duration of CMN release from alginate beads at 5 h. CMN release from beads was relatively slower than that observed with MET beads, this was probably mainly due to the lower solubility of the CMN and, to a limited extent, the difference in pH of the dissolution media. The lower solubility of the drug reduces the

diffusion rate of the drug out of the beads therefore, CMN release may be due more to the porosity of the beads than the solubility of CMN at this pH. At pH 4.0, CMN release was slower due to the low solubility of CMN at this pH (f_2 = 41- 53). There was no significant burst release from the beads at this pH and release of drug was complete between 6 - 10 h. The effect of drug – polymer ratio on drug release was also obvious at this pH with the beads containing most drug (C_{15}), having the slowest release profile.

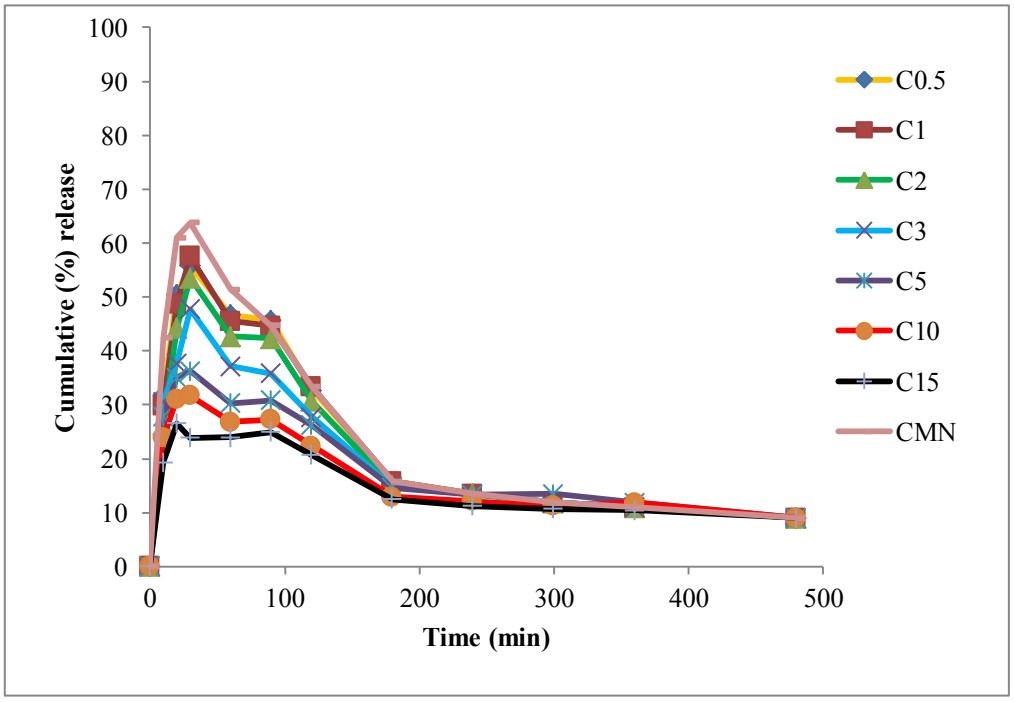

Figure 4-10: Release profile of CMN from beads at pH 2.0 without correction for degradation

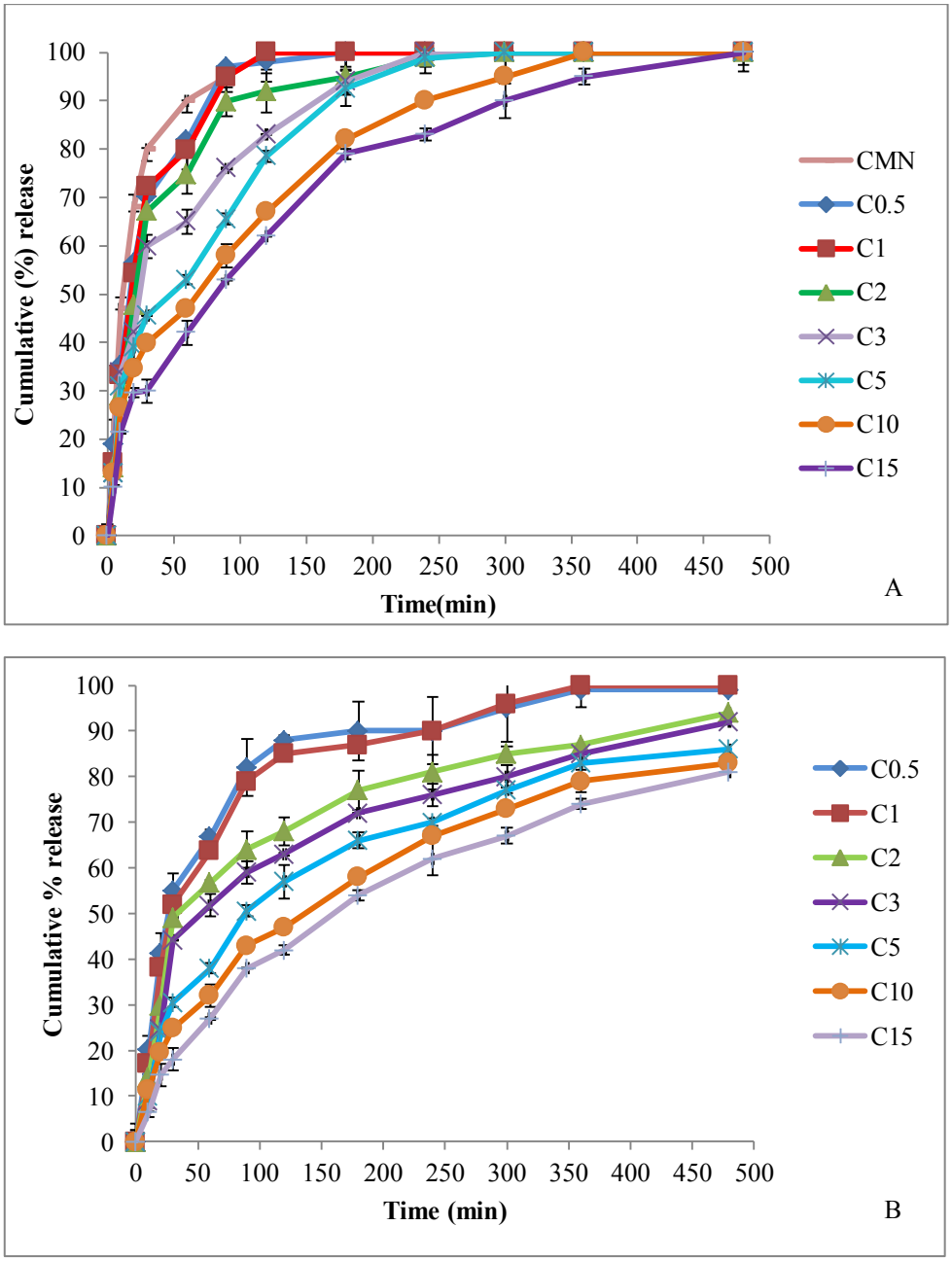

Figure 4-11: Release profile of CMN beads at A) pH 2.0 corrected for degradation and B) pH 4.0 corrected for degradation

Table 4-5: Release parameters of CMN loaded beads in acidic media

Beads	$t_{25\%}$(min)	$t_{50\%}$(min)	$t_{75\%}$ (min)	$t_{25\%}$(min)	$t_{50\%}$(min)	$t_{75\%}$ (min)
		pH 2.0			pH 4.0	
$C_{0.5}$	5 - 10	10 - 20	30 - 60	< 5	20 - 30	60 - 90
C_1	5 - 10	10 - 20	30 - 60	10 - 20	20 - 30	60 - 90
C_2	5 - 10	20 - 30	60	10 - 20	30	120 -180
C_3	5 - 10	30 - 60	60 - 90	20	30 - 60	180 - 240
C_5	5 - 10	30 - 60	90 - 120	20 - 30	90	240 - 300
C_{10}	5 - 10	60 - 90	120 - 180	30	120 - 180	300 - 360
C_{15}	10 - 20	60 - 90	120 - 180	30-60	300 - 360	360

4.3.2.9.2 Release kinetics of claritromycin from beads in acidic medium (pH 2.0)

The *in vitro* release data were in favour of Higuchi-diffusion kinetics (R^2 = 0.98 – 0.99), demonstating that rate of drug release is dependent on the rate of drug diffusion. Overall, n < 0.43, indicating Fickian diffusion (Table 4-6) for all the samples except C_2, (n = 0.69). These release kinetic results are similar to those observed with the MET beads, which further confirms that drug release from alginate beads is mainly diffusion controlled as already reported by other researchers (Murata *et al.*, 2000, Rajinikanth and Mishra, 2008, Bera *et al.*, 2009, Jahan *et al.*, 2012).

Table 4-6: Release kinetics of CMN beads in 0.1N HCl (pH 2.0)

Beads	Zero order		1st order		Higuchi		Hixson-Crowell		Peppas	
	$K_0(min^{-1})$	R^2	$K_1(min^{-1})$	R^2	$K(min^{1/2})$	R^2	k	R^2	n	R^2
C_2	2.072	0.993	0.016	0.992	16.123	0.997	0.048	0.996	0.693	0.939
C_3	1.691	0.928	0.013	0.952	13.295	0.993	0.037	0.949	0.389	0.912
C_5	0.399	0.965	0.004	0.927	5.196	0.994	0.012	0.903	0.328	0.988
C_{10}	0.361	0.963	0.003	0.931	4.696	0.995	0.009	0.912	0.340	0.989
C_{15}	0.358	0.981	0.003	0.979	5.101	0.995	0.008	0.971	0.395	0.971

4.3.2.9.3 Release of clarithromycin from beads in alkaline medium (pH 7.4)

CMN release was slow at the initial stages when compared with release in acidic medium, and this was probably due to the lower solubility of CMN. Subsequently at later stages as observed in Figure 4-12 and Table 4-7, drug release was faster because of the degradation of the polymer matrix. After ~ 2 h, the beads started to disintegrate and complete release was achieved at ~ 3h. This further supports the results obtained from the swelling studies (Figure 4-8), where degradation of the beads was observed at ~ 200 min. The release kinetics of CMN from the beads in PBS followed Higuchi kinetics (R^2 = 0.98 – 0.99) indicating drug release was diffusion controlled, however most of the other models also showed a high corelation coefficient ranging from 0.97 - 0.99 (Table 4-8). The ‘n’ value for most of the beads was > 0.85 indicating case-II transport, which involves polymer dissolution and

polymeric chain enlargement or relaxation, which is in agreement with the bead dissolution. For the other beads, $n < 0.85$, which is an indication of non-Fickian release, which involves both diffusion and swelling controlled drug release. In comparison, CMN release in PBS was more dependent on swelling and subsequent dissolution than MET release where release was more dependent on diffusion and swollen beads due to the initial slow release of CMN followed by a subsequent fast release due to beads swelling and dissolution.

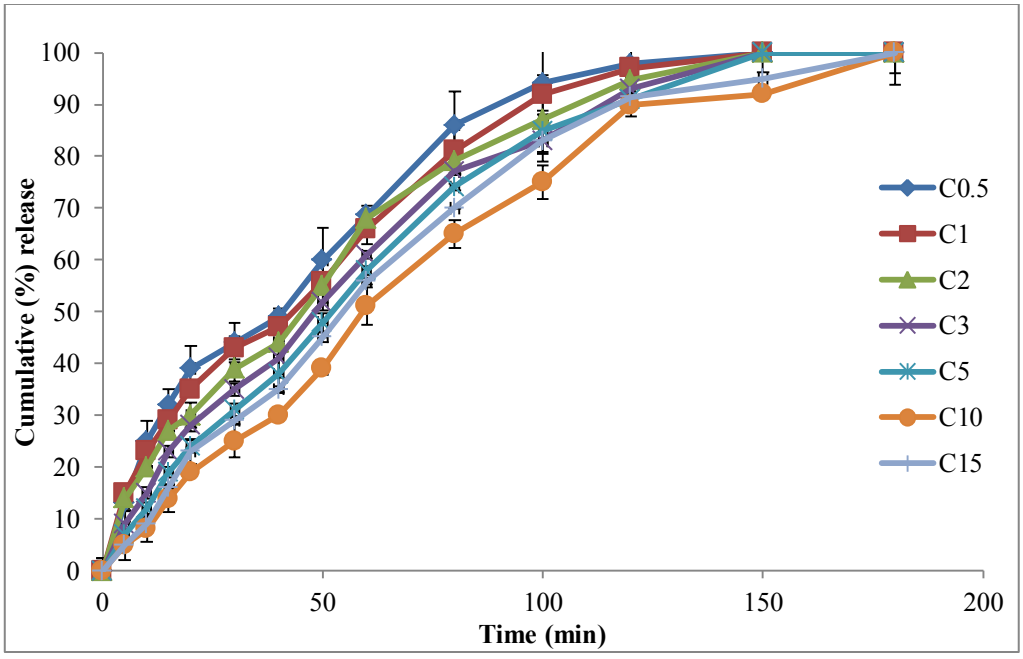

Figure 4-12: Release of CMN in PBS (pH 7.4)

Table 4-7: Release parameters of CMN-loaded beads in PBS

Beads	$t_{25\%}$(min)	$t_{50\%}$(min)	$t_{75\%}$ (min)
$C_{0.5}$	10	40 -50	60 - 80
C_1	10 -15	40 - 50	60 - 80
C_2	10 -15	40 - 50	60 - 80
C_3	15 -20	40 - 50	60 - 80
C_5	20 - 30	50 - 60	80 -100
C_{10}	20 - 30	50 - 60	80 -100
C_{15}	30	60	100

Table 4-8: Release kinetics of beads in PBS

Beads	Zero order		1st order		Higuchi		Hixson-Crowell		Peppas	
	$K_0(min^{-1})$	R^2	$K_1(min^{-1})$	R^2	$K(min^{1/2})$	R^2	k	R^2	n	R^2
C_2	0.859	0.985	0.006	0.986	8.156	0.987	0.018	0.981	0.881	0.995
C_3	0.898	0.981	0.006	0.984	9.137	0.985	0.019	0.977	0.751	0.993
C_5	0.889	0.993	0.006	0.983	9.001	0.995	0.018	0.990	0.836	0.995
C_{10}	0.886	0.989	0.005	0.988	8.225	0.994	0.018	0.985	0.961	0.989
C_{15}	0.797	0.993	0.006	0.969	8.846	0.997	0.017	0.981	0.933	0.992

4.3.2.9.4 *In vitro* release of clarithromycin from beads in mucin suspension

The saturated CMN solution had a concentration of 12.8 $mgml^{-1}$ at pH 2.0, and this was expected due to the low solubility of CMN. This concentration provides the necessary concentration gradient required for drug diffusion into the receiver cell (Table 4-9). Hence, a combination of this low concentration gradient and low solubility was responsible for the relatively lower flux of the saturated solution of CMN compared to that of MET under the same conditions. Encapsulation of CMN in the beads reduced its flux by ~ 43 % when compared with that of the saturated drug solution. The presence of mucin restricted the movement of drug as the CMN flux was ~ 40 % lower than the flux observed when CMN beads were immersed in 0.1N HCl. In addition, drug flux into PBS was ~ 9 % lower than what was observed in 0.1N HCl. The retardation of CMN permeation by mucin was also reported Grubel and Cave (1998). Lag times were evident for diffusion through mucin into the acidic media (~ 20 min) but were more pronounced at higher pH (~ 50 min), a likely consequence of the reduced solubility of CMN, but not significantly higher than the lag times observed for MET beads (Figure 4-13). These results did not show any form of drug binding to the mucin, with almost complete release observed from C_{10}, and these results are similar to the release profiles observed from the dissolution studies. The penetration of an antibiotic through the mucus network is reported to be dependent on factors such as the drug charge, hydration radius of the molecule and its ability to form hydrogen bonds with antibiotics of small molecular size and those with high mucus binding showing the poorest mucus penetration.

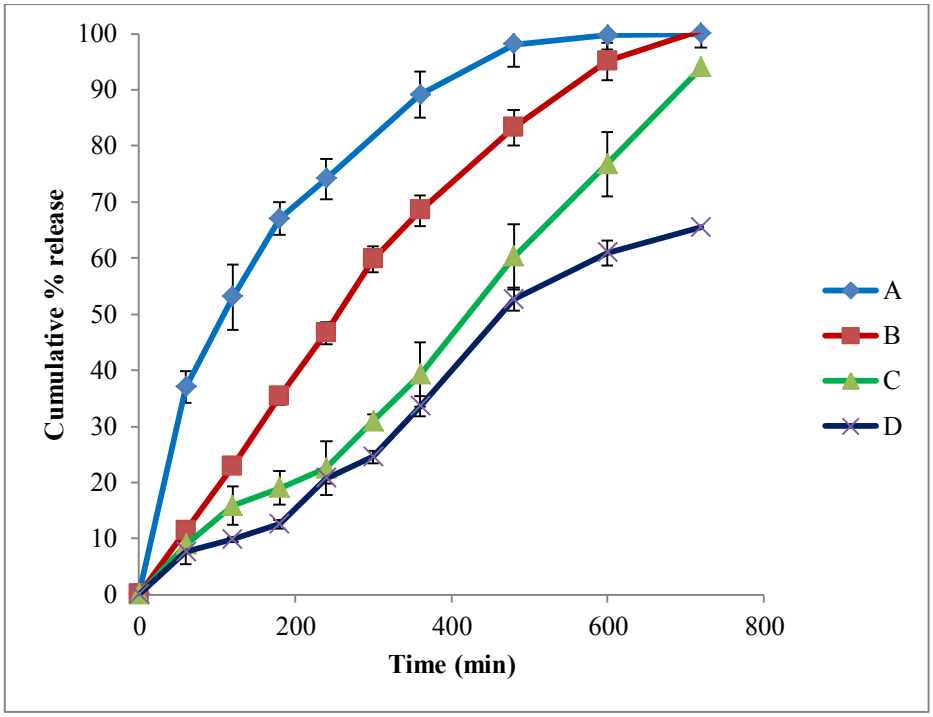

Figure 4-13: Franz cell diffusion studies with a) saturated CMN solution / 0.1N HCl receiver cell b) C_{10} in 0.1N HCl / 0.1N HCl (c) C_{10} in 3 % mucin (pH 2.0) / 0.1N HCl (d) C_{10} in 3 % mucin / PBS (pH 7.4)

Table 4-9: Franz cell diffusion studies of beads in mucin dispersion

Donor cell	Receiver cell	Sample	Flux ($mgcm^{-2}h^{-1}$)	Lag time (h)
Saturated solution	0.1N HCl (pH 2.0)	-	1.02	0
0.1N HCl (pH 2.0)	0.1N HCl (pH 2.0)	C_{10}	0.59	0.08
3 % Mucin (pH 2.0)	0.1N HCl (pH 2.0)	C_{10}	0.35	0.33
3 % Mucin (PBS)	PBS	C_{10}	0.32	0.83

4.4 Conclusion

The poorly water-soluble drug, CMN, was adequately loaded onto calcium alginate beads. Adequate drug loadings were achieved with CMN, even at low drug-polymer ratios, which was a major problem when loading a water-soluble drug such as MET in the beads. High DEE > 85 % was achieved in the beads across all drug-polymer ratios and this was enhanced due to the low solubility of CMN, which minimises the loss of CMN into the cross-linking solution. Solid state chracterisation showed no polymer-drug interaction and stability of CMN in the beads with the drug maintaining its crystallinity in the beads Drug release was complete within 6 – 8 h in acidic pH and in PBS; drug release was complete within 3h. Since complete drug, release was achieved in less than 12 h in acidic pH and there was limited buoyancy of the beads (< 24 h); these properties need to be modified to fit the controlled release profile expected of a gastro-retentive formulation. Therefore, in order to improve the buoyancy of these beads and control CMN release from the beads, there is a need for modification of the formulation.

Chapter 5 MODIFICATION OF ALGINATE BEADS TO IMPROVE BUOYANCY AND DRUG RELEASE

5.1 Chapter overview

In the previous chapters, two antibiotics used in the treatment of *H. pylori* infection were encapsulated into calcium alginate beads including both a water-soluble drug (MET) and a poorly soluble drug (CMN). The beads prepared especially MET beads exhibited fast release in the acidic pH of the stomach with drug release from both MET and CMN complete generally in less than 10 h. In addition, all the beads exhibited limited buoyancy with a small proportion of the beads floating for significantly less than 24 h. The aim of this study was to produce alginate beads that would exhibit high DEE, high drug content, and adequate floating characteristics with 100 % of the beads floating for ~ 24 h and with a controlled drug release to extend the lifetime of the drug delivery device to about ~ 12 h. This was attempted by including oil in the bead formulations. Olive oil (OO) was chosen as the preferred oil due to its inherent anti-*H. pylori* activity (Romero *et al*., 2007, Castro *et al*., 2012). Romero *et al* (2007) examined the effect of OO on eight different *H. pylori* isolates, including three different antibiotic-resistant strains, and observed the potent anti-*H. pylori* activity of OO against all the strains tested. In addition to the reported antibacterial activity, the active

phenolic compounds in OO can remain stable for several hours under harsh acidic environments of the stomach (Murali *et al.*, 2014).

5.2 Materials and methods

Olive oil (density = 0.91 g/cm^3) was obtained from Sigma UK and all other materials were sourced as previously stated.

5.2.1 Method for preparation of oil-modified beads

The required amount of SAL was dissolved in deionised water. Upon dissolution, 10 g of sodium alginate solution was weighed and then homogenised for 10 minutes with varying concentrations of olive oil (OO) (1 – 15 %w/w) and drug relative to the SAL concentration (Murata *et al.*, 2000). A range of formulation variables was explored as detailed in Table 5-1 using the method described in Section 3.2.2.

Table 5-1: Formulation table for oil-modified beads

Code	MET/CMN (w/w) %	Olive oil (w/w) (%)
S1 (MET/CMN)	3	1
S2 (MET/CMN)	3	3
S3 (MET/CMN)	3	5
S4 (MET/CMN)	3	10
S5 (MET/CMN)	3	15
S6 (MET/CMN)	5	1
S7 (MET/CMN)	5	3
S8 (MET/CMN)	5	5
S9 (MET/CMN)	5	10
S10 (MET/CMN)	5	15
S11 (MET/CMN)	10	1
S12 (MET/CMN)	10	3
S13 (MET/CMN)	10	5
S14 (MET/CMN)	10	10
S15 (MET/CMN)	10	15

5.3 Results and discussion

During the homogenization process, a fine dispersion of the oil and water phase was obtained. The homogenisation time was varied and an optimised homogenisation speed and duration (8,000 rpm for 10 minutes) was determined to obtain a stable oil in water emulsion. The homogenisation stage is very important, as without this, the oil and alginate phases will separate. Homogenisation ensures the disruption of the interface between the two phases, allowing them to blend. The emulsifying properties of SAL, through its surface-active ability

to reduce the interfacial tension between an oil and water phase, also contribute to the stability of the emulsion (Choudhury and Kar, 2005). There is generally no limitation on the type of oil that can be used in this type of formulation; however, the only requirement is that the oil should have a lower density than that of water. OO and corn oil have been reported to not leak during the preparation of alginate gels (Kawashima and Murata, 2001). The shape of the beads produced with the inclusion of OO was well rounded. With increasing concentrations of OO in the formulation, the viscosity of the emulsion increased and at concentrations greater than 15 %w/w OO, the emulsion formed became very viscous and quite difficult to pump through the needle into the gelling medium. In addition, the beads formed using high oil content were less spherical, with a tail at one end, Figure 3-9. Therefore, the working range of OO used in this study was between 1 - 15 %w/w. The beads have a yellowish colour, acquiring the colour of the oil while the unmodified beads were whiter.

5.3.1 Morphology and structure of oil - modified beads

Prominent features of these beads are the large pores visible within the core of the beads and the layered structure unique to these beads. These pores appear larger than those observed for the unmodified beads (Figure 5-1) with sizes > 100 μm. The uneven size of the pores could be due to the coalescence of the oil droplets during the gelling process.

5.3.2 Physical properties of the of oil - modified beads

The size, weight and true densities of the beads increased with an increase in concentration of oil in the formulations ($p < 0.05$). There was an increase of ~ 12 % in size with $S9_{MET}$

beads and ~ 10 % with $S9_{CMN}$ compared with the non oil-modified beads. The weights of the beads increased by ~ 44 % , 83 % in $S13_{MET}$ and $S14_{MET}$ beads respectively relative to the non oil-modified beads. These increases in size and weight of the beads due to the presence of OO have been reported by other researchers (Choudhury and Kar, 2005, Jaiswal *et al.*, 2009, Singhal *et al.*, 2010). The bulk densities of the beads was not affected significantly by the addition of oil as detailed in Table 5-2.

Table 5-2: Physical properties of CMN - loaded beads

Code	Diameter (mm)	True density (g/cm^3)	Weight (g) (*n=100*)	Bulk density (g/cm^3)	Porosity (%)
$S8_{MET}$	2.65 ± 0.3	1.12 ± 0.01	0.24 ±0.01	0.19 ± 0.02	89.5
$S9_{MET}$	2.75 ± 0.2	1.23 ± 0.01	0.33 ± 0.01	0.19 ± 0.01	84.5
$S10_{MET}$	2.89 ± 0.3	1.27 ± 0.01	0.35 ± 0.01	0.21 ± 0.03	83.5
$S13_{MET}$	2.74 ± 0.1	1.43 ± 0.01	0.33 ± 0.01	0.27 ± 0.02	81.1
$S14_{MET}$	2.89 ± 0.1	1.51 ± 0.01	0.42 ± 0.01	0.28 ± 0.02	81.5
$S15_{MET}$	2.97 ± 0.2	1.53 ± 0.01	0.45 ± 0.01	0.29 ± 0.04	81.1
$S8_{CMN}$	2.68 ± 0.3	1.16 ± 0.01	0.27 ± 0.01	0.21 ± 0.01	81.9
$S9_{CMN}$	2.73 ± 0.4	1.25 ± 0.01	0.36 ± 0.01	0.22 ± 0.01	82.4
$S10_{CMN}$	2.88 ± 0.3	1.28 ± 0.01	0.39 ± 0.01	0.22 ± 0.02	82.8
$S13_{CMN}$	2.78 ± 0.4	1.46 ± 0.01	0.37 ± 0.01	0.28 ± 0.01	80.8
$S14_{CMN}$	2.91 ± 0.2	1.50 ± 0.01	0.47 ± 0.01	0.29 ± 0.02	80.6
$S15_{CMN}$	2.95 ± 0.4	1.56 ± 0.01	0.49 ± 0.01	0.29 ± 0.01	81.4

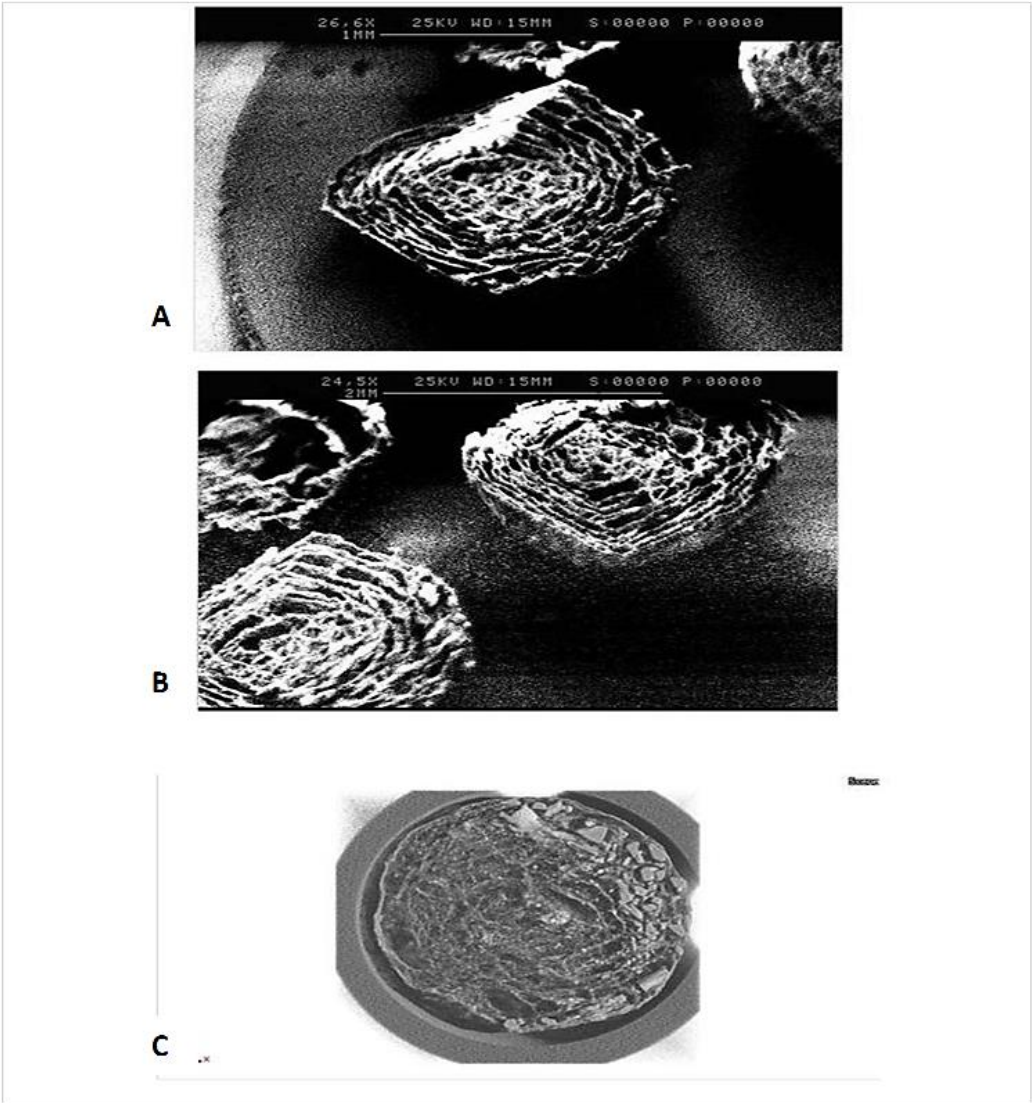

Figure 5-1: SEM images of cross-sectional surface of A) $S14_{MET}$; B) $S14_{CMN}$ and C) XµMT image of $S14_{MET}$ ($S14_{MET}$- beads loaded with 10 % MET and 10 % OO)

5.3.3 Drug content and DEE of oil - modified beads

The inclusion of OO enhanced the DEE of MET ($p < 0.05$) but did not have any effect on the DEE of CMN in the beads. The DEE of the MET beads increased by 15.32 ± 1.29 % on addition of 15 %w/w OO (Figure 5-2a) for all the different drug-polymer ratios, while the inclusion of the same amount of oil only enhanced the DEE of CMN in the beads by 5.92 ± 1.42 % (Figure 5-2b). The addition of oil produced an emulsion, which was slightly more viscous than SAL, thereby entrapping more drug in the bead. In addition, the entrapped oil droplets restricted drug diffusion back into the cross-linking solution and prevented loss during washing of the beads after curing. This result corresponds with the higher DEE observed on inclusion of oil in bead formulations (Murata *et al.*, 2000, Bera *et al.*, 2009). Some researchers have reported that inclusion of oil led to a reduction in the DEE of the beads because of the oil displacing the drug from the beads, thereby occupying most of the volume of the beads (Jaiswal *et al*, 2009). This suggests that there is an optimal volume of oil to be used in the beads and an ideal oil concentration has to be determined.

5.3.4 Differential scanning calorimetry of oil-modified beads

The $S14_{MET}$ and the $S14_{CMN}$ beads showed a single melting endotherm at 156.23 ± 0.57 ℃ (*n=3*) (Figure 5-3) and 225.17 ± 0.94 ℃ (*n=3*) (Figure 5-4) respectively with the absence of any extra peaks on the thermograms. The melting endotherms in the oil-modified beads was slightly lower than that observed in unmodified beads especially MET beads (MET (164.13 ± 0.81℃) and CMN (226.56 ± 0.89 ℃). Also, they were lower than those observed in the pure samples of MET (163.15 ± 0.52℃) and (CMN) 227.5 ± 0.32 ℃. This was probably due to the proportion of oil present in the formulation. These findings indicate that there was no interaction between the drug and oil during the process of bead formation and both drugs were stable in the formulation. Other researchers have reported similar results (Satishbabu *et al.*, 2010, Ahmed *et al.*, 2013).

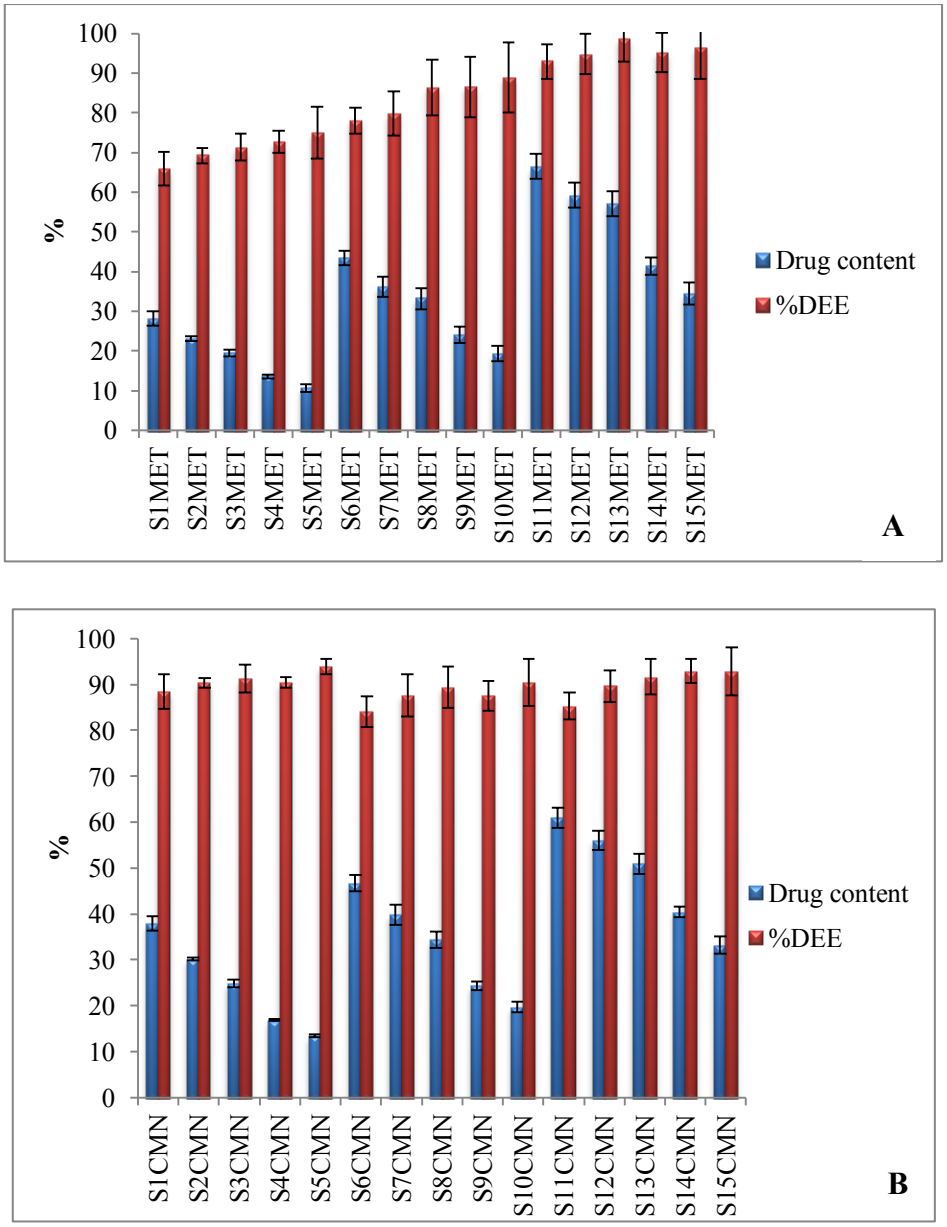

Figure 5-2: Drug content and DEE of A) MET and B) CMN oil-modified beads

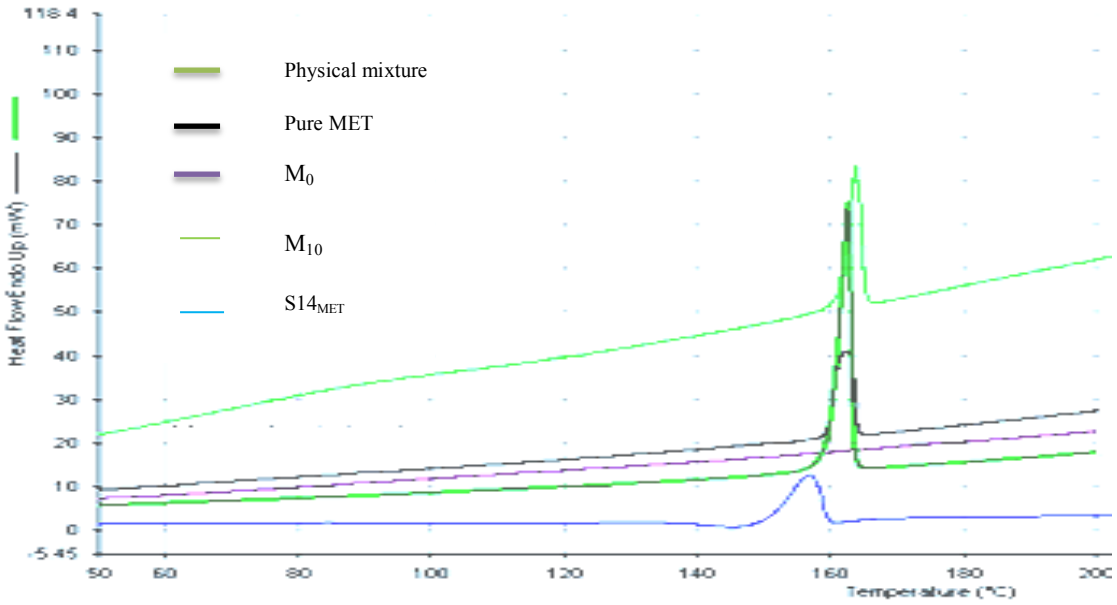

Figure 5-3**:** DSC thermograms of physical mixture of MET and SAL; pure MET; non oil modified and oil modified beads.

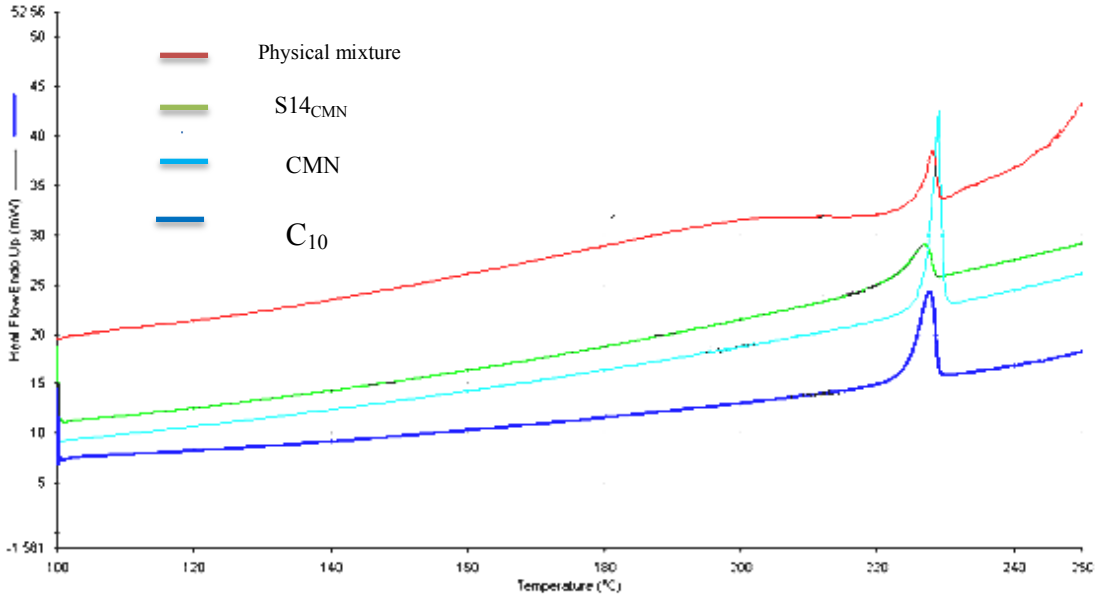

Figure 5-4: DSC thermograms of DSC thermograms of physical mixture of CMN and SAL; pure CMN; non oil modified and oil modified

5.3.5 Fourier transform infrared (FT-IR) analysis of oil-modified beads

The oil-modified beads showed characteristic peaks similar to those of the unmodified beads for both MET and CMN as shown in Figures 5-5 and 5-6, even though the peaks showed lower intensities compared to the pure drug, indicating there was no chemical interaction between the oil and/or the drugs or the polymer.

5.3.6 *In vitro* buoyancy and buoyancy profile of oil-modified beads

The addition of OO improved the buoyancy of the beads with an increasing concentration of the oil leading to an increase in the *in vitro* buoyancy ($p < 0.05$) over the period of analysis as shown in Figure 5-7 and Figure 5-8. The beads prepared at a concentration < 10 %w/w OO failed the test as a proportion of the beads sank during the analysis. However, there was an increase in the proportion of floating beads with an increase in concentration of oil added. The beads loaded with ≥ 10 %w/w OO provided the best buoyancy profiles as they remained buoyant at all drug-polymer ratios over all the different time intervals. The oil entrapped in the bead acts as a floating aid (Murata *et al.*, 2000) due to its hydrophobicity thereby prolonging the duration of floating. The oil acts as a dispersed phase to prepare a stable emulsion and creates multiple tiny pockets in the alginate matrix (as shown in the SEM and XμMT images (Figure 5-1)) for better buoyancy. For formulations containing ≥ 10 %w/w olive oil, the onset of floating was within 1 minute, compared to 3 minutes for equivalent formulations without oil. The lag time remained unchanged for the beads containing < 5 %w/w oil, but as the concentration of oil increased, the lag time reduced. A short lag time is important as this minimises the occurrence of premature evacuation of the beads from the stomach (Streubel *et al*., 2003a).

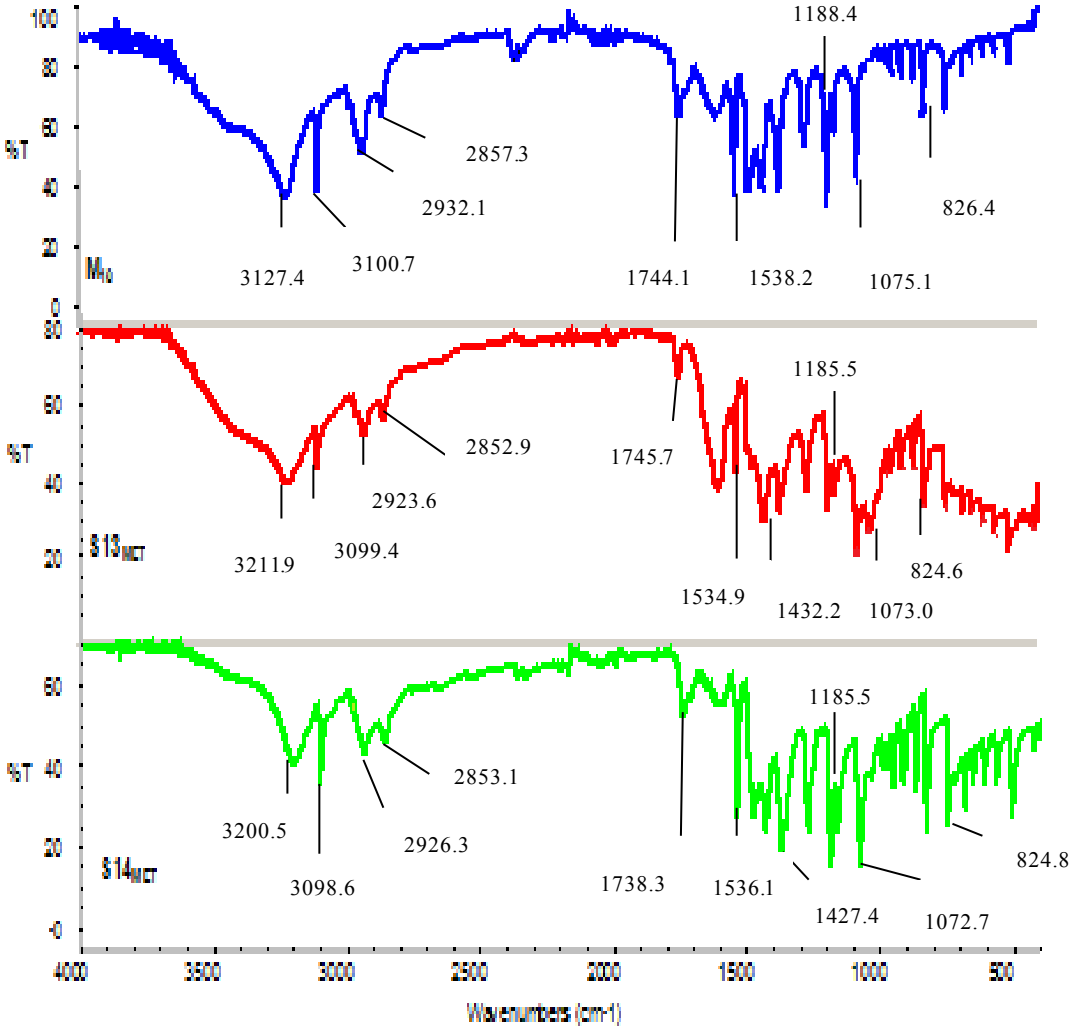

Figure 5-5: FTIR scans of unmodified and oil-modified MET beads

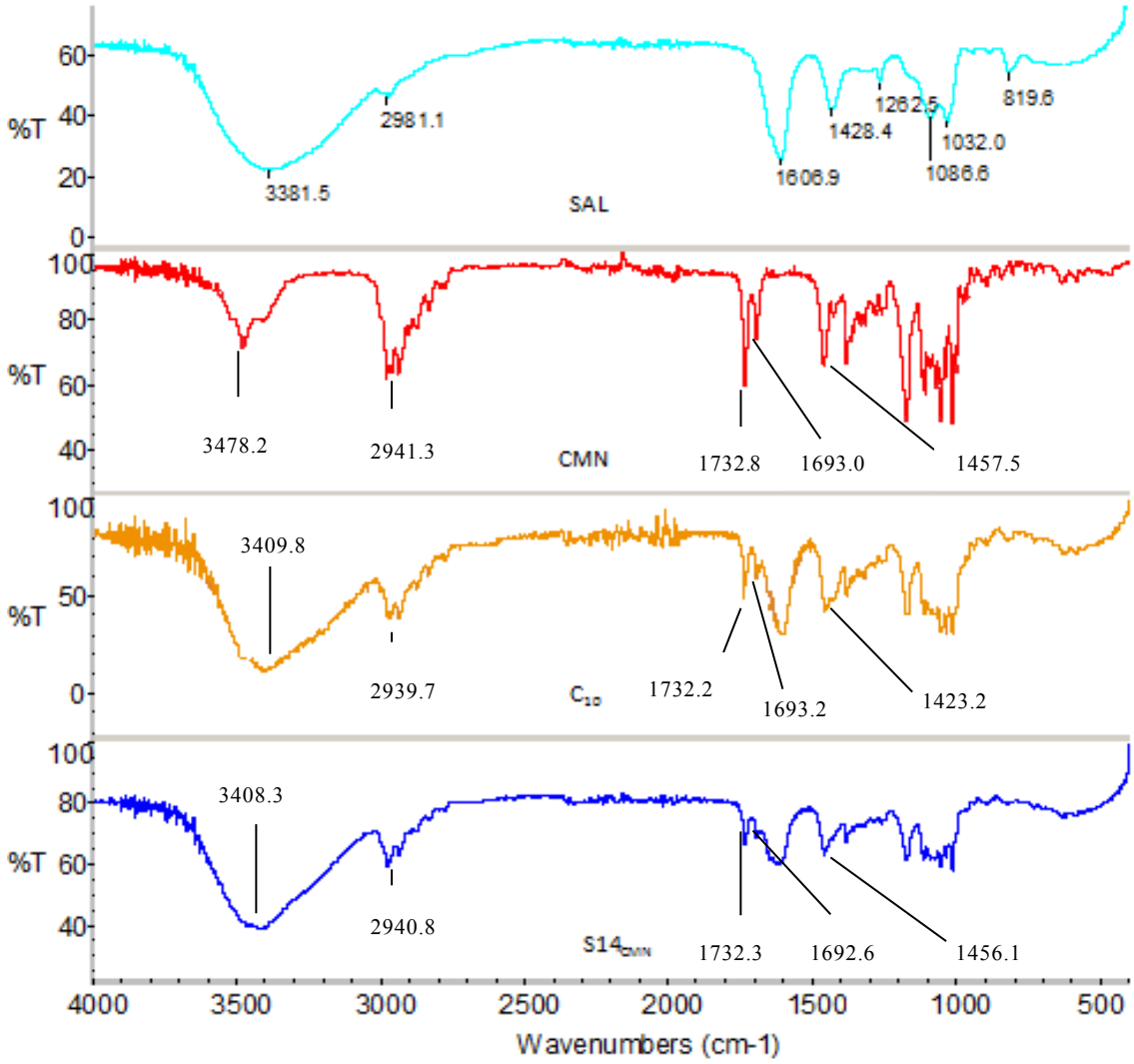

Figure 5-6: Comparison FTIR scans of unmodified and oil-modified CMN beads

A few studies have been able to achieve adequate buoyancy of alginate beads by incorporating concentrations of oil as low as 0.5 % in the formulation (Malviya *et al.*, 2013), however, in this study these concentrations had no impact. However, several studies have used concentrations as high as 15 – 30 %w/w to achieve buoyancy (Wu *et al.*, 1997, Morgner *et al.*, 2000, Ma *et al.*, 2008, Strubing *et al.*, 2008, Khan and Bajpai, 2011). Optimal concentrations of oil in this study were 10 - 15 % with higher levels potentially negatively affecting the DEE and the mechanical strength of the beads. In addition, oil leakage could occur from the beads at high concentrations after drying. The fact that the beads used in this study were freeze-dried rather than air-dried or oven-dried as in other studies gave the beads additional buoyancy, hence the requirement of a lower concentration of oil.

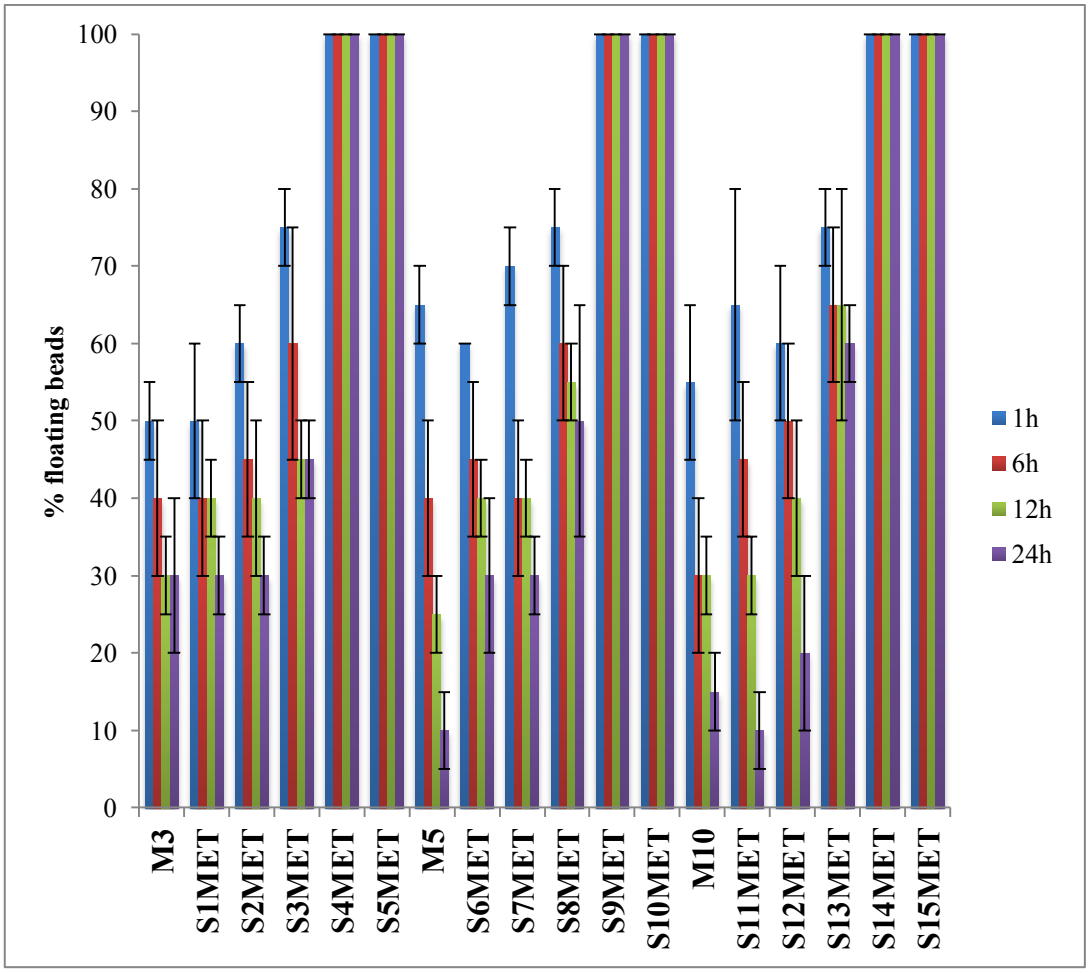

Figure 5-7: Buoyancy profile of oil modified metronidazole loaded beads

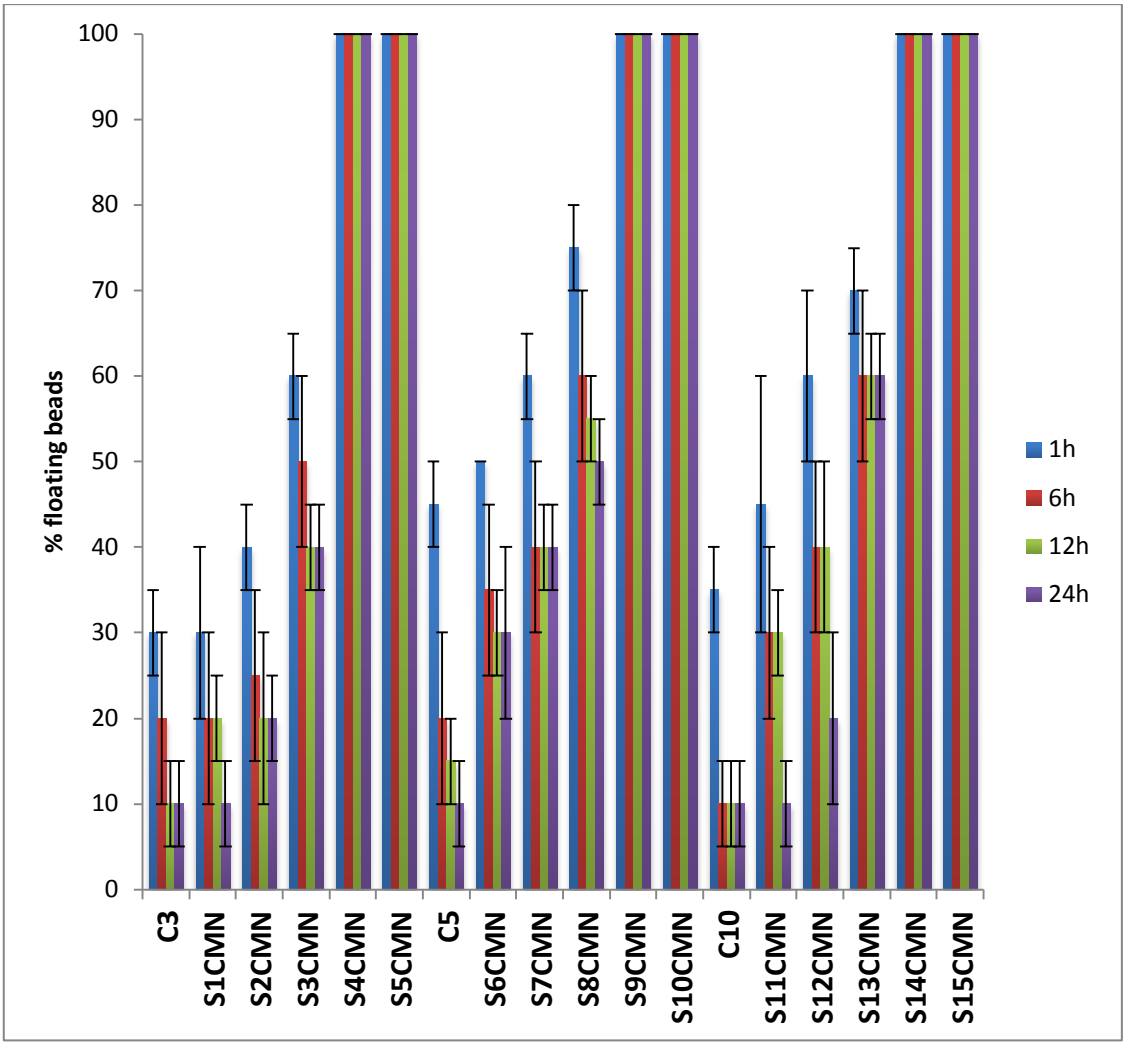

Figure 5-8: Buoyancy profile of oil modified clarithromycin loaded beads

5.3.7 Swelling profile of oil-modified beads

The oil-modified beads reached their maximum sizes after 100 - 150 minutes in both acidic and alkaline media irrespective of the drug loaded into the beads. In acidic media, the beads increased to a range of 50 – 200 % of their original weight depending on the drug and oil

content. Increasing oil content did not significantly affect the swelling ratio ($p > 0.05$) but the presence of oil had a significant effect on the swelling ratio when compared with unmodified beads ($p < 0.05$) (Figure 5-9). In PBS, there was a significant reduction in swelling ratio on addition of oil to the formulations with a reduction from about 2000 % (average swelling ratio of unmodified beads) to about 750 % (Figure 5-10). The oil serves as a barrier to the absorption of water and pores normally filled with water in the unmodified beads is assumed to be occupied by the oil, therefore limiting the volume of the beads available for water absorption and swelling in water. The observed reduction in swelling of oil modified beads has been reported by other researchers (Jaiswal *et al*., 2009, Patel *et al*., 2011). The disintegration of the oil-modified beads started at approximately 180 - 210 minutes, while for the unmodified beads the disintegration started at about 150 minutes and complete dissolution was between 300 - 360 minutes for oil-modified beads while the unmodified beads were completely dissolved at ~ 240 minutes. The oil probably delayed the uptake of water into the beads due to its hydrophobic nature and delayed the ionic exchange required for bead disintegration as previously discussed in section 3.3.3.8.

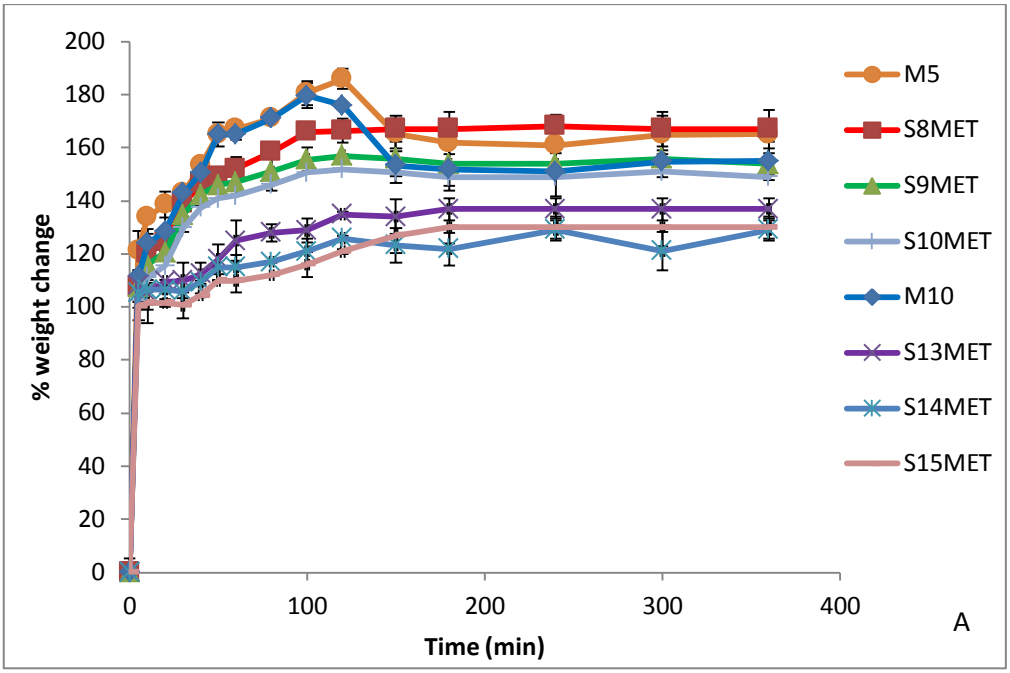

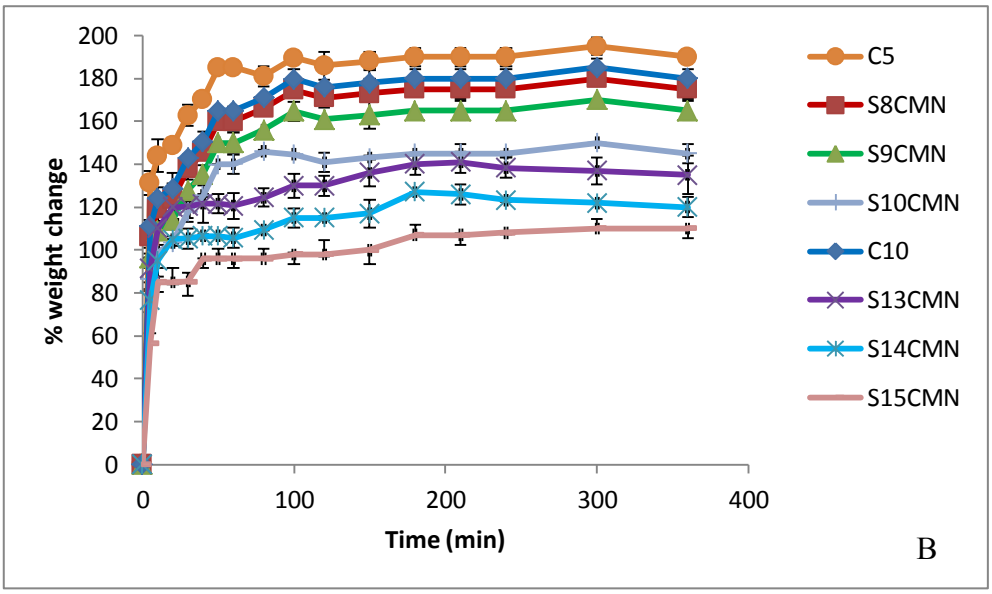

Figure 5-9: Swelling profile of oil-modified A) MET and B) CMN beads in acidic media

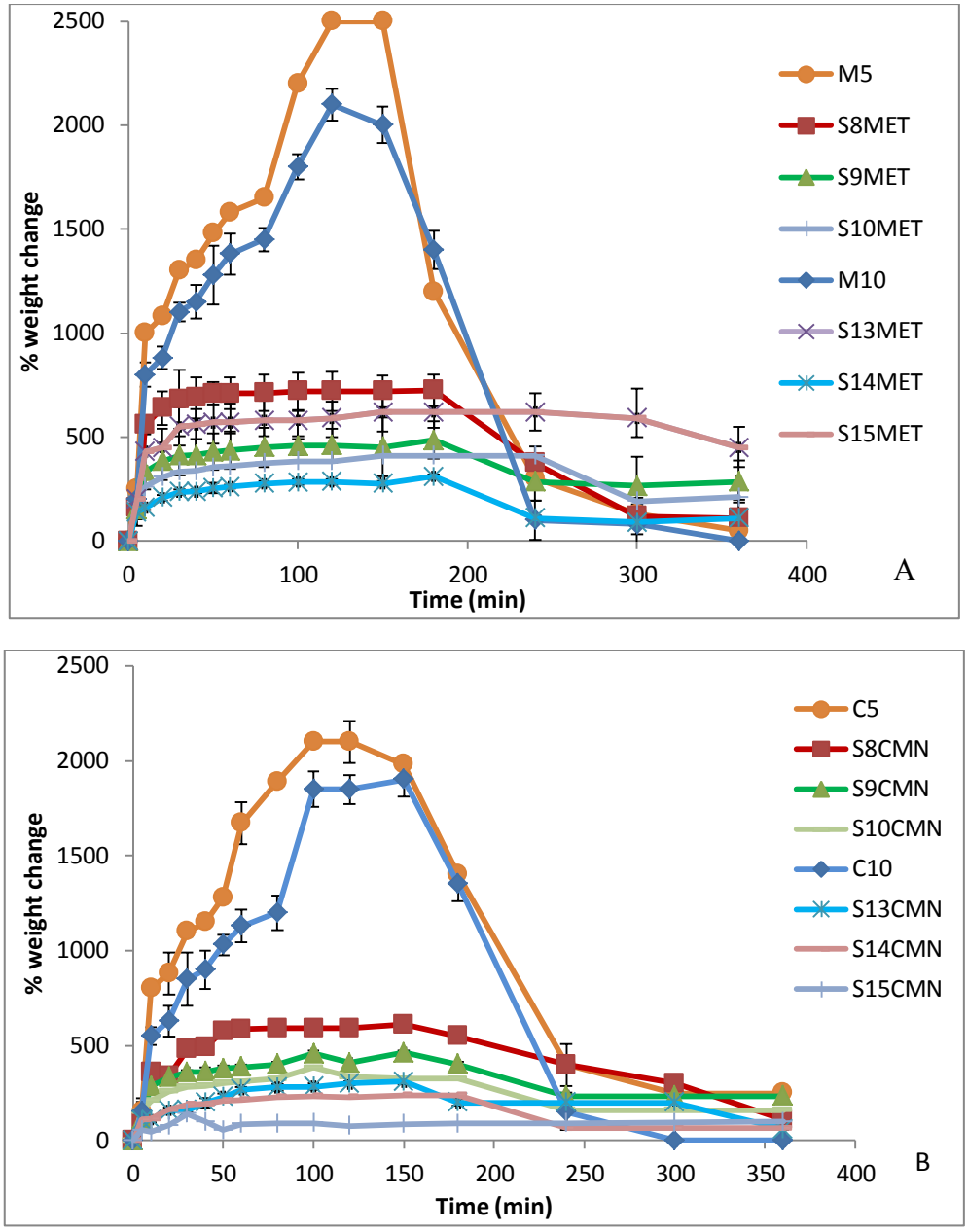

Figure 5-10: Swelling profile of oil-modified A) MET and B) CMN beads in PBS

5.3.8 *In vitro* drug release from oil-modified beads

5.3.8.1 Release in acidic media

Similarly, to unmodified beads, for both batches of oil-modified beads, there was a biphasic release pattern with an initial burst release followed by a slower release.

5.3.8.1.1 Modified MET beads

In acidic pH (pH 1.2), the inclusion of oil at low concentrations (< 10 %) in MET beads did not reduce the release rate of drug and at some time points drug release was even higher than the unmodified beads (60 >f_2 >53) . However, at concentrations > 10 % , there was a significant difference with the oil retarding drug release. In comparison, $S10_{MET}$ beads *versus* M_5 beads had a f_2 value of 30.3 and $S15_{MET}$ *versus* M_{10} had a f_2 value of 38.1. Similar effects were observed at low drug / high oil loading, *e.g.* $S4_{MET}$, release of MET was reduced significantly compared to the unmodified beads (40 >f_2 >30). Complete drug release was achieved within 6 h which is an extension of lifetime of the formulation by 3 h compared with the unmodified beads (Figure 5-11a).

5.3.8.1.2 Modified CMN beads

Addition of oil at concentrations ≥ 10 % significantly reduced CMN release from the modified beads (Figure 5-11b) (42 >f_2 >32). This is in contrast to results for MET beads, where more oil was required to modify MET release. This difference in effects might be due to the combined effect of a hydrophobic drug and oil, which led to the retardation of aqueous permeation and reduced swelling of the bead matrix. The limiting factors on drug release are dissolution and diffusion of drug passing through the oil pockets and the bead matrix. The oil

adds an additional diffusion barrier layer to the release of the drug from the beads. This barrier formed by the oil phase was more substantial for the CMN beads than the MET beads. The respective $t_{50\%}$ and $t_{75\%}$ (Table 5-3) all increasing with increasing concentrations of the olive oil ($p < 0.05$) (with the exception of modified beads loaded with 10 % CMN); the differences were more pronounced for CMN beads than MET beads.

The presence of oil in the formulation at < 10 % concentration did not significantly retard MET release but sustained release was achieved at concentrations > 10 %. However, due to the inherent low solubility of CMN, the presence of oil even at low concentrations retarded drug release (≥ 10 %). These release profiles concurred with the results obtained from Murata *et al*. (2010), where the oil-modified beads released their drug contents at a slower rate with only about 80 % of the drug released within 60 min when compared with the unmodified beads with complete release within 30 min.

Table 5-3: Release profiles of oil-modified beads in acidic and alkaline media

Formulation	$t_{25\%}$	$t_{50\%}$	$t_{75\%}$	$t_{25\%}$	$t_{50\%}$	$t_{75\%}$
Acidic media (0.1N HCl pH 1.2 (MET) and pH 2.0 (CMN))				**PBS (pH 7.4)**		
$S8_{MET}$	< 5	5 -10	40 - 50	< 5	10 -15	20 - 30
$S9_{MET}$	< 5	15 - 20	50 -60	< 5	10 -15	20 -30
$S10_{MET}$	5-10	30	80 -100	5	10 -15	30 -40
$S13_{MET}$	< 5	5-10	40-50	5	15-20	40-50
$S14_{MET}$	< 5	15-20	50-60	5-10	20-30	40-50
$S15_{MET}$	5-10	20-30	80-100	5-10	20-30	40-50
$S8_{CMN}$	10	60-90	120-180	20-30	50-60	80-100
$S9_{CMN}$	10-20	90-120	180-240	30	50-60	80-100
$S10_{CMN}$	30-60	120	360	30-40	60	80-100
$S13_{CMN}$	10-20	60-90	240-300	20-30	50-60	80-100
$S14_{CMN}$	20-30	90	300-360	30	60	80-100
$S15_{CMN}$	30	90-120	360	30-40	60-80	100

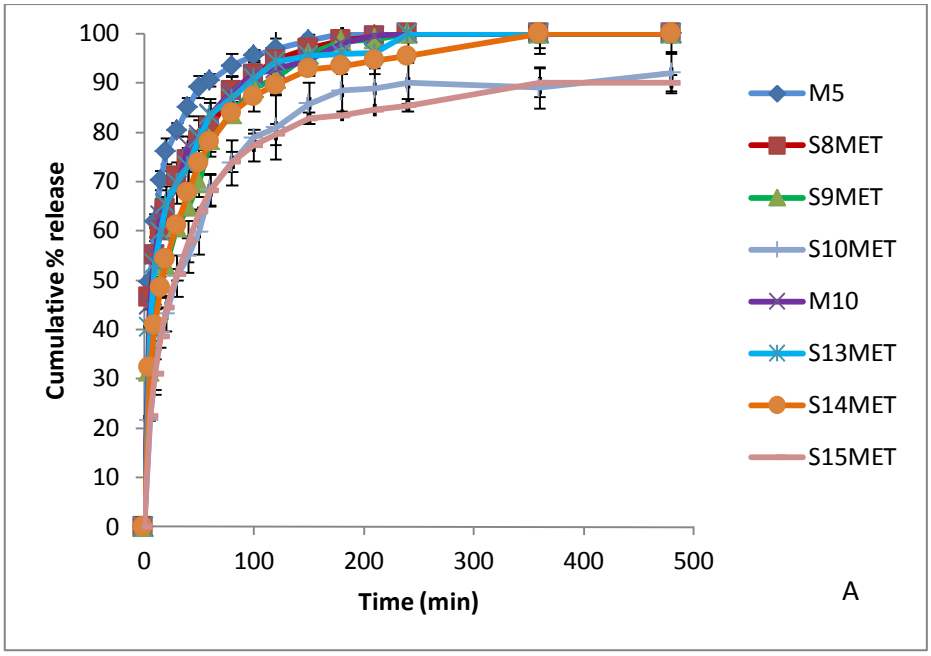

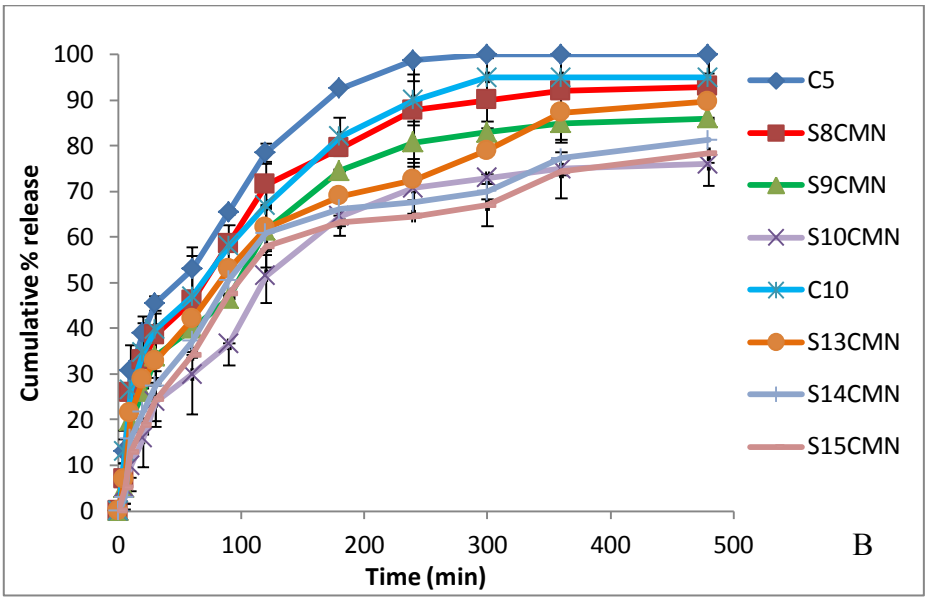

Figure 5-11: Drug release of oil-modified A) MET beads at pH 1.2 and B) CMN beads at pH 2.0

5.3.8.2 Release kinetics of oil-modified beads in acidic media

The release profiles of oil-modified beads were both in favour of Higuchi-diffusion kinetics (R^2 = 0.94 – 0.99 (MET) and R^2 = 0.95 – 0.98 (CMN) (Table 5-4). This is similar to the release kinetics observed with the unmodified beads, therefore it can be deduced that the oil did not change the drug release kinetics. For the modified MET beads, the release exponent 'n' was ≤ 0.43, indicating Fickian diffusion for the formulations containing up to 10 % OO, but at 15 % olive oil n > 0.43 indicating non-Fickian anomalous diffusion with drug release controlled by a combination of diffusion and polymer relaxation. For the modified CMN beads, the release exponent was 0.59 - 0.80, indicating non-Fickian anomalous diffusion (Table 5-5). There was a change in the release kinetics as the unmodified CMN beads exhibited Fickian diffusion while the oil-modified beads exhibited non-Fickian anomalous diffusion related to diffusion and swelling. Some oil-modified alginate formulations have been reported to exhibit a non-Fickian diffusion mechanism (Ahmed *et al.*, 2013, Malakar *et al.*, 2012).

Table 5-4: Release kinetics of MET beads in both acidic and alkaline media

pH 1.2										
Sample	**Zero order**		**1st order**		**Higuchi**		**Hixson-Crowell**		**Peppas**	
	K_0(%/min)	**R^2**	**K_1(min^{-1})**	**R^2**	**K(%/$min^{1/2}$)**	**R^2**	**k**	**R^2**	**n**	**R^2**
$S8_{MET}$	2.84	0.74	0.02	0.84	14.51	0.94	0.06	0.81	0.23	0.99
$S9_{MET}$	1.79	0.79	0.01	0.89	11.21	0.98	0.04	0.87	0.37	0.99
$S10_{MET}$	1.02	0.83	0.01	0.92	8.48	0.98	0.02	0.89	0.43	0.98
$S13_{MET}$	3.85	0.85	0.03	0.92	15.84	0.98	0.08	0.90	0.36	0.99
$S14_{MET}$	1.81	0.80	0.01	0.90	11.26	0.98	0.04	0.87	0.36	0.99
$S15_{MET}$	1.10	0.87	0.01	0.95	8.99	0.99	0.02	0.93	0.45	0.99
pH 7.4										
Sample	**Zero order**		**1st order**		**Higuchi**		**Hixson-Crowell**		**Peppas**	
	K_0(%/min)	**R^2**	**K_1(min^{-1})**	**R^2**	**K(%/$min^{1/2}$)**	**R^2**	**k**	**R^2**	**n**	**R^2**
$S8_{MET}$	3.80	0.89	0.03	0.95	15.42	0.99	0.08	0.93	0.41	0.99
$S9_{MET}$	3.12	0.90	0.02	0.97	14.82	0.99	0.07	0.95	0.50	0.99
$S10_{MET}$	3.11	0.95	0.02	0.98	14.41	0.99	0.06	0.98	0.65	0.98
$S13_{MET}$	1.97	0.88	0.01	0.96	11.79	0.99	0.04	0.94	0.51	0.99
$S14_{MET}$	1.86	0.91	0.03	0.98	10.94	0.99	0.02	0.99	0.52	0.99
$S15_{MET}$	2.06	0.96	0.01	0.99	11.77	0.99	0.02	0.99	0.65	0.99

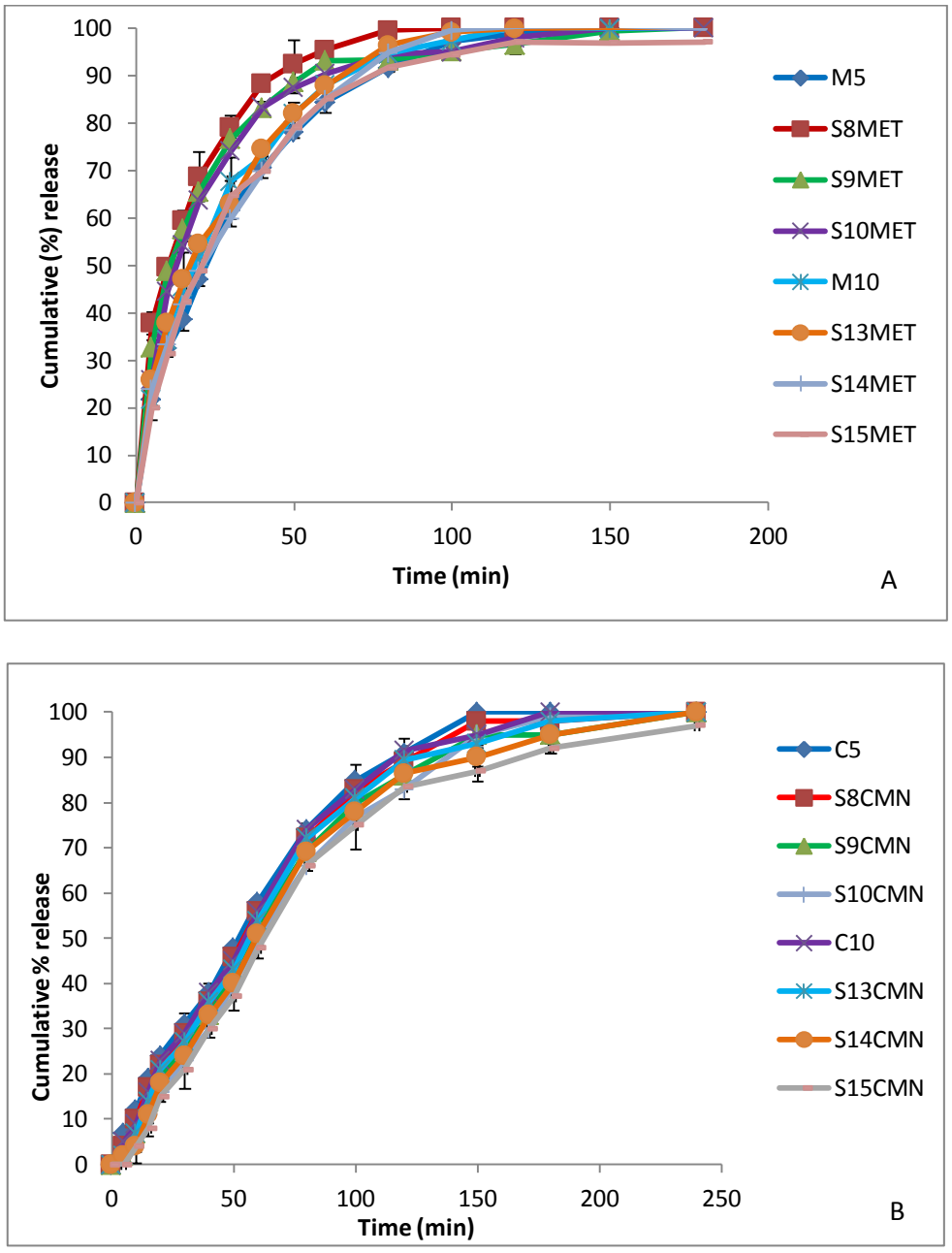

Figure 5-12: Drug release of oil-modified A) MET beads and B) CMN beads in PBS

5.3.8.3 Release of oil-modified beads in alkaline media

In PBS, calcium alginate was converted to a soluble salt of sodium alginate and the matrix disintegrated, completely releasing the drug encapsulated in the beads similar to the unmodified beads. Drug release was due more to the swelling and erosion of the beads than diffusion of the drug especially at the initial stages with the CMN beads due to the low solubility of CMN. The beads started to disintegrate /dissolve in PBS at ~ 180 - 210 minutes leading to fast drug release and complete dissolution was between 300 - 360 minutes, a time at which drug release was already complete for MET (~ 180 minutes (Figure 5-12a)) and CMN (~ 240 minutes (Figure 5-12b)). At some time points, drug release from oil-modified beads was faster than unmodified beads and this may be because the oil slightly reduced the extent of cross-linking of the beads or the cross-linked calcium was displaced faster from the cross-linked beads. From these results, it can be deduced that the addition of olive oil in this formulation did not significantly affect the drug release in PBS, though the disintegration and complete dissolution of the beads in PBS were delayed compared with unmodified beads. Therefore, the presence of oil will not have any significant effect on its route of elimination from the body.

5.3.8.4 Release kinetics of oil-modified beads in alkaline media

Drug release from oil modified MET beads followed Higuchi-diffusion kinetics (R^2 = 0.99). The release exponent ‘n’ was mostly between 0.49 – 0.65 (Table 5-4), with an exception of $S8_{MET}$ beads with a value of 0.41. Therefore, the beads exhibited anomalous drug diffusion related to swelling and diffusion. The CMN beads followed mostly zero-order drug release, which is due to low solubility of drug in the media and the presence of oil thereby presenting a hydrophobic drug within a hydrophobic polymer matrix in a hydrophilic media. The ‘n’ value was 1.01 - 1.30 (Table 5-5) indicating supercase II transport which means that the drug

release rate did not change over time and involves polymer relaxation and chain disentanglement (Harland *et al.*, 1988).

Table 5-5: Release kinetics of CMN beads in both acidic and alkaline media

pH 2.0										
Sample	**Zero order**		**1st order**		**Higuchi**		**Hixson-Crowell**		**Peppas**	
	K_0(%/min)	**R^2**	**K_1(min^{-1})**	**R^2**	**K(%/$min^{1/2}$)**	**R^2**	**k**	**R^2**	**n**	**R^2**
$S8_{CMN}$	0.571	0.817	0.004	0.903	6.238	0.949	0.012	0.877	0.632	0.829
$S9_{CMN}$	0.443	0.877	0.003	0.935	5.446	0.963	0.009	0.921	0.658	0.859
$S10_{CMN}$	0.344	0.960	0.002	0.984	4.864	0.987	0.007	0.981	0.678	0.983
$S13_{CMN}$	0.458	0.886	0.003	0.95	5.565	0.979	0.009	0.937	0.593	0.898
$S14_{CMN}$	0.4776	0.913	0.003	0.912	5.708	0.979	0.009	0.973	0.809	0.876
$S15_{CMN}$	0.355	0.919	0.002	0.966	5.157	0.985	0.007	0.954	0.674	0.968
pH 7.4										
Sample	**Zero order**		**1st order**		**Higuchi**		**Hixson-Crowell**		**Peppas**	
	K_0(%/min)	**R^2**	**K_1(min^{-1})**	**R^2**	**K(%/$min^{1/2}$)**	**R^2**	**k**	**R^2**	**n**	**R^2**
$S8_{CMN}$	0.891	0.993	0.002	0.981	7.418	0.931	0.006	0.969	1.012	0.984
$S9_{CMN}$	0.876	0.996	0.006	0.971	8.032	0.914	0.018	0.986	1.209	0.971
$S10_{C,MN}$	0.847	0.996	0.006	0.967	7.689	0.893	0.017	0.982	1.280	0.981
$S13_{CMN}$	0.903	0.992	0.005	0.987	7.299	0.915	0.017	0.992	1.261	0.965
$S14_{CMN}$	0.877	0.995	0.006	0.961	7.971	0.895	0.023	0.977	1.294	0.977
$S15_{CMN}$	0.847	0.994	0.006	0.957	7.629	0.877	0.023	0.978	1.301	0.984

5.4 Conclusion

Beads loaded with either MET or CMN were modified with OO, which has been documented to possess some anti-*H. pylori* activity and used to impart buoyancy to the beads. Beads loaded with ≥ 10 %w/w oil, showed excellent buoyancy with 100 % buoyancy over a 24 h period. In addition to these favourable buoyancy properties, the beads had a high DEE with the DEE of MET increasing, though this had no effect on DEE of CMN. Drug release from the oil-modified MET beads containing ≤ 10 % OO was not as controlled as CMN and was similar to unmodified beads. The inclusion of OO at a concentration > 10 %w/w and ≥ 10 %w/w were required to retard MET and CMN release, respectively. However, too much oil (> 15 %w/w) in the formulation may negatively influence the mechanical strength of the beads and cause oil leakage from the beads on drying, even though the oil may retard drug release. Therefore, formulations containing the right amount of oil (usually 10 - 15 %w/w oil) are likely to be buoyant for > 24 h, release drug in a controlled manner than the unmodified beads and may be retained long enough in the stomach for them to be able to release their drug contents before being removed from the stomach. Drug release from oil-modified MET beads containing 15 %w/w OO was extended to ~ 6 h and CMN release was extended to > 8 h.

Chapter 6 MODIFICATION OF ALGINATE BEADS TO CONTROL RELEASE AND MUCOADHESION PROFILE OF BEADS BY ADDITION OF CHITOSAN

6.1 Chapter overview

Despite the documented advantages of calcium alginate beads as drug delivery devices, there are a number of challenges to their application, which were observed in previous chapters. Such limitations include rapid drug release, low buoyancy in SGF and high solubility and instability in alkaline media (pH > 6). Therefore, in this chapter, further modifications were carried out to improve the gastro-retentive and drug release properties of the drug loaded alginate beads. The beads produced have been previously optimised based on their buoyancy properties in Chapter 5; however, it is proposed that an additional layer of a mucoadhesive polymer on the bead surface may improve the beads' gastro-retentive properties by converting the beads from a floating DDS into a floating-mucoadhesive DDS. This dual-functioning formulation is expected to bind to stomach mucosal layers, in addition to having the ability to float on gastric contents. This helps to further improve the opportunities for retention of the beads in the stomach. A mucoadhesive polymer, chitosan, was used in this study to extend the mucoadhesiveness of the beads beyond the adhesiveness imparted by

SAL (Chen and Cyr, 1970, Smart, 1984, Richardson *et al*, 2004, Esposito *et al*, 1994). This additional mucoadhesive layer is also expected to help further control drug release from the bead surface by extending the path length for drug to pass through before drug release from the beads, reduce the porosity at the bead surface and reducing the proportion of loosely associated surface drug. These effects might help to reduce the burst release and increase the lifetime of the DDS. Dual functioning systems can be exploited to achieve synergy and help to overcome the drawbacks associated with each of the floating and mucoadhesive systems. The theory of combining two or more gastro-retentive techniques has been explored by various researchers to improve gastro-retention of formulations (Chitnis *et al*, 1991, Umamaheswari *et al*, 2002, Zheng *et al*, 2006, Rajinikanth *et al*, 2008, Gattani *et al*, 2010, Sahasathian *et al*, 2010, Vaiciunas *et al*, 2010, Singh *et al*, 2012).

6.2 Materials and method

Chitosan (low molecular weight (LMW), 75 - 85 % deacetylated); medium molecular weight (MMW), 75 - 85 % deacetylated) and high molecular weight (HMW), 75 - 85 % deacetylated), glacial acetic acid, Cibacron Brilliant Red 3B-A, Glycine HCl buffer, Periodic acid solution, 1 % basic Fuschin and Sodium metabisulphite were obtained from Sigma (UK).

6.2.1 Preparation of coated beads

Following preparation of drug-loaded beads as described in section 3.2.2 and 5.2.1, the beads were cured for 15 minutes in a $CaCl_2$ solution. After curing and washing with deionized

water, the beads were blotted on absorbent paper to remove any residual water. The beads were immersed in chitosan solutions (pH 5) for 30 minutes with gentle stirring to allow formation of a polyelectrolyte complex membrane on the surface of the beads. The concentrations used are detailed in Table 6-1. This method was used to produce two categories of beads; a) coated non oil-modified (CNOM) and b) coated oil-modified (COM) beads. The beads were recovered, washed, snap frozen in liquid nitrogen and freeze-dried. The beads produced were then characterised as described in Section 2.3 as well as other evaluation methods described in this chapter.

Table 6-1: Formulation variables for coated beads. The G series contained MET and the D series contained CMN.

Code	Drug (%w/w)	Oil (%w/w)	Chitosan (%w/v)	Drug
G1/D1	5	-	0.5 (LMW)	MET/CMN
G2/D2	5	-	1 (LMW)	MET/CMN
G3/D3	5	-	0.5 (MMW)	MET/CMN
G4/D4	5	-	1 (MMW)	MET/CMN
G5/D5	5	-	0.5 (HMW)	MET/CMN
G6/D6	5	-	1 (HMW)	MET/CMN
G7/D7	10	-	0.5 (LMW)	MET/CMN
G8/D8	10	-	1 (LMW)	MET/CMN
G9/D9	10	-	0.5 (MMW)	MET/CMN
G10/D10	10	-	1 (MMW)	MET/CMN
G11/D11	10	-	0.5 (HMW)	MET/CMN
G12/D12	10	-	1 (HMW)	MET/CMN
G13/D13	5	10	0.5 (LMW)	MET/CMN
G14/D14	5	10	1 (LMW)	MET/CMN
G15/D15	5	10	0.5 (MMW)	MET/CMN
G16/D16	5	10	1 (MMW)	MET/CMN
G17/D17	5	10	0.5 (HMW)	MET/CMN
G18/D18	5	10	1 (HMW)	MET/CMN
G19/D19	5	15	0.5 (LMW)	MET/CMN
G20/D20	5	15	1 (LMW)	MET/CMN
G21/D21	5	15	0.5 (MMW)	MET/CMN
G22/D22	5	15	1 (MMW)	MET/CMN
G23/D23	5	15	0.5 (HMW)	MET/CMN
G24/D24	5	15	1 (HMW)	MET/CMN
G25/D25	10	10	0.5 (LMW)	MET/CMN
G26/D26	10	10	1 (LMW)	MET/CMN
G27/D27	10	10	0.5 (MMW)	MET/CMN
G28/D28	10	10	1 (MMW)	MET/CMN
G29/D29	10	10	0.5 (HMW)	MET/CMN
G30/D30	10	10	1 (HMW)	MET/CMN
G31/D31	10	15	0.5 (LMW)	MET/CMN
G32/D32	10	15	1 (LMW)	MET/CMN
G33/D33	10	15	0.5 (MMW)	MET/CMN
G34/D34	10	15	1 (MMW)	MET/CMN
G35/D35	10	15	0.5 (HMW)	MET/CMN
G36/D36	10	15	1 (HMW)	MET/CMN

6.2.2 Determination of amount of chitosan bound to alginate bead surface

6.2.2.1 Chitosan assay

Cibacron Brilliant Red 3B-A dye stock solution was prepared by dissolving 150 mg of the powder in 100 ml deionized water. 5 ml of this solution was diluted to 100 ml with 0.1 M Glycine HCl buffer to prepare a final dye concentration of 0.075 mg/ml (pH 2.8). Stock solutions of 0.5 %w/v chitosan in acetic acid were prepared and different volumes of these polymer solutions (30, 45, 60, 80, 100, 150, 200 and 250 µl) were filled into test tubes and made up to 300 µl with 0.1M Glycine HCl buffer. Aliquots of dye solution (3 ml) were added to each tube and the absorbance values were measured spectrophotometrically at 575 nm (Muzzarelli, 1998, Miralles *et al.*, 2011).

6.2.2.2 Bound chitosan per bead surface area

After washing, 50 beads were transferred directly into the chitosan solutions used for coating. The difference between the amount of chitosan in solution before and after coating was calculated as the amount of chitosan bound to the alginate beads.

The total surface area of all the beads was calculated using Equation 6-1:

Surface area of individual beads x total number of beads = $4\pi r^2$ x number of beads……..….Equation 6-1

The amount of bound chitosan was calculated using Equation 6-2:

$$Bound\ chitosan\ \left(\frac{\mu g}{mm^2}\right) = \frac{Bound\ chitosan\ (\mu g)}{total\ surface\ area\ of\ all\ beads\ (mm^2)} \quad \text{……. Equation 6-2}$$

6.2.3 Mucoadhesion tests

6.2.3.1 Mucin-particle method

6.2.3.1.1 Mucin sample preparation

Mucin suspensions (1 mg/ml) were prepared and the pH was adjusted to pH 3.0 with HCl and agitated overnight. The average hydrodynamic diameter of mucin in this suspension was determined (see section 6.2.3.1.2). The suspension was sonicated for 15 min and centrifuged at 4,000 rpm for 10 min to isolate mucin particles between ~ 200 – 300 nm. The supernatant was recovered and used in the experiment. Mucin suspension (1 ml) was mixed with chitosan solution at the same pH in different chitosan/mucin ratios (0.0125 - 10) by vortexing for 1 minute. All suspensions were incubated at 37 ℃ for 1 h before analysis (Sogias *et al.*, 2008, Takeuchi *et al.*, 2005)

6.2.3.1.2 Particle sizing of chitosan-mucin mixtures

The hydrodynamic diameter of the mucin before and after size reduction and the diameter of the polymer-mucin mixtures were measured using NTA (Nanosight LM 10). The samples were injected into the sample chamber using a disposable syringe. Suspended particles were irradiated by a laser source and as these particles scatter the light, the particle dynamics were visualized at 30 frames per second by the Coupled Charge Device (CCD) camera. The paths the particles take under Brownian motion over time were analysed using the NTA software. Each particle visible in the image was individually but simultaneously tracked. The samples were measured in triplicate and the results represent the mean hydrodynamic diameter.

6.2.3.1.3 Turbidity of chitosan-mucin mixtures

Turbidity of the polymer suspensions, mucin suspensions and the polymer-mucin mixtures was measured at 400 nm using a UV spectrophotometer (Jenway 6305 UV/VIS).

6.2.3.1.4 Zeta potential of chitosan-mucin mixtures

The *Zp* and pH of the polymer suspension, mucin suspension and polymer-mucin mixtures were measured with a Zetasizer Z (Malvern UK) using the capillary cell. All samples were controlled at 25 ± 0.1°C during the test. The measurements were repeated at least 5 times and the mean values and standard deviations were calculated.

6.2.3.2 Mucin adsorption assay

Mucin adsorption was studied using a periodic acid /Schiff colorimetric method described by Mantle and Allen (Mantle and Allen, 1978) to determine the free mucin concentration following incubation with beads.

6.2.3.2.1 Calibration curve of mucin using PAS/Schiff colorimetric assay

Standard calibration curves for mucin were prepared from 2 ml of mucin standard solutions of concentrations (0.125 mg/ml – 0.5 mg/ml). Periodic acid reagent (0.2 ml) was added to the mucin standard solutions and these mixtures were incubated at 37 ℃ for 2 h in a water bath. Periodic acid reagent was freshly prepared by adding 10 µl of 50 % of periodic acid solution to 7 ml of 7 % acetic acid solution (He *et al.*, 1998). Schiff reagent (0.2 ml) was added at room temperature and after 30 minutes, the absorbance of the solution was recorded at 555

nm using a UV Spectrophotometer (Gujarathi *et al*., 2012). The Schiff reagent contains 100 ml of 1 % basic Fuschin aqueous solution and 20 ml 1 M HCl. Sodium metabisulphite (0.1 g) was added to every 6 ml of Schiff reagent before use and the resultant solution was incubated at 37 ºC until it became colourless or pale yellow.

6.2.3.2.2 Adsorption of mucin on chitosan-coated beads

Mucin solutions (0.5, 1.0, 2.0 and 2.5 mg/ml) were prepared at pH 3. An average of 10 beads were dispersed in mucin solutions (10 ml) of each concentration and subjected to shaking at room temperature for 1 h (He *et al.*, 1998). The free mucin content was determined using the standard calibration curve.

6.2.3.2.3 Storage stability of coated beads

Beads were sealed in vials and stored at 4° C and room temperature (~ 20 ºC) over a period of three months. The drug loading, buoyancy, mucoadhesion and *in vitro* release were determined at the end of days 30, 60 and 90.

6.3 Results and discussion

Chitosan-coated alginate beads usually have a heterogenous structure with a chitosan surface, a chitosan-alginate inner layer and a calcium alginate core (Figure 6-1). The chitosan-alginate surface provides a thin membranous layer and with further coating, this chitosan alginate surface is itself surrounded by a layer of chitosan. The coating of alginate beads by chitosan

is achieved by electrostatic interaction (Murata *et al.*, 2003). The negatively charged carboxylic acid groups of the alginate bind with the positively charged amino groups on the chitosan leading to the formation of a polyelectrolyte complex on the basis of their opposite charges (Takahashi *et al.*, 1990, Coppi *et al.*, 2001, Douglas and Tabrizian, 2005). As a result of its mucoadhesive properties, chitosan also enhances the absorption of compounds across the mucosal barrier (Artursson *et al*, 1999).

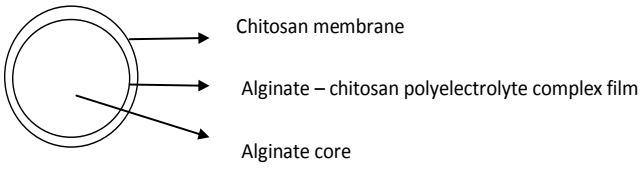

Figure 6-1: Schematic representation of chitosan-coated beads

It is expected that the chitosan membrane will be strong enough to resist osmotic swelling pressure in the beads and also reduce and control the permeability of the beads. pH has been reported to have a strong influence on the polyelectrolyte functional groups, yield and permeability of the formed membrane (Simsek-Ege *et al.*, 2003). Coating with chitosan was carried out at ~ pH 5, because this has been determined to be the optimum pH for the polyelectrolyte membrane formation (Simsek-Ege *et al.*, 2003). Increasing the pH of chitosan solutions from 4 to 6 has been reported to lead to an increase in the rate of chitosan complexation (Gåserød *et al.*, 1998b). This could be due to the fact that when pH approaches the pK_a of chitosan (*i.e.* 6.3 - 6.5), the charge density of the chitosan molecule will be significantly reduced leading to a less extended molecule with a high diffusion coefficient (Anthonsen *et al.*, 1993) enhancing the complexation. The complex is believed to be formed primarily by a coulombic force (King *et al.*, 1987, Huguet *et al.*, 1994). Other secondary forces believed to be responsible for the complex formation include hydrogen or covalent

bonding. Polyelectrolyte complexes have been proposed for the design of DDS (Ribeiro *et al*., 1999, Mi *et al*., 2002, Anal *et al*., 2003, Tapia *et al*., 2004, Anal and Stevens, 2005, Ribeiro *et al*., 2005).

6.3.1 Morphology and structure of coated beads

The beads were spherical with the outer surface of the beads appearing rough with a wrinkled structure (Figure 6 - 1a and c). The cross-sectional structure appeared sponge-like, similar to the unmodified beads with no distinct layer of coating evident on the beads due to the thinness of the layer of chitosan coating (Figure 6 – 1b and d). The rough surface of the coated beads may be due to dehydration of the chitosan during drying (Narkar *et al*., 2010, Dai *et al.*, 2008, Pasparakis and Bouropoulos, 2006). Some studies have shown a smoother surface with chitosan coating (Shi *et al.*, 2008, Suknuntha *et al*., 2011), however, this difference may be due to the method of bead preparation and the drying method employed.

6.3.2 Physical properties of coated beads

The size, weight and densities of the beads did not increase significantly (< 2 % change) after chitosan coating and an increase in chitosan molecular weight had no effect on these properties ($p > 0.05$) as observed in the coated MET beads in Table 6-2. This indicates the thin nature of the layer of chitosan on the surface of the beads. Bead diameters for this series of formulations was between 2.47 ± 0.21 mm and 3.05 ± 0.05 mm and the bulk densities were all less than 1 g/cm^3. The controlled method of production of the beads helped to achieve this size uniformity. A wide range of bead size would lead to non-uniformity in

surface area exposed for drug release and mucoadhesion testing leading to inconsistent and irreproducible data.

Table 6-2: Physical properties of coated MET beads

Code	Diameter (mm)	True density (g/cm^3)	Weight (g) (*n=100*)	Bulk density (g/cm^3)
G7	2.69 ± 0.3	1.44 ± 0.01	0.24 ±0.01	0.23 ± 0.02
G8	2.71 ± 0.2	1.43 ± 0.01	0.23 ± 0.01	0.22 ± 0.01
G9	2.70 ± 0.2	1.45 ± 0.01	0.25 ± 0.01	0.21 ± 0.03
G10	2.72 ± 0.3	1.43 ± 0.01	0.23 ± 0.01	0.23 ± 0.02
G11	2.70 ± 0.1	1.41 ± 0.01	0.22 ± 0.01	0.22 ± 0.02
G12	2.73 ± 0.2	1.43 ± 0.01	0.25 ± 0.01	0.21 ± 0.04
G25	2.92 ± 0.2	1.51 ± 0.01	0.46 ± 0.01	0.28 ± 0.01
G26	2.93 ± 0.3	1.53 ± 0.01	0.46 ± 0.01	0.27 ± 0.01
G27	2.91 ± 0.3	1.52 ± 0.01	0.47 ± 0.01	0.29 ± 0.02
G28	2.92 ± 0.4	1.53 ± 0.01	0.47 ± 0.01	0.28 ± 0.01
G29	2.93 ± 0.2	1.52 ± 0.01	0.47 ± 0.01	0.29 ± 0.02
G30	2.93 ± 0.1	1.51 ± 0.01	0.46 ± 0.01	0.29 ± 0.01
G31	2.94 ± 0.3	1.57 ± 0.01	0.51 ± 0.01	0.27 ± 0.01
G32	2.95 ± 0.2	1.56 ± 0.01	0.50 ± 0.01	0.27 ± 0.01
G33	2.95 ± 0.4	1.54 ± 0.01	0.51 ± 0.01	0.28 ± 0.02
G34	2.94 ± 0.2	1.54 ± 0.01	0.52 ± 0.01	0.28 ± 0.01
G35	2.95 ± 0.1	1.56 ± 0.01	0.53 ± 0.01	0.28 ± 0.02
G36	2.95 ± 0.2	1.55 ± 0.01	0.46 ± 0.01	0.29 ± 0.01

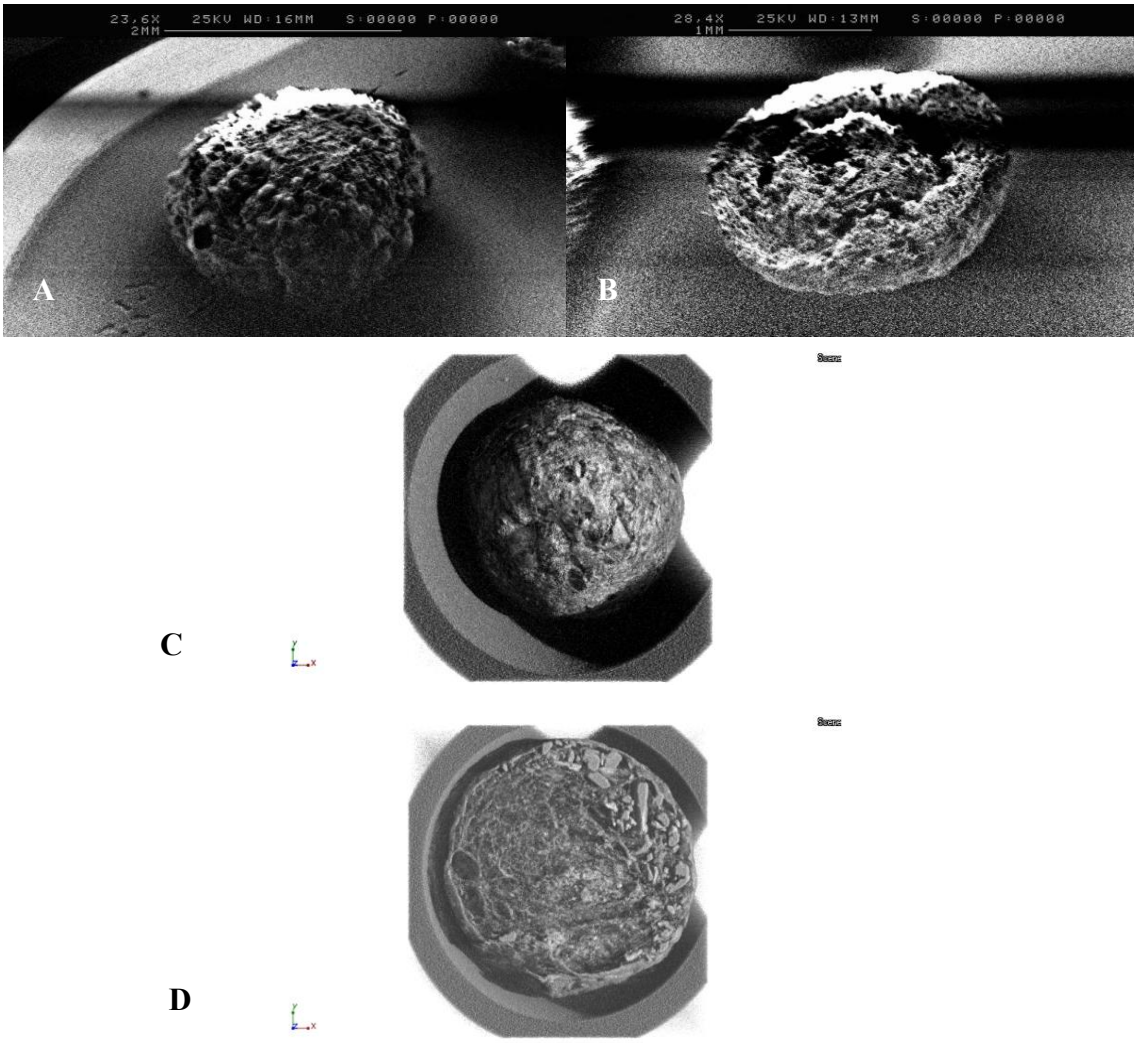

Figure 6-2: SEM images of A) G30; B) cross section of G30 bead; C) and D) XµMT image of G30.

(G30 beads loaded with 10 %w/w MET and 10 % olive oil coated with 1 % HMW Chitosan)

6.3.3 Drug content and DEE of coated beads

DEE of the coated beads for both drugs was high (> 55 %). The COM beads exhibited a higher DEE than the CNOM beads with the DEE range of COM beads being 87 - 96 % and the DEE range of CNOM being 54 – 85 %. The higher DEE of the COM beads corresponds with the observed high DEE of oil-modified beads in Chapter 5.

6.3.3.1 Metronidazole beads

The drug content and DEE of the CNOM (G1 – G12) beads were lower than what was observed in the uncoated beads (Figure 6-3a) with about 12 - 29 % reduction in DEE of the beads. This reduction was due to the extra time the beads are in contact with the aqueous medium during coating with associated drug loss due the high solubility of MET in aqueous medium. This was different from results obtained from previous studies where there was a higher DEE with chitosan coating (Ishak *et al.*, 2007, Tamilvanan and Karmegam, 2012). The COM beads had a slightly higher DEE than the unmodified beads and the uncoated oil modified beads, with increases between 2.5 - 8.3 % (G13 – G24), 0.3 - 1.6 % (G25 - G36) ($p > 0.05$) (Figure 6-3b and 3c). The presence of oil in the bead formulation prevented the leaching of drug into the coating medium and drug loss during washing after bead preparation.

6.3.3.2 Clarithromycin beads

There was a reduction in DEE of CNOM beads containing CMN, with about 3 - 15 % reduction observed for the D1 - D12 beads compared with the DEE of the uncoated beads (Figure 6-4a). This reduction in DEE was less than that observed with the MET coated beads based on the difference in the solubility and molecular weight of both drugs. There was no significant difference in the DEE of the COM beads ($p > 0.05$) (Figure 6-4b and 4c) with differences less than 3 %.

6.3.3.3 Effect of chitosan concentration and molecular weight on DEE of coated beads

Increasing the concentration of chitosan slightly increased the DEE of the beads with an average increase of 5.17 ± 2.37 % for G1 - G6 beads and 4.07 ± 1.88 % for G7 - G12 ($p > 0.05$) (MET beads) while there was an increase in DEE of 7.46 ± 3.73 % (D1 - D6 beads) and 5.06 ± 0.91 % (D7 - D12 beads) ($p > 0.05$) (CMN beads). For all the COM beads, there was less than 2 % difference in DEE. There was no significant difference in drug content and DEE on increasing the concentration of chitosan and molecular weight of the chitosan. This could be due to the high concentrations of chitosan used, if concentrations such as 0.1 or 0.2 %w/v were used, concentration and molecular weight may have had a larger impact on drug release.

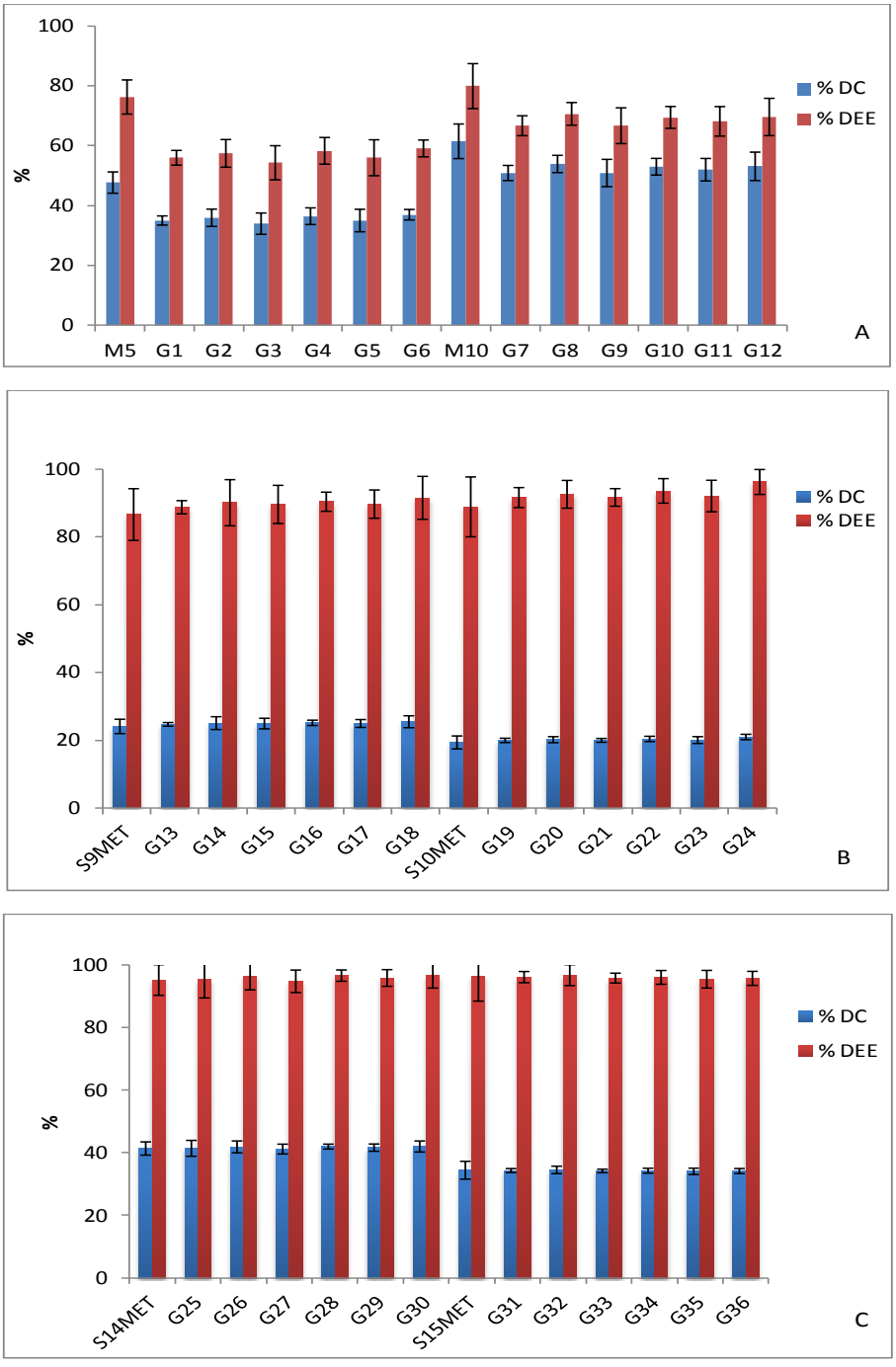

Figure 6-3: Effect of coating on DEE of A) coated non-oil modified MET beads and B, C) coated oil-modified MET loaded beads

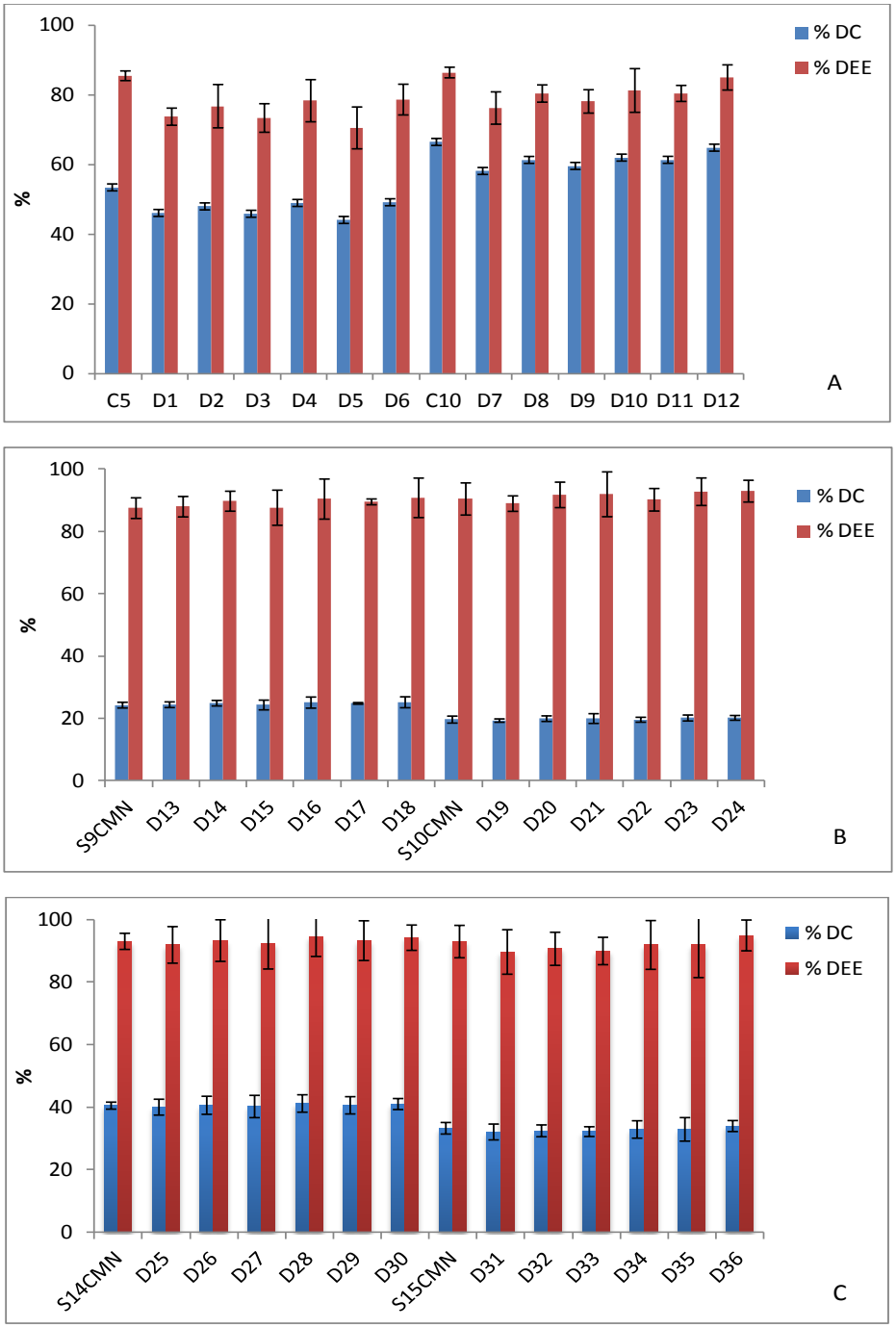

Figure 6-4: Effect of coating on DEE of A) coated non-oil modified CMN beads and B, C) coated oil-modified CMN loaded beads

6.3.4 Differential scanning calorimetry of coated beads

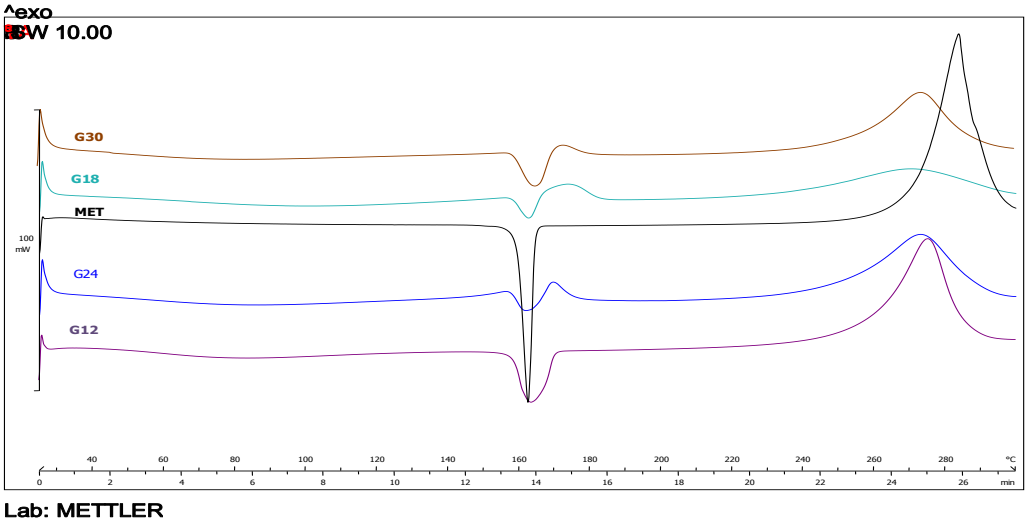

Figure 6-5: Comparison of DSC thermograms of pure MET and coated MET beads

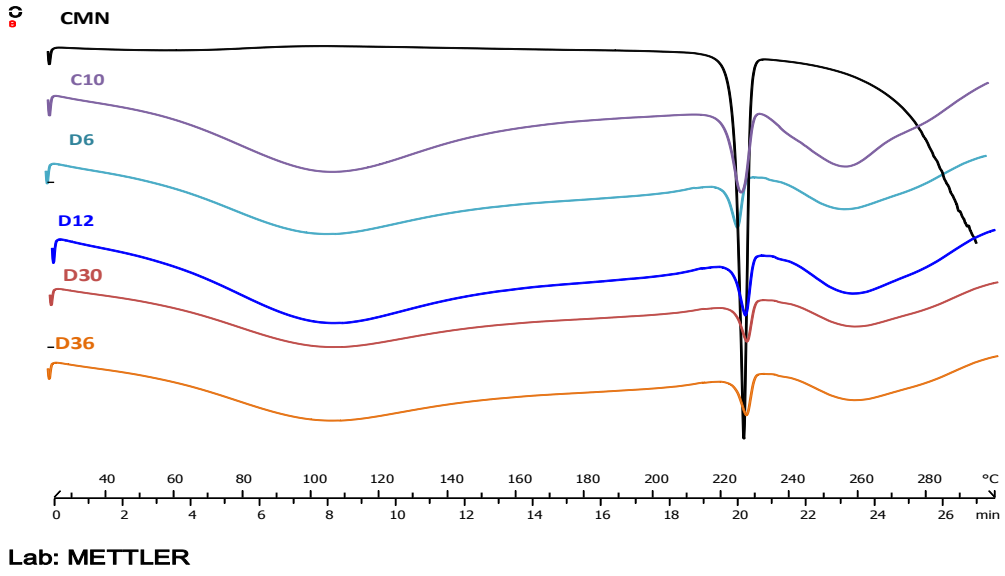

Figure 6-6: Comparison of DSC thermograms of pure CMN and coated CMN beads

CNOM MET (Figure 6-5) and CNOM CMN (Figure 6-6) beads had a single melting endotherms at an average temperature of 164.53 ± 0.79 ℃ and 225.45 ± 0.82 (*n=3*) respectively, confirming the presence of MET and CMN in the bead sample. The COM MET and COM CMN beads also showed melting endotherms at respectively similar temperatures ($p > 0.05$). These findings indicate the stability of the drug in the formulations and the absence of major interactions between the drug, oil, polymer and the coating material. These results were similar to those observed with the oil-modified beads and the unmodified beads.

6.3.5 Powder X-ray diffraction analysis of coated beads

The P-XRD patterns of the CNOM and COM CMN and MET beads showed displayed the characteristic drugs albeit at lower intensity as shown in Figure 6-7a and b. The coating process did not eliminate the presence of some crystalline material within the bead and this was supported by tomography images (Figure 6-2).

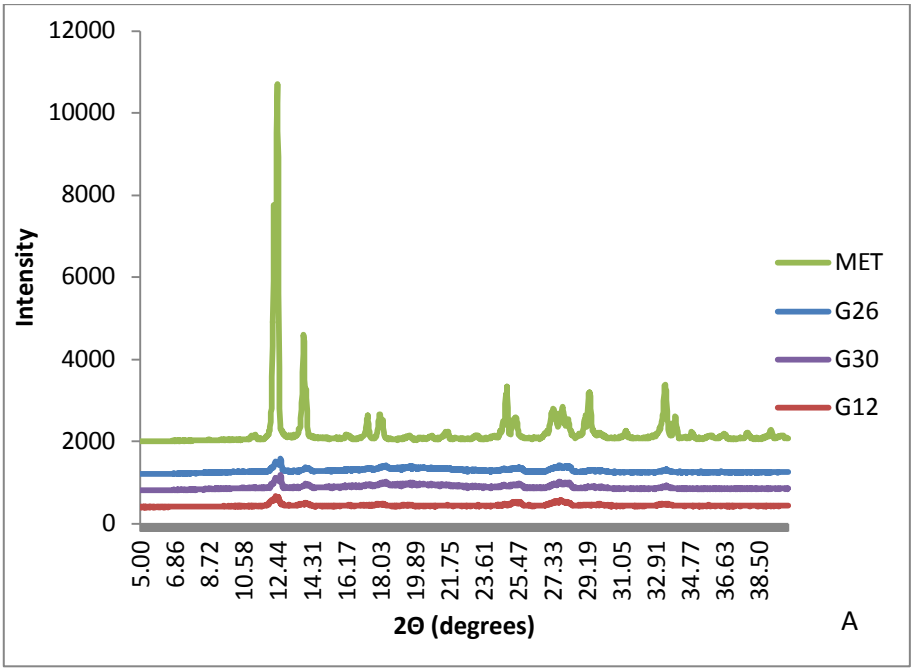

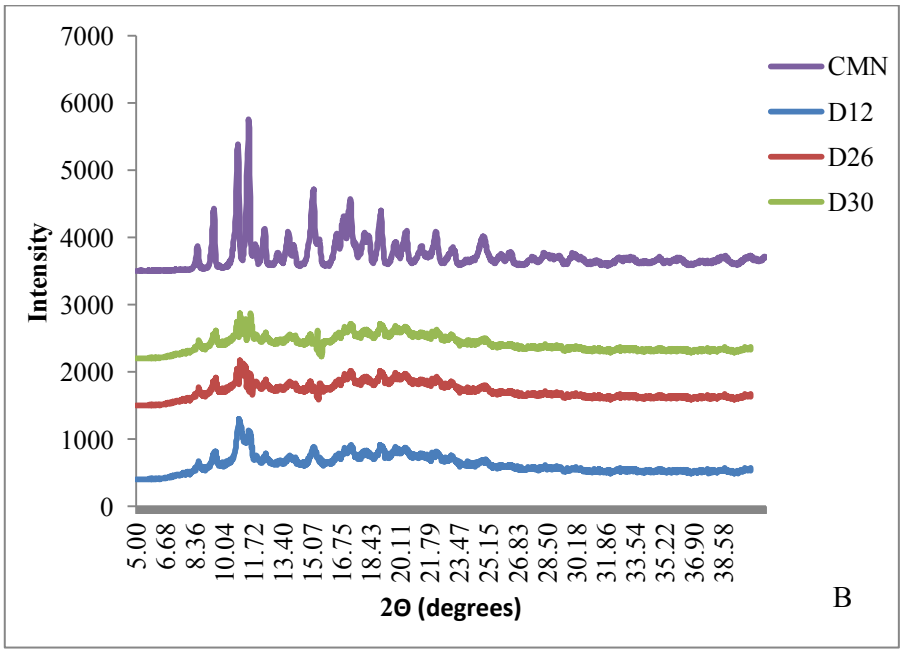

Figure 6-7: P-XRD patterns of coated A) MET beads and B) CMN beads

6.3.6 Fourier transform infra-red analysis of coated beads

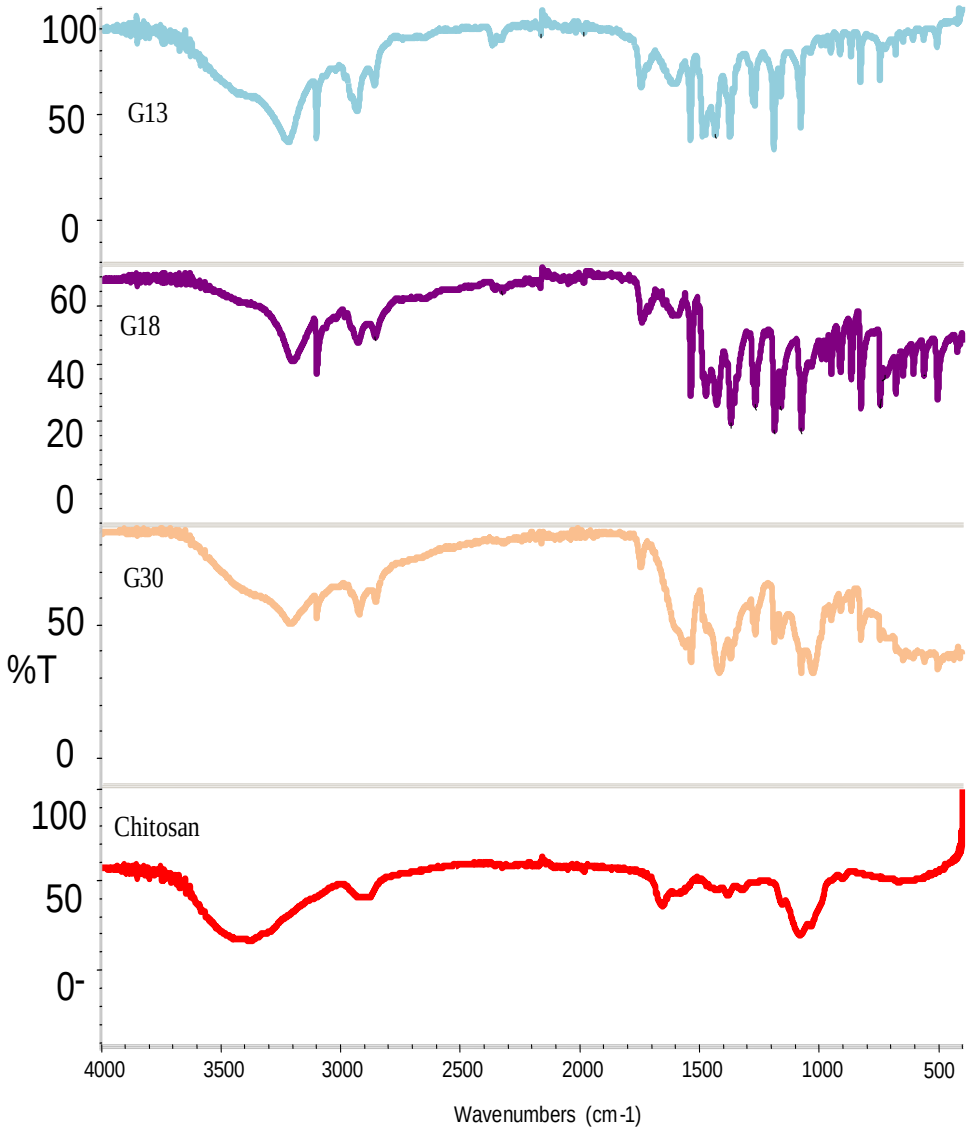

Figure 6-8: FTIR of coated MET beads

The CNOM and COM beads showed characteristic peaks similar to those observed for unmodified beads for both MET and CMN as shown in Figures 6-8 and 6-9 respectively, with the peaks exhibiting lower intensities, as expected, due to the presence of other components in the formulation. A peak at ~ 1603 cm^{-1} was observed for the coated beads as a result of the interaction between the negatively charged – COO^- groups of alginate and the positively charged -NH_3^+ groups of chitosan (Shi *et al.*, 2008). The absence of any major changes in the scans of unmodified and modified beads indicates the stability of the drugs in the formulation and the absence of chemical interaction between the oil and/or the drugs or the polymer.

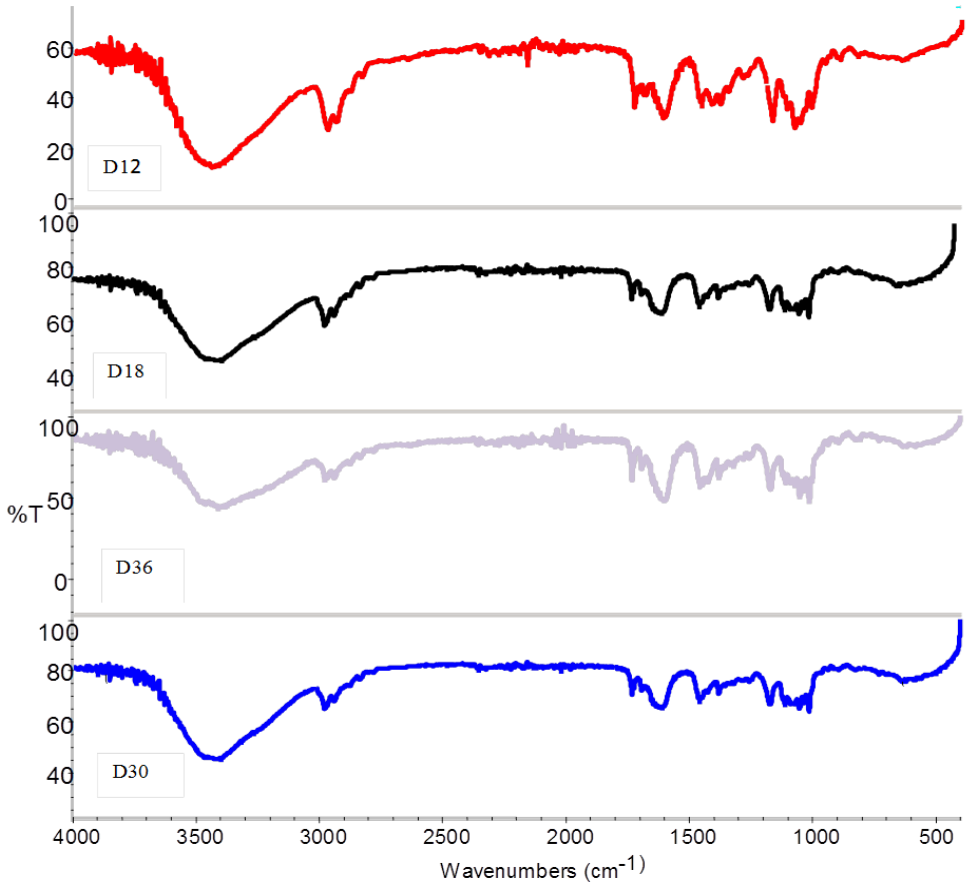

Figure 6-9: FTIR of coated CMN beads

6.3.7 Determination of bound chitosan on alginate bead surface

6.3.7.1 Chitosan assay and calibration curve

The protonated amino group on the chitosan structure can act as a cationic site which binds to anionic dyes such as Cibracron Brilliant Red dye, forming an uncharged dye-chitosan colloidal complex. This reaction causes a bathochromic shift, and when the absorbance of this dye-chitosan mixture is measured against a pure dye solution, a sharp peak is detected at ~575 nm (Wischke and Borchert, 2006, Mendelovits *et al.*, 2012) as a result of the complexation. The degree of protonation of both the chitosan and the dye is pH dependent; therefore pH was kept constant at ~ pH 2.8 by the addition of glycine buffer to prevent changes in protonation and ensure accurate evaluations (Mendelovits *et al.*, 2012). There was no major difference between the calibration curves of the different molecular weights of chitosan used (Figure 6-10a), therefore, they reacted similarly with the dye, irrespective of the molecular weight of the chitosan. This was similar to the results obtained by a previous research by Muzarelli (1998). The assay showed a high sensitivity with LOD and LOQ being 1.79 ± 0.07 µg/ml and 5.43 ± 0.21µg/ml, respectively with a high linearity ($R^2 > 0.99$) and reproducibility with RSD < 3 % (Figure 6-10a). Some studies have modified the method by Muzarelli (1998), due to its lack of sensitivity at low chitosan concentrations < 100 ppm (Wischke and Borchert, 2006, Mendelovits *et al.*, 2012). However, this issue was not encountered in this study and the only modification was the use of acetic acid instead of lactic acid and reducing the calibration points based on the detection limit observed for the assay method and equipment. It has been described in a previous study that there was no major difference in results obtained from the use of lactic acid or acetic acid in the dissolution of chitosan for analysis (Miralles *et al.*, 2011). Acetic acid was more preferred in this study because the coating of the beads was carried out in a chitosan-acetic acid solution, is less expensive and more common in laboratories.

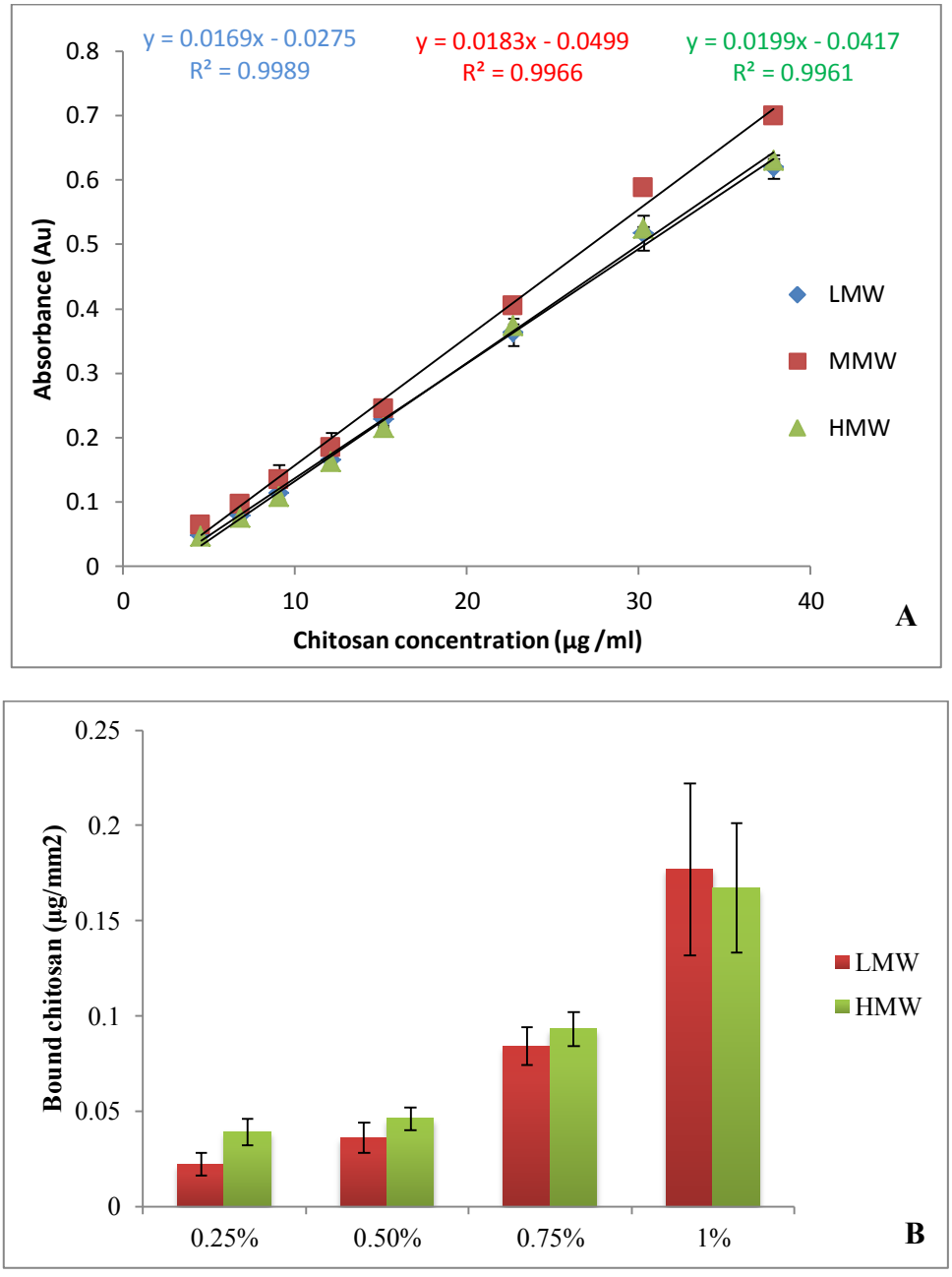

Figure 6-10: A) Calibration curve of chitosans of different molecular weights and B) Amount of bound chitosan on alginate bead surface

6.3.7.2 Bound chitosan on alginate bead surface

During coating, the chitosan molecules attach to the negative charge of alginate at the bead surface, forming a thick well-packed chitosan membrane layer around the alginate bead over a layer of polyelectrolyte complex between the alginate and the chitosan. There was no major difference between the amounts of bound chitosan across all molecular weights used ($p > 0.05$), but an increase in concentration of chitosan had an effect on the amount of chitosan bound onto the surface of the alginate beads ($p < 0.05$) (Figure 6-10 b). There was an increase of ~63 % in bound chitosan (LMW) on increasing concentration from 0.25 to 0.5 %w/v. A previous study observed that chitosan binding on alginate beads is favoured by high bead porosity (related to low concentrations of SAL) and low molecular size of chitosan (Gåserød *et al.*, 1998b), with low molecular weight chitosan providing a denser membrane than high molecular weight chitosan (McKnight *et al.*, 1988). The bead porosity and molecular size of the chitosan enhances the penetration of chitosan into the bead structure. The increase in variability at 1 %w/v chitosan may be due to loss of chitosan during the recovery of the coated beads from the chitosan solution as a result of the high viscosity of the polymer solution. Suspending beads in chitosan solution allows more chitosan to bind both onto the surface of the bead and the interior gel network and allows binding of more chitosan than the one stage coating process, because the two stage coating process, as used in this study, allows chitosan to diffuse into gel beads more rapidly (Gåserød *et al.*, 1998b). The one stage coating process involves dropping the alginate solution into a gelling/coating medium containing chitosan and $CaCl_2$.

6.3.8 Swelling profile and disintegration of coated beads

In order to study possible *in vivo* behaviour, formulations need to be exposed to a range of pHs mimicking those it will encounter on its journey through the GI tract. On exposure to acidic pH (Figure 6-11a and b), the coated beads absorbed water and underwent more swelling than uncoated beads. This is because chitosan, due to its hydrophilic nature, swells in acidic media and absorbs water. In addition to the hydration of hydrophilic groups of chitosan-coated beads, another important factor that contributes to the swelling profile in acidic pH is that protonization of the amino groups of chitosan creates a repulsive force, which leads to the swelling of the chitosan membrane (Mukhopadhyay *et al.*, 2013, Kim *et al.*, 2000). In CNOM beads, for both drugs, there was an average 13.12 ± 3.76 % increase in swelling of the beads, while for COM, there was an average of 6.17 ± 2.05 % increases in swelling ($p > 0.05$). This reduced swelling capacity of COM might be due to the presence of oil in the formulation, which makes it more hydrophobic and a slightly reduced tendency to swell. Increasing the concentration of chitosan led to an increase in swelling by 5.72 ± 1.48 % (CNOM beads) and 2.72 ± 1.13 % (COM beads) ($p > 0.05$). The swelling profile was similar to that of the uncoated beads with maximum swelling observed for both CNOM and COM beads between 120 - 150 minutes in acidic media (Figure 6-11a and b).

In alkaline media, maximal swelling was observed at ~150 minutes and, unlike the uncoated beads, coated beads were stable in PBS for longer than the uncoated beads. The CNOM beads also exhibited slightly more swelling than the uncoated beads with a maximum of ~ 2700 % weight change (Figure 6-12a and b). The COM beads did not swell as much in PBS, due to the oil but similar to results in acidic media, they swelled slightly more than the uncoated oil modified beads but the difference in swelling was not considered significant. Chitosan has been reported to swell considerably with up to 140 % swelling at neutral pH (Silva *et al.*, 2004). The COM swelled to an average maximum of about 500 % weight change and maintained this weight increase for the entire period of the study. Further degradation studies in PBS, which were carried for 12 h, showed the beads exhibited better

stability than unmodified beads. Bead disintegration occurred at an average of 9.5 ± 1.2 h, which is probably due to the combination of the oil and the coating. Disintegration of CNOM beads was observed after 5.4 ± 0.8 h and dissolution of the unmodified beads was complete in 3.8 ± 0.6 h. This enhanced stability in alkaline media extends the lifetime of the DDS and faciliates delivery of drugs to areas of higher pH, *e.g.* lower GI tract and in cases where the contents of the stomach becomes less acidic, *e.g.* use of antacids and alkali- forming foods. The unmodified beads are destabilised in the presence of chelators such as phosphate or non-gelling cations like sodium and magnesium. However, binding of chitosan to alginate beads has been described as almost irreversible because once the polyelectrolyte complex has been formed, exposure to solutions with higher concentrations of competing ions have limited influence on the complex (Gåserød *et al.*, 1999). Therefore, the coating not only enhances water uptake of the beads but also enhances the stability of the beads.

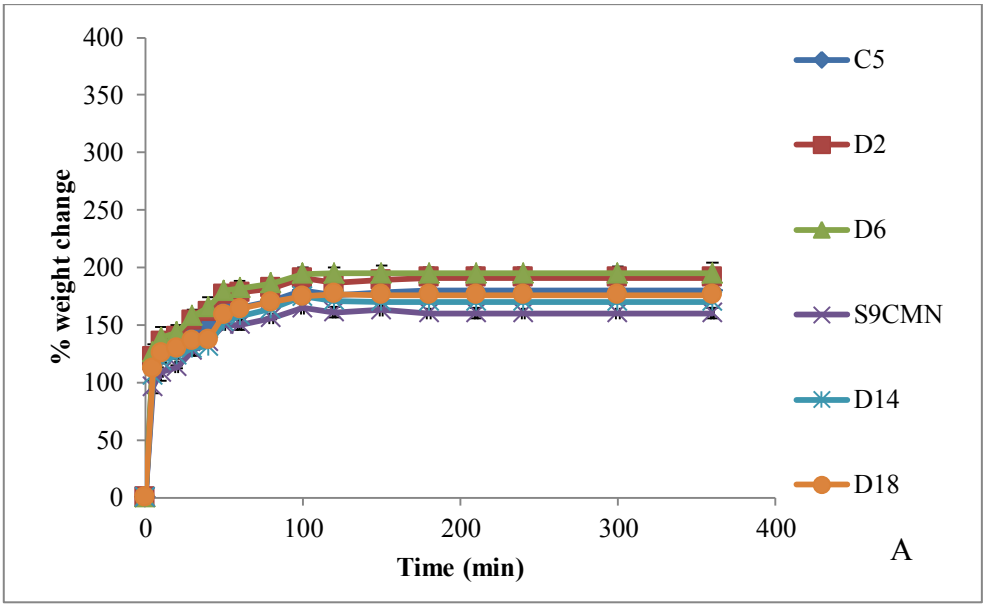

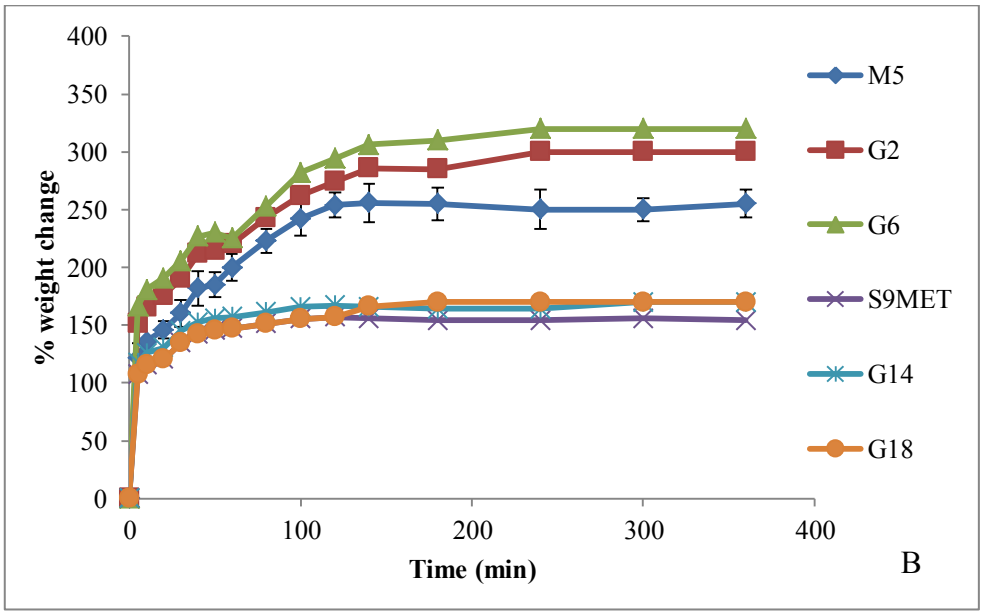

Figure 6-11: Swelling profiles of A) coated CMN beads; B) coated MET beads in acidic pH

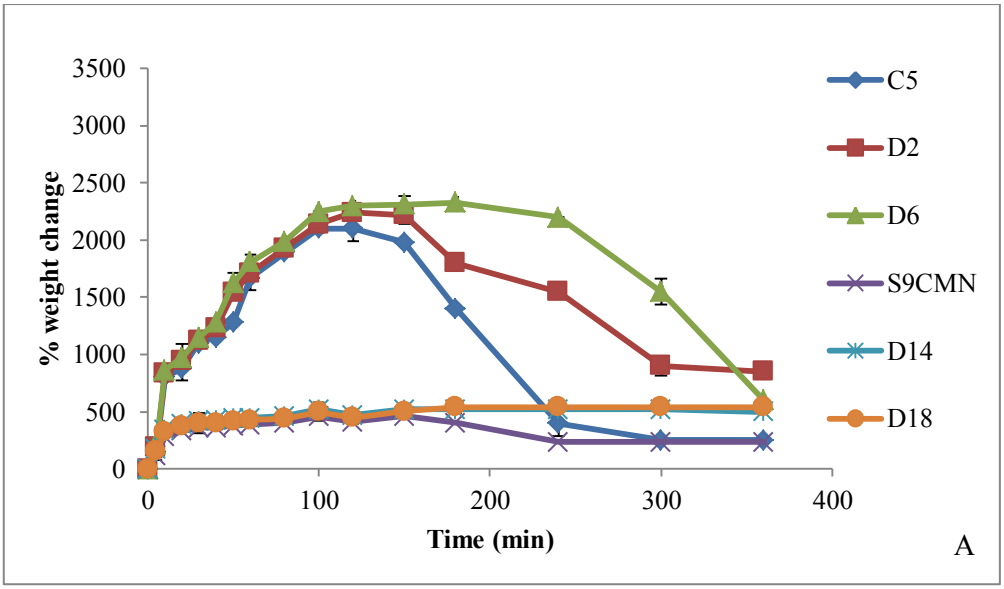

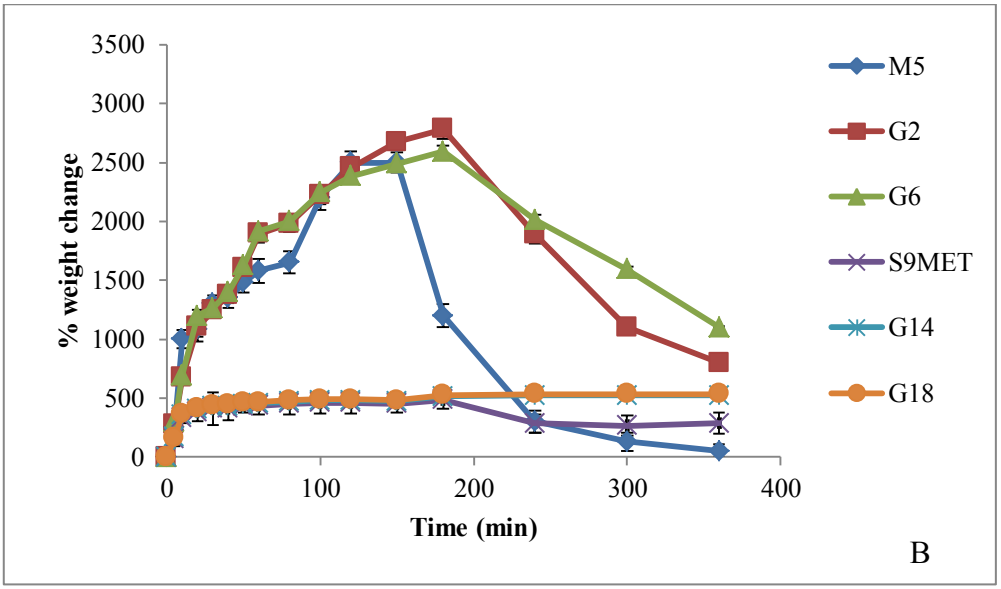

Figure 6-12: Swelling profiles of A) coated CMN beads; B) coated MET beads in alkaline pH

6.3.9 *In vitro* buoyancy of coated beads

The coating of the beads with chitosan did not have any effect on the buoyancy of the beads with similar lag times and duration, as uncoated beads (Figure 6 - 13) ($p > 0.05$). Studies by Ishak *et al* (2007) have shown that chitosan has no direct effect on the buoyancy of beads, but a combination of chitosan with other excipents such as magnesium stearate and κ-carrageenan can help achieve 100 % floatation. Chitosan microspheres prepared in another study exhibited non-floating properties in SGF (Kas, 1997). However, conflicting results have reported an increase in buoyancy of alginate beads on chitosan coating (Sahasathian *et al.*, 2010).

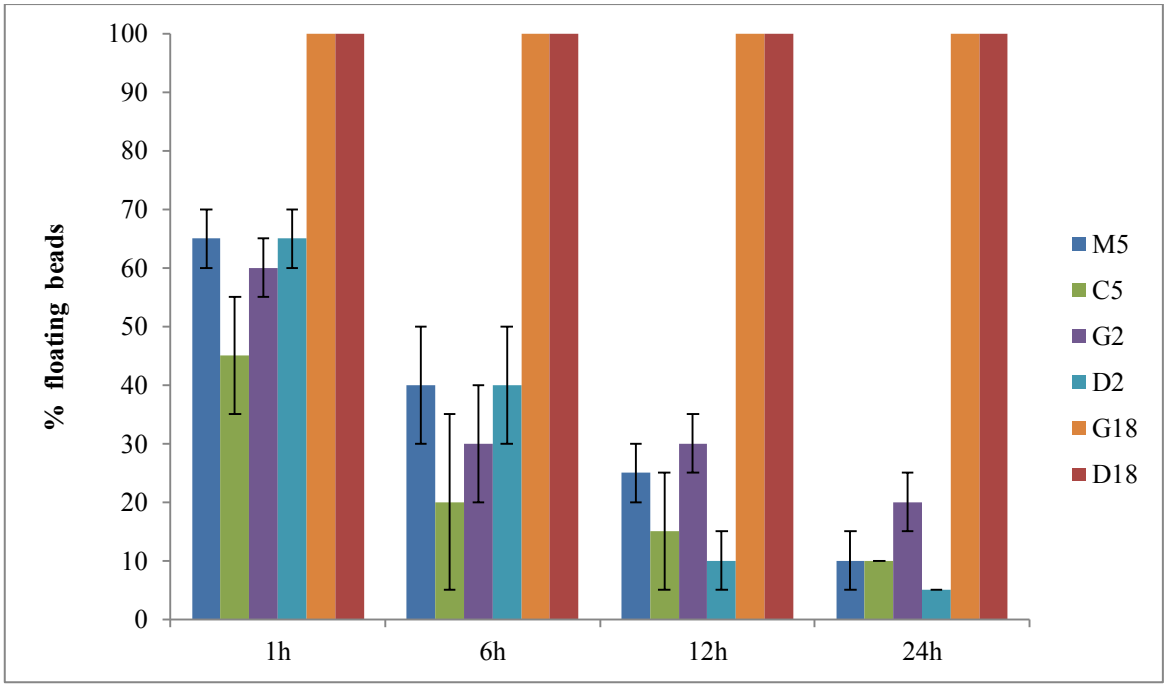

Figure 6-13: Buoyancy profile of coated beads

6.3.10 Mucoadhesion tests

6.3.10.1 Mucin-particle method

The interaction between mucin and chitosan was studied at pH 3 because at this pH, both mucin (mucin is ionized at pH > 2.6 (Peppas and Sahlin, 1996, Bansil and Turner, 2006)) and chitosan (pK_a = 6.3 - 6.5) are both ionized. This pH is also close to the average pH of the stomach, the intended target site for the DDS. Commercial mucins are often used in mucoadhesion experiments because they have less batch variability compared to fresh

extracted mucins resulting in improved reproducibility in early screening processes (Rossi *et al.*, 2000, Rossi *et al.*, 2001). Chitosan is a cationic polymer with a primary amino and hydroxyl group in each repeating polymer (see section 1.7.2) unit except for the acetylated units, which are without primary amines. Upon protonation, the primary amino groups have a positive charge, which helps facilitate electrostatic interactions with the negatively charged mucin but also other contributions such as hydrogen bonding, hydrophobic effects and chain entanglement might have an effect. When the amino groups are de-protonated at high pH levels, they can only react with mucin through hydrogen bonding.

6.3.10.1.1 Particle sizing of chitosan-mucin mixtures

The initial size of mucin upon dispersion and pH change was within a range of 143 to 635 nm as a result of a combination on small and large aggregates (Figure 6-14, Figure 6-16b). In order to reduce the extent of aggregation, the suspensions were sonicated and filtered and the particle size was reduced to a range of 161 to 197 nm. (Figure 6-14, Figure 6-16b). Chitosan was also mixed thoroughly to ensure complete dissolution, however chitosan tends to form intermolecular hydrophobic aggregates in aqueous solutions (Philippova *et al.*, 2001, Anthonsen *et al.*, 1994, Wu *et al.*, 1995) at concentrations ~ 1 mg/ml, which is the concentration used in this study. The average range of chitosan aggregate size observed was between 184 and 218 nm. On reaction of mucin with chitosan, particle size increased indicating chitosan binding to the mucin particle surface (Figure 6-15, Figure 6-16b). The increase in standard deviation (SD) indicates a broader size distribution in polymer-mucin mixtures relative to the mucin suspension. The modification of the particle size was as a result of the electrostatic interactions between the positively charged chitosan and the net negative charge of the mucin particles.

Initial mucin particle size

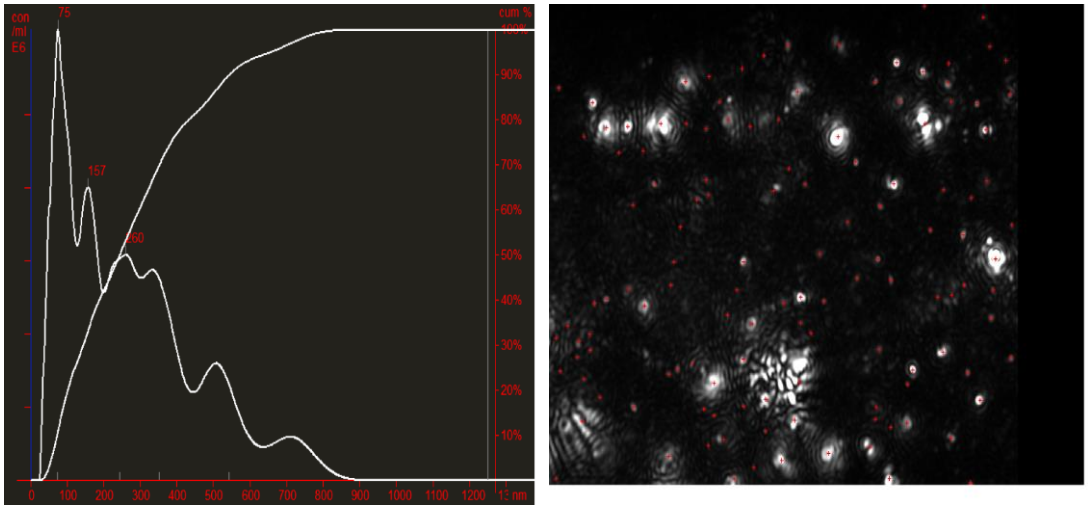

Micron sized mucin particles

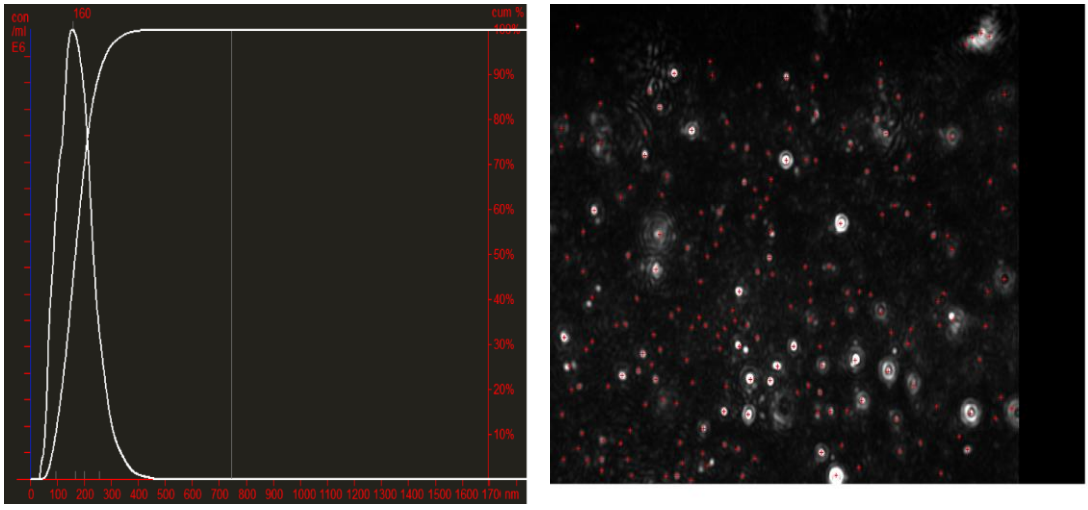

Figure 6-14: Particle size distribution of mucin before and after size reduction

Chitosan / mucin ratio 0.1

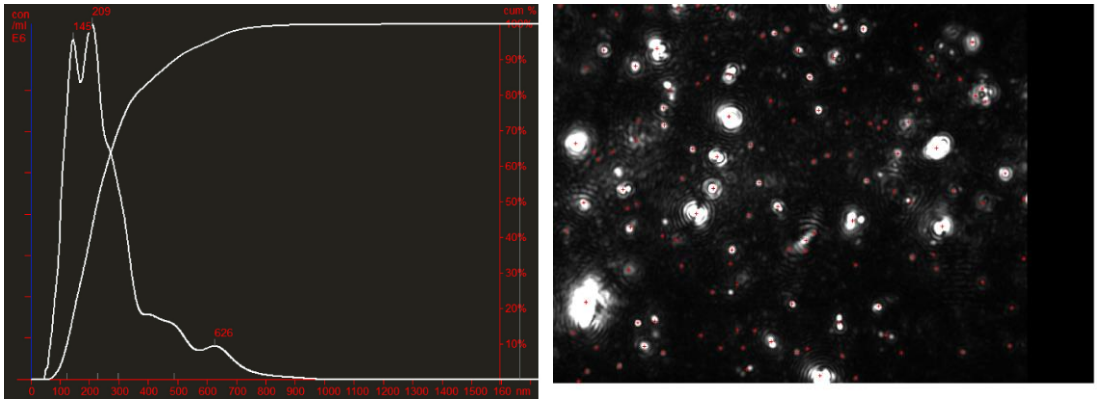

Chitosan / mucin ratio 1.5

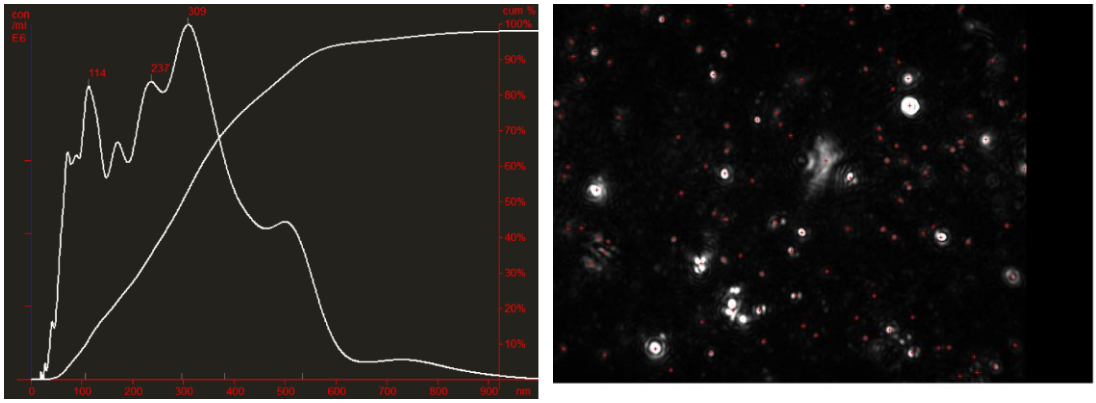

Chitosan/ mucin ratio 3

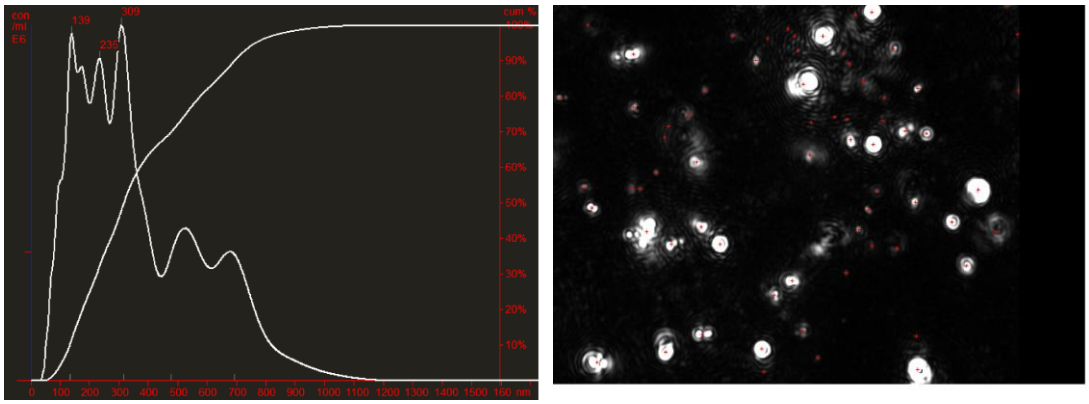

Figure 6-15: Particle size distribution of chitosan-mucin mixtures

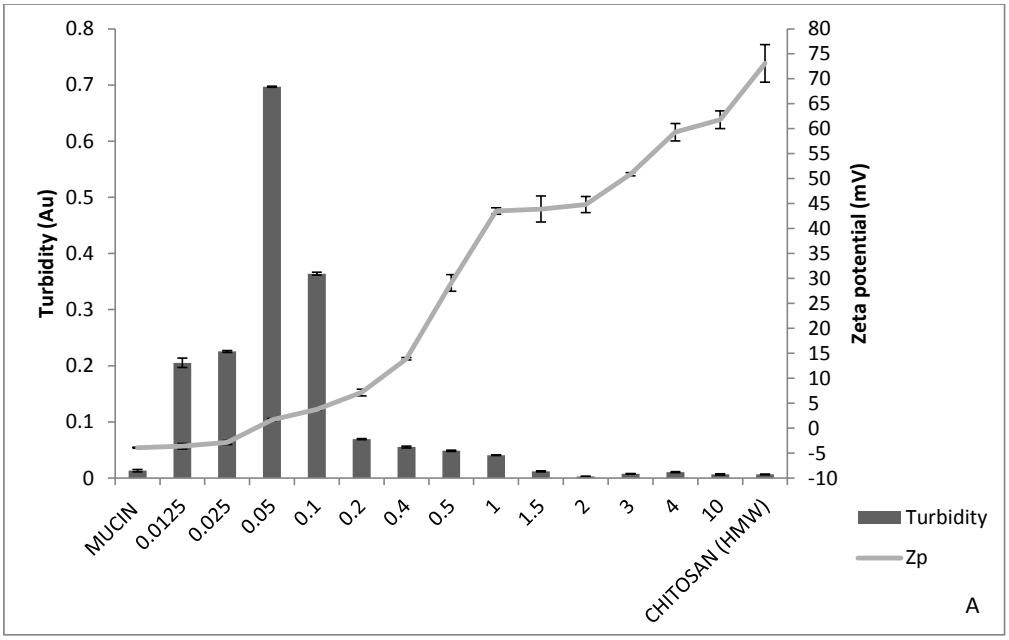

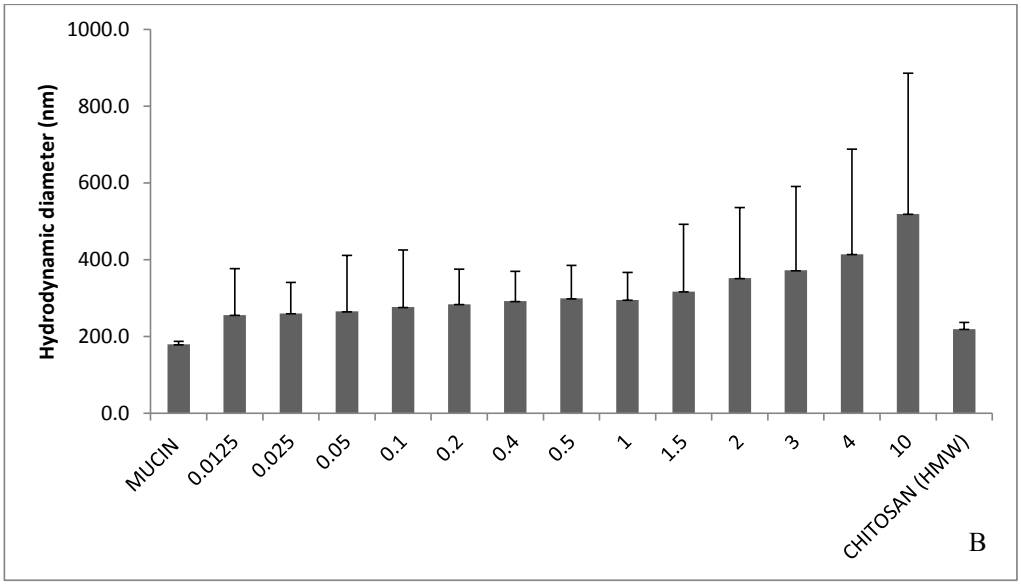

Figure 6-16: A) Turbidity and *Zp* of chitosan - mucin mixtures and B) Particle sizes of mucin in the chitosan-mucin mixtures

6.3.10.1.2 Zeta potential of chitosan-mucin mixtures

The estimation of the *Zp* of mucin in the presence of chitosan has been reported to be a good means of studying the mucoadhesive interactions of the chitosan – mucin mixtures (Fefelova *et al.*, 2007, Takeuchi *et al.*, 2005). Chitosan recharges the mucin particles, thereby confirming the adsorption of cationic chitosan onto the negative mucin surfaces (Figure 6-16a). The initial *Zp* of mucin particles, which was negative, changed to positive at a chitosan-mucin ratio of 0.05 and the positive *Zp* was further increased with increasing chitosan. This increase in *Zp* is as a result of the increasing aggregation tendency and the adsorption of chitosan on the mucin particles is responsible for the aggregation.

6.3.10.1.3 Turbidimetry measurements of chitosan-mucin mixtures

Turbidimetry provides another means of assessing mucin aggregation (He *et al.*, 1998, Fefelova *et al.*, 2007) and there was a marked increase in solution turbidity as the polymer ratio increased, up to a maximum polymer-mucin ratio 0.05, after which the turbidity started to decrease (Figure 6-16a). Aggregation of the mucin in the presence of small quantities of chitosan causes an increase in the turbidity of the mixture. Disaggregation occurs in the presence of excess chitosan, which was observed with the reduced turbidity due to dilution. The ratio at which the mixture exhibits maximum turbidity was similar to the ratio at which there was a *Zp* charge reversal of the polymer-mucin mixture from negative to positive.

In summary, the hydrodynamic diameter, *Zp* and turbidity mucin changed in the presence of chitosan (Figure 6-16). An inversion of *Zp* from the initial negative to a positive *Zp* was observed with increasing chitosan concentration. Also, there was a 190 % increase in particle size on increasing the chitosan/mucin ratios from 0 to 10. All these results indicate an interaction between mucin and chitosan.

6.3.10.2 Mucoadhesive beads

6.3.10.2.1 Adsorption of mucin on chitosan-coated beads

Mucin colorimetric assay and calibration curve

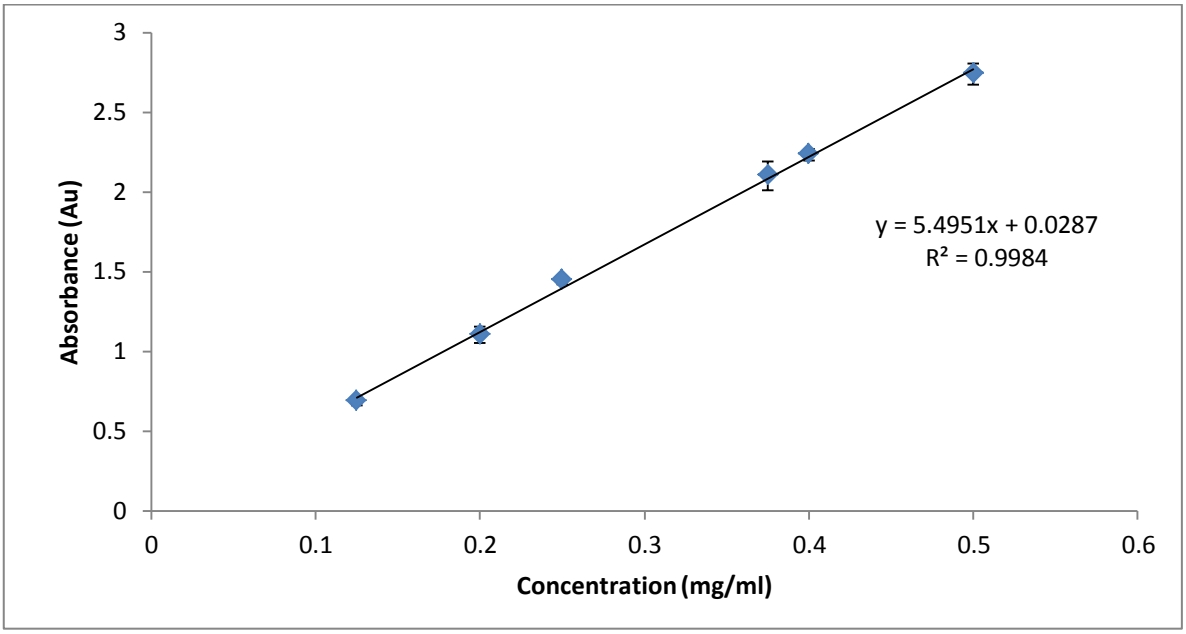

Figure 6-17: Calibration curve of mucin (*n=3*; mean ± SD)

Proteins are generally detected at UV 280 nm (Layne, 1957, Stoscheck, 1990), however mucins absorb UV light poorly, since they generally have no or negligible aromatic amino acid content (Wang and Granados, 1997, Thanka and Veluraja, 2001) but colorimetric assays provide a reliable method of detection and analysis of complex mucin glycoproteins. The assay showed a high sensitivity with LOD and LOQ being 0.062 ± 0.004 and 0.207 ± 0.014

mg/ml, respectively with a high linearity ($R^2 > 0.99$) and reproducibility with RSD < 4.5 % (Figure 6-17).

Amount of bound mucin on bead surface

Due to the interaction between mucin and chitosan, mucin is expected to spontaneously adsorb onto the surface of the chitosan-coated beads. The amount and proportion of mucin adsorbed onto the coated bead surface increased with an increase in mucin concentration; from 2.5 mg/ml to 12.5 mg/ml, the average increase was 45.63 ± 7.64 % (Figure 6-18). Mucin adsorption was lower for the uncoated bead with an average of up to 18 % of mucin adsorbed unto these beads. There was no significant difference between the adsorption of mucin on blank, drug-loaded and oil-modified beads ($p > 0.05$). The average amount of mucin bound on the surface of uncoated beads was 18.13 ± 7.32 µg mucin/mm^2 and for coated beads was 88.21 ± 21.85 µg mucin/mm^2. These results show that the coated beads are able to adsorb mucin, thus would be expected to exhibit a degree of mucoadhesion. SAL beads also demonstrated a certain level of mucoadhesion, albeit substantially less than with chitosan. The adsorption of mucin to the chitosan surface is expected to be due to electrostatic attraction between the positively charged chitosan and the negatively charged mucin. The negative charge of mucin is as a result of the ionization of sialic acid.

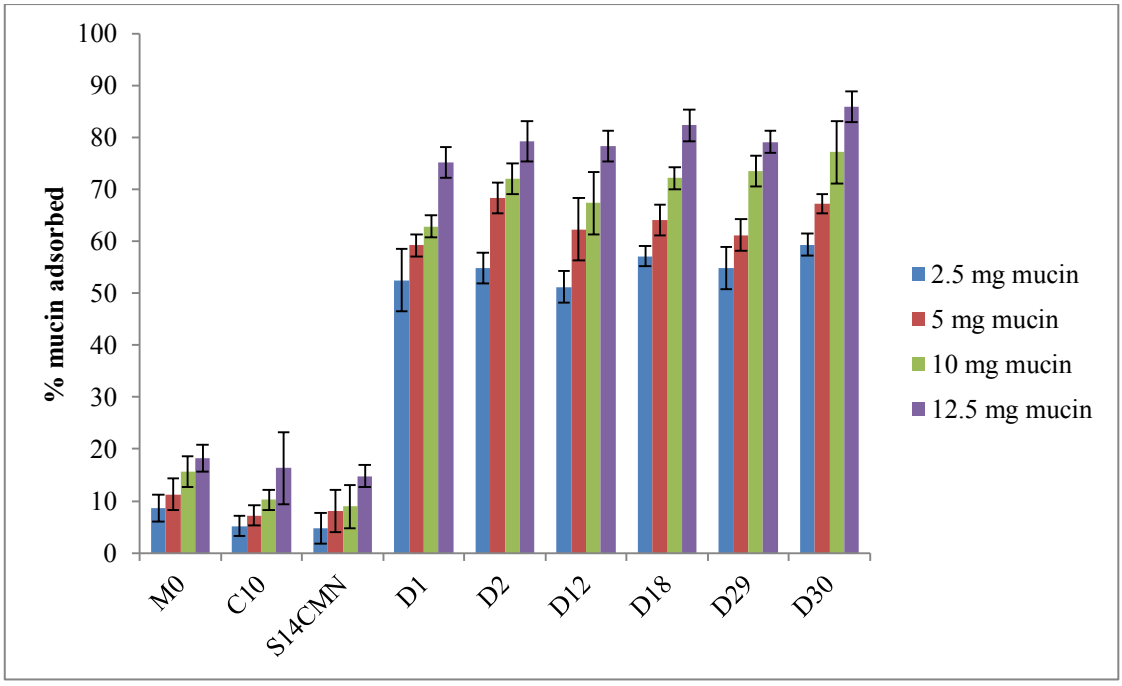

Figure 6-18: Adsorption of mucin on chitosan-coated beads

6.3.10.2.2 Mucoadhesion tests in the humidity chamber

Both freshly excised and frozen tissue samples have been used previously in mucoadhesion studies. Some studies have determined that there was no significant difference in the quantity and quality of mucus present on tissues, whether fresh or frozen (Nystrom and Bredenberg, 2006, Hibi *et al.*, 2002). Another study reported no difference in the mucoadhesion of a poly(acrylic acid) formulation either on the fresh or frozen tissues (Hibi *et al.*, 2002). In this thesis, frozen tissues were used in order to minimise tissue-to-tissue variation by obtaining replicate tissues from the same stock of animals. The appearance of the mucosal surfaces seemed unaffected during the freezing and thawing processes.

Almost 50 % of the uncoated beads detached from the mucosa after 1 h compared with a maximum of 30 % for coated beads (Figure 6-19a). After 6 h, only ~ 35 % uncoated beads remained on the mucosal surface compared with a minimum of 60 % observed with coated beads. The uncoated beads exhibited some mucoadhesive properties as 10 – 15 % uncoated beads were retained after 12 h indicating a lower level of mucoadhesion compared with the coated beads (Figure 6-19). It has been documented that SAL demonstrates some mucoadhesive properties (Shaikh *et al.*, 2012, Allamneni *et al.*, 2012) although it is not as highly mucoadhesive as chitosan. Increasing the concentration or the molecular weight of the coating material did not have a significant effect on the mucoadhesion of the beads as the coated beads D2 and D6 had similar mucoadhesive profiles in the acidic environment ($p > 0.05$). This is due to the high variability between the results. It has, however, been reported that a higher concentration of chitosan can lead to a reduction in the flexibility of the polymeric chains, thus causing a reduction in adhesive strength compared to lower chitosan concentrations which have more space to extend within the mucin (Govender *et al.*, 2005). Mucoadhesion was generally lower in alkaline media (Figure 6-20) than in acidic media and this may be due to the reduced interaction between the mucoadhesive polymer and the mucosal layer. It could also be as a result of the gradual loss of the calcium ions from the beads and the ionization of carboxyl and other functional groups in the polymers at this pH (Ikeda *et al*., 1992, Nayak *et al*., 2010a), even though this loss was quite reduced for the coated beads. Mucoadhesion occurs with an initial wetting process causing intimate contact between the mucus and the swelling mucoadhesive polymer. The polymer strands relax, followed by penetration of the polymer chains into the mucus network and finally the formation of secondary chemical bonds. Huang *et al* (2000) reported that the adhesive properties of hydrogels could be improved by tethering of long flexible chains to a particle surface. The hydrogels in this study also exhibited increased mucoadhesive properties due to enhanced anchoring of the flexible chains within the mucosa (Figure 6-21).

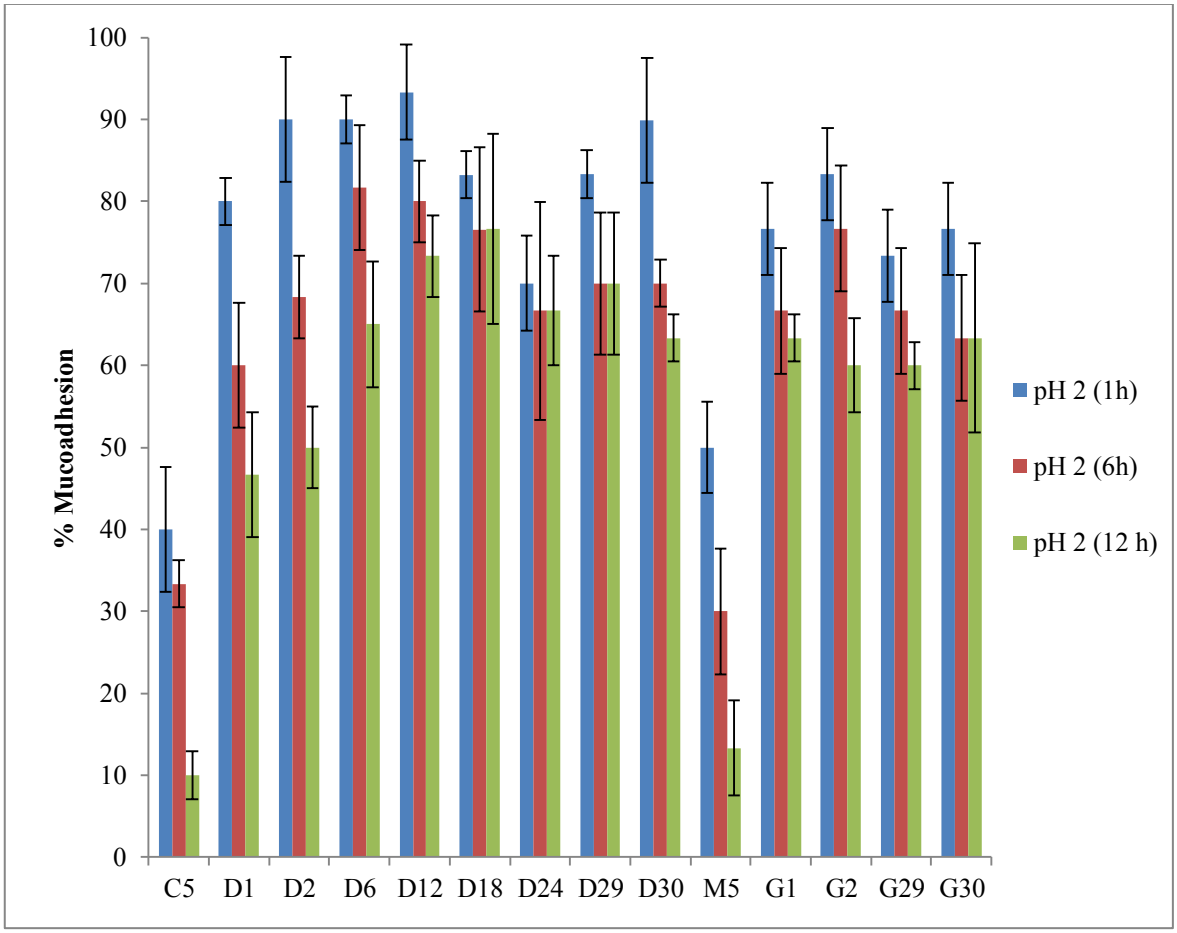

Figure 6-19: Mucoadhesion tests on coated MET and CMN beads in acidic media

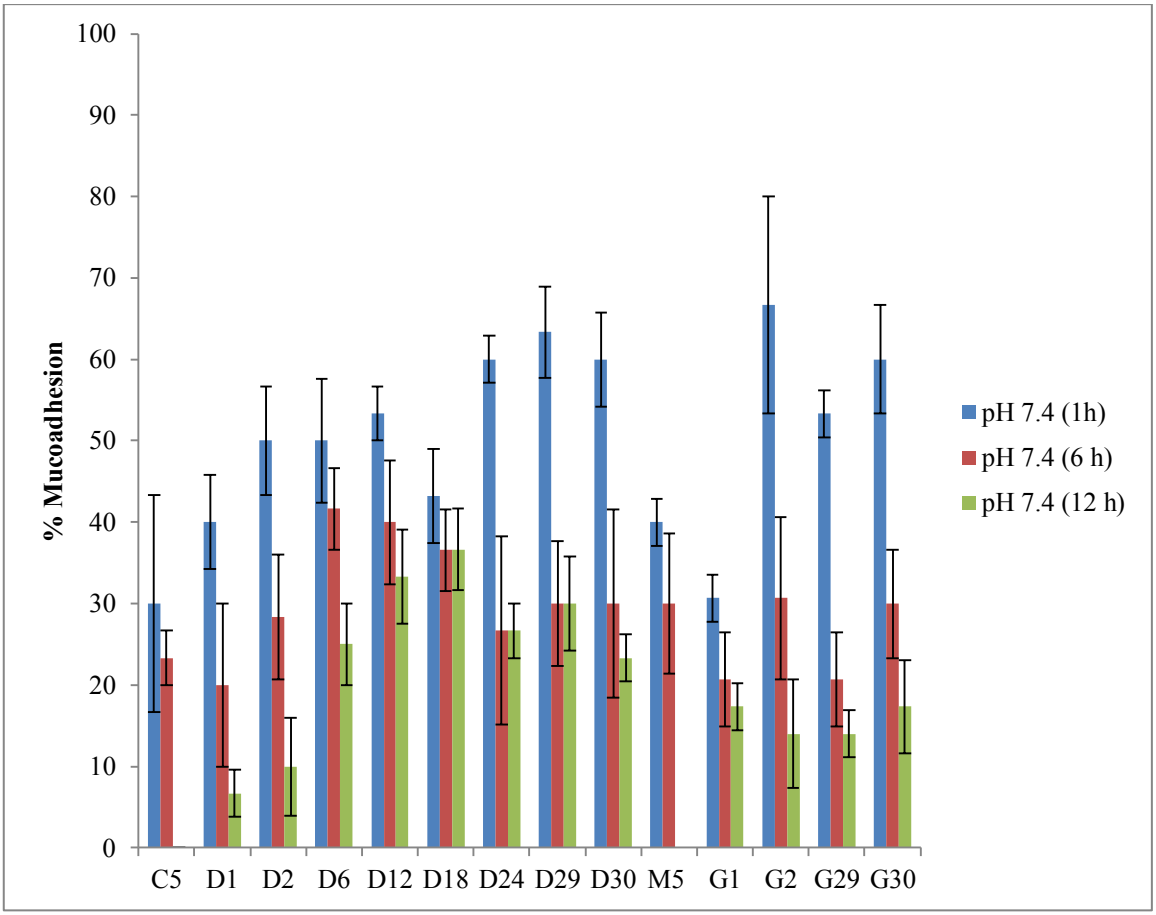

Figure 6-20: Mucoadhesion tests on coated MET and CMN beads in alkaline media

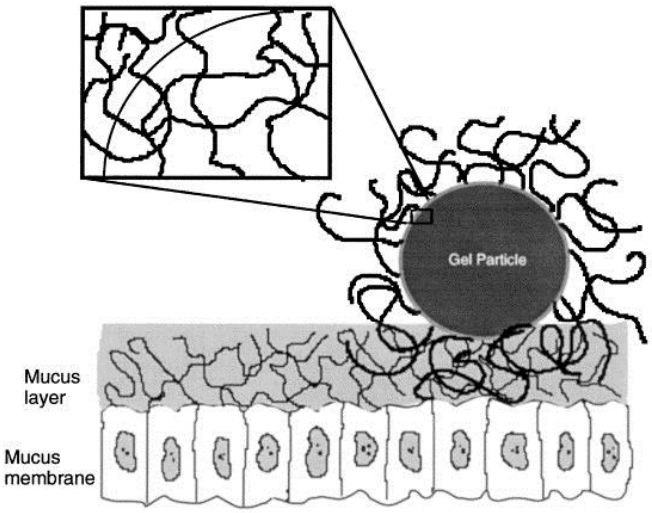

Figure 6-21 : A proposed mechanism of action of mucoadhesion of coated hydrogels (Huang *et al.*, 2000)

For this mucoadhesion test, several other factors apart from the chitosan and mucin molecular interactions may help retention of the beads on the tissue surface or even detachment from the tissue surface. Factors such as ridges on the tissue, surface tension, gravitational forces *etc*., all play a role in the outcome of these tests. However, as the coated and the uncoated beads showed significant differences in mucoadhesion with other conditions kept constant, it can be concluded that the observed increase in mucoadhesion was due to the presence of the chitosan coating. This study was also performed using a disintegration apparatus and it gave a similar trend with the uncoated beads being detached from the pig gastric mucosa faster than the coated beads.

6.3.10.2.3 Zeta potential of coated beads

It has been demonstrated that the positive charge on the bead surface due to the presence of chitosan could lead to a strong electrostatic interaction with a negatively charged mucosal surface (He *et al.*, 1999a, He *et al.*, 1999b).

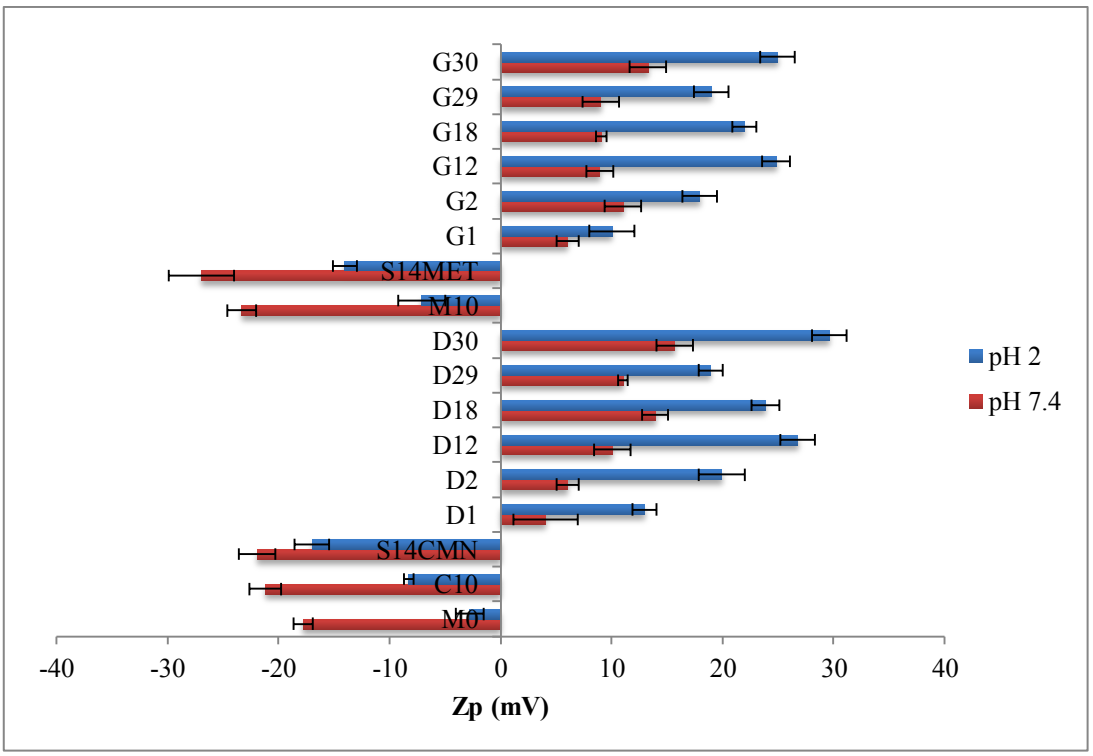

Figure 6-22: Zeta potential of uncoated and coated beads

In neutral and alkaline pH environments, uncoated beads have a negative surface charge due to the presence of ionized carboxylic groups of the alginate matrix, whereas in the acidic media the ionization is suppressed and *Zp* values are closer to zero. In acidic chitosan solution, the polymeric chains are positively charged and *Zp* of chitosan-coated beads is positive. The addition of drug in the bead matrix also increased the negativity of the *Zp* of the

drug-loaded beads (Huang *et al*, 2003, Martinac *et al*, 2005). These negatively charged beads could interact with the positively charged chitosan. On coating with chitosan, the beads became positively charged (Figure 6-22) as a result of neutralization of the charge by chitosan and the excessive amino groups present on the surface of the beads. The presence of oil also had a negative impact on the *Zp*, which was reversed by the coating. The *Zp* inversion strongly suggests successful chitosan coating on the bead surface with *Zp* becoming increasingly positive as chitosan concentration increased from 0.5 % to 1 % ($p < 0.05$).

6.3.11 *In vitro* drug release from coated beads

6.3.11.1 Drug release from coated beads in acidic media (pH 1.2 / 4.0)

6.3.11.1.1 Effect of coating on the release profile of beads

MET beads

Coating of alginate beads with chitosan is expected to reduce the porosity at the surface of the beads and increase the stability of the beads especially in alkaline media. This reduction in porosity reduced the rate of drug release from the bead surface. At early time points, there was a reduced burst effect in coated beads, compared with uncoated beads (Figure 6-23). This was due to the combination of reduced LSC, due to the coating process and the presence of an additional barrier layer, which reduces the rate of drug diffusion from the bead surface. It takes longer for the dissolution media to penetrate the surface environs before drug dissolution and diffusion can occur into the dissolution media. Drug release from the coated beads was more controlled than in both the unmodified beads and the oil-modified beads. For example, $t_{50\%}$ of M_{10}, $S15_{MET}$, G34 and G36 were 5-10 minutes; 20-30 minutes; 120-150

minutes and 120-150 minutes respectively (Table 6-3). There was a significant difference in the release profiles from the CNOM beads *versus* the unmodified beads with the f_2 values within the range of 27 - 33 (M_{10} beads *versus* G8/G10/G12 beads). With the COM beads, there was a similar pattern, with a significant difference in release profiles from coated *versus* uncoated oil modified beads with f_2 values within the range of 26 - 29 ($S15_{MET}$ beads *versus* G32/G34/G36 beads). In comparison with the unmodified beads, there was a significant difference in the release profiles of COM with f_2 values < 20. At pH 4.0, the f_2 values were > 60, therefore they presented almost identical release profiles, and therefore this pH difference was not enough to make a significant difference in the release pattern. Drug release from CNOM beads was extended to ~ 8 - 10 h as a result of the extra layer of coating on the bead surface. Similar results were observed for COM beads where duration of drug release was ≥ 12 h. This is an improvement on the duration of release observed from unmodified beads, which exhibited complete drug release at ~ 4 h.

CMN beads

CMN release from the coated beads was more controlled than both the unmodified beads and the oil-modified beads. For example, $t_{50\%}$ of C_{10}, $S15_{CMN}$, D34 and D36 were 60 - 90 minutes; 60 - 90 minutes; 300 minutes and 360 - 480 minutes respectively (Table 6-4). There was a significant difference between the release profiles from the CNOM beads *versus* the unmodified beads, with f_2 values within the range of 27 - 31 (C_{10} beads *versus* D8/D10/D12 beads). With the COM beads, there was a similar pattern, with a significant differences between release from coated *versus* uncoated oil modified beads (f_2 values ranged from 35 - 45 ($S15_{CMN}$ beads *versus* D32/D34/D36 beads)) (Figure 6-24). In comparison with the unmodified beads, there was a significant difference in the release profiles from COM (f_2 ranged from 23 to 28) but pH has less of an impact (f_2 values were > 55 for pH 2.0 and pH 4.0). The duration of drug release from CNOM beads was ~ 12 h as a result of the extra layer

of coating on the bead surface and findings were similar for COM beads where duration of drug release was > 12 h. Thus, the coating extended drug release from around 6 to 12 h.

6.3.11.1.2 Effect of chitosan concentration and molecular weight on drug release

Increasing concentration of chitosan from 0.5 % to 0.07 M led to a slight reduction in the release rate; however, based on f_2 analysis, drug release from all beads coated with chitosan with varying concentrations exhibited similar profiles with the f_2 values being all > 55. Therefore, increasing chitosan concentration across this concentration range did not cause dissimilarity in the release profiles of the coated beads. In contrast, however, release from beads coated with chitosan of low molecular weights was dissimilar to those coated with high molecular weight chitosan (f_2 values being $46 > f_2 < 48$). However, comparing low and medium molecular weight, the profiles were similar with $f_2 > 50$. This was also observed when comparing dissolution profiles of beads coated with medium and high molecular weight chitosan. This might be due to the high concentrations of chitosan used in coating the beads, because at these concentrations, highly viscous solutions were produced and a more significant difference between the different molecular weight chitosans may have been more obvious if lower concentrations such as 0.1 % were used for coating. A study has reported the complicated nature of the effect of chitosan coating on release of encapsulated drug (Shu and Zhu, 2002). It was observed that chitosan coating accelerated brilliant blue (BB) released in some cases with 64, 70, 76 and 79 % BB release in 3 h following coating of 1.5 % alginate beads with 0, 0.1, 0.3 and 0.5 %w/v chitosan. Chitosan coating only prolonged BB release slightly in 3 % alginate beads and chitosan coating had no effect on BB release, when 5 % alginate beads were coated with chitosan. Ishak *et al.* (2007), reported that increasing

chitosan concentration over 0.4 %w/v had little effect on the MET release from chitosan-coated alginate beads.

6.3.11.2 Drug release from coated beads in alkaline media (pH 7. 4)

6.3.11.2.1 MET beads

Drug release from the coated beads was more controlled than both the unmodified beads and the oil modified beads in alkaline media, similar to results in the acidic media. For example, $t_{50\%}$ of M_{10}, $S15_{MET}$, G34 and G36 were 15-20 minutes; 20-30 minutes; 60 minutes and 80 minutes respectively (Table 6-5). There was a significant difference in the release from CNOM beads *versus* uncoated unmodified beads with the f_2 values ranging from 38 - 46 (M_{10} beads *versus* G8/G10/G12 beads) (Figure 6-25a). There was a similar pattern from COM beads, with f_2 values within the range of 39 - 42 ($S15_{MET}$ beads *versus* G32/G34/G36 beads) (Figure 6-25b). There was a significant difference in the release profiles between COM and unmodified beads, with f_2 values < 28. The duration of drug release from CNOM beads was not extended in PBS; however, for the COM beads, the duration of drug release was extended to ~ 8 h, which also confirmed by the stability of the beads up to this time. This was an improvement on the release profile observed from unmodified beads, which exhibited complete drug release at 3 - 4 h.

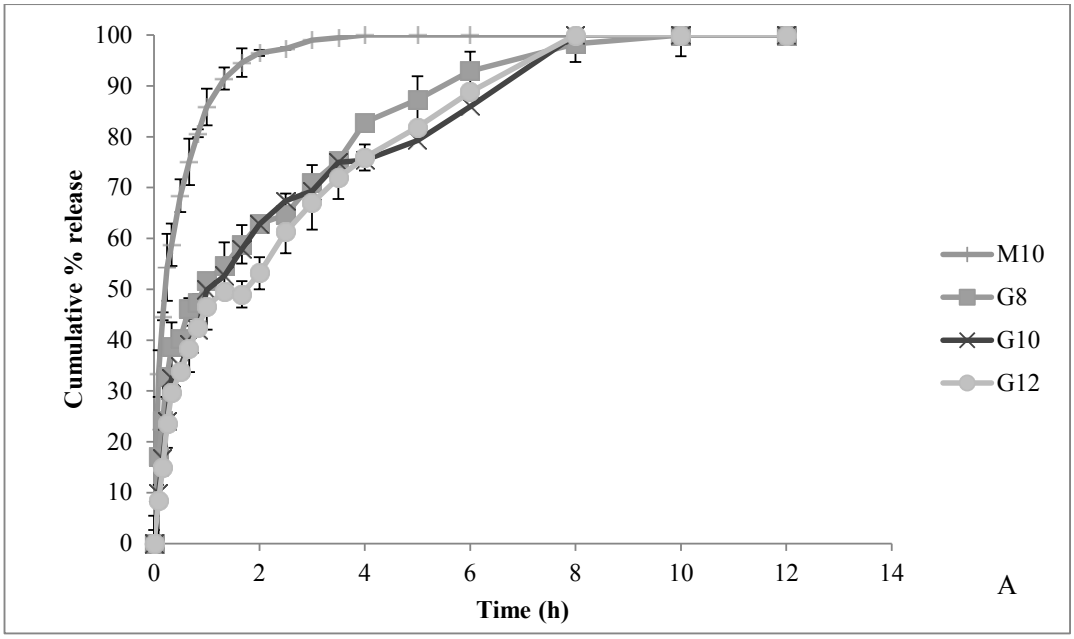

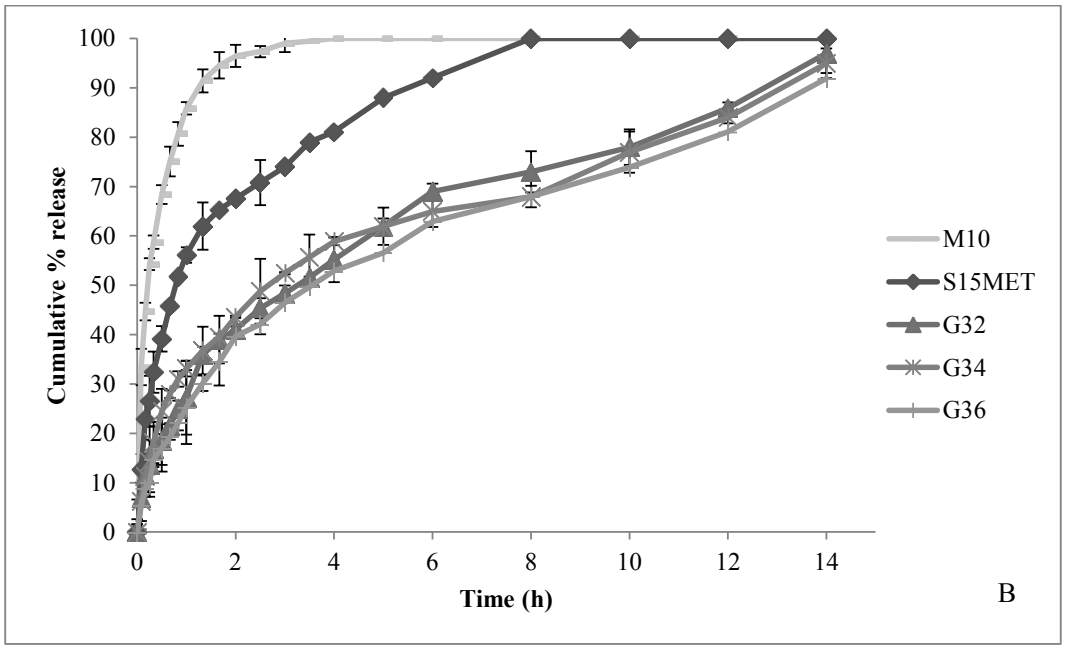

Figure 6-23: Release profile of MET loaded a) coated non oil-modified beads and b) coated oil-modified beads in acidic media (pH 1.2)

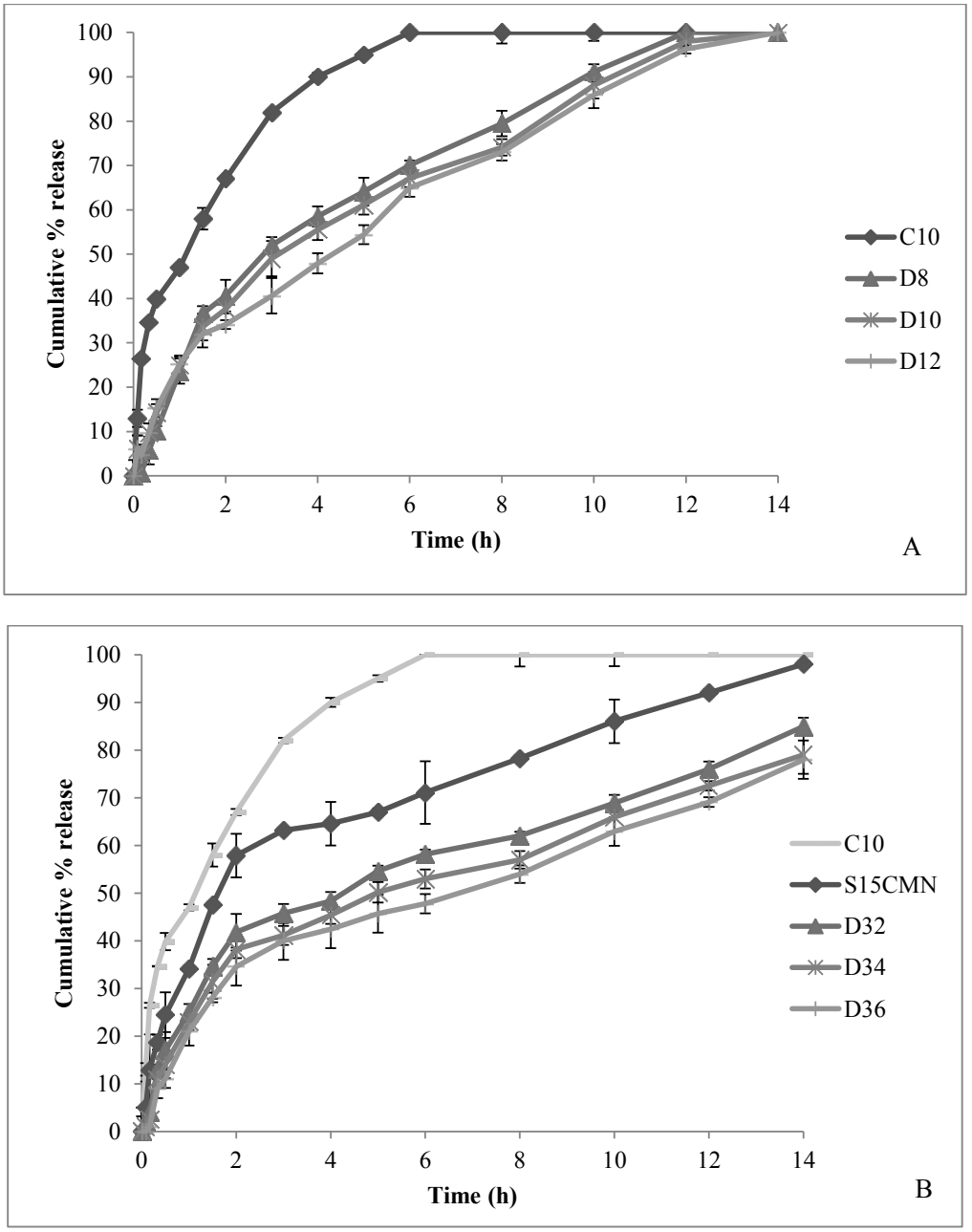

Figure 6-24: Release profile of CMN loaded a) coated non oil-modified beads and b) coated oil-modified beads in acidic media (pH 2.0)

Table 6-3: Release parameters of coated MET beads at pH 1.2

(Highlighted formulations exhibited significant changes in their drug release profiles compared to the unmodified formulations)

Formulation	$t_{25\%}$(min)	$t_{50\%}$ (min)	$t_{75\%}$ (min)
G_2	< 5	15 - 20	120
G_4	< 5	30	150
G_6	< 5	30	150 – 180
G_8	< 5	40-50	150 – 180
G_{10}	5-10	40-50	180-210
G_{12}	5-10	50-60	210-240
G_{14}	10-15	60	240-300
G_{16}	30	80	180-210
G_{18}	20-30	60-80	150 – 180
G_{20}	**30**	**80-100**	**360-480**
G_{22}	**50-60**	**100-120**	**360**
G_{24}	**40-50**	**100**	**300-360**
G_{26}	20-30	60-80	360-480
G_{28}	30-40	60-80	210-240
G_{30}	30	80-100	210-240
G_{32}	**40-50**	**120**	**480**
G_{34}	**50-60**	**120-150**	**360-480**
G_{36}	**50-60**	**120-150**	**360-480**

Table 6-4: Release parameters of coated CMN beads at pH 2.0

(Highlighted formulations exhibited significant changes in their drug release profiles compared to the unmodified formulations)

Formulation	$t_{25\%}$(min)	$t_{50\%}$ (min)	$t_{75\%}$ (min)
D_2	30 - 60	120	360 - 480
D_4	30 - 60	120	360
D_6	30 - 60	120 - 180	480
D_8	60 - 90	120 - 180	360 - 480
D_{10}	60	180 - 240	480 - 600
D_{12}	60	240 - 300	480 - 600
D_{14}	20 - 30	120 -180	240 - 300
D_{16}	20 - 30	120 -180	300
D_{18}	60	120 -180	360 - 480
D_{20}	**60 - 90**	**120 -180**	**360 - 480**
D_{22}	**60 - 90**	**180 - 240**	**480 - 600**
D_{24}	**120 -180**	**240 - 300**	**600 - 720**
D_{26}	30 - 60	120 -180	600 - 720
D_{28}	30 - 60	180 - 240	600 - 720
D_{30}	30 - 60	240 - 300	720
D_{32}	**60**	**240 - 300**	**600 - 720**
D_{34}	**60 - 90**	**300**	**720 - 840**
D_{36}	**60 - 90**	**360 - 480**	**720 - 840**

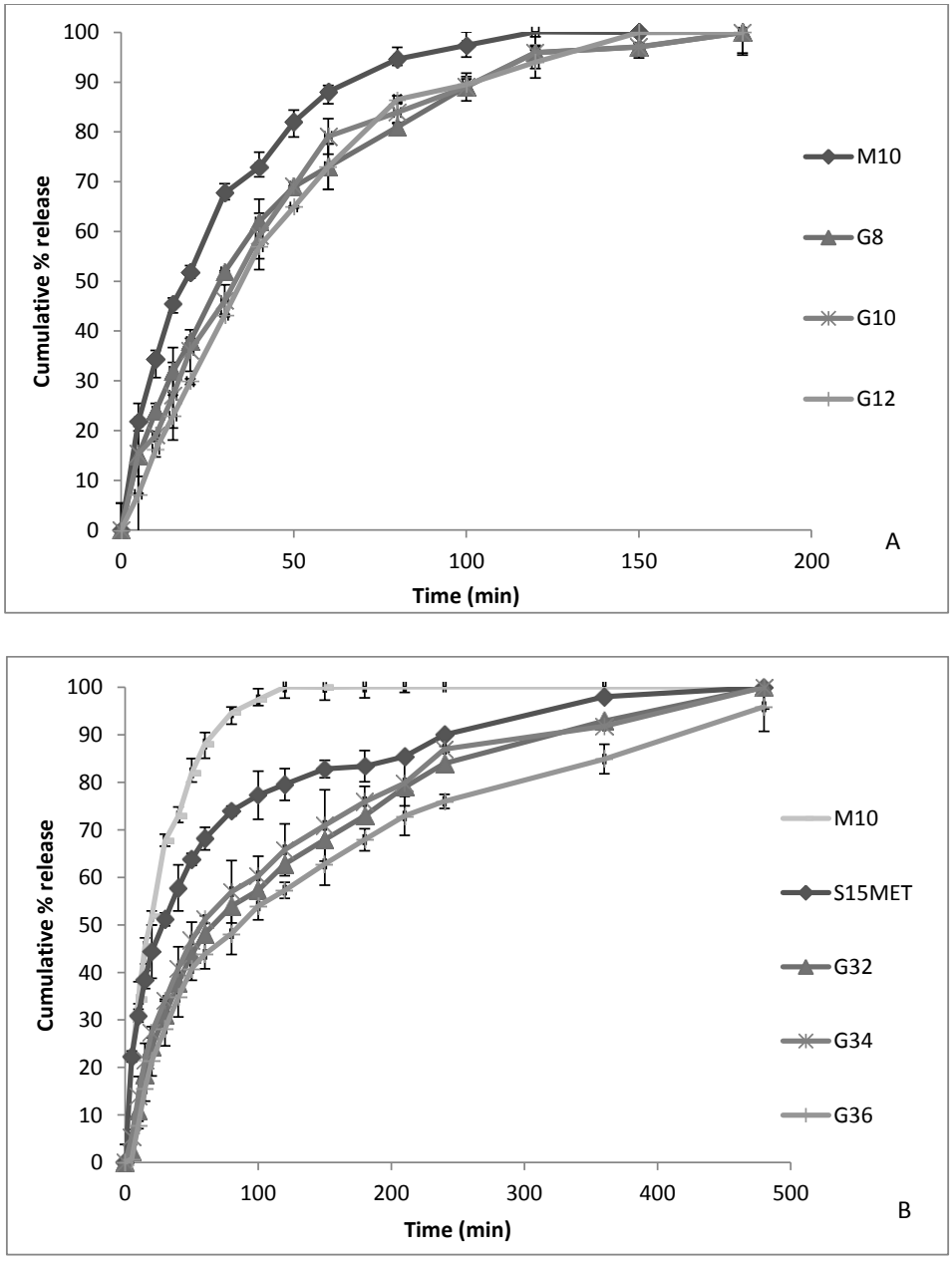

Figure 6-25: Release profile of MET-loaded A) coated non oil-modified beads and B) coated oil-modified beads in PBS

6.3.11.2.2 CMN beads

There was an initial lag time of about 5 to 10 minutes prior to CMN release, which was slightly more controlled than in alkaline media than observed in the acidic media. For example, $t_{50\%}$ of C_{10}, $S15_{CMN}$, D34 and D36 were 50 - 60 minutes, 60 - 80 minutes, 80 – 100 minutes and 80 minutes respectively (Table 6-6). There was a significant difference between release from CNOM beads and the uncoated unmodified beads, with f_2 values ranging from 30 - 40 (C_{10} beads *versus* $D_8/D_{10}/D_{12}$ beads) (Figure 6-26a). The pattern was similar for coated *versus* uncoated oil modified beads, with f_2 values between 41 and 47 ($S15_{CMN}$ beads *versus* D32/D34/D36 beads) (Figure 6-26b). There was a difference in release compared to uncoated beads (f_2 values < 38) and the duration of CMN release from CNOM beads was extended in PBS with complete drug release being at ~ 6 h and ~ 8 h for COM beads.

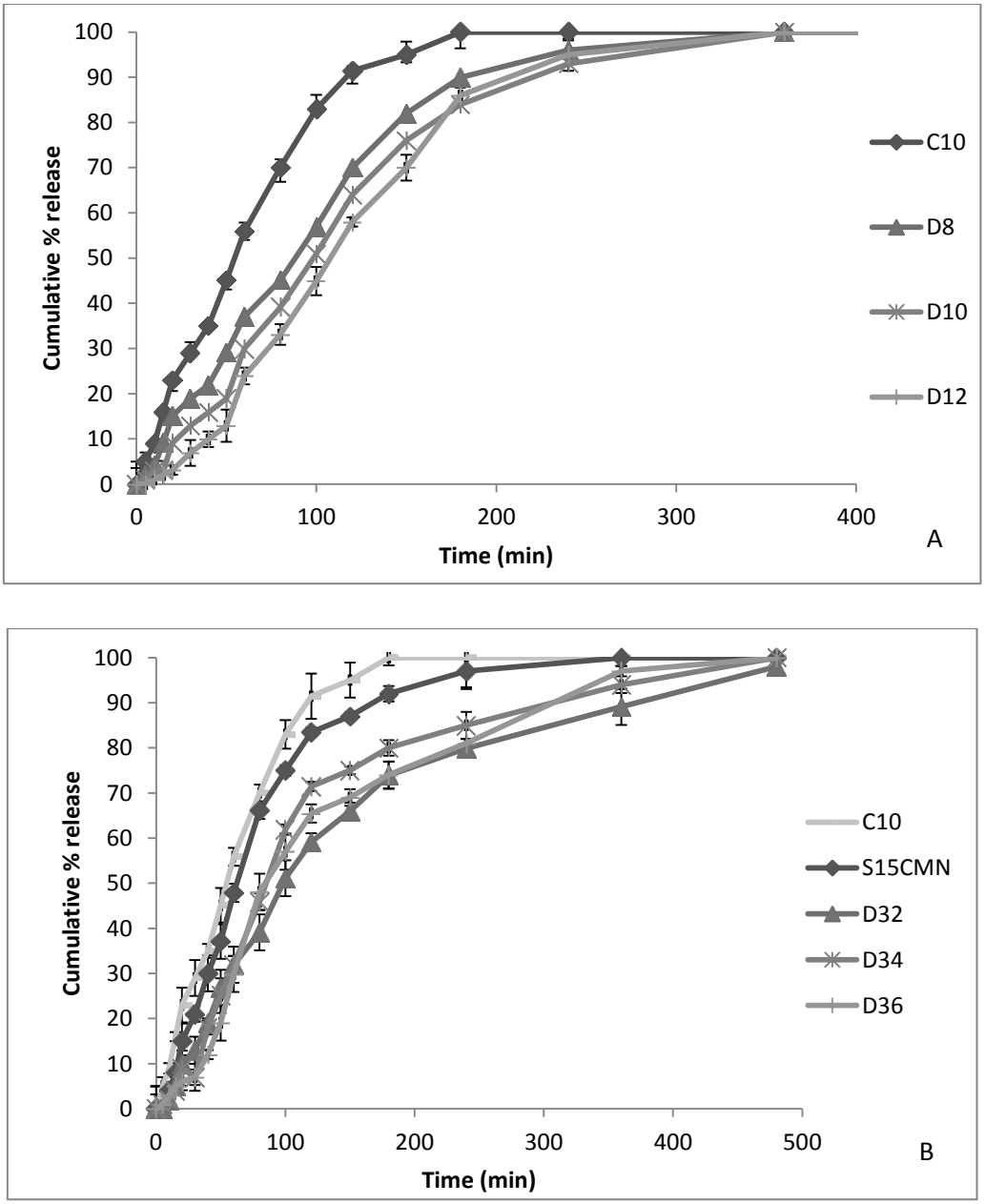

Figure 6-26: Release profile of CMN-loaded A) coated non oil-modified beads and B) coated oil-modified beads in PBS media

Table 6-5: Release parameters of coated MET beads in PBS

(Highlighted formulations exhibited significant changes in their drug release profiles compared to the unmodified formulations)

Formulation	$t_{25\%}$(min)	$t_{50\%}$ (min)	$t_{75\%}$ (min)
G_2	5 - 10	20 - 30	40 - 50
G_4	5 - 10	20 - 30	40 - 50
G_6	10	20 - 30	50 - 60
G_8	10 - 15	20 - 30	60 - 80
G_{10}	10 - 15	30 - 40	50 - 60
G_{12}	15 - 20	30 - 40	60 - 80
G_{14}	30 - 40	80 - 100	180 - 210
G_{16}	20 - 30	60 - 80	150 - 180
G_{18}	20 - 30	80	150 - 180
G_{20}	**40 - 50**	**100-120**	**210 - 240**
G_{22}	**20 - 30**	**80 - 100**	**150 - 180**
G_{24}	**30**	**80 - 100**	**180**
G_{26}	15 - 20	50 - 60	150 - 180
G_{28}	15	50	150
G_{30}	20	60 - 80	180 - 210
G_{32}	**20 - 30**	**60 - 80**	**180 - 210**
G_{34}	**15 - 20**	**50 - 60**	**180**
G_{36}	**20 - 30**	**80 - 100**	**210 - 240**

Table 6-6: Release parameters of coated CMN beads in PBS

(Highlighted formulations exhibited significant changes in their drug release profiles compared to the unmodified formulations)

Formulation	$t_{25\%(}$min)	$t_{50\%\ (}$min)	$t_{75\%}$ (min)
D_2	30	50 - 60	80 - 100
D_4	30 – 40	60 - 80	100 - 120
D_6	40 – 50	60 - 80	120 - 150
D_8	50	80 - 100	120 - 150
D_{10}	50 - 60	100	150
D_{12}	60 - 80	100 - 120	150 -180
D_{14}	30 - 40	60 - 80	100 - 120
D_{16}	40 - 50	60 - 80	120 - 150
D_{18}	50	60 - 80	150 -180
D_{20}	40 - 50	60 - 80	100 - 120
D_{22}	40 - 50	60 - 80	120 - 150
D_{24}	50 - 60	80 - 100	120 - 150
D_{26}	30 - 40	60 - 80	100 - 120
D_{28}	40 - 50	60 - 80	120
D_{30}	50 - 60	80	150 -180
D_{32}	**40 - 50**	**100**	**180 -240**
D_{34}	**50**	**80 - 100**	**150 -180**
D_{36}	**50 - 60**	**80 - 100**	**180 -240**

6.3.11.3 Drug release kinetics and release mechanism of coated beads

6.3.11.3.1 MET and CMN release in acidic media

Release from coated beads fitted best to Higuchi kinetics (R^2 = 0.98 – 0.99 (MET) and R^2 = 0.97 – 0.99 (CMN)) as did release from unmodified beads; therefore the modifications did not cause a change in the drug release kinetics (Table 6-7). For the CNOM MET beads, the release exponent 'n' was ≤ 0.43, indicating Fickian diffusion, however for the COM MET beads, n > 0.43 indicating non-Fickian anomalous diffusion with drug release controlled by a combination of diffusion and polymer relaxation. There was a change in the release kinetics as the unmodified CMN beads exhibited Fickian diffusion while the COM CMN beads (n = 0.72 - 0.81) exhibited non- Fickian anomalous diffusion related to diffusion and swelling. The release exponent of the CNOM CMN beads was 0.88 - 0.89 except for D_{12} which was 0.61, indicating most of the CNOM CMN beads exhibited case II transport, which involves polymer dissolution and polymeric chain enlargement or relaxation. The formation of a polyelectrolyte complex membrane altered the drug release mechanism towards anomalous diffusion indicating that drug was diffusing out through the beads with simultaneous polymer relaxation. Coated beads have been demonstrated to exhibit similar non-Fickian (anomalous) and case II diffusion kinetics (Basu and Rajendran, 2008, Sun *et al.*, 2013).

Table 6-7: Release kinetics of coated a) MET beads and b) CMN beads in acidic media

A

Sample	Zero order		1st order		Higuchi		Hixson-Crowell		Peppas	
	K_0(%/min)	R^2	K_1(/min^1)	R^2	K(%/min$^{1/2}$)	R^2	k	R^2	n	R^2
G_2	0.277	0.884	0.003	0.881	4.136	0.991	0.008	0.962	0.254	0.949
G_8	0.208	0.948	0.002	0.776	4.274	0.990	0.007	0.958	0.309	0.988
G_{12}	0.185	0.895	0.002	0.972	3.775	0.989	0.005	0.956	0.327	0.975
G_{14}	0.134	0.739	0.001	0.876	3.515	0.990	0.004	0.777	0.436	0.979
G_{20}	0.145	0.791	0.001	0.818	3.713	0.988	0.004	0.879	0.589	0.975
G_{26}	0.108	0.703	0.001	0.848	3.181	0.994	0.003	0.801	0.509	0.991
G_{30}	0.137	0.879	0.001	0.829	3.792	0.993	0.003	0.886	0.733	0.981
G_{32}	0.122	0.782	0.001	0.828	3.492	0.997	0.003	0.886	0.701	0.931

B

Sample	Zero order		1st order		Higuchi		Hixson-Crowell		Peppas	
	K_0(%/min)	R^2	K_1(/min^1)	R^2	K(%/min$^{1/2}$)	R^2	k	R^2	n	R^2
D_2	0.156	0.826	0.001	0.841	3.997	0.981	0.003	0.933	0.888	0.967
D_8	0.197	0.922	0.001	0.787	4.204	0.992	0.004	0.967	0.899	0.981
D_{12}	0.133	0.954	0.001	0.877	3.573	0.994	0.003	0.988	0.614	0.991
D_{14}	0.208	0.889	0.002	0.737	4.655	0.978	0.005	0.942	0.799	0.845
D_{20}	0.138	0.837	0.001	0.952	3.899	0.973	0.003	0.918	0.729	0.934
D_{26}	0.096	0.829	0.001	0.854	2.971	0.997	0.003	0.921	0.799	0.802
D_{30}	0.084	0.877	0.001	0.867	2.744	0.995	0.002	0.95	0.727	0.843
D_{32}	0.095	0.841	0.001	0.748	2.921	0.995	0.002	0.919	0.721	0.926

6.3.11.3.2 MET and CMN release in alkaline media

Both MET and CMN were released from CNOM following zero order drug release kinetics (R^2 = 0.99) (Table 6-8). The change in mechanism compared to unmodified beads is due to decreased solubility of drug at this pH and the extra layer of chitosan on the surface, which also has a low solubility in PBS, leading to an initial slow release of the drug from the beads. However, the COM MET and CMN beads followed Higuchi kinetics (R^2= 0.97- 0.99), similar to the unmodified beads and the oil-modified beads. For the CNOM MET beads, the release exponent 'n' was 0.68 - 0.72, indicating anomalous diffusion, however for the COM MET beads, 'n' was 0.86 - 0.95 indicating case II transport or zero order kinetics; one formulation, G_{20}, had a value > 1, indicating Supercase II transport. CNOM and COM CMN beads had a release exponent, n value > 1 also indicating Supercase II transport with the exception of one formulation D_{30} with, n value < 1 indicating case II transport approaching a zero order behaviour arising from a reduction in the attractive forces between polymer chains. Supercase II transport is controlled by swelling and relaxation of polymer chains and is characterized by accelerated solvent penetration. The rate of solvent diffusion in the matrix is much greater than the swelling, with this being the determining factor in the drug release.

Table 6-8: Release kinetics of coated A) MET beads and B) CMN beads in alkaline media

Sample	Zero order		1st order		Higuchi		Hixson-Crowell		Peppas	
	K_0(%/min)	R^2	K_1(/min^1)	R^2	K(%/min$^{1/2}$)	R^2	k	R^2	n	R^2
G_2	1.273	0.995	0.013	0.985	12.015	0.986	0.037	0.994	0.682	0.972
G_8	0.898	0.994	0.009	0.932	10.421	0.988	0.024	0.979	0.688	0.999
G_{12}	1.076	0.995	0.009	0.996	12.346	0.975	0.028	0.998	0.725	0.995
G_{14}	0.355	0.934	0.003	0.990	6.209	0.993	0.008	0.979	0.904	0.955
G_{20}	0.348	0.945	0.003	0.991	6.051	0.994	0.008	0.981	1.011	0.961
G_{26}	0.370	0.871	0.003	0.969	6.188	0.971	0.009	0.943	0.950	0.949
G_{30}	0.292	0.867	0.003	0.968	5.529	0.974	0.007	0.947	0.857	0.902
G_{32}	0.335	0.875	0.003	0.973	5.991	0.976	0.008	0.949	0.903	0.885

B

Sample	Zero order		1st order		Higuchi		Hixson-Crowell		Peppas	
	K_0(%/min)	R^2	K_1(/min^1)	R^2	K(%/min$^{1/2}$)	R^2	k	R^2	n	R^2
D_2	0.755	0.993	0.007	0.983	10.129	0.984	0.0192	0.994	1.12	0.989
D_8	0.558	0.994	0.005	0.958	8.043	0.964	0.013	0.981	1.068	0.981
D_{12}	0.514	0.991	0.004	0.922	7.871	0.928	0.012	0.961	1.695	0.992
D_{14}	0.741	0.986	0.006	0.985	9.861	0.993	0.017	0.977	1.489	0.982
D_{20}	0.727	0.987	0.006	0.984	9.675	0.992	0.017	0.971	1.469	0.993
D_{26}	0.746	0.988	0.006	0.981	9.918	0.991	0.018	0.971	1.471	0.982
D_{30}	0.392	0.898	0.004	0.964	7.102	0.978	0.009	0.945	0.966	0.965
D_{32}	0.377	0.941	0.003	0.912	6.796	0.993	0.009	0.982	1.316	0.979

6.3.11.4 Drug release in mucin suspension

6.3.11.4.1 MET beads

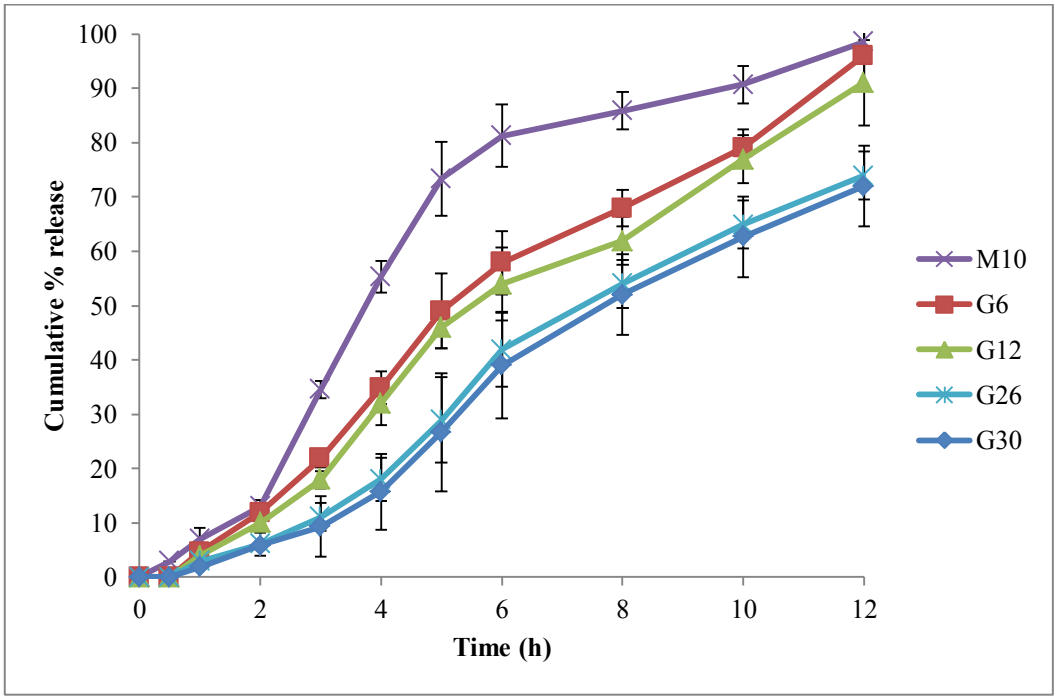

Figure 6-27: Franz cell diffusion studies of coated MET beads

Drug diffusion through mucin from coated beads of both drugs was sustained over the 12 h period studied (Figure 6-27). The CNOM MET beads exhibited no burst release and no significant lag times (10.34 ± 5.37 min). However, for COM MET beads, there was a lag of 41.45 ± 5.07 min. Drug flux decreased slightly following coating but this reduction was more pronounced for COM beads than CNOM beads (62.8 % decrease compared with 54.3 %) (Figure 6-28). Dissolution profiles from CNOM beads were dissimilar to those of M_{10} beads;

with f_2 being 38 – 43 and dissolution profiles of COM beads were also significantly different to M_{10} beads with f_2 values being < 30.

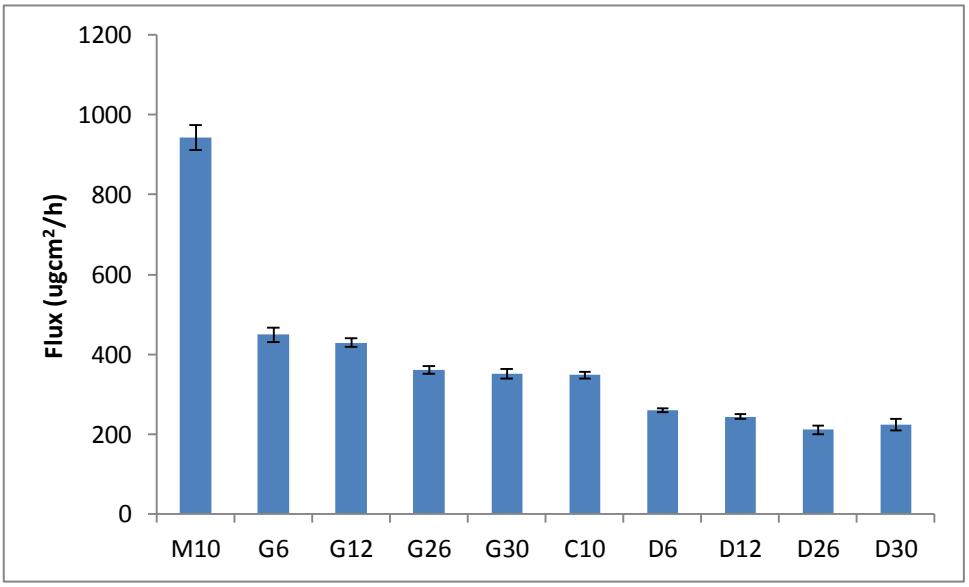

Figure 6-28: Fluxes of coated MET and CMN beads

6.3.11.4.2 CMN beads

The CNOM CMN beads exhibited no burst release, similar to the observation with MET beads, however, there were significant lag times (43.52 ± 2.01 min), most likely due to reduced aqueous solubility of CMN (Figure 6-29). Also, like the equivalent MET formulation, there was a lag of 50.47 ± 6.75 min before the start of drug release for COM CMN, which is only slightly different from the lag time observed for CNOM and significantly different from the unmodified CMN beads (~ 20 min). Drug flux decreased

slightly following coating but more so for COM beads than CNOM (55 % decrease *versus* 45 % decrease).

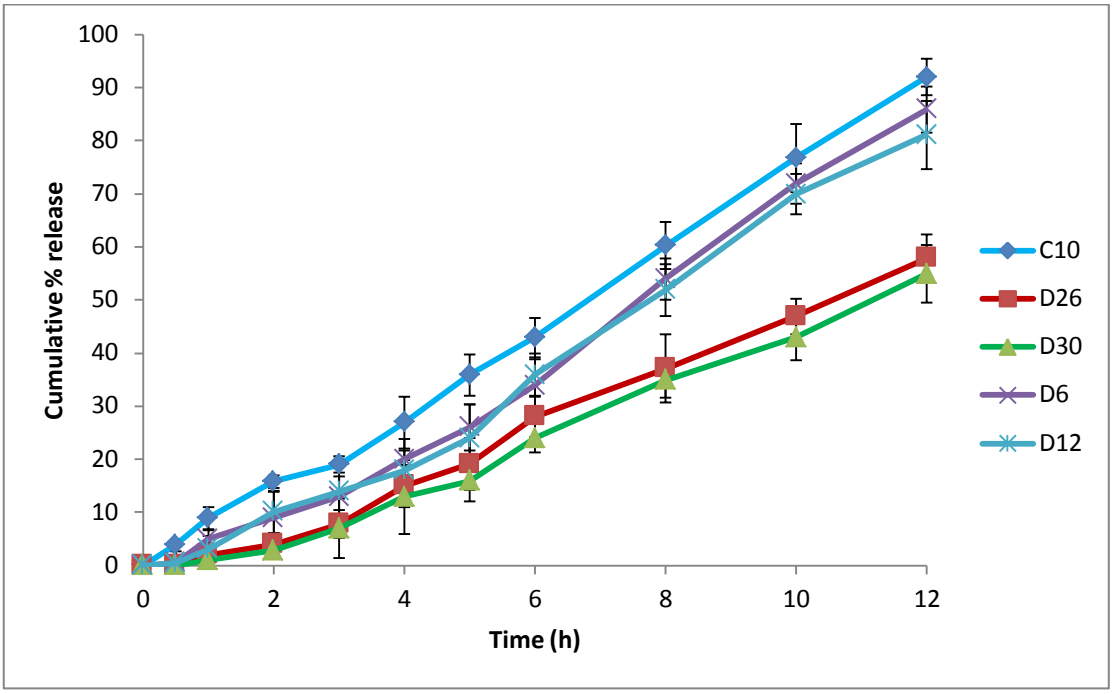

Figure 6-29: Franz cell diffusion studies of coated CMN beads

Dissolution from CNOM beads was dissimilar to that of M_{10} beads (f_2 being 38 – 43) and dissolution profiles from COM beads were also significantly different to M_{10} beads with f_2 values being < 30. Mucus is a primary barrier with which drugs must interact and diffuse through to be absorbed. Drug transport rate through mucus can be an important determinant of the efficacy of a formulation. Interspecies variations in mucus thickness limit the suitability of common laboratory animals for *in vivo* studies (Varum *et al.*, 2012). Drug release through mucin suspension demonstrated there was a sustained and adequate release of drug from the beads and the presence of chitosan on the surface of the beads did not hinder

drug release in the presence of mucin. This method may present a more realistic *in vitro* drug release model for mucoadhesive formulations as it better represents the *in vivo* environment especially in cases where *in vivo* models are absent.

6.3.12 Storage stability of coated beads

After 3 months storage at both 4 ℃ and 20 °C, there was no significant difference in the DEE, buoyancy, mucoadhesion ($p > 0.05$) and drug release ($f_2 > 50$) as shown in Table 6-9 and Figure 6-30 to Figure 6-32 (4 °C). On storage, the beads did not show any significant change in color and texture. There was no significant difference in all the other parameters therefore, the formulations were stable and could be stored at these temperatures without any need for special storage conditions.

	G30	G36	D30	D36
% DEE				
Day 0	88.67 (6.5)	92.13 (5.1)	94.09 (4.1)	94.82 (4.9)
Day 30	87.92 (7.4)	90.32 (6.8)	93.41 (5.2)	94.94 (5.1)
Day 60	88.13 (4.9)	91.17 (5.3)	89.98 (5.9)	94.93 (4.2)
Day 90	86.57 (5.1)	90.74 (5.4)	89.24 (6.2)	93.21 (5.9)
%Buoyancy				
Day 0	100	100	100	100
Day 30	100	100	100	100
Day 60	100	100	100	100
Day 90	100	100	100	100

Table 6-9: Stability of beads stored at 4 ℃ over a period of 3 months

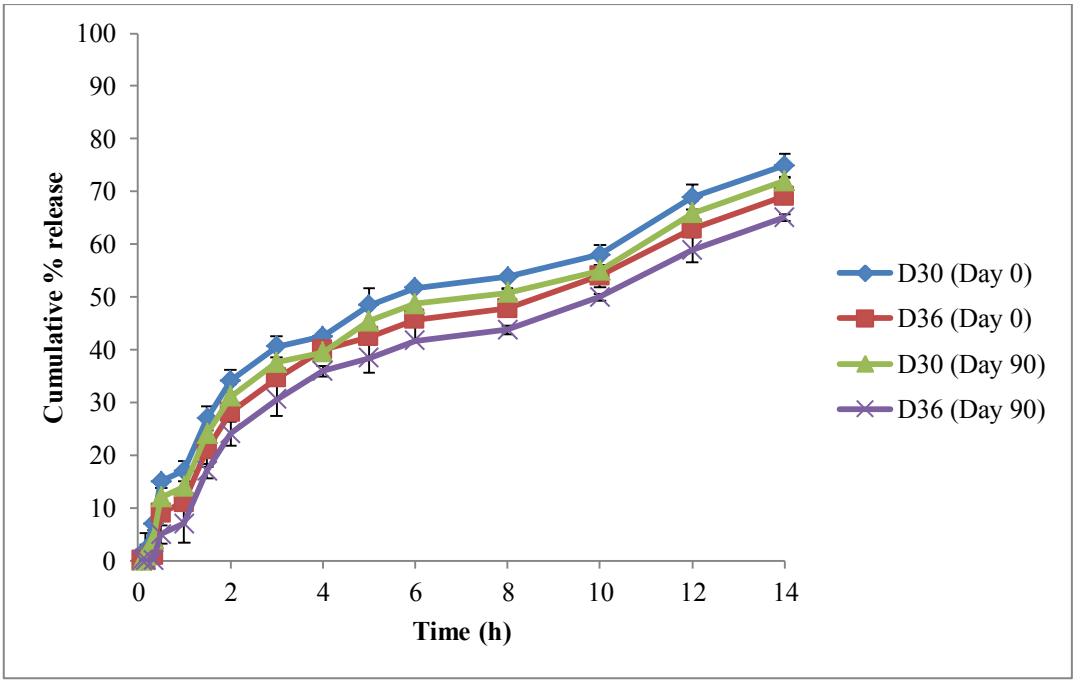

Figure 6-30: *In vitro* release of coated CMN beads in 0.1N HCl stored at 4 ℃

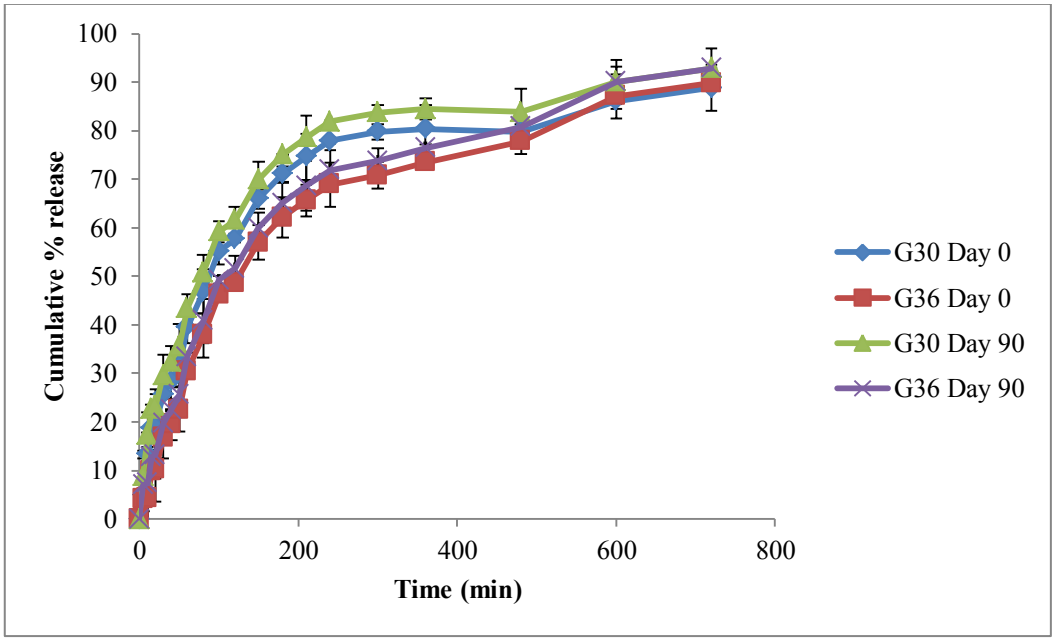

Figure 6-31: *In vitro* release of coated MET beads in 0.1N HCl stored at 4 ℃

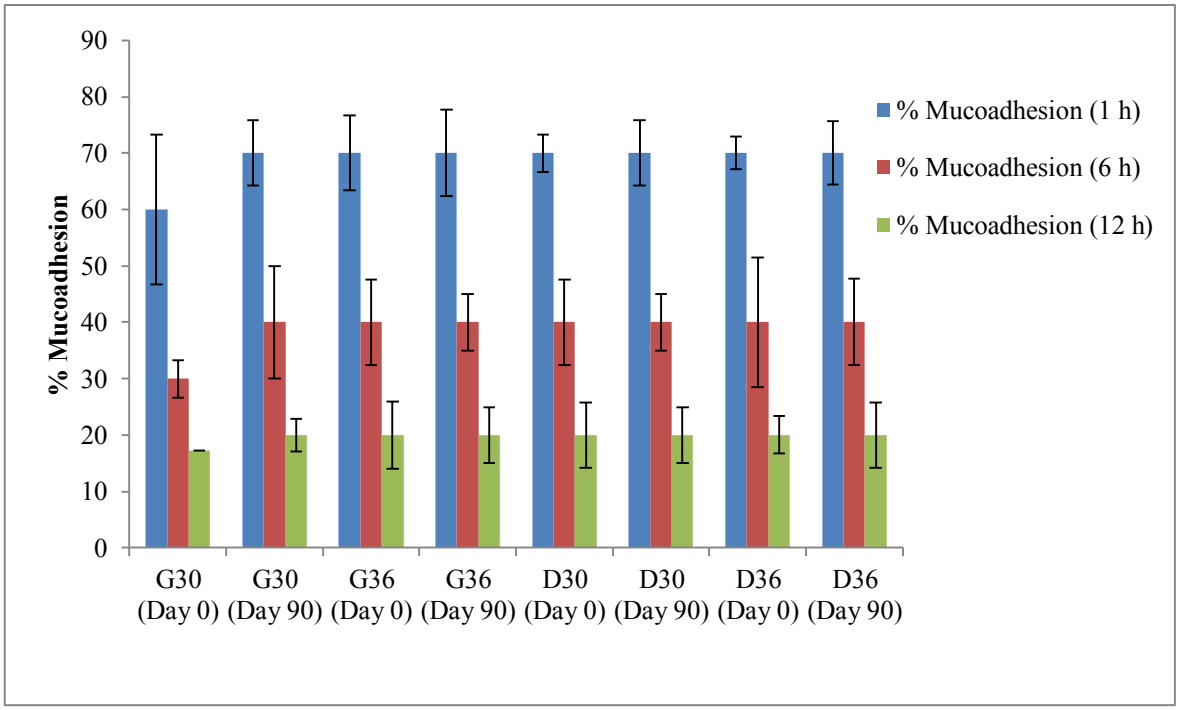

Figure 6-32: Mucoadhesion studies of coated MET and CMN beads stored at 4 ℃

6.4 Conclusion

The release of MET and CMN from alginate beads was modified by the addition of oil in the previous chapter (Chapter 5) and by coating of these oil-modified beads with chitosan- a mucoadhesive polymer. The coating of the beads with chitosan creates an additional barrier on the surface of the beads, to sustain the release of drug from the beads and create a mucoadhesive surface on the beads. The addition of oil improved the buoyancy of the beads, which is useful for gastro-retentive applications. Beads that were modified both with oil and coated with chitosan, provided the best-combined buoyancy, mucoadhesive and drug release

profiles, with the beads floating for at least 24 h and drug release sustained beyond 12 h. This shows a huge improvement especially for MET beads, where drug release from unmodified beads was ~ 3 h and 5 - 40 % beads floating after 12 h. In addition, a similar improvement in sustained drug release was observed for CMN beads where drug release from unmodified beads was initially ~ 8 h. Therefore, the modification of calcium alginate beads with oil and further chitosan coating can ensure the development of good sustained release devices and floating-mucoadhesive gastro-retentive drug delivery devices.

Chapter 7 LECTIN-CONJUGATED MICROSPHERES AND INTERACTION WITH MUCUS

7.1 Chapter overview

The common polymers used to achieve mucoadhesion have been classified into three main categories: a) polymers that are bioadhesive due to their stickiness; b) polymers that adhere through non-specific, non-covalent, primarily electrostatic interactions and c) polymers that bind to a specific receptor on the cell surface (Park and Robinson, 1984). Unlike the first-generation non-specific mucoadhesive polymers, where adhesion may occur at different sites in the GI tract, some second-generation mucoadhesive polymers are less susceptible to mucus turnover rates, with the potential to bind directly to mucosal surfaces through cyto-adhesion. This type of drug delivery, with attached mucus or cell-specific ligands, could offer the advantage of creating more targeted drug delivery systems. Site-specific targeting of drugs to a biological surface can be achieved through conjugate-receptor interactions. Labelling the surface of polymeric drug carriers, such as microspheres and nanoparticles, with appropriate conjugates enables targeting of surface receptors on selected target cell types. When such systems contact the relevant surface receptor, they can interact and potentially be retained at

the cell surface. Drug delivery directly to the site of interest can result in a lower required dose, leading to both cost savings and reduction of potential unwanted side effects. Lectins may provide a site-specific targeted drug delivery to mucosal cells due to the fact that they bind to carbohydrate residues specifically and non-covalently (Naisbett and Woodley, 1995, Chowdary and Rao, 2004) and are resistant to protease degradation (Kilpatrick *et al*, 1985, Gabor *et al*, 1997). In comparison with the non-specific interactions between polymer chains and mucin, lectin interactions with mucin are very specific. Lectins have been described as 'second generation mucoadhesives' (Kompella and Lee, 1992) and are found in organisms ranging from viruses and plants to animals (Barondes *et al*, 1994, Ezpeleta *et al*, 1999). Concanavalin A (Con A) is a lectin extracted from the jack bean, *Canavalia ensiformis*. It binds specifically to certain structures found in various sugars, glycoproteins, and glycolipids, mainly internal and non-reducing terminal α-D-mannosyl and α-D-glucosyl groups (Sumner *et al*, 1938, Goldstein and Poretz, 1986). This helps in their role in biological-recognition events (Rini, 1995).

In this chapter, floating-mucoadhesive microparticles containing ethylcellulose (EC) and chitosan were loaded with clarithromycin (CMN) and characterized. The microspheres were conjugated with Con A to form a lectin-drug carrier complex to ensure both controlled and targeted delivery of drug to improve the eradication of *H. pylori*. This research studies the effect of formulation variables such as grades of EC and ratios of Con A on conjugation efficiency (CE). In addition, the impact of conjugation on drug loading, drug entrapment, drug release and mucoadhesion was assessed. The impact of gastric environment should be considered when developing such systems (Noqieira *et al*, 2013) so in addition, robust *in-vitro* mucoadhesion tests were performed which can be useful in cases where *in vivo* models are not readily available. The use of second-generation mucoadhesives may enhance the targeting of antibiotics for eradication of *H. pylori* from the stomach for the treatment of peptic ulcer.

7.2 Materials and methods

EC-10 (low viscosity EC), EC-46 (high viscosity EC), chitosan (high molecular weight), polyvinyl alcohol (PVA), CMN, Con A (Type IV) and FITC-Con A, N-hydroxysuccinimide (NHS) and 1-ethyl-3, 3-(dimethylaminopropyl) carbodiimide (EDAC) were obtained from Sigma Aldrich (UK). All other chemicals used were of analytical grade and were used as received.

7.2.1 Preparation of floating microspheres

Microspheres were prepared using an emulsification/solvent evaporation method (Zheng *et al*., 2006, Jain and Jangdey, 2009). CMN, the polymers (EC-10 or EC-46) and chitosan were initially dissolved in the organic solvent, dichloromethane, which is immiscible with water and more volatile than water. An aqueous solution of 1 %w/v PVA was prepared and the polymer-drug solution was added to the aqueous solution as defined in Table 7-1. The emulsion formed was stirred continuously at 2,000 rpm for 1 h using a mechanical stirrer equipped with a three-blade propeller. The microsphere suspension was heated to 40 °C under reduced pressure, recovered by filtration, washed and dried at 40 °C for 24 h.

7.2.1.1 Characterisation of floating microspheres

These microspheres were characterised similarly to the beads (see section 3.3.3) unless otherwise stated.

Table 7-1: Formulation variables (S-10 and S-46 series were made with EC-10 and EC-46 polymers respectively

Code	EC (%w/w)	Chitosan (%w/w)	CMN (%w/w)	Con A (%w/v)
S0-10	4	-	-	-
S1-10	4	0.6	-	-
S2-10	2	0.6	4	-
S3-10	4	0.6	4	-
S4-10	8	0.6	4	-
S5-10	12	0.6	4	-
S0-46	4	-	-	-
S1-46	4	0.6	-	-
S2-46	2	0.6	4	-
S3-46	4	0.6	4	-
S4-46	8	0.6	4	-
S5-46	12	0.6	4	-
Con S1-10	4	0.6	-	0.1
Con S3-10a	4	0.6	4	0.025
Con S3-10b	4	0.6	4	0.05
Con S3-10c	4	0.6	4	0.1
Con S1-46	4	0.6	-	0.1
Con S3-46a	4	0.6	4	0.025
Con S3-46b	4	0.6	4	0.05
Con S3-46c	4	0.6	4	0.1
Con S4-46	8	0.6	4	0.1

7.2.1.2 Morphology and micromeritics of microspheres

The morphology and surface structure of the microspheres were examined by SEM using a Cambridge Instruments Stereoscan 90 microscope. Particle size was determined using a Malvern Mastersizer 2000 (Malvern Instruments Ltd, Worcestershire, UK) laser diffraction particle size analyser using a Hydro SM.

7.2.1.2.1 Bulk and tapped density of microspheres

The microspheres were poured through a glass funnel into a graduated measuring cylinder cut exactly to the 10 ml mark (V_o). Excess sample was removed using a spatula and the weight of the cylinder containing the microspheres was measured and recorded (M) without disturbing the sample bed. The cylinder was then tapped approximately 100 times manually from a height of approximately 2 cm and the final volume (V_t) was also recorded. The bulk density (ρ_b) and tapped density (ρ_t) were calculated using the equations 7-1 and 7-2 respectively:

$$\rho b = \frac{M}{V_0} \quad \text{..... Equation 7-1}$$

$$\rho t = \frac{M}{V_t} \quad \text{..... Equation 7-2}$$

7.2.1.2.2 Hausner ratio (H_r) and Carr index (I_C)

Hausner ratio (H_r) (equation 7-3) and Carr index (I_C) (equation 7-4) were calculated according to the following equations:

$$H_r = \frac{\rho_t}{\rho_b} \text{.....Equation 7-3}$$

$$I_c = \frac{\rho_t - \rho_b}{\rho_t} \; x\,100 \text{……..……..Equation 7-4}$$

7.2.1.2.3 Angle of repose (θ)

The angle of repose was determined using the fixed funnel method (Rahman *et al.*, 2006). A funnel with the end of the stem cut perpendicular to the axis of symmetry was secured with its tip approximately 2 cm height (H) above the graph paper placed on a flat horizontal surface. The microspheres were carefully poured through this funnel (cone diameter 5.5 cm, orifice diameter 1 cm) until the apex of the conical pile formed almost reaches the tip of the funnel. The mean diameter, 2R, of H, base of the powder cone was determined and the tangent of the angle of repose was calculated using Equation 7-5:

$$Tan\ \theta = \frac{H}{R} \text{…….……Equation 7-5}$$

7.2.1.3 CMN assay in methanol

Stock solutions of CMN were prepared by dissolving 5 mg drug in 10 ml methanol. Standards solutions of CMN were prepared in concentrations between 10 µg/ml and 100 µg/ml by diluting the stock solution and were analysed in triplicate by UV spectroscopy at a wavelength of 211 nm.

7.2.1.4 Yield, drug content and DEE of floating microspheres

Microspheres (20 mg) were agitated for 12 h in methanol to allow extraction of the drug from the polymer. The drug solution was filtered, diluted and analysed by UV spectroscopy at 211 nm and the quantity of drug content was determined from the equation of the regression line of the standard calibration curve of CMN in methanol. No interferences were found due to the presence of dissolved microsphere components was observed at this wavelength. This was performed in triplicate. The DEE and yield were calculated using equations 7-6 and 7-7 respectively:

$$\%\ Drug\ entrapment = \frac{actual\ drug\ content}{theoretical\ drug\ content}\ x\ 100 \quad \text{..... Equation 7-6}$$

$$\%\ Yield = \frac{weight\ of\ microspheres}{weight\ of\ drug\ polymer\ and\ other\ non\ volatile\ solids}\ x\ 100 \text{.....Equation 7-7}$$

7.2.1.5 *In vitro* buoyancy lag time and duration of floating microspheres

Microspheres (500 mg) were placed in 900 ml of simulated gastric fluid (SGF) pH 2.0 and pH 5.0 buffer containing 0.02 %w/v Tween 80 in a USP dissolution apparatus II (paddle). This dispersion was stirred continuously at 100 rpm for 12 hours after which time buoyant microspheres and the settled microspheres were collected, dried at 40 ºC and weighed. The buoyancy was determined by the weight ratio of buoyant microspheres to the sum of both the buoyant and settled particles (equation 7-8):

$$\%\ Buoyancy = \frac{Wf}{(Wf+Ws)}\ X\ 100 \quad \text{..... .Equation 7-8}$$

where, W_f and W_s are the weights of the floating and settled microspheres, respectively. All the tests were carried out in triplicate.

7.2.1.6 *In vitro* release studies of floating microspheres

Drug release from the microspheres was carried out using a USP II (paddle) dissolution apparatus. Microspheres, equivalent to 100 mg of CMN, were packed in hard gelatin capsules and immersed in 900 ml SGF (pH 2.0) and acetate buffer (pH 5.0) containing 0.02 %w/v Tween 80. The solution was maintained at 37 ± 1°C and at a rotation speed of 100 rpm. Samples were analysed by HPLC with a correction applied for degradation using the degradation rate constant *k* (Chun *et al.*, 2005) of CMN as detailed in Chapter 4.

7.2.2 Floating-mucoadhesive microspheres

7.2.2.1 Conjugation of Concanavalin A to microsphere surfaces

Activation of the carboxyl group of EC microspheres was carried out by the addition of 10 ml 0.1M EDAC and 10 ml of 0.11 M NHS in phosphate buffer (pH 5.8) (Irache *et al*., 1994, Damink *et al*., 1996). After incubation for ~ 3 hours, excess activating agents were removed by washing with phosphate buffer. The microspheres were re-suspended in Con A solution in phosphate buffer. This suspension was left overnight (~ 12 h) and microspheres collected by centrifugation at 4,000 rpm for 5 min, to remove any free unbound lectin, washed with distilled water, dried at room temperature and stored at 4 °C until required for use.

7.2.2.2 Determination of CE of conjugated blank microspheres

The amount of bound Con A and CE was calculated as the difference between the Con A added initially and the Con A recovered after incubation with the microspheres, using a Folin- Ciocalteu phenol assay as described in section 2.3.26.1.

10 ml of Reagent C was added to a suspension containing 100 mg of conjugated microspheres, mixed thoroughly and allowed to stand for 30 minutes. 1 ml of Reagent D was added and mixed rapidly. After 30 minutes, the solution was filtered and absorbance was measured against a blank (microspheres without lectin) using a UV-Vis spectrophotometer at 750 nm. The amount of bound lectin was determined using the standard calibration curve of Con A in phosphate buffer using the method above (presented in Section 2.3.26.1).

7.2.2.3 Determination of CE of conjugated drug loaded microspheres

For drug - loaded microspheres, FITC-labelled Con A was used to determine the CE and amount of bound lectin. The fluorescence of the FITC-Con A solution before and after conjugation were measured at excitation and emission wavelengths of 493 nm and 526 nm respectively and the concentration of the solutions determined from the standard calibration curve of FITC-Con A solution in phosphate buffer (presented in Section 2.3.26.2). The CE determined from the concentration of free lectin in the supernatant (Ezpeleta *et al.*, 1999) and was determined using equation 7-9:

$$\%\ CE = \frac{Con\ A\ (pre{-}incubation) - Con\ A\ (post{-}incubation)}{Con\ A\ (pre{-}incubation)}\ X\ 100 \quad \text{.....Equation 7-9}$$

7.2.2.4 Effect of amount of lectin loaded on CE

Varying concentrations of Con A (0.25 – 1 mg/ml) were incubated with the microspheres to determine its effect on CE.

7.2.2.5 Storage stability studies of microspheres

The microspheres were sealed in capsules and stored at room temperature (approximately 20° C) and 4° C over a period of three months. The average diameters, *Zp*, DEE, mucoadhesion and *in vitro* drug release were determined by methods described previously.

7.3 Results and discussion

EC-based microparticles have been used for the encapsulation of different drugs, such as amoxicillin (Das and Rao, 2006) and theophylline (Zinutti *et al.*, 1994) prepared by solvent evaporation. In this study, CMN microspheres were prepared using an oil-in-water emulsion solvent evaporation method. The drug was encapsulated in a gastric-resistant polymer film of EC, which can act as a physical barrier and prevent the degradation of CMN in the acidic pH of the stomach. EC, being a water insoluble polymer, helps to modify encapsulated drug release and prolong the action of CMN in the acidic environment of the stomach. Chitosan in this formulation acts as a mucoadhesive polymer. When the polymeric solution was poured into the aqueous continuous phase, emulsion droplets were formed. The dichloromethane was then removed from the system causing the droplets to solidify to form polymeric microspheres.

7.3.1 Characterisation of ethylcellulose microspheres

7.3.1.1 Micromeritics and morphology of ethylcellulose microspheres

The prepared microspheres were smooth and spherical in shape as seen in Figure 7-1. The shape of the microspheres became more spherical and the surface became smoother and less porous with an increase in EC concentration. Distinct pores were present on the surface of microspheres and these may be subsequently responsible for drug release (Tanwar *et al.*, 2007). The surface porosity was found to be crucial for drug release from EC microspheres by dissolution and diffusion allowing water to permeate the microsphere surface without dissolving in it (Lee *et al.*, 2000a). The pores at the surface are suspected to be the result of rapid evaporation of the solvent, dichloromethane, relative to the evaporation of water. During the solvent evaporation process, a crust initially formed on the surface of the droplets prevents the evaporation of the solvent causing the building up of vapour pressure, leading to

the formation of small eruption openings (Wang and Wang, 2002). There was evidence of collapsed particles at low EC concentrations (see Figure 7-1b) but this diminished with an increase in polymer concentration, with little aggregation of particles and absence of un-encapsulated drug crystals (Figure 7-1c and d). The microspheres ranged in size from 50 -183 µm (S-10 series) and 59 - 211 µm (S-46 series) with the particle sizes being significantly different ($p < 0.05$) due to the difference in molecular weight of EC polymers and thus viscosity of the droplets. The mean particle sizes of the floating microspheres significantly increased ($p < 0.05$) with increasing polymer concentration as shown in Table 7-2. The low concentrations of polymer resulted in a low viscosity of the polymer solution which in turn resulted in smaller emulsion droplets in the aqueous phase (Chaisri *et al.*, 2009, Parashar *et al.*, 2010) leading to smaller microsphere sizes. As the concentrations increase, there is an associated increase in viscosity and microsphere size. All the microspheres showed good flow properties represented in terms of angle of repose, which were all less than 40° and the Carr Index were all less than 20 (Shan-Yang and Yuh-Horng, 1989). The Hausner's ratio decreased with increasing EC concentration, which suggested good flow. Bulk and tapped density determinations also demonstrated good compaction and packing properties of the floating microspheres suggesting the microparticles would be amenable to pharmaceutical processing (Table 7-3).

7.3.1.2 Yield of ethylcellulose microspheres

The yield of the microspheres increased with an increase in polymer concentration and ranged from 54 to 83 % (Table 7-2). The low yield at low polymer /drug ratio and higher yield at high polymer/drug ratio may be due to the loss of smallest and lightest particles during microsphere preparation with the particles sticking to the blades and container. In addition, microsphere loss may occur during the filtration and the washing processes, even

though this was carefully controlled in this study. Several studies have reported lower yields at low polymer concentrations (Abdallah *et al.*, 2012, Trivedi *et al.*, 2008).

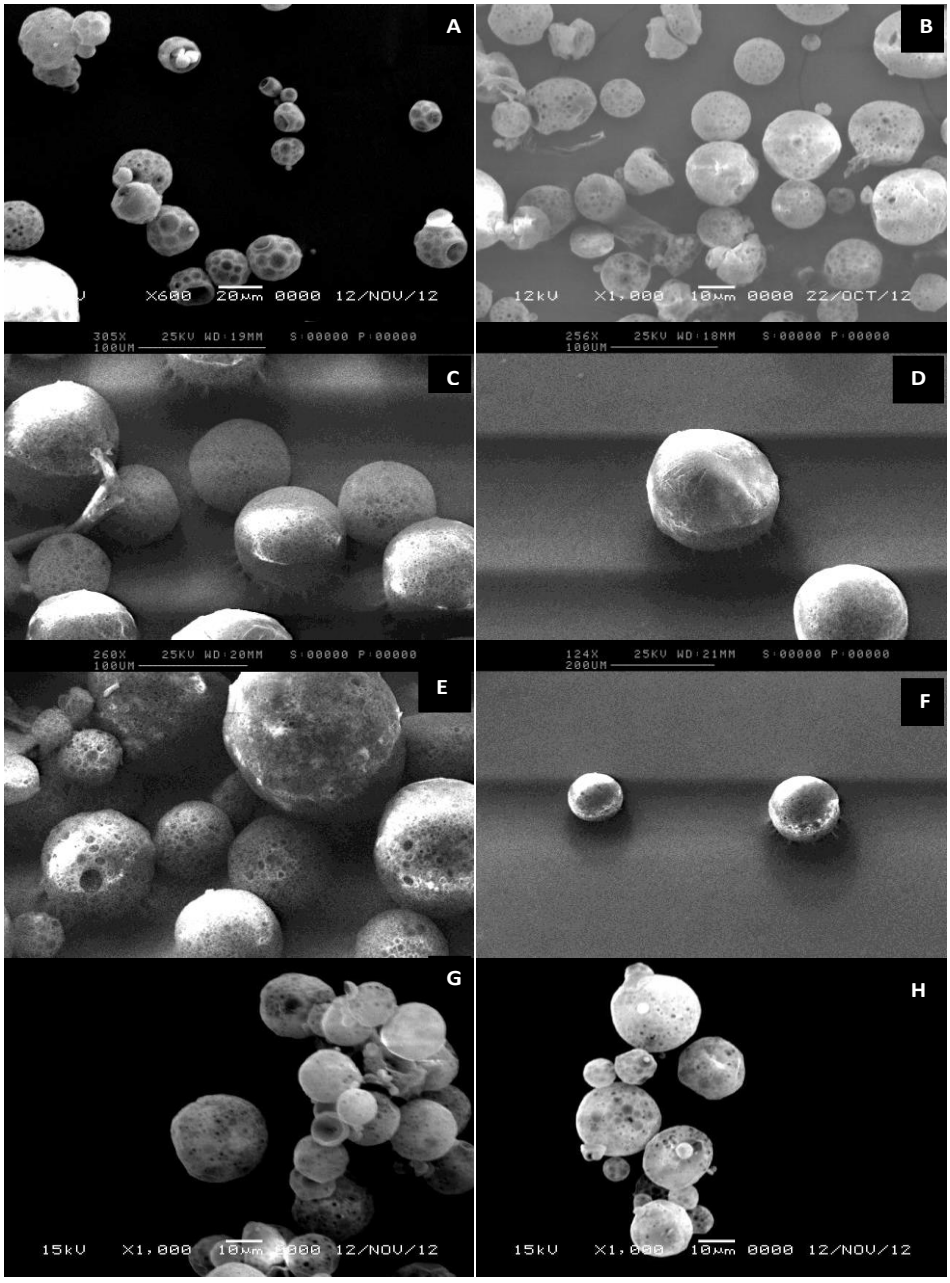

Figure 7-1: SEM images of A) S1-10, B) S1-46, C & D) S5-46 , E& F) S3-46, G) Con S1-10 and H) Con S1-46

Table 7-2: Properties of microspheres, results presented as mean ± SD (*n=3*)

Code	% Yield	Particle size (µm)	% Drug loading	% DEE	% Buoyancy
S0-10	54.21±6.3	50.21±3.28	-	-	93.1±4.31
S1-10	56.7±4.8	51.67±2.56	-	-	95.9±5.9
S2-10	62.9±2.8	60.65±3.65	35.5±2.3	58.58±3.83	80.8±2.9
S3-10	68.8±6.9	95.47±5.62	30.7±2.6	66.1±3.94	81.7±5.4
S4-10	76.9±2.7	131.73±4.74	22.9±1.7	72.15±2.35	87.9±3.9
S5-10	79.7±3.9	183.17±8.12	20.1±1.6	83.51±1.91	86.8± 4.8
S0-46	57.8±5.7	59.21±5.23	-	-	94.5±3.4
S1-46	69.9±3.7	66.75±6.32	-	-	92.8±3.6
S2-46	78.2±2.6	75.54±8.76	39.3±3.2	64.85±4.93	75.8±3.8
S3-46	75.8±4.6	104.18±7.96	35.9±2.2	77.18±3.24	78.9±5.8
S4-46	81.3±5.6	148.45±10.51	25.6±1.2	80.65±5.32	84.8±4.9
S5-46	82.6±6.5	211.44±8.28	22.1±2.3	91.86±4.68	93.2±4.9
ConS1-10	ND	82.82± 5.9	-	-	92.7±2.7
Con S3-10a	ND	-	21.11±3.1	45.38±6.8	80.3±5.6
Con S3-10b	ND	-	21.95±2.6	47.16±5.51	82.4±6.7
ConS3-10c	ND	113.93±6.3	21.7±3.9	46.65±7.9	79.8±4.9
ConS1-46	ND	107.45± 3.6	-	-	90.5±4.5
Con S3-46a	ND	-	30.45±3.6	65.49±5.49	82.5±6.2
Con S3-46b	ND	-	29.67±4.6	63.79±7.2	78.8±5.2
ConS3-46c	ND	129.38±8.3	30.9±1.3	66.43±5.5	79.9±5.8
Con S4-46	ND	162.24±10.32	23.9±2.5	75.29±7.87	83.92±6.3

Table 7-3: Flow properties of microspheres

Formulation	Bulk density (g/cm^3)	True density (g/cm^3)	Hausner's ratio	Compressibility index	Angle of repose (°)
S3-10	0.13 ± 0.02	0.15 ± 0.02	1.17 ± 0.03	14.64 ± 1.76	23.32 ± 0.15
S4-10	0.16 ± 0.04	0.19 ± 0.02	1.15 ± 0.01	15.79 ± 2.11	25.52 ± 2.69
S5-10	0.18 ± 0.02	0.22 ± 0.03	1.12 ± 0.02	18.18 ± 1.73	21.62 ± 1.32
S3-46	0.15 ± 0.01	0.18 ± 0.03	1.26 ± 0.02	16.67 ± 0.57	22.18 ± 1.62
S4-46	0.18 ± 0.02	0.21 ± 0.03	1.20 ± 0.03	14.28 ± 2.12	23.87 ± 1.03
S5-46	0.23 ± 0.01	0.28 ± 0.04	1.14 ± 0.01	17.86 ± 1.15	22.82 ± 0.64

7.3.1.3 Drug content and DEE of ethylcellulose microspheres

7.3.1.3.1 CMN calibration in methanol

The assay showed a high sensitivity with LOD and LOQ being 4.34 ± 0.21 and 13.02 ± 0.63 µg/ml, respectively with a high linearity ($R^2 > 0.99$) across the concentration range used. The inter-day and intra-day RSD were less than 4 % (Figure 7-2).

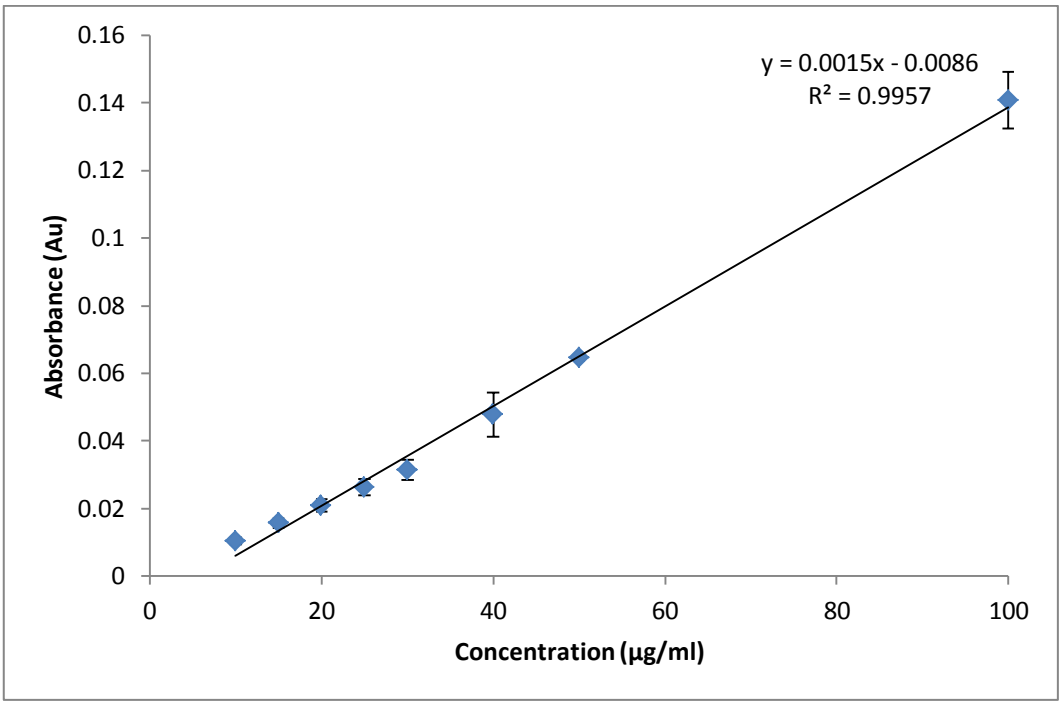

Figure 7-2: Calibration curve of CMN in methanol

7.3.1.3.2 DEE and drug content of ethylcellulose microspheres

Similar to the yield, DEE also increased with an increase in polymer/drug ratio with the DEE of unconjugated microspheres being between 58 – 92 % ($p < 0.05$). Low polymer/drug ratios

typically result in lower DEE due to higher concentration gradients causing the drug to diffuse out of the polymer/solvent droplets into the external processing medium. With an increase in polymer/drug ratio, the increase in viscosity enables more efficient drug entrapment. Similarly, increased viscosity associated with higher molecular weight also increased DEE ($p < 0.05$). The drug content in the microspheres was between 20 - 40 %w/w depending on the polymer/drug ratio. This result is similar to previous studies with reported increases in DEE with increases in polymer-drug ratio (Mehta *et al.*, 1996, Rafati *et al.*, 1997, Jelvehgari *et al.*, 2011).

7.3.1.4 Differential scanning calorimetry and thermogravimetric analysis of ethylcellulose microspheres

DSC for pure CMN showed a sharp symmetrical melting endotherm at 227.5 ± 0.2 ℃ which corresponds to the recorded melting temperature of CMN (Gómez-Burgaz *et al.*, 2009, Tozuka *et al.*, 2002). There was no shift in the melting endotherm of the physical mixture indicating that there was no chemical interaction between the CMN and EC in the physical mixture. There was a slight reduction in the melting endotherm and broadening of CMN peak in the drug-loaded microspheres (Figure 7-4a and b), suggesting a less ordered drug crystal structure and reduced crystallinity existing in the microspheres. This demonstrates that the drug was compatible with the polymer and neither drug decomposition nor drug-polymer interactions occurred in the microspheres. The TGA curves for pure CMN, EC, physical mixture and the microspheres are shown in Figure 7-3. Pure EC showed a significant weight loss around 310 ℃ with about 89 % decrease between 300 -350 °C. CMN also showed 97 % weight loss between 250 - 400 °C. This was similar to earlier reports that CMN exhibits about 91 % loss at temperature values above 300 ºC (Salem, 1996). The blank microspheres

appeared to be slightly more thermally stable than pure EC probably due to the formulation and this was further observed as the drug-loaded microspheres were more stable than the physical mixture, polymer and drug itself, with the onset of decomposition of microspheres being higher than that of the physical mixtures alone The decomposition onset temperature of the physical mixture was similar to that of the pure drug indicating that the decomposition of the drug was not influenced by the presence of ethyl cellulose. The drug-loaded EC microspheres decomposed at approximately the same temperature as pure drug and since the melting point of drug was not altered, it indicates the absence of any chemical interaction of drug with the polymer. Thus, the thermal stability of the drug was maintained in the microspheres. The moisture content of the microspheres was determined to be less than 2 %w/w from the TGA curve

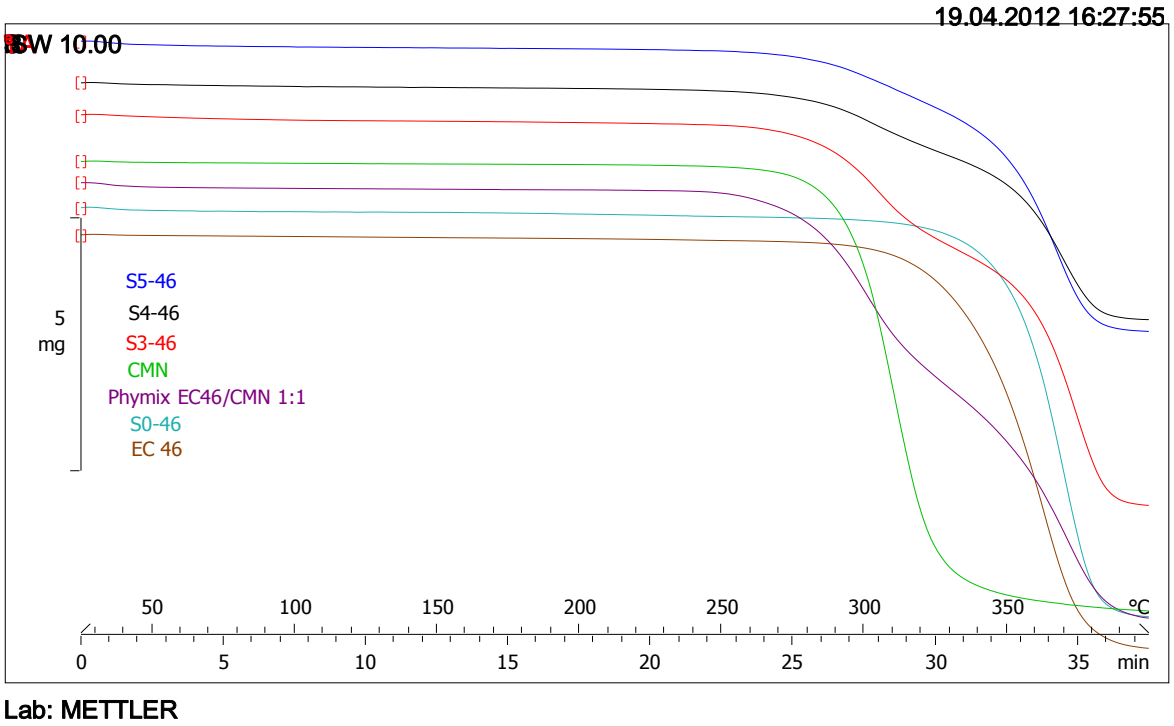

Figure 7-3: TGA curves of S-46 microspheres

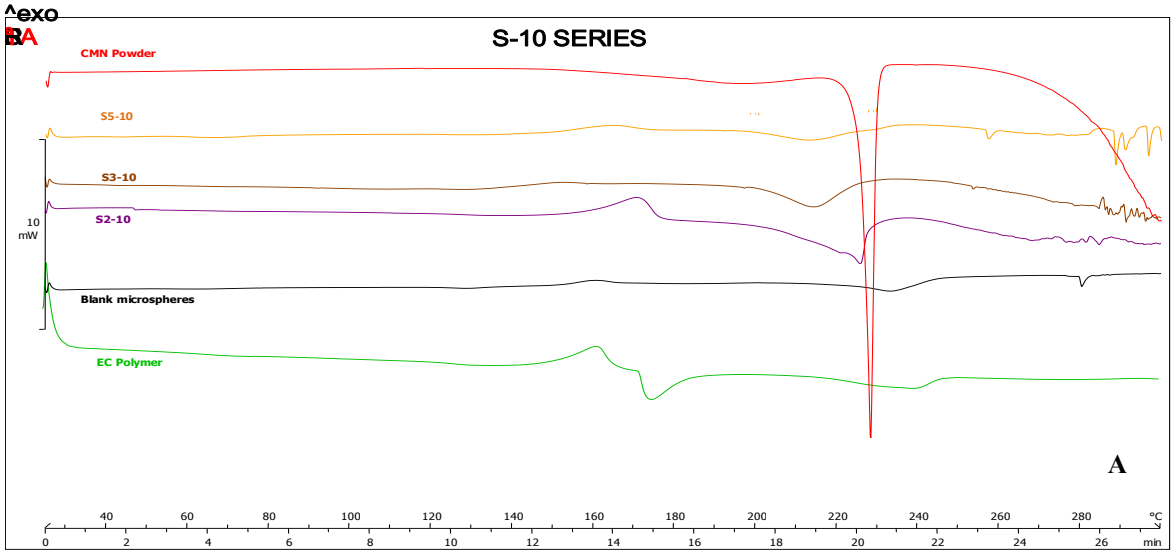

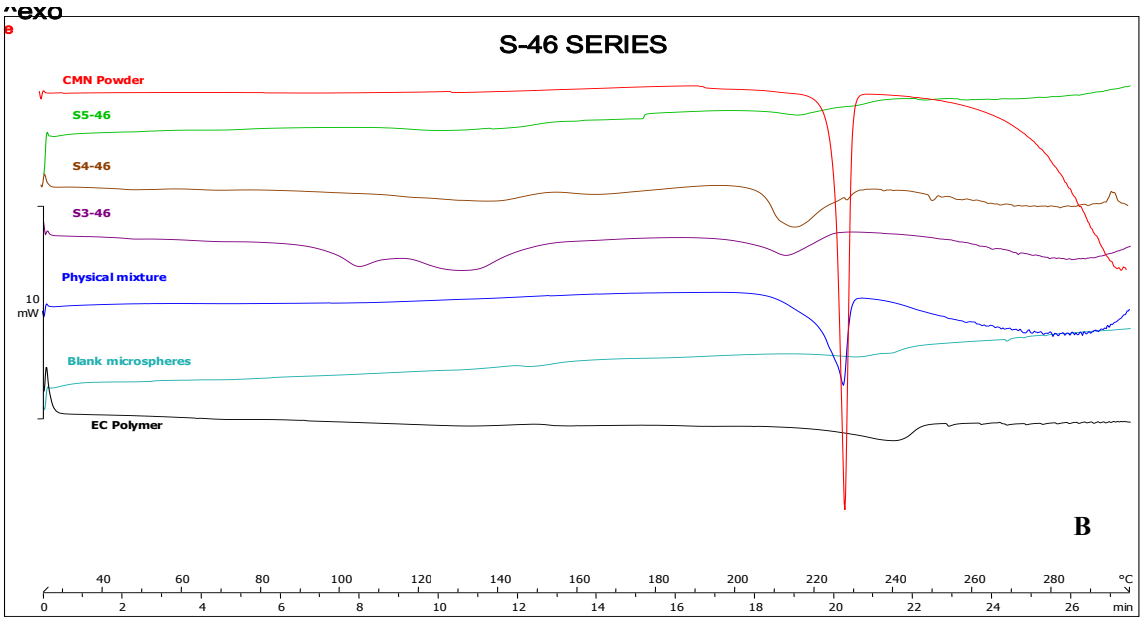

Figure 7-4: DSC scans of floating A) S-10 and B) S-46 EC microspheres

7.3.1.5 Fourier transform infra-red analysis of ethylcellulose microspheres

The IR spectra of CMN (Figure 7-5) showed the characteristic band of hydrogen bonds between –OH groups vibration at 3479.1 cm^{-1}. The characteristic C=O vibration of the lactone group was at 1732.6 cm^{-1} and a strong absorption band at 1692.8 cm^{-1} belonged to the carbonyl ketone peak and for N-CH_3 stretching of aromatic ring was evident at 1423.0 cm^{-1}. The IR spectra for EC shows a distinct peak at 3479.0 cm^{-1} which is due to the –OH groups present on the closed ring structure of the repeating units and the intra- and intermolecular hydrogen bonds (Ravindra *et al.*, 1999). The asymmetric peak observed between 2974.2-2870.6 cm^{-1} may be due to–CH stretching. The peak present at 1375.2 cm^{-1} is due to –CH_3 bending and the smaller peak at 1444 cm^{-1} is due to the –CH_2 bending. The broad peak at 1103.8 cm^{-1} may be due to the C-O-C stretch in the cyclic ether (Desai *et al.*, 2006). The formulations showed characteristic peaks, which were close to the principal IR peaks of the drug, confirming the presence of CMN in the microspheres indicating no strong interactions between the drug and the polymers used, and the stability of the drug during the microencapsulation process.

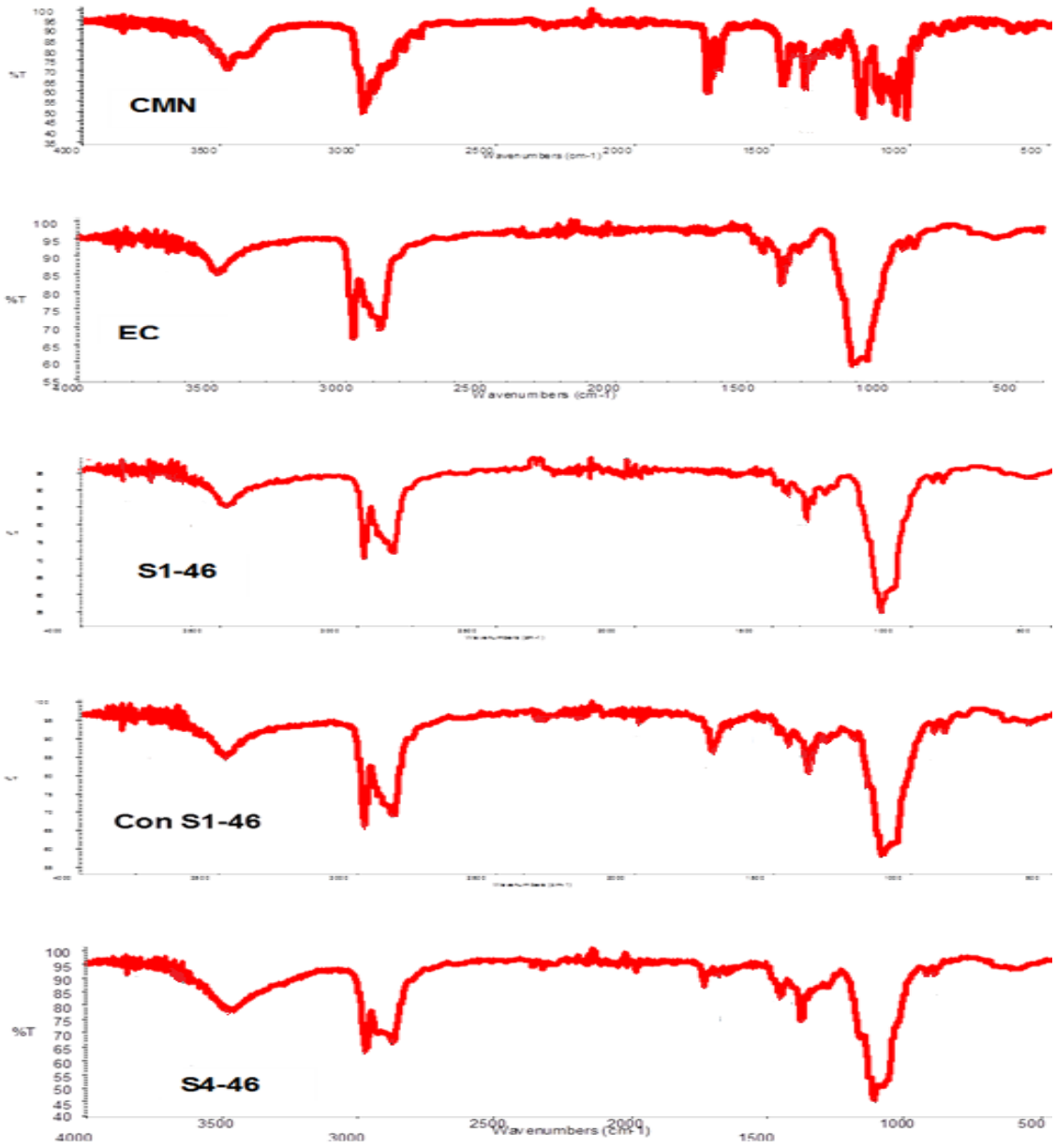

Figure 7-5: FTIR scans of CMN, EC polymer, unconjugated and conjugated microspheres

7.3.1.6 Powder X-ray diffraction analysis of ethylcellulose microspheres

EC and chitosan showed their amorphous nature while CMN was highly crystalline (Figure 7-6). CMN exhibited a pattern characteristic of a highly crystalline material with peaks appearing at 2θ values of 8.52 ° / 9.57 ° / 10.94 ° / 11.55 °/ 12.35 °/ 13.27 ° /13.81 °/ 15.27 °/ 16.70 °/ 17.39 °/ 18.33 ° / 19.12 °/ 20.58 °/ 21.54 °/ 22.31 °/ 24.84 °. The diffraction patterns of the physical mixture and the drug-loaded microspheres showed similar peaks of the CMN, however they were broader and had reduced intensities relative to that of the pure drug. This could be ascribed to the crystalline nature of the drug in the microspheres. These results further confirm the results obtained in DSC and FTIR analysis indicating the stability of CMN in the formulations.

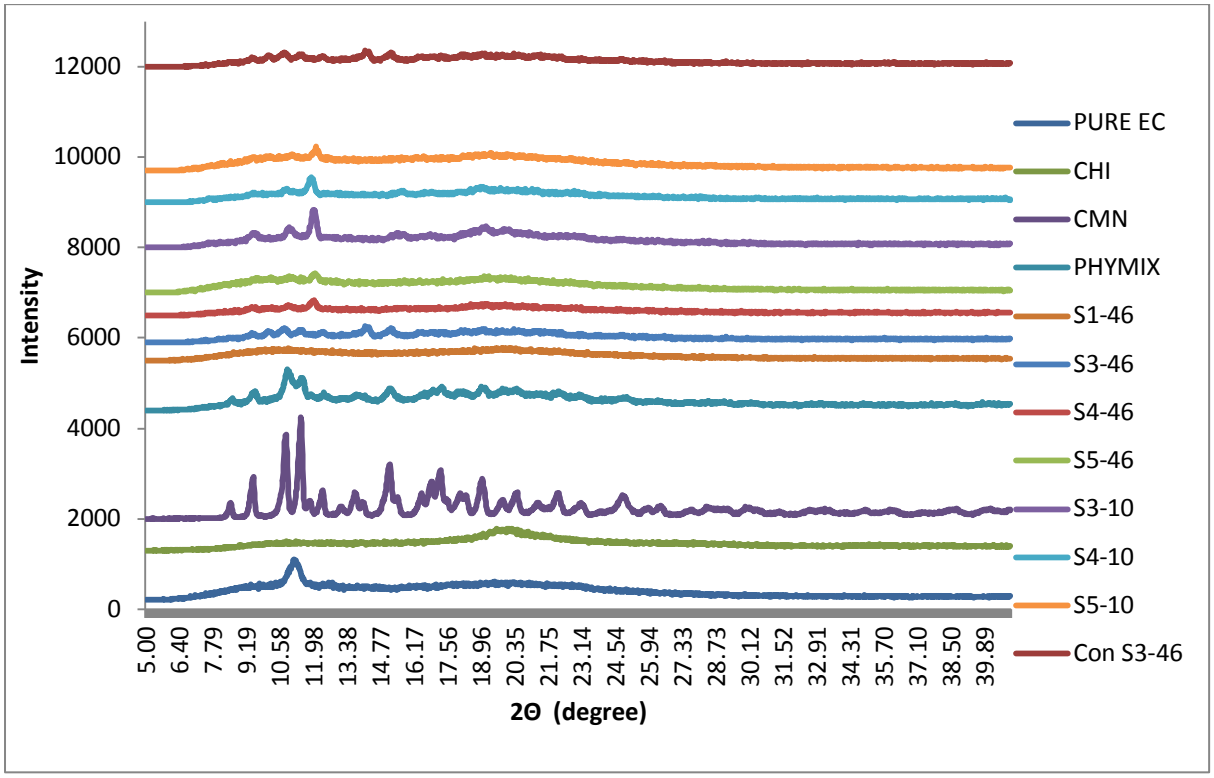

Figure 7-6: P-XRD of CMN, EC polymer, unconjugated and conjugated microspheres

7.3.1.7 *In vitro* buoyancy profile of ethylcellulose microspheres

Good *in vitro* percentage buoyancy was observed for all the microsphere formulations, between 75 to 96 % microspheres remained floating after 12 h, and increasing slightly with an increase in polymer concentration ($p > 0.05$). Floating occurred immediately on contact with the dispersion media with negligible lag time (Table 7-2). EC microspheres being insoluble and unswellable do not take up water significantly therefore, remained floating on the media. The absence of any lag time indicates the low density of the microspheres in

simulated media. The buoyancy of EC microspheres have been reported by other researchers (Mastiholimath *et al.*, 2008, Pande *et al.*, 2010, Vaghani *et al.*, 2010).

7.3.1.8 *In vitro* release studies of ethylcellulose microspheres

Drug release from microspheres was determined in SGF pH= 2.0 (Figure 7-7a) and acetate buffer at pH = 5.0 (Figure 7-7b) to cover the pH range for when CMN is used alone or in combination with omeprazole (Gustavson *et al.*, 1995). In addition, this covers potential variations in stomach pH in the absence and presence of food, respectively. Tween 80 was added to the dissolution medium to increase the wetting and hydration of the polymers (El-Kamel *et al.*, 2001). At pH 2.0, the dissolution of the unencapsulated drug was rapid and complete within 3 hours (Figure 7-7a). Drug release was biphasic with an initial burst release followed by a second moderate rate of release, a characteristic feature of matrix diffusion kinetics. The burst release and CMN release rates were reduced with increasing EC concentration and viscosity ($p < 0.05$), probably due to a change in distribution of drug in the particles, with less being located at the surface and better entrapment (Figure 7-7a and 7-7b). Also, an increase in polymer/drug ratio led to an increase in the particle size, decrease in surface/volume ratio, increase in polymer density and an increase in diffusional path length, all of which can contribute to prolonging drug release (Muramatsu and Kondo, 1995). The effect of polymer-drug ratio on drug release was observed on comparison of f_2 values of S3-10 *versus* S5-10 (41.5) and S3-46 *versus* S5-46 (42.3). EC has a low water permeability, while both chitosan and CMN are relatively soluble at low pH, therefore formulations containing more drug will most likely have a higher initial burst release (S2-10 / S2-46) than those with less drug (S5-10 / S5-46) as observed in these results. Also, dissolution of chitosan may lead to increased permeability of the microspheres, especially at later times. At pH 5.0,

solubility of CMN and chitosan was reduced and drug release was much slower from the microspheres with an average f_2 of 51. Drug release rate was also slower with an increase in polymer viscosity and polymer concentration (Figure 7-7b).

7.3.1.9 Drug release kinetics and mechanisms of floating microspheres

Drug release at pH 2.0 from all formulations fitted well to Higuchi kinetics (R^2= 0.97 to 0.99), indicating a diffusion controlled release dominated. The release mechanism denoted by the release exponent 'n' of all the formulations was between 0.23 – 0.44, indicating Fickian diffusion-controlled release (Table 7-4). This supports the formation of monolithic microspheres that release their drug content by Fickian diffusion. This release mechanism has been used to describe drug release from EC microspheres by other researchers (Maiti *et al.*, 2009, Nath *et al.*, 2010)

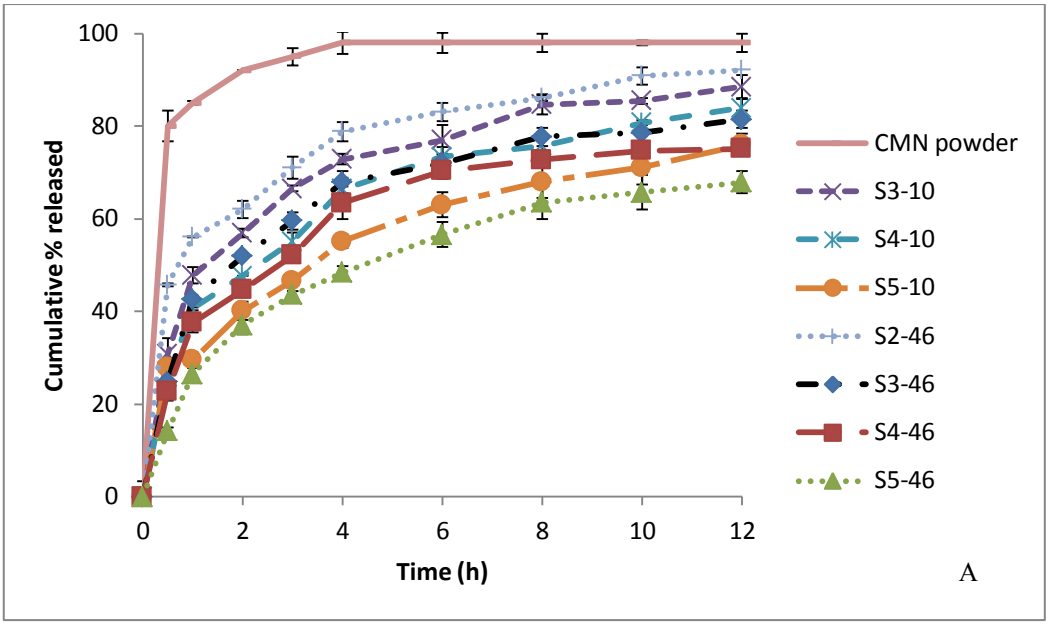

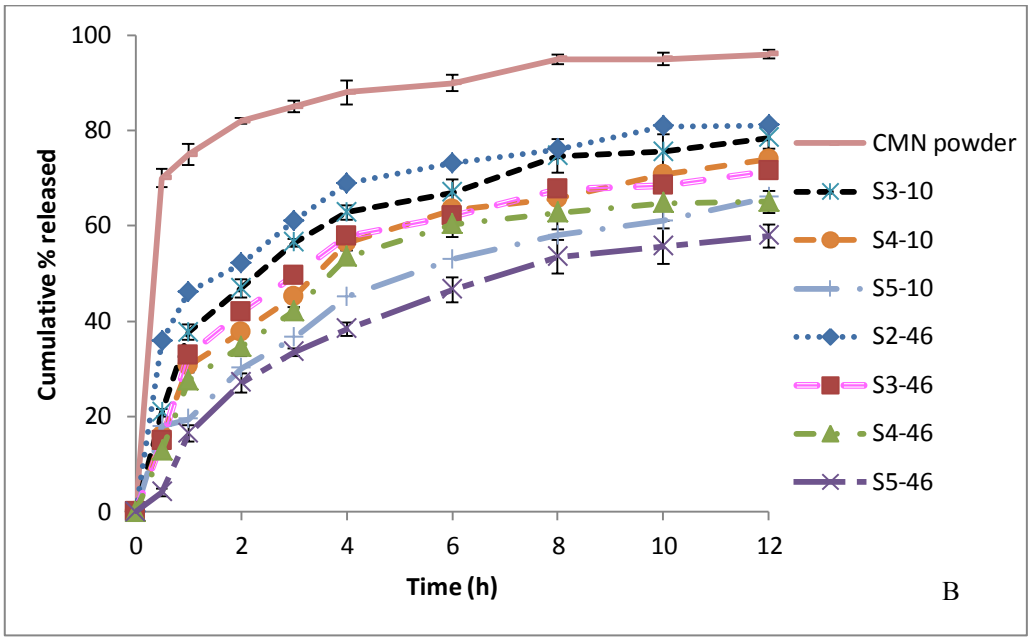

Figure 7-7: *In- vitro* release profiles of microspheres in SGF pH =2.0 (A) and pH 5.0 (B).

Table 7-4: Release kinetics of the microspheres (pH 2.0)

Release kinetics models								
Code	Zero order		First order		Higuchi model		Korsmeyer-Peppas	
	R^2	K_o (h^{-1})	R^2	K_1(h^{-1})	R^2	K_h ($h^{-1/2}$)	R^2	n
S2-10	0.9025	13.09	0.9082	0.112	0.9824	43.76	0.9132	0.24
S3-10	0.9204	11.06	0.9759	0.109	0.9787	38.66	0.9877	0.27
S4-10	0.9456	10.39	0.9672	0.089	0.9815	31.99	0.9764	0.31
S5-10	0.9683	7.05	0.9913	0.057	0.9903	22.67	0.9907	0.37
S2-46	0.9513	9.35	0.9849	0.110	0.9746	28.62	0.9848	0.23
S3-46	0.9987	8.30	0.9662	0.097	0.9942	24.85	0.9873	0.29
S4-46	0.9635	6.83	0.9715	0.074	0.968	23.25	0.9707	0.44
S5-46	0.9544	4.99	0.9883	0.042	0.9942	19.84	0.9921	0.39
Con S3-46c	0.9667	6.17	0.9873	0.069	0.9936	21.71	0.9844	0.56
Con S4-46	0.9611	6.04	0.9823	0.051	0.9913	20.56	0.9882	0.64

7.3.2 Characterisation of conjugated microspheres

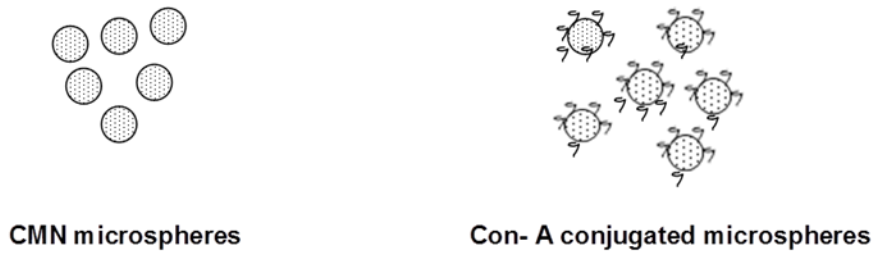

Figure 7-8: Schematic representation of the unconjugated and conjugated CMN microspheres

The conjugation (Figure 7-8) reaction involves the use of water-soluble carbodiimide, which reacts with the carboxyl group on EC, leading to the formation of an amine reactive O-acylisourea intermediate. The intermediate may react with an amine on the lectin forming a stable amide bond. This intermediate is susceptible to some side reactions such as hydrolysis or can form a stable compound through re-arrangement; therefore, the solutions are stabilized with the addition of NHS by converting it to an amine reactive NHS ester, thus increasing the efficiency of the coupling reaction. The optimum pH for this EDAC and NHS reaction is between pH 4 - 6. The use of the carbodiimide method is preferable to cross-linking agents such as glutaraldehyde because it minimises the risk of structural modification of the conjugated ligands at locations, which may be critical to their binding activity.

7.3.2.1 Morphology and micromeritics of conjugated microspheres

The conjugation process did not affect the microsphere morphology or the structural integrity with the surface appearing similar to that of the unconjugated microspheres (Figure 7-1g and h). The particle size of the microspheres increased on conjugation with S1-10 and S1-46 increasing from about 50µm and 65 µm to about 83 µm and 108 µm, respectively (Table 7-2). This was similarly observed with drug-loaded microspheres ($p < 0.05$). This may be due to the presence of a layer of Con A on the surface of the microspheres and also probably due to swelling of the microspheres on exposure to fluids during the conjugation process. All results presented are of microspheres conjugated with 0.1 %w/v Con A unless otherwise stated.

7.3.2.2 Conjugation efficiency and amount of bound lectin

The initial method used to determine the CE of blank microspheres was not feasible with drug loaded microspheres because CMN reacts with Folin-Ciocalteu reagent in an alkaline medium and has been used as a reagent in the determination of its concentration in various formulations (Nama *et al.*, 2008). Folin Ciocalteu reagent measures the total reducing capacity of a sample as well as the concentration of the phenolic content of a sample not just the level of phenolic compounds. Therefore, the use of this method for quantifying CE could overestimate conjugation of Con A to the microspheres as it would detect any surface bound or released CMN during the test. This justified the need of another method to estimate CE of drug loaded microspheres. It has been reported that the CE of Con A binding can be determined using UV analysis at 280 nm (Chern *et al.*, 2001) but due to interference from the various reagents and drug this was also not an ideal analytical method to use for this analysis. Therefore, FITC conjugated lectin was used and the binding analysed by fluorescence spectroscopy (see section 2.3.26.2).

The amount of Con–A bound onto the surface of the microspheres was between 1.8 ± 0.2 and 15.3 ± 1.4 µg Con A / mg microspheres with a CE of 36 - 77 % of the initial amount of lectin added. Residual PVA present on the microsphere surface (and associated –OH groups) can act as a steric barrier to a higher conjugation (Scholes *et al.*, 1999). There was a reduction in CE following incorporation of drug and this may be due to the presence of drug on the surface of microspheres rendering some of the –COOH unavailable for conjugation. The CE of Con A to the microsphere increased significantly ($p < 0.05$) with increasing lectin added (Figure 7-9). This contrasts with WGA conjugation efficiency to PLGA nanospheres (Weissenbock *et al.*, 2004) which was found to be independent of lectin concentration.

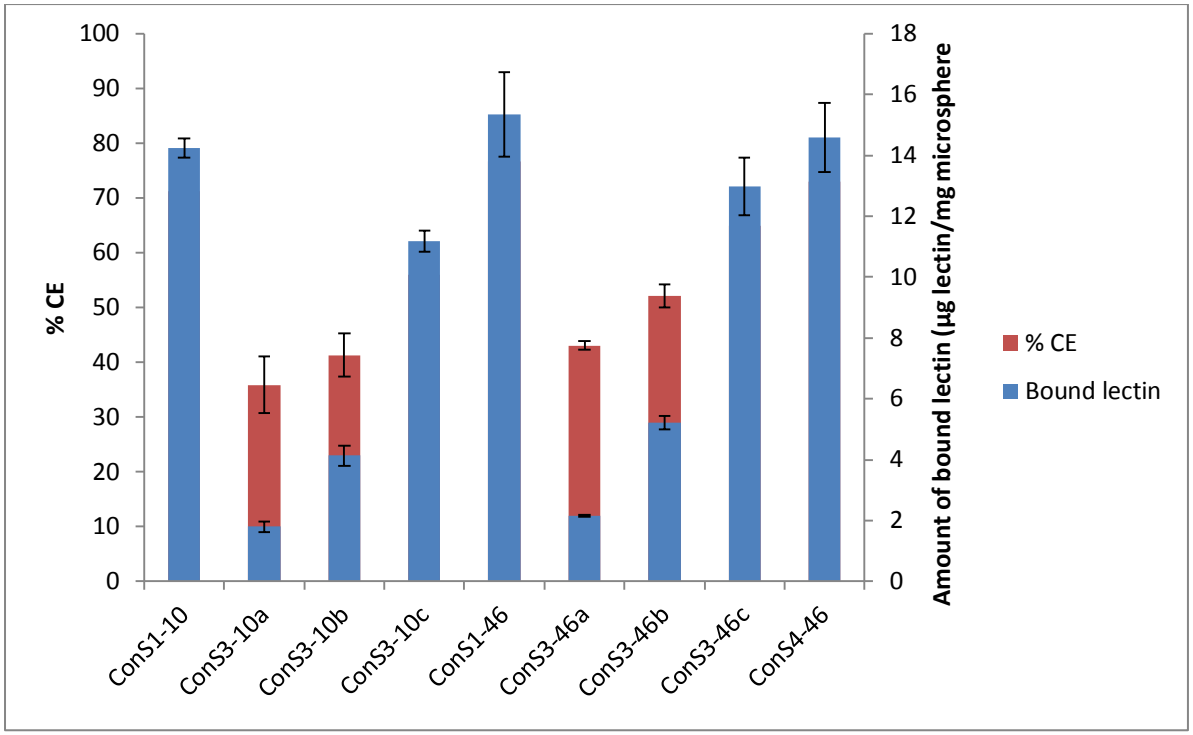

Figure 7-9: Effect of Con A loading on CE and amount of bound Con A

7.3.2.3 Effect of EC molecular weight on CE of lectin

Using different grades of EC did not have a significant effect on the CE of blank microspheres, as the CE of both Con S1-46 and Con S1-10 were similar, however for drug-loaded microspheres there was an average increase of 20.7 ± 5.1 % in CE with Con S3-46c than observed with Con S3-10c (Figure 7-9). This might be because the presence of drug reduced the available sites for conjugation and this effect was more obvious in EC of lower viscosity grade than at relatively high viscosity grade probably with more available conjugation sites.

7.3.2.4 DEE of conjugated microspheres

The coupling process and washing led to the loss of loosely encapsulated surface-associated drug with a reduction in drug content of Con S3-46 by about 14 % compared to S3-46 and a loss of about 7 % in Con S4-46 relative to S4-46 (Table 7-2). There was more drug loss observed with S3-10 with a loss of about 30 % in Con S3-10, which was more than double the loss observed in Con S3-46 and quadruple that observed in ConS4-46. The DEE of these conjugated microspheres was above 45 % in all cases. This shows that high viscosity EC microspheres were able to retain more drug within the microsphere matrix than the corresponding lower viscosity EC microspheres.

7.3.2.5 DSC of conjugated microspheres

The absence of any extra peaks on the thermograms (such as peaks of EDAC or NHS) and no major differences between the scans of the conjugated and the unconjugated microspheres confirms that there were no excess conjugation chemicals left in the microspheres and that conjugation did not cause any significant changes in the microspheres (Figure 7-10).

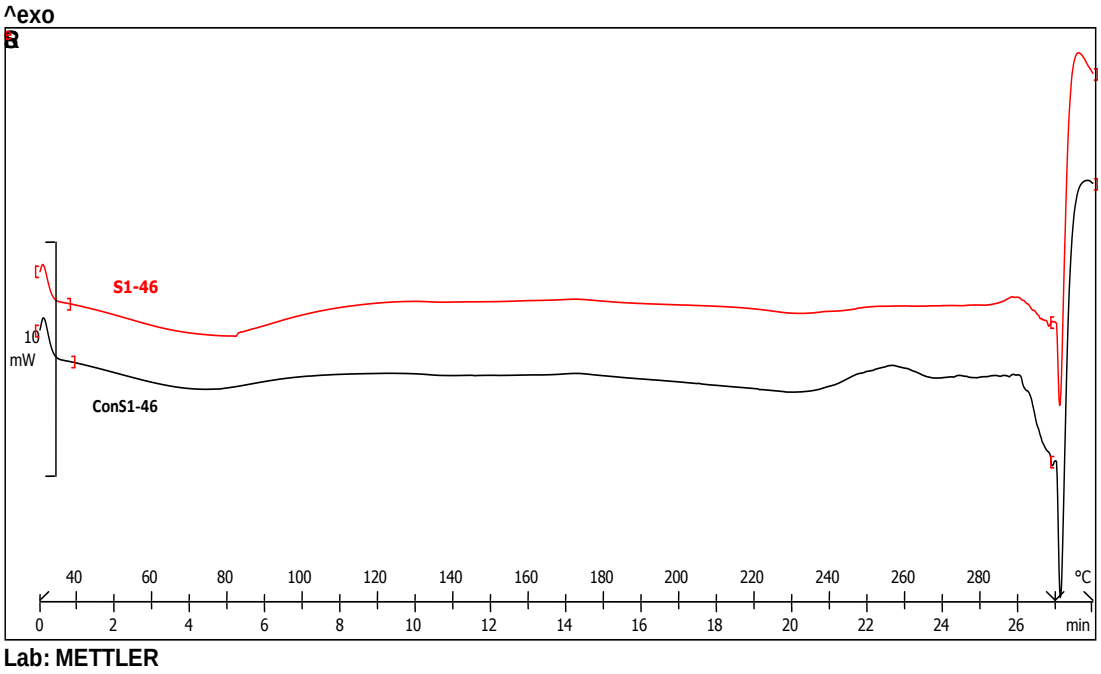

Figure 7-10: DSC scans of the unconjugated and conjugated blank microspheres

7.3.2.6 FTIR of conjugated microspheres

Conjugation of Con-A was through the formation of amide bonds between the -NH_2 groups of Con A and –COOH on EC. This was confirmed with the presence of two amide bonds (I and II) with peaks at 1716.1, 1651.1 and 1538.6 cm^{-1} which are characteristics of amides mainly in proteins (Anande *et al.*, 2008, Jain and Jangdey, 2009). These peaks were noticeably absent in the unconjugated microspheres (Figure 7-5).

7.3.2.7 *In vitro* buoyancy of conjugated microspheres

Conjugation and pH of dispersion media had no significant effect on the buoyancy of the microspheres ($p > 0.05$). The conjugated microspheres all exhibited good buoyancy with the buoyancy of conjugated microspheres being > 70 % after 12 h (Table 7-2).

7.3.2.8 Zeta potential of conjugated microspheres

Zp for S0-46, S1-46 and Con S1-46 were -14.6 ± 2.4 mV, -10.8 ± 0.6 mV and +29.4 ± 1.07 mV respectively, while S3-46 had values of -13.4 ± 1.5 mV and Con S3-46 was +18.3 ± 1.5 mV. The negative *Zp* of the unconjugated microspheres was due to the presence of uncapped end carboxyl groups present at the surface of EC due to EC deprotonation at pH 7.0. The presence of chitosan in the formulation reduced the negative *Zp* of the microspheres. The conjugation of Con A on the microsphere surface normally causes a positive increase in the *Zp* of microspheres (Anande *et al.*, 2008). The presence of drug had a negative effect on the *Zp* of the microspheres and the negative influence of drug on *Zp* of microspheres has been reported (Huang *et al*., 2003, Martinac *et al.*, 2005). Lectin coating on gliadin microparticles positively increased the *Zp* of the microparticles (Umamaheshwari and Jain, 2003). The positive *Zp* is crucial for effective electrostatic interaction of the microspheres with the negatively charged sialic acid of the gastric mucosa leading to prolonged gastro-retention.

7.3.2.9 *In vitro* drug release of conjugated microspheres

Drug release from Con S3-46 and Con S4-46 microspheres was slower than the corresponding unconjugated S3-46 and S4-46 microspheres at pH 2.0, with no associated burst release as seen with S3-46 (f_2 = 47.4) and S4-46 (f_2 = 41.0) (Figure 7-11). This may be due to the loss of the surface associated drug and the reaction at the surface of the microspheres, rendering it slightly less permeable than unconjugated microspheres. Drug

release kinetics followed Higuchi kinetics similar to the unconjugated microspheres. The ‘n’ values for the conjugated drug loaded microspheres were 0.43 > n < 0.85 which indicate anomalous non-Fickian transport kinetics. This change in drug release kinetics may be due to the conjugation effects on the microsphere surface.

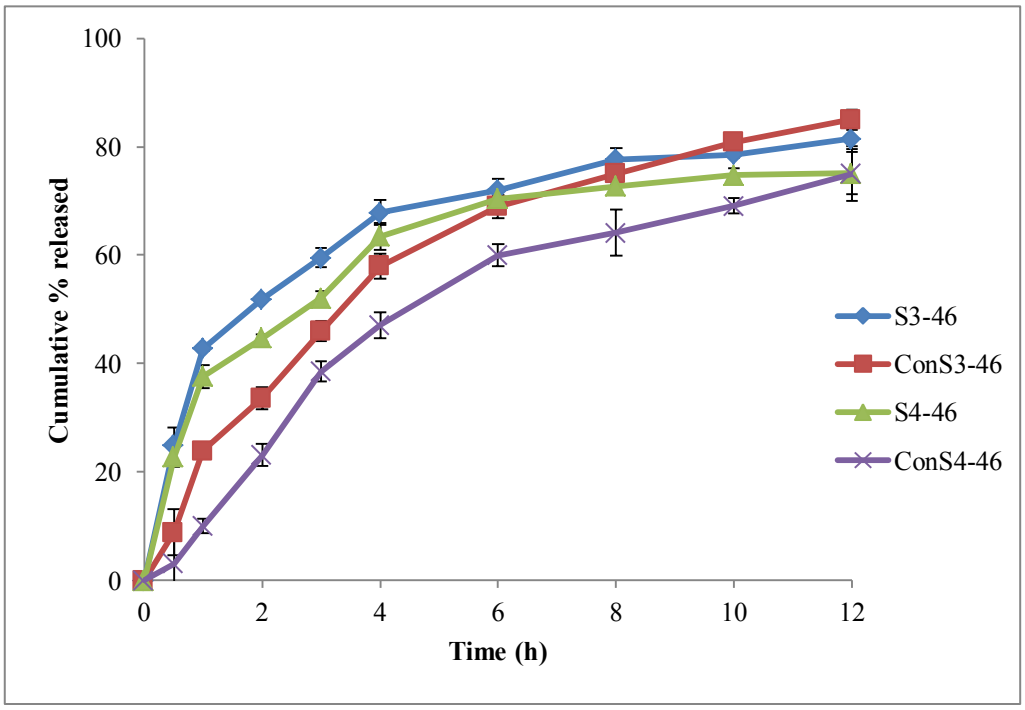

Figure 7-11: *In vitro* release profiles of conjugated microspheres in SGF (pH 2.0)

7.3.2.10 *In vitro* interactions of conjugated microspheres with PGM

The Con A conjugated microspheres have a higher affinity for pig gastric mucin than unconjugated EC microspheres (Figure 7- 12a). Mucin binding to S1-10 / S1-46 *versus* Con S1-10/Con S1-46 as a function of time is shown in Figure 7-12b. The amount of mucin bound to the ConS1-46 was about 81 % more than that bound to S1-46. An increase in bound mucin of about 79 % was observed with Con S1-10 (Figure 7-12a). The equilibrium for the interaction was reached after incubation between 60 to 120 minutes (Figure 7-12b) and the adsorption process was not affected by the different temperatures used ($p > 0.05$). The amount of bound mucin depended on the amount of lectin on the surface of the microspheres with approximately 10 - 22 % mucin binding on doubling Con A concentration..

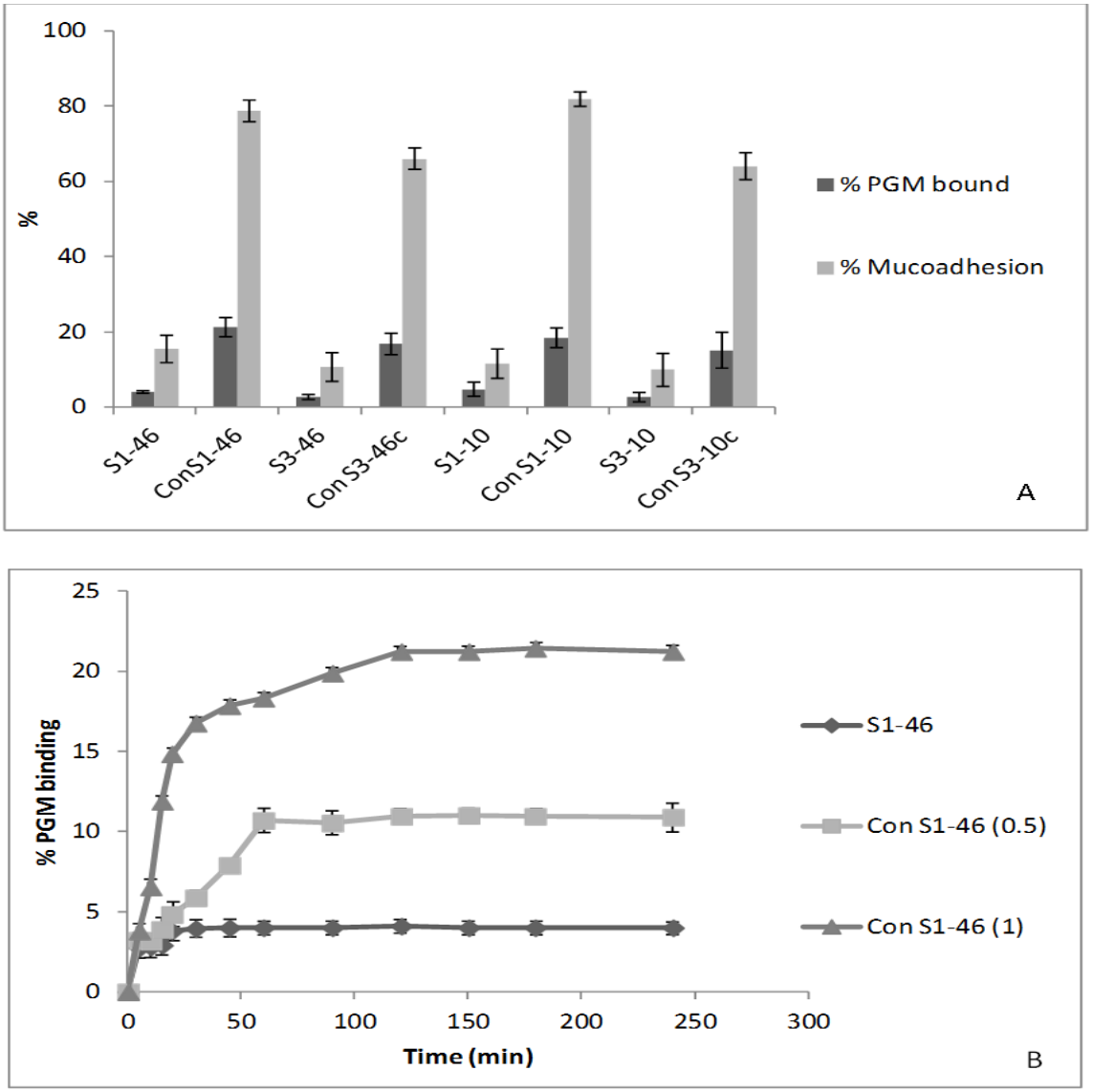

Figure 7-12: A) PGM binding of conjugated and non-conjugated microspheres; B) Lectin-mucin interaction kinetics. Results presented as mean ± SD (*n=3*), with Con S1-46 (0.5) and Con S1-46 (1) represemting microspheres conjugated with 0.05 and 0.1 %w/v Con A

7.3.2.11 *Ex vivo* wash off test

Mucoadhesion of the Con A conjugated microspheres to porcine gastric mucosa at pH 2.0 was 64.0 ± 3.58 % to 78.7 ± 2.87 % compared with 9.9 ± 4.37 to 15.5 ± 3.64 % of the unconjugated microspheres, which corresponds to an average enhancement in mucoadhesion of 85 % (Figure 7-12a). On increasing the pH to pH 5.0, there was a similar increase in mucoadhesion of the conjugated microspheres with ~ 90 % increase in mucoadhesion. This increase in mucoadhesion was due to the Con A coating on the microsphere surface ($p < 0.05$) due to the affinity of Con A to the mucin glycoproteins of the stomach mucus and mucosa. Increasing amount of surface lectin also increased the mucoadhesion with ~ 32 % increase in mucoadhesion in Con S3-46c compared with the mucoadhesion of Con S3-46b (Figure 7-12a).

7.3.2.12 *In vitro* drug diffusion of clarithromycin through PGM

The release of drug from the microspheres and its diffusion through a 3 % mucin suspension was sustained over a period of 12 h at pH 2 and 5. There was no obvious burst release and there was an initial lag time of approximately 110 minutes observed with Con S3-46, while there was no lag time observed for the saturated solution and the S3-46 (Figure 7-13). The absence of a burst release and the sustained release of CMN from the microspheres may be due to the loss of the surface-associated drug. The sustained release may also be due to binding of the mucin to the surface of the microspheres, thus presenting a further barrier to CMN diffusion from the microsphere surface. S3-46 did not also show an obvious burst release, however, the release rate was significantly higher than that of the equivalent conjugated formulation. The flux of the drug through the mucin dispersion and membrane was 145.8 ± 5.73 $\mu gcm^{-2}h^{-1}$ (ConS3-46) and 243.9± 8.85 $\mu gcm^{-2}h^{-1}$ (S3-46) compared with 1020.1 ± 30.11 $\mu gcm^{-2}h^{-1}$ from a saturated solution at pH 2.0. Encapsulation reduced flux of CMN by over 300 % (Saturated solution *versus* S3-46). There was also a reduction of about

40 % in drug flux for the conjugated formulation due to reduced drug availability at the particle surface, increased diffusional path-length and changes to the microsphere surface. At pH 5.0, the fluxes were significantly lower than those at pH 2.0 ($p < 0.05$) as expected with the decrease in CMN solubility at this pH. In the presence of mucin, there was still a sustained and adequate release of drug from the conjugated microspheres and the presence of lectin on the surface of the microsphere did not hinder the release of drug from the microspheres in the presence of mucin.

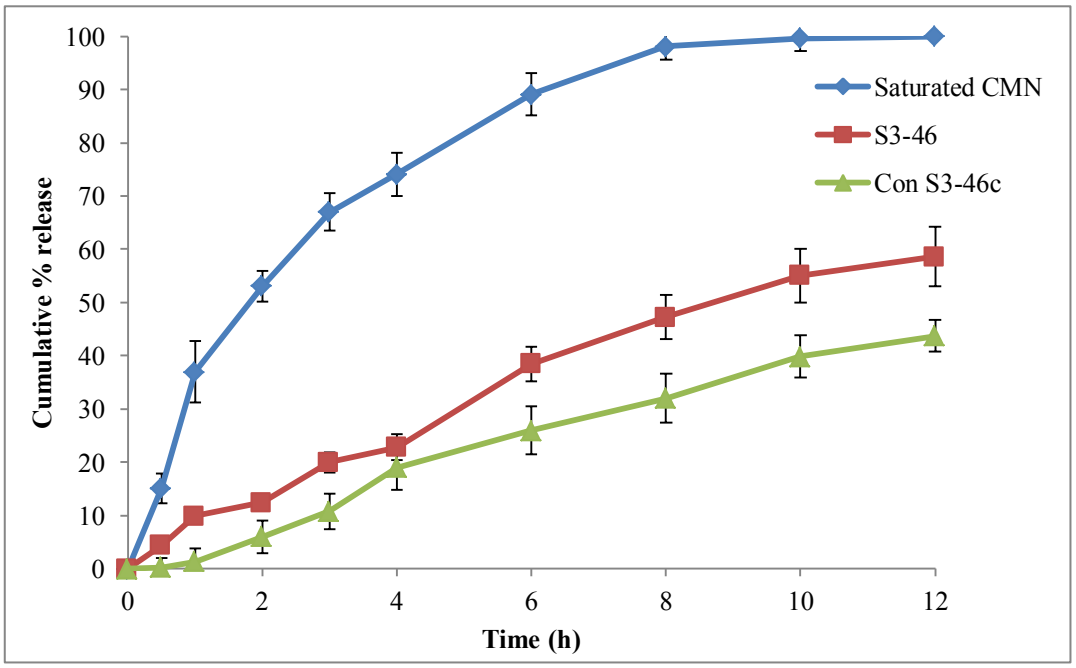

Figure 7-13: Franz cell diffusion profiles of microspheres in mucin suspension (pH 2). Results presented as mean ± SD (*n=3*).

7.3.2.13 Storage stability of microspheres

After 3 months of storage at 4 ℃, there was no significant difference in the particle size, zeta potential, DEE, drug release ($70 < f2 < 80$) and the mucoadhesion of the formulations as shown in Figure 7-14 to Figure 7-16. The activity of the lectin was still maintained whilst stored at this temperature since there was no significant change in the proportion of microparticles adhered to the porcine gastric mucosa. However, storage at room temperature led to a slight change only in the mucoadhesion with all the other parameters remaining consistent. Drug release from these microspheres was unaffected by storage but to preserve lectin binding efficiency, lower storage temperatures may need to be used.

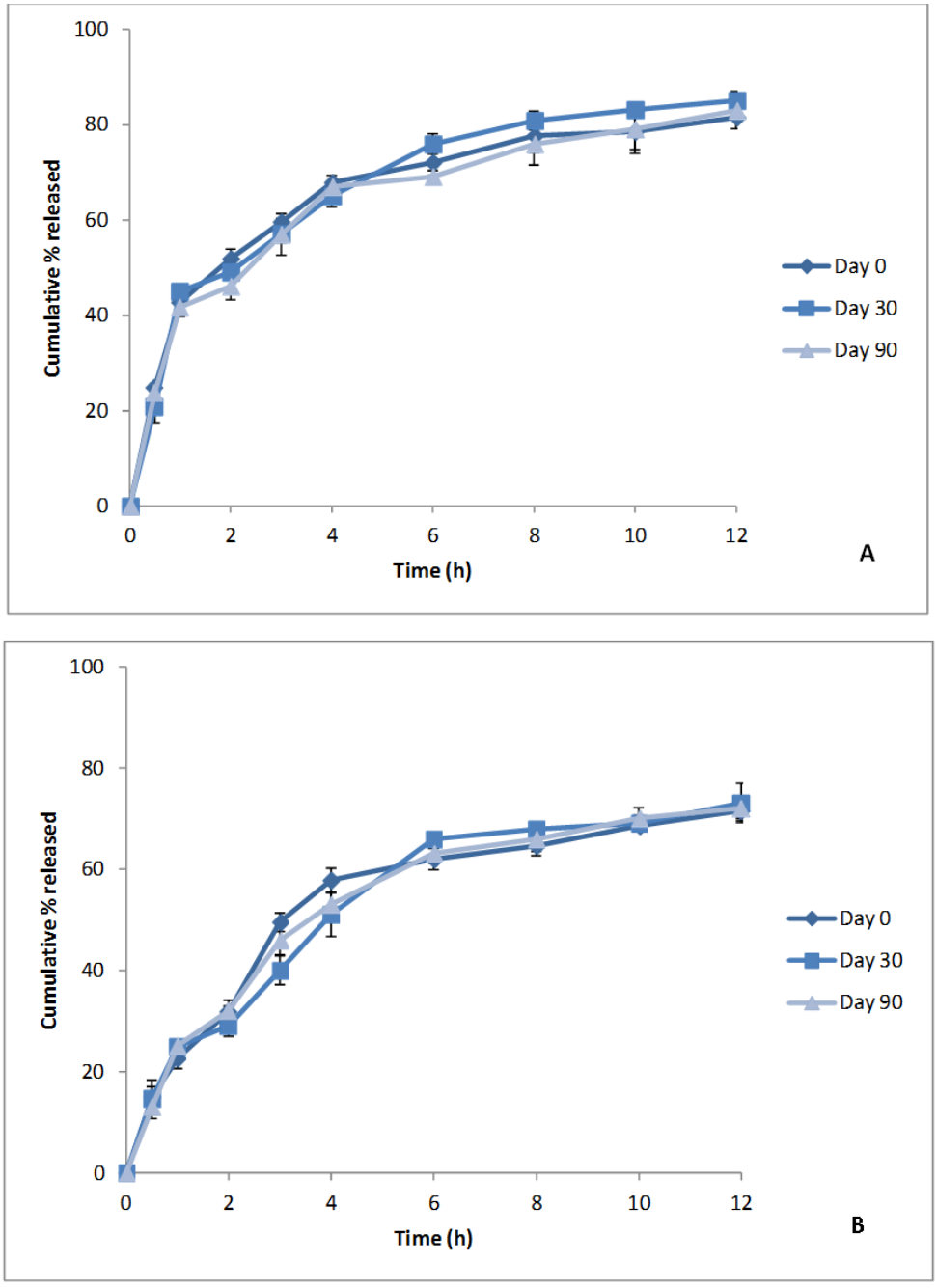

Figure 7-14: *In vitro* release profiles of microspheres stored at 4 °C: A) S3-46; B) Con S3-46

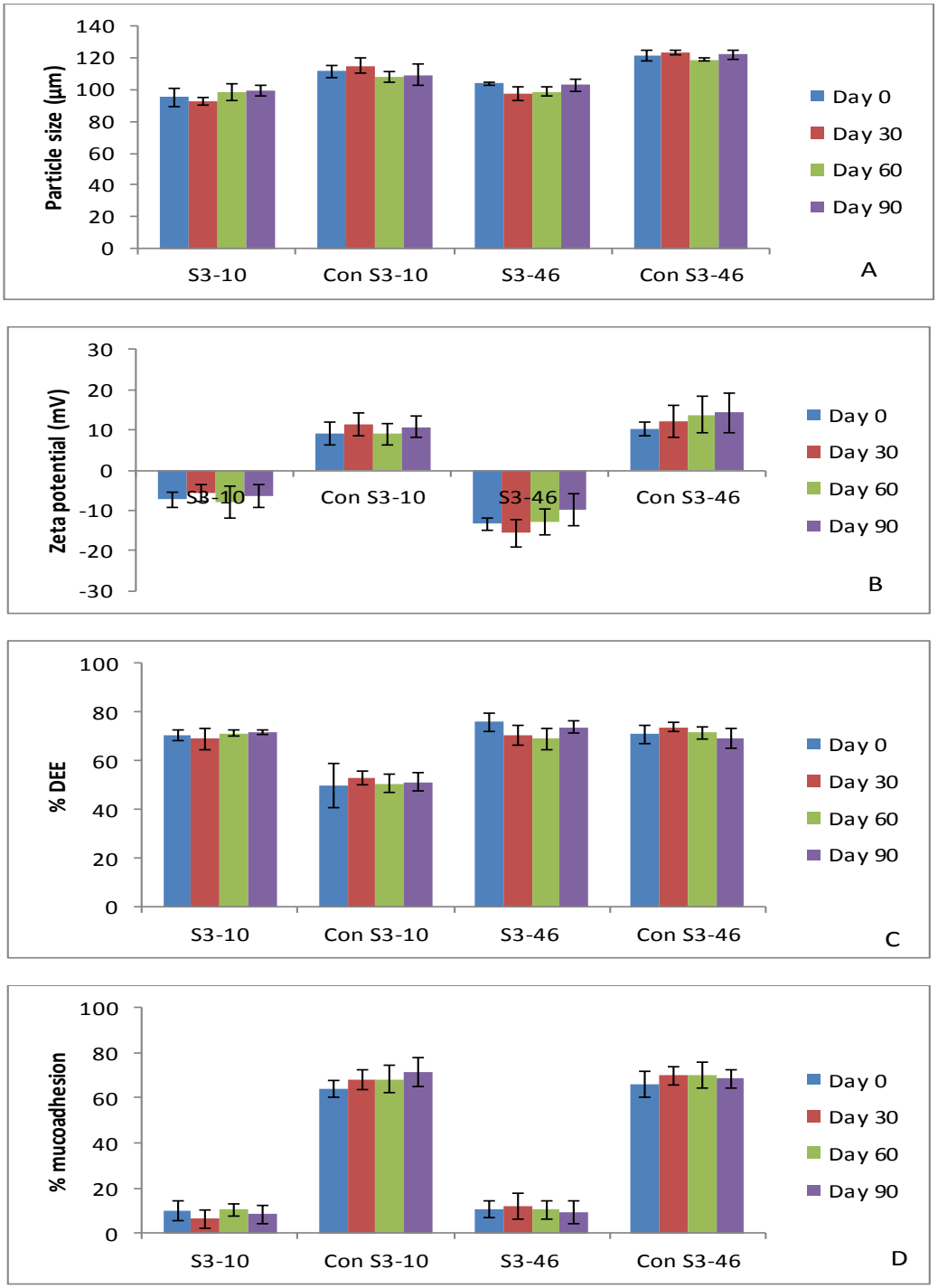

Figure 7-15: Stability of microspheres stored at 4 °C over 3 months

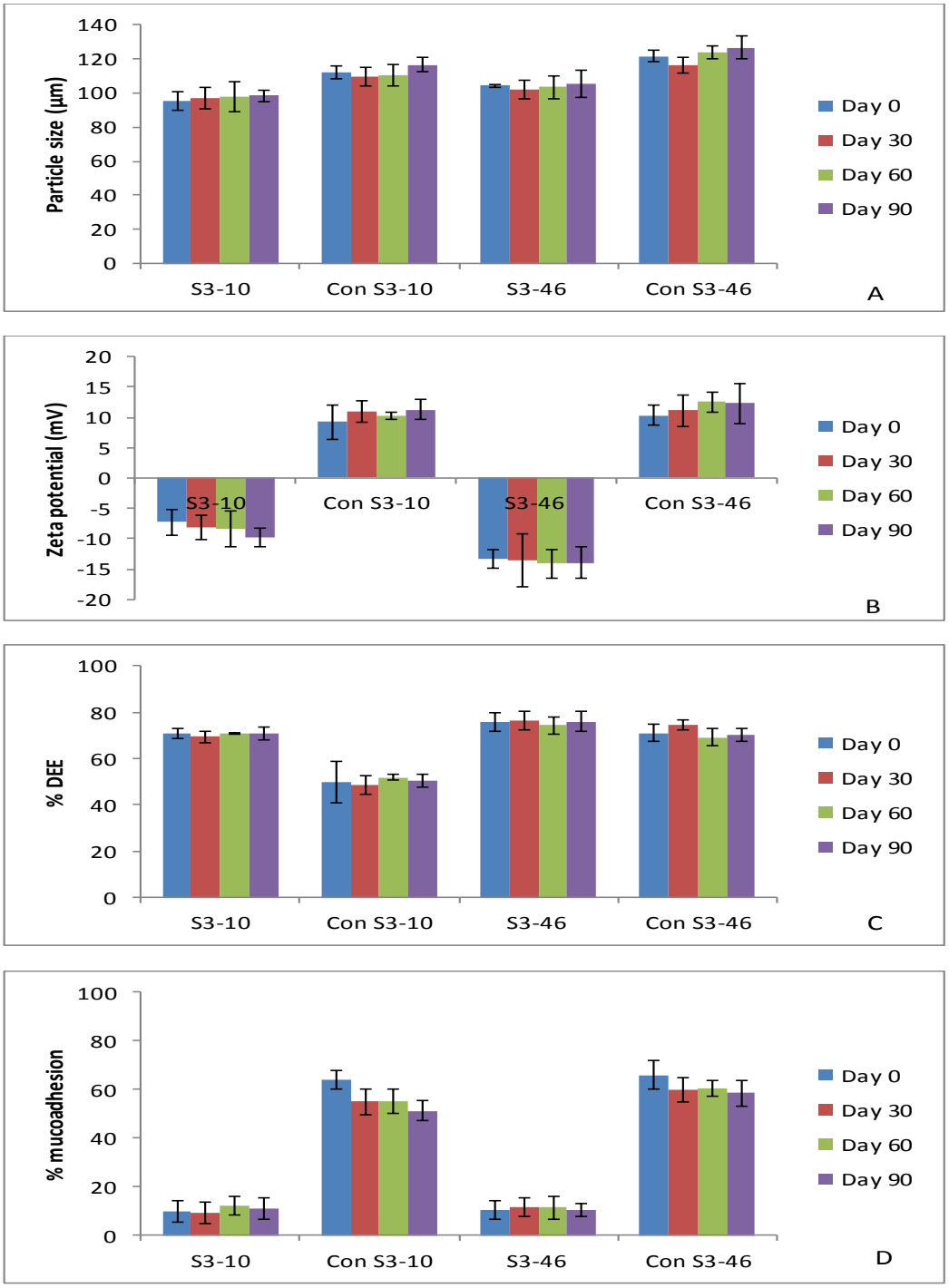

Figure 7-16: Stability of microspheres stored at room temperature (20 °C) over 3 months

7.4 Conclusion

CMN-loaded ethylcellulose microspheres were prepared using the solvent evaporation method and the mucin binding lectin, Concanavalin A, was successfully attached to the microspheres up to a maximum of 15.3 µg Con A per mg microsphere. The inclusion of CMN did not significantly reduce the amount of Con A bound to the surface of the microspheres, however, conjugation led to a reduction in the DEE of the microspheres with more drug loss being observed with the S-10 series than the S-46 series. *In vitro* mucodhesion studies confirmed the enhancement of mucoahesion due to the presence of lectin. The drug loading, DEE, buoyancy and *in vitro* drug release in both the dissolution media and mucin dispersion were not compromised by the conjugation process. A combined approach of a floating – mucoadhesive formulation with a high buoyancy and high mucoadhesion may enhance the delivery of antibiotics to the target site in the stomach.

Chapter 8 FINAL CONCLUSIONS

The aim of this research was to develop gastro-retentive drug delivery devices that can potentially be retained in the stomach for a prolonged period compared to conventional drug delivery systems. In this thesis, two different multi-unit formulations were prepared – calcium alginate beads and ethylcellulose microspheres. Both formulations combine two gastroretentive techniques, which include floating and mucoadhesive techniques in order to explore the synergistic effect of both techniques and improve the chances of the formulation to be retained in the stomach. In addition to these gastroretentive properties, drug release from these formulations was sustained over a period of at least 12 h.

The calcium alginate beads were produced through the ionotropic-gelation method and encapsulation of drugs (MET and CMN) into the beads was simple and straightforward, producing spherical beads with an average size of 2 -3 mm. The limitations of these beads are the fact that they release their drug contents quickly – MET within 3 h and CMN within 8h (the difference in release profile being dependent on the aqueous solubilities of the drugs) and the limited buoyancy of the beads when in contact with simulated gastric fluids. These beads were modified by addition of olive oil (an oil demonstrated to have anti-*H. pylori* activities) to primarily improve the buoyancy of the beads and secondarily sustain drug release due to the increase in hydrophobicity of the bead matrix due to the presence of oil in the formulation. It was observed that beads modified with ≥ 10 % olive oil exhibited 100 % buoyancy with lag times < 1 minute, thereby improving the gastro-retentive potential of the

beads. Drug release of MET from the beads was not sustained until > 10 %w/w oil was included in the formulation, while for CMN beads, drug release was sustained on inclusion of ≥ 10 %w/w olive oil. The addition of oil at high concentrations (> 15 %w/w) had a detrimental effect on the mechanical strength and structure of the beads, therefore, the use of high concentrations of oil as a means of further sustaining MET release from the beads were discarded. Chitosan, a mucoadhesive polymer, was used to coat oil-modified beads to convert the beads from a floating formulation to a floating-mucoadhesive formulation. Chitosan also provides an additional barrier, which reduces the rate of drug diffusion from the bead surface, thereby sustaining drug release from the beads. Solid-state characterisation indicated the stability of both drugs in the beads. Coating of these oil-modified beads led to the production of beads with high DEE, 100 % buoyancy over a 24 h period and drug release from beads loaded with either MET and CMN over a 12 h period, thereby fulfilling all the characteristics desired in a gastro-retentive formulation.

There is further work that can be done to improve this formulation and this includes a means of reducing the sizes of the beads, ideally to within the nano/micron size range; this will help with the packing and formulation administration issues. This can be achieved with electro-spray techniques where small droplets are generated through the use of electric field between a nozzle and a eletroconductive solution underneath. The droplet size will depend on factors such as the electric field strength, the nozzle diameter and the flow rate of liquid, as well as liquid properties such as viscosity, electrical conductivity and surface tension (Ku and Kim, 2002). Performance of the developed formulation in GI tract can be also visualized by gamma scintigraphy in animal models to further determine the effectiveness of the formulation. In addition, the bead formulation can also be further evaluated for their effectiveness in eradicating *H. pylori*, by exposing strains of *H. pylori* to these formulations and comparing its effectiveness with that of plain drug through assessment of *H. pylori* growth inhibition. Also, another area of research is to try to incorporate two antibiotic drugs into alginate beads to be able to determine if both drugs will be sufficiently loaded into the beads and the effect of the physicochemical properties of the drugs on the entrapment efficiencies of the drug in the beads. This approach is due to the multiple drug therapy

required in the eradication of the bacteria; the combination of 2 antibiotics in the same formulation will help reduce the total number of drugs to be used thereby improving patient compliance.

Ethylcellulose microspheres were prepared using an emulsification/solvent evaporation method with two grades of ethylcellulose (10 cps and 46 cps). The particles sizes were within the range of 50 – 211 µm with the DEE increasing with increasing polymer-drug ratio. Buoyancy of these microspheres was high due to the hydrophobic nature of ethylcellulose demonstrating good gastro-retentive potential. Conjugation efficiency of lectin to the microspheres was high with a maximum of ~ 77 % and it increased with increasing lectin added. DEE of S-46 series were higher than that of S-10 series and conjugation of the microspheres did not affect the buoyancy of the microspheres. Conjugation with lectin improved the mucoadhesion of the microspheres (with > 60 % mucoadhesion in conjugated microspheres *versus* < 15 % mucoadhesion observed in unconjugated microspheres) and this combined with the high buoyancy of the microspheres produced a formulation with a high gastro-retentive potential. Clarithromycin release was sustained beyond 12 h and conjugation with lectin reduced release rate, which may be due to the conjugation effects on the surface on the microspheres. Solid-state characterisation indicated the stability of clarithromycin in the unconjugated and conjugated microspheres.

Further work can be done by direct compression and formulating the microspheres into fast disintegrating tablets, which can be subjected to *in vivo* studies in animal models for assessment of the effectiveness of the formulation. Also, the microspheres can be further evaluated for their effectiveness in eradicating *H. pylori*, by exposing strains of *H. pylori* to these formulations and comparing its effectiveness with that of plain drug through assessment of *H. pylori* growth inhibition.

APPENDIX

PUBLICATIONS FROM THIS THESIS

ADEBISI, A. O. & CONWAY, B. R. 2010. Development of gastro-retentive systems for the eradication of *H. pylori* infections in the treatment of peptic ulcer. *Journal of Pharmacy and Pharmacology,* 62**,** 1201-1516.

ADEBISI, A. & CONWAY, B. R. 2011. Gastroretentive microparticles for drug delivery applications. *Journal of Microencapsulation,* 28**,** 689-708.

ADEBISI, A. O. & CONWAY, B. R. 2014. Lectin-conjugated microspheres for eradication of *Helicobacter-pylori* infection and interaction with mucus. *International Journal of Pharmaceutics,* 470**,** 28-40.

ADEBISI, A. O. & CONWAY, B. R. 2014. Preparation and characterisation of gastroretentive alginate beads for targeting *H. pylori*. *Journal of Microencapsul,* 31**,** 58-67.

ADEBISI, A. O. & CONWAY, B. R.. Formulation and evaluation of floating-mucoadhesive alginate beads for targeting *H. pylori, Journal of Pharmacy and Pharmacology* (Accepted)

REFERENCES

ABDALLAH, M. H., SAMMOUR, O. A., EL-GHAMRY, H. A., EL-NAHAS, H. M. & BARAKAT, W. 2012. Development and Characterization of Controlled Release Ketoprofen Microspheres. *Journal of Applied Pharmaceutical Science,* 2**,** 60-67.

ABDI, Y., GUSTAFSSON, L., ERICSSON, O. & HELLGREN, U. 1995. Metronidazole. *Handbook of drugs for tropical parasitic infections.* 2nd ed. London: Taylor & Francis.

ABDOU, H. M. 1989. Theory of dissolution. *In:* GENNARO, A., MIGDALOF, B., HASSERT , G. L. & MEDWICK, T. (eds.) *Dissolution, Bioavailability & Bioequivalence.* Easton, PA.: Mack Publishing Company.

ADEBISI, A. O. & CONWAY, B. R. 2010. Development of gastro-retentive systems for the eradication of H-pylori infections in the treatment of peptic ulcer. *Journal of Pharmacy and Pharmacology,* 62**,** 1417-1418.

ADEBISI, A. O. & CONWAY, B. R. 2014. Preparation and characterisation of gastroretentive alginate beads for targeting H. pylori. *Journal of Microencapsulation,* 31**,** 58-67.

AGRAWAL, A. M., MANEK, R. V., KOLLING, W. M. & NEAU, S. H. 2003. Studies on the interaction of water with ethylcellulose: effect of polymer particle size. *AAPS PharmSciTech,* 4**,** E60.

AGUDO, S., ALARCON, T., CIBRELUS, L., URRUZUNO, P., MARTINEZ, M. J. & LOPEZ-BREA, M. 2009. High percentage of clarithromycin and metronidazole resistance in Helicobacter pylori clinical isolates obtained from Spanish children. *Revista española de quimioterapia : publicación oficial de la Sociedad Española de Quimioterapia,* 22**,** 88-92.

AHAD, H. A., SREERAMULU, J., REDDY, N. D., PRAKASH, G. P. & RAMYASREE, P. 2012. Fabrication and In vitro Evaluation of High density Gastro retentive

Microspheres of Famotidine with Synthetic and Natural Polymers. *Indian Journal of Pharmaceutical Education and Research,* 46**,** 45-51.

AHAD, H. A., SREERAMULU, J., SREENIVASULU, R., SRAVANTHI, M. & PRAKASH, G. 2011. Preparation and in vitro evaluation of altered density gastro retentive microspheres of Famotidine with synthetic and natural polymers. *Der Pharmacia Sinica,* 2**,** 110-118.

AHMED, O. A. A., BADR-ELDIN, S. M. & AHMED, T. A. 2013. Kinetic study of the in vitro release and stability of theophylline floating beads. *International Journal of Pharmacy and Pharmaceutical Sciences,* 5**,** 179-184.

AKRE, H. S., MUNDHADA, D. R., BHASKARAN, S., ASGHAR, S. & GANDHI, G. S. 2012. Dry Suspension Formulation of Taste Masked Antibiotic Drug for Pediatric Use. *Journal of Applied Pharmaceutical Science,* 2**,** 166-171.

AL-ABDULLA, S. A. A., AL-ASSADY, N. A. H. & SYYAH, S. G. 2012. Preparation and In Vitro Evaluation of Mucoadhesive Films Containing Metronidazole. *Journal of Thi-Qar Science,* 3**,** 129-140.

AL-KASSAS, R. S., AL-GOHARY, O. M. & AL-FAADHEL, M. M. 2007. Controlling of systemic absorption of gliclazide through incorporation into alginate beads. *International Journal of Pharmaceutics,* 341**,** 230-237.

ALLAMNENI, Y., REDDY, B. V. V. K., CHARY, P. D., RAO, V. B., KUMAR, S. C. & KALEKAR, A. K. 2012. Performance Evaluation of Mucoadhesive Potential of Sodium Alginate on Microspheres Containing an Anti-Diabetic Drug: Glipizide. *International Journal of Pharmaceutical Sciences and Drug Research,* 4**,** 115-122.

ALLÉMANN, E., LEROUX, J.-C. & GURNY, R. 1998. Polymeric nano- and microparticles for the oral delivery of peptides and peptidomimetics. *Advanced Drug Delivery Reviews,* 34**,** 171-189.

ALLEN, A. 1981. Structure and function of gastrointestinal mucus. *In:* JOHNSON, L. R. (ed.) *Physiology of the gastrointestinal tract.* New York: Raven Press.

ALLEN, A. & SNARY, D. 1972. The structure and function of gastric mucus. *Gut,* 13**,** 666-672.

ALVAREZ-ELCORO, S. & ENZLER, M. J. 1999. The macrolides: erythromycin, clarithromycin, and azithromycin. *Mayo Clinical Proceedings,* 74**,** 613-634.

ANAL, A. K., BHOPATKAR, D., SEIICHI, T., HIROSHI, T. & STEVENS, W. F. 2003. Chitosan-alginate multilayer beads for gastric passage and controlled intestinal release of protein. *Drug Development and Industral Pharmacy,* 29**,** 713-724.

ANAL, A. K. & STEVENS, W. F. 2005. Chitosan-alginate multilayer beads for controlled release of ampicillin. *International Journal of Pharmaceutics,* 290**,** 45-54.

ANANDE, N. M., JAIN, S. K. & JAIN, N. K. 2008. Con-A conjugated mucoadhesive microspheres for the colonic delivery of diloxanide furoate. *International Journal of Pharmaceutics,* 359**,** 182-189.

ANILKUMAR, S. J. 2008. Gastro retentive Drug Delivery Systems: An Overview. *Pharminfo.net* [Online], 6. Available: http://www.pharmainfo.net/reviews/gastroretentive-drug-delivery-system-overview [Accessed 12 October 2010].

ANNESE, V., BASSOTTI, G., NAPOLITANO, G., FRUSCIANTE, V., BRUNO, M., CONOSCITORE, P., GERMANI, U., MORELLI, A. & ANDRIULLI, A. 1995. Gastric emptying of solids in patients with nonobstructive Crohn's disease is sometimes delayed. *Journal of Clinical Gastroenterology,* 21**,** 279-282.

ANTHONSEN, M. W., VÅRUM, K. M., HERMANSSON, A., SMIDSRØD, O. & BRANT, D. A. 1994. Aggregates in acidic solutions of chitosans detected by static laser light scattering. *Carbohydrate Polymers,* 25**,** 13-23.

ANTHONSEN, M. W., VÅRUM, K. M. & SMIDSRØD, O. 1993. Solution properties of chitosans: conformation and chain stiffness of chitosans with different degrees of N-acetylation. *Carbohydrate Polymers,* 22**,** 193-201.

ARAKAWA, T., PRESTRELSKI, S. J., KENNEY, W. C. & CARPENTER, J. F. 2001. Factors affecting short-term and long-term stabilities of proteins. *Advanced Drug Delivery Reviews,* 46**,** 307-26.

ARORA, S., ALI, J., AHUJA, A., KHAR, R. K. & BABOOTA, S. 2005. Floating drug delivery systems: a review. *AAPS PharmSciTech,* 6**,** E372-E390.

ARZA, R. A., GONUGUNTA, C. S. & VEERAREDDY, P. R. 2009. Formulation and evaluation of swellable and floating gastroretentive ciprofloxacin hydrochloride tablets. *AAPS PharmSciTech,* 10**,** 220-226.

ASHOKA, C., M, KUMARAN, S. K. & HIRAMAN, G. H. 2013. Development and in vitro evaluation of gastroretentive high density tablet of Propafenone HCl. *Asian Journal of Pharmaceutical Research and Health Care,* 5**,** 89-99.

ASHWELL, G. & HARFORD, J. 1982. Carbohydrate-specific receptors of the liver. *Annual Review of Biochemistry,* 51**,** 531-554.

ASLANI, P. & KENNEDY, R. A. 1996. Effect of gelation conditions and dissolution media on the release of paracetamol from alginate gel beads. *Journal of Microencapsulation,* 13**,** 601-14.

ATHERTON, J. C. 2006. The pathogenesis of Helicobacter pylori-induced gastro-duodenal diseases. *Annual Review of Pathology,* 1**,** 63-96.

ATHERTON, J. C., COCKAYNE, A., BALSITIS, M., KIRK, G. E., HAWKEY, C. J. & SPILLER, R. C. 1995. Detection of the intragastric sites at which Helicobacter pylori evades treatment with amoxycillin and cimetidine. *Gut.,* 36**,** 670-674.

BADWAN, A. A., ABUMALOOH, A., SALLAM, E., ABUKALAF, A. & JAWAN, O. 1985. A Sustained Release Drug Delivery System Using Calcium Alginate Beads. *Drug Development and Industrial Pharmacy,* 11**,** 239-256.

BAI, Y. X. & LI, Y. F. 2006. Preparation and characterization of crosslinked porous cellulose beads. *Carbohydrate Polymers,* 64**,** 402-407.

BAJPAI, S. K. & SHARMA, S. 2004. Investigation of swelling/degradation behaviour of alginate beads crosslinked with Ca^{2+} and Ba^{2+} ions. *Reactive and Functional Polymers,* 59**,** 129-140.

BAJPAI, S. K. & TANKHIWALE, R. 2006. Investigation of water uptake behavior and stability of calcium alginate/chitosan bi-polymeric beads: Part-1. *Reactive & Functional Polymers,* 66**,** 645-658.

BANNISTER, L. H. 1995. Alimentary system. *In:* WILLIAMS, P. L. (ed.) *Gray's Anatomy.* New York: Churchill Livingstone.

BANSIL, R., CELLI, J., HARDCASTLE, J. & TURNER, B. 2013. The influence of mucus microstructure and rheology in H. pylori infection. *Frontiers in Immunology,* 4.

BANSIL, R. & TURNER, B. S. 2006. Mucin structure, aggregation, physiological functions and biomedical applications. *Current Opinion in Colloid & Interface Science,* 11**,** 164-170.

BARDONNET, P. L., FAIVRE, V., PUGH, W. J., PIFFARETTI, J. C. & FALSON, F. 2006. Gastroretentive dosage forms: overview and special case of Helicobacter pylori. *Journal of Controlled Release,* 111**,** 1-18.

BASU, P. P., RAYAPUDI, K., PACANA, T., SHAH, N. J., KRISHNASWAMY, N. & FLYNN, M. 2011. A randomized study comparing levofloxacin, omeprazole, nitazoxanide, and doxycycline versus triple therapy for the eradication of Helicobacter pylori. *American Journal of Gastroenterology,* 106**,** 1970-1975.

BASU, S. K. & RAJENDRAN, A. 2008. Studies in the development of nateglinide loaded calcium alginate and chitosan coated calcium alginate beads. *Chemical and Pharmaceutical Bulletin (Tokyo),* 56**,** 1077-1084.

BATCHELOR, H., CONWAY, B. & WILLIAMS, R. O. 2007. Targeting the infections within the gastro- intestinal tract. *In:* WILLIAMS, R. O., TAFT, D. R. & MCCONVILLLES, J. T. (eds.) *Advanced drug formulation design to optimize therapeutic outcomes (Drugs and the Pharmaceutical Sciences).* New York: Informa Healthcare.

BATCHELOR, H. K., BANNING, D., DETTMAR, P. W., HAMPSON, F. C., JOLLIFFE, I. G. & CRAIG, D. Q. M. 2002. An in vitro mucosal model for prediction of the

bioadhesion of alginate solutions to the oesophagus. *International Journal of Pharmaceutics,* 238**,** 123-132.

BAZZOLI, F., BIANCHI PORRO, G., MACONI, G., MOLTENI, M., POZZATO, P. & ZAGARI, R. M. 2002. Treatment of Helicobacter pylori infection. indications and regimens: an update. *Digestive and Liver Disease,* 34**,** 70-83.

BECHGAARD, H. & LADEFOGED, K. 1978. Distribution of pellets in the gastrointestinal tract. The influence on transit time exerted by the density or diameter of pellets. *Journal of Pharmacy and Pharmacology,* 30**,** 690-692.

BELL, A. E., SELLERS, L. A., ALLEN, A., CUNLIFFE, W. J., MORRIS, E. R. & ROSSMURPHY, S. B. 1985. Properties of Gastric and Duodenal Mucus - Effect of Proteolysis, Disulfide Reduction, Bile, Acid, Ethanol, and Hypertonicity on Mucus Gel Structure. *Gastroenterology,* 88**,** 269-280.

BEMPONG, D. K., MANNING, R. G., MIRZA, T. & BHATTACHARYYA, L. 2005. A stability-indicating HPLC assay for metronidazole benzoate. *Journal of Pharmacy and Biomedical Analysis,* 38**,** 776-80.

BERA, R., MANDAL, B., BHOWMIK, M., BERA, H., DEY, S. K., NANDI, G. & GHOSH, L. K. 2009. Formulation and in vitro evaluation of sunflower oil entrapped within buoyant beads of furosemide. *Scientia Pharmaceutica,* 77**,** 669-678.

BERNKOP-SCHNÜRCH, A., GABOR, F., SZOSTAK, M. P. & LUBITZ, W. 1995. An adhesive drug delivery system based on K99-fimbriae. *European Journal of Pharmaceutical Sciences,* 3**,** 293-299

BERRY, M., ELLINGHAM, R. B. & CORFIELD, A. P. 1996. Polydispersity of normal human conjunctival mucins. *Investigative Ophthalmology and Visual Science,* 37**,** 2559-2571.

BHARDWAJ, V. & HARIKUMAR, N. S. L. 2013. Floating Drug Delivery System: A review. *Pharmacophore,* 4**,** 26-38.

BHASKARA, R. S. & SHARMA, C. P. 1997. Use of chitosan as biomaterial:studies on its safety and hemostatic potential. *Journal of Biomedical Materials Research,* 34**,** 21-28.

BLANDINO, A., MACíAS, M. & CANTERO, D. 2000. Glucose oxidase release from calcium alginate gel capsules. *Enzyme and Microbial Technology,* 27**,** 319-324.

BLASER, M. J. 1992. Hypotheses on the pathogenesis and natural history of Helicobacter pylori-induced inflammation. *Gastroenterology,* 102**,** 720-727.

BLOOM, S. R. & POLAK, J. M. 1980. Physiology of gastrointestinal hormones. *Biochemical Society transactions,* 8**,** 15-17.

BODDUPALLI, B. M., MOHAMMED, Z. N., NATH, R. A. & BANJI, D. 2010. Mucoadhesive drug delivery system: An overview. *Journal of Advanced Pharmaceutical Technology and Research,* 1**,** 381-387.

BODMEIER, R. & PAERATAKUL, O. 1989. Spherical agglomerates of water-insoluble drugs. *Journal of Pharmaceutical Sciences,* 78**,** 964-967.

BONE, W., YEUNG, C. H., SKUPIN, R., HAUFE, G. & COOPER, T. G. 1997. Toxicity of ornidazole and its analogues to rat spermatozoa as reflected in motility parameters. *International Journal of Andrology,* 20**,** 347-355.

BOUYSSOU, C. 2014. Helicobacter pylori : l'essentiel pour comprendre. *Actualités Pharmaceutiques,* 53**,** 20-24.

BOWMAN, W. C., RAND, M. J. & WEST, G. B. 1968. *Textbook of pharmacology,* Oxford, Edinburgh,, Blackwell Scientific.

BOYANOVA, L., MITOV, I. & VLADIMIROV, B. 2011. Helicobacter. pylori resistance to antibiotics. *In:* BOYANOVA, L. (ed.) *Helicobacter pylori.* Norfolk, UK: Caister Academic Press.

BRECKAN, R. K., PAULSSEN, E. J., ASFELDT, A. M., MORTENSEN, L., STRAUME, B. & FLORHOLMEN, J. 2009. The impact of body mass index and Helicobacter pylori infection on gastro-oesophageal reflux symptoms: a population-based study in Northern Norway. *Scandinavian Journal of Gastroenterology,* 44**,** 1060-1066.

BROWN, L. M. 2000. Helicobacter pylori: epidemiology and routes of transmission. *Epidemiology Reviews,* 22**,** 283-297.

BU, H., KJØNIKSEN, A.-L. & NYSTRÖM, B. 2005. Effects of pH on dynamics and rheology during association and gelation via the Ugi reaction of aqueous alginate. *European Polymer Journal,* 41**,** 1708-1717.

CABALLERO, F., FORADADA, M., MIÑARRO, M., PÉREZ-LOZANO, P., GARCÍA-MONTOYA, E., TICÓ, J. R. & SUÑÉ-NEGRE, J. M. 2014. Characterization of alginate beads loaded with ibuprofen lysine salt and optimization of the preparation method. *International Journal of Pharmaceutics,* 460**,** 181-188.

CAMARGO, M. C., GARCIA, A., RIQUELME, A., OTERO, W., CAMARGO, C. A., HERNANDEZ-GARCIA, T., CANDIA, R., BRUCE, M. G. & RABKIN, C. S. 2014. The Problem of Helicobacter pylori Resistance to Antibiotics: A Systematic Review in Latin America. *American Journal of Gastroenterology,* 109**,** 485-495.

CAMERON, P. 1997. *Good pharmaceutical freeze-drying practice,* Buffalo Grove, Taylor & Francis.

CAMMAROTA, G., PASCERI, V., PAPA, A., CIANCI, R., GASBARRINI, A., FEDELI, P., CREMONINI, F., FEDELI, G., MASERI, A. & GASBARRINI, G. 1998. Helicobacter pylori infection and ischaemic heart disease. *Italian Journal of Gastroenterology and Hepatology,* 30 S304-S306.

CAMMAROTA, G., SANGUINETTI, M., GALLO, A. & POSTERARO, B. 2012. Review article: biofilm formation by Helicobacter pylori as a target for eradication of resistant infection. *Alimentary Pharmacology & Therapeutics,* 36**,** 222-230.

CAMPBELL, I. 2012. The mouth, stomach and intestines. *Anaesthesia & Intensive Care Medicine,* 13**,** 56-58.

CARR, B. & WRIGHT, M. 2013. *Nanoparticle Tracking Analysis - A Review of Application and Usage 2010-2012,* United Kingdom, NanoSight Ltd.

CASTRO, M., ROMERO, C., DE CASTRO, A., VARGAS, J., MEDINA, E., MILLAN, R. & BRENES, M. 2012. Assessment of Helicobacter pylori eradication by virgin olive oil. *Helicobacter,* 17**,** 305-11.

CH'NG, H. S., PARK, H., KELLY, P. & ROBINSON, J. R. 1985. Bioadhesive polymers as platforms for oral controlled drug delivery II: synthesis and evaluation of some swelling, water-insoluble bioadhesive polymers. *Journal of Pharmaceutical Sciences,* 74**,** 399-405.

CHAISRI, W., HENNINK, W. E. & OKONOGI, S. 2009. Preparation and characterization of cephalexin loaded PLGA microspheres. *Current Drug Delivery,* 6**,** 69-75.

CHAN, E.-S., LIM, T.-K., VOO, W.-P., POGAKU, R., TEY, B. T. & ZHANG, Z. 2011a. Effect of formulation of alginate beads on their mechanical behavior and stiffness. *Particuology,* 9**,** 228-234.

CHAN, E.-S., WONG, S.-L., LEE, P.-P., LEE, J.-S., TI, T. B., ZHANG, Z., PONCELET, D., RAVINDRA, P., PHAN, S.-H. & YIM, Z.-H. 2011b. Effects of starch filler on the physical properties of lyophilized calcium–alginate beads and the viability of encapsulated cells. *Carbohydrate Polymers,* 83**,** 225-232.

CHANG, F. Y., LU, C. L., CHEN, C. Y., LUO, J. C., JIUM, K. L. & LEE, S. D. 2003. Effect of Helicobacter pylori eradicated therapy on water gastric emptying in patients with active duodenal ulcer. *Journal of Gastroenterology and Hepatology,* 18**,** 1250-1256.

CHANG, W. L., SHEU, B. S., CHENG, H. C., YANG, Y. J., YANG, H. B. & WU, J. J. 2009. Resistance to metronidazole, clarithromycin and levofloxacin of Helicobacter pylori before and after clarithromycin-based therapy in Taiwan. *Journal of Gastroenterology and Hepatology,* 24**,** 1230-1235.

CHATAP, V. K., MAURYA, A. R., DESHMUKH, P. K. & ZAWAR, L. R. 2013. Formulation and Evaluation of Nisoldipne Sublingual Tablets Using Pullulan & Chitosan for Rapid Oromucosal Absorption. *Advances in Pharmacology and Pharmacy* 1**,** 18-25.

CHAUDHURI, S., CHOWDHURY, A., DATTA, S., MUKHOPADHYAY, A. K., CHATTOPADHYA, S., SAHA, D. R., DHALI, G., SANTRA, A., NAIR, G. B., BHATTACHARYA, S. & BERG, D. E. 2003. Anti-Helicobacter pylori therapy in

India: differences in eradication efficiency associated with particular alleles of vacuolating cytotoxin (vacA) gene. *Journal of Gastroenterology and Hepatology,* 18**,** 190-195.

CHAWLA, G., GUPTA, P., KORADIA, V. & BANSAL, A. K. 2003. Gastroretention- A means to address regional variability in intestinal drug absorption. *Pharmaceutical Technology,* 27**,** 50-68.

CHEN, J., BLEVINS, W. E., PARK, H. & PARK, K. 2000. Gastric retention properties of superporous hydrogel composites. *Journal of Controlled Release,* 64**,** 39-51.

CHEN, J. & PARK, K. 2000. Synthesis and characterization of superporous hydrogel composites. *Journal of Controlled Release,* 65**,** 73-82.

CHEN, J. P. & WANG, L. 2001. Characterization of a Ca-alginate based ion-exchange resin and its applications in lead, copper, and zinc removal. *Separation Science and Technology,* 36**,** 3617-3637.

CHEN, Y.-C., HO, H.-O., LEE, T.-Y. & SHEU, M.-T. 2013. Physical characterizations and sustained release profiling of gastroretentive drug delivery systems with improved floating and swelling capabilities. *International Journal of Pharmaceutics,* 441**,** 162-169.

CHERN, C. S., LEE, C. K. & TSAI, Y. J. 2001. Interactions between dextran-modified poly(methyl methacrylate) latex particles and concanavalin A. *Colloid & Polymer Science,* 279**,** 420-426.

CHI, C. H., LIN, C. Y., SHEU, B. S., YANG, H. B., HUANG, A. H. & WU, J. J. 2003. Quadruple therapy containing amoxicillin and tetracycline is an effective regimen to rescue failed triple therapy by overcoming the antimicrobial resistance of Helicobacter pylori. *Alimentary Pharmacology and Therapeutics,* 18**,** 347-353.

CHITNIS, V. S., MALSHE, V. S. & LALLA, J. K. 1991. Bioadhesive Polymers - Synthesis, Evaluation and Application in Controlled Release Tablets. *Drug Development and Industrial Pharmacy,* 17**,** 879-892.

CHICKERING, D. E. & MATHIOWITZ, E. 1999. Definitions, mechanisms, and theories of bioadhesion. *In:* MATHIOWITZ, E., CHICKERING, D. E. & LEHR, C. M. (eds.) *Bioadhesive Drug Delivery Systems: Fundamentals, Novel Approaches, and Development.* New York Marcel Dekker.

CHOI, B. Y., PARK, H. J., HWANG, S. J. & PARK, J. B. 2002. Preparation of alginate beads for floating drug delivery system: effects of CO2 gas-forming agents. *International Journal of Pharmaceutics,* 239**,** 81-91.

CHOUDHURY, P. K. & KAR, M. 2005. Preparation of Alginate Gel Beads Containing Metformin Hydrochloride Using Emulsion- Gelation Method. *Tropical of Journal Pharmaceutical Research,* 4**,** 489-493.

CHOUDHURY, P. K., MURTHY, P. N., TRIPATHY, N. K., PANIGRAHI, R. & BEHERA, S. 2012. Investigation of Drug Polymer Compatibility: Formulation and

Characterization of Metronidazole Microspheres for Colonic Delivery. *WebmedCentral Pharmaceutical sciences,* 3**,** WMC003253.

CHOWDARY, K. P. & RAO, Y. S. 2003. Design and in vitro and in vivo evaluation of mucoadhesive microcapsules of glipizide for oral controlled release: a technical note. *AAPS PharmSciTech,* 4**,** E39.

CHOWDARY, K. P. & RAO, Y. S. 2004. Mucoadhesive microspheres for controlled drug delivery. *Biological and Pharmaceutical Bulletin,* 27**,** 1717-1724.

CHOWDHURY, J. K., JAHAN, S. T., MORSHED, M. M., MALLICK, J., NATH, A. K., UDDIN, M. Z., DUTTA, M., ISLAM, M. K. & KAWSAR, M. H. 2011. Development and Evaluation of Diclofenac Sodium Loaded Alginate Cross-Linking Beads. *Bangladesh Pharmaceutical Journal,* 14**,** 41-48.

CHUN, M. K., SAH, H. & CHOI, H. K. 2005. Preparation of mucoadhesive microspheres containing antimicrobial agents for eradication of H. pylori. *International Journal of Pharmacetics,* 297**,** 172-179.

CLARKE, G. M., NEWTON, J. M. & SHORT, M. D. 1993. Gastrointestinal transit of pellets of differing size and density. *International Journal of Pharmaceutics,* 100**,** 81-92.

COHEN, S., LOBEL, E., TREVGODA, A. & PELED, Y. 1997. A novel in situ-forming ophthalmic drug delivery system from alginates undergoing gelation in the eye. *Journal of Controlled Release,* 44**,** 201-208.

CONWAY, B. R. 2005. Drug delivery strategies for the treatment of Helicobacter pylori infections . *Current Pharmaceutical Design,* 11**,** 775-790.

COPPI, G., IANNUCCELLI V FAU - LEO, E., LEO E FAU - BERNABEI, M. T., BERNABEI MT FAU - CAMERONI, R. & CAMERONI, R. 2001. Chitosan-alginate microparticles as a protein carrier. *Drug Development and Industrial Pharmacy,* 27**,** 393-400.

COSTA, P. & LOBO, J. M. S. 2001. Influence of dissolution medium agitation on release profiles of sustained-release tablets. *Drug Development and Industrial Pharmacy,* 27**,** 811-817.

CUI, S. W. 2005. Structural analysis of polysaccharides. *In:* CUI, S. W. (ed.) *Food Carbohydrates: Chemistry, Physical Properties, and Applications.* Boca Raton, Florida: Taylor and Francis.

CUÑA, M., ALONSO, M. J. & TORRES, D. 2001. Preparation and in vivo evaluation of mucoadhesive microparticles containing amoxycillin-resin complexes for drug delivery to the gastric mucosa. *European Journal of Pharmaceutics and Biopharmaceutics,* 51**,** 199-205.

CZINN, S. J. 2005. Helicobacter pylori infection: detection, investigation, and management. *Journal of Pediatrics,* 146**,** S21-S26.

DAI, Y. N., LI, P., ZHANG, J. P., WANG, A. Q. & WEI, Q. 2008. Swelling characteristics and drug delivery properties of nifedipine-loaded pH sensitive alginate-chitosan hydrogel beads. *Journal of Biomedical Material Research. Part B, Applied Biomaterials,* 86**,** 493-500.

DAIGO, K., WADA, Y., YAMADA, C., YAMAJI, M., OKUDA, S., OKADA, M. & MIYAZATO, T. 1981. Pharmacological studies of sodium alginate. I. Protective effect of sodium alginate on mucous membranes of upper-gastrointestinal tract. *Yakugaku Zasshi: Journal of the Pharmaceutical Society of Japan,* 101**,** 452-457.

DAMINK, L. H. H. O., DIJKSTRA, P. J., VANLUYN, M. J. A., VANWACHEM, P. B., NIEUWENHUIS, P. & FEIJEN, J. 1996. Cross-linking of dermal sheep collagen using a water-soluble carbodiimide. *Biomaterials,* 17**,** 765-773.

DARANDALE, S. S. & VAVIA, P. R. 2012. Design of a gastroretentive mucoadhesive dosage form of furosemide for controlled release. *Acta Pharmaceutica Sinica B,* 2**,** 509-517.

DAS, M. K. & RAO, K. R. 2006. Evaluation of zidovudine encapsulated ethylcellulose microspheres prepared by water-in-oil-in-oil (w/o/o) double emulsion solvent diffusion technique. *Acta Poloniae Pharmaceutica,* 63**,** 141-148.

DAVE, B. S., AMIN, A. F. & PATEL, M. M. 2004. Gastroretentive drug delivery system of ranitidine hydrochloride: formulation and in vitro evaluation. *AAPS PharmSciTech,* 5**,** E34.

DAVEY, P. G. 1991. The pharmacokinetics of clarithromycin and its 14-OH metabolite. *The Journal of Hospital Infections,* 19 Suppl A**,** 29-37.

DAVIS, D. W. 1968. *Method of swallowing a pill*. US patent application US Patent No.3418999.

DAVIS, S. S. 2005. Formulation strategies for absorption windows. *Drug Discovery Today,* 10**,** 249-257.

DAVIS, S. S., ILLUM, L. & HINCHCLIFFE, M. 2001. Gastrointestinal transit of dosage forms in the pig. *Journal of Pharmacy and Pharmacology,* 53**,** 33-39.

DAVIS, S. S., STOCKWELL, A. F., TAYLOR, M. J., HARDY, J. G., WHALLEY, D. R., WILSON, C. G., BECHGAARD, H. & CHRISTENSEN, F. N. 1986. The effect of density on the gastric emptying of single- and multiple-unit dosage forms. *Pharmaceutical Research,* 3**,** 208-213.

DE BOER, W. A. 2001. A novel therapeutic approach for Helicobacter pylori infection: the bismuth-based triple therapy monocapsule. *Expert Opinion on Investigational Drugs,* 10**,** 1559-1566.

DE FRANCESCO, V., GIORGIO, F., HASSAN, C., MANES, G., VANNELLA, L., PANELLA, C., IERARDI, E. & ZULLO, A. 2010. Worldwide H. pylori antibiotic resistance: a systematic review. *Journal of Gastrointestinal and Liver Disease.,* 19**,** 409-414.

DE FRANCESCO, V., ZULLO, A., IERARDI, E. & VAIRA, D. 2009. Minimal inhibitory concentration (MIC) values and different point mutations in the 23S rRNA gene for clarithromycin resistance in Helicobacter pylori. *Digestive and Liver Disease,* 41**,** 610-611.

DENNIS, A. & TIMMINS, P. 1992. *Buoyant controlled release powder formulations* . US patent application US Patent 5169638. December 8th ,1992.

DERJAGUIN, B. V., ALEINIKOVA, I. N. & TOPOROV, Y. P. 1994. On the role of electrostatic forces in the adhesion of polymer particles to solid surfaces. *Progress in Surface Science,* 45**,** 119-123.

DERJAGUIN, B. V., TOPOROV, Y. P., MULLER, V. M. & ALEINIKOVA, I. N. 1977. On the relationship between the electrostatic and the molecular component of the adhesion of elastic particles to a solid surface. *Journal of Colloid and Interface Science,* 58**,** 528-533.

DESAI, J., ALEXANDER, K. & RIGA, A. 2006. Characterization of polymeric dispersions of dimenhydrinate in ethyl cellulose for controlled release. *International Journal of Pharmaceutics,* 308**,** 115-123.

DESAI, J. U. 2007. Floating Drug Delivery Systems : An approach to gastroretention. *Pharminfo.net* [Online], 5. Available: http://www.pharmainfo.net/reviews/floating-drug-delivery-systemsan-approach-gastro-retention [Accessed 15/11/2010].

DESAI, M. A., NICHOLAS, C. V. & VADGAMA, P. 1991. Electrochemical determination of the permeability of porcine mucus to model solute compounds. *Journal of Pharmacy and Pharmacology,* 43**,** 124-127.

DESAI, S. J., SINGH, P., SIMONELLI, A. P. & HIGUCHI, W. I. 1966. Investigation of factors influencing release of solid drug dispersed in inert matrices. 3. Quantitative studies involving the polyethylene plastic matrix. *Journal of Pharmaceutical Sciences,* 55**,** 1230-1234.

DESHPANDE, A. A., RHODES, C. T., SHAH, N. H. & MALICK, A. W. 1996. Controlled-Release Drug Delivery Systems for Prolonged Gastric Residence : An Overview. *Drug Development and Industrial Pharmacy.,* 22**,** 531-539.

DHALIWAL, S., JAIN, S., SINGH, H. P. & TIWARY, A. K. 2008. Mucoadhesive microspheres for gastroretentive delivery of acyclovir: in vitro and in vivo evaluation. *AAPS Journal,* 10**,** 322-330.

DODD, S., PLACE, G. A., HALL, R. L. & HARDING, S. E. 1998. Hydrodynamic properties of mucins secreted by primary cultures of guinea-pig tracheal epithelial cells: Determination of diffusion coefficients by analytical ultracentrifugation and kinetic analysis of mucus gel hydration and dissolution. *European Biophysics Journal,* 28**,** 38-47.

DONATI, I., HOLTAN, S., MORCH, Y. A., BORGOGNA, M., DENTINI, M. & SKJAK-BRAEK, G. 2005. New hypothesis on the role of alternating sequences in calcium-alginate gels. *Biomacromolecules,* 6**,** 1031-1040.

DOUGLAS, K. L. & TABRIZIAN, M. 2005. Effect of experimental parameters on the formation of alginate-chitosan nanoparticles and evaluation of their potential application as DNA carrier. *Journal of Biomaterial Science. Polymer Edition,* 16**,** 43-56.

DRAGET, K. I. & TAYLOR, C. 2011. Chemical, physical and biological properties of alginates and their biomedical implications. *Food Hydrocolloids***,** 251-256.

DUBE, C., NKOSI, T. C., CLARKE, A. M., MKWETSHANA, N., GREEN, E. & NDIP, R. N. 2009. Helicobacter pylori antigenemia in an asymptomatic population of Eastern Cape Province, South Africa: public health implications. *Reviews on Environmental Health,* 24**,** 249-255.

DUNN, B. E., COHEN, H. & BLASER, M. J. 1997. Helicobacter pylori. *Clinical Microbiology Reviews,* 10**,** 720-741.

DUPUY, B., ARIEN, A. & PERROT MINNOT, A. 1994. FT-IR of membranes made with alginate/polylysine complexes. Variations with the mannuronic or guluronic content of the polysaccharides. *Artifical Cells, Blood Substitute and Immobilization Biotechnology,* 22**,** 71-82.

EHRLEIN, H. J. 1988. Motility of the pyloric sphincter studied by the inductograph method in conscious dogs. *American Journal of Physiology,* 254**,** G650-G657.

EL-GIBALY, I. 2002. Development and in vitro evaluation of novel floating chitosan microcapsules for oral use: comparison with non-floating chitosan microspheres. *International Journal of Pharmaceutics,* 249**,** 7-21.

EL-KAMEL, A. H., AL-GOHARY, O. M. & HOSNY, E. A. 2003. Alginate-diltiazem hydrochloride beads: optimization of formulation factors, in vitro and in vivo availability. *Journal of Microencapsulation,* 20**,** 211-225.

EL-KAMEL, A. H., SOKAR, M. S., AL GAMAL, S. S. & NAGGAR, V. F. 2001. Preparation and evaluation of ketoprofen floating oral delivery system. *International Journal of Pharmaceutics,* 220**,** 13-21.

ELTOM, M., HOFVANDER, Y., TORELM, I. & FELLSTROM, B. 1984. Endemic goitre in the Darfur region (Sudan). Epidemiology and aetiology. *Acta Medica Scandinavica,* 215**,** 467-475.

EMEJE, M. O., KUNLE, O. O. & OFOEFULE, S. I. 2006. Compaction characteristics of ethylcellulose in the presence of some channeling agents: technical note. *AAPS PharmSciTech,* 7**,** 58.

ERAH, P. O., BARRETT, D. A. & SHAW, P. N. 1996. Ion-pair high-performance liquid chromatographic assay method for the assessment of clarithromycin stability in

aqueous solution and in gastric juice. *Journal of Chromatography B: Biomedical Sciences and Applications,* 682**,** 73-78.

ERAH, P. O., GODDARD, A. F., BARRETT, D. A., SHAW, P. N. & SPILLER, R. C. 1997. The stability of amoxycillin, clarithromycin and metronidazole in gastric juice: relevance to the treatment of Helicobacter pylori infection. *Journal of Antimicrobial Chemotherapy,* 39**,** 5-12.

ERNI, W. & HELD, K. 1987. The hydrodynamically balanced system: a novel principle of controlled drug release. *European Neurology,* 27 Suppl 1**,** 21-27.

ERNST, P. B. & GOLD, B. D. 2000. The disease spectrum of Helicobacter pylori: the immunopathogenesis of gastroduodenal ulcer and gastric cancer. *Annual Review of Microbiology,* 54**,** 615-640.

EVANS, C. M. & KOO, J. S. 2009. Airway mucus: The good, the bad, the sticky. *Pharmacology & Therapeutics,* 121**,** 332-348.

EVERS, P. 2001. Drug Delivery: Market Perspectives. *In:* HILLERY, A. M., LLOYD, A. W. & SWARBRICK, J. (eds.) *Drug Delivery and Targeting for Pharmacists and Pharmaceutical Scientists.* London and New York: Taylor & Francis.

EZPELETA, I., ARANGOA, M. A., IRACHE, J. M., STAINMESSE, S., CHABENAT, C., POPINEAU, Y. & ORECCHIONI, A.-M. 1999. Preparation of Ulex europaeus lectin-gliadin nanoparticle conjugates and their interaction with gastrointestinal mucus. *International Journal of Pharmaceutics,* 191**,** 25-32.

FABREGAS, J. L., CLARAMUNT, J., CUCALA, J., POUS, R. & SILES, A. 1994. "In-Vitro" Testing of an Antacid Formulation with Prolonged Gastric Residence Time (Almagate Flot-Coat®). *Drug Development and Industrial Pharmacy,* 20**,** 1199-1212.

FARTHING, M. J. 1998. Helicobacter pylori infection: an overview. *British Medical Bulletin,* 54**,** 1-6.

FEFELOVA, N. A., NURKEEVA, Z. S., MUN, G. A. & KHUTORYANSKIY, V. V. 2007. Mucoadhesive interactions of amphiphilic cationic copolymers based on [2-(methacryloyloxy)ethyl]trimethylammonium chloride. *International Journal of Pharmaceutics,* 339**,** 25-32.

FENNEMA, O. R. 1975. *Principles of food science, Part II: Physical principles of food preservation.,* New York, Marcel Dekker, Inc.

FIX, J. A., CARGILL, R. & ENGLE, K. 1993. Controlled gastric emptying. III. Gastric residence time of a nondisintegrating geometric shape in human volunteers. *Pharmaceutical Research,* 10**,** 1087-1089.

FONTES, G. C., CALADO, V. A. C., ROSSI, A. M. & ROCHA-LEAO, M. H. M. 2013. Characterization of Antibiotic-Loaded Alginate-Osa Starch Microbeads Produced by Ionotropic Pregelation. *BioMed Research International,* 2013**,** 11.

FORD, A. C. & AXON, A. T. R. 2010. Epidemiology of Helicobacter pylori infection and Public Health Implications. *Helicobacter,* 15**,** 1-6.

FOX, J. G. 1995. Non-human reservoirs of Helicobacter pylori. *Alimentary Pharmacology & Therapeutics,* 9 Suppl 2**,** 93-103.

FRANKS, F. 1992. Freeze-drying: From empiricism to predictability. The significance of glass transitions. *Developments in Biological Standardization,* 74**,** 9-18.

FRANZ, M. R. & OTH, M. P. 1992. *Sustained release: Bilayer buoyant dosage form.* US patent application US Patent 5232704.

FREITAS, S., MERKLE, H. P. & GANDER, B. 2005. Microencapsulation by solvent extraction/evaporation: reviewing the state of the art of microsphere preparation process technology. *Journal of Controlled Release,* 102**,** 313-332.

FROHOFF-HÜLSMANN, M. A., LIPPOLD, B. C. & MCGINITY, J. W. 1999. Aqueous ethyl cellulose dispersion containing plasticizers of different water solubility and hydroxypropyl methyl-cellulose as coating material for diffusion pellets II: properties of sprayed films. *European Journal of Pharmaceutics and Biopharmaceutics,* 48**,** 67-75.

GABOR, F., WIRTH, M., JURKOVICH, B., HABERL, I., THEYER, G., WALCHER, G. & HAMILTON, G. 1997. Lectin-mediated bioadhesion: Pro-teolytic stability and binding-characteristics of wheat germagglu-tinin and Solanum tuberosumlectin on Caco-2, HT-29 and human colonocytes. *Journal of Controlled Release,* 49**,** 27-37.

GAD, S. C. 2008. Pharmaceutical Manufacturing Handbook. *In:* GAD, S. C. (ed.) *Production and Processes.* New York: Wiley Interscience.

GAL, A. & NUSSINOVITCH, A. 2007. Hydrocolloid carriers with filler inclusion for diltiazem hydrochloride release. *Journal of Pharmaceutical Sciences,* 96**,** 168-178.

GALINDO-RODRIGUEZ, S. A., ALLEMANN, E., FESSI, H. & DOELKER, E. 2005. Polymeric Nanoparticles for Oral Delivery of Drugs and Vaccines: A Critical Evaluation of In Vivo Studies. *Critical Reviews in Therapeutic Drug Carrier Systems,* 22**,** 419-464.

GANGA, S. & BAFNA, M. 2007. Mucosal drug delivery - A review. *Pharmaceutical Reviews* [Online], 5. Available: http://www.pharmainfo.net/reviews/mucosal-drug-delivery-review [Accessed 01/04/2013].

GAO, W., CHENG, H., HU, F., LI, J., WANG, L., YANG, G., XU, L. & ZHENG, X. 2010. The evolution of Helicobacter pylori antibiotics resistance over 10 years in Beijing, China. *Helicobacter,* 15**,** 460-466.

GARG, R. & GUPTA, G. D. 2008. Progress in controlled gastroretentive delivery systems. *Tropical Journal of Pharmaceutical Research,* 7**,** 1055-1066.

GARG, S. & SHARMA, S. 2003. Gastroretentive drug delivery systems. Business Briefing. *Pharmatech,* 5**,** 160-166.

GÅSERØD, O., JOLLIFFE, I. G., HAMPSON, F. C., DETTMAR, P. W. & SKJÅK-BRÆK, G. 1998a. The enhancement of the bioadhesive properties of calcium alginate gel beads by coating with chitosan. *International Journal of Pharmaceutics,* 175**,** 237-246.

GÅSERØD, O., SANNES, A. & SKJÅK-BRÆK, G. 1999. Microcapsules of alginate–chitosan. II. A study of capsule stability and permeability. *Biomaterials,* 20**,** 773-783.

GÅSERØD, O., SMIDSRØD, O. & SKJÅK-BRÆK, G. 1998b. Microcapsules of alginate-chitosan – I: A quantitative study of the interaction between alginate and chitosan. *Biomaterials,* 19**,** 1815-1825.

GATES, K. A. 1999. *Controlled Drug Delivery Using Bioerodible Polymeric Systems for the Treatment of Periodontitis.* Doctor of Philosophy, University of Toronto.

GATTANI, S. G., SAVALIYA, P. J. & BELGAMWAR, V. S. 2010. Floating-mucoadhesive beads of clarithromycin for the treatment of Helicobacter pylori infection. *Chemical and Pharmaceutical Bulletin (Tokyo),* 58**,** 782-787.

GEORGOPOULOS, S. D., LADAS, S. D., KARATAPANIS, S., TRIANTAFYLLOU, K., SPILIADI, C., MENTIS, A., ARTIKIS, V. & RAPTIS, S. A. 2002. Effectiveness of two quadruple, tetracycline- or clarithromycin-containing, second-line, Helicobacter pylori eradication therapies. *Alimentary pharmacology & therapeutics,* 16**,** 569-575.

GEORGOPOULOS, S. D., PAPASTERGIOU, V. & KARATAPANIS, S. 2012. Helicobacter pylori Eradication Therapies in the Era of Increasing Antibiotic Resistance: A Paradigm Shift to Improved Efficacy. *Gastroenterology Research and Practice,* 2012**,** 9-18.

GIRI, T. K., VERMA, S., ALEXANDER, A., BADWAIK, A. H., TRIPATHI, M. & TRIPATHI, D. K. 2013. Crosslinked biodegradable alginate hydrogel floating beads for stomach site specific controlled delivery of metronidazole. *Farmacia,* 61**,** 533-550.

GLASS, G. B. 1964. Proteins, Mucosubstances, and Biologically Active Components of Gastric Secretion. *In:* HARRY, S. & STEWART, C. P. (eds.) *Advances in Clinical Chemistry.* United States: Elsevier.

GÓMEZ-BURGAZ, M., TORRADO, G. & TORRADO, S. 2009. Characterization and superficial transformations on mini-matrices made of interpolymer complexes of chitosan and carboxymethylcellulose during in vitro clarithromycin release. *European Journal of Pharmaceutics and Biopharmaceutics,* 73**,** 130-139.

GOTOH, T., MATSUSHIMA, K. & KIKUCHI, K. 2004. Preparation of alginate-chitosan hybrid gel beads and adsorption of divalent metal ions. *Chemosphere,* 55**,** 135-140.

GOUDANAVAR, P. S., BAGALI, R. S., CHANDRASHEKHARA.S & PATIL, S. M. 2010. Design and characterization of diclofenac sodium microbeads by ionotropic gelation technique. *International Journal of Pharma and Bio Sciences,* 1**,** 1-10.

GOVENDER, S., PILLAY, V., CHETTY, D. J., ESSACK, S. Y., DANGOR, C. M. & GOVENDER, T. 2005. Optimisation and characterisation of bioadhesive controlled release tetracycline microspheres. *International Journal of Pharmaceutics,* 306**,** 24-40.

GRAHAM, D. Y. & FISCHBACH, L. 2010. Helicobacter pylori treatment in the era of increasing antibiotic resistance. *Gut,* 59**,** 1143-1153.

GRANT, G. T., MORRIS, E. R., REES, D. A., SMITH, P. J. C. & THOM, D. 1973. Biological interactions between polysaccharides and divalent cations: The egg-box model. *FEBS Letters,* 32**,** 195-198.

GRASDALEN, H. 1979. A p.m.r. study of the composition and sequence of uronate residues in alginates. *Carbohydrate research,* 68**,** 23-31.

GRASDALEN, H. 1981. ^{13}C-N.M.R. studies of monomeric composition and sequence in alginate. *Carbohydrate research,* 89**,** 179-191.

GRASDALEN, H. 1983. High-field, ^{1}H-N.M.R. spectroscopy of alginate: sequential structure and linkage conformations. *Carbohydrate Research,* 118**,** 255-260.

GRASSI, M., COLOMBO, I. & LAPASIN, R. 2001. Experimental determination of the theophylline diffusion coefficient in swollen sodium-alginate membranes. *Journal of Controlled Release,* 76**,** 93-105.

GREGORIADIS, G. & FLORENCE, A. T. 1993. Liposomes in drug delivery, Clinical, diagnostic and ophthalmic potential. *Drugs,* 145**,** 15-28.

GRILL, B. B., LANGE, R., MARKOWITZ, R., HILLEMEIER, A. C., MCCALLUM, R. W. & GRYBOSKI, J. D. 1985. Delayed gastric emptying in children with Crohn's disease. *Journal of Clinical Gastroenterology,* 7**,** 216-226.

GRÖNING, R., CLOER, C., GEORGARAKIS, M. & MULLER, R. S. 2007. Compressed collagen sponges as gastroretentive dosage forms: in vitro and in vivo studies. *European Journal of Pharmaceutical Sciences,* 30**,** 1-6.

GRÖNING, R. & HEUN, G. 1984. Oral Dosage Forms with Controlled Gastrointestinal Transit. *Drug Development and Industrial Pharmacy,* 10**,** 527-539.

GRUBEL, P. & CAVE, D. R. 1998. Factors affecting solubility and penetration of clarithromycin through gastric mucus. *Alimentary Pharmacology & Therapeutics,* 12**,** 569-576.

GRUBER, P., RUBENSTEIN, A., LI, V. H., BASS, P. & ROBINSON, J. R. 1987. Gastric emptying of non-digestible solids in the fasted dog. *Journal of Pharmaceutical Sciences,* 76**,** 117-122.

GU, J. M., ROBINSON, J. R. & LEUNG, S. H. 1988. Binding of acrylic polymers to mucin/epithelial surfaces: structure-property relationships. *Critical Reviews in Therapeutic Drug Carrier Systems,* 5**,** 21-67.

GU, T. H., CHEN, S. X., ZHU, J. B., SONG, D. J., GUO, J. Z. & HOU, H. M. 1992. Pharmacokinetics and pharmacodynamics of diltiazem floating tablets. *Zhongguo yao li xue bao (Acta pharmacologica Sinica),* 13**,** 527-531.

GUJARATHI, N. A., RANE, B. R. & PATEL, J. K. 2012. pH sensitive polyelectrolyte complex of O-carboxymethyl chitosan and poly (acrylic acid) cross-linked with calcium for sustained delivery of acid susceptible drugs. *International Journal of Pharmaceutics,* 436**,** 418-425.

GUSLER, G., GORSLINE, J., LEVY, G., ZHANG, S. Z., WESTON, I. E., NARET, D. & BERNER, B. 2001. Pharmacokinetics of metformin gastric-retentive tablets in healthy volunteers. *Journal of Clinical Pharmacology,* 41**,** 655-661.

GUSTAVSON, L. E., KAISER, J. F., EDMONDS, A. L., LOCKE, C. S., DEBARTOLO, M. L. & SCHNECK, D. W. 1995. Effect of omeprazole on concentrations of clarithromycin in plasma and gastric tissue at steady state. *Antimicrobial Agents and Chemotherapy,* 39**,** 2078-2083.

HAAS, J. & LEHR, C. M. 2002. Developments in the area of bioadhesive drug delivery systems. *Expert Opinion on Biological Therapy,* 2**,** 287-298.

HADI, M. A., SRINIVASA RAO, A., MARTHA, S., SIRISHA, Y. & UDAYA CHANDRIKA, P. 2013. Development of a floating multiple unit controlled-release beads of zidovudine for the treatment of AIDS. *Journal of Pharmacy Research,* 6**,** 78-83.

HAEBERLE, S., NAEGELE, L., BURGER, R., STETTEN, F. V., ZENGERLE, R. & DUCRÉE, J. 2008. Alginate bead fabrication and encapsulation of living cells under centrifugally induced artificial gravity conditions. *Journal of Microencapsulation,* 25**,** 267-274.

HALDER, A., MAITI, S. & SA, B. 2005. Entrapment efficiency and release characteristics of polyethyleneimine-treated or untreated calcium alginate beads loaded with propranolol–resin complex. *International Journal of Pharmaceutics,* 302**,** 84-94.

HANCOCK, B. C. & MULLARNEY, M. P. 2005. Xray Microtomography of solid dosage forms. *Pharmaceutical Technology* [Online]. Available: http://www.pharmtech.com/pharmtech/data/articlestandard//pharmtech/172005/156853/article.pdf [Accessed 12/12/2013].

HARDING, S. E., DAVIS, S. S., DEACON, M. P. & FIEBRIG, I. 1999. Biopolymer mucoadhesives. *Biotechnology and Genetic Engineering Reviews, 6,* 16**,** 41-86.

HARDY, D. J., GUAY, D. R. & JONES, R. N. 1992. Clarithromycin, a unique macrolide. A pharmacokinetic, microbiological, and clinical overview. *Diagnostic Microbiology and Infectious Disease,* 15**,** 39-53.

HARI, P. R., CHANDY, T. & SHARMA, C. P. 1996. Chitosan/calcium alginate microcapsules for intestinal delivery of nitrofurantoin. *Journal of Microencapsulation,* 13**,** 319-329.

HARLAND, R. S., GAZZANIGA, A., SANGALLI, M. E., COLOMBO, P. & PEPPAS, N. A. 1988. Drug/polymer matrix swelling and dissolution. *Pharmaceutical Research,* 5**,** 488-494.

HARRIGAN, R. M. 1977. *Drug delivery device for preventing contact of undissolved drug with the stomach lining.* United States patent application. October 25, 1977.

HAUG, A. 1974. Uronic acid sequence in alginate from different sources. *Carbohydrate research,* 32**,** 217-225.

HAUG, A., LARSEN, B. & SMIRSROD, O. 1963. The degradation of alginate at different pH values. *Acta Chemica Scandinavica,* 17**,** 1466-1468.

HE, P., DAVIS, S. S. & ILLUM, L. 1998. In vitro evaluation of the mucoadhesive properties of chitosan microspheres. *International Journal of Pharmaceutics,* 166**,** 75-88.

HE, P., DAVIS, S. S. & ILLUM, L. 1999a. Chitosan microspheres prepared by spray drying. *International Journal of Pharmaceutics,* 187**,** 53-65.

HE, P., DAVIS, S. S. & ILLUM, L. 1999b. Sustained release chitosan microspheres prepared by novel spray drying methods. *Journal of Microencapsulation,* 16**,** 343-355.

HENRIKSEN, I., GREEN, K. L., SMART, J. D., SMISTAD, G. & KARLSEN, J. 1996. Bioadhesion of hydrated chitosans: An in vitro and in vivo study. *International Journal of Pharmaceutics,* 145**,** 231-240.

HERRERA, A. G. 2004. Helicobacter pylori and food products: a public health problem. *Methods in Molecular Biology,* 268**,** 297-301.

HESSEY, S. J., SPENCER, J., WYATT, J. I., SOBALA, G., RATHBONE, B. J., AXON, A. T. & DIXON, M. F. 1990. Bacterial adhesion and disease activity in Helicobacter associated chronic gastritis. *Gut.,* 31**,** 134-8.

HEYRAUD, A., GEY, C., LEONARD, C., ROCHAS, C., GIROND, S. & KLOAREG, B. 1996. NMR spectroscopy analysis of oligoguluronates and oligomannuronates prepared by acid or enzymatic hydrolysis of homopolymeric blocks of alginic acid. Application to the determination of the substrate specificity of Haliotis tuberculata alginate lyase. *Carbohydrate Research,* 289**,** 11-23.

HIBI, T., OGATA, H. & SAKURABA, A. 2002. Animal models of inflammatory bowel disease. *Journal of Gastroenterology,* 37**,** 409-417.

HICKS, S. J., CORFIELD, A. P., KASWAN, R. L., HIRSH, S., STERN, M., BARA, J. & CARRINGTON, S. D. 1998. Biochemical Analysis of Ocular Surface Mucin Abnormalities in Dry Eye: The Canine Model. *Experimental Eye Research,* 67**,** 709-718.

HIGUCHI, T. 1963. Mechanism of sustained-action medication. Theoretical analysis of rate of release of solid drugs dispersed in solid matrices. *Journal of Pharmaceutical Sciences,* 52**,** 1145-1149.

HIRAI, I., SASAKI, T., FUJIMOTO, S., MORIYAMA, T., AZUMA, T. & YAMAMOTO, Y. 2009. A method for assessment of Helicobacter pylori genotype using stool specimens. *FEMS Immunology & Medical Microbiology,* 56**,** 63-66.

HIXSON, A. W. & CROWELL, J. H. 1931. Dependence of Reaction Velocity upon surface and Agitation. *Industrial & Engineering Chemistry,* 23**,** 923-931.

HOFFMAN, A. 1998. Pharmacodynamic aspects of sustained release preparations. *Advanced Drug Delivery Reviews,* 33**,** 185-199.

HOFFMAN, A. S. 2002. Hydrogels for biomedical applications. *Advanced Drug Delivery Reviews,* 54**,** 3-12.

HOICHMAN, D., GROMOVA, I. & SELA, J. 2004. Gastro-retentive controlled release drugs. *Pharmaceutical Chemistry Journal,* 38**,** 621-624.

HOPKINS, R. J., VIAL, P. A., FERRECCIO, C., OVALLE, J., PRADO, P., SOTOMAYOR, V., RUSSELL, R. G., WASSERMAN, S. S. & MORRIS, J. G., JR. 1993. Seroprevalence of Helicobacter pylori in Chile: vegetables may serve as one route of transmission. *Journal of Infectious Diseases,* 168**,** 222-226.

HORIKI, N., OMATA, F., UEMURA, M., SUZUKI, S., ISHII, N., IIZUKA, Y., FUKUDA, K., FUJITA, Y., KATSURAHARA, M., ITO, T., CESAR, G. E., IMOTO, I. & TAKEI, Y. 2009. Annual change of primary resistance to clarithromycin among Helicobacter pylori isolates from 1996 through 2008 in Japan. *Helicobacter,* 14**,** 86-90. .

HOROWITZ, M., WISHART, J. M., JONES, K. L. & HEBBARD, G. S. 1996. Gastric emptying in diabetes: an overview. *Diabetic Medicine,* 13**,** S16-S22.

HSU, P. I., WU, D. C., CHEN, A., PENG, N. J., TSENG, H. H., TSAY, F. W., LO, G. H., LU, C. Y., YU, F. J. & LAI, K. H. 2008. Quadruple rescue therapy for Helicobacter pylori infection after two treatment failures. *European Journal of Clinical Investigation,* 38**,** 404-409.

HUANG, K., LEE, B. P., INGRAM, D. R. & MESSERSMITH, P. B. 2002. Synthesis and characterization of self-assembling block copolymers containing bioadhesive end groups. *Biomacromolecules,* 3**,** 397-406.

HUANG, X. & BRAZEL, C. S. 2001. On the importance and mechanisms of burst release in matrix-controlled drug delivery systems. *Journal of Controlled Release,* 73**,** 121-136.

HUANG, Y., LEOBANDUNG, W., FOSS, A. & PEPPAS, N. A. 2000. Molecular aspects of muco- and bioadhesion:: Tethered structures and site-specific surfaces. *Journal of Controlled Release,* 65**,** 63-71.

HUANG, Y. C., CHIANG, C. H. & YEH, M. K. 2003. Optimizing formulation factors in preparing chitosan microparticles by spray-drying method. *Journal of Microencapsulation,* 20**,** 247-260.

HUDSON, S. M. & JENKINS, D. W. 2001. Chitin and Chitosan. *In***:** MARKS, H. F., KROSCHWITZ, J. T., & BIKALES, N. (ed.) *Encyclopedia of polymer science and technology.* New York: John Wiley and Sons.

HUGUET, M. L., GROBOILLOT, A., NEUFELD, R. J., PONCELET, D. & DELLACHERIE, E. 1994. Hemolglobin encapsulation in chitosan/calcium alginate beads. *Journal of Applied Polymer Science,* 51**,** 1427-1432.

HULTEN, K., HAN, S. W., ENROTH, H., KLEIN, P. D., OPEKUN, A. R., GILMAN, R. H., EVANS, D. G., ENGSTRAND, L., GRAHAM, D. Y. & EL-ZAATARI, F. A. 1996. Helicobacter pylori in the drinking water in Peru. *Gastroenterology,* 110**,** 1031-1035.

HUNT, J. N. & KNOX, M. T. 1968. Regulation of gastric emptying. *In:* CODE, C. F. (ed.) *Handbook of Physiology.* Washington DC: American Physiology Society.

HWANG, S. J., PARK, H. & PARK, K. 1998. Gastric retentive drug-delivery systems. *Critical Reviews in Therapeutic Drug Carrier Systems,* 15**,** 243-284.

HWANG, S. J., RHEE, G. J., JO, H. B., LEE, K. M. & KIM, C. K. 1993. Alginate beads as controlled release polymeric drug delivery system. *Journal of Korean Pharmaceutical Science,* 23**,** 19-26.

IANNUCCELLI, V., COPPI, G., BERNABEI, M. T. & CAMERONI, R. 1998. Air compartment multiple-unit system for prolonged gastric residence. Part I. Formulation study. *International Journal of Pharmaceutics,* 174**,** 47-54.

ICHIKAWA, M., KATO, T., KAWAHARA, M., WATANABE, S. & KAYANO, M. 1991. A new multiple-unit oral floating dosage system. II: In vivo evaluation of floating and sustained-release characteristics with p-aminobenzoic acid and isosorbide dinitrate as model drugs. *Journal of Pharmaceutical Sciences,* 80**,** 1153-1156.

IIJIMA, K., SEKINE, H., KOIKE, T., IMATANI, A., OHARA, S. & SHIMOSEGAWA, T. 2004. Long-term effect of Helicobacter pylori eradication on the reversibility of acid secretion in profound hypochlorhydria. *Alimentary Pharmacology & Therapeutics,* 19**,** 1181-1188.

IKEDA, K., MURATA, K., KOBAYASHI, M. & NODA, K. 1992. Enhancement of bioavailability of dopamine via nasal route in beagle dogs. *Chemical and Pharmaceutical Bulletin (Tokyo),* 40**,** 2155-2158.

ILLUM, L. 1998. Chitosan and its use as a pharmaceutical excipient. *Pharmaceutical Research,* 15**,** 1326-1331.

ILLUM, L., FARAJ, N. F., CRITCHLEY, H., JOHANSEN, B. R. & DAVIS, S. S. 1989. Enhanced nasal absorption of insulin in rats using lysophosphatidylcholine. *International Journal of Pharmaceutics,* 57**,** 49-54.

IMRIE, C., ROWLAND, M., BOURKE, B. & DRUMM, B. 2001. Is Helicobacter pylori infection in childhood a risk factor for gastric cancer? *Pediatrics,* 107**,** 373-380.

INOUE, Y., YOSHIMURA, S., TOZUKA, Y., MORIBE, K., KUMAMOTO, T., ISHIKAWA, T. & YAMAMOTO, K. 2007. Application of ascorbic acid 2-glucoside as a solubilizing agent for clarithromycin: solubilization and nanoparticle formation. *International Journal of Pharmaceutics,* 331**,** 38-45.

IRACHE, J. M., DURRER, C., DUCHENE, D. & PONCHEL, G. 1994. Preparation and characterization of lectin-latex conjugates for specific bioadhesion. *Biomaterials,* 15**,** 899-904.

ISHAK, R. A., AWAD, G. A., MORTADA, N. D. & NOUR, S. A. 2007. Preparation, in vitro and in vivo evaluation of stomach-specific metronidazole-loaded alginate beads as local anti-Helicobacter pylori therapy. *Journal of Controlled Release,* 119**,** 207-214.

JAHAN, S. T., SADAT, S. M. A., ISLAM, M. R., AZAM, A. T. M. Z. & CHOWDHURY, J. A. 2012. Effect of Various Electrolytes on Theophylline Loaded Sodium Alginate Beads Prepared by Ionic Cross Linking Technique. *Dhaka University Journal of Pharmaceutical Sciences,* 11**,** 181-189.

JAIN, S. K. & JANGDEY, M. S. 2009. Lectin Conjugated Gastroretentive Multiparticulate Delivery System of Clarithromycin for the Effective Treatment of Helicobacter pylori. *Molecular Pharmaceutics,* 6**,** 295-304.

JAISWAL, D., BHATTACHARYA, A., YADAV, D. K., SINGH, H. P., CHANDRA, D. & JAIN, D. A. 2009. Formulation and evaluation of oil entrapped floating alginate beads of ranitidine hydrochloride. *International Journal of Pharmacy and Pharmaceutical Sciences,,* 1, Suppl 1**,** 128-140.

JANG, S. W., LEE, J. W., PARK, S. H., KIM, J. H., YOO, M., NA, D. H. & LEE, K. C. 2008. Gastroretentive drug delivery system of DA-6034, a new flavonoid derivative, for the treatment of gastritis. *International Journal of Pharmaceutics,* 356**,** 88-94.

JANSSEN, M. J., HENDRIKSE, L., DE BOER, S. Y., BOSBOOM, R., DE BOER, W. A., LAHEIJ, R. J. & JANSEN, J. B. 2006. Helicobacter pylori antibiotic resistance in a Dutch region: trends over time. *Netherlands Journal of Medicine,* 64**,** 191-195.

JAVADZADEH, Y., HAMEDEYAZDAN, S., ADIBKIA, K., KIAFAR, F., ZARRINTAN, M. H. & BARZEGAR-JALALI, M. 2010. Evaluation of drug release kinetics and

physico-chemical characteristics of metronidazole floating beads based on calcium silicate and gas-forming agents. *Pharmaceutical Development and Technology,* 15**,** 329-338.

JAVADZADEH, Y., MUSAALREZAEI, L. & NOKHODCHI, A. 2008. Liquisolid technique as a new approach to sustain propranolol hydrochloride release from tablet matrices. *International Journal of Pharmaceutics,* 362**,** 102-108.

JELVEHGARI, M., HASSANZADEH, D., KIAFAR, F., DELF LOVEYM, B. & AMIRI, S. 2011. Preparation and Determination of Drug-Polymer Interaction and In-vitro Release of Mefenamic Acid Microspheres Made of CelluloseAcetate Phthalate and/or Ethylcellulose Polymers. *Iranian Journal of Pharmaceutical Research,* 10**,** 457-467.

JOHNSON, L. R., CHRISTENSEN, J., JACKSON, M., J., JACOBSON , E. D. & WALSH, J. H. 1987. *Physiology of the gastrointestinal tract,* United Kingdom, Raven Press.

JOSHI, H. N. & WILSON, T. D. 1993. Calorimetric studies of dissolution of hydroxypropyl methylcellulose E5 (HPMC E5) in water. *Journal of Pharmaceutical Sciences,* 82**,** 1033-1038.

KANIWA, N., AOYAGI, N., OGATA, H., EJIMA, A., MOTOYAMA, H. & YASUMI, H. 1988. Gastric emptying rates of drug preparations. II. Effects of size and density of enteric-coated drug preparations and food on gastric emptying rates in humans. *Journal of Pharmacobiodynamics,* 11**,** 571-575.

KAMBA, M., SETA, Y., KUSAI, A., IKEDA, M. & NISHIMURA, K. 2000. A unique dosage form to evaluate the mechanical destructive force in the gastrointestinal tract. *International Journal of Pharmaceutics,* 208**,** 61-70.

KAO, C.-Y., LEE, A.-Y., HUANG, A.-H., SONG, P.-Y., YANG, Y.-J., SHEU, S.-M., CHANG, W.-L., SHEU, B.-S. & WU, J.-J. 2014. Heteroresistance of Helicobacter pylori from the same patient prior to antibiotic treatment. *Infection, Genetics and Evolution,* 23**,** 196-202.

KAS, H. S. 1997. Chitosan: properties, preparations and application to microparticulate systems. *Journal of Microencapsulation,* 14**,** 689-711.

KAWAHARA, Y., MIZUNO, M., YOSHINO, T., YOKOTA, K., OGUMA, K., OKADA, H., FUJIKI, S. & SHIRATORI, Y. 2005. HLA-DQA1*0103-DQB1*0601 haplotype and Helicobacter pylori-positive gastric mucosa-associated lymphoid tissue lymphoma. *Clinical of Gastroenterology and Hepatology,* 3**,** 865-868.

KAWASHIMA, S. I., JP), & MURATA, Y. I., JP). 2001. *Gel compositions*. United States patent application US 09/396,988.

KAWASHIMA, Y., NIWA, T., TAKEUCHI, H., HINO, T. & ITO, Y. 1991. Preparation of multiple unit hollow microspheres (microballoons) with acrylic resin containing tranilast and their drug release characteristics (in vitro) and floating behavior (in vivo). *Journal of Controlled Release,* 16**,** 279-289.

KEDZIEREWICZ, F., THOUVENOT, P., LEMUT, J., ETIENNE, A., HOFFMAN, M. & MAINCENT, P. 1999. Evaluation of peroral silicone dosage forms in humans by gamma-scintigraphy. *Journal of Controlled Release,* 58**,** 195-205.

KHAMES, A., ABDELAZEEM, A. H., HABASH, M. & TAHA, M. O. 2014. Preparation and in vitro characterization of glibenclamide-loaded alginate hexyl-amide beads: a novel drug delivery system to improve the dissolution rate. *Pharmaceutical Development and Technology,* 19**,** 881-890.

KHAN, A. D. & BAJPAI, M. 2011. Formulation and Evaluation of Floating beads of Verapamil hydrochloride. *International Journal of PharmTech Research,* 3**,** 1537-1546.

KHANDAI, M., CHAKRABORTY, S., SHARMA, A., PATTNAIK, S., PATRA, C. N., DINDA, S. C. & SEN, K. K. 2010. Preparation and evaluation of algino-secrin mucoadhesive microspheres: An approach for sustained drug delivery. *Journal of Advanced Pharmaceutical Research,* 1**,** 48-60.

KHANVILKAR, K., DONOVAN, M. D. & FLANAGAN, D. R. 2001. Drug transfer through mucus. *Advanced Drug Delivery Reviews,* 48**,** 173-193.

KHOSLA, R. & DAVIS, S. S. 1987. The effect of polycarbophil on the gastric emptying of pellets. *Journal of Pharmacy and Pharmacology,* 39**,** 47-49.

KHOSLA, R., FEELY, L. C. & DAVIS, S. S. 1989. Gastrointestinal transit of non-disintegrating tablets in fed subjects. *International Journal of Pharmaceutics,* 53**,** 107-117.

KIERSTAN, M. & BUCKE, C. 2000. Immobilization of microbial cells, subcellular organelles, and enzymes in calcium alginate gels. *Biotechnology and Bioengineering,* 67**,** 726-736.

KIKUCHI, A., KAWABUCHI, M., WATANABE, A., SUGIHARA, M., SAKURAI, Y. & OKANO, T. 1999. Effect of Ca2+-alginate gel dissolution on release of dextran with different molecular weights. *Journal of Controlled Release,* 58**,** 21-28.

KIM, C.-K. & LEE, E.-J. 1992. The controlled release of blue dextran from alginate beads. *International Journal of Pharmaceutics,* 79**,** 11-19.

KIM, S. Y., CHO, S. M., LEE, Y. M. & KIM, S. J. 2000. Thermo- and pH-responsive behaviors of graft copolymer and blend based on chitosan and N-isopropylacrylamide. *Journal of Applied Polymer Science,* 78**,** 1381-1391.

KIM, T. H. & PARK, T. G. 2004. Critical effect of freezing/freeze-drying on sustained release of FITC-dextran encapsulated within PLGA microspheres. *International Journal of Pharmaceutics,* 271**,** 207-214.

KING, G., DAUGULIS, A., FAULKNER, P. & GOOSEN, M. 1987. Alginate-Polylysine Microcapsules of Controlled Membrane Molecular Weight Cutoff for Mammalian Cell Culture Engineering. *Biotechnology Progress,* 3**,** 231-240.

KINLOCH, A. J. 1980. The Science of Adhesion - Part 1 Surface and interfacial aspects. *Journal of Materials Science,* 15**,** 2141-2166.

KISS, D., ZELKÓ, R., NOVÁK, C. & ÉHEN, Z. 2006. Application of DSC and NIRS to study the compatibility of metronidazole with different pharmaceutical excipients. *Journal of Thermal Analysis and Calorimetry,* 84**,** 447-451.

KLAUSNER, E. A., EYAL, S., LAVY, E., FRIEDMAN, M. & HOFFMAN, A. 2003a. Novel levodopa gastroretentive dosage form: in-vivo evaluation in dogs. *Journal of Controlled Release,* 88**,** 117-126.

KLAUSNER, E. A., LAVY, E., BARTA, M., CSEREPES, E., FRIEDMAN, M. & HOFFMAN, A. 2003b. Novel gastroretentive dosage forms: evaluation of gastroretentivity and its effect on levodopa absorption in humans. *Pharmaceutical Research,* 20**,** 1466-1473.

KLAUSNER, E. A., LAVY, E., FRIEDMAN, M. & HOFFMAN, A. 2003c. Expandable gastroretentive dosage forms. *Journal of Controlled Release,* 90**,** 143-162.

KLAUSNER, E. A., LAVY, E., STEPENSKY, D., CSEREPES, E., BARTA, M., FRIEDMAN, M. & HOFFMAN, A. 2003d. Furosemide pharmacokinetics and pharmacodynamics following gastroretentive dosage form administration to healthy volunteers. *Journal of Clinical Pharmacology,* 43**,** 711-720.

KLAUSNER, E. A., LAVY, E., STEPENSKY, D., FRIEDMAN, M. & HOFFMAN, A. 2002. Novel gastroretentive dosage forms: evaluation of gastroretentivity and its effect on riboflavin absorption in dogs. *Pharmaceutical Research,* 19**,** 1516-1523.

KLOKK, T. I. & MELVIK, J. E. 2002. Controlling the size of alginate gel beads by use of a high electrostatic potential. *Journal of Microencapsulation,* 19**,** 415-424.

KNEAFSEY, B., O'SHAUGHNESSY, M. & CONDON, K. C. 1996. The use of calcium alginate dressings in deep hand burns. *Burns,* 22**,** 40-43.

KOLETZKO, S., RICHY, F., BONTEMS, P., CRONE, J., KALACH, N., MONTEIRO, M. L., GOTTRAND, F., CELINSKA-CEDRO, D., ROMA-GIANNIKOU, E., ORDERDA, G., KOLACEK, S., URRUZUNO, P., MARTINEZ-GOMEZ, M. J., CASSWALL, T., ASHORN, M., BODANSZKY, H. & MEGRAUD, F. 2006. Prospective multicentre study on antibiotic resistance of Helicobacter pylori strains obtained from children living in Europe. *Gut,* 55**,** 1711-1716.

KORJAMO, T., HEIKKINEN, A. T. & MÖNKKÖNEN, J. 2009. Analysis of unstirred water layer in in vitro permeability experiments. *Journal of Pharmaceutical Sciences,* 98**,** 4469-4479.

KOTESHWARA, K. B., THOPPIL, S. C. & NAHA, A. 2011. Design and development of multiparticulate drug delivery of metronidazole for targeted delivery to colon. *International Journal of Pharmacy & Technology,* 3**,** 3580-3589.

KROGEL, I. & BODMEIER, R. 1999. Development of a multifunctional matrix drug delivery system surrounded by an impermeable cylinder. *Journal of Controlled Release,* 61**,** 43-50.

KU, B. K. & KIM, S. S. 2002. Electrospray characteristics of highly viscous liquids. *Journal of Aerosol Science,* 33**,** 1361-1378.

KULKARNI, A. R., SOPPIMATH, K. S. & AMINABHAVI, T. M. 1999. Controlled release of diclofenac sodium from sodium alginate beads crosslinked with glutaraldehyde. *Pharmaceutica Acta Helvetiae,* 74**,** 29-36.

KULKARNI, A. R., SOPPIMATH, K. S., AMINABHAVI, T. M. & RUDZINSKI, W. E. 2001. In-vitro release kinetics of cefadroxil-loaded sodium alginate interpenetrating network beads. *European Journal of Pharmaceutics and Biopharmaceutics,* 51**,** 127-133.

LABY, R. H. 1974. *Device for administration to ruminants*. US patent application 3844285.

LAHEIJ, ROSSUM, L. G. M. V., JANSEN, STRAATMAN & VERBEEK 1999. Evaluation of treatment regimens to cure Helicobacter pylori infection - a meta-analysis. *Alimentary Pharmacology & Therapeutics,* 13**,** 857-864.

LAI, S. K., WANG, Y.-Y. & HANES, J. 2009. Mucus-penetrating nanoparticles for drug and gene delivery to mucosal tissues. *Advanced Drug Delivery Reviews,* 61**,** 158-171.

LARHED, A. W., ARTURSSON, P. & BJÖRK, E. 1998. The influence of intestinal mucus components on the diffusion of drugs. *Pharmaceutical Research,* 15**,** 66-71.

LAWRIE, G., KEEN, I., DREW, B., CHANDLER-TEMPLE, A., RINTOUL, L., FREDERICKS, P. & GRØNDAHL, L. 2007. Interactions between Alginate and Chitosan Biopolymers Characterized Using FTIR and XPS. *Biomacromolecules,* 8**,** 2533-2541.

LAYNE, E. 1957. Spectrophotometric and turbidimetric methods for measuring proteins. *Methods in Enzymology*. London: Academic Press.

LEE, B.-J. & MIN, G.-H. 1995. Preparation and release characteristics of polymer-reinforced and coated alginate beads. *Archives of Pharmacal Research,* 18**,** 183-188.

LEE, B. J., MIN, G. H. & CUI, J. H. 1999. Correlation of drug solubility with trapping efficiency and release characteristics of alginate beads. *Pharmacy and Pharmacology Communications,* 5**,** 85-89.

LEE, J.-H., PARK, T. G. & CHOI, H.-K. 2000a. Effect of formulation and processing variables on the characteristics of microspheres for water-soluble drugs prepared by

w/o/o double emulsion solvent diffusion method. *International Journal of Pharmaceutics,* 196**,** 75-83.

LEE, J. W., PARK, J. H. & ROBINSON, J. R. 2000b. Bioadhesive-based dosage forms: the next generation. *Journal of Pharmaceutical Sciences,* 89**,** 850-866.

LEE, S. P. & NICHOLLS, J. F. 1987. Diffusion of Charged Ions in Mucus Gel - Effect of Net Charge. *Biorheology,* 24**,** 565-569.

LEHMANN, F. S., TERRACCIANO, L., CARENA, I., BAERISWYL, C., DREWE, J., TORNILLO, L., DE LIBERO, G. & BEGLINGER, C. 2002. In situ correlation of cytokine secretion and apoptosis in Helicobacter pylori-associated gastritis. *American Journal of Physiology. Gastrointestinal Liver Physiology,* 283**,** G481-G488.

LEHR, C.-M., BODDÉ, H. E., BOUWSTRA, J. A. & JUNGINGER, H. E. 1993. A surface energy analysis of mucoadhesion II. Prediction of mucoadhesive performance by spreading coefficients. *European Journal of Pharmaceutical Sciences,* 1**,** 19-30.

LEHR, C.-M., BOUWSTRA, J. A., SCHACHT, E. H. & JUNGINGER, H. E. 1992a. In vitro evaluation of mucoadhesive properties of chitosan and some other natural polymers. *International Journal of Pharmaceutics,* 78**,** 43-48.

LEHR, C.-M., POELMA, F. G. J., JUNGINGER, H. E. & TUKKER, J. J. 1991. An estimate of turnover time of intestinal mucus gel layer in the rat in situ loop. *International Journal of Pharmaceutics,* 70**,** 235-240.

LEHR, C. M., BOUWSTRA, J. A., BODDE, H. E. & JUNGINGER, H. E. 1992b. A surface energy analysis of mucoadhesion: contact angle measurements on polycarbophil and pig intestinal mucosa in physiologically relevant fluids. *Pharmaceutical Research,* 9**,** 70-5.

LEOR, J., ABOULAFIA-ETZION, S., DAR, A., SHAPIRO, L., BARBASH, I. M., BATTLER, A., GRANOT, Y. & COHEN, S. 2000. Bioengineered cardiac grafts: A new approach to repair the infarcted myocardium? *Circulation,* 102**,** III56-III61.

LEUNG, S.-H. S. & ROBINSON, J. R. 1990. Polymer structure features contributing to mucoadhesion. II. *Journal of Controlled Release,* 12**,** 187-194.

LI, Y., HU, M., DU, Y., XIAO, H. & MCCLEMENTS, D. J. 2011. Control of lipase digestibility of emulsified lipids by encapsulation within calcium alginate beads. *Food Hydrocolloids,* 25**,** 122-130.

LIM, L. Y. & WAN, L. S. C. 1997. Propranolol hydrochloride binding in calcium alginate beads. *Drug Development and Industrial Pharmacy,* 23**,** 973-980.

LIN, Y. H., LIANG, H. F., CHUNG, C. K., CHEN, M. C. & SUNG, H. W. 2005. Physically crosslinked alginate/N,O-carboxymethyl chitosan hydrogels with calcium for oral delivery of protein drugs. *Biomaterials,* 26**,** 2105-2113.

LINDMARK, D. G. & MULLER, M. 1976. Antitrichomonad action, mutagenicity, and reduction of metronidazole and other nitroimidazoles. *Antimicrobial Agents and Chemotherapy,* 10**,** 476-482.

LIOU, J.-M., LIN, J.-T., CHANG, C.-Y., CHEN, M.-J., CHENG, T.-Y., LEE, Y.-C., CHEN, C.-C., SHENG, W.-H., WANG, H.-P. & WU, M.-S. 2010. Levofloxacin-based and clarithromycin-based triple therapies as first-line and second-line treatments for Helicobacter pylori infection: a randomised comparative trial with crossover design. *Gut,* 59**,** 572-578.

LIS, H. & SHARON, N. 1986. Lectins as molecules and as tools. *Annual Review of Biochemistry,* 55**,** 35-67.

LIU, J. H. & RILEY, D. A. 1998. Preparation of crystal form II of clarithromycin. US Patent 5844105 A, 1st December 1998.

LIU, X. D., BAO, D. C., XUE, W. M., XIONG, Y., YU, W. T., YU, X. J., MA, X. J. & YUAN, Q. 2003. Preparation of uniform calcium alginate gel beads by membrane emulsification coupled with internal gelation. *Journal of Applied Polymer Science,* 87**,** 848-852.

LIU, Z., LU, W., QIAN, L., ZHANG, X., ZENG, P. & PAN, J. 2005. In vitro and in vivo studies on mucoadhesive microspheres of amoxicillin. *Journal of Controlled Release,* 102**,** 135-144.

LOGAN, R. P., GUMMETT, P. A., SCHAUFELBERGER, H. D., GREAVES, R. R., MENDELSON, G. M., WALKER, M. M., THOMAS, P. H., BARON, J. H. & MISIEWICZ, J. J. 1994. Eradication of Helicobacter pylori with clarithromycin and omeprazole. *Gut,* 35**,** 323-326.

LOWRY, O. H., ROSEBROUGH, N. J., FARR, A. L. & RANDALL, R. J. 1951. Protein measurement with the Folin phenol reagent. *Journal of Biology and Chemistry,* 193**,** 265-275.

MA, N., XU, L., WANG, Q., ZHANG, X., ZHANG, W., LI, Y., JIN, L. & LI, S. 2008. Development and evaluation of new sustained-release floating microspheres. *International Journal of Pharmaceutics,* 358**,** 82-90.

MACADAM, A. 1993. The effect of gastro-intestinal mucus on drug absorption. *Advanced Drug Delivery Reviews,* 11**,** 201-220.

MACHIDA, Y., INOUYE, K., TOKUMURA, T., IWATA, M. & NAGAI, T. 1989. Preparation and evaluation of intragastric buoyant preparations. *Drug Design and Delivery,* 4**,** 155-161.

MAHFOUZ, N. M. & HASSAN, M. A. 2001. Synthesis, chemical and enzymatic hydrolysis, and bioavailability evaluation in rabbits of metronidazole amino acid ester prodrugs

with enhanced water solubility. *Journal of Pharmacy and Pharmacology,* 53**,** 841-848.

MAI, T. T. T., HA, P. T., PHAM, H. N., LE, T. T. H., PHAM, H. L., PHAN, T. B. H., TRAN, D. L. & NGUYEN, X. P. 2012. Chitosan and O-carboxymethyl chitosan modified Fe 3 O 4 for hyperthermic treatment. *Advances in Natural Sciences: Nanoscience and Nanotechnology,* 3 (015006)**,** 1-5.

MAITI, A. K., DHARA, A. K. & NANDA, A. 2012. Preparation and Evaluation of Starch coated Alginate Microsphere of Diclofenac potassium. *International Journal of PharmTech Research,* 4**,** 630-636.

MAITI, S., DEY, P., KAITY, S., RAY, S., MAJI, S. & SA, B. 2009. Investigation on Processing Variables for the Preparation of Fluconazole-Loaded Ethyl Cellulose Microspheres by Modified Multiple Emulsion Technique. *AAPS PharmSciTech,* 10**,** 703-715.

MALAKAR, J., NAYAK, A. K. & PAL, D. 2012. Development of cloxacillin loaded multiple-unit alginate-based floating system by emulsion-gelation method. *International Journal of Biological Macromolecules,* 50**,** 138-147.

MALAKAR, J., NAYAK, A. K., PAL, D. & JANA, P. 2013. Potato starch-blended alginate beads for prolonged release of tolbutamide: Development by statistical optimization and in vitro characterization. *Asian Journal of Pharmaceutics,* 7**,** 43-51.

MALFERTHEINER, P., MEGRAUD, F., O'MORAIN, C., BAZZOLI, F., EL-OMAR, E., GRAHAM, D., HUNT, R., ROKKAS, T., VAKIL, N. & KUIPERS, E. J. 2007. Current concepts in the management of Helicobacter pylori infection: the Maastricht III Consensus Report. *Gut,* 56**,** 772-781.

MALVIYA, S., PANDEY, J. & DWIVED, S. 2013. Formulation and evaluation of floating microbeads of Ciprofloxacin HCl by emulsion gelation method. *International Journal of Pharmacy & Life Science,* 4**,** 2876-2884.

MANDAL, S., KUMAR, S. S., KRISHNAMOORTHY, B. & BASU, S. K. 2010. Development and evaluation of calcium alginate beads prepared by sequential and simultaneous methods. *Brazilian Journal of Pharmaceutical Sciences,* 46**,** 785-793.

MANISHA, P., RANJANA, G., ASHOK, R., MAMMAN, K., SARAF, K. & SHUBHINI, A. 2010. A controlled release Theophylline loaded bouyant Sodium alginate microbeads for prolonged drug delivery to gastric mucosa. *Journal of Pharmaceutical Research,* 3**,** 758-762.

MANJANNA, K. M., RAJESH, K. S. & SHIVAKUMAR, B. 2013. Formulation and Optimization of Natural Polysaccharide Hydrogel Microbeads of Aceclofenac Sodium for Oral Controlled Drug Delivery. *American Journal of Medical Sciences and Medicine,* 1**,** 5-17.

MANO, J. F., KONIAROVA, D. & REIS, R. L. 2003. Thermal properties of thermoplastic starch/synthetic polymer blends with potential biomedical applicability. *Journal of Materials Science: Materials in Medicine,* 14**,** 127-135.

MANSOUR, K. B., BURUCOA, C., ZRIBI, M., MASMOUDI, A., KAROUI, S., KALLEL, L., CHOUAIB, S., MATRI, S., FEKIH, M., ZARROUK, S., LABBENE, M., BOUBAKER, J., CHEIKH, I., HRIZ, M., SIALA, N., AYADI, A., FILALI, A., MAMI, N., NAJJAR, T., MAHERZI, A., SFAR, M. & FENDRI, C. 2010. Primary resistance to clarithromycin, metronidazole and amoxicillin of Helicobacter pylori isolated from Tunisian patients with peptic ulcers and gastritis: a prospective multicentre study. *Annals of Clinical Microbiology and Antimicrobials,* 9**,** 22.

MANTLE, M. & ALLEN, A. 1978. A colorimetric assay for glycoproteins based on the periodic acid/Schiff stain [proceedings]. *Biochemical Society Transactions,* 6**,** 607-609.

MARSHALL, B. J. & WARREN, J. R. 1984. Unidentified curved bacilli in the stomach of patients with gastritis and peptic ulceration. *Lancet,* 1**,** 1311-1315.

MARTINAC, A., FILIPOVIĆ-GRČIĆ, J., VOINOVICH, D., PERISSUTTI, B. & FRANCESCHINIS, E. 2005. Development and bioadhesive properties of chitosan-ethylcellulose microspheres for nasal delivery. *International Journal of Pharmaceutics,* 291**,** 69-77.

MARTINSEN, A., SKJÅK-BRÆK, G. & SMIDSRØD, O. 1989. Alginate as immobilization material: I. Correlation between chemical and physical properties of alginate gel beads. *Biotechnology and Bioengineering,* 33**,** 79-89.

MASTIHOLIMATH, V. S., DANDAGI, P. M., GADAD, A. P., MATHEWS, R. & KULKARNI, A. R. 2008. In vitro and in vivo evaluation of ranitidine hydrochloride ethyl cellulose floating microparticles. *Journal of Microencapsulation,* 25**,** 307-14.

MATHARU, R. S. & SANGHAVI, N. M. 1992. Novel drug delivery system for captopril. *Drug Development and Industrial Pharmacy,* 18**,** 1567-1574.

MCHUGH, D. J. 1987. Production, properties and uses of alginates. *In:* MCHUGH, D. J. (ed.) *Production and Utilization of Products from Commercial Seaweeds.* Rome: Food and Agriculture Organization of the United Nations

MCKNIGHT, C. A., KU, A., GOOSEN, M. F. A., SUN, D. & PENNEY, C. 1988. Synthesis of Chitosan-Alginate Microcapsule Membranes. *Journal of Bioactive and Compatible Polymers,* 3**,** 334-355.

MEGRAUD, F. 1995. Transmission of Helicobacter pylori: faecal-oral versus oral-oral route. *Alimentary Pharmacology & Therapeutics,* 9 Suppl 2**,** 85-91.

MEGRAUD, F. 2004. Basis for the management of drug-resistant Helicobacter pylori infection. *Drugs,* 64**,** 1893-904.

MEGRAUD, F. 2007. Helicobacter pylori and antibiotic resistance. *Gut,* 56**,** 1502.

MEHTA, R. C., THANOO, B. C. & DELUCA, P. P. 1996. Peptide containing microspheres from low molecular weight and hydrophilic poly(d,l-lactide-co-glycolide). *Journal of Controlled Release,* 41**,** 249-257.

MENDALL, M. A., GOGGIN, P. M., MOLINEAUX, N., LEVY, J., TOOSY, T., STRACHAN, D., CAMM, A. J. & NORTHFIELD, T. C. 1994. Relation of Helicobacter pylori infection and coronary heart disease. *British Heart Journal,* 71**,** 437-439.

MENDELOVITS, A., PRAT, T., GONEN, Y. & RYTWO, G. 2012. Improved Colorimetric Determination of Chitosan Concentrations by Dye Binding. *Applied Spectroscopy,* 66**,** 979-982.

MENON, A., RITSCHEL, W. A. & SAKR, A. 1994. Development and evaluation of a monolithic floating dosage form for furosemide. *Journal of Pharmaceutical Sciences,* 83**,** 239-245.

MEURER, L. N. & BOWER, D. J. 2002. Management of Helicobacter pylori infection. *American Family Physician,* 65**,** 1327-1336.

MEYER, F. A. & SILBERBER, A. Structure and function of mucus. *In:* NUGENT, J. & O'CONNOR, M., eds. Respiratory Tract Mucus, Ciba Foundation Symposium, 1978 Amsterdam. Elsevier, 203–211.

MI, F.-L., SUNG, H.-W. & SHYU, S.-S. 2002. Drug release from chitosan–alginate complex beads reinforced by a naturally occurring cross-linking agent. *Carbohydrate Polymers,* 48**,** 61-72.

MIDOLO, P. D., TURNIDGE, J. D. & MUNCKHOF, W. J. 1996. Is bactericidal activity of amoxicillin against Helicobacter pylori concentration dependent? *Antimicrobial Agents and Chemotherapy,* 40**,** 1327-1328.

MILLER, L. J., MALAGELADA, J. R., LONGSTRETH, G. F. & GO, V. L. 1980. Dysfunctions of the stomach with gastric ulceration. *Digestive Diseases and Sciences,* 25**,** 857-864.

MINAMI, H. & MCCALLUM, R. W. 1984. The physiology and pathophysiology of gastric emptying in humans. *Gastroenterology,* 86**,** 1592-1610.

MIRALLES, B., MENGÍBAR, M., HARRIS, R. & HERAS, A. 2011. Suitability of a colorimetric method for the selective determination of chitosan in dietary supplements. *Food Chemistry,* 126**,** 1836-1839.

MLADENOVSKA, K., CRUAUD, O., RICHOMME, P., BELAMIE, E., RAICKI, R. S., VENIER-JULIENNE, M. C., POPOVSKI, E., BENOIT, J. P. & GORACINOVA, K. 2007. 5-ASA loaded chitosan–Ca–alginate microparticles: Preparation and physicochemical characterization. *International Journal of Pharmaceutics,* 345**,** 59-69.

MOAYYEDI, P., SAHAY, P., TOMPKINS, D. S. & AXON, A. T. 1995. Efficacy and optimum dose of omeprazole in a new 1-week triple therapy regimen to eradicate Helicobacter pylori. *European Journal of Gastroenterology & Hepatology,* 7**,** 835-640.

MOJAVERIAN, P. 1996. Evaluation of gastrointestinal pH and gastric residence time via the Heidelberg radiotelemetry capsule: Pharmaceutical application. *Drug Development Research,* 38**,** 73-85.

MOJAVERIAN, P., VLASSES, P. H., KELLNER, P. E. & ROCCI, M. L., JR. 1988. Effects of gender, posture, and age on gastric residence time of an indigestible solid: pharmaceutical considerations. *Pharmaceutical Research,* 5**,** 639-644.

MONTISCI, M. J., DEMBRI, A., GIOVANNUCI, G., CHACUN, H., DUCHENE, D. & PONCHEL, G. 2001. Gastrointestinal transit and mucoadhesion of colloidal suspensions of Lycopersicon esculentum L. and Lotus tetragonolobus lectin-PLA microsphere conjugates in rats. *Pharmaceutical Research,* 18**,** 829-837.

MOORE, J. W. & FLANNER, H. H. 1996. Mathematical comparison of curves with an emphasis on in vitro dissolution profiles. *Pharmaceutical Technology,* 20**,** 64-74.

MOREIRA, A. P. D., SADER, M. R. S., SOARES, G. D. D. A. & LEÃ£O, M. H. M. R. 2014. Strontium Incorporation on Microspheres of Alginate/β-tricalcium Phosphate as Delivery Matrices. *Materials Research* [Online], 17. Available: http://www.scielo.br/scielo.php?script=sci_arttext&pid=S151614392014005000095&nrm=iso [Accessed 03/07/2014].

MORENO, S. N. J., MASON, R. P., MUNIZ, R. P. A., CRUZ, F. S. & DOCAMPO, R. 1983. Generation of free radicals from metronidazole and other nitroimidazoles by Tritrichomonas foetus. *Journal of Biological Chemistry,* 258**,** 4051-4054.

MORGNER, A., BAYERDORFFER, E., NEUBAUER, A. & STOLTE, M. 2000. Gastric MALT lymphoma and its relationship to Helicobacter pylori infection: management and pathogenesis of the disease. *Microscopy Research and Technique,* 48**,** 349-356.

MORIMOTO, K., YAGAMUCHI, H., IWAKURA, Y., MORISAKA, K., OHASHI, Y. & Y., N. 1991. Effects of viscous hyaluronate sodium solutions on the nasal absorption of vasopressin and an analogue . *Pharmaceutical Research,* 8**,** 471-474.

MORIMOTO, S., MISAWA, Y., ASAKA, T., KONDOH, H. & WATANABE, Y. 1990. Chemical modification of erythromycins. VI. Structure and antibacterial activity of acid degradation products of 6-O-methylerythromycins A. *Journal of Antibiotics (Tokyo),* 43**,** 570-573.

MOSTAFAVI, A., EMAMI, J., VARSHOSAZ, J., DAVIES, N. M. & REZAZADEH, M. 2011. Development of a prolonged-release gastroretentive tablet formulation of

ciprofloxacin hydrochloride: Pharmacokinetic characterization in healthy human volunteers. *International Journal of Pharmaceutics,* 409**,** 128-136.

MUKHOPADHYAY, P., SARKAR, K., SOAM, S. & KUNDU, P. P. 2013. Formulation of pH-responsive carboxymethyl chitosan and alginate beads for the oral delivery of insulin. *Journal of Applied Polymer Science,* 129**,** 835-845.

MURALI, M. R., VASUDEVARAJ NAVEEN, S., GUE SON, C. & RAO BALAJI RAGHAVENDRAN, H. 2014. Current knowledge on alleviating Helicobacter pylori infections through the use of some commonly known natural products: bench to bedside. *Integrative Medicine Research,* 3**,** 111-118.

MURAMATSU, N. & KONDO, T. 1995. An approach to prepare microparticles of uniform size. *Journal of Microencapsulation,* 12**,** 129-136.

MURATA, Y., KOFUJI, K. & KAWASHIMA, S. 2003. Preparation of floating alginate gel beads for drug delivery to the gastric mucosa. *Journal of Biomaterials Science. Polymer Edition,* 14**,** 581-588.

MURATA, Y., SASAKI, N., MIYAMOTO, E. & KAWASHIMA, S. 2000. Use of floating alginate gel beads for stomach-specific drug delivery. *European Journal of Pharmaceutics and Biopharmaceutics,* 50**,** 221-226.

MURATA, Y., TONIWA, S., MIYAMOTO, E. & KAWASHIMA, S. 1999. Preparation of alginate gel beads containing chitosan nicotinic acid salt and the functions. *European Journal of Pharmaceutics and Biopharmaceutics,* 48**,** 49-52.

MURRAY, C. J. & LOPEZ, A. D. 1997. Mortality by cause for eight regions of the world: Global Burden of Disease Study. *Lancet,* 349**,** 1269-1276.

MURTAZA, G., AHMAD, A., WAHEED ASGHAR, A. & NAEEM AAMIR, M. 2009. Salbutamol sulphate-ethylcellulose microparticles: formulation and in-vitro evaluation with emphasis on mathematical approaches. *DARU Journal of Pharmaceutical Sciences,* 17**,** 209-216.

MUZZARELLI, R. A. A. 1998. Colorimetric Determination of Chitosan. *Analytical Biochemistry,* 260**,** 255-257.

NAGAHARA, N., AKIYAMA, Y., NAKAO, M., TADA, M., KITANO, M. & OGAWA, Y. 1998. Mucoadhesive microspheres containing amoxicillin for clearance of Helicobacter pylori. *Antimicrobial Agents and Chemotherapy,* 42**,** 2492-2494.

NAGAI, T., NISHIMOTO, Y., NAMBU, N., SUZUKI, Y. & SEKINE, K. 1984. Powder dosage form of insulin for nasal administration. *Journal of Controlled Release,* 1**,** 15-22.

NAGAR, H., BERGER, S. A., HAMMAR, B. & GOREA, A. 1989. Penetration of clindamycin and metronidazole into the appendix and peritoneal fluid in children. *European Journal of Clinical Pharmacology,* 37**,** 209-210.

NAHAR, S., KIBRIA, K. M., HOSSAIN, M. E., SULTANA, J., SARKER, S. A., ENGSTRAND, L., BARDHAN, P. K., RAHMAN, M. & ENDTZ, H. P. 2009. Evidence of intra-familial transmission of Helicobacter pylori by PCR-based RAPD fingerprinting in Bangladesh. *European Journal of Clinical Microbiology & Infectious Diseases* 28**,** 767-773.

NAISBETT, B. & WOODLEY, J. 1995. The potential use of tomato lectin for oral drug delivery:3.Bioadhesion in vivo. *International Journal of Pharmaceutics,* 114**,** 227-236.

NAJIB, N. & SULEIMAN, M. S. 1985. The Kinetics of Drug Release from Ethylcellulose Solid Dispersions. *Drug Development and Industrial Pharmacy,* 11**,** 2169-2181.

NAKAGAWA, Y., ITAI, S., YOSHIDA, T. & NAGAI, T. 1992. Physicochemical properties and stability in the acidic solution of a new macrolide antibiotic, clarithromycin, in comparison with erythromycin. *Chemical and Pharmaceutical Bulletin (Tokyo),* 40**,** 725-728.

NAMA, M., GONUGUNTA, C. S. & REDDY VEERAREDDY, P. 2008. Formulation and evaluation of gastroretentive dosage forms of Clarithromycin. *AAPS PharmSciTech,* 9**,** 231-237.

NARKAR, M., SHER, P. & PAWAR, A. 2010. Stomach-Specific Controlled Release Gellan Beads of Acid-Soluble Drug Prepared by Ionotropic Gelation Method. *AAPS PharmSciTech,* 11**,** 267-277.

NARRA, K., DHANALEKSHMI, U., RANGARAJ, G., RAJA, D., SENTHIL KUMAR, C., NEELAKANTA REDDY, P. & BARAN MANDAL, A. 2012. Effect of formulation variables on rifampicin loaded alginate beads. *Iranian Journal of Pharmaceutical Research,* 11**,** 715-721.

NASSAR, E. J., CIUFFI, K. J., RIBEIRO, S. J. L. & MESSADDEQ, Y. 2003. Europium incorporated in silica matrix obtained by sol-gel: luminescent materials. *Materials Research,* 6**,** 557-562.

NATH, B., KANTA NATH, L., MAZUMDER, B., KUMAR, P., SHARMA, N. & PRATAP SAHU, B. 2010. Preparation and Characterization of Salbutamol Sulphate Loaded Ethyl Cellulose Microspheres using Water-in-Oil-Oil Emulsion Technique. *Iranian Journal of Pharmaceutical Research,* 9**,** 97-105.

NAU, R., SORGEL, F. & EIFFERT, H. 2010. Penetration of drugs through the blood-cerebrospinal fluid/blood-brain barrier for treatment of central nervous system infections. *Clinical Microbiology Reviews,* 23**,** 858-883.

NAYAK, A. K., HASNAIN, M. S., BEG, S. & ALAM, M. I. 2010a. Mucoadhesive beads of gliclazide: Design, development, and evaluation. *Science Asia,* 36**,** 319-325.

NAYAK, A. K., MAJI, R. & DAS, B. K. 2010b. Gastro retentive drug delivery systems: a review. *Journal of Pharmaceutical and Clinical Research* 3**,** 2-10.

NAYAK, A. K., DAS, B. & MAJI, R. 2013. Gastroretentive hydrodynamically balanced systems of ofloxacin: In vitro evaluation. *Saudi Pharmaceutical Journal,* 21**,** 113-117.

NEU, H. C. 1991. The development of macrolides: clarithromycin in perspective. *Journal of Antimicrobial Chemotherapy,* 27 Suppl A**,** 1-9.

NIMASE, P. K. & VIDYASAGAR, G. 2010. Preparation and evaluation of floating calsium alginate beads of clarithromycin. *Der Pharmacia Sinica,* 1**,** 29-35.

NORRIS, D. A., PURI, N. & SINKO, P. J. 1998. The effect of physical barriers and properties on the oral absorption of particulates. *Advanced Drug Delivery Reviews,* 34**,** 135-154.

NOVOA, G. A. G., HEINÄMÄKI, J., MIRZA, S., ANTIKAINEN, O., IRAIZOZ COLARTE, A., SUZARTE PAZ, A. & YLIRUUSI, J. 2005. Physical solid-state properties and dissolution of sustained-release matrices of polyvinylacetate. *European Journal of Pharmaceutics and Biopharmaceutics,* 59**,** 343-350.

NUR, A. O. & ZHANG, J. S. 2000. Captopril floating and/or bioadhesive tablets: design and release kinetics. *Drug Development and Industrial Pharmacy,* 26**,** 965-969.

NUSSINOVITCH, A. & ZVITOV-MARABI, R. 2008. Unique shape, surface and porosity of dried electrified alginate gels. *Food Hydrocolloids,* 22**,** 364-372.

NYSTROM, C. & BREDENBERG, S. 2006. Rapid-acting pharmaceutical composition. Patent Number WO2004067004 A1.

O'NEIL , M. J. (ed.) 2006. *The Merck Index: An Encyclopedia of Chemicals, Drugs and Biologicals.,* New Jersey: Merck.

OLUKMAN, M., ŞANLı, O. & SOLAK, E. 2012. Release of Anticancer Drug 5-Fluorouracil from Different Ionically Crosslinked Alginate Beads. *Journal of Biomaterials and Nanobiotechnology,* 3**,** 469-479.

ØSTBERG, T., LUND, E. M. & GRAFFNER, C. 1994. Calcium alginate matrices for oral multiple unit administration: IV. Release characteristics in different media. *International Journal of Pharmaceutics,* 112**,** 241-248.

OTH, M., FRANZ, M., TIMMERMANS, J. & MOES, A. 1992. The bilayer floating capsule: a stomach-directed drug delivery system for misoprostol. *Pharmaceutical Research,* 9**,** 298-302.

OWEN, R. J. 1998. Helicobacter--species classification and identification. *British Medical Bulletin,* 54**,** 17-30.

OZDEMIR, N., ORDU, S. & OZKAN, Y. 2000. Studies of floating dosage forms of furosemide: in vitro and in vivo evaluations of bilayer tablet formulations. *Drug development and industrial pharmacy,* 26**,** 857-866.

PANDE, A. V., VAIDYA, P. D., ARORA, A. & DHOKA, M. V. 2010. In vitro and in vivo evaluation of ethyl cellulose based floating microspheres of cefpodoxime proxetil. *International Journal of Pharmaceutical & Biomedecical Research,* 1**,** 122-128.

PANDYA, S. J. 2008. An attractive biocompartible polymer for pharmaceutical application in various dosage forms : Chitosan. *Pharm.info.net* [Online], 8. Available: http://www.pharmainfo.net/pharma-student-magazine/attractive-biocompatible-polymer-pharmaceutical-application-various-dosage--0 [Accessed 28/10/2013]

PARASHAR, V., AHMAD, D., GUPTA, S. P., UPMANYU, N., PARASHAR, N. & MUDGAL, V. 2010. Formulation and evaluation of biodegradable microspheres of tinidazole. *International Journal of Drug Delivery,* 2**,** 238-241.

PARK, H. & ROBINSON, J. R. 1985. Physico-chemical properties of water insoluble polymers important to mucin/epithelial adhesion. *Journal of Controlled Release,* 2**,** 47-57.

PARK, H. & ROBINSON, J. R. 1987. Mechanisms of mucoadhesion of poly(acrylic acid) hydrogels. *Pharmaceutical Research,* 4**,** 457-464.

PARK, K. & ROBINSON, J. R. 1984. Bioadhesive polymers as platforms for oral-controlled drug delivery: method to study bioadhesion. *International Journal of Pharmaceutics,* 19**,** 107-127.

PARK, W. S. W. & SHARABY, H. P. 1993. *Physical Gels,* Lancaster, PA, Technomic Publishing.

PASPARAKIS, G. & BOUROPOULOS, N. 2006. Swelling studies and in vitro release of verapamil from calcium alginate and calcium alginate-chitosan beads. *International Journal of Pharmaceutics,* 323**,** 34-42.

PATEL, G. M. 2007. Floating Drug Delivery System: An innovative approach to prolong gastric retention. *Pharminfo.net* [Online], 5. http://www.pharmainfo.net/reviews/floating-drug-delivery-system-innovative-approach-prolong-gastric-retention [Accessed 03/04/2013].

PATEL, K. T., MAHAJAN, A. N. & SHAH, D. A. 2011. Studies in formulation development of chronotherapeutics dosage of model drug. *Der Pharmacia Lettre,* 3**,** 227-240.

PATEL, R., BATHE, R. S., KHOBRAGADE, D. & JADHAV, S. 2014. Formulation and evaluation of gastroretentive beads of ranitidine hydrochloride. *International Journal of Pharmacy and Pharmaceutical Sciences,,* 6**,** 237-242.

PATEL, R. P., DADHANI, B., LADANI, R., BARIA, A. H. & PATEL, J. 2010. Formulation, evaluation and optimization of stomach specific in situ gel of clarithromycin and metronidazole benzoate. *International Journal of Drug Delivery,* 2**,** 141-153.

PATEL, Y. L., SHER, P. & PAWAR, A. P. 2006. The effect of drug concentration and curing time on processing and properties of calcium alginate beads containing metronidazole by response surface methodology. *AAPS PharmSciTech,* 7**,** 86.

PATEL, J. K. & CHAVDA, J. R. 2008. Formulation and evaluation of stomach-specific amoxicillin-loaded carbopol-934P mucoadhesive microspheres for anti-Helicobacter pylori therapy. *Journal of Microencapsulation,,* 21**,** 1-12.

PATEL, J. K. & PATEL, M. M. 2007. Stomach specific anti-helicobacter pylori therapy: preparation and evaluation of amoxicillin-loaded chitosan mucoadhesive microspheres. *Current Drug Delivery,* 4**,** 41-50.

PATIL, P., CHAVANKE, D. & WAGH, M. 2012. A review on ionotropic gelation method: Novel approach for controlled gastroretentive gelispheres. *International Journal of Pharmacy and Pharmaceutical Sciences,,* 4**,** 27-32.

PATIL, S., SHARMA, S., NIMBALKAR, A. & PAWAR, A. 2006. Study of Formulation Variables on Properties of Drug-Gellan Beads by Factorial Design. *Drug Development and Industrial Pharmacy,* 32**,** 315-326.

PAWAR, A. P., GADHE, A. R., VENKATACHALAM, P., SHER, P. & MAHADIK, K. R. 2008. Effect of core and surface cross-linking on the entrapment of metronidazole in pectin beads. *Acta Pharmaceutica,* 58**,** 78-85.

PAWAR, V. K., KANSAL, S., GARG, G., AWASTHI, R., SINGODIA, D. & KULKARNI, G. T. 2011. Gastroretentive dosage forms: a review with special emphasis on floating drug delivery systems. *Drug Delivery,* 18**,** 97-110.

PEEUSH, S., KAPIL K, MANISHA & S, S. A. 2010. Evaluation of Acyclovir Loaded oil entrapped Calcium alginate Beads Prepared by Ionotropic Gelation Method. *International Journal of ChemTech Research,* 2**,** 2076-2085.

PENMAN, A. 1972. A method for the determination of uronic acid sequence in alginates. *Carbohydrate Research,* 25**,** 273-282.

PENNERS, G., LUSTIG, K. & JORG, P. V. G. 1997. *Expandable pharmaceutical forms*. US Patent 5,651,985. July 29, 1997.

PEPPAS, N. A. & BURI, P. A. 1985. Surface, interfacial and molecular aspects of polymer bioadhesion on soft tissues. *Journal of Controlled Release,* 2**,** 257-275.

PEPPAS, N. A. & SAHLIN, J. J. 1996. Hydrogels as mucoadhesive and bioadhesive materials: a review. *Biomaterials,* 17**,** 1553-1561.

PEREIRA, L., SOUSA, A., COELHO, H., AMADO, A. M. & RIBEIRO-CLARO, P. J. A. 2003. Use of FTIR, FT-Raman and 13C-NMR spectroscopy for identification of some seaweed phycocolloids. *Biomolecular Engineering,* 20**,** 223-228.

PETERSEN, A. M. & KROGFELT, K. A. 2003. Helicobacter pylori: an invading microorganism? A review. *FEMS Immunology & Medical Microbiology,* 36**,** 117-126.

PETERSON, W. L. 1991. Helicobacter pylori and Peptic Ulcer Disease. *New England Journal of Medicine,* 324**,** 1043-1048.

PHILIPPIDIS, A. 2013. NanoSight Sets Sights on Exosomes. *Genetic Engineering and Biotechnology News* [Online], 33. Available: http://www.genengnews.com/gen-articles/nanosight-sets-sights-on-exosomes/4912/ [Accessed 15/09/2014].

PHILIPPOVA, O. E., VOLKOV, E. V., SITNIKOVA, N. L., KHOKHLOV, A. R., DESBRIERES, J. & RINAUDO, M. 2001. Two Types of Hydrophobic Aggregates in Aqueous Solutions of Chitosan and Its Hydrophobic Derivative. *Biomacromolecules,* 2**,** 483-490.

PIKAL, M. J. 1990. Freeze-drying of proteins. Part II: formulation selection. *Biopharmaceutics,* 3**,** 18-27.

PIKAL, M. J. 2002. *Freeze drying,* New York, Marcel Dekker.

PILLAY, V. & FASSIHI, R. 1999. In vitro release modulation from crosslinked pellets for site-specific drug delivery to the gastrointestinal tract: II. Physicochemical characterization of calcium–alginate, calcium–pectinate and calcium–alginate–pectinate pellets. *Journal of Controlled Release,* 59**,** 243-256.

PISCITELLI, S. C., DANZIGER, L. H. & RODVOLD, K. A. 1992. Clarithromycin and azithromycin: new macrolide antibiotics. *Clinical Pharmacy,* 11**,** 137-152.

PONCHEL, G. & IRACHE, J. 1998. Specific and non-specific bioadhesive particulate systems for oral delivery to the gastrointestinal tract. *Advanced Drug Delivery Reviews,* 34**,** 191-219.

PUND, S., JOSHI, A., VASU, K., NIVSARKAR, M. & SHISHOO, C. 2011. Gastroretentive delivery of rifampicin: In vitro mucoadhesion and in vivo gamma scintigraphy. *International Journal of Pharmaceutics,* 411**,** 106-112.

RAFATI, H., COOMBES, A. G. A., ADLER, J., HOLLAND, J. & DAVIS, S. S. 1997. Protein-loaded poly(dl-lactide-co-glycolide) microparticles for oral administration: formulation, structural and release characteristics. *Journal of Controlled Release,* 43**,** 89-102.

RAHMAN, Z., K, K., RK, K., M, A., NA, C. & AA, S. 2006. Characterization of 5-fluorouracil microspheres for colonic delivery. *AAPS PharmSciTech,* 7**,** E113-E121.

RAJ, K. & PILLAI, K. 2013. Formulation And Evaluation Of Calcium Pectinate Floating Beads Of Clarithromycin. *International Journal of PharmTech Research,* 5**,** 781-789.

RAJALAKSHMI, G., DHULIPATI, R. & DAMODHARAN, N. 2013. Design and characterization of Ambroxol Hydrochloride sustained release microbeads. *International Journal of Biological & Pharmaceutical Research,* 4**,** 655-662.

RAJENDRAN, A. & BASU, S. K. 2009. Alginate-Chitosan Particulate System for Sustained Release of Nimodipine. *Tropical Journal of Pharmaceutical Research,* 8**,** 433-440.

RAJINIKANTH, P. S., ARUNAGARAN, L. N., BALASUBRAMANIAM, J. & MISHRA, B. 2008. Formulation and Evaluation of Clarithromycin Microspheres for Eradication of Helicobacter pylori. *Chemical and Pharmaceutical Bulletin,* 56**,** 1658-1664.

RAJINIKANTH, P. S. & MISHRA, B. 2008. Floating in situ gelling system for stomach site-specific delivery of clarithromycin to eradicate H-pylori. *Journal of Controlled Release,* 125**,** 33-41.

RAJINIKANTH, P. S. & MISHRA, B. 2009. Stomach-site specific drug delivery system of clarithromycin for eradication of Helicobacter pylori. *Chemical and Pharmaceutical Bulletin (Tokyo),* 57**,** 1068-1075.

RALPH, E. 1983. Clinical Pharmacokinetics of Metronidazole. *Clinical Pharmacokinetics,* 8**,** 43-62.

RAMACHANDRAN, S., SHAHEEDHA, S. M., THIRUMURUGAN, G. & DHANARAJU, M. D. 2010. Floating controlled drug delivery system of famotidine loaded hollow microspheres (microballoons) in the stomach. *Current Drug Delivery,* 7**,** 93-97.

RAMTEKE, S., RB UMAMAHESHWARI, R., B. & JAIN, N. K. 2006. Clarithromycin based oral sustained release nanoparticulate drug delivery system. *Indian Journal of Pharmaceutical Science,* 68**,** 479-484.

RAMUKUTTY, S. & RAMACHANDRAN, E. 2012. Crystal growth by solvent evaporation and characterization of metronidazole. *Journal of Crystal Growth,* 351**,** 47-50.

RASEL, M. A. T. & HASAN, M. 2012. Formulation and Evaluation of Floating Alginate Beads of Diclofenac Sodium. *Dhaka University Journal of Pharmaceutical Sciences,* 11**,** 29-35.

RASTELLO DE BOISSESON, M., LEONARD, M., HUBERT, P., MARCHAL, P., STEQUERT, A., CASTEL, C., FAVRE, E. & DELLACHERIE, E. 2004. Physical alginate hydrogels based on hydrophobic or dual hydrophobic/ionic interactions: Bead formation, structure, and stability. *Journal of Colloid and Interface Science,* 273**,** 131-139.

RASTOGI, R., SULTANA, Y., AQIL, M., ALI, A., KUMAR, S., CHUTTANI, K. & MISHRA, A. K. 2007. Alginate microspheres of isoniazid for oral sustained drug delivery. *International Journal of Pharmaceutics,* 334**,** 71-77

RAVINDRA, R., RAO, A. K. & KHAN, A. A. 1999. A qualitative evaluation of water and monomethyl hydrazine in ethylcellulose membrane. *Journal of Applied Polymer Science,* 72**,** 689-700.

REDDY, L. H. & MURTHY, R. S. 2002. Floating dosage systems in drug delivery. *Critical Reviews in Therapeutic Drug Carrier Systems,* 19**,** 553-585.

REDNICK, A. B. & TUCKER, S. J. 1970. *Sustained release bolus for animal husbandry.* United States patent application. 04/21/1970.

REYNOLDS, J. F. 1993. Metronidazole. *In:* MARTINDALE, W. (ed.) *The extra pharmacopoeia.* London, United Kingdom: Pharmaceutical Press (UK).

RIBEIRO, A. J., NEUFELD, R. J., ARNAUD, P. & CHAUMEIL, J. C. 1999. Microencapsulation of lipophilic drugs in chitosan-coated alginate microspheres. *International Journal of Pharmaceutics,* 187**,** 115-123.

RIBEIRO, A. J., SILVA, C., FERREIRA, D. & VEIGA, F. 2005. Chitosan-reinforced alginate microspheres obtained through the emulsification/internal gelation technique. *European Journal of Pharmaceutical Sciences,* 25**,** 31-40.

RILEY, R. G., SMART, J. D., TSIBOUKLIS, J., YOUNG, S. A., HAMPSON, F., DAVIS, A., KELLY, G., DETTMAR, P. W. & WILBER, W. R. 2002. An in vitro model for investigating the gastric mucosal retention of 14C-labelled poly(acrylic acid) dispersions. *International Journal of Pharmaceutics,* 236**,** 87-96.

RILLOSI, M. & BUCKTON, G. 1995. Modelling mucoadhesion by use of surface energy terms obtained from the Lewis acid-Lewis base approach. II. Studies on anionic, cationic, and unionisable polymers. *Pharmaceutical Research,* 12**,** 669-675.

RITGER, P. L. & PEPPAS, N. A. 1987. A simple equation for description of solute release II. Fickian and anomalous release from swellable devices. *Journal of Controlled Release,* 5**,** 37-42.

ROMERO, C., MEDINA, E., VARGAS, J., BRENES, M. & DE CASTRO, A. 2007. In vitro activity of olive oil polyphenols against Helicobacter pylori. *Journal of Agriculture and Food Chemistry,* 55**,** 680-686.

ROSSI, S., FERRARI, F., BONFERONI, M. C. & CARAMELLA, C. 2000. Characterization of chitosan hydrochloride-mucin interaction by means of viscosimetric and turbidimetric measurements. *European Journal of Pharmaceutical Sciences,* 10**,** 251-257.

ROSSI, S., FERRARI, F., BONFERONI, M. C. & CARAMELLA, C. 2001. Characterization of chitosan hydrochloride--mucin rheological interaction: influence of polymer concentration and polymer:mucin weight ratio. *European Journal of Pharmaceutical Sciences,* 12**,** 479-485.

ROTHENBACHER, D. & BRENNER, H. 2003. Burden of Helicobacter pylori and H. pylori-related diseases in developed countries: recent developments and future implications. *Microbes and Infection,* 5**,** 693-703.

ROUGE, N., ALLEMANN, E., GEX-FABRY, M., BALANT, L., COLE, E. T., BURI, P. & DOELKER, E. 1998. Comparative pharmacokinetic study of a floating multiple-unit capsule, a high-density multiple-unit capsule and an immediate-release tablet containing 25 mg atenolol. *Pharmaceutica acta Helvetiae,* 73**,** 81-87.

ROUGE, N., LEROUX, J.-C., COLE, E. T., DOELKER, E. & BURI, P. 1997. Prevention of the sticking tendency of floating minitablets filled into hard gelatin capsules. *European Journal of Pharmaceutics and Biopharmaceutics,* 43**,** 165-171.

ROWE, R. C., SHESKEY, P. J. & WELLER, P. J. 2003. *Handbook of pharmaceutical excipients,* London, Pharmaceutical Press.

ROWLAND, M., DALY, L., VAUGHAN, M., HIGGINS, A., BOURKE, B. & DRUMM, B. 2006. Age-specific incidence of Helicobacter pylori. *Gastroenterology,* 130**,** 65-72.

RUBINSTEIN, A. & FRIEND, D. R. 1994. *Polymeric Site-Specific Pharmacotherapy,* Chichester, Wiley-Blackwell

SAHASATHIAN, T., PRAPHAIRAKSIT, N. & MUANGSIN, N. 2010. Mucoadhesive and floating chitosan-coated alginate beads for the controlled gastric release of amoxicillin. *Archives of Pharmacal Research,* 33**,** 889-899.

SAKR, F. M. 1999. A programmable drug delivery system for oral administration. *International Journal of Pharmaceutics,* 184**,** 131-139.

SAKUGAWA, K., IKEDA, A., TAKEMURA, A. & ONO, H. 2004. Simplified method for estimation of composition of alginates by FTIR. *Journal of Applied Polymer Science,* 93**,** 1372-1377.

SALEM, I. I. 1996. Clarithromycin. *In:* BRITTAIN, H. G. (ed.) *Analytical Profiles of Drug Substances and Excipients.* London: Academic Press.

SALIH, B. A. 2009. Helicobacter pylori infection in developing countries: the burden for how long? *Saudi Journal of Gastroenterologyl,* 15**,** 201-207.

SANFORD, P. A. & BAIRD, J. 1983. *Industrial utilization of polysaccharides The Polysaccharides,* New York, Academic.

SANKALIA, M. G., MASHRU, R. C., SANKALIA, J. M. & SUTARIYA, V. B. 2005. Papain entrapment in alginate beads for stability improvement and site-specific delivery: physicochemical characterization and factorial optimization using neural network modeling. *AAPS PharmSciTech,* 6**,** E209-E222.

SANTOS, I. S., BOCCIO, J., DAVIDSSON, L., HERNANDEZ-TRIANA, M., HUANCA-SARDINAS, E., JANJETIC, M., MOYA-CAMARENA, S. Y., PAEZ-VALERY, M. C., RUIZ-ALVAREZ, V., VALENCIA, M. E., VALLE, N. C., VARGAS-PINTO, G., SOLANO, L. & THOMAS, J. 2009. Helicobacter pylori is not associated with anaemia in Latin America: results from Argentina, Brazil, Bolivia, Cuba, Mexico and Venezuela. *Public Health Nutrition,* 12**,** 1862-1870.

SATISHBABU, B. K., SANDEEP, V. R., RAVI, R. B. & SHRUTINAG, R. 2010. Formulation and evaluation of floating drug delivery system of famotidine. *Indian Journal of Pharmaceutical Science,* 72**,** 738-744.

SATTAR, M. A., SANKEY, M. G., CAWLEY, M. I., KAYE, C. M. & HOLT, J. E. 1982. The penetration of metronidazole into synovial fluid. *Postgraduate Medical Journal,* 58**,** 20-24.

SCHNURRER, J. & LEHR, C.-M. 1996. Mucoadhesive properties of the mussel adhesive protein. *International Journal of Pharmaceutics,* 141**,** 251-256.

SCHOLES, P. D., COOMBES, A. G. A., ILLUM, L., DAVIS, S. S., WATTS, J. F., USTARIZ, C., VERT, M. & DAVIES, M. C. 1999. Detection and determination of surface levels of poloxamer and PVA surfactant on biodegradable nanospheres using SSIMS and XPS. *Journal of Controlled Release,* 59**,** 261-278.

SCHWARTZ, D. E., JORDAN, J. C., VETTER, W. & OESTERHELT, G. 1979. Metabolic studies of ornidazole in the rat, in the dog and in man. *Xenobiotica,* 9**,** 571-581.

SEARLE, A. J. & WILLSON, R. L. 1976. Metronidazole (Flagyl): degradation by the intestinal flora. *Xenobiotica,* 6**,** 457-464.

SELLERS, L. A., ALLEN, A., MORRIS, E. R. & ROSS-MURPHY, S. B. 1987. Mechanical characterization and properties of gastrointestinal mucus gel. *Biorheology,* 24**,** 615-623.

SEZER, A. D. & AKBUGA, J. 1999. Release characteristics of chitosan treated alginate beads: I. Sustained release of a macromolecular drug from chitosan treated alginate beads. *Journal of Microencapsulation,* 16**,** 195-203.

SHAH, S., QAQISH, R., PATEL, V. & AMIJI, M. 1999. Evaluation of the factors influencing stomach-specific delivery of antibacterial agents for Helicobacter pylori infection. *Journal of Pharmacy and Pharmacology,* 51**,** 667-672.

SHAH, S. H., PATEL, J. K. & PATEL, N. V. 2009a. Gastroretentive floating drug delivery systems with potential herbal drugs for Helicobacter pylori eradication: a review. *Zhong Xi Yi Jie He Xue Bao (Journal of Chinese integrative medicine),* 7**,** 976-982.

SHAH, S. H., PATEL, J. K. & PATEL, N. V. 2009b. Stomach specific floating drug delivery system : A review. *International Journal of PharmTech Research,* 1**,** 623-633.

SHAH, V., TSONG, Y., SATHE, P. & LIU, J.-P. 1998. In Vitro Dissolution Profile Comparison—Statistics and Analysis of the Similarity Factor, f2. *Pharmaceutical Research,* 15**,** 889-896.

SHAIKH, A. A., PAWAR, Y. D. & KUMBHAR, S. T. 2012. Effect of Chitosan and Sodium Alginate on Mucoadhesion and Drug Release of Itraconazole Tablets. *International Journal of Research in Pharmaceutical and Biomedical Sciences,* 3**,** 293-298.

SHAIKH, R., RAJ SINGH, T. R., GARLAND, M. J., WOOLFSON, A. D. & DONNELLY, R. F. 2011. Mucoadhesive drug delivery systems. *Journal of Pharmacy and Bioallied Science,* 3**,** 89-100.

SHAN-YANG, L. & YUH-HORNG, K. 1989. Solid particulates of drug-β-cyclodextrin inclusion complexes directly prepared by a spray-drying technique. *International Journal of Pharmaceutics,* 56**,** 249-259.

SHELL, J. W., LOUIE-HELM, J. & MARKEY, M. 2002. *Extending the duration of drug release within the stomach during the fed mode*. US Patent 6340475. January 22, 2002.

SHERMAN, P. M. 2004. Appropriate strategies for testing and treating Helicobacter pylori in children: when and how? *The American Journal of Medicine,* 117 Suppl 5A**,** 30S-35S.

SHETH, P. R. & TOSSOUNIAN, J. 1984. The Hydrodynamically Balanced System (Hbs™): A Novel Drug Delivery System for Oral Use. *Drug Development and Industrial Pharmacy,* 10**,** 313-339.

SHETH, P. R. & TOSSOUNIAN, J. L. 1979. *Novel sustained release tablet formulations* . US patent application US Patent 4167558. September 11,1979.

SHI, J., ALVES, N. M. & MANO, J. F. 2008. Chitosan coated alginate beads containing poly(N-isopropylacrylamide) for dual-stimuli-responsive drug release. *Journal of Biomedical Materials Research Part B: Applied Biomaterials,* 84B**,** 595-603.

SHILPA, A., AGRAWAL, S. S. & RAY, A. R. 2003. Controlled Delivery of Drugs from Alginate Matrix. *Journal of Macromolecular Science, Part C,* 43**,** 187-221.

SHISHU, GUPTA, N. & AGGARWAL, N. 2007. Stomach-specific drug delivery of 5-fluorouracil using floating alginate beads. *AAPS PharmSciTech.,* 8**,** Article 48.

SHU, X. Z. & ZHU, K. J. 2002. The release behavior of brilliant blue from calcium-alginate gel beads coated by chitosan: the preparation method effect. *European Journal of Pharmaceutics and Biopharmaceutics,* 53**,** 193-201.

SIEPMANN, F., HOFFMANN, A., LECLERCQ, B., CARLIN, B. & SIEPMANN, J. 2007a. How to adjust desired drug release patterns from ethylcellulose-coated dosage forms. *Journal of Controlled Release,* 119**,** 182-189.

SIEPMANN, F., MUSCHERT, S., ZACH, S., LECLERCQ, B., CARLIN, B. & SIEPMANN, J. 2007b. Carrageenan as an Efficient Drug Release Modifier for Ethylcellulose-Coated Pharmaceutical Dosage Forms. *Biomacromolecules,* 8**,** 3984-3991.

SIEPMANN, F., WAHLE, C., LECLERCQ, B., CARLIN, B. & SIEPMANN, J. 2008. pH-sensitive film coatings: Towards a better understanding and facilitated optimization. *European Journal of Pharmaceutics and Biopharmaceutics,* 68**,** 2-10.

SIEPMANN, J. & PEPPAS, N. A. 2001. Modeling of drug release from delivery systems based on hydroxypropyl methylcellulose (HPMC). *Advanced Drug Delivery Reviews,* 48**,** 139-157.

SIGURDSSON, H. H., KIRCH, J. & LEHR, C.-M. 2013. Mucus as a barrier to lipophilic drugs. *International Journal of Pharmaceutics,* 453**,** 56-64.

SILVA, R. M., SILVA, G. A., COUTINHO, O. P., MANO, J. F. & REIS, R. L. 2004. Preparation and characterisation in simulated body conditions of glutaraldehyde

crosslinked chitosan membranes. *Journal of Material Science. Materials in Medicine,* 15**,** 1105-1112.

SILVERSTEIN, M. & WEBSTER, X. 1996. *Spectrometric identification of organic compounds,* New York, USA, John Wiley & Sons.

SIMENSEN, M. K., DRAGET, K., SMIDSROED, O. & HJELLAND, F. 1998. *Procedure for producing uronic acid blocks from alginate*. WO1998051710 A1. 19 Nov 1998.

SIMSEK-EGE, F. A., BOND, G. M. & STRINGER, J. 2003. Polyelectrolyte complex formation between alginate and chitosan as a function of pH. *Journal of Applied Polymer Science,* 88**,** 346-351.

SINGH, B., CHAKKAL, S. & AHUJA, N. 2006. Formulation and optimization of controlled release mucoadhesive tablets of atenolol using response surface methodology. *AAPS PharmSciTech,* 7**,** E19-E28.

SINGH, B. N. & KIM, K. H. 2000. Floating drug delivery systems: an approach to oral controlled drug delivery via gastric retention. *Journal of Controlled Release,* 63**,** 235-259.

SINGH, J. & ROBINSON, D. H. 1988. Controlled release captopril microcapsules: effect of non-ionic surfactants on release from ethyl cellulose microcapsules. *Journal of Microencapsulation,* 5**,** 129-137.

SINGH, R., MAITY, S. & SA, B. 2014. Effect of ionic crosslink on the release of metronidazole from partially carboxymethylated guar gum tablet. *Carbohydrate Polymers,* 106**,** 414-421.

SINGHAL, P., KUMAR, K., PANDEY, M. & SARAF, S. A. 2010. Evaluation of Acyclovir Loaded oil entrapped Calcium alginate Beads Prepared by Ionotropic Gelation Method. *International Journal of ChemTech Research,* 2**,** 2076-2085.

SMART, J. D. 2005. The basics and underlying mechanisms of mucoadhesion. *Advanced Drug Delivery Reviews,* 57**,** 1556-1568.

SMIDSRØD, O. 1974. Molecular basis for some physical properties of alginates in the gel state. *Faraday Discussions of the Chemical Society,* 57**,** 263-274.

SMIDSROD, O. & SKJAK-BRAEK, G. 1990. Alginate as immobilization matrix for cells. *Trends in Biotechnology,* 8**,** 71-78.

SMRDEL, P., BOGATAJ, M., PODLOGAR, F., PLANINSEK, O., ZAJC, N., MAZAJ, M., KAUCIC, V. & MRHAR, A. 2006. Characterization of calcium alginate beads containing structurally similar drugs. *Drug Development and Industrial Pharmacy,* 32**,** 623-33.

SMRDEL, P., BOGATAJ, M., ZEGA, A., PLANINSEK, O. & MRHAR, A. 2008a. Shape optimization and characterization of polysaccharide beads prepared by ionotropic gelation. *Journal of Microencapsulation,* 25**,** 90-105.

SMRDEL, P., BOGATAJ, M. & MRHAR, A. 2008b. The influence of selected parameters on the Size and Shape of Alginate beads prepared by ionotropic gelation. *Scientia Pharmaceutica,* 76**,** 77–89.

SOGIAS, I. A., WILLIAMS, A. C. & KHUTORYANSKIY, V. V. 2008. Why is chitosan mucoadhesive? *Biomacromolecules,* 9**,** 1837-1842.

SOHN, Y. T., RHEE, J. K. & IM, W. B. 2000. Polymorphism of Clarithromycin. *Archives of Pharmacal Research,* 23**,** 381-384.

SONI, M. L., KUMAR, M. & NAMDEO, K. P. 2010. Sodium alginate microspheres for extending drug release: formulation and in vitro evaluation. *International Journal of Drug Delivery,* 2**,** 64-68.

SOPPIMATH, K. S., KULKARNI, A. R., RUDZINSKI, W. E. & AMINABHAVI, T. M. 2001. Microspheres as floating drug-delivery systems to increase gastric retention of drugs. *Drug Metabolism Reviews,* 33**,** 149-160.

SORBERG, M., HANBERGER, H., NILSSON, M., BJORKMAN, A. & NILSSON, L. E. 1998. Risk of development of in vitro resistance to amoxicillin, clarithromycin, and metronidazole in Helicobacter pylori. *Antimicrobial Agents and Chemotherapy,* 42**,** 1222-1228.

SRAVANI, B., DEVESWARAN, R., BHARATH, S., BASAVARAJ, B. V. & MADHAVAN, V. 2011. Studies on Vigna Mungo Mucilage as a pharmaceutical excipient. *Journal of Chemical and Pharmaceutical Research,* 3**,** 118 -125.

SRIAMORNSAK, P., THIRAWONG, N. & PUTTIPIPATKHACHORN, S. 2004. Morphology and buoyancy of oil-entrapped calcium pectinate gel beads. *AAPS Journal,* 6**,** E24.

STOCKERT, R. J. & MORELL, A. G. 1983. Hepatic binding protein: the galactose-specific receptor of mammalian hepatocytes. *Hepatology,* 3**,** 750-757.

STOCKWELL, A. F., DAVIS, S. S. & WALKER, S. E. 1986. In vitro evaluation of alginate gel systems as sustained release drug delivery systems. *Journal of Controlled Release,* 3**,** 167-175.

STOPS, F., FELL, J. T., COLLETT, J. H. & MARTINI, L. G. 2008. Floating dosage forms to prolong gastro-retention--the characterisation of calcium alginate beads. *International Journal of Pharmaceutics,* 350**,** 301-311.

STORSKRUBB, T., ARO, P., RONKAINEN, J., WREIBER, K., NYHLIN, H., BOLLING-STERNEVALD, E., TALLEY, N. J., ENGSTRAND, L. & AGREUS, L. 2006. Antimicrobial susceptibility of Helicobacter pylori strains in a random adult Swedish population. *Helicobacter,* 11**,** 224-30.

STOSCHECK, C. M. 1990. Quantitation of protein. *In:* MURRAY, P. D. (ed.) *Methods in Enzymology*. London: Academic Press.

STREUBEL, A., SIEPMANN, J. & BODMEIER, R. 2002. Floating microparticles based on low density foam powder. *International Journal of Pharmaceutics,* 241**,** 279-292.

STREUBEL, A., SIEPMANN, J. & BODMEIER, R. 2003a. Multiple unit gastroretentive drug delivery systems: a new preparation method for low density microparticles. *Journal of Microencapsulation,* 20**,** 329-47.

STREUBEL, A., SIEPMANN, J. & BODMEIER, R. 2003b. Floating matrix tablets based on low density foam powder: effects of formulation and processing parameters on drug release. *European Journal of Pharmaceutical Sciences*, 18**,** 37-45.

STREUBEL, A., SIEPMANN, J. & BODMEIER, R. 2006. Drug delivery to the upper small intestine window using gastroretentive technologies. *Current Opinion in Pharmacology,* 6**,** 501-508.

STRUBING, S., ABBOUD, T., CONTRI, R. V., METZ, H. & MADER, K. 2008. New insights on poly(vinyl acetate)-based coated floating tablets: characterisation of hydration and CO2 generation by benchtop MRI and its relation to drug release and floating strength. *European Journal of Pharmaceutics and Biopharmaceutics,* 69**,** 708-717.

STURGILL, M. G. & RAPP, R. P. 1992. Clarithromycin: review of a new macrolide antibiotic with improved microbiologic spectrum and favorable pharmacokinetic and adverse effect profiles. *Annals of Pharmacotherapy,* 26**,** 1099-1108.

SUERBAUM, S. & MICHETTI, P. 2002. Helicobacter pylori Infection. *New England Journal of Medicine,* 347**,** 1175-1186.

SUGAWARA, S., IMAI, T. & OTAGIRI, M. 1994. The controlled release of prednisolone using alginate gel. *Pharmaceutical Research,* 11**,** 272-277.

SUKNUNTHA, K., TANTISHAIYAKUL, V., WORAKUL, N. & TAWEEPREDA, W. 2011. Characterization of muco- and bioadhesive properties of chitosan, PVP, and chitosan/PVP blends and release of amoxicillin from alginate beads coated with chitosan/PVP. *Drug Development and Industrial Pharmacy,* 37**,** 408-418.

SULTANA, S., BHAVNA, IQBAL, Z., PANDA, B. P., TALEGAONKAR, S., BHATNAGAR, A. & AHMAD, F. J. 2009. Lacidipine encapsulated gastroretentive microspheres prepared by chemical denaturation for Pylorospasm. *Journal of Microencapsulation,* 26**,** 385-393.

SUN, X., SHI, J., XU, X. & CAO, S. 2013. Chitosan coated alginate/poly(N-isopropylacrylamide) beads for dual responsive drug delivery. *International Journal of Biological Macromolecules,* 59**,** 273-281.

SUNGTHONGJEEN, S., PAERATAKUL, O., LIMMATVAPIRAT, S. & PUTTIPIPATKHACHORN, S. 2006. Preparation and in vitro evaluation of a multiple-unit floating drug delivery system based on gas formation technique. *International Journal of Pharmaceutics,* 324**,** 136-143.

SUZUKI, H. & ISHII, H. 2000. Role of apoptosis in Helicobacter pylori-associated gastric mucosal injury. *Journal of Gastroenterology and Hepatology,* 15**,** D46-D54.

SÝKORA, J., SIALA, K., VARVAŘOVSKÁ, J., PAZDIORA, P., POMAHAČOVÁ, R. & HUML, M. 2009. Epidemiology of Helicobacter pylori Infection in Asymptomatic Children: A Prospective Population-Based Study from the Czech Republic. Application of a Monoclonal-Based Antigen-in-Stool Enzyme Immunoassay. *Helicobacter,* 14**,** 286-297.

TABBAKHIAN, M., HASANZADEH, F., TAVAKOLI, N. & JAMSHIDIAN, Z. 2014. Dissolution enhancement of glibenclamide by solid dispersion: solvent evaporation versus a supercritical fluid-based solvent -antisolvent technique. *Research in Pharmaceutical Sciences,* 9**,** 337-350.

TAFAGHODI, M., TABASI, S. A. S. & JAAFARI, M. R. 2006. Formulation, characterization and release studies of alginate microspheres encapsulated with tetanus toxoid. *Journal of Biomaterials Science, Polymer Edition,* 17**,** 909-924.

TAKAFUMI, I. & KAZUHIKO, I. 2011. Protective Effects of Gastric Mucus. *In:* TONINO, P. (ed.) *Gastritis and Gastric Cancer - New Insights in Gastroprotection, Diagnosis and Treatments.* Croatia: InTech.

TAKAHASHI, T., TAKAYAMA, K., MACHIDA, Y. & NAGAI, T. 1990. Characteristics of polyion complexes of chitosan with sodium alginate and sodium polyacrylate. *International Journal of Pharmaceutics,* 61**,** 35-41.

TAKEUCHI, H., THONGBORISUTE, J., MATSUI, Y., SUGIHARA, H., YAMAMOTO, H. & KAWASHIMA, Y. 2005. Novel mucoadhesion tests for polymers and polymer-coated particles to design optimal mucoadhesive drug delivery systems. *Advanced Drug Delivery Reviews,* 57**,** 1583-1594.

TAKKA, S., OCAK, O. H. & ACARTURK, F. 1998. Formulation and investigation of nicardipine HCl-alginate gel beads with factorial design-based studies. *European Journal of Pharmaceutical Sciences,* 6**,** 241-246.

TALWAR, N., SEN, H. & STANIFORTH, J. N. 2001. *Orally administered controlled drug delivery system providing temporal and spatial control.* US Patent 6261601.

TAMILVANAN, S. & KARMEGAM, S. 2012. In vitro evaluation of chitosan coated- and uncoated-calcium alginate beads containing methyl salicylate-lactose physical mixture. *Pharmaceutical Development and Technology,* 17**,** 494-501.

TANG, Y.-D., VENKATRAMAN, S. S., BOEY, F. Y. C. & WANG, L.-W. 2007. Sustained release of hydrophobic and hydrophilic drugs from a floating dosage form. *International Journal of Pharmaceutics,* 336**,** 159-165.

TANWAR, Y. S., NARUKA, P. S. & OJHA, G. R. 2007. Development and evaluation of floating microspheres of verapamil hydrochloride. *Brazilian Journal of Pharmaceutical Sciences,* 43**,** 529-534.

TAPIA, C., ESCOBAR, Z., COSTA, E., SAPAG-HAGAR, J., VALENZUELA, F., BASUALTO, C., NELLA GAI, M. A. & YAZDANI-PEDRAM, M. 2004. Comparative studies on polyelectrolyte complexes and mixtures of chitosan–alginate and chitosan–carrageenan as prolonged diltiazem clorhydrate release systems. *European Journal of Pharmaceutics and Biopharmaceutics,* 57**,** 65-75.

TAVAKOL, M., VASHEGHANI-FARAHANI, E. & HASHEMI-NAJAFABADI, S. 2013. The effect of polymer and CaCl2 concentrations on the sulfasalazine release from alginate-N,O-carboxymethyl chitosan beads. *Progress in Biomaterials,* 2**,** 10.

THANKA, C. T. H. & VELURAJA, K. 2001. Database analysis of O-glycosylation sites in proteins. *Biophysical Journal,* 80**,** 952-960.

THOMPSON, J. E. & DAVIDOW, L. W. 2009. *A Practical Guide to Contemporary Pharmacy Practice*, Philadelphia, PA : Lippincott Williams & Wilkins.

TIMMERMANS, J. & MOES, A. J. 1994. Factors controlling the buoyancy and gastric retention capabilities of floating matrix capsules: new data for reconsidering the controversy. *Journal of Pharmaceutical Sciences,* 83**,** 18-24.

TIMMERMANS, J. & MOËS, A. J. 1990. How well do floating dosage forms float? *International Journal of Pharmaceutics,* 62**,** 207-216.

TOMIDA, H., NAKAMURA, C., YOSHITOMI, H. & KIRYU, S. 1993. Preparation of Theophylline-Loaded Calcium Alginate Gel Capsules and Evaluation of Their Drug Release Characteristics. *Chemical & Pharmaceutical Bulletin,* 41**,** 2161-2165.

TORRADO, S., PRADA, P. & DE LA TORRE, P. M. 2004. Chitosan-poly(acrylic) acid polyionic complex: in vivo study to demonstrate prolonged gastric retention. *Biomaterials,* 25**,** 917-23.

TORRE, M. L., MAGGI, L., VIGO, D., GALLI, A., BORNAGHI, V., MAFFEO, G. & CONTE, U. 2000. Controlled release of swine semen encapsulated in calcium alginate beads. *Biomaterials,* 21**,** 1493-1498.

TOZUKA, Y., ITO, A., SEKI, H., OGUCHI , T. & YAMAMOTO, K. 2002. Characterization and Quantitation of Clarithromycin Polymorphs by Powder X-Ray Diffractometry and Solid-State NMR Spectroscopy. *Chemical and Pharmaceutical Bulletin,* 50**,** 1128 -1130.

TRIVEDI, P., VERMA, A. M. L. & GARUD, N. 2008. Preparation and characterization of aceclofenac microspheres. *Asian Journal of Pharmaceutics,* 2**,** 110-115.

UMAMAHESHWARI, R. B. & JAIN, N. K. 2003. Receptor mediated targeting of lectin conjugated gliadin nanoparticles in the treatment of Helicobacter pylori. *Journal of Drug Targeting,* 11**,** 415-423

UMAMAHESHWARI, R. B., JAIN, S., BHADRA, D. & JAIN, N. K. 2003. Floating microspheres bearing acetohydroxamic acid for the treatment of Helicobacter pylori. *Journal of Pharmacy and Pharmacology,* 55**,** 1607-1613.

UMAMAHESWARI, R. B., JAIN, S., TRIPATHI, P. K., AGRAWAL, G. P. & JAIN, N. K. 2002. Floating-bioadhesive microspheres containing acetohydroxamic acid for clearance of Helicobacter pylori. *Drug Delivery,* 9**,** 223-31.

UMEZAWA, H. 1978. *Pepstatin floating minicapsules*. United States patent application 05/785268.

URGUHART, J. & THEEUWES, F. 1994. *Drug delivery system comprising a reservoir containing a plurality of tiny pills*. United States Patent 4434153.

VAGHANI, S., VASANTI, S., CHATURVEDI, K., SATISH, C. S. & JIVANI, N. P. 2010. Stomach-specific drug delivery of 5-Fluorouracil using ethylcellulose floating microspheres. *Pharmaceutical Development and Technology,* 15**,** 154-161.

VAICIUNAS, S., OLIVEIRA, M. A., BEZERRA, I. L., OLIVEIRA, E. G., SOUZA, C. M. & LOIOLA, C. F. N. 2010. M1137 Floating-Bioadhesive Microspheres of Clarithromycin Versus Antibacterial Agent Ceragenin CsA-13 for Eradication of Helicobacter pylori Resistant: Meta-Analysis. *Gastroenterology,* 138**,** S339-S340.

VAN GANSBEKE, B., TIMMERMANS, J., SCHOUTENS, A. & MOES, A. J. 1991. Intragastric positioning of two concurrently ingested pharmaceutical matrix dosage forms. *International Journal of Radiation Applications and Instrumentation. Part B, Nuclear Medicine and Biology,* 18**,** 711-718.

VARUM, F. J., VEIGA, F., SOUSA, J. S. & BASIT, A. W. 2012. Mucus thickness in the gastrointestinal tract of laboratory animals. *Journal of Pharmacy and Pharmacology,* 64**,** 218-227.

VASIR, J. K., TAMBWEKAR, K. & GARG, S. 2003. Bioadhesive microspheres as a controlled drug delivery system. *International Journal of Pharmaceutics,* 255**,** 13-32.

VENKATESWARAMURTHY, N., SAMBATHKUMAR, R. & PERUMAL, P. 2012. Controlled release mucoadhesive microspheres of clarithromycin for the treatment of Helicobacter Pylori infection. *Der Pharmacia Lettre,* 4**,** 993-1004.

VENUGOPAL, V. 2011. *Marine Polysaccharides: Food Applications,* Boca Raton, Florida, Taylor & Francis.

VERMA, A., SHARMA, A., VERMA, N. & PANDIT, J. K. 2013. Floating alginate beads: studies on formulation factors for improved drug entrapment efficiency and in vitro release. *Farmacia,* 61**,** 143-160.

VYAS, S. P. & KHAR, R. K. 2006. *Gastroretentive systems. In: Controlled drug Delivery,* Delhi, India, Vallabh Prakashan.

WAGNER, J. G. 1977. Drug bioavailability studies. *Hospital Practice,* 12**,** 119-127.

WAN, L. Q., JIANG, J., ARNOLD, D. E., GUO, X. E., LU, H. H. & MOW, V. C. 2008. Calcium Concentration Effects on the Mechanical and Biochemical Properties of Chondrocyte-Alginate Constructs. *Cellular and Molecular Bioengineering,* 1**,** 93-102.

WANG, F.-J. & WANG, C.-H. 2002. Sustained release of etanidazole from spray dried microspheres prepared by non-halogenated solvents. *Journal of Controlled Release,* 81**,** 263-280.

WANG, J., TAUCHI, Y., DEGUCHI, Y., MORIMOTO, K., TABATA, Y. & IKADA, Y. 2000. Positively charged gelatin microspheres as gastric mucoadhesive drug delivery system for eradication of H. pylori. *Drug Deliv.,* 7**,** 237-43.

WANG, P. & GRANADOS, R. P. 1997. An intestinal mucin is the target substrate for a baculovirus enhancin. *Proceedings of the National Academy of Science of the United States of America,* 94**,** 6977–6982.

WANG, W. 2000. Lyophilization and development of solid protein pharmaceuticals. *International Journal of Pharmaceutics,* 203**,** 1-60.

WARD, K., GASTER, T. & WOOD, R. 2008. Freeze drying Technology. *Biopharma Technology Ltd,* Lulu**,** C19.8-C19.22.

WAUGH, A., GRANT, A. W. & ROSS, J. S. 2001. *Ross and Wilson anatomy and physiology in health and illness,* New York, London, Churchill Livingstone.

WEE, S. & GOMBOTZ, W. R. 1998. Protein release from alginate matrices. *Advanced Drug Delivery Reviews,* 31**,** 267-285.

WEISSENBOCK, A., WIRTH, M. & GABOR, F. 2004. WGA-grafted PLGA-nano spheres: preparation and association with Caco-2 single cells. *Journal of Controlled Release,* 99**,** 383-392.

WHITEHEAD, L., COLLETT, J. H. & FELL, J. T. 2000. Amoxycillin release from a floating dosage form based on alginates. *International Journal of Pharmaceutics,* 210**,** 45-49.

WHITEHEAD, L., FELL, J. T. & COLLETT, J. H. 1996. Preparation of a gastroretentive dosage form. *European Journal of Pharmaceutical Sciences***,** S182.

WHITEHEAD, L., FELL, J. T., COLLETT, J. H., SHARMA, H. L. & SMITH, A. 1998. Floating dosage forms: an in vivo study demonstrating prolonged gastric retention. *Journal of Controlled Release,* 55**,** 3-12.

WILLEMER, H. 1992. Measurements of temperatures, ice evaporation rates and residual moisture contents in freeze-drying. *Developments in Biological Standardization,* 74**,** 123-134.

WISCHKE, C. & BORCHERT, H. H. 2006. Increased sensitivity of chitosan determination by a dye binding method. *Carbohydrate Research,* 341**,** 2978-2979.

WU, C., ZHOU, S. & WANG, W. 1995. A dynamic laser light-scattering study of chitosan in aqueous solution. *Biopolymers,* 35**,** 385-392.

WU, W., YANG, Y. & SUN, G. 2012. Recent Insights into Antibiotic Resistance in Helicobacter pylori Eradication. *Gastroenterology Research and Practice,* 2012**,** 723183.

WU, W., ZHOU, Q., ZHANG, H. B., MA, G. D. & FU, C. D. 1997. Studies on nimodipine sustained-release tablet capable of floating on gastric fluid with prolonged gastric resident time. *Yao Xue Xue Bao (Acta pharmaceutica Sinica),* 32**,** 786-790.

WU, Y. & FASSIHI, R. 2005. Stability of metronidazole, tetracycline HCl and famotidine alone and in combination. *International Journal of Pharmaceutics,* 290**,** 1-13.

YANG, L., ESHRAGHI, J. & FASSIHI, R. 1999. A new intragastric delivery system for the treatment of Helicobacter pylori associated gastric ulcer: in vitro evaluation. *Journal of Controlled Release,* 57**,** 215-222.

YELLANKI, S. K., SINGH, J., SYED, J. A., BIGALA, R., GORANTI, S. & NERELLA, N. K. 2010. Design and characterization of amoxicillin trihydrate mucoadhesive microspheres for prolonged gastric retention. *International Journal of Pharmaceutical Sciences and Drug Research,* 2**,** 112-114.

YIN, Y., CHEN, D., QIAO, M., LU, Z. & HU, H. 2006. Preparation and evaluation of lectin-conjugated PLGA nanoparticles for oral delivery of thymopentin. *Journal of Controlled Release,* 116**,** 337-345.

YOTSUYANAGI, T., OHKBO, T., OHHASHI, T. & IKEDA, K. 1987. Calcium induced gelation of alginic acid and pH sensitive re-swelling of dried gels. *Chemical and Pharmaceutical Bulletin,* 35**,** 1555-1563.

YOTSUYANAGI, T., YOSHIOKA, I., SEGI, N. & IKEDA, K. 1991. Acid-Induced and Calcium-Induced Gelation of Alginic Acid : Bead Formation and pH-Dependent Swelling. *Chemical and Pharmaceutical Bulletin,* 39**,** 1072-1074.

YOUNG, S. A. & SMART, J. D. 1998. A novel in-vitro apparatus for evaluating the mucoadhesion of liquid and semi-solid formulations. *Journal of Pharmacy and Pharmacology,* 50**,** 167-167.

YUASA, H., TAKASHIMA, Y. & KANAYA, Y. 1996. Studies on the development of intragastric floating and sustained release preparation I, Application of calcium silicate as a floating carrier. *Chemical and Pharmaceutical Bulletin,* 44**,** 1361-1366.

ZHANG, D. H., ZHOU, L. Y., LIN, S. R., DING, S. G., HUANG, Y. H., GU, F., ZHANG, L., LI, Y., CUI, R. L., MENG, L. M., YAN, X. E. & ZHANG, J. 2009. Recent changes in the prevalence of Helicobacter pylori infection among children and adults in high- or low-incidence regions of gastric cancer in China. *Chinese Medical Journal (Engl),* 122**,** 1759-1763.

ZHENG, J., LIU, C., BAO, D., ZHAO, Y. & MA, X. 2006. Preparation and evaluation of floating-bioadhesive microparticles containing clarithromycin for the eradication of Helicobacter pylori. *Journal of Applied Polymer Science,* 102**,** 2226-2232.

ZINUTTI, C., KEDZIEREWICZ, F., HOFFMAN, M. & MAINCENT, P. 1994. Preparation and characterization of ethylcellulose microspheres containing 5-fluorouracil. *Journal of Microencapsulation,* 11**,** 555-563.